

APPLICATION OF DEWAR HETEROCYCLES AND VINYL
CARBOCATIONS IN ORGANIC SYNTHESIS

Thesis by

Sepand K. Nistanaki

In Partial Fulfillment of the Requirements

for the Degree of

Doctor of Philosophy

The logo for the California Institute of Technology (Caltech), featuring the word "Caltech" in a bold, orange, sans-serif font.

CALIFORNIA INSTITUTE OF TECHNOLOGY

Pasadena, California

2023

(Defended June 5, 2023)

© 2023

Sepand K. Nistanaki

ORCID: 0000-0002-5252-803X

All Rights Reserved

For my family.

ACKNOWLEDGEMENTS

I would first like to acknowledge my family for their continued love and support. My brother, who is my biggest supporter and best friend, has always been there for me. I could always count on him for a good laugh to lift my spirits during the more challenging moments of my PhD. My mother believed in me way more than I could ever believe in myself, and she is owed tremendous credit for any success I have ever achieved. My father is one of the hardest working individuals I know—he worked hard to give me a better life, and I am eternally grateful for his support and sacrifices.

Next, I would like to thank my PhD advisor, Hosea Nelson, for all his support and mentorship. I was in Hosea's third class of students when I joined the group, and he taught me many things in lab, from the preparation of organomagnesium reagents to setting up reaction screens. But beyond the lessons I learned about lab techniques and tackling research problems, I think the most valuable thing I have learned from Hosea is the importance of entertaining scientific possibilities—the idea that a likely impossible outcome may not be as impossible as you might think. This is a lesson that I hope to carry with me throughout the rest of my scientific career and personal life.

I would next like to thank my committee members, both at UCLA and at Caltech. Professors Neil Garg, Patrick Harran, and Chong Liu were very supportive during my early graduate career at UCLA, and they provided thoughtful feedback on my proposals. Neil was always a great person to talk to and provided great scientific and career-related advice—I am grateful for his continued support beyond my time at UCLA. I would also like to thank Professors Brian Stoltz, Greg Fu, and Jonas Peters who were willing to serve on my thesis committee fairly late in my PhD after transferring to Caltech. During my two

years at Caltech, they have been incredibly supportive and have provided insightful feedback on my proposals and invaluable career advice. I am very fortunate to have gotten to know them and discuss chemistry with them.

I would like to thank Professor Heather Maynard, who has also been a mentor to me during my graduate career given her role as director of the Chemistry-Biology Interface (CBI) training program at UCLA, which I was very fortunate to be a part of. Heather was very dedicated to making CBI an amazing community for chemists and biologists to talk science together, and I learned a lot of challenging biology topics through all the meetings and conferences organized for CBI trainees.

I would like to thank my undergraduate research advisor, Professor Christopher Chang, for welcoming me into his lab to do research at UC Berkeley. My experience in his group was profound, and I was provided opportunities to work on many projects and present my results to the whole group twice a year. I was surrounded by many friendly graduate students and postdocs who were willing to talk to me about anything from chemistry advice to life. It was here that I first learned that chemistry research involves community, a team of individuals united by a shared academic interest. I would also like to thank my graduate student research mentor in the Chang Lab, Eva Nichols, who took me under her wing and spent countless hours weekly to teach me how to make molecules, address unexpected challenges in the lab, and how to think more like a scientist. During my time working with her, she made sure to remind me that although a project may not be going well at a given time, it's important to be optimistic and still have fun doing chemistry. I am very grateful to have worked with her during my undergraduate career, and she has taught me many lessons that I continue to use to this day.

I next want to acknowledge all members of the Nelson lab that I have worked with during my PhD. Alex Bagdasarian (aka “Bags”) was a third-year graduate student (and one of the first members of the Nelson Lab) when I joined the group. We both shared a mutual enjoyment of carbonated Iranian yogurt drinks called “Doogh,” and we frequently indulged in Iranian cuisine, Zankou Chicken (often referred to as “Zank Dank”), and In-N-Out. Alex has also taught me a lot of bench chemistry techniques, including how to run a silica column like a “non-loser.” Brian Shao (aka “Big Man”) was also a third-year graduate student when I joined the group, and he worked in the fume hood right next to me. From him I learned many things, including proper Schlenk technique and the joys of listening to comedy podcasts while at your hood (this has carried me throughout the rest of my PhD). I was very sad when Alex and Brian graduated from our group, because they were mentors as well as great friends. They had incredible work ethic and loyalty to the group, and this had a profound influence on me.

I want to thank Stasik Popov, who is one of the most selfless people I know. Stasik always stopped what he was doing to help me with anything, ranging from the interpretation of my NMR spectra to planning out an experiment. I learned a lot about chemistry and problem solving from Stasik, and he continues to be an important mentor to me to this day. Sydnee Green was also a good friend during graduate school, and I learned a lot from her about how to better communicate science results and how to work with biomolecules such as DNA and RNA.

I want to thank Ben (aka “Methyl Wigs”) Wigman, a good friend throughout graduate school whom I have had the privilege of working on a project with. Ben was always a very hard worker, and being in the same class I think we found ourselves naturally

competing with one another at times (in a healthy way). We share mutual interests in awkward humor and indie music, which has been central to our friendship throughout graduate school and beyond.

I want to thank Chloe Williams, one of my project mates and best friends during graduate school. Chloe is one of the kindest people I know and one of the most skilled purification chemists in our group (she is very good at columns). Chloe is also a great team player, and has always been very dedicated to making our lab a better place for everyone, frequently putting others before herself. I have especially realized this having worked on several research projects with Chloe and together experiencing the joys (?) of moving a lab across town. I think that any lab is lucky to have a person like Chloe around.

Chris Jones, Lee Joon Kim, and Jessica Burch are all admirable lab mates who helped start a new and important subgroup in our lab focused on electron diffraction crystallography with essentially no prior expertise in the discipline. I am fortunate to have experienced the evolution of the structural chemistry subgroup led by their hard work and bravery. I would also like to thank Steven Zhao for being a great lab mate and basically a walking textbook of chemistry knowledge. Woojin Lee, our group's computational chemist, has been great to know over the years—he is a very kind person, and always willing to help in any way that he can.

I want to thank all other members of the Nelson lab not directly mentioned above who I have had the privilege of working with over the years. They are all great co-workers, people who have spent countless hours reading my proposals or chatting with me about science. The Nelson Lab is a fantastic place to be a graduate student, and a big reason for that is the people who make it what it is.

ABSTRACT

High-energy molecules are frequently employed in the construction of organic molecules and materials in both academic and industrial settings. This thesis will address the application of two distinct classes of reactive molecules in organic synthesis: (1) Dewar heterocycles, which contain a highly strained bicyclic structure; (2) vinyl cations, a class of dicoordinated carbocations containing an electron-deficient carbon center bound to only two atoms. While both these classes of molecules are relatively high in energy for distinct reasons (ring strain or electron deficiency), they are united in their potential to undergo powerful chemical reactions as a means to overcome their instability.

To begin, the history and reported applications of Dewar heterocycles and vinyl carbocations in organic synthesis will be discussed through literature examples. A description of our experimental work relevant to this thesis commences with the exploration of Dewar pyrone in the total synthesis of (\pm)-vibrallactone. Specifically, a concise four-step route towards the natural product is enabled by the ability to rapidly install the key β -lactone moiety and all-carbon quaternary center in the photochemical valence isomerization of a prenylated pyrone derivative. Next, the application of Dewar heterocycles to the synthesis of new strained-ring polymers will be discussed, including examples of post-polymerization strategies to access soluble poly(acetylene) derivatives and β -amino acid type polymers. Finally, the development of a catalytic asymmetric C–H insertion reaction of vinyl carbocations will be described, with an emphasis on reaction development, scope, and mechanism. This transition metal-free C–H functionalization methodology is demonstrated in the construction of complex nitrogen-containing bicyclic scaffolds through intramolecular C(sp^3)–H insertion.

PUBLISHED CONTENT AND CONTRIBUTIONS

Portions of the work described herein were disclosed in the following publications:

1. Nistanaki, S. K.; Boralsky, L. A.; Pan, R. D.; Nelson, H. M. A Concise Total Synthesis of (\pm)-Vibralactone. *Angew. Chem. Int. Ed.* **2019**, *58*, 1724–1726. DOI: 10.1002/anie.201812711, Copyright © 2019 Wiley–VCH.

S. K. N. participated in project design, execution of experiments, data analysis, and preparation of manuscript.

2. Nistanaki, S. K.; Nelson, H. M. Dewar Heterocycles as Versatile Monomers for Ring-Opening Metathesis Polymerization. *ACS Macro Lett.* **2020**, *9*, 731–735. DOI: 10.1021/acsmacrolett.0c00227, Copyright © 2020 American Chemical Society.

S. K. N. participated in project design, execution of experiments, data analysis, and preparation of manuscript.

3. Nistanaki, S. K.; Williams, C. G.; Wigman, B.; Wong J. J.; Haas, B. C.; Popov, S.; Werth, J.; Sigman, M. S.; Houk, K. N.; Nelson, H. M. Catalytic asymmetric C–H insertion reactions of vinyl carbocations. *Science* **2022**, *378*, 1085–1091. DOI: 10.1126/science.ade5320, Copyright © 2022 American Association for the Advancement of Science.

S. K. N. participated in project design, execution of experiments, data analysis, and preparation of manuscript.

TABLE OF CONTENTS

Dedication	iii
Acknowledgements	iv
Abstract.....	viii
Published Content and Contributions	ix
Table of Contents	x
List of Abbreviations	xv
CHAPTER 1	1
<i>Application of High-Energy Molecules in Organic Synthesis: Dewar Heterocycles and Vinyl Carbocations</i>	
1.1 INTRODUCTION.....	1
1.2 DEWAR HETEROCYCLES: HISTORY AND REACTIVITY	3
1.2.1 Dewar Pyrone.....	4
1.2.2 Dewar Azacycles: Pyridone, Pyridine, and Azaborine.....	6
1.2.3 Application of Dewar Heterocycles in Small Molecule Synthesis	9
1.2.4 Application of Dewar Heterocycles in Polymer Synthesis	16
1.3 VINYL CARBOCATIONS.....	18
1.3.1 Early History of Vinyl Carbocations.....	19
1.3.2 C–H Insertion Reactions of Vinyl Carbocations	22
1.4 CONCLUSION.....	27

1.5 REFERENCES	28
CHAPTER 2	38
<i>A Concise Total Synthesis of (±)-Vibralactone</i>	
2.1 INTRODUCTION.....	38
2.1.1 Bioactivity.....	38
2.1.2 Biosynthetic Proposal.....	40
2.1.3 Previous Syntheses.....	41
2.1.4 Retrosynthetic Analysis	43
2.2 SYNTHESIS OF (±)-VIBRALACTONE.....	44
2.2.1 Forward Synthesis	44
2.2.2 Attempts to Catalyze Pyrone Photoisomerization	49
2.3 CONCLUSION	51
2.4 EXPERIMENTAL SECTION.....	52
2.4.1 Materials & Methods.....	52
2.4.2 Experimental Procedures & Characterization	53
2.5 REFERENCES	58

APPENDIX 1	62
Spectra Relevant to Chapter 2	
APPENDIX 2	73
X-Ray Data Relevant to Chapter 2	
CHAPTER 3	78
<i>Dewar Heterocycles as Versatile Monomers for Ring-Opening Metathesis Polymerization</i>	
3.1 INTRODUCTION.....	78
3.2 POLYMERIZATION OF DEWAR HETEROCYCLE DERIVATIVES.....	80
3.2.1 Polymerization of Dewar Pyridone Derivatives	82
3.2.2 Polymerization of Dewar Dihydropyridine Derivatives	84
3.2.3 Synthesis of Substituted Poly(acetylene) from α -Pyrone.....	86
3.3 CONCLUSION.....	88
3.4 EXPERIMENTAL SECTION.....	89
3.4.1 Materials & Methods.....	89
3.4.2 Preparation of ROMP Monomers	91
3.4.3 Polymerization Reactions.....	94
3.4.5 FT-IR and UV-Vis Data for Polymer 198	102
3.4.6 GPC Data for Determination of M_n and \bar{M}_w	103
3.5 REFERENCES	109

APPENDIX 3	115
Spectra Relevant to Chapter 3	
CHAPTER 4	122
<i>Catalytic Asymmetric C–H Insertion Reactions of Vinyl Carbocations</i>	
4.1 INTRODUCTION.....	122
4.1.1 Carbocations in Asymmetric Catalysis.....	122
4.1.2 C–H Insertion Reactions of Vinyl Carbocations	125
4.2 REACTION DEVELOPMENT.....	127
4.2.1 Catalyst Discovery	127
4.2.2 Reaction Optimization.....	129
4.2.3 Reaction Scope Studies	130
4.3 MECHANISTIC STUDIES.....	131
4.3.1 Evidence for Vinyl Carbocation Intermediate	131
4.3.2 Origin of Stereoselectivity	133
4.4 ATTEMPTS AT INTERMOLECULAR INSERTION	137
4.5 CONCLUSION.....	140
4.6 EXPERIMENTAL SECTION.....	141
4.6.1 Materials & Methods.....	141
4.6.2 Preparation of Vinyl Tosylate Substrates.....	143
4.6.3 Preparation of Allyl Silane.....	205
4.6.4 Preparation of Catalysts.....	206

4.6.5 Catalytic Asymmetric C–H Insertion Reactions.....	215
4.6.6 Isotopic Labeling Studies.....	238
4.6.7 Chiral HPLC Traces of Racemic and Enantioenriched Products.....	240
4.7 REFERENCES	256
 APPENDIX 4	 264
Spectra Relevant to Chapter 4	
 APPENDIX 5	 512
X-Ray Data Relevant to Chapter 4	
 ABOUT THE AUTHOR	 522

LIST OF ABBREVIATIONS

Å	angstrom(s)
Ac	acetyl
acac	acetylacetonate
AcOH	acetic acid
add'n	addition
aq	aqueous
Ar, (het)Ar	generic aryl, heteroaryl group
ASP	L-aspartic acid
ATP	adenosine triphosphate
β	beta
BINOL	1,1'-bi(2-naphthol)
Boc	<i>tert</i> -butoxycarbonyl
BPin	pinacol boronic ester
Bn	benzyl
bp	boiling point
br	broad
Bu	butyl
¹³ C	carbon-13 isotope
°C	degrees Celsius
ca.	about (Latin <i>circa</i>)
cat.	catalytic
<i>cis</i>	on the same side

cm ⁻¹	wavenumber(s)
COD	1,5-cyclooctadiene
conc.	concentrated
CPME	cyclopentyl methyl ether
Cy	cyclohexyl
CyH	cyclohexane
δ	delta
Δ	heat or difference
d	doublet
D	deuterium
<i>D</i>	dispersity
dba	dibenzylideneacetone
DBU	1,8-diazabicyclo[5.4.0]undec-7-ene
dd	doublet of doublet
DIBAL	diisobutylaluminum hydride
DP	degree of polymerization
dt	doublet of triplet
ddd	doublet of doublet of doublet
DCE	1,2-dichloroethane
DCM	dichloromethane
DMAP	4-dimethylaminopyridine
DMF	<i>N,N</i> -dimethylformamide
DMSO	dimethylsulfoxide

dppf	1,1'-bis(diphenylphosphino)ferrocene
DTBP	di- <i>tert</i> -butyl peroxide
d.r.	diastereomeric ratio
<i>E</i>	trans (entgegen) olefin geometry
EDC(I)	<i>N</i> -(3-dimethylaminopropyl)- <i>N</i> '-ethylcarbodiimide hydrochloride
<i>ee</i>	enantiomeric excess
elim	elimination
es	enantiospecificity
equiv	equivalents(s)
ESI	electrospray ionization
esp	$\alpha,\alpha,\alpha',\alpha'$ -tetramethyl-1,3-benzenedipropionic acid
Et	ethyl
<i>et. al.</i>	and others (Latin: <i>et alii</i>)
EtOAc	ethyl acetate
FD	field desorption
γ	gamma
g	gram
<i>G</i>	Gibbs free energy
G2	Grubbs catalyst 2 nd generation
G3	Grubbs catalyst 3 rd generation
GC-(FID)	gas chromatography (flame ionization detector)
gCOSY	gradient-selected correlation spectroscopy
GPC	gel permeation chromatography

^1H	proton
hr	hour(s)
HIS	L-histidine
HMBC	heteronuclear multiple bond correlation
HMDS	hexamethyldisilazide
$h\nu$	light
HPLC	high-performance liquid chromatography
HRMS	high-resolution mass spectroscopy
HSQC	heteronuclear single quantum correlation
Hz	hertz
IC ₅₀	half maximal inhibitory concentration (50%)
IDPi	imidodiphosphorimidate
i.e.	that is (Latin: <i>id est</i>)
<i>i</i> -Pr	isopropyl
<i>in situ</i>	in the reaction mixture
<i>in vitro</i>	in glass
IPA	isopropanol, 2-propanol
IR	infrared (spectroscopy)
J	coupling constant
k	rate constant
K	Kelvin(s) (absolute temperature)
kcal	kilocalorie
kDa	kilodalton

L	liter
LA	Lewis acid
LDA	lithium diisopropylamide
μ	micro
m	multiplet; milli
<i>m</i>	meta
M	metal; molar; molecular ion
M_n	number average molecular weight
m/z	mass to charge ratio
Me	methyl
Mes	mesityl, mesitylene
mg	milligram(s)
MHz	megahertz
min	minute(s)
mol	mole(s)
MOM	methoxymethyl acetal
Ms	methanesulfonyl (mesyl)
MS	molecular sieves or mass spectrometry
MTBE	methyl <i>tert</i> -butyl ether
n	nano
<i>n</i> -Bu	butyl
<i>n</i> -Pr	propyl
NMR	nuclear magnetic resonance

NOESY	nuclear Overhauser effect spectroscopy
Nu	nucleophile
<i>o</i>	ortho
[Ox.]	oxidation
<i>o</i> -DCB	1,2-dichlorobenzene
<i>o</i> -DFB	1,2-difluorobenzene
obs	observe
OTf	trifluoromethanesulfonate (triflate)
OTs	<i>p</i> -toluenesulfonate (tosylate)
<i>p</i>	para
PCC	pyridinium chlorochromate
PDI	polydispersity index
Ph	phenyl
Piv	trimethylacetyl, pivaloyl
PMP	<i>p</i> -methoxyphenyl
ppm	parts per million
Pr	propyl
py	pyridine
q	quartet
qd	quartet of doublets
R	generic for any atom or functional group
R _f	retention factor
Ref.	reference

ROMP	ring-opening metathesis polymerization
rt	room temperature
σ_p	substituent constant
s	singlet
S ¹	first singlet excited state
sat.	saturated
SER	L-serine
SM	starting material
%T	% transmittance
t	triplet
$t_{1/2}$	half-life
td	triplet of doublet
<i>t</i> -Bu	<i>tert</i> -butyl
TBAF	tetrabutylammonium fluoride
TBS	<i>tert</i> -butyldimethylsilyl
temp.	temperature
TES	triethylsilyl
Tf	trifluoromethanesulfonyl (triflyl)
TFA	trifluoroacetic acid
TFE	2,2,2-trifluoroethanol
TfOH	trifluoromethanesulfonic acid
THF	tetrahydrofuran
TIPS	triisopropylsilyl

TLC	thin-layer chromatography
TMS	trimethylsilyl
TOF	time-of-flight
Tol	tolyl
t_R	retention time
<i>trans</i>	on the opposite side
Ts	<i>p</i> -toluenesulfonyl (tosyl)
UV	ultraviolet
V-65	2,2'-Azobis(2,4-dimethylvaleronitrile)
vib-PT	vibralactone prenyl transferase enzyme
vibC	vibralactone cyclase enzyme
<i>vide infra</i>	see below
λ	wavelength
WCA	weakly coordinating anion
X	anionic ligand or halide
Z	cis (zusammen) olefin geometry

Chapter 1

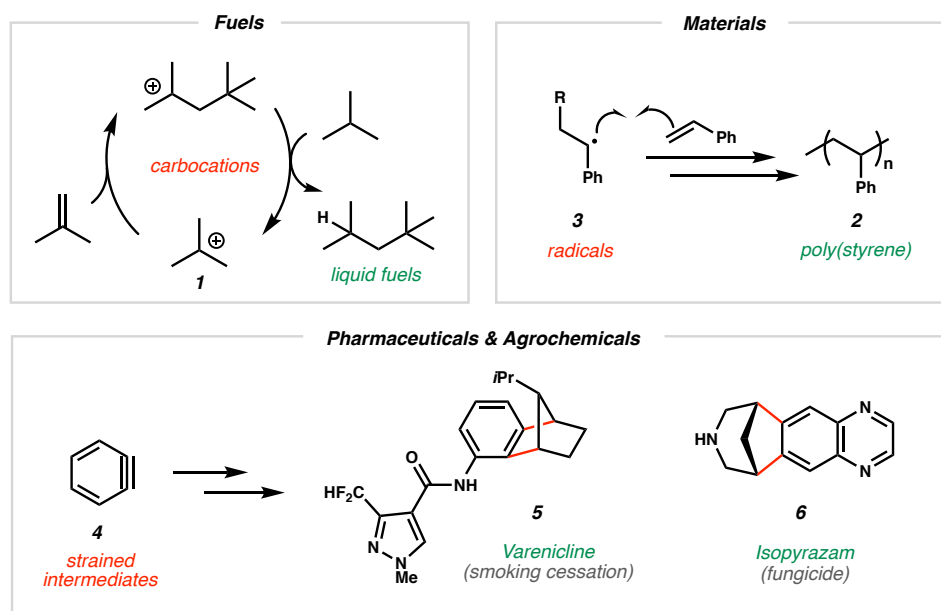
Application of High-Energy Molecules in Organic Synthesis: Dewar Heterocycles and Vinyl Carbocations

1.1 INTRODUCTION

High-energy organic molecules can contain alluring chemical structures, resulting from unusual bonding patterns, geometries, or electron deficiency imparted by charge or low valency. Such molecules can display high reactivity, capable of forming challenging bonds in chemical processes. As such, reactive intermediates are commonly employed in synthetic organic chemistry, in both academic research and industrial processes alike. For example, the petroleum industry heavily utilizes carbocations like **1** (Scheme 1.1) for the synthesis of over 1.5 million barrels of branched hydrocarbons per day.¹ These electron-deficient intermediates have been invoked in various other petrochemical processes, such as Mobil's methanol-to-olefins (MTO) and methanol-to-gasoline (MTG) system.²⁻⁵ Poly(styrene) (**2**), a material found in everyday life, is synthesized through the use of reactive free radical species (**3**) in the polymerization of styrene (Scheme 1.1).⁶⁻⁸ Strain-

induced reactive intermediates, such as arynes (4), are also frequently utilized in the synthesis of pharmaceuticals and agrochemicals, as highlighted by the medicinal chemistry route towards Pfizer's Varenicline (5) (smoking cessation)⁹ and the multi-kilogram scale synthesis of Syngenta's Isopyrazam (6) (fungicide)¹⁰ via aryne cycloaddition reactions.¹¹ These select examples highlight the utility of various classes of reactive molecules in numerous important industrial processes, and shed light on the potential utility of new reactive molecules in organic synthesis.

Scheme 1.1. Application of reactive intermediates in industrial processes



This document is focused on the discussion of two distinct classes of reactive molecules that have been the subject of my PhD research. The first class is in relation to Dewar heterocycles such as 7, which are highly-strained valence isomers of their more familiar aromatic heterocycles, such as pyrone (Scheme 1.2). The second class pertains to

vinyl carbocations (**8**). These are highly reactive intermediates given their cationic charge localized on an electron-deficient *sp*-hybridized carbon center. While both these classes of molecules are “frustrated” by unique structural or electronic features that result in their instability (ring strain *vs* cationic charge), they are united in their utility in undergoing powerful chemical reactions as a means to overcome their high energy. This document will highlight some applications of these intermediates in organic synthesis to date.

Scheme 1.2. Overview of Dewar heterocycles and carbocations

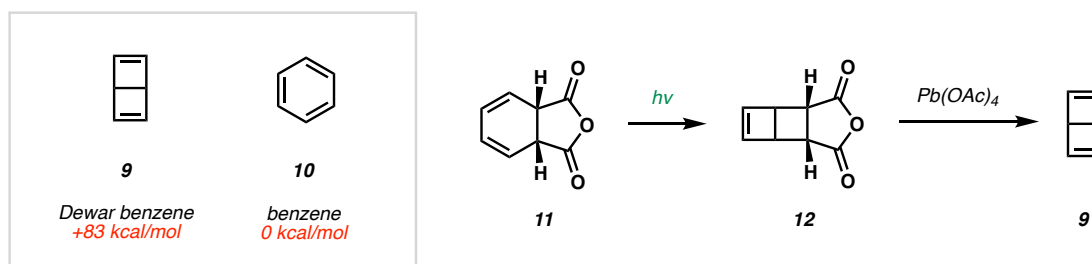


1.2 DEWAR HETEROCYCLES: HISTORY AND REACTIVITY

What is currently referred to as “Dewar benzene” (**9**) was suggested as a potential isomer of C_6H_6 over 150 years ago by James Dewar (Scheme 1.3).^{12,13} Perhaps contrary to popular belief, Dewar never proposed the structure as an alternative to Kekulé’s benzene (**10**) itself, but rather one of seven theoretical isomers of C_6H_6 . In fact, Dewar expressed agreement with August Kekulé’s 1865 proposal of a 6-membered ring with arranged tricoordinate carbon atoms as the likely structure of benzene.¹³ It was not until over 100 years later that the strained bicyclic structure, eventually termed “Dewar benzene”, was synthesized by Eugene van Tamelen (Scheme 1.3).¹⁴ This was achieved through a multistep sequence, involving photochemical valence isomerization of dihydrophthalic anhydride **11**

and subsequent Pb-mediated oxidation of **12**. While this isomer of benzene is significantly more energetic (calculated 81 kcal/mol higher in energy than benzene)^{15,16}, its isomerization back to benzene is kinetically challenged ($t_{1/2} \approx 2$ days at room temperature) given that the necessary disrotatory process is thermally forbidden by the Woodward-Hoffman rules.¹⁴

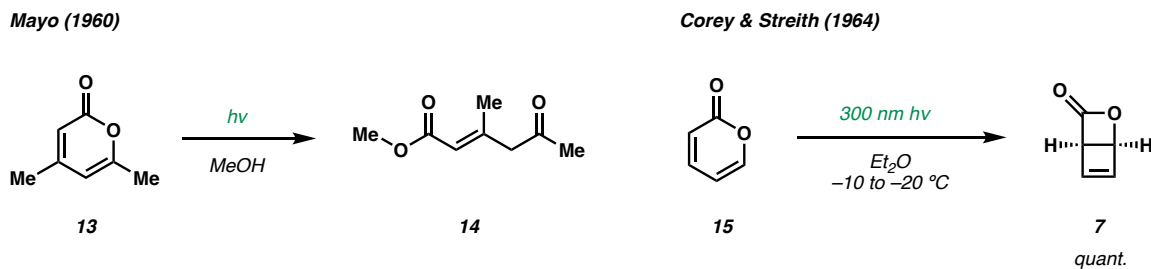
Scheme 1.3. Dewar structure in 1962 synthesis by Tamelen



1.2.1 Dewar Pyrone

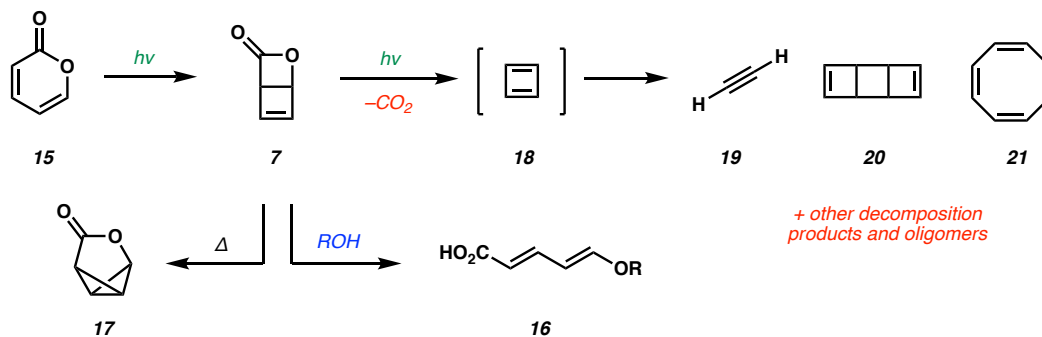
In the same decade that Dewar benzene was first synthesized, reports on the photochemical reactions of heterocyclic compounds were surfacing. Following Mayo's disclosure that α -pyrone **13** could be converted to enoate **14** upon irradiation in methanol solvent^{17,18}, Corey *et al.* disclosed the photochemical valence isomerization of α -pyrone (**15**) to its Dewar isomer (**7**) in diethyl ether (Scheme 1.4).¹⁹ The high energy of Dewar pyrone is embedded in the text of this 1964 report, describing the molecule as "pyrophoric in air at room temperature and which can explode on warming in air."

Scheme 1.4. Early reports of pyrone photochemistry



The thermal instability of Dewar pyrone is attributed to its high strain energy imparted by the fusion of two already-strained 4-membered rings: a β -lactone and a cyclobutene. Unlike Dewar benzene, which lacks polarizing heteroatoms, Dewar pyrone has the capacity to undergo various chemical reactions that result in a range of products. For example, exposure of Dewar pyrone (**7**) to protic solvents results in opening of the β -lactone, followed by 4π electrocyclic ring-opening to form **16** (Scheme 1.5).¹⁸ In polar aprotic solvents, it undergoes thermal isomerization to tricycle **17**.²⁰ Dewar pyrone can also undergo decarboxylation to form antiaromatic cyclobutadiene (**18**), which rapidly decomposes to a range of products such as **19–21**.²¹ One of the most interesting applications of Dewar pyrone is in Cram's study on the room temperature encapsulation of cyclobutadiene in a supramolecular complex.²² This was achieved through the photolysis of encapsulated α -pyrone in a hemicarcerand capsule, which initially converts pyrone to Dewar pyrone (**7**), then ultimately to cyclobutadiene **18** upon loss of CO_2 .

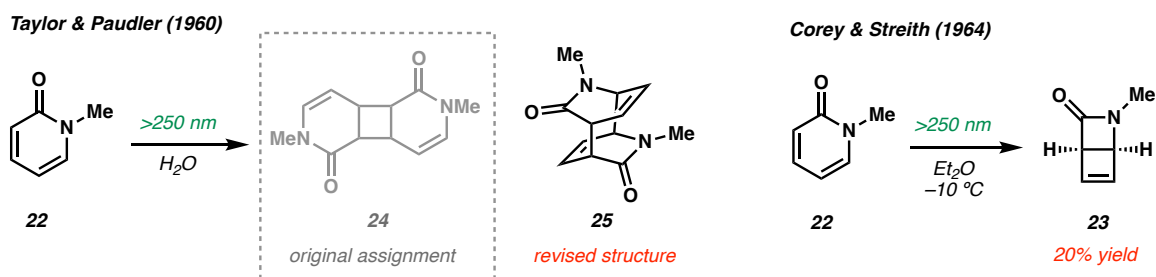
Scheme 1.5. Reactivity of Dewar pyrone



1.2.2. Dewar Azacycles: Pyridone, Pyridine, and Azaborine

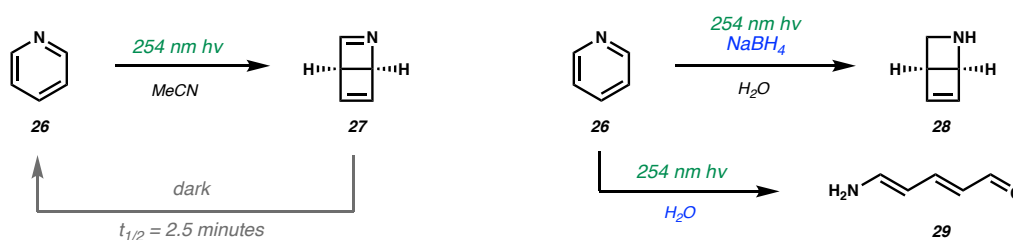
In Corey and Streith's 1964 paper on the valence isomerization of pyrone, the photoisomerization of pyridone **22** to form the β -lactam containing Dewar heterocycle (**23**) was also reported under identical conditions (Scheme 1.6).¹⁹ Interestingly, earlier reports on the photochemistry of pyridone did not mention the formation of bicycle **23**, but rather a dimeric structure assigned originally as **24**, which was later reassigned as **25**.^{23–25} The selectivity for dimerization vs unimolecular valence isomerization was found to be dependent on various factors, including solvent identity, reaction concentration, and substrate structure.

Scheme 1.6. Initial reports of pyridone photochemistry



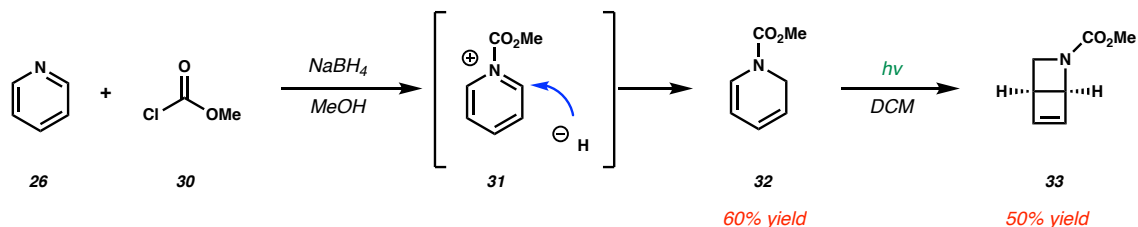
Wilzbach and Rausch reported the photochemical isomerization of pyridine (**26**) to Dewar pyridine (**27**) (Scheme 1.7).²⁶ However, this imine-containing molecule readily converts back to pyridine with a half-life ($t_{1/2}$) of only 2.5 minutes at 25 °C. Conducting the photochemistry in the presence of NaBH_4 could trap the reactive species *via* imine reduction to form azetidine **28**, which was isolable. Photolysis in water produced linear diene **29** resulting from imine hydrolysis followed by 4π electrocyclic ring-opening of the amino cyclobutene.

Scheme 1.7. Wilzbach and Rausch's report of Dewar pyridine and its reactivity



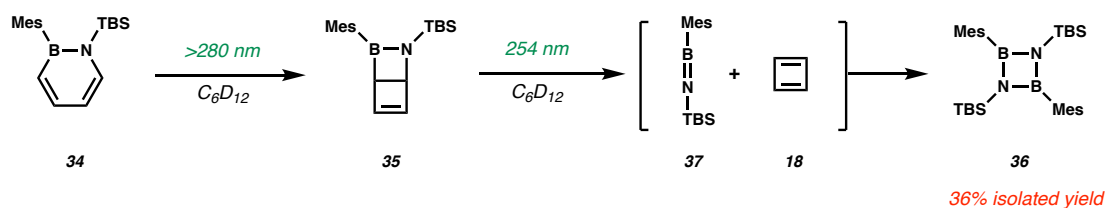
Given Dewar pyridine's fleeting lifetime, another interesting strategy involves prior dearomatization of pyridine in such a way that photoisomerization does not produce an imine-containing product. Fowler demonstrated that the reaction of pyridine with chloroformate electrophiles (**30**) in the presence of NaBH_4 delivered N-protected 1,2-dihydropyridine (**32**) upon N-acyl pyridinium (**31**) reduction (Scheme 1.8).^{27,28} Photolysis of this diene delivered its Dewar isomer (**33**), which could be isolated and was reportedly more stable than its dearomatized precursor (**32**).

Scheme 1.8. Fowler's report of Dewar pyridine and its reactivity



More recently, boron-containing heterocycles have also been studied in the context of Dewar isomerism. Bettinger and Liu found that azaborine **34** underwent photochemical valence isomerization to afford **35** (Scheme 1.9).²⁹ This molecule was reported to be stable at room temperature for weeks, reverting back to **34** over time. Interestingly, irradiation of intermediate **35** with higher energy light (254 nm) resulted in the formation of diazadiboretidine **36**, which was characterized by X-ray crystallography. It was proposed that compound **36** formed from the direct dimerization of iminoborane **37**. While this structure is an isoelectronic analogue to cyclobutadiene, the authors reported that this molecule was isolable by silica column chromatography.

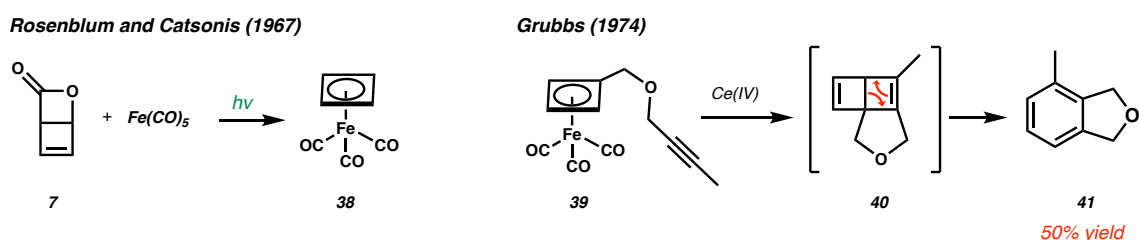
Scheme 1.9. Bettinger and Liu's report of Dewar dihydroazaborinine and reactivity



1.2.3. Application of Dewar Heterocycles in Small Molecule Synthesis

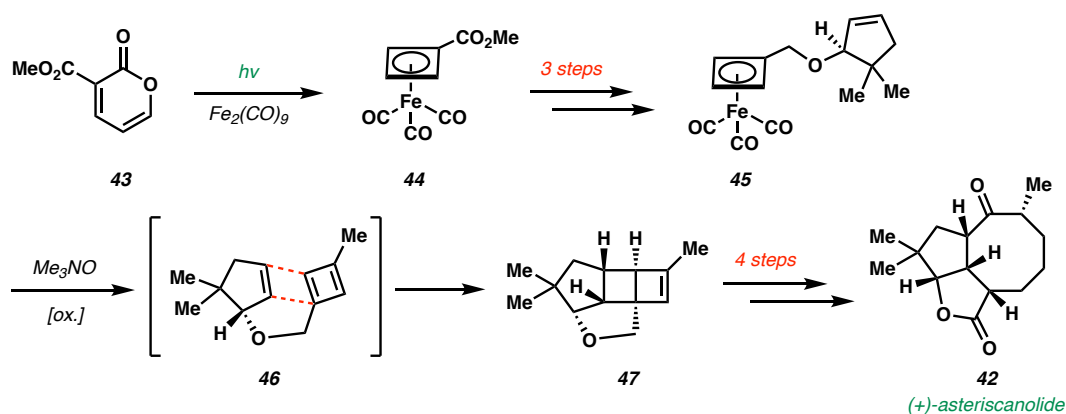
Despite their high energy, Dewar heterocycles are attractive molecules from the perspective of organic synthesis because they can be readily accessed in one step from abundant precursors in a process which installs precise stereochemical features and reactive handles for further synthetic manipulation (i.e., cyclobutene, β -lactone, allylic carboxylate, etc.). It is therefore no surprise that Dewar heterocycles have been applied in various synthetic contexts. An early application of Dewar pyrone was in the preparation of transition metal cyclobutadiene complexes through decarboxylation.^{30,31} It was shown by Rosenblum and Catsonis that the irradiation of Dewar pyrone (**7**) in the presence of $\text{Fe}(\text{CO})_5$ produces iron complex **38** (Scheme 1.10).³⁰ $\text{Fe}(\text{C}_4\text{H}_4)(\text{CO})_3$ has utility as a reagent in organic synthesis, as it can serve as a cyclobutadiene precursor upon chemical oxidation. Cyclobutadiene can be trapped in cycloaddition reactions to construct strained polycyclic molecules. Grubbs *et al.* have demonstrated this in the Ce(IV)-mediated oxidation of **39**, which generated strained Dewar benzene derivative **40** upon cycloaddition with a pendant alkyne, followed by 4π ring-opening to form substituted arene **41**.³²

Scheme 1.10. Synthesis and reactivity of $\text{Fe}(\text{C}_4\text{H}_4)\text{CO}_3$ in cycloaddition chemistry



Snapper and co-workers applied this to the total synthesis of the sesquiterpene natural product (+)-asteriscanolide (**42**) (Scheme 1.11).³³ Photochemical valence isomerization of pyrone **43** in the presence of $\text{Fe}_2(\text{CO})_9$ afforded iron complex **44**. After further synthetic elaboration to install the pendant cyclopentene (**45**), oxidation with trimethylamine N-oxide ejects the reactive cyclobutadiene intermediate, which undergoes intramolecular cycloaddition (**46**) to forge the strained cyclobutene **47**. This reaction rapidly generates stereocomplexity, installing four contiguous stereocenters in a single step. Intermediate **47** was manipulated to forge the requisite cyclooctyl moiety by ring-opening metathesis, followed by spontaneous Cope rearrangement. Further elaboration to Wender's intermediate³⁴ completed the formal synthesis of asteriscanolide (**42**) in 9 steps.

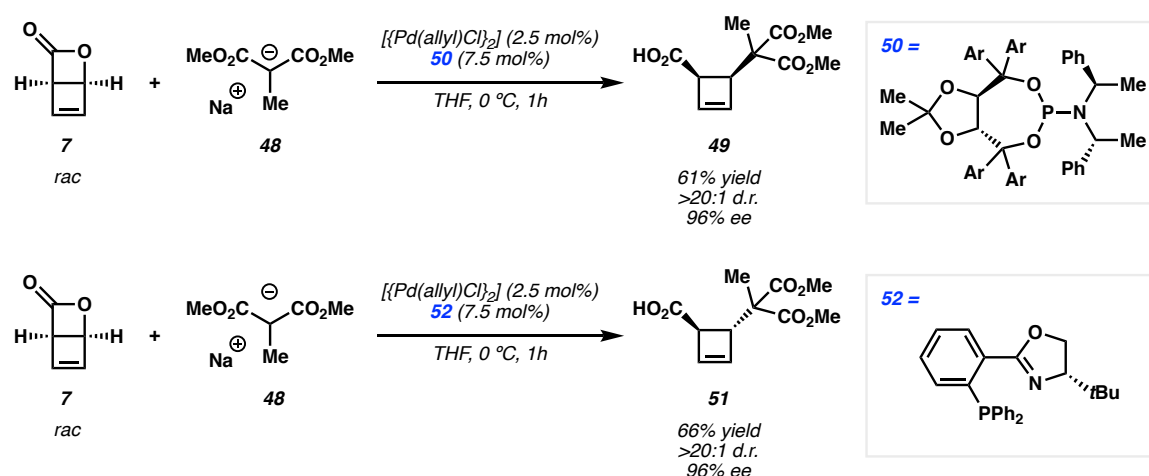
Scheme 1.11. Snapper's synthesis of (+)-asteriscanolide



Maulide and co-workers have reported several creative applications of Dewar pyrones to the stereoselective synthesis of substituted cyclobutenes.³⁵ Four-membered carbocycles are featured in various complex natural products along with pharmaceutical drugs, and are useful building blocks given the potential for synthetic elaboration imparted

by their ring strain.^{36–38} In an early report, they have shown that Pd-catalyzed asymmetric allylic alkylation of soft carbon-based nucleophiles such as **48** with racemic Dewar pyrone can form substituted cyclobutenes (**49**, **51**) with high enantio- and diastereoselectivity (Scheme 1.12).^{39–41} Interestingly, the diastereoselectivity of this process can be controlled through the use of either a phosphoramidite (**50**) or phosphinooxazoline (**52**) ligand.

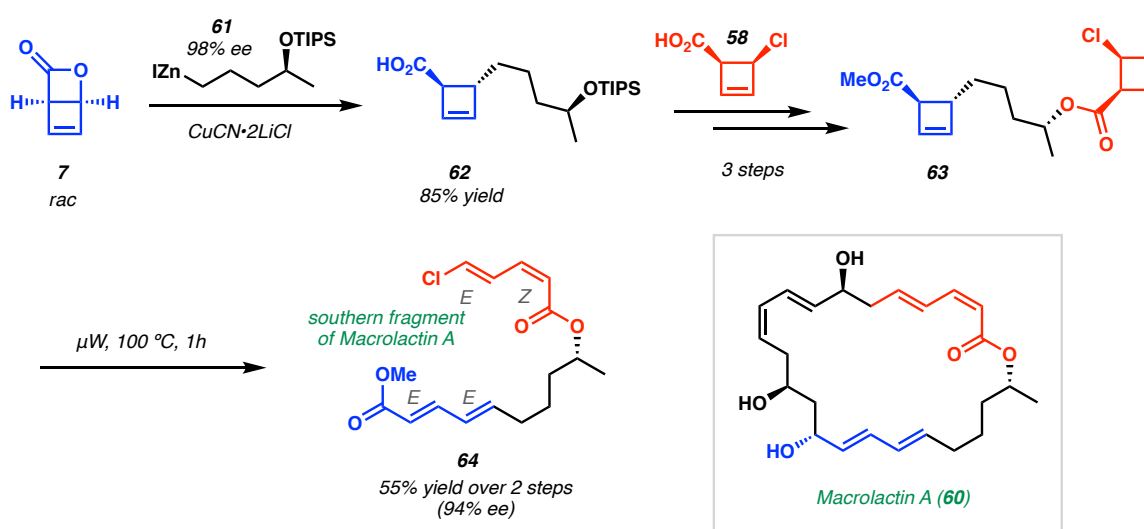
Scheme 1.12. Pd-catalyzed asymmetric allylic alkylation with Dewar pyrones



Maulide and co-workers have also demonstrated an efficient strategy to synthesize polyene motifs in a stereocontrolled fashion from Dewar pyrone.³⁵ Given the prevalence of geometrically precise polyene substructures in natural products and the potential to control stereoselectivity of Dewar pyrone substitution, this presents an efficient strategy to access polyene motifs through 4π electrocyclic ring-opening of substituted cyclobutenes, which undergo a thermal conrotatory opening consistent with the Woodward-Hoffman rules. In a demonstration of this, Maulide and co-workers reported the stereoinvertive Pd-catalyzed Suzuki-Miyaura alkenylation of β -chloro ester **53** (Scheme 1.13).⁴² The

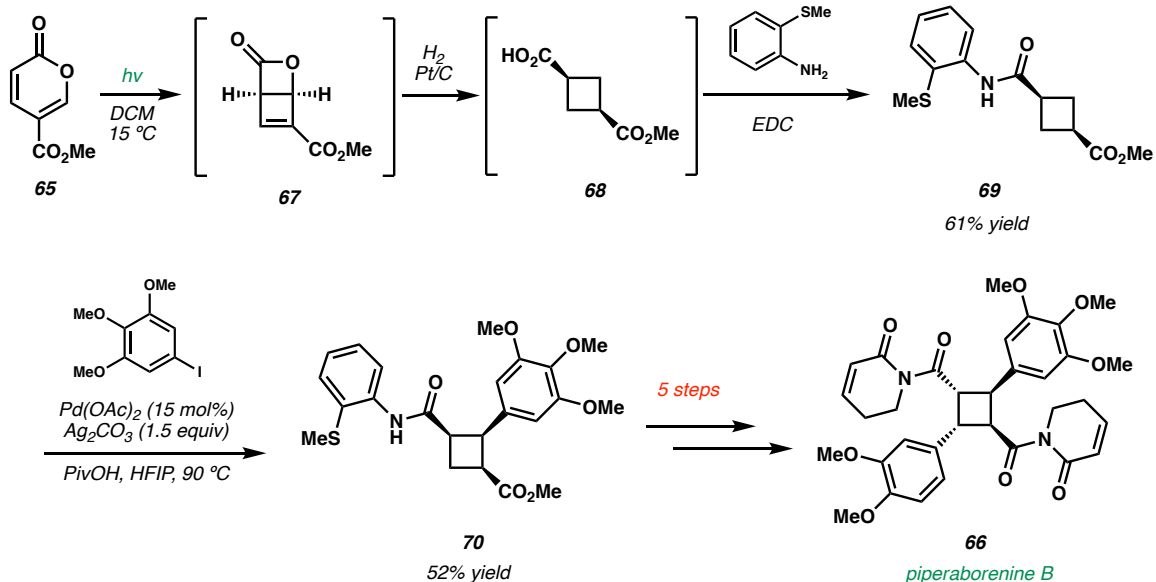
installation of a second Dewar pyrone derivate (**58**) furnished stereodefined intermediate **63**, which underwent global thermal 4π electrocyclic ring-opening to form the southern fragment of macrolactin A (**64**), with precise control over the geometry of all four olefins in the two diene systems.

Scheme 1.14. Maulide's synthesis of the southern fragment of Macrolactin A

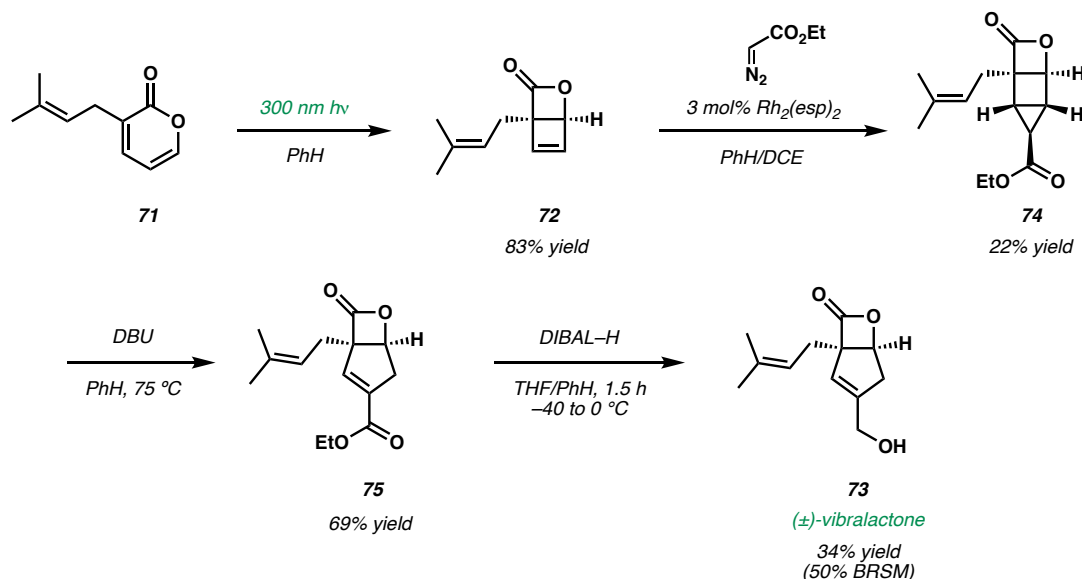


Baran and co-workers leveraged coumalic ester **65** in their synthesis of piperaborenine B (**66**) (Scheme 1.15).⁴⁴ Photolysis to Dewar pyrone **67**, followed by direct hydrogenation and amidation delivered key cyclobutane **69**. Successive Pd-catalyzed C–H arylation enabled stereoselective aryl group installation towards **66** upon epimerization. Importantly, valence isomerization of pyrone **65** enabled rapid access to cyclobutane **69**.

Scheme 1.15. Baran's synthesis of piperaborenine B

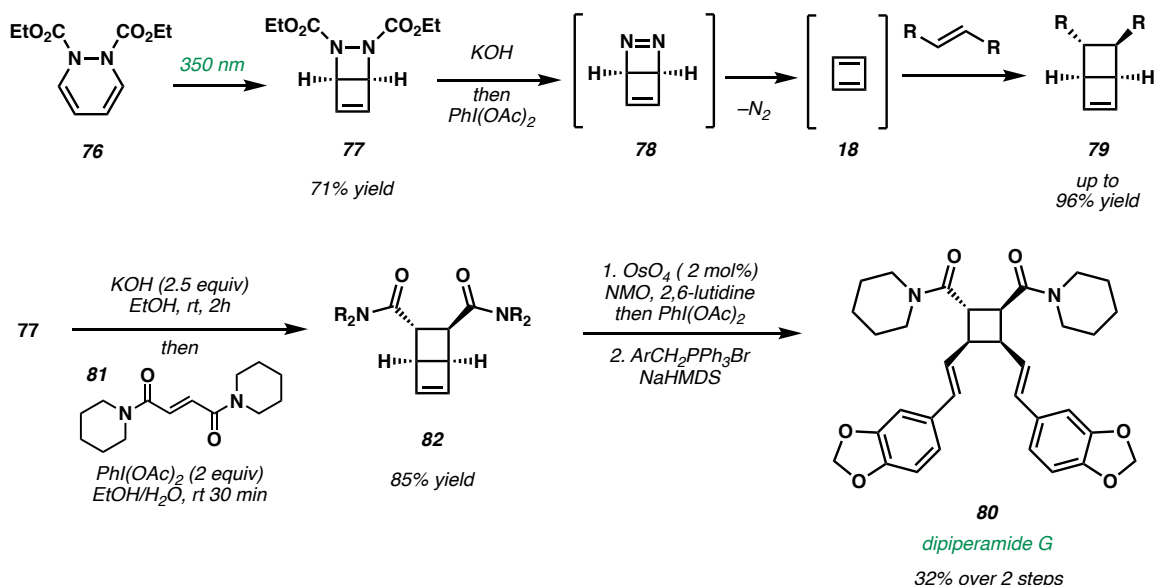


Nelson and co-workers employed a prenylated Dewar pyrone derivative **72** for the expedient synthesis of vibrallactone (**73**), an inhibitor of pancreatic lipase and caseinolytic peptidase ClpP, a conserved enzyme responsible for bacterial virulence (Scheme 1.16).⁴⁵ A Rh-catalyzed cyclopropanation of Dewar pyrone intermediate **72** afforded stereocomplex housane **74**. Ring expansion of **74** under basic conditions followed by reduction of the exocyclic ester in **75** under kinetic control furnished the natural product in four steps from known pyrone **71**. Utilizing pyrone's valence isomer was critical in rapidly assembling the key β -lactone moiety, all-carbon quaternary center, and cyclobutenyl olefin necessary for one-carbon homologation chemistry.

Scheme 1.16. Nelson's synthesis of (\pm)-vibralactone

Recently, Burns *et al.* have devised a clever strategy for generating cyclobutadiene from photochemically-derived Dewar azacycle **77** (Scheme 1.17).⁴⁶ Hydrolysis of the diazabicyclohexene diester followed by $PhI(OAc)_2$ -mediated oxidation furnishes Dewar pyridazine (**78**), which undergoes spontaneous N_2 -elimination to form cyclobutadiene (**18**), which is trapped by a range of reaction partners *via* intermolecular cycloaddition reactions to forge strained bicyclohexenes (**79**). This strategy is attractive because it could avoid the use of stoichiometric $Fe(C_4H_4)(CO)_3$ (**38**), which is laborious to synthesize and requires toxic reagents. This methodology was applied to the total synthesis of dipiperamide **G** (**80**) through the cycloaddition of diamide **81** with cyclobutadiene to form bicyclohexene **82**.

Scheme 1.17. Burns' synthesis of dipiperamide **G** via a Dewar dihydropyridazine



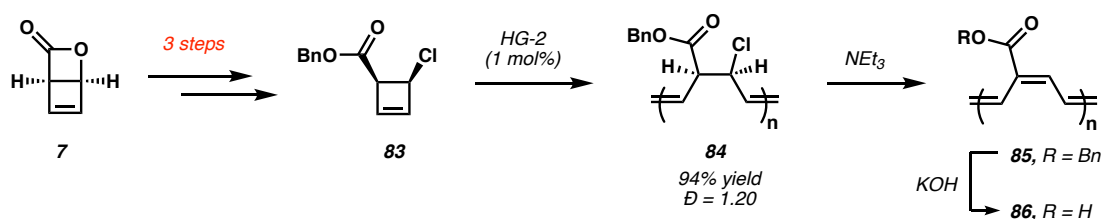
1.2.4. Application of Dewar Heterocycles in Polymer Synthesis

Strain is often leveraged as a driving force in polymerization reactions, and cyclobutenes are known to be reactive monomeric units for ring-opening metathesis polymerization (ROMP).⁴⁷ The cyclobutene motif of Dewar heterocycles therefore could serve as a highly reactive handle for ROMP chemistry. However, application of Dewar heterocycles to polymer synthesis has been explored to a lesser extent when compared to small molecule synthesis.

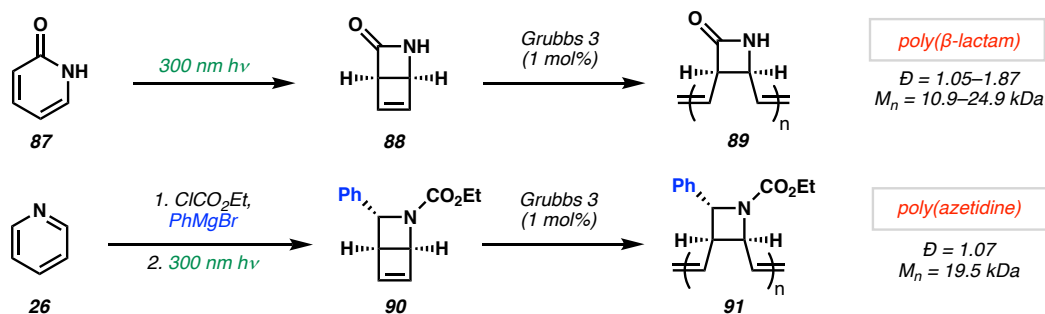
Bielawski and co-workers reported the polymerization of cyclobutene substrates (**83**) derived from Dewar pyrone to form β -chloroester-containing polymers (**84**) (Scheme 1.18).⁴⁸ These could easily be converted to soluble poly(acetylene) derivatives (**85**) through base-mediated elimination. Moreover, hydrolysis of the ester moiety delivered a water-soluble poly(acetylene) derivative **86**. While poly(acetylene) possesses conductive

properties when doped, it is a notoriously insoluble material, rendering it difficult for processing in the application to electronic devices.^{49,50} Several strategies have been devised to address this, including the synthesis of more soluble block co-polymers consisting of poly(acetylene)^{51,52}, synthesis of a soluble polymer precursor to poly(acetylene)^{53–55}, and synthesis of substituted poly(acetylene)s *via* monomer-derivatization.^{56,57} The strategy reported by Bielawski *et al.*⁴⁸ demonstrates the ability to access various substituted poly(acetylene)s through appendage of functional groups onto the ester of cyclobutene **83**.

Scheme 1.18. Bielawski's synthesis of poly(acetylene) derivatives



Nelson and co-workers similarly utilized the strain energy of cyclobutenes in Dewar heterocycles for polymer synthesis.⁵⁸ Unlike Bielawski's report, wherein prior β -lactone ring-opening precedes polymerization, Nelson and co-workers directly polymerized Dewar heterocycles to access polymers with strained rings embedded in their backbone (Scheme 1.19). Dewar pyridones such as **88** were polymerized with Grubbs 3 catalyst to yield poly(β -lactam)s such as **89**. Poly(azetidines) such as **91** could be accessed from pyridine through prior nucleophilic addition to acylated pyridinium ions. The resulting polymers were obtained with low dispersity (D), and their molecular weights could be reliably tuned by controlling the catalyst loading.

Scheme 1.19. Synthesis of strained-ring polymers via ROMP of Dewar Heterocycles

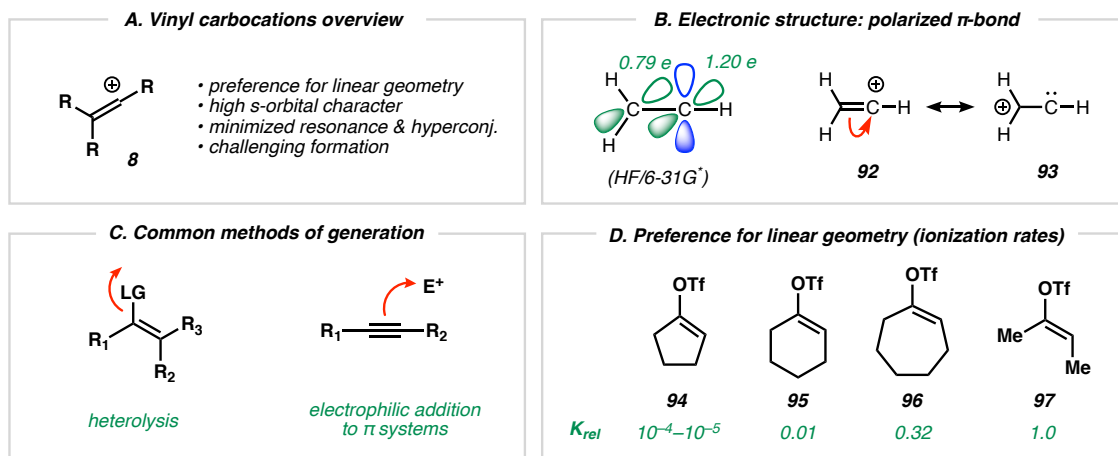
1.3 VINYL CARBOCATIONS

The second class of reactive molecules pertains to carbocations. These “classic” intermediates are highly electrophilic given their electron-deficiency, prompting reactivity with even weakly nucleophilic reacting partners. There are several classifications of carbocations, the most common being that of tricoordinated carbocations. These feature a cationic carbon center bonded to three atoms; typically, these are characterized by trigonal planar geometry and sp^2 -hybridization, and overall they have found tremendous utility in synthetic organic chemistry.⁵

This section will be focused on another class of carbocations known as vinyl carbocations, which are described by a cationic carbon center bound to two groups (Scheme 1.20).⁵⁹ Historically, vinyl cations have been more difficult to generate than their tricoordinated counterparts, and their higher s -orbital character renders them highly electrophilic. The electronic structure of a vinyl carbocation is also unique given the existence of a π -bond, which has been computed to be highly polarized towards the cationic carbon center, as depicted by resonance structures **92** and **93** (Scheme 1.20b).⁶⁰ While there have been various approaches towards generating these reactive intermediates, two

common approaches involve heterolysis of a vinyl (pseudo)halide or electrophilic addition to a π -bond such as an alkyne (Scheme 1.20c).^{59,61} Moreover, vinyl cations prefer to adopt a linear geometry, and early experimental evidence for this arises from the significant rate differences in solvolysis reactions of vinyl triflates **94–97** (Scheme 1.20d).⁶¹ Overall, vinyl cations have seen significantly less attention in synthesis, likely given their more challenging formation and difficulty in subjection to selective chemical reactions.

Scheme 1.20. Overview of vinyl carbocations

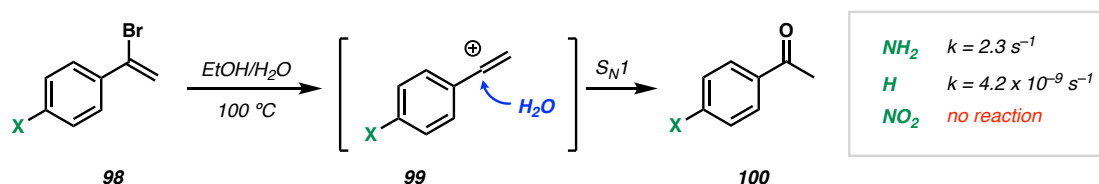


1.3.1. Early History of Vinyl Carbocations

Early reports by Jacobs and Searles on the hydration of acetylenic ethers under acidic conditions pointed towards the possible intermediacy of a heteroatom-stabilized vinyl carbocation which undergoes S_N1 -type trapping with solvent.⁶² Eventually, work by Grob and co-workers provided mechanistic support for the intermediacy of a vinyl carbocation in the solvolysis of vinyl bromides (Scheme 1.21).^{63,64} They found that heating

vinyl bromides of type **98** in aqueous ethanol at 100 °C resulted in the formation of ketone **100**, presumably through the trapping of a vinyl carbocation intermediate (**99**) by water.⁶³ The influence of substituents on rate is consistent with the development of positive charge in the rate-determining transition state, wherein electron-donating groups resulted in significantly faster reactions, while strong electron-withdrawing groups essentially halted the reaction (Scheme 1.21). Addition of triethylamine base did not perturb the reaction rate, which would be expected if an acid-catalyzed olefin hydration/elimination pathway through a benzylic carbocation intermediate was operative. Generation of phenylacetylene as a side product *via* E1 elimination of a putative vinyl cation also supports its intermediacy.

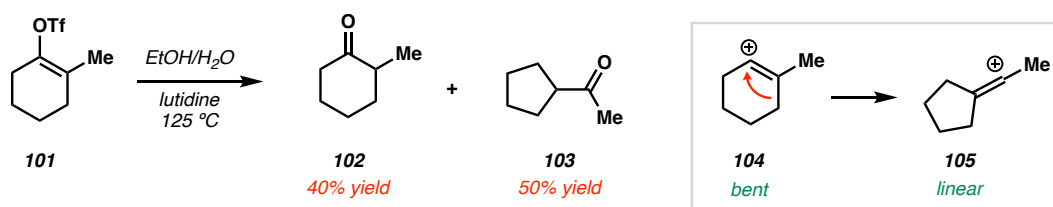
Scheme 1.21. Early solvolysis studies of vinyl bromides by Grob



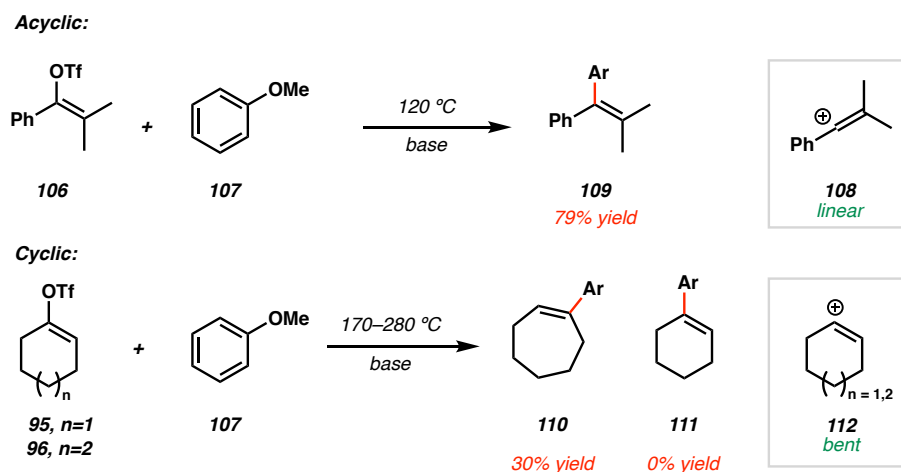
Following these early studies by Grob, various reports of solvolysis reactions involving putative vinyl carbocation intermediates were surfacing, and “vinyl cations have finally become acceptable members of the ‘reactive intermediate’ community.”^{61,65} For example, Noyce *et al.* reported the acid-catalyzed hydration of alkynes, wherein a rate-determining alkyne protonation to a vinyl carbocation intermediate was invoked.⁶⁶ Stang, Schleyer, and Hanack reported the ring-contraction reactions of cyclic vinyl triflates (Scheme 1.22). Heating vinyl triflate **101** in the presence of lutidine base in aqueous media resulted in the formation of solvolysis product **102**, along with ring-contracted

acyclopentane **103**, which presumably arises from a 1,2-alkyl shift across a cyclic vinyl cation **104** to the linear vinyl cation **105** prior to trapping with water.

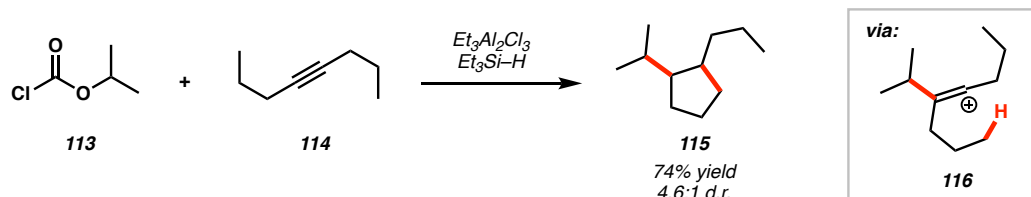
Scheme 1.22. Ring-contraction reactions of cyclic vinyl carbocations



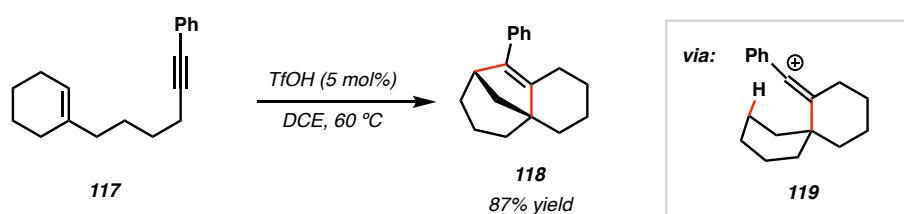
While most early reports of reactions invoking vinyl carbocations involve C–O bond formation (from quenching with aqueous solvent), reports of C–C bond-formation *via* Friedel-Crafts reactions of vinylic substrates were also known.^{67–70} Ultimately, mechanistic studies by Roberts *et al.*⁶⁹ and Stang *et al.*⁷¹ supported the intermediacy of a vinyl carbocation in Friedel-Crafts reactions. In Stang's studies, it was found that acyclic vinyl triflate **106** underwent Friedel-Crafts arylation with anisole (**107**) *via* a proposed linear vinyl cation intermediate (**108**) in non-aqueous media (Scheme 1.23). However, cyclic substrates required significantly higher temperatures to react, wherein cycloheptenyl triflate (**96**) reacted at 170 °C to form adduct **110** in 30% yield, while the smaller cyclohexenyl triflate (**95**) was unreactive up to 280 °C. These data are consistent with a preferred linear geometry of vinyl carbocations, as cyclic vinyl triflates possessing larger ring sizes can achieve greater linearity in the vinyl cation intermediate (**112**).⁷²

Scheme 1.23. Friedel-Crafts reactions of vinyl carbocations**1.3.2. C–H Insertion Reactions of Vinyl Carbocations**

Perhaps one of the most interesting aspects of vinyl carbocations is their propensity to undergo insertion into unactivated $C(sp^3)\text{--}H$ bonds. This is a fundamentally unique reactivity profile associated with this class of carbocations that is not known with tricoordinated carbocations. While C–H insertion is typically associated with metal-based reaction platforms, the C–H insertion reactivity of vinyl cations presents an attractive metal-free approach towards C–H functionalization. The key to accessing this reactivity is the generation of a vinyl carbocation under non-polar conditions such that traditional solvolysis reactions could be avoided. Lewis acid-mediated vinyl cation generation has been particularly useful in this regard. An early report by Metzger and co-workers highlighted the formation of cyclopentane **115** through the reaction of a chloroformate ester **113** with an alkyne (**114**) in the presence of Al-based Lewis acid (Scheme 1.24).⁷³ It is proposed that addition of an isopropyl cation to an alkyne results in vinyl carbocation **116**, which undergoes insertion into the terminal methyl C–H bond.

Scheme 1.24. Early report of vinyl cation C–H insertion by Metzger

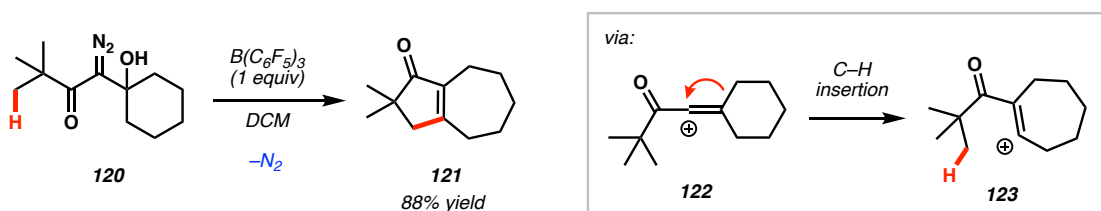
Yamamoto and co-workers demonstrated that alkynes could similarly be engaged in intramolecular cyclization through alkylation of a pendant alkyne in a catalytic fashion (Scheme 1.25).⁷⁴ In this reaction, a putative tricoordinated carbocation is generated by protonation of **117** by a strong Brønsted acid TfOH ($\text{pK}_a = 0.7$ in MeCN⁷⁵). Similar to Metzger's report, a vinyl carbocation was proposed to undergo insertion into an appended cyclohexyl ring to generate tricyclic product **118**. This report demonstrates the ability to efficiently generate complex polycyclic scaffolds from simple precursors.

Scheme 1.25. Cascade alkyne alkylation/C–H insertion via Brønsted acid catalysis

Brewer and co-workers reported the decomposition of β -hydroxy diazoketone **120** in the presence of stoichiometric strong Lewis acid $\text{B}(\text{C}_6\text{F}_5)_3$ to furnish an intermediate acyclic vinyl carbocation **122** after loss of N_2 gas (Scheme 1.26).⁷⁶ Ring-expansion to

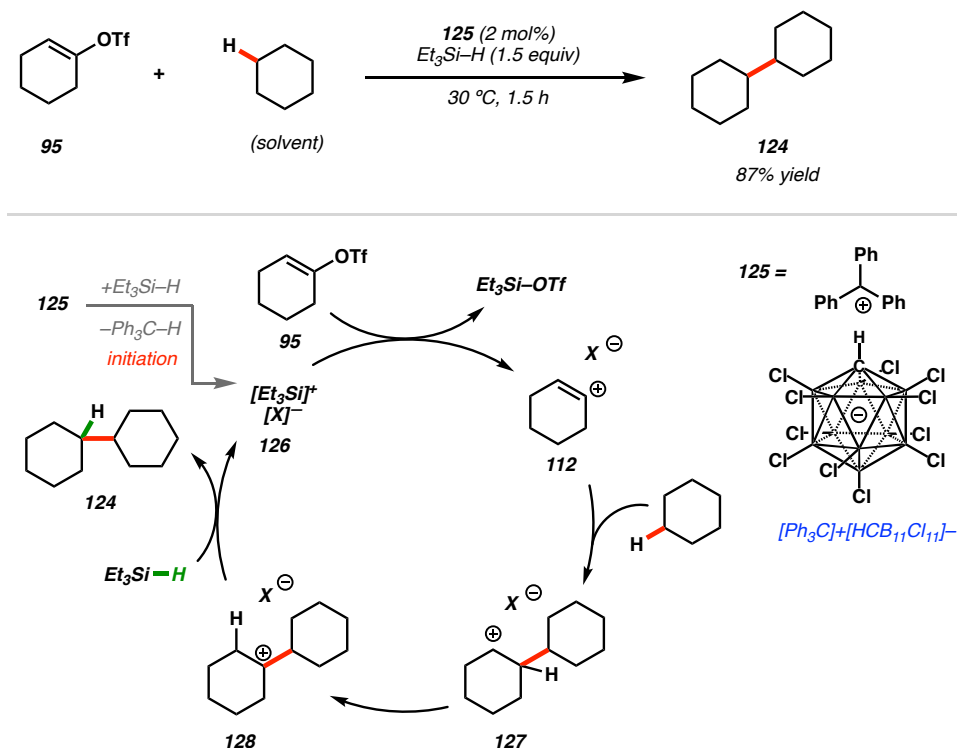
cycloheptyl cation **123** enables quenching of the vinyl cation through intramolecular C–H insertion to the pendant *t*Bu group to furnish [3.5.0]bicyclodecenone **121**.

Scheme 1.26. Brewer's Lewis acid-mediated vinyl carbocation generation

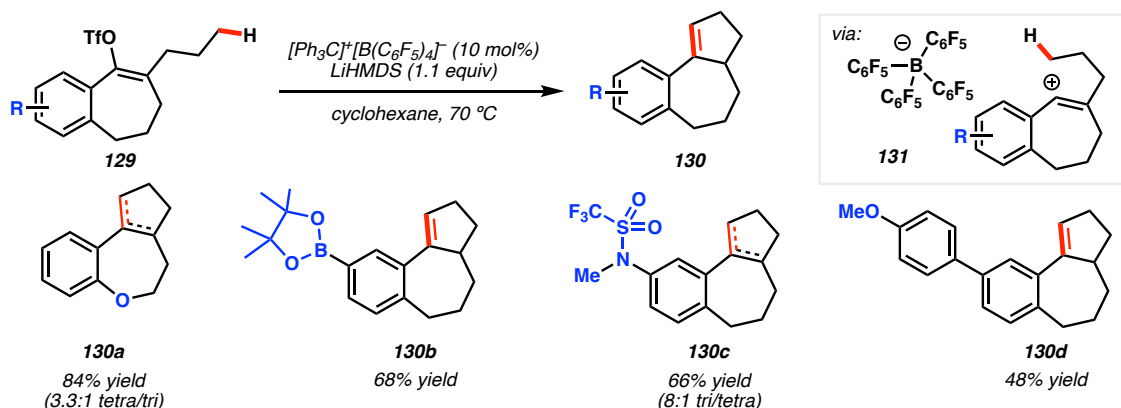


Nelson and co-workers developed a catalytic platform for the intermolecular C–H insertion reactions of vinyl carbocations utilizing Lewis acids comprised of weakly coordinating carborane anions.⁷⁷ In this system, vinyl triflate **95** alkylates cyclohexane (solvent) at room temperature in the presence of catalytic **125** and silane (Scheme 1.27). It is proposed that the reaction of **125** with silane *via* a Bartlett-Condon-Schneider hydride exchange generates a silylium species **126** paired with the weakly coordinating carborane anion. The high Lewis acidity of this species enables triflate abstraction from **95** to produce vinyl cation **112**, which has previously been difficult to generate thermally in polar media. Intermolecular C–H insertion followed by sequential hydride shift to **128** and quench by silane forms the alkylated product (**124**) and regenerates catalytic silylium (**126**). The role of the weakly coordinating anion in this system is to enhance the Lewis acidity of the silylium ion, while also preventing unproductive E1 or S_N1 pathways that would traditionally arise from a more basic counter anion.

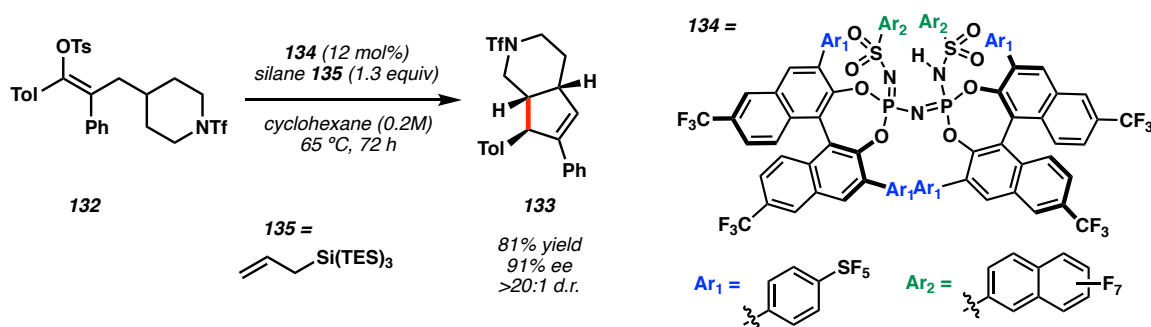
Scheme 1.27. Catalytic intermolecular C–H insertion of cyclic vinyl cations



Nelson *et al.* later reported a catalytic platform for intramolecular C–H insertion under basic conditions (Scheme 1.28).⁷⁸ Notably, this system showed markedly improved functional group tolerance by employing a milder Li-based Lewis acid catalyst, which is derived from a commercially-available borate salt. This was applied to the synthesis of 6-7-5 tricyclic systems (**130**) *via* the insertion of vinyl cation **131** into an appended alkyl chain. Select examples of substrates with tolerated heteroatom functionality, such as boronic esters (**130b**) and sulfonamides (**130c**), are shown in Scheme 1.28.

Scheme 1.28. Li-catalyzed vinyl cation generation under basic conditions

More recently, Nelson and co-workers developed a catalytic asymmetric C–H insertion reaction by leveraging List’s chiral imidodiphosphorimidate (IDPi) scaffold (**134**) as a strong acid catalyst (Scheme 1.29).^{73,79} Here, silylation of IDPi **134** generates a strong Lewis acid catalyst capable of ionizing tosylate **132** to generate a vinyl carbocation which undergoes insertion into an appended piperidine ring. Three contiguous stereocenters are set with high enantioselectivity (up to 93% *ee*) and diastereoselectivity (>20:1 d.r.), demonstrating the ability to generate stereocomplex nitrogen-containing polycyclic scaffolds, which are found in numerous bioactive natural products.⁸⁰

Scheme 1.29. Catalytic asymmetric C–H insertion of vinyl cations

1.4 CONCLUSION

High-energy molecules continue to capture the attention of chemists who are fascinated by their exotic chemical structures and high reactivities. Highly strained Dewar heterocycles and electrophilic vinyl carbocations are discussed in this chapter as two distinct classes of reactive molecules that have proven useful in bond-forming reactions.

While Dewar heterocycles have already found extensive utility in synthetic organic chemistry, such as in natural product total synthesis and polymer synthesis, new strategies for their preparation and synthetic elaboration will continue to broaden their utility. For example, the development of catalytic asymmetric methods for accessing enantioenriched Dewar heterocycles, perhaps through an enantioselective photoisomerization process, would further expand the utility of these chiral building blocks in the synthesis of organic molecules and materials.

Vinyl carbocations, given their ability to undergo C–H insertion, have considerable utility as intermediates relevant to metal-free C(*sp*³)–H functionalization reactions. However, catalytic asymmetric platforms for the intermolecular reactions of vinyl cations are currently undeveloped, despite its potential utility in organic synthesis. Issues surrounding vinyl cation persistence and C–H functionalization site selectivity will likely be some of the primary challenges in this area. It is expected that the development of more acidic chiral catalysts will enable not only intermolecular reactivity, but ultimately expand the scope of vinyl carbocations that can be generated. Therefore, it is anticipated that catalyst development will drive further advancement in this area.

1.5 REFERENCES

- (1) Olah, G. A. *Hypercarbon Chemistry*, 2nd ed.; J. Wiley & Sons: Hoboken, N.J, 2011.
- (2) Tian, P.; Wei, Y.; Ye, M.; Liu, Z. Methanol to Olefins (MTO): From Fundamentals to Commercialization. *ACS Catal.* **2015**, *5*, 1922–1938.
- (3) Li, J.; Wei, Y.; Chen, J.; Tian, P.; Su, X.; Xu, S.; Qi, Y.; Wang, Q.; Zhou, Y.; He, Y.; Liu, Z. Observation of Heptamethylbenzenium Cation over SAPO-Type Molecular Sieve DNL-6 under Real MTO Conversion Conditions. *J. Am. Chem. Soc.* **2012**, *134*, 836–839.
- (4) McCann, D. M.; Lesthaeghe, D.; Kletnieks, P. W.; Guenther, D. R.; Hayman, M. J.; Van Speybroeck, V.; Waroquier, M.; Haw, J. F. A Complete Catalytic Cycle for Supramolecular Methanol-to-Olefins Conversion by Linking Theory with Experiment. *Angew. Chem. Int. Ed.* **2008**, *47*, 5179–5182.
- (5) Naredla, R. R.; Klumpp, D. A. Contemporary Carbocation Chemistry: Applications in Organic Synthesis. *Chem. Rev.* **2013**, *113*, 6905–6948.
- (6) Flory, P. J. The Mechanism of Vinyl Polymerizations¹. *J. Am. Chem. Soc.* **1937**, *59*, 241–253.
- (7) Mayo, F. R. Chain Transfer in the Polymerization of Styrene. VIII. Chain Transfer with Bromobenzene and Mechanism of Thermal Initiation¹. *J. Am. Chem. Soc.* **1953**, *75*, 6133–6141.
- (8) Khuong, K. S.; Jones, W. H.; Pryor, W. A.; Houk, K. N. The Mechanism of the Self-Initiated Thermal Polymerization of Styrene. Theoretical Solution of a Classic Problem. *J. Am. Chem. Soc.* **2005**, *127*, 1265–1277.

- (9) Coe, J. W.; Brooks, P. R.; Wirtz, M. C.; Bashore, C. G.; Bianco, K. E.; Vetelino, M. G.; Arnold, E. P.; Lebel, L. A.; Fox, C. B.; Tingley, F. D.; Schulz, D. W.; Davis, T. I.; Sands, S. B.; Mansbach, R. S.; Rollema, H.; O'Neill, B. T. 3,5-Bicyclic Aryl Piperidines: A Novel Class of A4 β 2 Neuronal Nicotinic Receptor Partial Agonists for Smoking Cessation. *Bioorg. Med. Chem. Lett.* **2005**, *15*, 4889–4897.
- (10) Schleth, F.; Vettiger, T.; Rommel, M.; Tobler, H. Process for the Preparation of Pyrazole Carboxylic Acid Amides. International Patent WO2011131544A1, 2011.
- (11) Anthony, S. M.; Wonilowicz, L. G.; McVeigh, M. S.; Garg, N. K. Leveraging Fleeting Strained Intermediates to Access Complex Scaffolds. *JACS Au* **2021**, *1*, 897–912.
- (12) Dewar, J. 5. On the Oxidation of Phenyl Alcohol, and a Mechanical Arrangement Adapted to Illustrate Structure in the Nonsaturated Hydrocarbons. *Proc. R. Soc. Edinb.* **1869**, *6*, 82–86.
- (13) Baker, W.; Rouvray, D. H. Para-Bond or “Dewar” Benzene? *J. Chem. Educ.* **1978**, *55*, 645.
- (14) Van Tamelen, E. E.; Pappas, S. P. Bicyclo [2.2.0]Hexa-2,5-Diene. *J. Am. Chem. Soc.* **1963**, *85*, 3297–3298.
- (15) Johnson, R. P.; Daoust, K. J. Electrocyclic Ring Opening Modes of Dewar Benzenes: Ab Initio Predictions for Möbius Benzene and *Trans* -Dewar Benzene as New C₆H₆ Isomers. *J. Am. Chem. Soc.* **1996**, *118*, 7381–7385.
- (16) Kelleghan, A. V.; Bulger, A. S.; Witkowski, D. C.; Garg, N. K. Strain-Promoted Reactions of 1,2,3-Cyclohexatriene and Its Derivatives. *Nature* **2023**.
<https://doi.org/10.1038/s41586-023-06075-8>.

- (17) De Mayo, P. *Advan. Org. Chem.* **1960**, *2*, 394.
- (18) Pirkle, W. H.; McKendry, L. H. Photochemical Reactions of 2-Pyrone and Thermal Reactions of the 2-Pyrone Photoproducts. *J. Am. Chem. Soc.* **1969**, *91*, 1179–1186.
- (19) Corey, E. J.; Streith, Jacques. Internal Photoaddition Reactions of 2-Pyrone and N-Methyl-2-Pyridone: A New Synthetic Approach to Cyclobutadiene. *J. Am. Chem. Soc.* **1964**, *86*, 950–951.
- (20) Corey, E. J.; Pirkle, W. H. Tricyclo[23,6.1.1.0]Pyran-2-One. *Tetrahedron Lett.* **1967**, *8*, 5255–5256.
- (21) Chapman, O. L.; McIntosh, C. L.; Pacansky, J. Photochemical Transformations. XLVIII. Cyclobutadiene. *J. Am. Chem. Soc.* **1973**, *95*, 614–617.
- (22) Cram, D. J.; Tanner, M. E.; Thomas, R. The Taming of Cyclobutadiene. *Angew. Chem. Int. Ed.* **1991**, *30*, 1024–1027.
- (23) Taylor, E. C.; Paudler, W. W. *Tetrahedron Lett.* **1960**, *25*, 1–3.
- (24) Slomp, G.; MacKellar, F. A.; Paquette, L. A. Structure Studies by Nuclear Magnetic Resonance Spectroscopy. I. The Photodimer of n-Methyl-2-pyridone. *J. Am. Chem. Soc.* **1961**, *83*, 4472–4473.
- (25) Ayer, W. A.; Hayatsu, R.; De Mayo, P.; Reid, S. T.; Stothers, J. B. The Photodimers of α -Pyridones. *Tetrahedron Lett.* **1961**, *2*, 648–653.
- (26) Wilzbach, K. E.; Rausch, D. J. Photochemistry of Nitrogen Heterocycles. Dewar Pyridine and Its Intermediacy in Photoreduction and Photohydration of Pyridine. *J. Am. Chem. Soc.* **1970**, *92*, 2178–2179.
- (27) Fowler, F. W. Synthesis of 1,2- and 1,4-Dihydropyridines. *J. Org. Chem.* **1972**, *37*, 1321–1323.

- (28) Beeken, P.; Bonfiglio, J. N.; Hasan, I.; Piwinski, J. J.; Weinstein, B.; Zollo, K. A.; Fowler, F. W. Synthesis and Study of N-Substituted 1,2-Dihydropyridines. *J. Am. Chem. Soc.* **1979**, *101*, 6677–6682.
- (29) Edel, K.; Yang, X.; Ishibashi, J. S. A.; Lamm, A. N.; Maichle-Mössmer, C.; Giustra, Z. X.; Liu, S.; Bettinger, H. F. The Dewar Isomer of 1,2-Dihydro-1,2-azaborinines: Isolation, Fragmentation, and Energy Storage. *Angew. Chem. Int. Ed.* **2018**, *57*, 5296–5300.
- (30) Rosenblum, Myron.; Gatsonis, Christos. New Synthesis of Cyclobutadiene Iron Tricarbonyl. *J. Am. Chem. Soc.* **1967**, *89*, 5074–5075.
- (31) Rosenblum, M.; North, B. Photochemical Synthesis of Cyclobutadiene(Cyclopentadienyl)Cobalt. *J. Am. Chem. Soc.* **1968**, *90*, 1060–1061.
- (32) Grubbs, R. H.; Pancoast, T. A.; Grey, R. A. Intramolecular Trapping of Cyclobutadiene. *Tetrahedron Lett.* **1974**, *15*, 2425–2426.
- (33) Limanto, J.; Snapper, M. L. Sequential Intramolecular Cyclobutadiene Cycloaddition, Ring-Opening Metathesis, and Cope Rearrangement: Total Syntheses of (+)- and (–)-Asteriscanolide. *J. Am. Chem. Soc.* **2000**, *122*, 8071–8072.
- (34) Wender, P. A.; Ihle, N. C.; Correia, C. R. D. Nickel-Catalyzed Intramolecular [4+4] Cycloadditions. 4. Enantioselective Total Synthesis of (+)-Asteriscanolide. *J. Am. Chem. Soc.* **1988**, *110*, 5904–5906.
- (35) Misale, A.; Niyomchon, S.; Maulide, N. Cyclobutenes: At a Crossroad between Diastereoselective Syntheses of Dienes and Unique Palladium-Catalyzed Asymmetric Allylic Substitutions. *Acc. Chem. Res.* **2016**, *49*, 2444–2458.

- (36) Namyslo, J. C.; Kaufmann, D. E. The Application of Cyclobutane Derivatives in Organic Synthesis. *Chem. Rev.* **2003**, *103*, 1485–1538.
- (37) Lee-Ruff, E.; Mladenova, G. Enantiomerically Pure Cyclobutane Derivatives and Their Use in Organic Synthesis. *Chem. Rev.* **2003**, *103*, 1449–1484.
- (38) Li, J.; Gao, K.; Bian, M.; Ding, H. Recent Advances in the Total Synthesis of Cyclobutane-Containing Natural Products. *Org. Chem. Front.* **2020**, *7*, 136–154.
- (39) Luparia, M.; Oliveira, M. T.; Audisio, D.; Frébault, F.; Goddard, R.; Maulide, N. Catalytic Asymmetric Diastereodivergent Deracemization. *Angew. Chem. Int. Ed.* **2011**, *50*, 12631–12635.
- (40) Frébault, F.; Luparia, M.; Oliveira, M. T.; Goddard, R.; Maulide, N. A Versatile and Stereoselective Synthesis of Functionalized Cyclobutenes. *Angew. Chem. Int. Ed.* **2010**, *49*, 5672–5676.
- (41) Audisio, D.; Luparia, M.; Oliveira, M. T.; Klütt, D.; Maulide, N. Diastereodivergent De-Epimerization in Catalytic Asymmetric Allylic Alkylation. *Angew. Chem. Int. Ed.* **2012**, *51*, 7314–7317.
- (42) Chen, Y.; Coussanes, G.; Souris, C.; Aillard, P.; Kaldre, D.; Runggatscher, K.; Kubicek, S.; Di Mauro, G.; Maryasin, B.; Maulide, N. A Domino 10-Step Total Synthesis of FR252921 and Its Analogues, Complex Macrocyclic Immunosuppressants. *J. Am. Chem. Soc.* **2019**, *141*, 13772–13777.
- (43) Souris, C.; Misale, A.; Chen, Y.; Luparia, M.; Maulide, N. From Stereodefined Cyclobutenes to Dienes: Total Syntheses of Ieodomycin D and the Southern Fragment of Macrolactin A. *Org. Lett.* **2015**, *17*, 4486–4489.

- (44) Gutekunst, W. R.; Baran, P. S. Total Synthesis and Structural Revision of the Piperarborenes via Sequential Cyclobutane C–H Arylation. *J. Am. Chem. Soc.* **2011**, *133*, 19076–19079.
- (45) Nistanaki, S. K.; Boralsky, L. A.; Pan, R. D.; Nelson, H. M. A Concise Total Synthesis of (±)-Vibrallactone. *Angew. Chem. Int. Ed.* **2019**, *58*, 1724–1726.
- (46) Boswell, B. R.; Mansson, C. M. F.; Cabrera, G. E.; Hansen, C. R.; Oliver, A. G.; Burns, N. Z. A Metal-Free Cyclobutadiene Reagent for Intermolecular [4 + 2] Cycloadditions. *J. Am. Chem. Soc.* **2023**, *145*, 5631–5636.
- (47) Bielawski, C. W.; Grubbs, R. H. Living Ring-Opening Metathesis Polymerization. *Prog. Polym. Sci.* **2007**, *32*, 1–29.
- (48) Seo, J.; Lee, S. Y.; Bielawski, C. W. Dewar Lactone as a Modular Platform to a New Class of Substituted Poly(Acetylene)s. *Polym. Chem.* **2019**, *10*, 6401–6412.
- (49) Berets, D. J.; Smith, D. S. Electrical Properties of Linear Polyacetylene. *Trans. Faraday Soc.* **1968**, *64*, 823.
- (50) Watson, W. H.; McMordie, W. C.; Lands, L. G. Polymerization of Alkynes by Ziegler-Type Catalyst. *J. Polym. Sci.* **1961**, *55*, 137–144.
- (51) Chen, Z.; Mercer, J. A. M.; Zhu, X.; Romaniuk, J. A. H.; Pfattner, R.; Cegelski, L.; Martinez, T. J.; Burns, N. Z.; Xia, Y. Mechanochemical Unzipping of Insulating Polyladderene to Semiconducting Polyacetylene. *Science* **2017**, *357*, 475–479.
- (52) Yoon, K.-Y.; Lee, I.-H.; Kim, K. O.; Jang, J.; Lee, E.; Choi, T.-L. One-Pot in Situ Fabrication of Stable Nanocaterpillars Directly from Polyacetylene Diblock Copolymers Synthesized by Mild Ring-Opening Metathesis Polymerization. *J. Am. Chem. Soc.* **2012**, *134*, 14291–14294.

- (53) Swager, T. M.; Dougherty, D. A.; Grubbs, R. H. Strained Rings as a Source of Unsaturation: Polybenzvalene, a New Soluble Polyacetylene Precursor. *J. Am. Chem. Soc.* **1988**, *110*, 2973–2974.
- (54) Feast, W. J.; Tsibouklis, J.; Pouwer, K. L.; Groenendaal, L.; Meijer, E. W. Synthesis, Processing and Material Properties of Conjugated Polymers. *Polymer* **1996**, *37*, 5017–5047.
- (55) Safir, A. L.; Novak, B. M. Air- and Water-Stable 1,2-Vinyl-Insertion Polymerizations of Bicyclic Olefins: A Simple Precursor Route to Polyacetylene. *Macromolecules* **1993**, *26*, 4072–4073.
- (56) Gorman, C. B.; Ginsburg, E. J.; Grubbs, R. H. Soluble, Highly Conjugated Derivatives of Polyacetylene from the Ring-Opening Metathesis Polymerization of Monosubstituted Cyclooctatetraenes: Synthesis and the Relationship between Polymer Structure and Physical Properties. *J. Am. Chem. Soc.* **1993**, *115*, 1397–1409.
- (57) Lam, J. W. Y.; Tang, B. Z. Functional Polyacetylenes. *Acc. Chem. Res.* **2005**, *38*, 745–754.
- (58) Nistanaki, S. K.; Nelson, H. M. Dewar Heterocycles as Versatile Monomers for Ring-Opening Metathesis Polymerization. *ACS Macro Lett.* **2020**, *9*, 731–735.
- (59) Rappoport, Z., Stang, P. J. *Dicoordinated Carbocations*; Wiley: Chichester ; New York, **1997**.
- (60) Glaser, R. Diazonium Ions: A Theoretical Study of Pathways to Automerization, Thermodynamic Stabilities, and Topological Electron Density Analysis of the Bonding. *J. Phys. Chem.* **1989**, *93*, 7993–8003.

- (61) Hanack, M. Vinyl Cations in Solvolysis Reactions. *Acc. Chem. Res.* **1970**, *3*, 209–216.
- (62) Jacobs, T. L.; Searles, S. Acetylenic Ethers. IV.¹ Hydration. *J. Am. Chem. Soc.* **1944**, *66*, 686–689.
- (63) Grob, C. A.; Cseh, G. Die Solvolyse von α -Bromstyrolen Substitution am ungesättigten trigonalen Kohlenstoffatom. *Helv. Chim. Acta* **1964**, *47*, 194–203.
- (64) Grob, C. A.; Csapilla, J.; Cseh, G. Die solvolytische Decarboxylierung von α , β -ungesättigten β -Halogensäuren Fragmentierungsreaktionen, 9. Mitteilung. *Helv. Chim. Acta* **1964**, *47*, 1590–1602.
- (65) Jones, W. M.; Maness, D. D. Solvolysis of Sulfonic Acid Esters of Triphenylvinyl Alcohol by a Heterolytic Mechanism. *J. Am. Chem. Soc.* **1969**, *91*, 4314–4315.
- (66) Noyce, D. S.; Matesich, M. A.; Melvyn, O. P.; Schiavelli, D.; Peterson, P. E. Concerning the Acid-Catalyzed Hydration of Acetylenes. *J. Am. Chem. Soc.* **1965**, *87*, 2295–2296.
- (67) Schmerling, L.; West, J. P.; Welch, R. W. Condensation of Benzene with Unsaturated Chlorides¹. *J. Am. Chem. Soc.* **1958**, *80*, 576–579.
- (68) Anschütz, R. Beiträge zur Kenntniss der Wirkung des Aluminiumchlorids. *Justus Liebigs Ann. Chem.* **1886**, *235* (1–2), 150–229.
- (69) Roberts, R. M.; Abdel-Baset, M. B. New Friedel-Crafts Chemistry. XXXII. Friedel-Crafts Alkylations with Vinyl Halides. Vinyl Cations and Spirobiindans. *J. Org. Chem.* **1976**, *41*, 1698–1701.

- (70) Cook, O. W.; Chambers, V. J. The Condensation Of Acetylene With Benzene And Its Derivatives In The Presence Of Aluminum Chloride. *J. Am. Chem. Soc.* **1921**, *43*, 334–340.
- (71) Stang, P. J.; Anderson, A. G. Preparation and Chemistry of Vinyl Triflates. 16. Mechanism of Alkylation of Aromatic Substrates. *J. Am. Chem. Soc.* **1978**, *100*, 1520–1525.
- (72) Sustmann, R.; Williams, J. E.; Dewar, M. J. S.; Allen, L. C.; Schleyer, P. V. R. Molecular Orbital Calculations on Carbonium Ions. II. Methyl, Ethyl, and Vinyl Cations. The Series C₃H₇⁺. *J. Am. Chem. Soc.* **1969**, *91*, 5350–5357.
- (73) Biermann, U.; Koch, R.; Metzger, J. O. Intramolecular Concerted Insertion of Vinyl Cations into C–H Bonds: Hydroalkylating Cyclization of Alkynes with Alkyl Chloroformates To Give Cyclopentanes. *Angew. Chem. Int. Ed.* **2006**, *45*, 3076–3079.
- (74) Jin, T.; Himuro, M.; Yamamoto, Y. Brønsted Acid-Catalyzed Cascade Cycloisomerization of Enynes via Acetylene Cations and Sp³-Hybridized C–H Bond Activation. *J. Am. Chem. Soc.* **2010**, *132*, 5590–5591.
- (75) Kütt, A.; Tshepelevitsh, S.; Saame, J.; Lõkov, M.; Kaljurand, I.; Selberg, S.; Leito, I. Strengths of Acids in Acetonitrile. *Eur. J. Org. Chem.* **2021**, *2021*, 1407–1419.
- (76) Cleary, S. E.; Hensinger, M. J.; Brewer, M. Remote C–H Insertion of Vinyl Cations Leading to Cyclopentenones. *Chem. Sci.* **2017**, *8*, 6810–6814.
- (77) Popov, S.; Shao, B.; Bagdasarian, A. L.; Benton, T. R.; Zou, L.; Yang, Z.; Houk, K. N.; Nelson, H. M. Teaching an Old Carbocation New Tricks: Intermolecular C–H Insertion Reactions of Vinyl Cations. *Science* **2018**, *361*, 381–387.

- (78) Wigman, B.; Popov, S.; Bagdasarian, A. L.; Shao, B.; Benton, T. R.; Williams, C. G.; Fisher, S. P.; Lavallo, V.; Houk, K. N.; Nelson, H. M. Vinyl Carbocations Generated under Basic Conditions and Their Intramolecular C–H Insertion Reactions. *J. Am. Chem. Soc.* **2019**, *141*, 9140–9144.
- (79) Nistanaki, S. K.; Williams, C. G.; Wigman, B.; Wong, J. J.; Haas, B. C.; Popov, S.; Werth, J.; Sigman, M. S.; Houk, K. N.; Nelson, H. M. Catalytic Asymmetric C–H Insertion Reactions of Vinyl Carbocations. *Science* **2022**, *378*, 1085–1091.
- (80) Fattorusso, E.; Tagliatela-Scafati, O. *Modern Alkaloids: Structure, Isolation, Synthesis and Biology*; Wiley-VCH: Weinheim, 2008.

Chapter 2

A Concise Total Synthesis of (\pm)-Vibralactone¹

2.1 INTRODUCTION

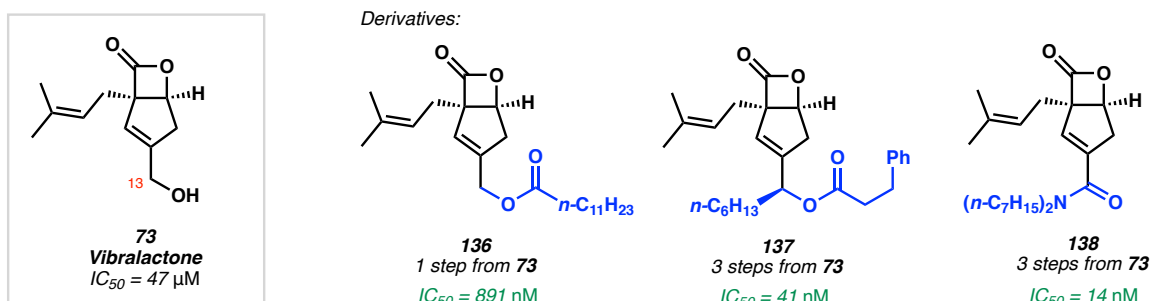
2.1.1 Bioactivity

Vibralactone (**73**) was isolated in 2006 by Liu and co-workers from the basidiomycete fungus *Boreostereum vibrans*.¹ In its initial isolation report, vibralactone was identified as an inhibitor of pancreatic lipase with notable *in vitro* potency (IC₅₀ vibralactone = 47 μ M) (Scheme 2.1). This bioactivity renders vibralactone as a potential therapeutic for targeting obesity through modulation of fat absorption, similarly to Orlistat, an FDA-approved anti-obesity medication that is also a lipase inhibitor.² In a study by Liu

¹ Portions of this chapter have been adapted from Nistanaki, S. K.; Boralsky, L. A.; Pan, R. D.; Nelson, H. M. *Angew. Chem. Int. Ed.* **2019**, *58*, 1724–1726. © Wiley–VCH.

and co-workers, it was found that synthetic elaboration of isolated vibralactone at the C13 position enhanced its inhibitory potency against pancreatic lipase *in vitro*, with the best reported example (**138**) demonstrating a 3,000-fold increase in activity (Scheme 2.1).³ While only post-isolation synthetic modification of vibralactone was explored in this study, it demonstrated the potential to further tune its bioactivity through derivative synthesis. Importantly, obesity is a growing worldwide epidemic affecting over a billion adults worldwide, and it is known to dramatically increase risk of other health issues, including cardiovascular disease, hypertension, and diabetes.^{4,5} New therapeutics targeting obesity are therefore of great interest.

Scheme 2.1. Vibralactone (**73**) and synthetic derivatives



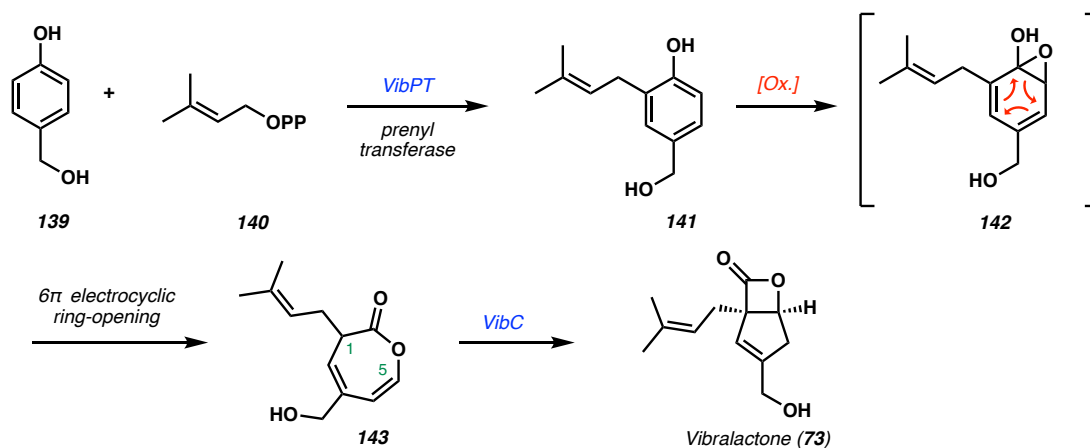
Vibralactone was also recently identified as a potent covalent inhibitor of caseinolytic peptidase ClpP, a highly conserved bacterial enzyme responsible for virulence in *Listeria monocytogenes*.^{6,7} Interestingly, unlike most β -lactone-containing molecules that target solely the ClpP2 isoform of the ClpP complex, vibralactone is particularly unique in its ability to bind both the ClpP1 and ClpP2 isoforms. Given that antibiotics are facing a decline in efficacy due to rapid multidrug resistance development⁸, an alternative approach to combatting antibiotic-resistant bacterial infections could involve medicines

that target virulence factors, which are responsible for the negative health effects experienced during infection. Therefore, vibralactone could serve as an attractive lead for the development of novel antibiotics. Ultimately, the development of a modular and efficient synthetic route towards the natural product could enable further exploration of its biological activity and bioactivity optimization through derivatization.

2.1.2 Biosynthetic Proposal

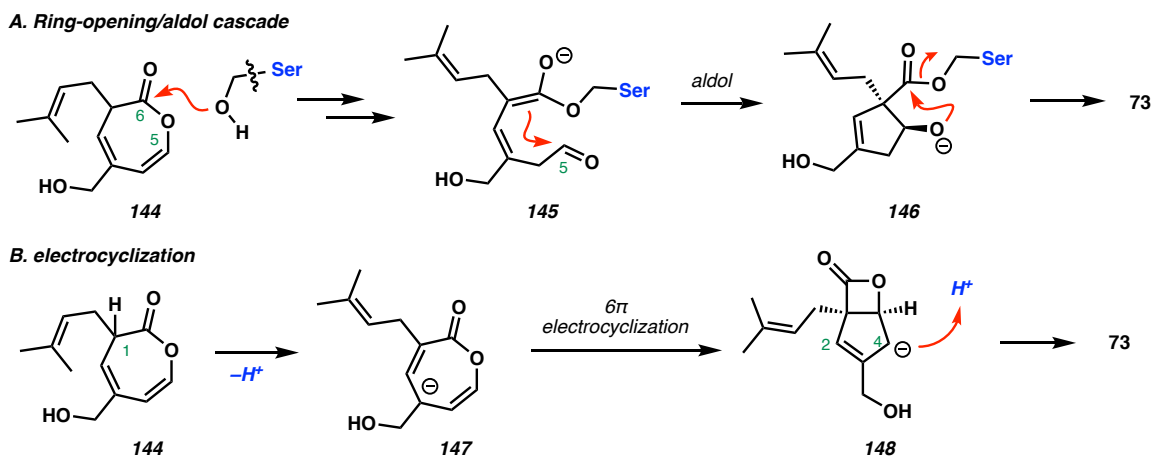
A proposed biosynthetic pathway put forth by Zeng, Liu, and Huang commences with the prenylation of benzylic alcohol **139** with prenyl pyrophosphate (**140**) catalyzed by a prenyl transferase enzyme (Scheme 2.2).^{9,10} Oxidation of **141** to arene oxide **142** sets the stage for a thermal 6π -electrocyclic ring opening to form oxepinone **143**. A final transannular C1–C5 bond formation forges the β -lactone-fused bicyclic structure in vibralactone. Interestingly, while studying the potential biosynthetic mechanism of this cyclization, it was discovered that a hydrolase (termed “VibC”) catalyzes the cyclization likely through a Ser-His-Asp catalytic triad, as shown by site-specific mutagenesis studies.

Scheme 2.2. Proposed biosynthesis of vibralactone (**73**)



Unlike known β -lactone synthetases and non-ribosomal peptide synthetases that convert β -hydroxy acids to β -lactone in an ATP-dependent process, it was suggested that β -lactone formation by VibC occurs through a distinct mechanism (Scheme 2.3).^{9,11} Zeng, Liu, and Huang propose two potential pathways that are consistent with their mechanistic experiments: (1) ring-opening of oxepinone **144** by a serine residue at C6, followed by aldol addition to the resulting C5 aldehyde of **145** and subsequent lactonization of **146**; or (2) disrotatory 6π electrocyclicization of a generated pentadienyl anion (**147**) to form allyl anion **148**, which undergoes selective protonation at C4 to form vibralactone. In the latter pathway, it is proposed that the catalytic triad facilitates deprotonation of the C1 proton.

Scheme 2.3. Potential biosynthetic mechanisms for VibC-catalyzed cyclization

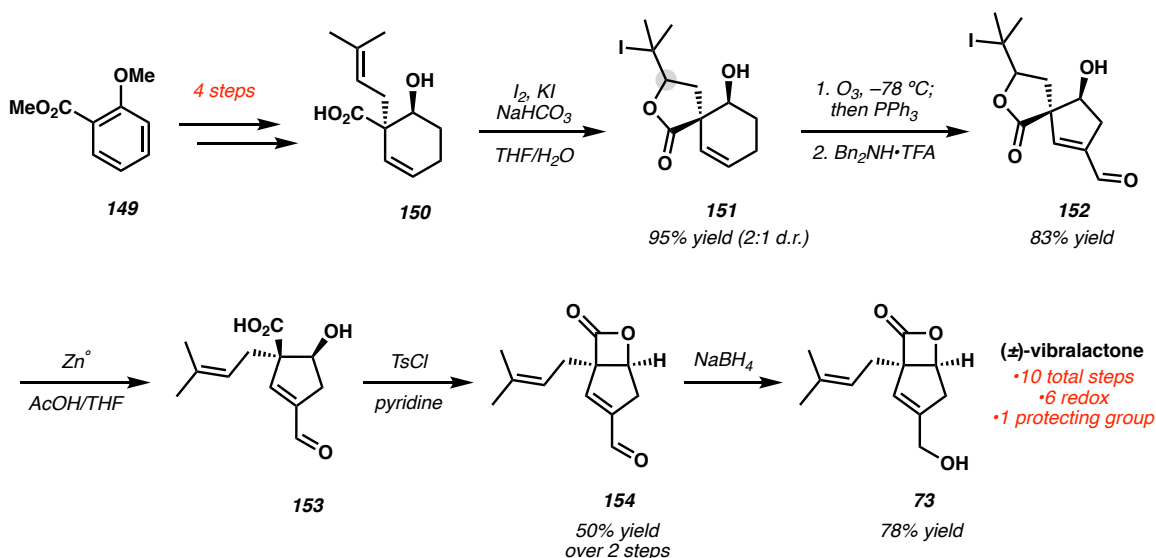


2.1.3 Previous Syntheses

The first synthesis of (\pm)-vibralactone was reported by Snider and co-workers in 2008, and their route consisted of ten steps from benzoate **149** (Scheme 2.4).¹² β -hydroxy acid **150** was accessed in four steps *via* a Birch reductive alkylation/hydrolysis sequence,

followed by diastereoselective reduction. Protection of the pendant prenyl group *via* iodolactonization was necessary prior to the two-step ring-contraction to cyclopentene **152** *via* sequential ozonolysis followed by intramolecular aldol cyclization. Reductive deprotection of the prenyl group followed by lactonization and aldehyde reduction furnished the natural product (**73**) in 10 total steps and 9% overall yield. A total of six redox manipulations and one protecting group strategy were required for this synthesis. An enantioselective variant of this synthesis was achieved later *via* an early-stage diastereoselective Birch reductive alkylation of a chiral auxiliary-appended variant of **149**.¹³

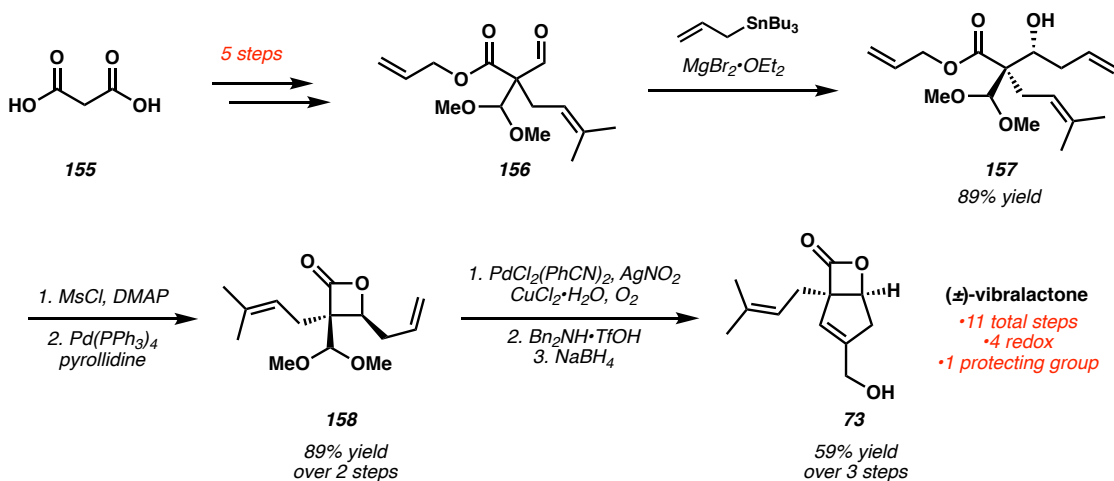
Scheme 2.4. Snider's synthesis of vibralactone (**73**)



In 2016, Brown and co-workers reported an alternative route to (\pm)-vibralactone in 11 steps starting from malonic acid (**155**) (Scheme 2.5).¹⁴ A five-step sequence to malonaldehyde **156** was followed by a Mg-mediated diastereoselective allylation with allyl tributyltin to afford **157**. The β -lactone moiety was then constructed through mesylation of

the secondary alcohol, followed by Pd-catalyzed de-allylation to reveal a nucleophilic carboxylate that could cyclize to forge the lactone ring through an S_N2-type mesylate displacement. Subsequent aldehyde-selective Wacker oxidation, aldol condensation, and reduction afforded (\pm)-vibralactone in 11 steps and 16% overall yield. This synthesis contained four redox manipulations and one protecting group strategy, although no enantioselective variant has been reported.

Scheme 2.5. Brown's synthesis of vibralactone (**73**)

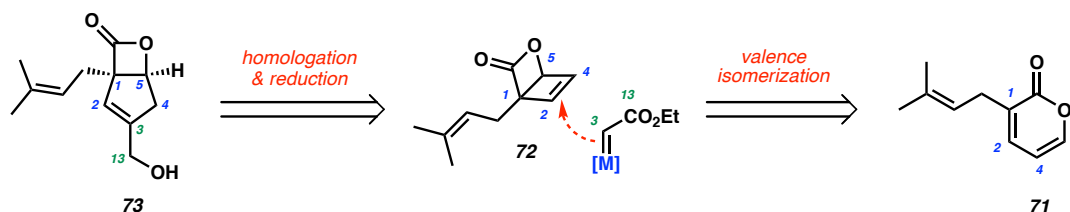


2.1.4 Retrosynthetic Analysis

With the previously reported synthetic routes in mind, we became interested in developing a more concise route to (\pm)-vibralactone.¹⁵ Our retrosynthetic hypothesis pointed towards Dewar pyrone **72** as a strategic intermediate, which would require one-carbon homologation to access the carbocyclic core of vibralactone (Scheme 2.6). Compound **72** would be readily accessed photochemically from the corresponding prenylated pyrone (**71**). We envisioned that this approach would be expedient given that

the photochemical valence isomerization of pyrone **71** would install the β -lactone moiety and all-carbon quaternary stereocenter in a single step, while simultaneously revealing a reactive cyclobutene moiety that would be key for homologation chemistry.

Scheme 2.6. Retrosynthetic hypothesis



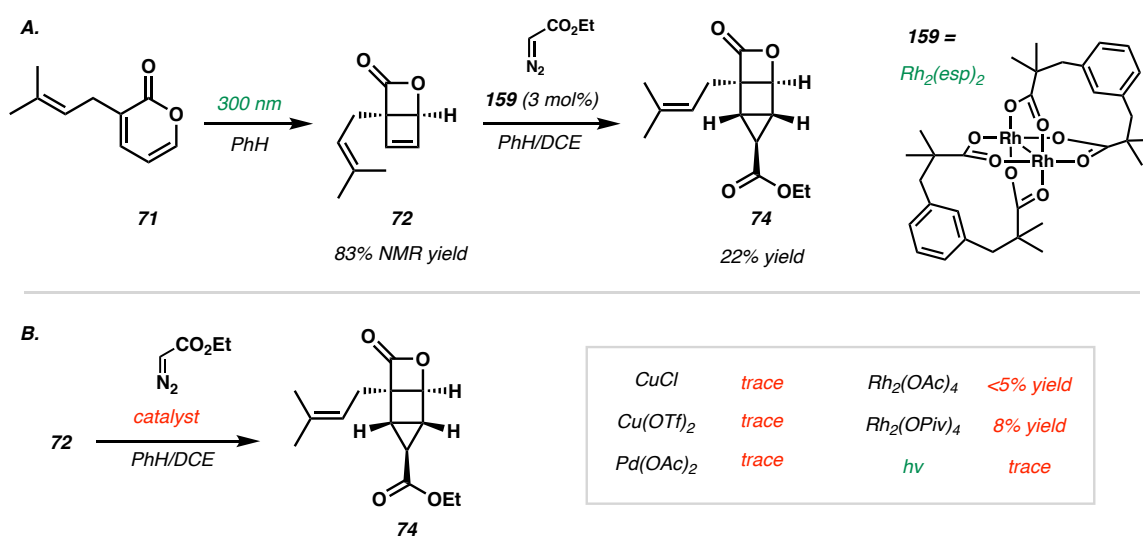
2.2 SYNTHESIS OF (\pm)-VIBRALACTONE

2.2.1 Forward Synthesis

Our forward synthesis commenced with the preparation of known prenylated pyrone **71** via a protocol reported by Maulide and co-workers.¹⁶ Valence isomerization of **71** via irradiation with 300 nm light afforded oxabicyclo[2.2.0]hexenone **72** in 83% yield, determined by ¹H NMR (Scheme 2.7). Given the high instability of this compound, it was used immediately in the next step without further purification or complete removal of solvent.¹⁷ The high instability of this compound was evident in its gradual decomposition even when frozen as a matrix in benzene. We then investigated the cyclopropanation of the cyclobutenyl olefin of bicycle **72** (Scheme 2.7). This reaction was challenged by potential selectivity issues arising from competitive cyclopropanation of the pendant prenyl olefin, along with other side reactions that may arise from the highly reactive substrate. After screening various transition metal-mediated carbene transfer reactions, we found that

$\text{Rh}_2(\text{esp})_2$ (**159**)¹⁸ afforded the desired cyclopropane **74** in 22% yield as a single diastereomer. We found that this Rh catalyst was uniquely effective in affording acceptable yields of the desired product, while other explored catalysts gave disappointing results (Scheme 2.7). We attributed the poor reactivity of the [2.2.0]bicycle (**72**) to the sterically congested environment surrounding the reactive olefin, along with challenges associated with employing such a highly unstable molecule. Nevertheless, we were gratified to install the final two carbons of the natural product, furnishing the strained “housane” **74**, which was characterized by X-ray crystallography.

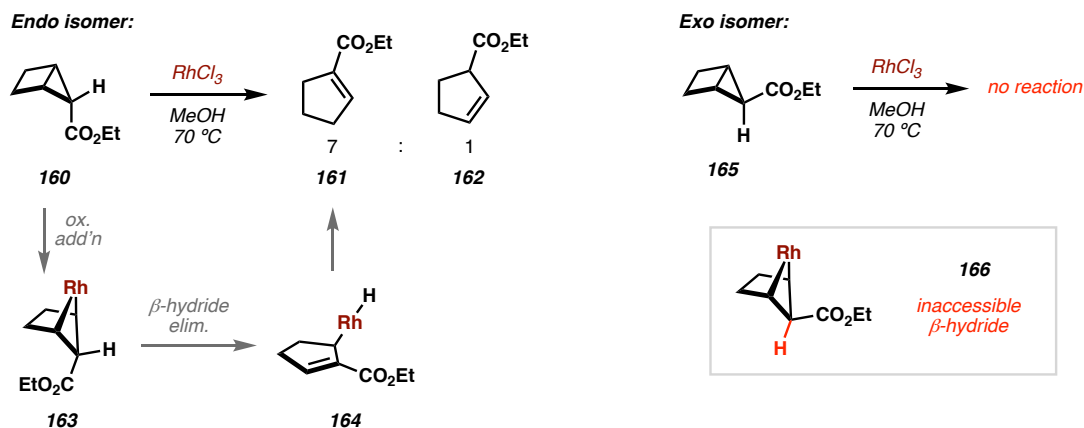
Scheme 2.7. Cyclopropanation of prenylated Dewar pyrone intermediate (**72**)



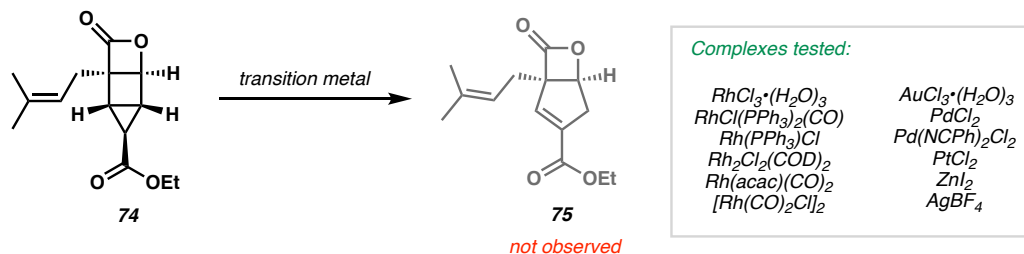
At this stage of the synthesis, we found ourselves one isomerization away from arriving at the carbocyclic core of the natural product. We therefore turned our attention to early reports by Bishop and co-workers in which similar bicyclo[2.1.0]pentane scaffolds (**160**) were converted to cyclopentenones (**161,162**) by rhodium catalysis (Scheme 2.8).¹⁹ It

was proposed by Bishop that oxidative addition of the strained cyclopropyl C–C bond to rhodium (**163**), followed by β -hydride elimination affords rhodium allyl intermediate **164**. However, the lack of reactivity with the *exo* isomer (**165**) highlights the necessity for the *syn*-relationship of the β -hydrogen to the metal center for successful ring expansion.

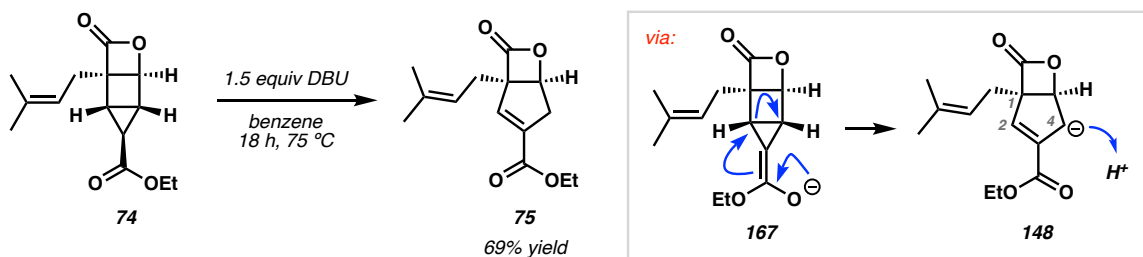
Scheme 2.8. Bishop's Ru-catalyzed ring-expansion of bicyclo[2.1.0]pentanes



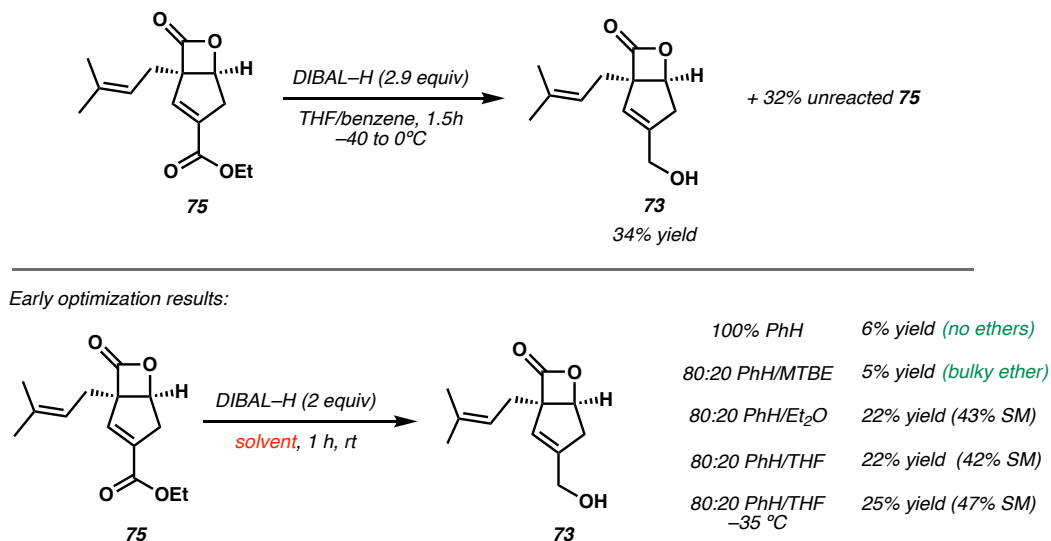
Analogous to Bishop's work, we initially envisioned a transition metal-catalyzed approach for ring expansion of housane **74**, recognizing that in our system oxidative addition would likely lead to an *anti*-configuration between the metal center and β -hydride. Nevertheless, we attempted this transformation in the hope that outer-sphere elimination could be achieved, but failed to observe ring expansion of **74** to cyclopentene **75** in the presence of various transition metal complexes tested (Scheme 2.9). In most cases, no reactivity was observed at low temperatures, while decomposition to complex mixtures was observed at elevated temperatures. While unsuccessful, the putative mechanism of Bishop's system pointed towards a strategic opportunity to exploit an analogous allyl intermediate to achieve ring expansion.

Scheme 2.9. Failed attempts at metal-catalyzed ring expansion

Seeking to harness the natural reactivity of the molecule, we recognized that the acidic α -proton of the exocyclic ester in **74** could be deprotonated to afford ester enolate **167**, which could perhaps facilitate cleavage of the strained bridging C–C bond (Scheme 2.10). While 4π electrocyclic ring-opening of cyclopropyl anions is known, the necessity for a disrotatory process with **167** is formally forbidden by the Woodward-Hoffman rules.²⁰ Nonetheless, we hypothesized that the high strain energy of the system would drive the ring expansion forward through some mechanism, and that selective protonation of the resulting allyl anion in **148** could deliver the desired cyclopentene (**75**). To this end, we found that ring expansion of housane **74** could be achieved by heating it in the presence of stoichiometric 1,8-diazabicyclo[5.4.0]undec-7-ene (DBU) base, affording α,β -unsaturated ester **75** as a single allyl isomer in 69% yield. We attributed selective formation of the desired isomer to kinetic protonation of allyl anion **148** at the C4 carbon distal to the sterically congested C1 all-carbon quaternary center. Notably, such an allylic anion was invoked as a potential intermediate in the biosynthetic pathway of vibralactone.⁹

Scheme 2.10. Base-mediated ring expansion of housane intermediate (**74**)

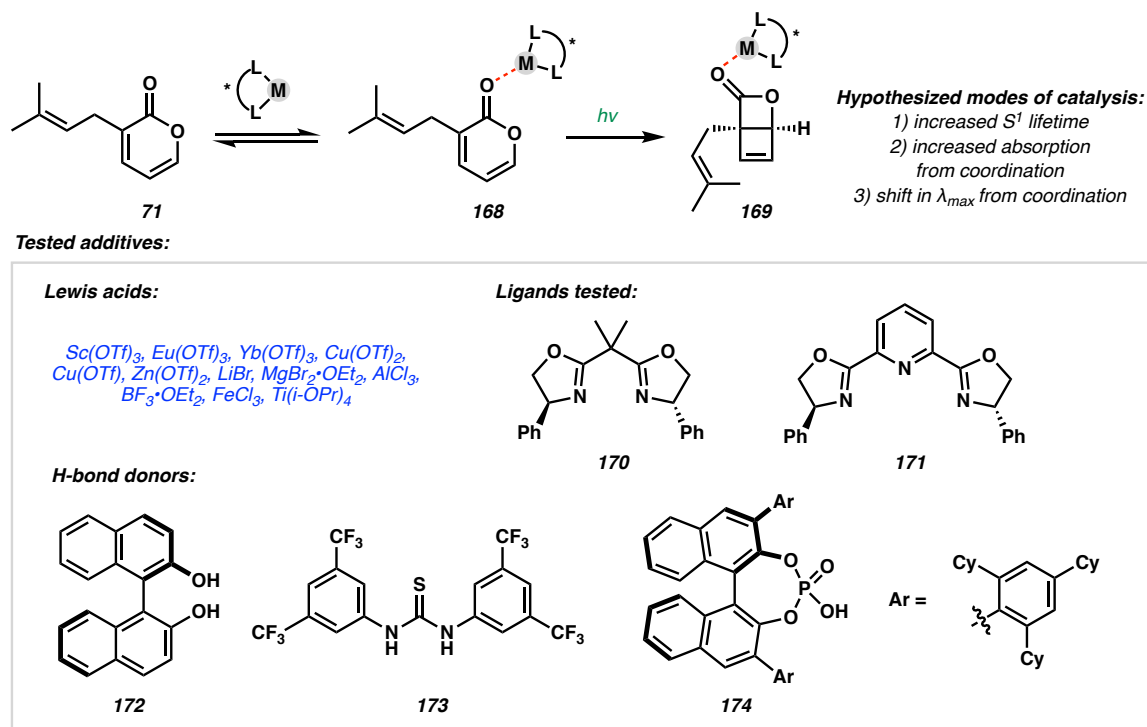
At this stage, we were faced with the endeavor of selectively reducing the exocyclic α,β -unsaturated ester in a 1,2 fashion while in the presence of the strained β -lactone moiety installed in the first step of the synthesis. Despite our trepidation with this step, we reasoned that kinetic control could enable the selective reduction of the less sterically-encumbered exocyclic ester in **75**, given that both the β -lactone moiety and β -carbon of the enoate system contained an adjacent all-carbon quaternary center. Through extensive optimization, we found that reduction of the ethyl ester to afford vibralactone (**73**) could be achieved in 34% yield through the use of excess diisobutylaluminum hydride (DIBAL-H), with 32% unreacted starting material recovered (Scheme 2.11). Key to successful execution of this step was precise control of the reaction time and temperature, along with employment of coordinating ether solvents. For example, conducting the reduction in non-coordinating solvents (like benzene) or sterically hindered ethers (like MTBE) resulted in low yields of vibralactone and detection of over-reduced products (Scheme 2.11). We attributed this to attenuated reactivity of DIBAL when complexed with coordinating solvents, which may be key for achieving selectivity; coordination of ethers to the Al center also introduces steric bulk around the Al-H bond, which may contribute as well. Ultimately, this step concluded our synthesis of vibralactone in four steps from pyrone **71**.

Scheme 2.11. Reduction of exocyclic ester and completion of synthesis**2.2.2 Attempts to Catalyze Pyrone Photoisomerization**

During our studies we made various attempts to develop a catalytic asymmetric route to vibralactone, with considerable focus on the possibility of catalyzing the photochemical valence isomerization of prochiral **71** to chiral Dewar pyrone **72**. From previous work, it has been supported that the photoisomerization of α -pyrone occurs *via* the singlet excited state.²¹ Most known examples of asymmetric photochemical reactions of organic substrates involve systems that occur through the triplet excited state manifold; asymmetric organic reactions directly through the singlet excited state continues to be a challenge.^{22–27} To this end, we reasoned that pyrone photoisomerization could serve as a good platform for exploring this, given that the photophysical properties of the pyrone could perhaps be altered through coordination to the carbonyl (**168**) by some chiral additive (Scheme 2.12). It has been shown that the singlet excited state chemistry of related coumarin molecules could be accelerated *via* Lewis acid coordination.^{28,29} We therefore

hypothesized that chiral Lewis acids, hydrogen bond donors, or Brønsted acids could perhaps accelerate the valence isomerization reaction either by (1) increasing singlet excited state lifetime; (2) increasing the chromophore absorption (more facile excitation when the chiral complex **168** is formed); (3) shifting the wavelength of absorption, such that the complexed pyrone (**168**) could be selectively excited by careful selection of wavelength.

Scheme 2.12. Attempts to catalyze the pyrone photoisomerization



In order to study the rate acceleration of this step in the presence of additives, we studied the kinetics of the reaction in the presence of Lewis acids and hydrogen bond donors (**172–174**) via 1H NMR, which unfortunately showed no signs of rate acceleration

(Scheme 2.12). In cases where inorganic salts were employed as Lewis acids, pre-mixing with chiral ligands (**170,171**) was also tested, but with no success. In some experiments, we would observe conversion of starting material to complex product mixtures in the presence of acidic additives. This was perhaps unsurprising, given the notorious lack of stability of Dewar pyrone, first reported by Corey and Streith.¹⁷ UV-Vis experiments were conducted to probe the change in photophysical properties in the presence of these activators, which appeared to show essentially no influence on the absorption features of pyrone **71** under the conditions tested. Though unsuccessful in our hands, development of such a catalytic asymmetric photoisomerization would be transformative for both our synthesis of vibralactone, but also for the field of asymmetric photochemistry broadly.

2.3 CONCLUSION

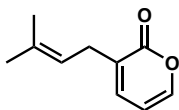
In conclusion, (\pm)-vibralactone (**73**) was prepared in four steps from prenyl pyrone (**71**) in a protecting group-free fashion with a single redox manipulation. Through a key photochemical valence isomerization, the all-carbon quaternary center and β -lactone moiety were installed at an early stage. In the subsequent two steps, the carbocyclic core of the natural product was forged through a sequential cyclopropanation and ring expansion strategy. In the fourth and final step of the synthesis, a selective reduction of the exocyclic ester over the strained β -lactone completed the natural product. Early installation of the C1 quaternary center proved critical in imparting kinetic selectivity in both the ring expansion and reduction steps.

2.4 EXPERIMENTAL SECTION

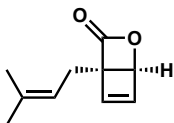
2.4.1 Materials & Methods

Unless otherwise stated, all reactions were performed in flame-dried glassware under nitrogen atmosphere using dry, deoxygenated solvents. Solvents were dried in a JC Meyer solvent system. Ethyl diazoacetate (Sigma-Aldrich), 1,8-diazabicyclo[5.4.0]undec-7-ene (TCI), and diisobutylaluminum hydride (Sigma-Aldrich) were used as purchased. Photochemistry was performed in a Rayonet RPR-200 photochemical reactor. 300nm bulbs were purchased from Rayonet (model RPR-3000A). Disposable Pyrex tubes were used for photochemistry (Fisherbrand borosilicate glass, 18x150mm). Thin layer chromatography (TLC) was performed using E. Merck silica gel 60 F254 precoated plates (0.25mm) and visualized by UV fluorescence quenching, *p*-anisaldehyde, KMnO₄, or cerium-ammonium-molybdate (CAM) staining. SiliaFlash P60 Silica gel (230–400 mesh) was used for flash chromatography. ¹H and ¹³C NMR spectra were recorded on a Bruker DRX-500 (¹H), Bruker AV-400 (¹H), and Bruker AV-500 (¹H, ¹³C). All ¹H NMR spectra are reported relative to CDCl₃ (7.26ppm). Data for ¹H NMR spectra are as follows: s = singlet, d = doublet, t = triplet, dd = doublet, ddd = doublet of doublet of doublet, qd = quartet of doublet, m = multiplet. All ¹³C NMR spectra are reported relative to CDCl₃ (77.16 ppm). IR spectra were recorded on a Perkin Elmer 100 spectrometer and are reported in terms of absorption frequency (cm⁻¹). High resolution mass spectra (HR-MS) were recorded on an Agilent 7250 Quadrupole TOF GC-MS, Waters LCT Premier TOF-ESI Mass Spectrometer, and a Thermo Scientific Q Exactive Plus Hybrid Quadrupole-Orbitrap Mass Spectrometer. Crystallographic data were obtained by the UCLA J.D. McCullough Laboratory of X-ray Crystallography.

2.4.2 Experimental Procedures & Characterization



3-(3-methylbut-2-en-1-yl)-2H-pyran-2-one (71). Prepared according to literature.¹⁶ All spectra matched the reported literature.



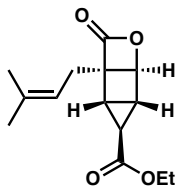
4-(3-methylbut-2-en-1-yl)-2-oxabicyclo[2.2.0]hex-5-en-3-one (72). To a degassed solution of benzene (120 mL) in a flame-dried round bottom flask under N₂ was added prenyl pyrone **71** (750 mg, 4.57 mmol). The solution was divided into six oven-dried Pyrex tubes capped with a septum and further sparged with N₂ for 10 minutes with vigorous stirring. The tubes were then irradiated at 300nm at room temperature for 24 hours or until complete. The reaction was monitored by ¹H NMR by taking crude aliquots. Once complete, the solutions were combined and yield of product was 83% (620 mg, 3.78 mmol) by ¹H NMR. The material was carried further to the next step without any further purification or concentration due to its instability. Note: extensive removal of solvent was avoided due to reported explosions of similar photo-pyrones.¹⁷

¹H NMR (500 MHz, CDCl₃) δ 6.73 (dd, $J = 4.2, 2.3$ Hz, 1H), 6.57 (d, $J = 2.5$ Hz, 1H), 5.16 (d, $J = 4.3$, 1H), 5.17–5.11 (m, 2H), 2.62 (dd, $J = 15.2, 7.5$ Hz, 1H), 2.51 (dd, $J = 15.3, 7.3$ Hz, 1H), 1.72 (s, 3H), 1.64 (s, 3H)

^{13}C NMR (125 MHz, CDCl_3) δ 172.3, 145.0, 140.2, 136.1, 117.1, 74.5, 70.9, 25.8, 24.9, 18.0

FT-IR (Neat Film NaCl) 2917, 1808, 1274, 828, 734 cm^{-1}

HR-MS: (MS-EI) m/z calc'd for $\text{C}_{10}\text{H}_{12}\text{O}_2$: 164.0832; measured 164.0835.



Ethyl-1-(3-methylbut-2-en-1-yl)-7-oxo-6-oxatricyclo[3.2.0.0.2,4]heptane-3-

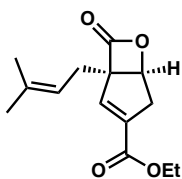
carboxylate (74). To a flame-dried flask equipped with a magnetic stir bar was added bicycle **72** (84 mg, 0.51 mmol) as a 0.03M solution in benzene (15 mL) under N_2 atmosphere. 15 mL of dry DCE was subsequently added to this, followed by $\text{Rh}_2(\text{esp})_2^{30}$ (12 mg, 15.3 μmol , 0.03 equiv). To this homogeneous solution was added ethyl diazoacetate (EDA) (1.75 g, 15.4 mmol, 30 equiv) dropwise by syringe pump over 6 hours at room temperature. The green-yellow reaction solution was allowed to stir overnight, concentrated by rotary evaporation, and loaded directly onto a silica column for purification (5% \rightarrow 15% ethyl acetate in hexanes on SiO_2). Further purification was often deemed necessary, which was accomplished by column chromatography eluting with DCM on SiO_2 affording 28mg (22% yield) of **74** as a white solid.

^1H NMR (500 MHz, CDCl_3) δ 5.07 (t, $J = 7.5$ Hz, 1H), 4.57 (d, $J = 4.3$ Hz, 1H), 4.19–4.13 (q, $J = 7.1$ Hz, 2H), 2.73 (d, $J = 3.7$ Hz, 1H), 2.67 (dd, $J = 4.4, 3.7$ Hz, 1H), 2.46 (dd, $J = 15.3, 7.6$ Hz, 1H), 2.25 (dd, $J = 15.2, 7.4$ Hz, 1H), 2.13 (s, 1H), 1.27 (t, 7.1 Hz, 3H)

^{13}C NMR (125 MHz, CDCl_3) δ 170.9, 169.1, 136.4, 116.5, 74.5, 69.3, 61.3, 30.0, 29.1, 29.0, 25.8, 25.2, 18.0, 14.2

FT-IR (Neat Film NaCl) 2981, 2917, 1824, 1727, 1447, 1383, 1266, 1182, 1035, 909 cm^{-1}

HR-MS (MS-EI) m/z calc'd for $\text{C}_{14}\text{H}_{18}\text{O}_4$: 250.1205; measured 250.1195.



Ethyl-1-(3-methylbut-2-en-1-yl)-7-oxo-6-oxabicyclo[3.2.0]hept-2-ene-3-carboxylate

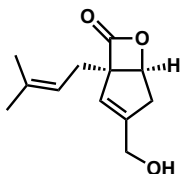
(**75**). To a flame dried schlenk flask equipped with a magnetic stir bar under N_2 atmosphere was added housane **74** (135 mg, 0.54 mmol). To this was added dry benzene (35 mL), followed by DBU (123 mg, 0.81 mmol, 1.5 equiv). The reaction flask was heated at $75\text{ }^\circ\text{C}$ for 18 hours or until complete by TLC (20% ethyl acetate in hexanes on SiO_2). The slightly yellow/brown-colored reaction solution was then loaded directly onto a silica plug, washed through with DCM, and then concentrated by rotary evaporation. The crude oil was then further purified by column chromatography (20% ethyl acetate in hexanes on SiO_2) to afford 93 mg (69%) of **75** as a colorless oil.

^1H NMR (500 MHz, CDCl_3) δ 6.58 (t, $J = 1.9$ Hz, 1H), 5.09 (t, $J = 7.4$ Hz, 1H), 4.82 (d, $J = 5.6$ Hz, 1H), 4.22 (qd, $J = 7.1, 2.5$ Hz, 2H), 3.04 (dd, $J = 19.3, 1.8$ Hz, 1H), 2.94 (ddd, $J = 19.3, 5.7, 2.3$ Hz, 1H), 2.66 (dd, $J = 15.1, 7.4$ Hz, 1H), 2.49 (dd, $J = 15.1, 7.3$ Hz, 1H), 1.71 (s, 3H), 1.63 (s, 3H), 1.39 (t, $J = 7.1$ Hz, 3H)

^{13}C NMR (125 MHz, CDCl_3) δ 170.9, 163.8, 137.7, 137.7, 136.9, 116.6, 78.2, 76.3, 61.1, 36.8, 27.5, 25.9, 18.1, 14.3

FT-IR (Neat Film NaCl) 2923, 1823, 1716, 1627

HR-MS (TOF MS-ES)⁺ m/z calc'd for $\text{C}_{14}\text{H}_{18}\text{O}_4+\text{Na}$: 273.1103; measured: 273.1116.



(\pm)-vibralactone (**73**). To a flame-dried flask equipped with a magnetic stir bar was added ester **75** as a solution in benzene (24.6 mg, 0.052 M, 1.9 mL). To this was added dry THF (7 mL) and this was cooled to -40 °C. Next, a solution of DIBAL-H in THF (2.9 mL, 0.1M, 0.285 mmol, 2.9 equiv) was added dropwise, and the reaction was allowed to stir for 1 hour. Then the reaction was warmed to 0 °C and stirred for an additional 30 minutes. The reaction flask was then warmed to room temperature and quenched with a solution of acetic acid in ethyl acetate (2.5 mL, 0.23M, 6 equiv). This solution was allowed to stir for 10 minutes, then loaded onto a short silica plug, eluting with 100% ethyl acetate. The eluent was collected and concentrated in vacuo and purified by flash chromatography (15% \rightarrow 30% ethyl acetate in hexanes on SiO_2) affording 6.9 mg (34% yield) of (\pm)-vibralactone **73** as a colorless oil. Spectroscopic data are consistent with previous reports.^{1,12} Additionally, 7.8 mg (32%) of starting material (**75**) was also recovered.

^1H NMR (500 MHz, CDCl_3) δ 5.62 (t, $J=7.4$, 1H), 5.12 (m, 1H), 4.80 (dd, $J=4.7$, 1.4 Hz, 1H), 4.25 (d, $J=4.7$ Hz, 2H), 2.81–2.71 (m, 2H), 2.62 (dd, $J=15.1$, 7.4 Hz, 1H), 2.43 (dd, $J=15.1$, 7.4 Hz, 1H), 1.72 (s, 3H), 1.64 (s, 3H)

¹³C NMR (125 MHz, CDCl₃) δ 173.0, 146.6, 136.1, 122.7, 117.4, 78.5, 75.3, 61.5, 37.5, 27.7, 25.9, 18.1

FT-IR (Neat Film NaCl): 3419, 2917, 1815, 1111, 833 cm⁻¹

HR-MS (MS-ESI)⁺ m/z calc'd for C₁₂H₁₆O₃+H: 209.1172; measured: 209.1171.

2.5 REFERENCES

- (1) Liu, D.-Z.; Wang, F.; Liao, T.-G.; Tang, J.-G.; Steglich, W.; Zhu, H.-J.; Liu, J.-K. Vibralactone: A Lipase Inhibitor with an Unusual Fused β -Lactone Produced by Cultures of the Basidiomycete *Boreostereum Vibrans*. *Org. Lett.* **2006**, *8*, 5749–5752.
- (2) Hochuli, E.; Kupfer, E.; Maurer, R.; Meister, W.; Mercadal, Y.; Schmidt, K. Lipstatin, an Inhibitor of Pancreatic Lipase, Produced by *Streptomyces Toxytricini*. II. Chemistry and Structure Elucidation. *J. Antibiot. (Tokyo)* **1987**, *40*, 1086–1091.
- (3) Wei, K.; Wang, G.-Q.; Bai, X.; Niu, Y.-F.; Chen, H.-P.; Wen, C.-N.; Li, Z.-H.; Dong, Z.-J.; Zuo, Z.-L.; Xiong, W.-Y.; Liu, J.-K. Structure-Based Optimization and Biological Evaluation of Pancreatic Lipase Inhibitors as Novel Potential Antiobesity Agents. *Nat. Prod. Bioprospecting* **2015**, *5*, 129–157.
- (4) Tucci, S. The Role of Lipid and Carbohydrate Digestive Enzyme Inhibitors in the Management of Obesity: A Review of Current and Emerging Therapeutic Agents. *Diabetes Metab. Syndr. Obes. Targets Ther.* **2010**, 125.
- (5) Bray, G. A. Medical Consequences of Obesity. *J. Clin. Endocrinol. Metab.* **2004**, *89*, 2583–2589.
- (6) Böttcher, T.; Sieber, S. A. β -Lactones as Specific Inhibitors of ClpP Attenuate the Production of Extracellular Virulence Factors of *Staphylococcus Aureus*. *J. Am. Chem. Soc.* **2008**, *130*, 14400–14401.
- (7) Zeiler, E.; Braun, N.; Böttcher, T.; Kastenmüller, A.; Weinkauff, S.; Sieber, S. A. Vibralactone as a Tool to Study the Activity and Structure of the ClpP1P2 Complex from *Listeria Monocytogenes*. *Angew. Chem. Int. Ed.* **2011**, *50*, 11001–11004.

- (8) Burlak, C.; Hammer, C. H.; Robinson, M.-A.; Whitney, A. R.; McGavin, M. J.; Kreiswirth, B. N.; DeLeo, F. R. Global Analysis of Community-Associated Methicillin-Resistant *Staphylococcus Aureus* Exoproteins Reveals Molecules Produced in Vitro and during Infection. *Cell. Microbiol.* **2007**, *9*, 1172–1190.
- (9) Feng, K.; Yang, Y.; Xu, Y.; Zhang, Y.; Feng, T.; Huang, S.; Liu, J.; Zeng, Y. A Hydrolase-Catalyzed Cyclization Forms the Fused Bicyclic β -Lactone in Vibralactone. *Angew. Chem. Int. Ed.* **2020**, *59*, 7209–7213.
- (10) Zhao, P.-J.; Yang, Y.-L.; Du, L.; Liu, J.-K.; Zeng, Y. Elucidating the Biosynthetic Pathway for Vibralactone: A Pancreatic Lipase Inhibitor with a Fused Bicyclic β -Lactone. *Angew. Chem. Int. Ed.* **2013**, *52*, 2298–2302.
- (11) Robinson, S. L.; Christenson, J. K.; Wackett, L. P. Biosynthesis and Chemical Diversity of β -Lactone Natural Products. *Nat. Prod. Rep.* **2019**, *36*, 458–475.
- (12) Zhou, Q.; Snider, B. B. Synthesis of (\pm)-Vibralactone. *Org. Lett.* **2008**, *10*, 1401–1404.
- (13) Zhou, Q.; Snider, B. B. Synthesis of (\pm)- and ($-$)-Vibralactone and Vibralactone C. *J. Org. Chem.* **2008**, *73*, 8049–8056.
- (14) Leeder, A. J.; Heap, R. J.; Brown, L. J.; Franck, X.; Brown, R. C. D. A Short Diastereoselective Total Synthesis of (\pm)-Vibralactone. *Org. Lett.* **2016**, *18*, 5971–5973.
- (15) Nistanaki, S. K.; Boralsky, L. A.; Pan, R. D.; Nelson, H. M. A Concise Total Synthesis of (\pm)-Vibralactone. *Angew. Chem. Int. Ed.* **2019**, *58*, 1724–1726.
- (16) Frébault, F.; Oliveira, M. T.; Wöstefeld, E.; Maulide, N. A Concise Access to 3-Substituted 2-Pyrones. *J. Org. Chem.* **2010**, *75*, 7962–7965.

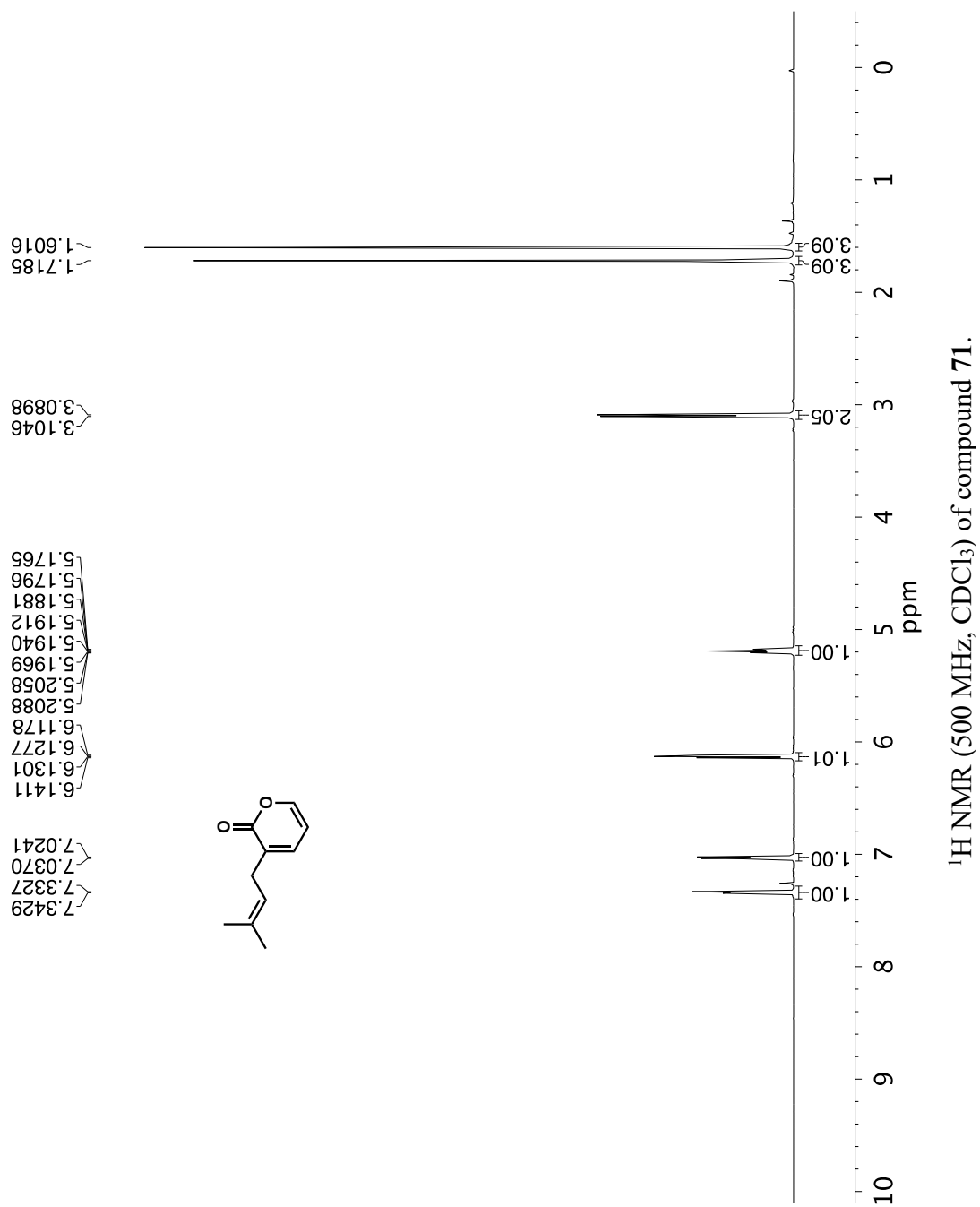
- (17) Corey, E. J.; Streith, Jacques. Internal Photoaddition Reactions of 2-Pyrone and N-Methyl-2-Pyridone: A New Synthetic Approach to Cyclobutadiene. *J. Am. Chem. Soc.* **1964**, *86*, 950–951.
- (18) Espino, C. G.; Fiori, K. W.; Kim, M.; Du Bois, J. Expanding the Scope of C–H Amination through Catalyst Design. *J. Am. Chem. Soc.* **2004**, *126*, 15378–15379.
- (19) Wiberg, K. B.; Bishop, K. C. Transition Metal Catalyzed Isomerization of Substituted Bicyclo[2.1.0] Pentanes. *Tetrahedron Lett.* **1973**, *14*, 2727–2730.
- (20) Boche, G.; Martens, D. Ring Opening of a Cyclopropyl Anion and Cycloaddition of the Allyl Anion. *Angew. Chem. Int. Ed. Engl.* **1972**, *11*, 724–725.
- (21) Arnold, B. R.; Brown, C. E.; Luszyk, J. Solution Photochemistry of 2H-Pyran-2-One: Laser Flash Photolysis with Infrared Detection of Transients. *J. Am. Chem. Soc.* **1993**, *115*, 1576–1577.
- (22) Großkopf, J.; Kratz, T.; Rigotti, T.; Bach, T. Enantioselective Photochemical Reactions Enabled by Triplet Energy Transfer. *Chem. Rev.* **2022**, *122*, 1626–1653.
- (23) Yoon, T. P. Photochemical Stereocontrol Using Tandem Photoredox–Chiral Lewis Acid Catalysis. *Acc. Chem. Res.* **2016**, *49*, 2307–2315.
- (24) Blum, T. R.; Miller, Z. D.; Bates, D. M.; Guzei, I. A.; Yoon, T. P. Enantioselective Photochemistry through Lewis Acid–Catalyzed Triplet Energy Transfer. *Science* **2016**, *354*, 1391–1395.
- (25) Daub, M. E.; Jung, H.; Lee, B. J.; Won, J.; Baik, M.-H.; Yoon, T. P. Enantioselective [2+2] Cycloadditions of Cinnamate Esters: Generalizing Lewis Acid Catalysis of Triplet Energy Transfer. *J. Am. Chem. Soc.* **2019**, *141*, 9543–9547.

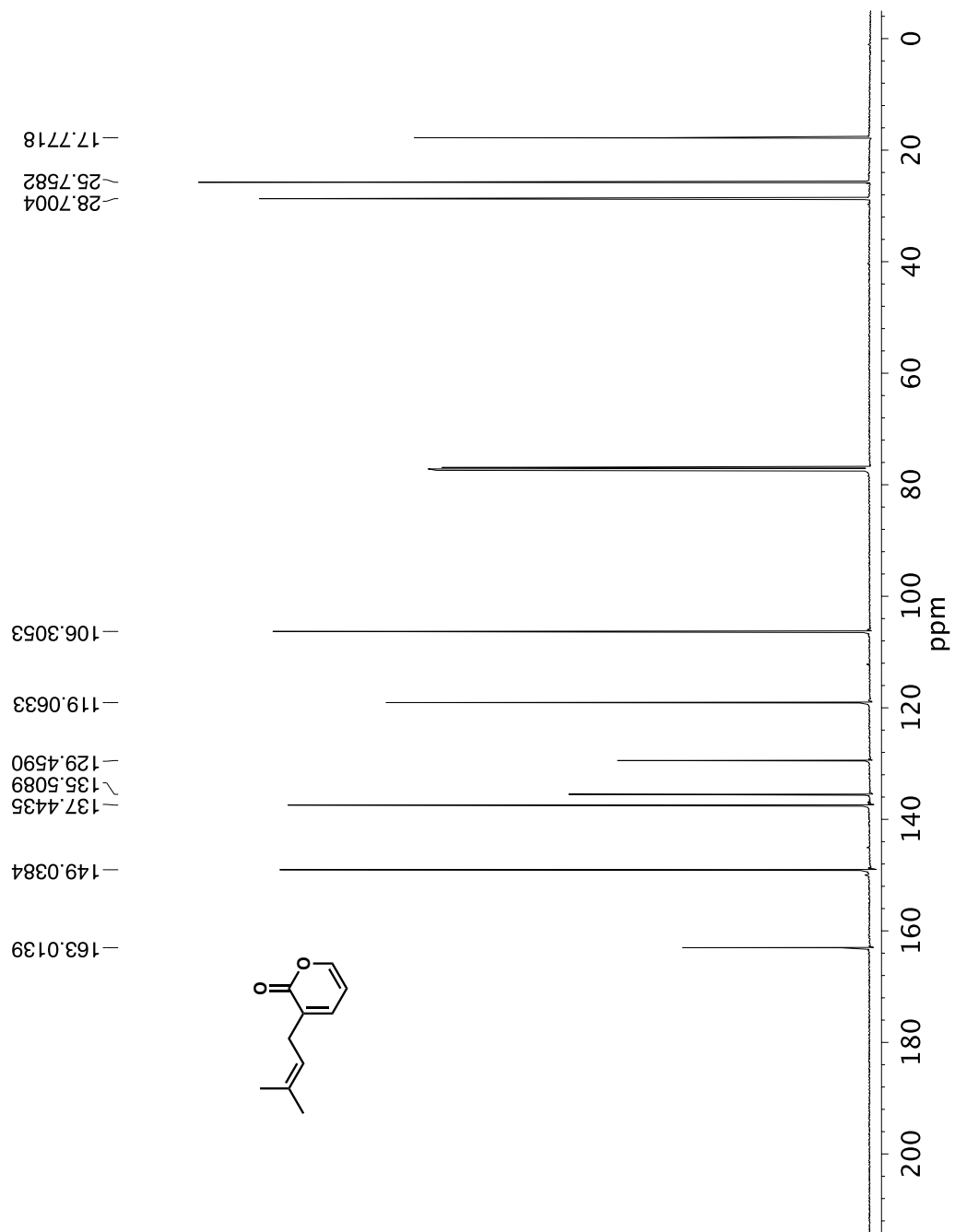
- (26) Zhou, Q.; Zou, Y.; Lu, L.; Xiao, W. Visible-Light-Induced Organic Photochemical Reactions through Energy-Transfer Pathways. *Angew. Chem. Int. Ed.* **2019**, *58*, 1586–1604.
- (27) Brimiouille, R.; Bach, T. Enantioselective Lewis Acid Catalysis of Intramolecular Enone [2+2] Photocycloaddition Reactions. *Science* **2013**, *342*, 840–843.
- (28) Lewis, F. D.; Barancyk, S. V. Lewis Acid Catalysis of Photochemical Reactions. 8. Photodimerization and Cross-Cycloaddition of Coumarin. *J. Am. Chem. Soc.* **1989**, *111*, 8653–8661.
- (29) Lewis, F. D.; Howard, D. K.; Oxman, J. D. Lewis Acid Catalysis of Coumarin Photodimerization. *J. Am. Chem. Soc.* **1983**, *105*, 3344–3345.
- (30) Taber, D. F.; Meagley, R. P.; Louey, J. P.; Rheingold, A. L. Molecular Complex Design: Bridging the Tetrakis(carboxylato)dirhodium Core. *Inorganica Chim. Acta* **1995**, *239* (1–2), 25–28.

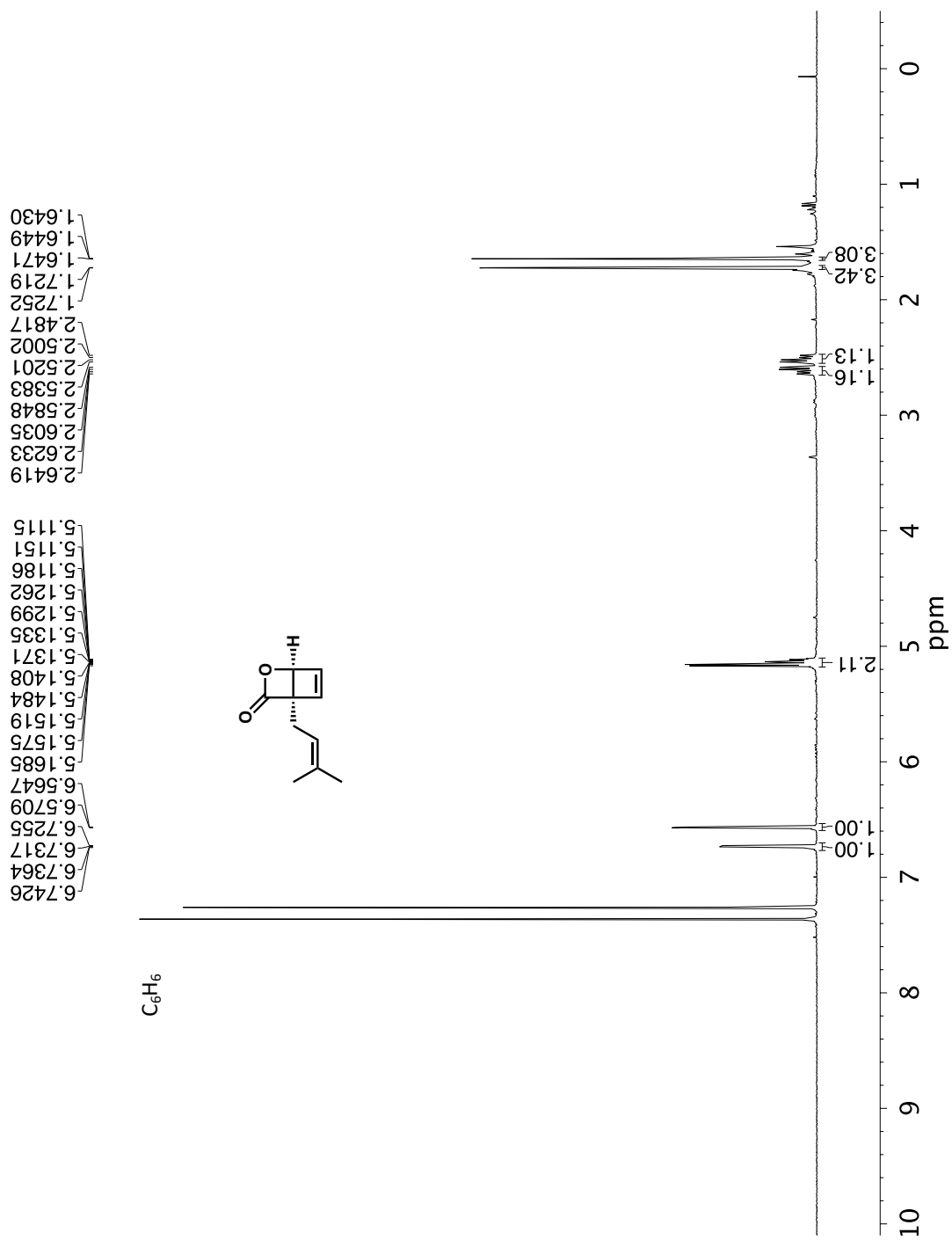
Appendix 1

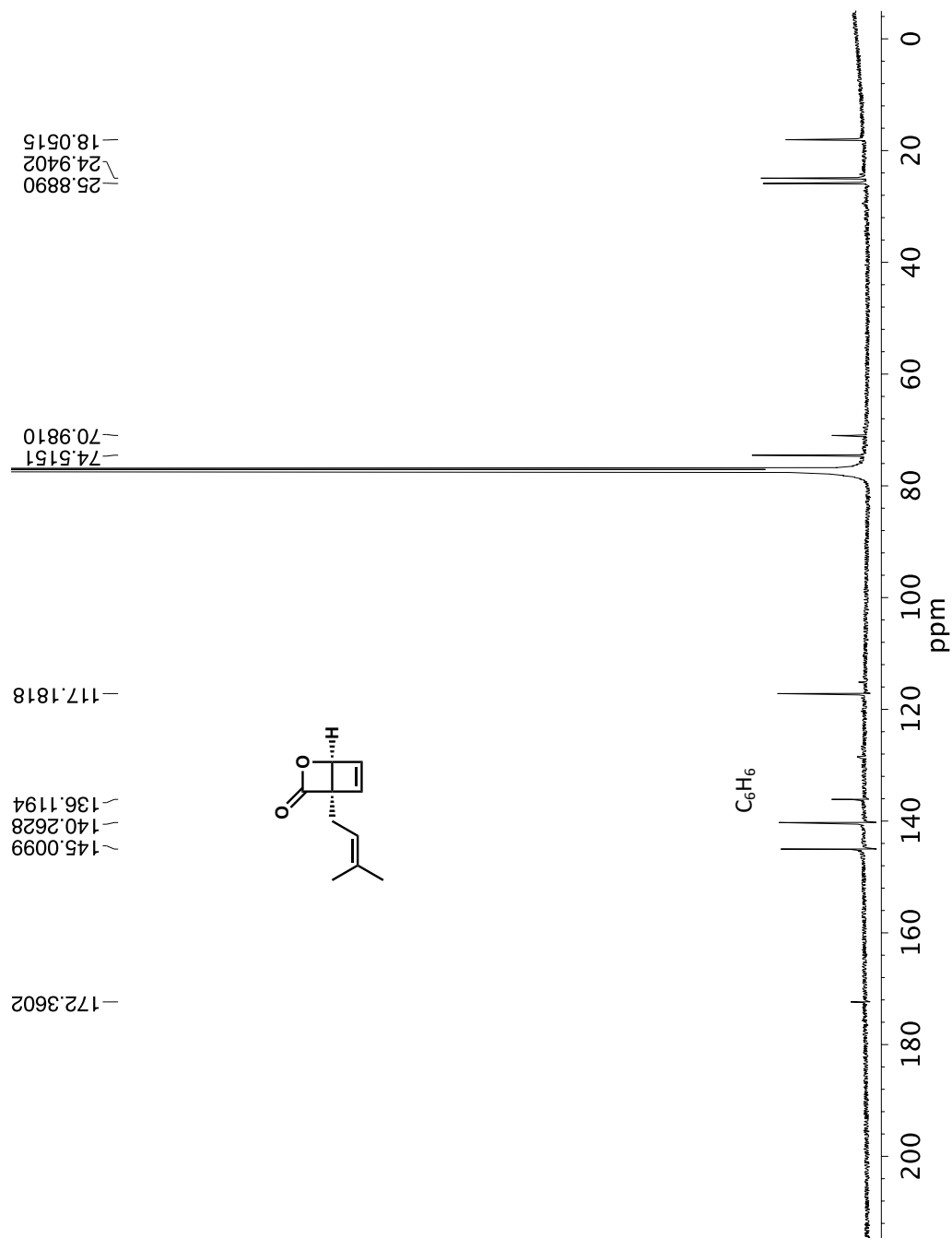
Spectra Relevant to Chapter 2: A Concise Total Synthesis of (±)-

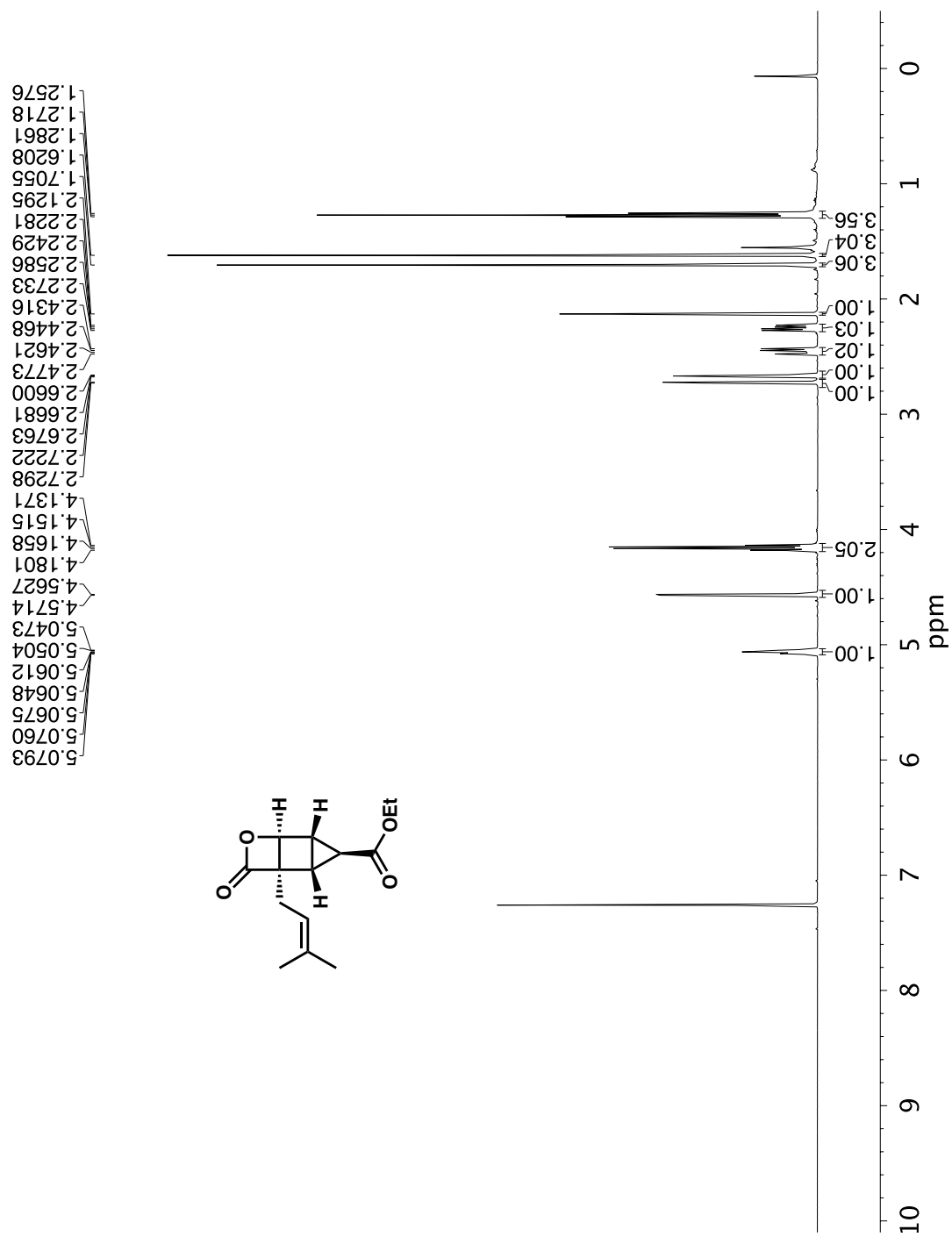
Vibralactone

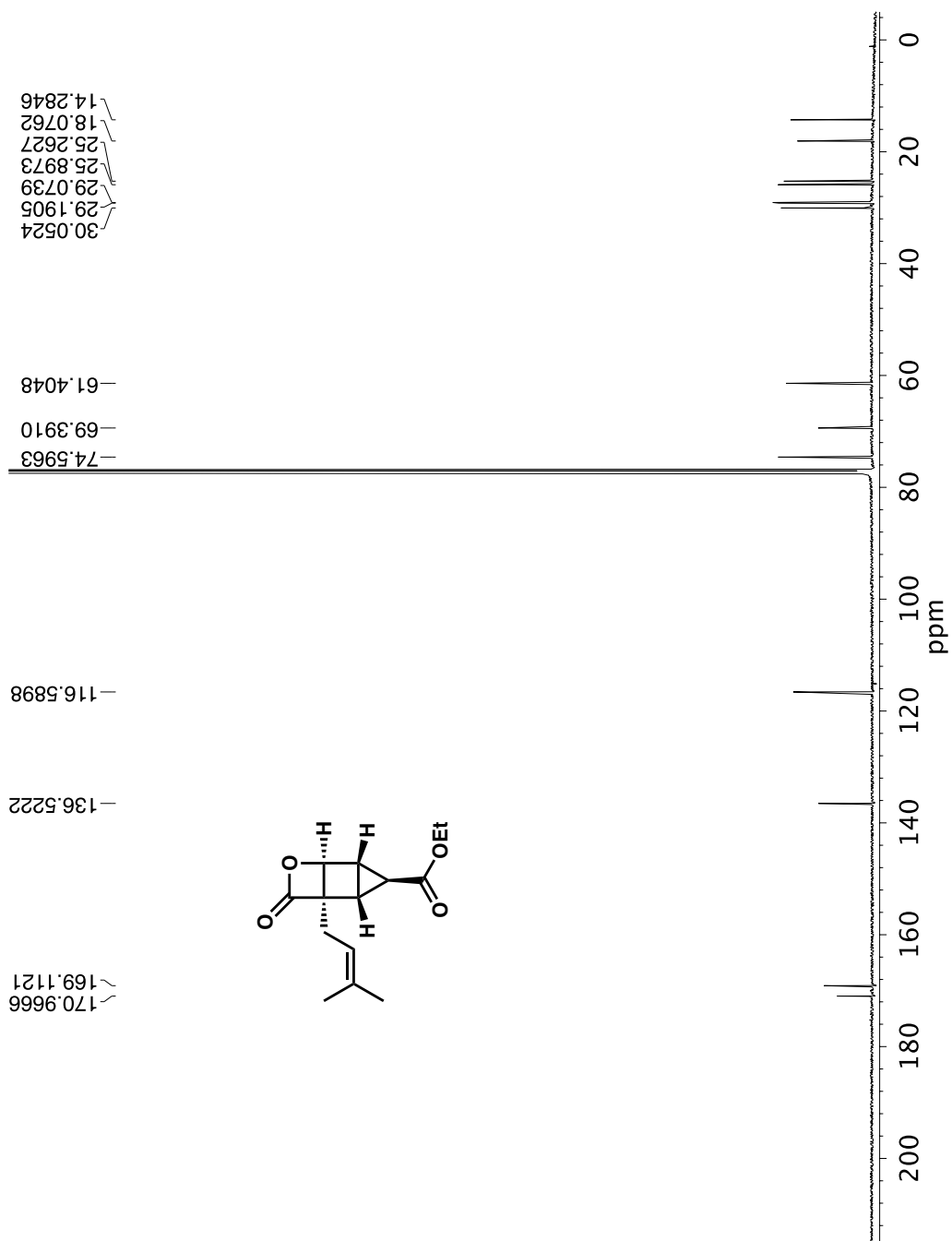


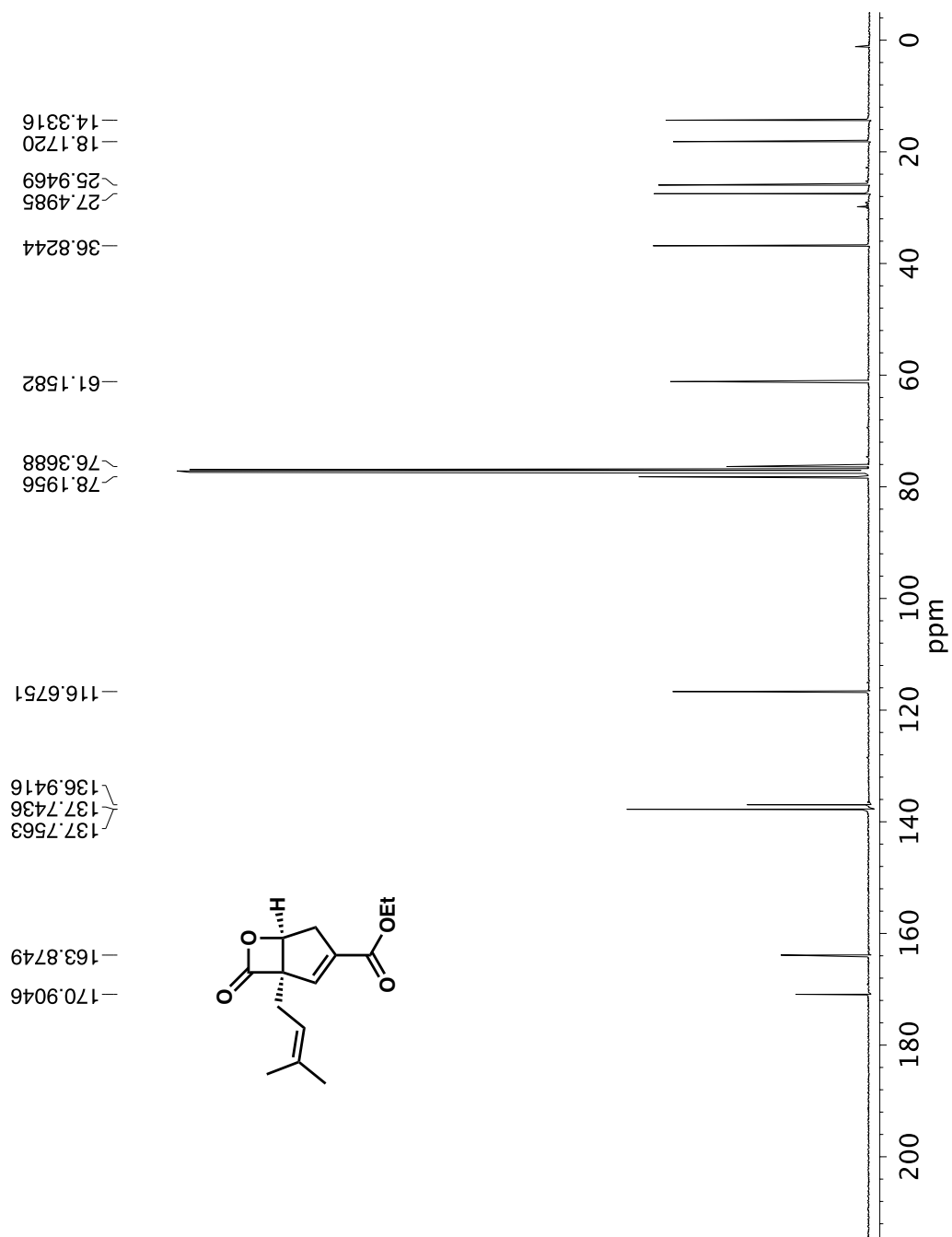


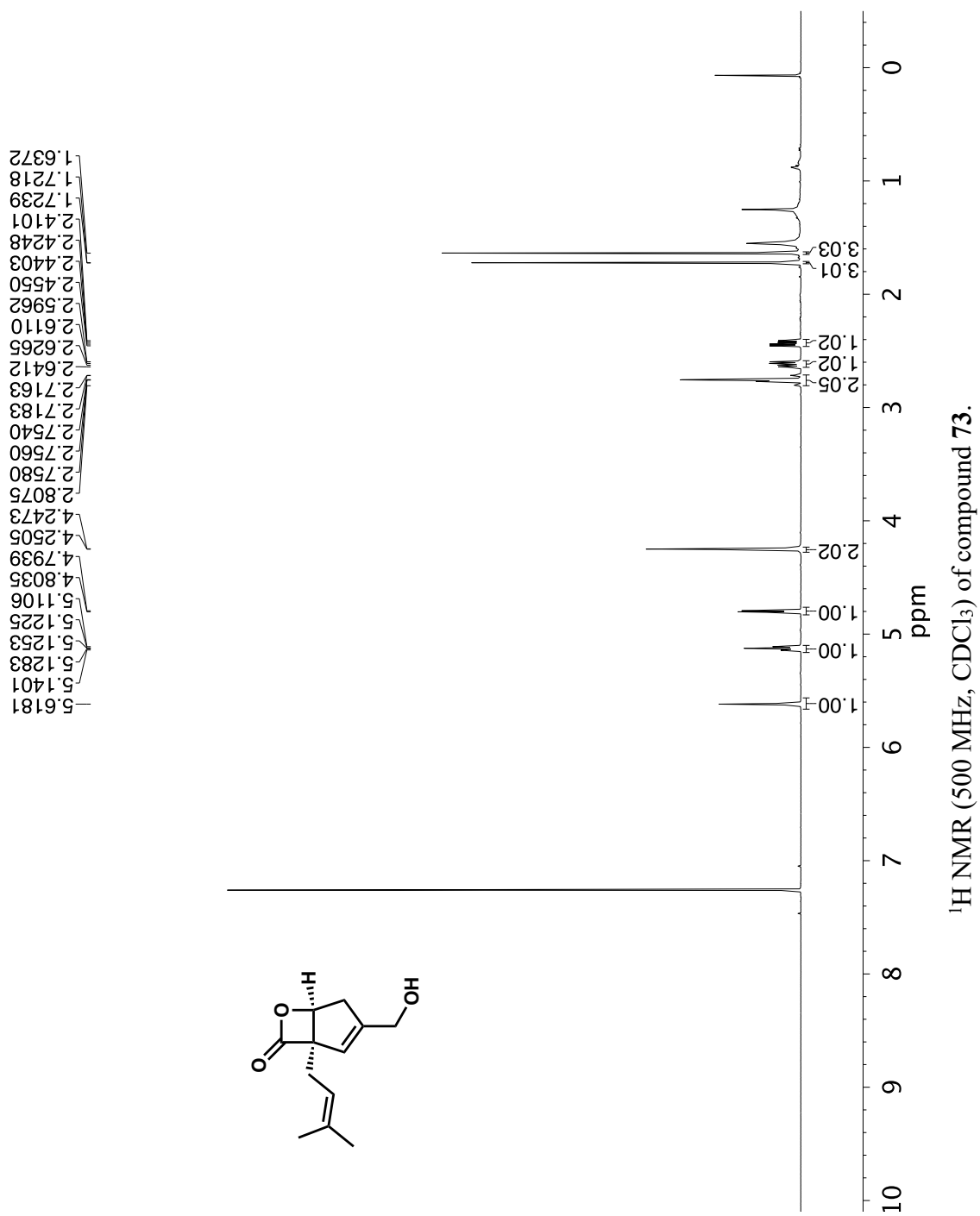


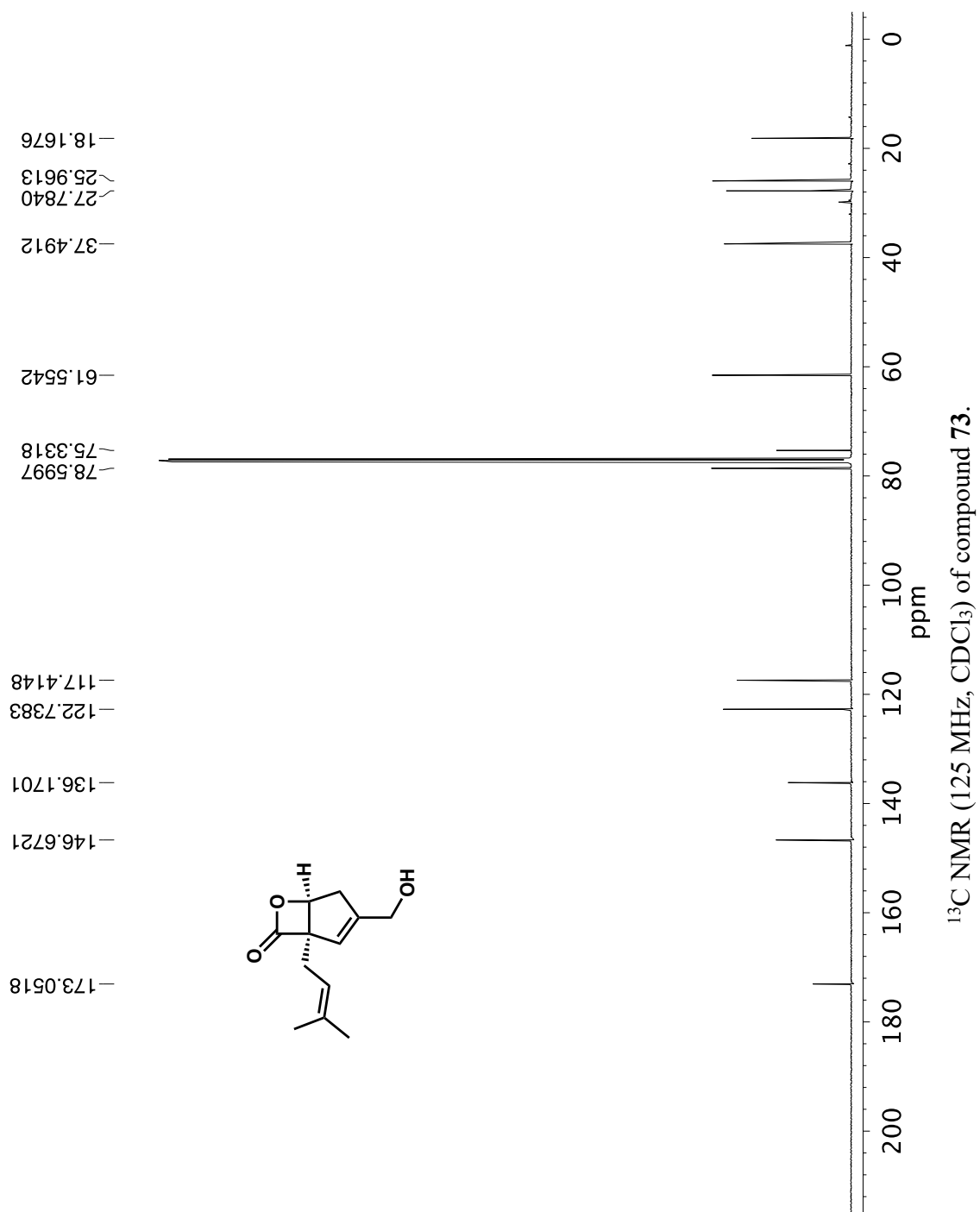












Appendix 2

X-Ray Data Relevant to Chapter 2: A Concise Total Synthesis of (±)-

Vibrallactone

A2.1. GENERAL EXPERIMENTAL

The diffraction data were measured at 100K(2) on a Bruker Smart Apex2 CCD-based X-ray diffractometer system equipped with a Cu-K α radiation ($\lambda = 1.54178 \text{ \AA}$). The frames were integrated with the Bruker Saint software package using a narrow-frame integration algorithm. The structure was solved and refined using the Bruker SHELXTL Software Package. All atoms were refined anisotropically, and hydrogen atoms were placed at calculated positions. Structure was solved by Dr. Saeed Khan (UCLA).

The crystallographic data have been deposited in the Cambridge Database (CCDC). The deposition number is 1867750.

A2.1.1 X-Ray Crystal Structure Analysis for 74

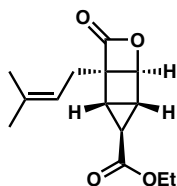


Figure A2.1 X-Ray Crystal Structure for 74

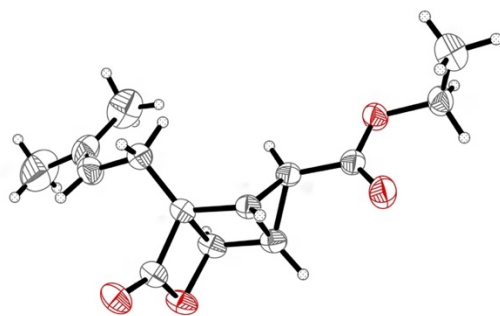


Table A2.1. Crystal data & structure refinement

Refined formula	$C_{14}H_{18}O_4$
Formula weight	250.28
Crystallization solvent	Hexanes
Crystal shape	Platelets
Crystal color	Colorless
Crystal size	0.400 x 0.050 x 0.020 mm

Data Collection

Type of diffractometer	Bruker APEX-II CCD	
Wavelength	$CuK\alpha$ ($\lambda = 1.54178$)	
Data collecting temperature	293(2) K	
Theta range for 5987 reflections used in lattice determination	4.05 to 68.74	
Unit cell dimensions	$a = 11.867(2)$	$\alpha = 90$
	$b = 5.3190(10)$	$\beta = 93.82(2)$
	$c = 43.735(8)$	$\gamma = 90$
	$2754.3(9) \text{ \AA}^3$	
Z	8	
Crystal system	monoclinic	
Space group	I 2/a	

Calculated density	1.207 g/cm ³
Linear absorption coefficient	0.722
F(000)	1072
2 θ range for data collection	2.025 to 69.712
Completeness to theta = 69.712	0.988
Index ranges	-14 \leq h \leq 13 -6 \leq h \leq 6 -52 \leq h \leq 53
Data collection scan type	ω and ϕ scan
Reflections collected	18802
Independent reflections	2587 [$R_{\text{int}} = 0.0493$, $R_{\text{sigma}} = 0.0286$]
Reflections > 2 σ (I)	2045
Average of σ (I)/(net I)	0.0286
Absorption coefficient	0.722 mm ⁻¹
Absorption correction	Multi scan
Max. and min. transmission	0.761 and 0.986

Structure solution & Refinement

Primary solution method	SHELXL-2014
Secondary solution method	SHELXL-2014

Hydrogen placement	geom	
Refinement method	Bruker SHELXTL	
Goodness-of-fit on F^2	1.081	
Final R indices [$I > 2\sigma(I)$]	$R_1 = 0.0610$	$wR_2 = 0.1511$
R indices (all data)	$R_1 = 0.0752$	$wR_2 = 0.1598$
Max shift/error	0.000	
Average shift/error	0.000	
Largest diff. peak and hole / $e \text{ \AA}^{-3}$	0.286/-0.174	

Programs used

Cell refinement	Bruker SAINT
Data collection	Bruker APEX2
Data reduction	Bruker SAINT
Structure solution	SHELXS-97 (Sheldrick 2008)
Structure refinement	SHELXL-2014/6 (Sheldrick, 2014)
Graphics	Bruker SHELXTL

Chapter 3

Dewar Heterocycles as Versatile Monomers for Ring-Opening Metathesis Polymerization¹

3.1 INTRODUCTION

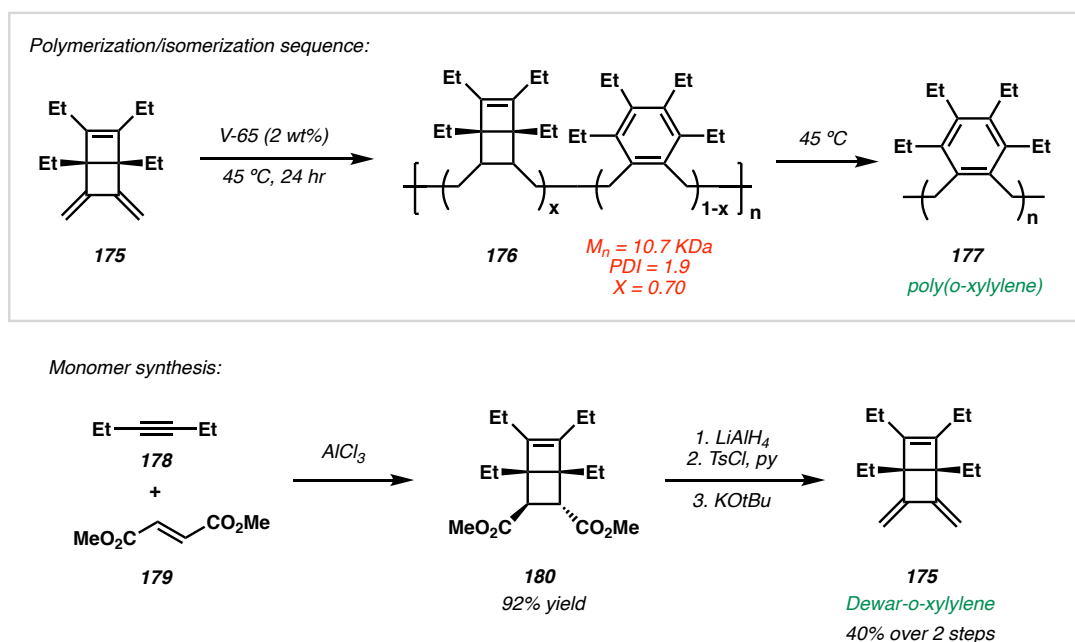
Heterocyclic compounds have long been known to undergo photochemical valence isomerization reactions to generate their dearomatized Dewar isomers.¹⁻³ This process affords molecules with compact stereocomplexity from readily available “flat” heterocyclic precursors. The photoproducts formed in such valence isomerization reactions are often quite reactive given the strained nature of their cyclobutene substructures, and in some cases rapid thermal reversion to the heterocyclic precursor challenges isolation, as

¹ Portions of this chapter have been adapted from Nistanaki, S. K.; Nelson, H. M. *ACS Macro Lett.* **2020**, *9*, 731–735. © American Chemical Society.

seen in the case of Dewar pyridine.² While Dewar heterocycles have been employed in the context of small molecule synthesis^{4–8}, their utility as substrates for polymerization reactions is underexplored.

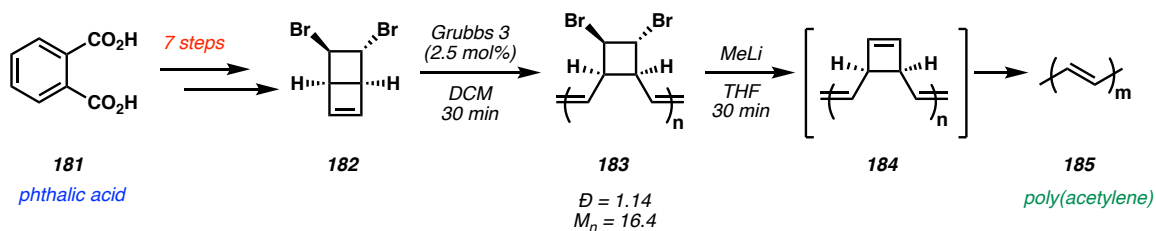
Synthetic strategies involving Dewar benzene derivatives have found recent utility in polymer synthesis. Swager and co-workers demonstrated in 2018 that Dewar *o*-xylylene (**175**) can undergo radical polymerization utilizing radical initiator V-65 to yield high molecular weight poly(*o*-xylylene) (**177**) via post-polymerization isomerization of **176** (Scheme 3.1).⁹ Accessing poly(*o*-xylylene) from *o*-xylylene itself has previously been a formidable challenge, given the propensity for *o*-xylylene to undergo form [4+2] and [4+4] dimerization. Swager's strategy highlights the utility of employing *o*-xylylene's Dewar isomer, which was prepared through a four-step cycloaddition/elimination sequence from a disubstituted alkyne (**178**) and dialkyl fumarate (**179**) precursor.

Scheme 3.1. Swager's study of poly(Dewar-*o*-xylylene)s



Bielawski and co-workers demonstrated in 2019 that a dibrominated derivative of Dewar benzene (**182**) could be polymerized and subsequently modified in two steps to access poly(acetylene) **185** (Scheme 3.2).¹⁰ Poly(acetylene), while a promising material for electronics applications, is notoriously insoluble and difficult to prepare in a controlled and tunable fashion.^{11–13} The controlled ring-opening metathesis polymerization (ROMP) of **182** (accessed in 7 steps from phthalic acid **181**) to **183** utilizing Grubbs 3rd generation (G3) catalyst enabled a method for accessing poly(acetylene) (**185**) with high *trans*-olefin content, along with triblock copolymers containing poly(acetylene) segments. These highly strained monomers were, however, challenging to access, involving many synthetic steps and harsh conditions. More recently, Bielawski and co-workers reported the polymerization of cyclobutene substrates derived in two steps from Dewar pyrone, which were then converted to substituted poly(acetylene) derivatives using post-polymerization chemistry (Chapter 1, Scheme 1.18).¹⁴

Scheme 3.2. Bielawski's synthesis of poly(acetylene) from Dewar benzene derivative

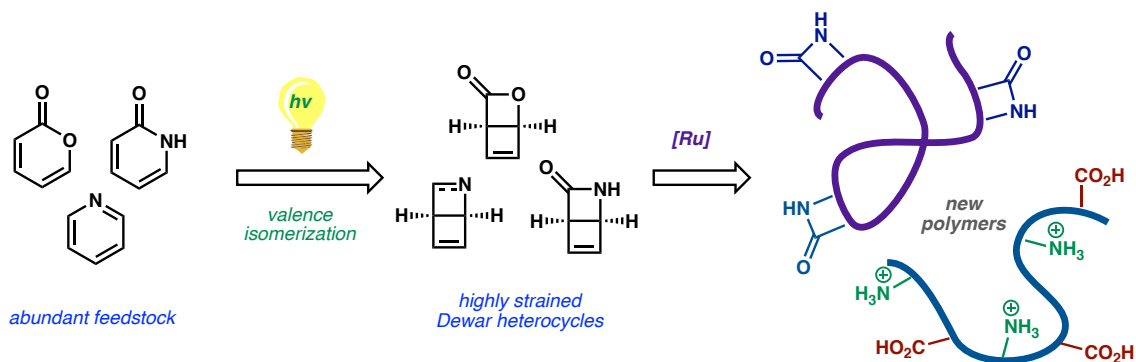


3.2 POLYMERIZATION OF DEWAR HETEROCYCLE DERIVATIVES

The synthesis of Dewar benzene and its derivatives requires multiple synthetic steps to access material in sufficient quantities. On the other hand, the photochemical valence

isomerization of heterocycles to their Dewar isomer is synthetically efficient, requiring only one step. Moreover, many aromatic heterocycles are known to undergo selective photoisomerization reactions, including abundant feedstock chemicals like pyridines and pyrones. This process introduces a strained cyclobutene moiety as a reactive handle for ring-opening metathesis polymerization (ROMP), and we reasoned that direct polymerization of the Dewar heterocycle could deliver unique polymers bearing strained heterocycles in their backbones. Furthermore, such polymers could possess unique physical properties given their structural rigidity, chirality, and capacity to undergo post-polymerization modification. This chapter describes our studies on the polymerization of Dewar heterocycles derived from pyrone, pyridine, and pyridone, along with their post-polymerization modification (Scheme 3.3). This strategy enables an expedient route to polymers bearing strained azacyclic rings in their backbone, water-soluble β -amino acid-type polymers, and soluble poly(acetylene) derivatives.

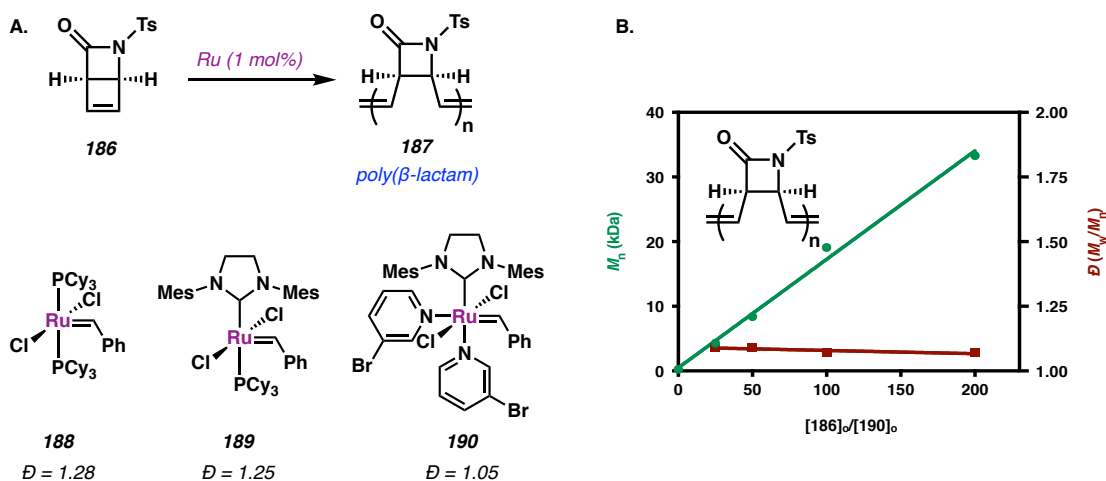
Scheme 3.3. Overview of Dewar heterocycle polymerization strategy



3.2.1 Polymerization of Dewar Pyridone Derivatives

We initiated our investigation by targeting pyridones, which are known to undergo photochemical valence isomerization to yield β -lactam-fused cyclobutenes.¹ Initial experiments with N-tosyl protected Dewar pyridone (**186**) demonstrated polymerization with commercial Grubbs catalysts (**188–190**), with Grubbs 3rd generation (G3) catalyst (**190**) affording poly(β -lactam) **187** with the lowest dispersity ($\mathcal{D} = 1.05$) (Scheme 3.4a). To study the influence of catalyst loading on polymer molecular weight, the initial monomer-to-catalyst ratio ($[\mathbf{186}]_0/[\mathbf{G3}]_0$) was varied from 25 to 200, which showed a linear increase in molecular weight from 4.3 to 33.3 kDa based on GPC analysis (Scheme 3.4b). The dispersity of these polymers remained low regardless of the feed ratio (\mathcal{D} between 1.05 to 1.09), demonstrating the controlled nature of these polymerization reactions.

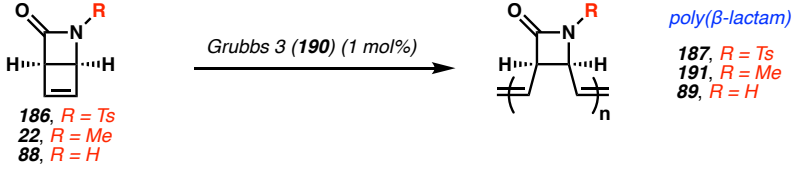
Scheme 3.4. Polymerization of N-tosylated Dewar pyridone with Grubbs catalysts

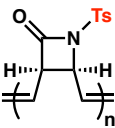
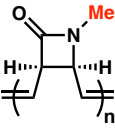
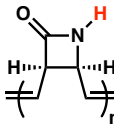


We next explored other Dewar pyridone derivatives, which were derived photochemically from their aromatic precursor and polymerized using G3 catalyst to afford

new poly(β -lactam) polymers with low dispersity ($\mathcal{D} < 1.30$) (Table 3.1). Along with N-sulfonylated monomer **186** (entry 1), polymerization was also observed with N-alkylated monomer **22** (entry 2) and unprotected lactam **88** (entry 3). In all cases, the β -lactam functionality is preserved with no sign of ring-opening by IR and NMR spectroscopy. β -lactams have traditionally been viewed as reactive functional groups for ring-opening polymerization to generate polyamide-type polymers.^{15–19} However, the synthesis of polymers with incorporated β -lactam functionality directly in the backbone is rarer, with limited examples in the literature.²⁰

Table 3.1. Polymerization of Dewar pyridone derivatives

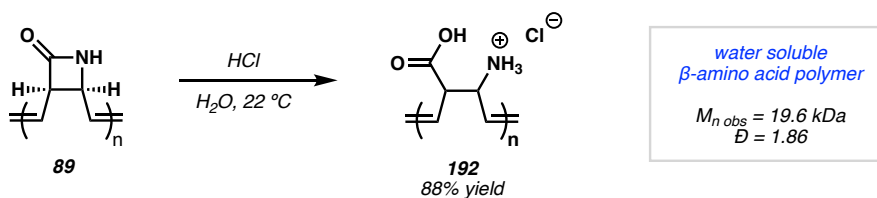


Entry	Polymer	Solvent	Time	M_n theory	M_n obs	\mathcal{D}	DP	Yield (%)
1		DCM	2 hr	24.9 kDa	19.1 kDa	1.05	77	95
2		DCM	4 hr	10.9 kDa	23.3 kDa	1.12	213	92
3		DMF	3 hr	19.0 kDa	29.9 kDa	1.87	315	81

We also investigated the post-polymerization modification of polymer **89**, with the hypothesis that the strained β -lactam could be leveraged to facilitate chemistry. We found that hydrolysis of the β -lactam under acidic conditions cleanly yielded water-soluble

polymer **192** bearing a β -amino acid motif, which could be an attractive material for biomedical applications (Scheme 3.5).^{21–23}

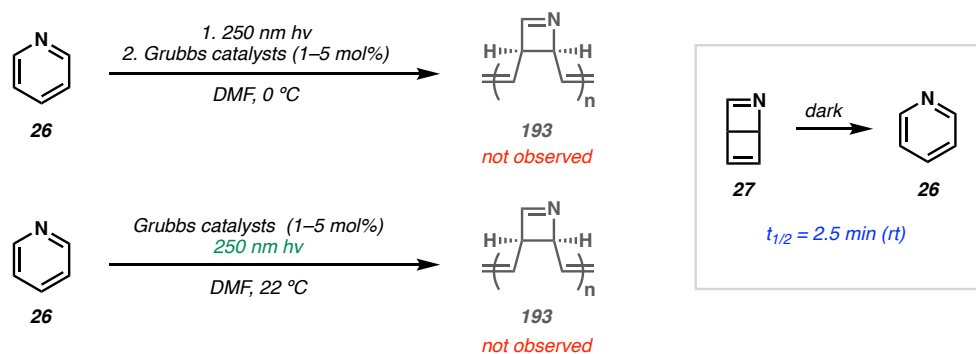
Scheme 3.5. Post-polymerization hydrolysis of β -lactam



3.2.2 Polymerization of Dewar Dihydropyridine Derivatives

Unlike pyridones, the formation of the azetidine-fused cyclobutene structure in Dewar pyridine (**27**) renders these intermediates highly reactive, with a reported half-life of only 2.5 minutes at room temperature (Scheme 3.6).² Attempts to polymerize these intermediates directly or to conduct the photo-isomerization and polymerization in one pot were unsuccessful.

Scheme 3.6. Failed attempts at Dewar pyridine polymerization



Given these difficulties, we reasoned that pyridine could still be incorporated into a polymer synthesis platform through dearomatization of pyridinium ions. Drawing from prior work by Fowler and Comins, selective NaBH_4 reduction or addition of Grignard reagents into N-acyl pyridinium ions resulted in dienamines.^{24–27} These intermediates could be isomerized photochemically to furnish protected bicyclic azetidines, formally the Dewar isomer of dihydropyridine (Table 3.2). We found that strained molecules **90** and **194** also readily engage in ROMP chemistry, yielding poly(azetidine)s **91** and **195** in a controlled fashion with polydispersity index values ranging from 1.07 to 1.09.

Table 3.2. Polymerization of Dewar dihydropyridine derivatives

Entry	Polymer	Solvent	Time	M_n theory	M_n obs	\bar{D}	DP	Yield (%)
1		DCM	4.5 hr	15.3 kDa	14.7 kDa	1.07	94	91%
2		DCM	4.5 hr	22.9 kDa	19.5 kDa	1.07	85	97%

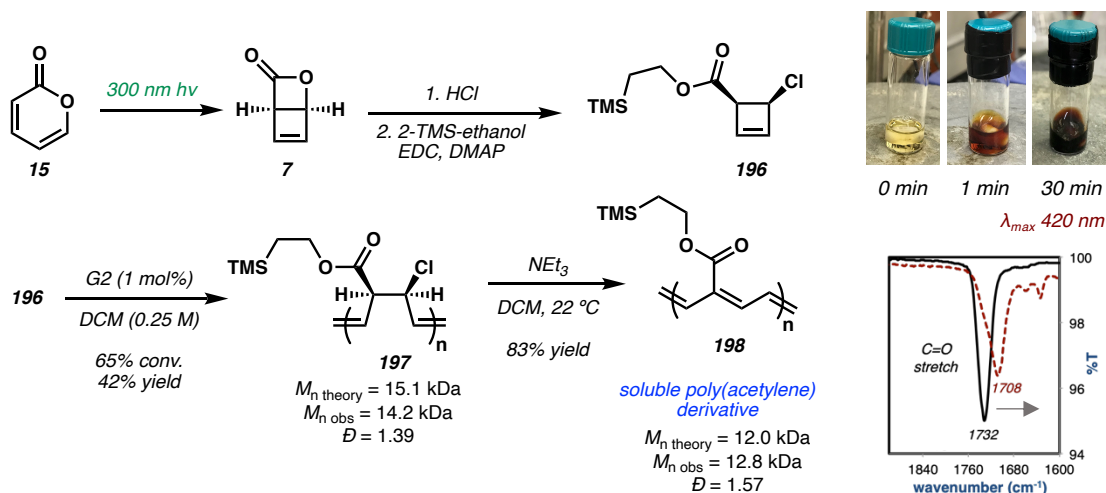
The initial monomer-to-catalyst ratio ($[\mathbf{194}]_0/[\mathbf{190}]_0$) was varied from 25 to 200, which showed a linear increase in molecular weight from 5.0 to 26.0 kDa with minimal change in the dispersity (Table 3.2). This confirms the ability to tune the molecular weight of the polymer through selection of catalyst loading, while maintaining low dispersity. These results represent another example of strained-ring polymers that could be derived from cheap and abundant compounds, like pyridine. The ability to add in different nucleophiles into the intermediate pyridinium ion towards Dewar dihydropyridine offers an approach for facile installation of various functional groups onto the structurally rigid azetidine scaffold. While azetidine functional groups have frequently been used in ring-opening polymerization reactions to yield polyamine-type polymers²⁸, the direct incorporation of the strained four-membered azacyclic ring in the polymer backbone is rarer.^{29,30}

3.2.3 Synthesis of Substituted Poly(acetylene) from α -Pyrone

We recognized that pyrones also pose as an interesting polymer precursor given that they could be derived from biomass feedstock. For example, α -pyrone (**15**) can be derived from malic acid, which is generated from glucose fermentation.^{31,32} Attempts to polymerize Dewar pyrone **7** directly were unfruitful – exposing a solution of freshly prepared monomer to Grubbs 3 catalyst led to rapid precipitation of an insoluble material (assigned as oligomer based on solid-state NMR), with recovered unreacted monomer in the filtrate. Attempts to synthesize a more soluble polymer by functionalizing the precursor pyrone with substituents at either C3 or C5 were also unsuccessful, as no polymerization was observed even at elevated temperatures. Instead, we opted to open up the β -lactone

ring, generating an ester moiety that could help solubilize the resulting polymer. To this end, we found that *cis* β -chloro ester **196** polymerized using Grubbs generation 2 catalyst to give polymer **197** after 24 hours at room temperature (Scheme 3.7).

We hypothesized that polymer **197** could be converted to a substituted poly(acetylene)s through a base-mediated elimination reaction and found that exposure of polymer **197** to triethylamine at room temperature resulted in the generation of organic-soluble poly(acetylene) derivative **198** and triethylammonium chloride, as determined by NMR (Scheme 3.7). A shift in the C=O IR absorption from 1732 to 1708 cm^{-1} is consistent with the formation of an α,β -unsaturated carbonyl system, which would be expected from the elimination of the β -chloride. Interestingly, the reaction immediately forms a vibrant burgundy color in solution, with strong absorption at 425 nm, as determined by UV-Vis spectroscopy. Given the difficulty in the controlled synthesis of substituted poly(acetylene) that are soluble in organic solvents^{11,33–35}, these results present a promising avenue towards accessing soluble conjugated materials that could be readily derived from pyrones. We note here that a similar approach was also reported by Bielawski and co-workers for accessing ester-substituted poly(acetylene)s.¹⁴ Interestingly, the authors also observed poor polymerization using Grubbs 3 catalyst and opted to use Hoveyda-Grubbs generation 2 catalyst to obtain high conversion in an hour on a similar β -chloroester monomer. Our experimental observations and recorded spectra are also consistent with their reported results.

Scheme 3.7. Synthesis of substituted poly(acetylene) derivatives from α -pyrone

3.3 CONCLUSION

We have demonstrated that Dewar heterocycles can serve as versatile monomers for ring-opening metathesis polymerization, resulting in new polymers with strained rings embedded in their backbones. The monomers can be accessed in one step from the requisite aromatic heterocycle using light as the energy source. In the case of Dewar pyridones and dihydropyridines, polymers with strained azacyclic rings (β -lactam and azetidine motifs) can be accessed. Pyrone-derived monomers can also be polymerized to give β -chloroester polymers. We have demonstrated that the resulting polymers could also be modified post-polymerization to access water-soluble β -amino acid-type polymers or organic-soluble poly(acetylene) derivatives, which could have potential applications in biomedical or conductive materials, respectively. Moreover, given that the strained polymers in this study are derived from unstrained aromatic precursors, it is enticing to consider opportunities for depolymerization chemistry to revert back to the thermodynamically-favored aromatic heterocycle for incorporation into a closed-loop system for recyclable materials.³⁶

3.4 EXPERIMENTAL SECTION

3.4.1 Materials & Methods

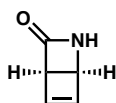
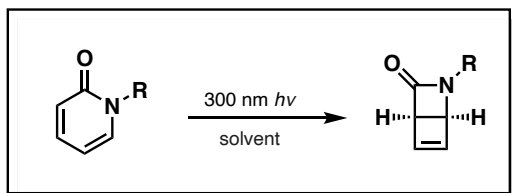
Unless otherwise stated, all polymerization reactions were performed in an MBraun glovebox under nitrogen atmosphere with < 0.5 ppm O₂ levels. All glassware and stir-bars were dried in a 160 °C oven for at least 12 hours and allowed to cool in vacuo before use. Monomers were dried over P₂O₅ before use. Unless otherwise noted, all solvents were dried and degassed in a JC Meyer solvent system. Grubbs generation 3 catalyst was synthesized according to the reported procedure from Grubbs generation 2 and freshly distilled 3-bromopyridine.³⁷ Grubbs generation 2 catalyst was purchased from Sigma-Aldrich and used as received. Poly(styrene) standards were obtained from Alfa Aesar (5.200 kDa and 13.000 kDa standards) and Wyatt (30.000 kDa and 200.000 kDa standards). All other chemical reagents were purchased from Sigma-Aldrich or Oakwood Chemicals and used as received. Photochemistry was performed in a Rayonet RPR-200 photochemical reactor. 300nm bulbs were purchased from Rayonet (model RPR-3000A). Disposable Thin layer chromatography (TLC) was performed using E. Merck silica gel 60 F254 precoated plates (0.25mm) and visualized by UV fluorescence quenching, *p*-anisaldehyde, KMnO₄, or cerium-ammonium-molybdate (CAM) staining. SiliaFlash P60 Silica gel (230–400 mesh) was used for flash chromatography. NMR spectra were recorded on a Bruker DRX-500, Bruker AV-500, or Bruker AV-400. All ¹H NMR spectra are reported relative to the deuterated solvent used. Data for ¹H NMR spectra are as follows: m = multiplet, br s = broad singlet, br m = broad multiplet. Gel Permeation Chromatography (GPC) for THF-soluble polymers was conducted on a Shimadzu Prominence-i LC 2030C 3D (UCLA) with MZ Analysentechnik MZ-Gel SDplus LS 5 μm, 300 × 8 mm linear column, a Wyatt DAWN

HELEOS-II, and a Wyatt Optilab T-rEX. Column temperature was 40 °C, with a flow rate of 0.70 mL min⁻¹. THF was used as the mobile phase and solvent for sample preparation. Polymer samples not soluble in THF were analyzed by the Materials Research Laboratory (MRL) at UCSB, using either DMF, CHCl₃, or aqueous GPC. DMF-soluble polymers were analyzed on a Waters Alliance HPLC system (2695 separation module) equipped with 2 Tosoh TSKgel Super HM-M columns, a Waters 2414 Differential Refractometer (RI) and Waters 2998 Photodiode Array Detector (PDA) using DMF solvent (0.01% LiBr). The flow rate was 0.3 mL/min, with an injection volume of 40 uL. Chloroform-soluble polymers were analyzed on a Waters Alliance HPLC system (2690 separation module) equipped with Agilent, PLgel, 5 μm MiniMIX-D, 250 x 4.6 mm column, a Waters 2410 Differential Refractometer (RI) and Waters 2998 Photodiode Array Detector (PDA) using chloroform solvent (0.25% triethylamine). The flow rate was 0.35 mL/min, with an injection volume of 40 uL. Water-soluble polymers were analyzed on a Waters Alliance HPLC system (2695 separation module) equipped with Tosoh TSKgel G3000PWXL (7um) and TSKgel G5000PWXL (10um) columns, Wyatt DAWN HELEOS-II (laser 663.1 nm) detector, Wyatt Optilab rEX (RI) detector, and Waters 2996 Photodiode Array (PDA) detector. Mobile phase consisted of water with 10 mM NaH₂PO₄ and 1.5 mM NaN₃, with a flow rate of 1 mL/min and 100 uL injection. IR spectra were recorded on a Perkin Elmer 100 spectrometer and are reported in terms of absorption frequency (cm⁻¹). UV-Vis experiments were conducted on a HP-8453 spectrophotometer.

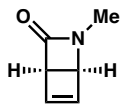
3.4.2 Preparation of ROMP Monomers

Representative scheme for photochemical valence isomerization of pyridines

*These procedures have not been optimized.

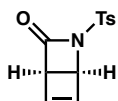


cis-2-azabicyclo[2.2.0]hex-5-en-3-one (88). Prepared according to literature.³⁸ A solution of 2-hydroxypyridine (.02M) in MeCN was degassed by freeze-pump-thaw (three cycles) in a flame-dried Schlenk flask. The flask was then sealed and irradiated using 300 nm light bulbs until the starting material was consumed (24–96 hours), as determined by TLC (8% MeOH in DCM). The solvent was then removed by rotary evaporation and purified by column chromatography (30% → 75% EtOAc in hexanes on SiO₂). Further purification was achieved by recrystallization from EtOAc/Hex to obtain a crystalline white solid. All NMR spectra matched the reported literature.



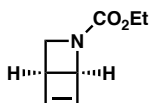
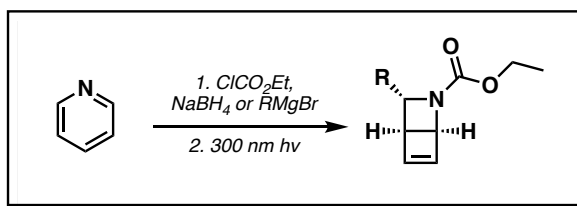
cis-2-methyl-2-azabicyclo[2.2.0]hex-5-en-3-one (22). Prepared according to literature.³⁹ A solution of N-Methyl-2-pyridone (.02M) in EtOAc was degassed by freeze-pump-thaw

(three cycles) in a flame-dried Schlenk flask. The flask was then sealed and irradiated using 300 nm light bulbs until the starting material was consumed (24–96 hours), as determined by TLC (6% MeOH in DCM). The solvent was then removed by rotary evaporation and purified by column chromatography (75% EtOAc in hexanes on SiO₂) to obtain a colorless oil. All NMR spectra matched the reported literature.



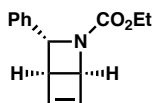
cis-2-tosyl-2-azabicyclo[2.2.0]hex-5-en-3-one (186). Prepared from Dewar pyridone **88** according to literature.^{38,40} All NMR spectra matched the reported literature.

Representative scheme for synthesis of Dewar dihydropyridines



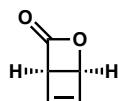
Ethyl-2-azabicyclo[2.2.0]hex-5-ene-2-carboxylate (194). Prepared according to literature.^{25,41} N-(ethoxycarbonyl)-1,2-dihydropyridine was prepared by the reaction of pyridine with ethyl chloroformate and sodium borohydride in methanol solvent according to the reported literature,⁴¹ and was carried forward after aqueous workup without

purification. A 1 g/L solution of the crude material was photolyzed in a flame-dried Schlenk flask in DCM (degassed by three freeze-pump-thaw cycles) until starting material was consumed (12–72 hours) by TLC (30% EtOAc in hexanes). The solvent was then removed by rotary evaporation and purified by column chromatography (25% EtOAc in hexanes on SiO₂) to obtain a colorless oil. All NMR spectra matched the reported literature.



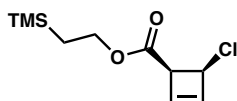
Ethyl-3-phenyl-2-azabicyclo[2.2.0]hex-5-ene-2-carboxylate (90). Prepared according to literature.^{26,41} N-(ethoxycarbonyl)-2-phenyl-1,2-dihydropyridine was prepared by the reaction of pyridine with ethyl chloroformate and PhMgBr in THF solvent according to the reported literature and was carried forward after aqueous workup without purification. A 1 g/L solution of the crude material was photolyzed in a flame-dried Schlenk flask in DCM (degassed by three freeze-pump-thaw cycles) until starting material was consumed (12–72 hours) by TLC (40% EtOAc in hexanes). The solvent was then removed by rotary evaporation and purified by column chromatography (30% → 65% EtOAc in hexanes on SiO₂) to obtain a yellow oil. All NMR spectra matched the reported literature.

Synthesis of pyrone-derived monomers:



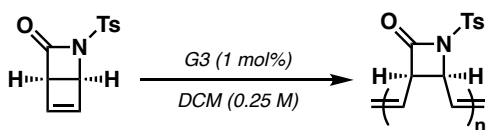
cis-2-oxabicyclo[2.2.0]hex-5-en-3-one (7). Prepared from 2-pyrone according to a modified procedure, using degassed DCM solvent instead of diethyl ether.⁴² Upon

completion of reaction (determined by NMR), the solution was concentration under vacuum and backfilled with nitrogen to maintain solution under inert atmosphere to achieve a concentration of 0.11M (as determined by NMR spectroscopy). This solution was used immediately in polymerization reaction, due to the molecule's instability. All NMR spectra matched the reported literature.



***trans*-2-(trimethylsilyl)ethyl-4-chlorocyclobut-2-ene-1-carboxylate (196).** Prepared from 2-pyrone according to literature.⁴³ All NMR spectra matched the reported literature.

3.4.3 Polymerization Reactions



Polymer 187. In a nitrogen glovebox, monomer **186** (50mg, 0.20 mmol) was added to a 4 mL dram vial equipped with a magnetic stir bar and dissolved in 0.8 mL dry DCM. Grubbs 3 catalyst (1.8 mg, 15.8 μmol , 1 mol %), dissolved in 40 μL DCM, was inject quickly into the solution containing monomer while vigorously stirring. The polymerization reaction was allowed to progress for 2 hours, by which time >95% conversion was reached as determined by ^1H NMR. The reaction was brought out of glovebox, and 0.1 mL ethyl vinyl ether was added to the reaction and allowed to stir for 30 minutes. Then, the reaction was

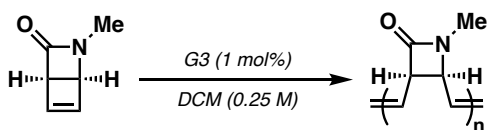
concentrated to half the original volume on the rotary evaporator, then precipitated with diethyl ether and dried under high vacuum to afford a 47.4 mg (95% yield) of polymer **187** as a light tan solid. For M_n and PDI vs. $[\mathbf{186}]_0/[\mathbf{G3}]_0$ experiments, where various loadings of Grubbs 3 catalyst are used to observe the effect on M_n and PDI of **187**, identical experimental procedures are followed (0.25M monomer in DCM, 2 hour reaction time, room temperature), but with varying G3 catalyst added as the only deviation from experimental procedure.

$^1\text{H NMR}$ (500 MHz, CDCl_3) δ 8.06–7.56 (br m, 2H), 7.50–7.10 (br m, 2H), 6.09–5.23 (br m, 2H), 5.21–3.67 (br m, 2H), 2.61–2.06 (br s, 3H).

$M_n = 19.1$ kDa.

$\mathcal{D} = 1.05$.

FT-IR (Neat Film NaCl) 1786 cm^{-1} (carbamate C=O), 1361 (sulfonamide S=O).



Polymer 191. In a nitrogen glovebox, monomer **22** (100 mg, 916 μmol) was added to a 4 mL dram vial equipped with a magnetic stir bar and dissolved in 3 mL dry DCM. Grubbs 3 catalyst (8.1mg, 9.1 μmol , 1 mol %), dissolved in 20 μL DCM, was injected quickly into solution containing monomer while vigorously stirring. The polymerization reaction was allowed to progress for 4 hours, by which time >95% conversion was reached as determined by $^1\text{H NMR}$. The reaction was brought out of glovebox, and 0.1 mL ethyl vinyl ether was added to the reaction and allowed to stir for 30 minutes. Then, the reaction was

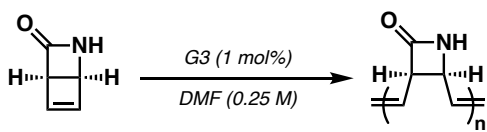
concentrated to half the original volume on the rotary evaporator, then precipitated with diethyl ether and dried under high vacuum to afford a 92 mg (92% yield) of polymer **191** as a light tan solid.

$^1\text{H NMR}$ (500 MHz, CDCl_3) δ 5.83–5.36 (br m, 2H), 4.70–3.82 (br m, 2H), 2.90–2.48 (br s, 3H).

$M_n = 23.3$ kDa.

$D = 1.12$.

FT-IR (Neat Film NaCl) 1732 cm^{-1} (β -lactam C=O stretch).



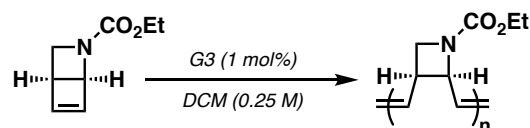
Polymer 89. In a flame-dried Schlenk flask, monomer **88** (300 mg, 3.15 mmol) was dissolved in 5 mL dry, degassed (*via* freeze-pump-thaw) DMF while under N_2 atmosphere. In a separate flame-dried Schlenk flask equipped with a magnetic stir bar, Grubbs 3 catalyst (14 mg, 15.8 μmol , 0.5 mol %) was dissolved in 8 mL dry, degassed (*via* freeze-pump-thaw) DMF under N_2 atmosphere. The solution of monomer was then rapidly injected into solution containing Grubbs catalyst and allowed to stir under N_2 atmosphere at room temperature. The polymerization reaction was allowed to progress for 3 hours, by which time >95% conversion was reached as determined by $^1\text{H NMR}$. The reaction was quenched by the addition of 0.3 mL ethyl vinyl ether and allowed to stir for 30 minutes. Then, the polymer was precipitated with diethyl ether, collected, and dried under high vacuum at 50 $^\circ\text{C}$ overnight to afford 242 mg (81% yield) of polymer **89** as an olive-tan solid.

$^1\text{H NMR}$ (500 MHz, d_6 -DMSO) δ 8.40–8.07 (br s, 1H), 5.80–5.37 (br m, 2H), 4.64–3.87 (br m, 2H).

$M_n = 29.9$ kDa.

$D = 1.87$.

FT-IR (Neat Film NaCl) 3229 (β -lactam N–H), 1725 cm^{-1} (β -lactam C=O).



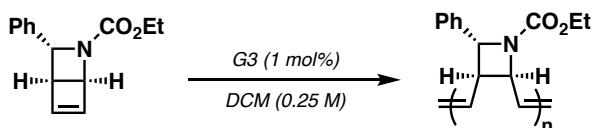
Polymer 195. In a nitrogen glovebox, monomer **194** (139 mg, 0.91 mmol) was added to an 8 mL dram vial equipped with a magnetic stir bar and dissolved in 3 mL dry DCM. Grubbs 3 catalyst (8.0 mg, 9.1 μmol , 0.5 mol %), dissolved in 40 μL DCM, was injected quickly into solution containing monomer while vigorously stirred. The polymerization reaction was allowed to progress for 4.5 hours, by which time >95% conversion was reached as determined by $^1\text{H NMR}$. The reaction was brought out of glovebox, and 0.1 mL ethyl vinyl ether was added to the reaction and allowed to stir for 30 minutes. Then, the reaction was concentrated to half the original volume on the rotary evaporator, then precipitated with diethyl ether, collected, and dried under high vacuum to afford a 127 mg (91% yield) of polymer **195** as a bronze-colored solid. For M_n and PDI vs. $[\mathbf{194}]_0/[\mathbf{G3}]_0$ experiments, where various loadings of Grubbs 3 catalyst are used to observe the effect on M_n and PDI of polymer **195**, identical experimental procedures are followed (0.25M monomer in DCM, 2 hour reaction time, room temperature), but with varying G3 catalyst added as the only deviation from experimental procedure.

$^1\text{H NMR}$ (500 MHz, CDCl_3) δ 5.90–5.39 (br m, 2H), 5.34–4.67 (br m, 2H), 4.24–3.95 (br m, 3H), 3.88–3.22 (br m, 2H), 1.32–1.12 (br m, 3H).

$M_n = 14.7$ kDa.

$D = 1.07$.

FT-IR (Neat Film NaCl) 1701 cm^{-1} (carbamate C=O).



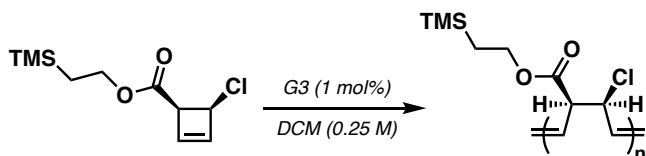
Polymer 91. In a nitrogen glovebox, monomer **90** (65 mg, 0.28 mmol) was added to a 4 mL dram vial equipped with a magnetic stir bar and dissolved in 1.1 mL dry DCM. Grubbs 3 catalyst (2.5 mg, 2.8 μmol , 1 mol %), dissolved in 40 μL DCM, was injected quickly into solution containing monomer while vigorously stirred. The polymerization reaction was allowed to progress for 4.5 hours, by which time >95% conversion was reached as determined by $^1\text{H NMR}$. The reaction was brought out of the glovebox, and 0.1 mL ethyl vinyl ether was added to the reaction and allowed to stir for 30 minutes. Then, the reaction was concentrated to half the original volume on the rotary evaporator, then precipitated with diethyl ether, collected, and dried under high vacuum to afford a 63 mg (97% yield) of polymer **91** as a bronze-colored solid.

$^1\text{H NMR}$ (500 MHz, CDCl_3) δ 7.58–6.43 (br m, 5H), 6.09–4.34 (br m, 4H), 4.30–3.00 (br m, 3H), 1.40–0.78 (br m, 3H), 1.32–1.12 (br m, 3H).

$M_n = 19.5$ kDa.

$D = 1.07$.

FT-IR (Neat Film NaCl) 1698 cm^{-1} (carbamate C=O).



Polymer 197. In a nitrogen glovebox, monomer **196** (6.0 mg, 26 μmol) was added to a 4 mL dram vial equipped with a magnetic stir bar and dissolved in 0.6 mL dry DCM. Grubbs 2 catalyst (1.3 mg, 1.5 μmol , 1 mol %), dissolved in 40 μL DCM, was injected quickly into solution containing monomer while vigorously stirred. The polymerization reaction was allowed to progress for 24 hours, by which time 65% conversion was reached as determined by ^1H NMR. The reaction was brought out of glovebox, and 0.1 mL ethyl vinyl ether was added to the reaction and allowed to stir for 30 minutes. Then, the reaction was concentrated to half the original volume on the rotary evaporator, then precipitated with cold methanol. The precipitate was then redissolved in 0.1 mL of ether, and reprecipitated with cold methanol, then dried under high vacuum to afford 4.2 mg (42% yield) of polymer **197**. The NMR and IR spectrum of this polymer are similar to those recently reported by the Bielawski lab.¹⁴

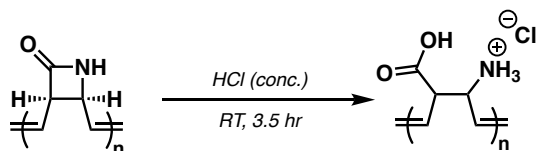
^1H NMR (500 MHz, CDCl_3) δ 6.06–5.50 (br m, 2H), 5.23–4.52 (br m, 1H), 4.36–4.00 (br m, 2H), 3.85–3.11 (br m, 1H), 1.13–0.84 (br m, 2H), 0.20–0.00 (br s, 9H).

M_n = 14.2 kDa.

D = 1.39.

FT-IR (Neat Film NaCl) 1732 cm^{-1} (ester C=O), 1250, 837 (Si–Me).

3.4.4 Post-Polymerization Modification Reactions



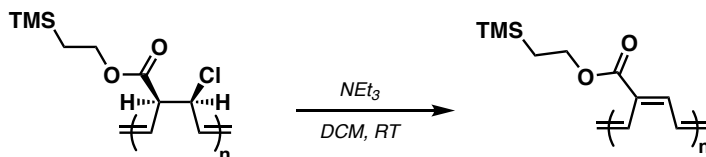
β -amino acid polymer 192. β -lactam polymer **87** (85 mg, 0.89 mmol) was suspended in 2 mL of concentrated HCl (12.1 M) in a dram vial equipped with a magnetic stir bar. The suspension was stirred at room temperature capped with a screw cap. The material went into solution slowly over time (around 30 minutes), but then slowly became cloudy after 2 more hours of stirring. After 3.5 hours, the solvent was removed by rotary evaporation and dried under high vacuum to give 118 mg (88% yield) of polymer **192** as pearl-tinted flakes.

$^1\text{H NMR}$ (500 MHz, D_2O) δ 5.90–5.39 (br m, 2H), 5.34–4.67 (br m, 2H), 4.24–3.95 (br m, 3H), 3.88–3.22 (br m, 2H), 1.32–1.12 (br m, 3H).

$M_n = 19.6$ kDa.

$D = 1.86$.

FT-IR (Neat Film NaCl) 2864 (N–H and O–H), 1709 cm^{-1} (acid C=O).



Poly(acetylene) polymer 198. In an oven-dried 4 mL dram vial equipped with an oven-dried stir bar with a rubber septum cap under N_2 atmosphere, β -chloroester polymer **197** (6.0 mg, 26 μmol) was dissolved in 0.6 mL of dry DCM . To this was added dropwise 20 μL of freshly distilled NEt_3 and allowed to stir at room temperature overnight (18 hours)

while under N₂. An immediate color change to dark red was observed. The solvent was then removed, and the excess triethylamine was removed on high vacuum. The polymer was then dissolved in ~0.1 mL DCM, and precipitated with methanol to obtain dark red flakes. This was repeated once more, then dried under high vacuum to afford 4.2 mg (83%) of dark burgundy flakes. Spectra are consistent with those reported on a similar polymer by Bielawski *et al.*¹⁴

¹H NMR (500 MHz, CDCl₃) δ 7.1–4.5 (br m, 2H), 4.45–4.00 (br m, 2H), 1.80–1.50 (br m, 1H), 1.18–0.91 (br m, 2H), 0.13–0.00 (br m, 9H).

***M*_n** = 12.8 kDa.

D = 1.57.

FT-IR (Neat Film NaCl) 1708 cm⁻¹ (ester C=O), 1250, 836 (Si–Me).

3.4.5 FT-IR and UV-Vis Data for Polymer 198

Figure 3.1. Carbonyl (C=O) stretch of polymers **197** and **198**. The shift in the C=O stretch is consistent with the formation of an α,β -unsaturated ester.

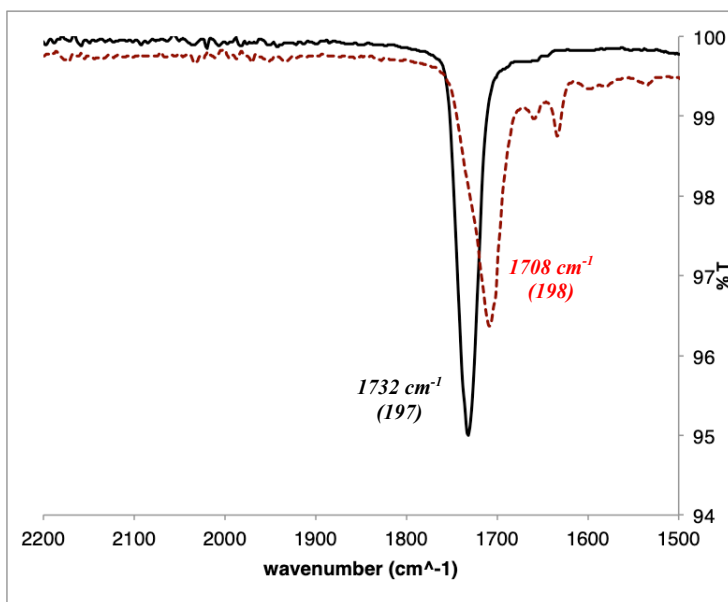
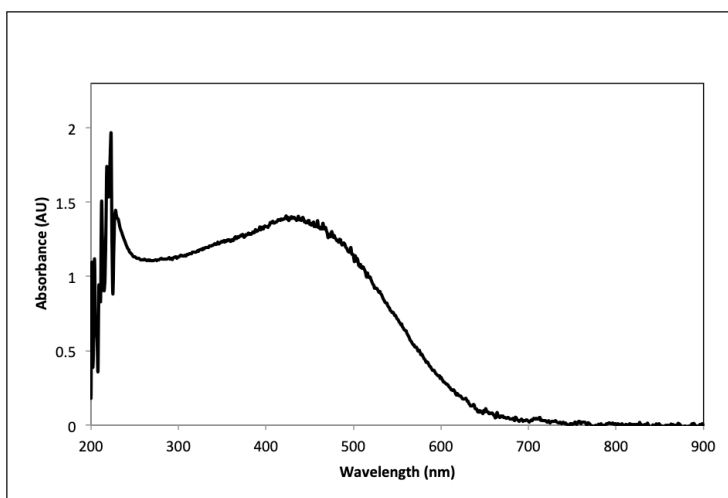
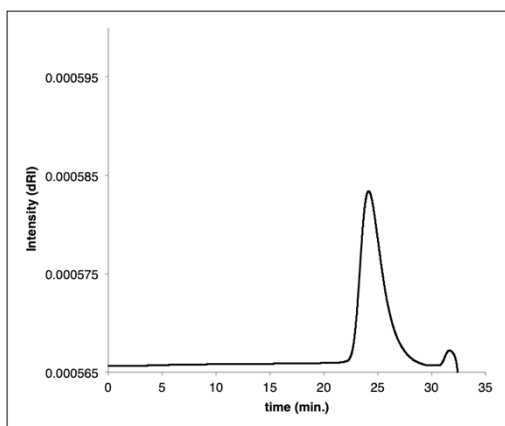


Figure 3.2. UV-Vis spectrum of polymer **198**.

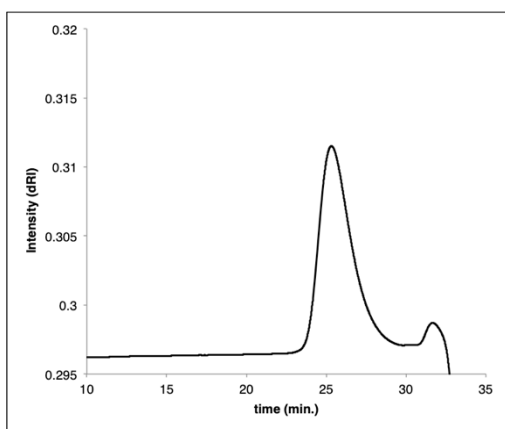


3.4.6 GPC Data for Determination of M_n and \bar{D}

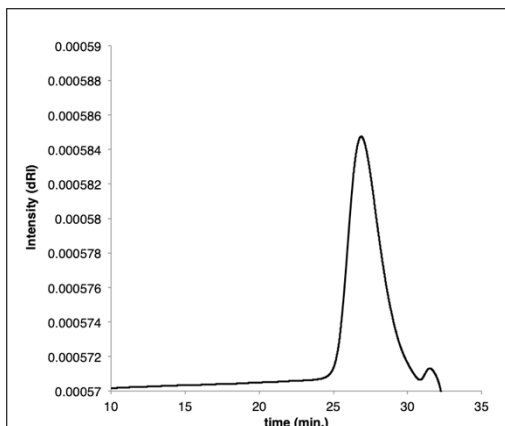
All THF-soluble polymers were analyzed by THF GPC. M_n was estimated through use of calibration curve derived from known molecular weight polystyrene standards.



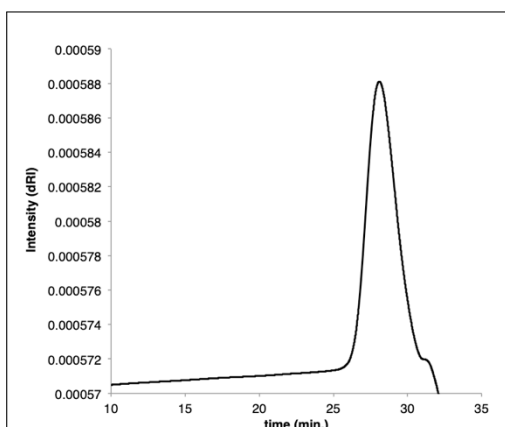
GPC trace 187 in THF with a $[186]_0/[G3]_0$ ratio of 200:1.



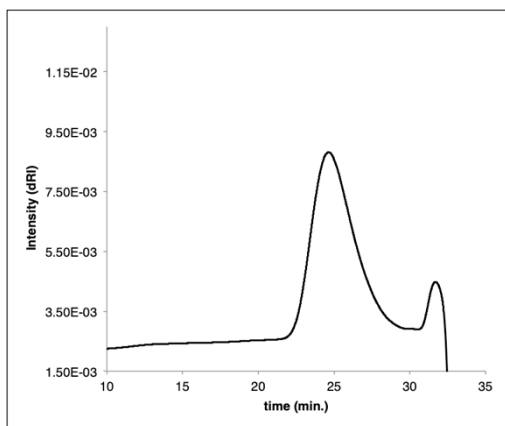
GPC trace of 187 in THF with a $[186]_0/[G3]_0$ ratio of 100:1.



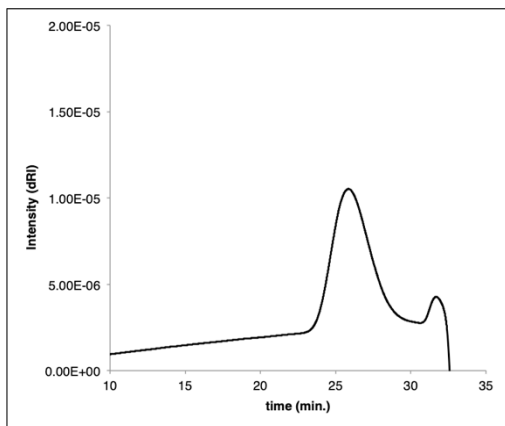
GPC trace of 187 in THF with a [186]₀/[G3]₀ ratio of 50:1.



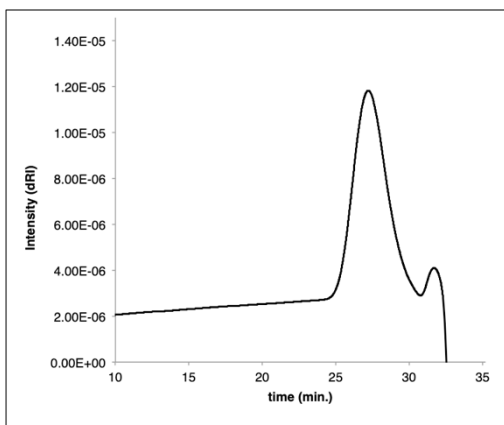
GPC trace of 187 in THF with a [186]₀/[G3]₀ ratio of 25:1.



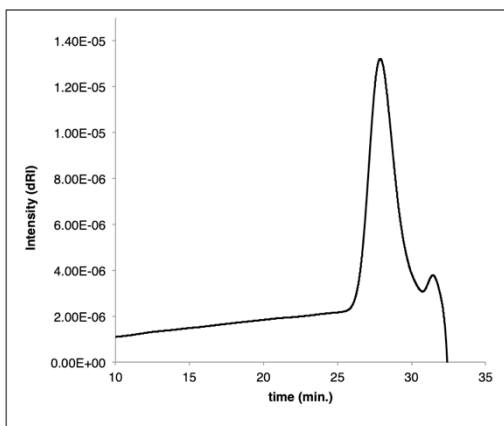
GPC trace of 195 in THF with a [194]₀/[G3]₀ ratio of 200:1.



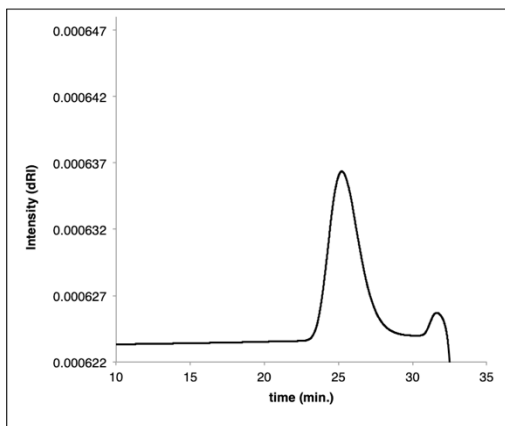
GPC trace of 195 in THF with a [194]₀/[G3]₀ ratio of 100:1.



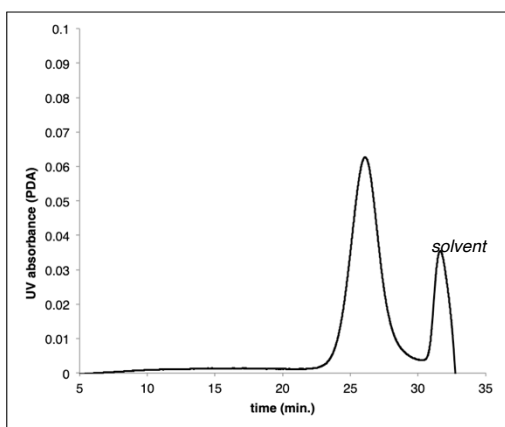
GPC trace of 195 in THF with a [194]₀/[G3]₀ ratio of 50:1.



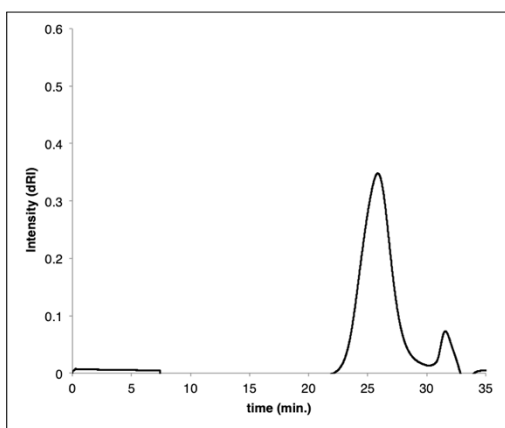
GPC trace of 195 in THF with a [194]₀/[G3]₀ ratio of 25:1.



GPC trace of 91 in THF with a [90]₀/[G3]₀ ratio of 100:1.

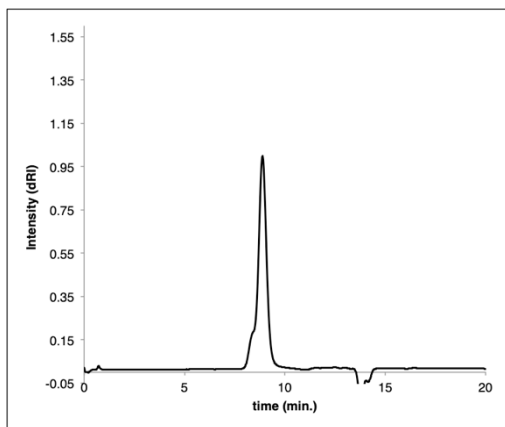


GPC trace of 197 in THF with a [196]₀/[G3]₀ ratio of 100:1.

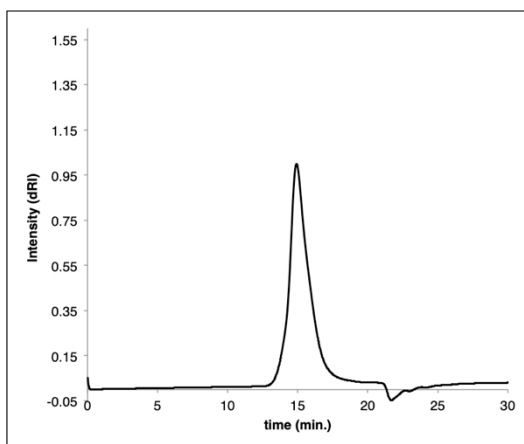


GPC trace of 198 in THF.

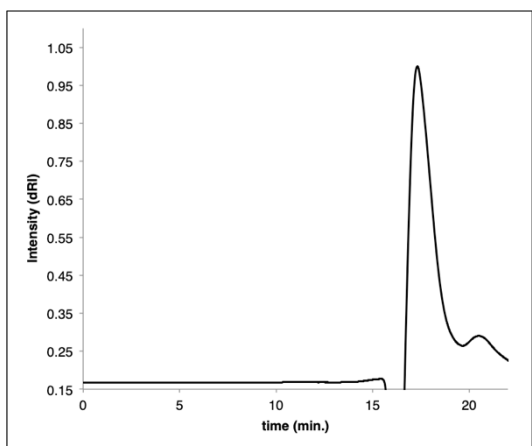
Other GPC traces: for polymers not soluble in THF.



GPC trace of 191 in CHCl₃ with a [22]₀/[G3]₀ ratio of 100:1.



GPC trace of 89 in DMF with a [87]₀/[G3]₀ ratio of 100:1.



Aqueous GPC trace of 192 in water with 10 mM NaH₂PO₄ + 1.5 mM NaN₃. M_n was determined using MALS detector.

*We thank the Materials Research Laboratory (MRL) at UC Santa Barbara for assistance with running GPC samples for polymers insoluble in THF (DMF, CHCl₃, and aqueous).

3.5 REFERENCES

- (1) Corey, E. J.; Streith, Jacques. Internal Photoaddition Reactions of 2-Pyrone and N-Methyl-2-Pyridone: A New Synthetic Approach to Cyclobutadiene. *J. Am. Chem. Soc.* **1964**, *86*, 950–951.
- (2) Wilzbach, K. E.; Rausch, D. J. Photochemistry of Nitrogen Heterocycles. Dewar Pyridine and Its Intermediacy in Photoreduction and Photohydration of Pyridine. *J. Am. Chem. Soc.* **1970**, *92*, 2178–2179.
- (3) Kobayashi, Y.; Kumadaki, I. Dewar Heterocycles and Related Compounds. In *Advances in Heterocyclic Chemistry*; Elsevier, 1982; Vol. 31, pp 169–206.
- (4) Nistanaki, S. K.; Boralsky, L. A.; Pan, R. D.; Nelson, H. M. A Concise Total Synthesis of (±)-Vibrallactone. *Angew. Chem. Int. Ed.* **2019**, *58*, 1724–1726.
- (5) Gutekunst, W. R.; Baran, P. S. Total Synthesis and Structural Revision of the Piperarborenines via Sequential Cyclobutane C–H Arylation. *J. Am. Chem. Soc.* **2011**, *133*, 19076–19079.
- (6) Souris, C.; Misale, A.; Chen, Y.; Luparia, M.; Maulide, N. From Stereodefined Cyclobutenes to Dienes: Total Syntheses of Ieodomycin D and the Southern Fragment of Macrolactin A. *Org. Lett.* **2015**, *17*, 4486–4489.
- (7) Souris, C.; Frébault, F.; Patel, A.; Audisio, D.; Houk, K. N.; Maulide, N. Stereoselective Synthesis of Dienyl-Carboxylate Building Blocks: Formal Synthesis of Inthomycin C. *Org. Lett.* **2013**, *15*, 3242–3245.
- (8) Chen, Y.; Coussanes, G.; Souris, C.; Aillard, P.; Kaldre, D.; Rungtatscher, K.; Kubicek, S.; Di Mauro, G.; Maryasin, B.; Maulide, N. A Domino 10-Step Total

- Synthesis of FR252921 and Its Analogues, Complex Macrocyclic Immunosuppressants. *J. Am. Chem. Soc.* **2019**, *141*, 13772–13777.
- (9) Zhu, R.; Swager, T. M. Polymer Valence Isomerism: Poly(Dewar- *o* -Xylylene)s. *J. Am. Chem. Soc.* **2018**, *140*, 5211–5216.
- (10) Seo, J.; Lee, S. Y.; Bielawski, C. W. Unveiling a Masked Polymer of Dewar Benzene Reveals *Trans* -Poly(Acetylene). *Macromolecules* **2019**, *52*, 2923–2931.
- (11) Lopyrev, V. A.; Myachina, G. F.; Shevalevskii, O. I.; Khidekel, M. L. Polyacetylene. Review. *Polym. Sci. USSR* **1988**, *30*, 2151–2173.
- (12) Swager, T. M.; Dougherty, D. A.; Grubbs, R. H. Strained Rings as a Source of Unsaturation: Polybenzvalene, a New Soluble Polyacetylene Precursor. *J. Am. Chem. Soc.* **1988**, *110*, 2973–2974.
- (13) Feast, W. J.; Tsibouklis, J.; Pouwer, K. L.; Groenendaal, L.; Meijer, E. W. Synthesis, Processing and Material Properties of Conjugated Polymers. *Polymer* **1996**, *37*, 5017–5047.
- (14) Seo, J.; Lee, S. Y.; Bielawski, C. W. Dewar Lactone as a Modular Platform to a New Class of Substituted Poly(Acetylene)s. *Polym. Chem.* **2019**, *10*, 6401–6412.
- (15) Graf, R.; Lohaus, G.; Börner, K.; Schmidt, E.; Bestian, H. β -Lactame, Polymerisation und Verwendung als Faserrohstoffe. *Angew. Chem.* **1962**, *74*, 523–530.
- (16) Zhang, J.; Gellman, S. H.; Stahl, S. S. Kinetics of Anionic Ring-Opening Polymerization of Variously Substituted β -Lactams: Homopolymerization and Copolymerization. *Macromolecules* **2010**, *43*, 5618–5626.
- (17) Hashimoto, K. Ring-Opening Polymerization of Lactams. Living Anionic Polymerization and Its Applications. *Prog. Polym. Sci.* **2000**, *25*, 1411–1462.

- (18) Eisenbach, C. D.; Lenz, R. W. Synthesis and Polymerization of Substituted β -Propiolactams. *Macromolecules* **1976**, *9*, 227–230.
- (19) Cheng, J.; Deming, T. J. Controlled Polymerization of β -Lactams Using Metal–Amido Complexes: Synthesis of Block Copoly(β -Peptides). *J. Am. Chem. Soc.* **2001**, *123*, 9457–9458.
- (20) Sudo, A.; Endo, T. A Novel Reactive Polymer Having 2-Azetidinone-Structure on the Main Chain: Development of Its Convenient Synthetic Method Based on [2 + 2]Cycloaddition of Bisketene with Bisimine. *Macromolecules* **1998**, *31*, 7996–7998.
- (21) Cheng, R. P.; Gellman, S. H.; DeGrado, W. F. β -Peptides: From Structure to Function. *Chem. Rev.* **2001**, *101*, 3219–3232.
- (22) Appella, D. H.; Christianson, L. A.; Klein, D. A.; Powell, D. R.; Huang, X.; Barchi, J. J.; Gellman, S. H. Residue-Based Control of Helix Shape in β -Peptide Oligomers. *Nature* **1997**, *387*, 381–384.
- (23) Gademann, K.; Ernst, M.; Hoyer, D.; Seebach, D. Synthesis and Biological Evaluation of a Cyclo--Tetrapeptide as a Somatostatin Analogue. *Angew. Chem. Int. Ed.* **1999**, *38*, 1223–1226.
- (24) Fowler, F. W. Synthesis of 1,2- and 1,4-Dihydropyridines. *J. Org. Chem.* **1972**, *37*, 1321–1323.
- (25) Beeken, P.; Bonfiglio, J. N.; Hasan, I.; Piwinski, J. J.; Weinstein, B.; Zollo, K. A.; Fowler, F. W. Synthesis and Study of N-Substituted 1,2-Dihydropyridines. *J. Am. Chem. Soc.* **1979**, *101*, 6677–6682.

- (26) Comins, D. L.; Abdullah, A. H. Regioselective Addition of Grignard Reagents to 1-Acylpyridinium Salts. A Convenient Method for the Synthesis of 4-Alkyl(Aryl)Pyridines. *J. Org. Chem.* **1982**, *47*, 4315–4319.
- (27) Fraenkel, G.; Cooper, J. W.; Fink, C. M. One-Step Synthesis of 2-Substituted N-Ethoxycarbonyl-1,2-Dihydropyridines. *Angew. Chem. Int. Ed. Engl.* **1970**, *9*, 523–523.
- (28) Gleede, T.; Reisman, L.; Rieger, E.; Mbarushimana, P. C.; Rugar, P. A.; Wurm, F. R. Aziridines and Azetidines: Building Blocks for Polyamines by Anionic and Cationic Ring-Opening Polymerization. *Polym. Chem.* **2019**, *10*, 3257–3283.
- (29) Deming, T. J.; Fournier, M. J.; Mason, T. L.; Tirrell, D. A. Structural Modification of a Periodic Polypeptide through Biosynthetic Replacement of Proline with Azetidine-2-Carboxylic Acid. *Macromolecules* **1996**, *29*, 1442–1444.
- (30) Sudo, A.; Iitaka, Y.; Endo, T. Selective Reduction of Main-Chain 2-Azetidinone Moieties into Azetidines for Polymer Modification. *J. Polym. Sci. Part Polym. Chem.* **2002**, *40*, 1912–1917.
- (31) Lee, J. J.; Pollock Iii, G. R.; Mitchell, D.; Kasuga, L.; Kraus, G. A. Upgrading Malic Acid to Bio-Based Benzoates via a Diels–Alder-Initiated Sequence with the Methyl Coumalate Platform. *RSC Adv* **2014**, *4*, 45657–45664.
- (32) Zelle, R. M.; De Hulster, E.; Van Winden, W. A.; De Waard, P.; Dijkema, C.; Winkler, A. A.; Geertman, J.-M. A.; Van Dijken, J. P.; Pronk, J. T.; Van Maris, A. J. A. Malic Acid Production by *Saccharomyces Cerevisiae*: Engineering of Pyruvate Carboxylation, Oxaloacetate Reduction, and Malate Export. *Appl. Environ. Microbiol.* **2008**, *74*, 2766–2777.

- (33) Gorman, C. B.; Ginsburg, E. J.; Grubbs, R. H. Soluble, Highly Conjugated Derivatives of Polyacetylene from the Ring-Opening Metathesis Polymerization of Monosubstituted Cyclooctatetraenes: Synthesis and the Relationship between Polymer Structure and Physical Properties. *J. Am. Chem. Soc.* **1993**, *115*, 1397–1409.
- (34) Masuda, T. Substituted Polyacetylenes. *J. Polym. Sci. Part Polym. Chem.* **2007**, *45*, 165–180.
- (35) Lam, J. W. Y.; Tang, B. Z. Functional Polyacetylenes. *Acc. Chem. Res.* **2005**, *38*, 745–754.
- (36) Hong, M.; Chen, E. Y.-X. Chemically Recyclable Polymers: A Circular Economy Approach to Sustainability. *Green Chem.* **2017**, *19*, 3692–3706.
- (37) Love, J. A.; Morgan, J. P.; Trnka, T. M.; Grubbs, R. H. A Practical and Highly Active Ruthenium-Based Catalyst That Effects the Cross Metathesis of Acrylonitrile. *Angew. Chem. Int. Ed.* **2002**, *41*, 4035–4037.
- (38) Gauvry, N.; Huet, F. A Short Stereoselective Preparation of Dienamides from Cyclobutene Compounds. Application in the Synthesis of a New Cyclohexene Nucleoside. *J. Org. Chem.* **2001**, *66*, 583–588.
- (39) Matsushima, R.; Terada, K. Photoreactions of Alkylated 2-Pyridones. *J. Chem. Soc. Perkin Trans. 2* **1985**, No. 9, 1445.
- (40) Aït Youcef, R.; Boucheron, C.; Guillarme, S.; Legoupy, S.; Dubreuil, D.; Huet, F. Stereoselective Synthesis of Dienic Nitrogen Compounds. *Synthesis* **2006**, *2006*, 633–636.
- (41) Krow, G. R.; Lee, Y. B.; Lester, W. S.; Liu, N.; Yuan, J.; Duo, J.; Herzon, S. B.; Nguyen, Y.; Zacharias, D. 2-Azabicyclo[2.1.1]Hexanes. 2. Substituent Effects on the

Bromine-Mediated Rearrangement of 2-Azabicyclo[2.2.0]Hex-5-Enes. *J. Org. Chem.* **2001**, *66*, 1805–1810.

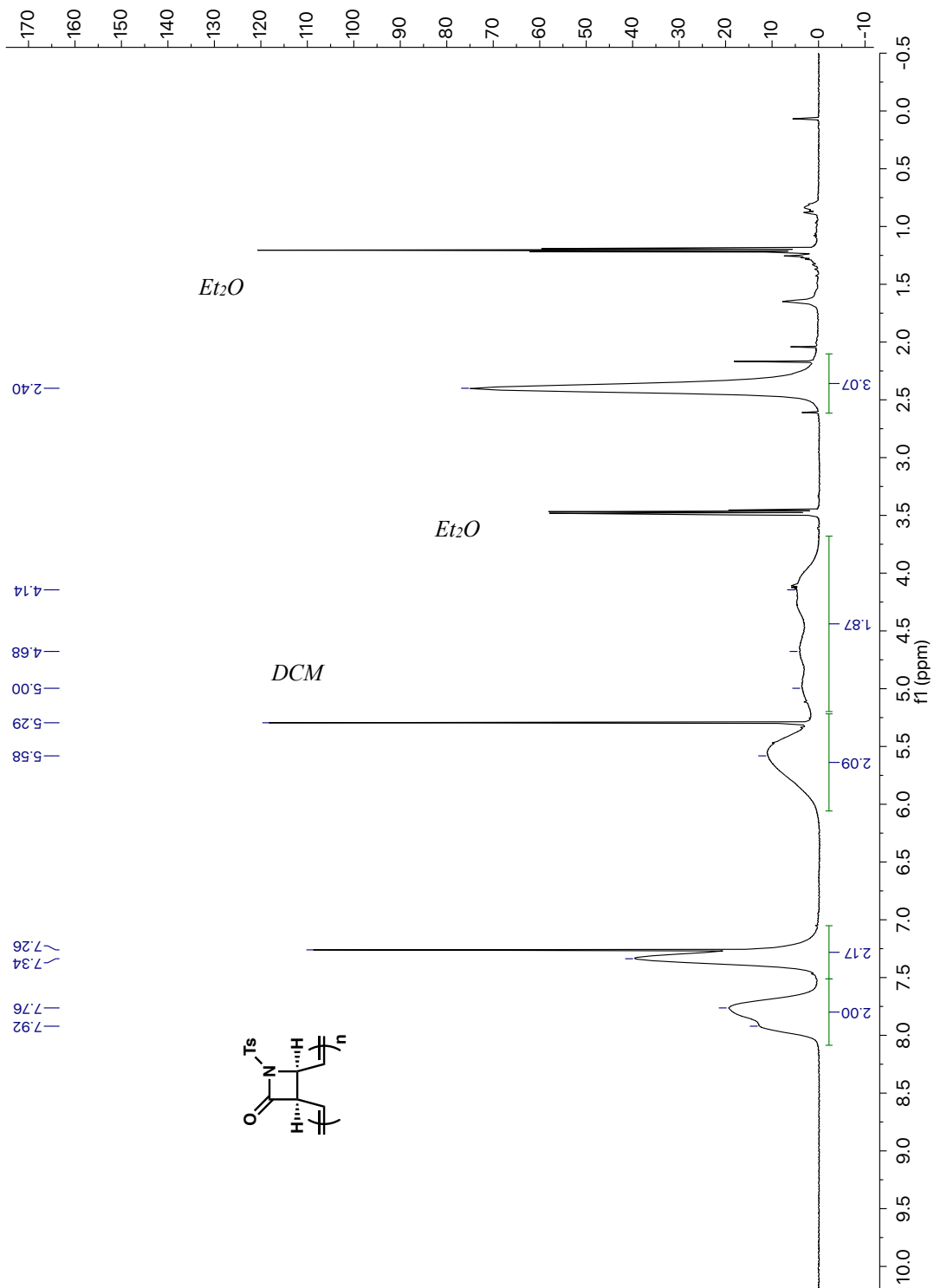
(42) Bauer, A.; Nam, J.-H.; Maulide, N. A Short, Efficient, and Stereoselective Synthesis of Piperine and Its Analogues. *Synlett* **2019**, *30*, 413–416.

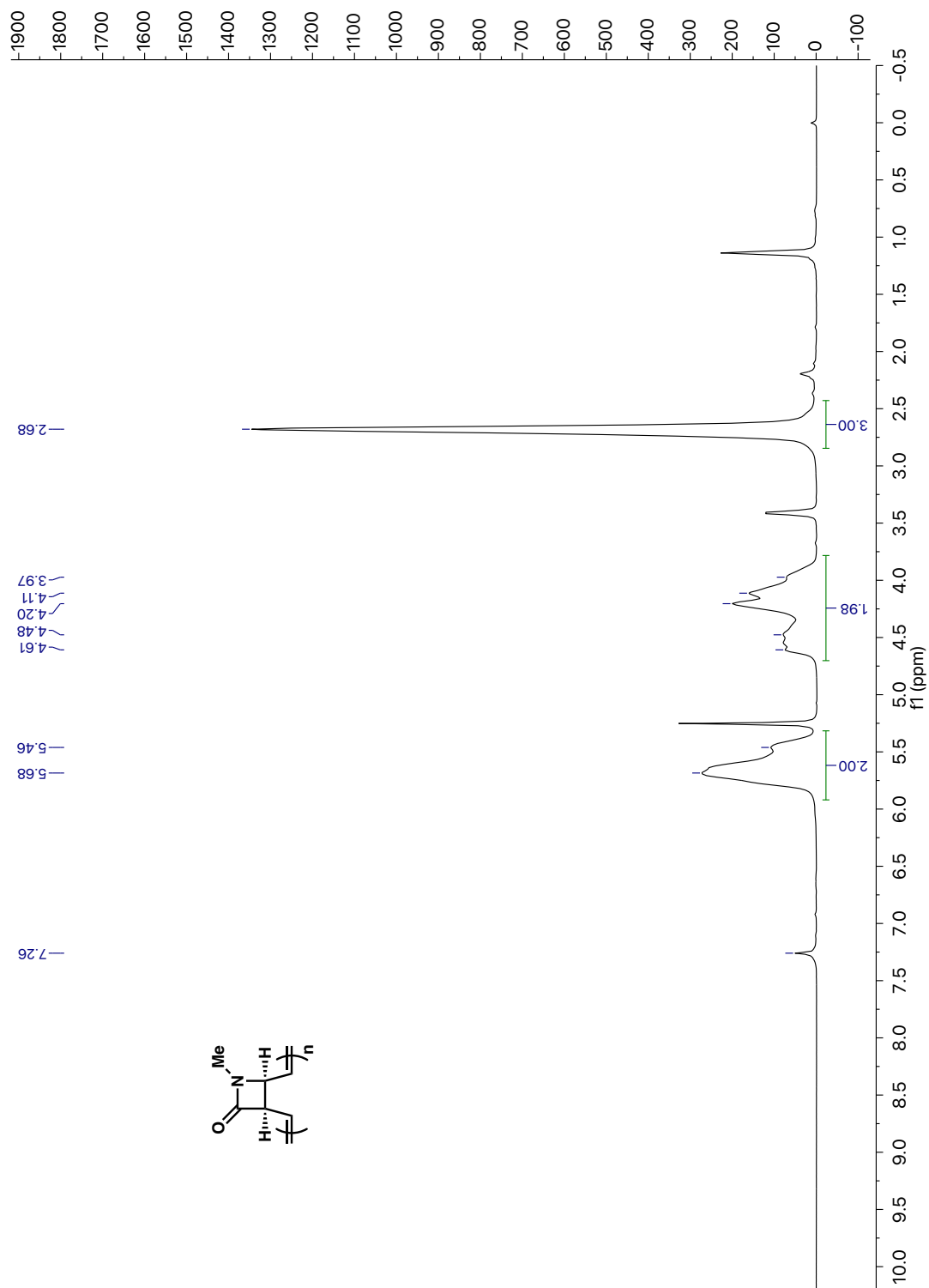
(43) Audisio, D.; Luparia, M.; Oliveira, M. T.; Klütt, D.; Maulide, N. Diastereodivergent De-Epimerization in Catalytic Asymmetric Allylic Alkylation. *Angew. Chem. Int. Ed.* **2012**, *51*, 7314–7317.

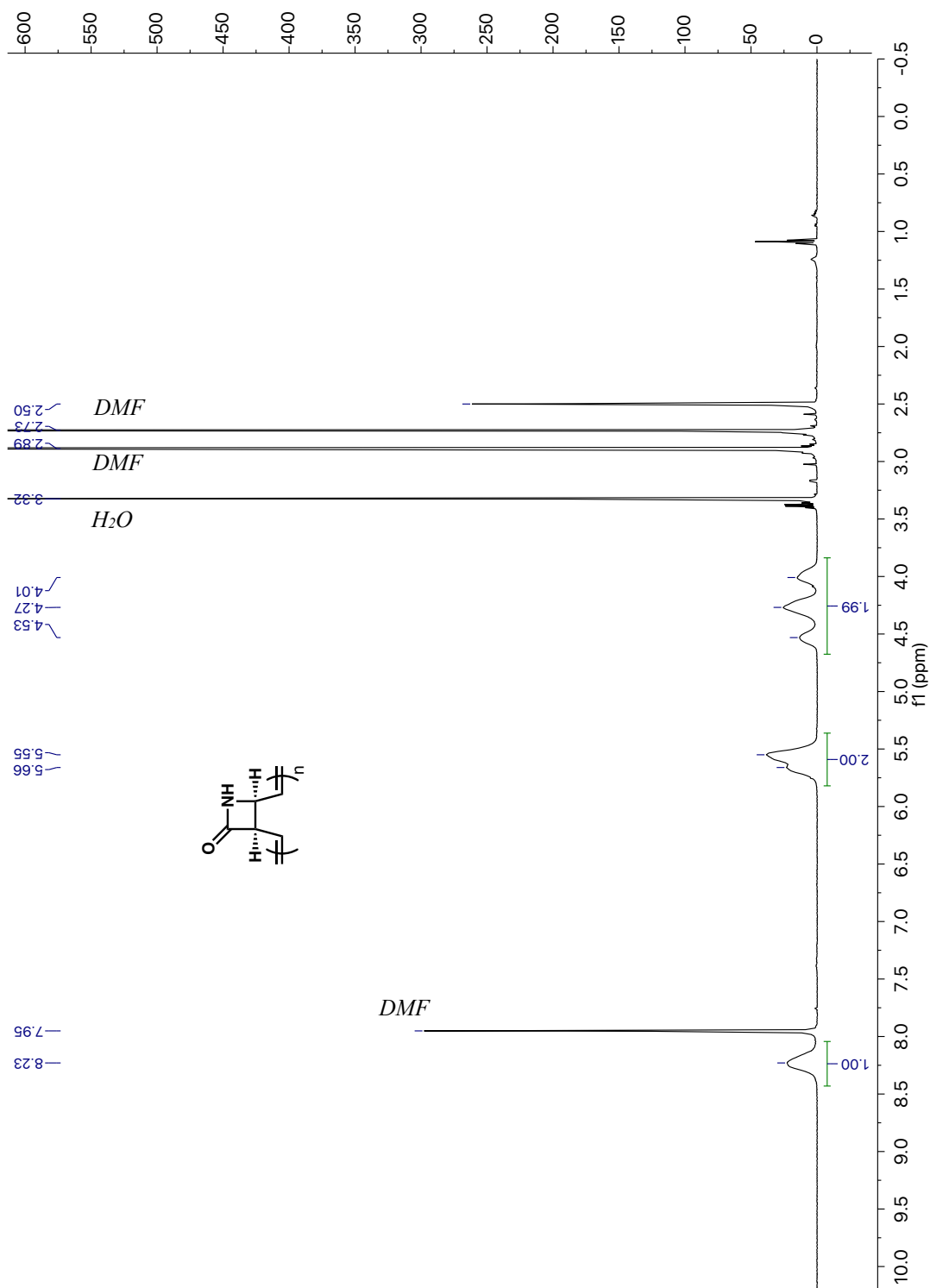
Appendix 3

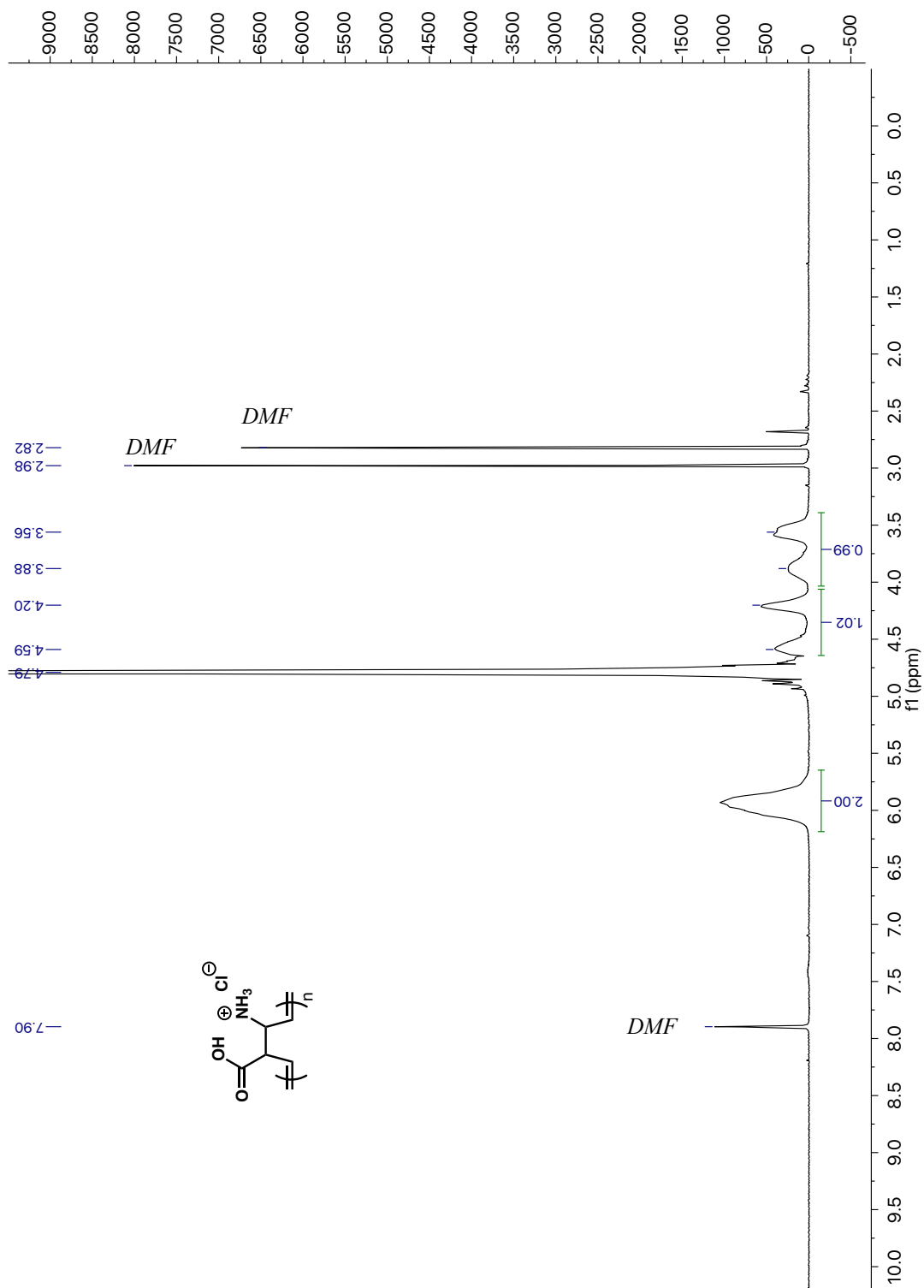
NMR Spectra Relevant to Chapter 3: Dewar Heterocycles as Versatile

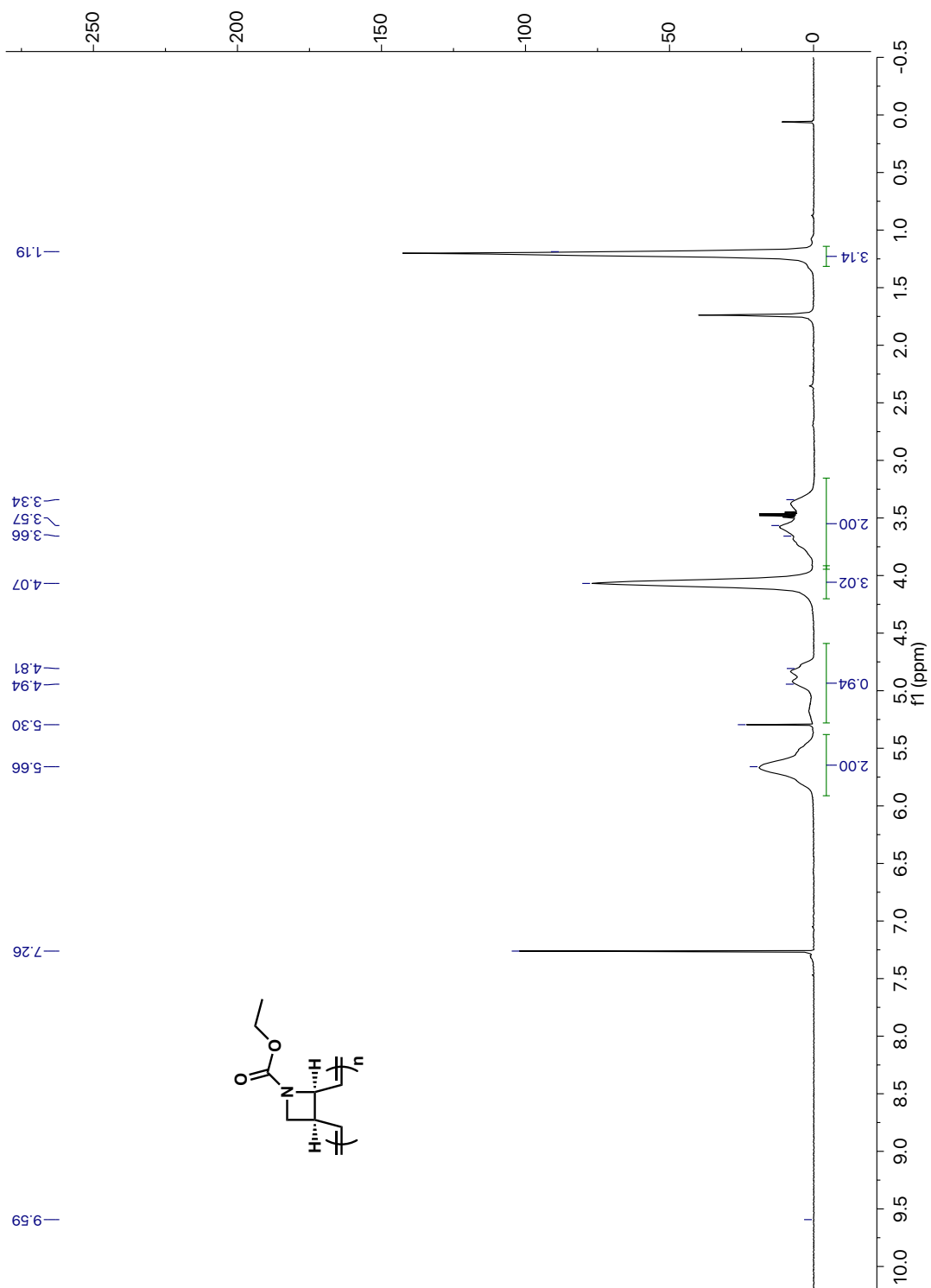
Monomers for Ring-Opening Metathesis

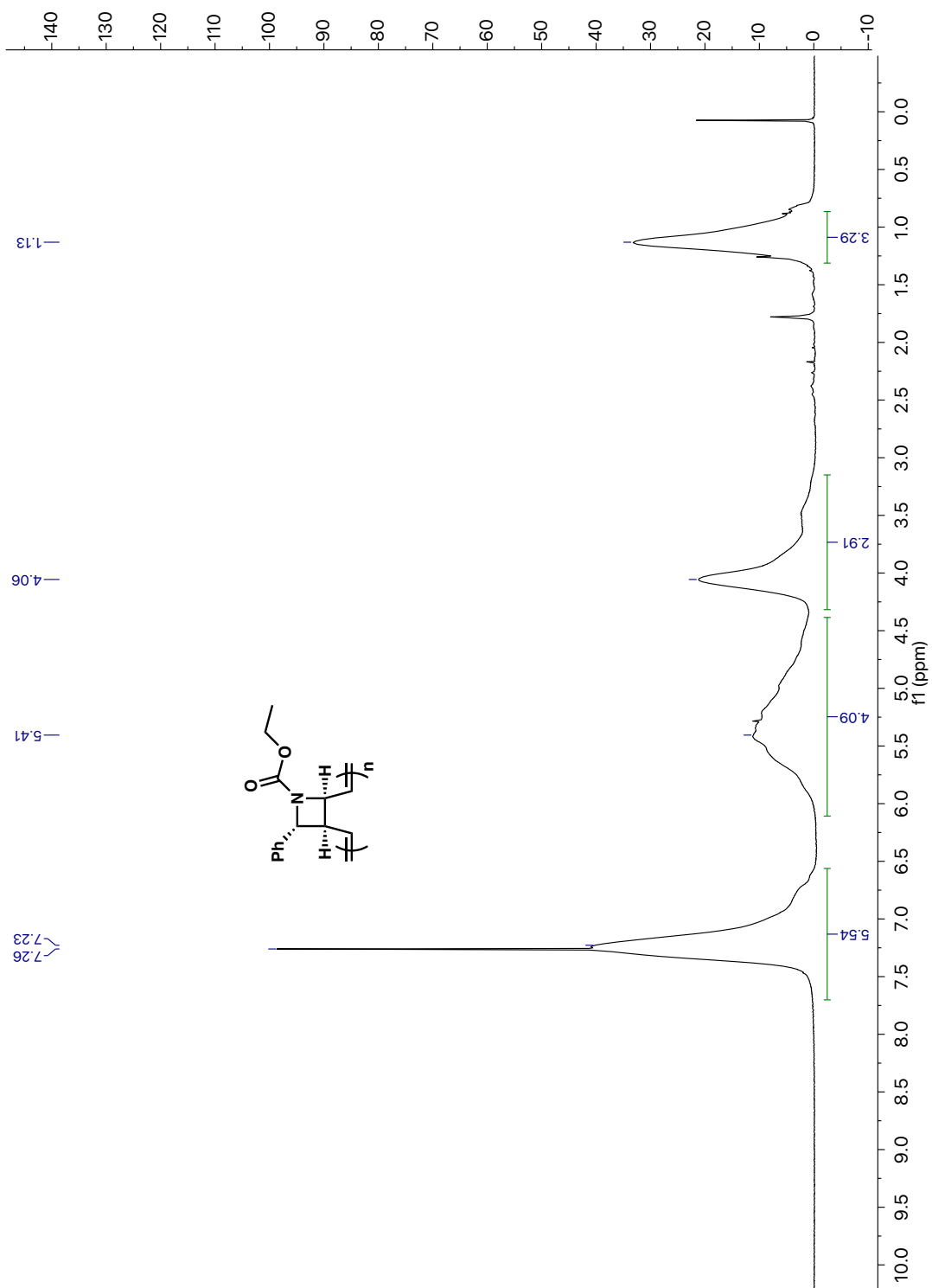












Chapter 4

*Catalytic Asymmetric C–H Insertion Reactions of Vinyl Carbocations*¹

4.1 INTRODUCTION

4.1.1 Carbocations in Asymmetric Catalysis

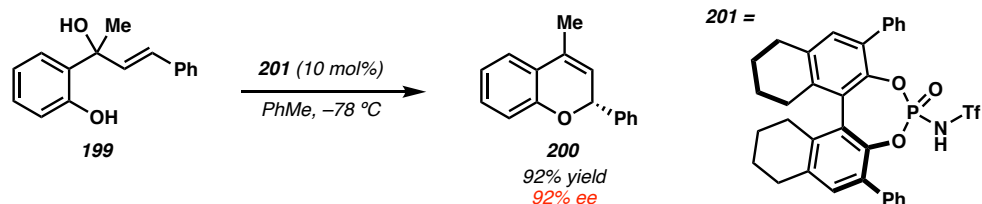
Carbocations are ubiquitous in organic chemistry, invoked in many important chemical processes and as intermediates in biosynthesis.^{1–4} However, controlling these high-energy intermediates in catalytic reactions has proven challenging, especially in the context of asymmetric catalysis, wherein a prochiral reactive intermediate must proceed through energetically differentiated diastereomeric transition states to obtain synthetically useful enantiomeric excesses. This is a difficult task for reactive intermediates, as

¹ Portions of this chapter have been adapted from Nistanaki, S. K.; Williams, C. G.; Wigman, B.; Wong, J. J.; Haas, B. C.; Popov, S.; Werth, J.; Sigman, M. S.; Houk, K. N.; Nelson, H. M. *Science* **2022**, 378, 1085–1091. © American Association for the Advancement of Science.

productive bond-formation can proceed *via* relatively low energetic barrier. Moreover, the propensity for such intermediates to engage in unproductive side reactions such as E1 elimination, rearrangement, and S_N1 substitution with other potential nucleophiles further complicates the development of selective reactions. This fundamental challenge is manifested in modern carbocation chemistry, where high levels of selectivity are routinely realized in the reactions of heteroatom-stabilized carbocations such as iminium and oxocarbenium ions.^{5–7} Selective catalytic reactions of non-stabilized carbocations are limited, with most reported examples involving significant stabilization through π -resonance.

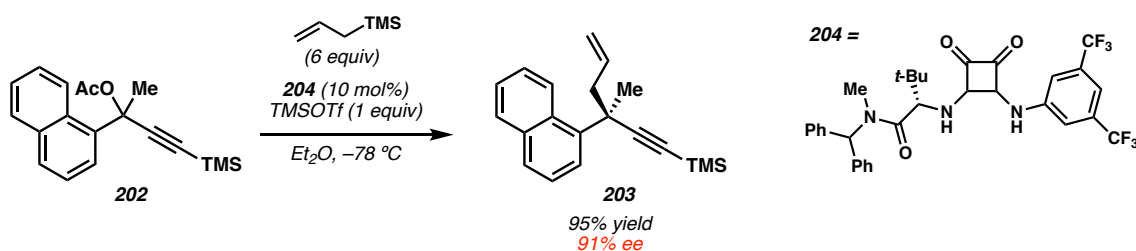
Early reports involved reactions of symmetric dibenzylic carbocations with chiral enamine intermediates, though these systems do not produce stereocenters at the carbocationic center.^{8–10} In 2011, Reuping reported the intramolecular cyclization reaction of allyl alcohol **199** catalyzed by chiral Brønsted acid **201** (Scheme 4.1).¹¹ Some mechanistic evidence is provided to support the intermediacy of an allyl cation intermediate, though such an intermediate possesses significant charge delocalization across an extensive heteroatom-containing π -system. Similar reactions invoking allyl cations have also been reported by Gong and Cozzi.^{12,13}

Scheme 4.1. Reuping's report of enantioselective allyl cation cyclization

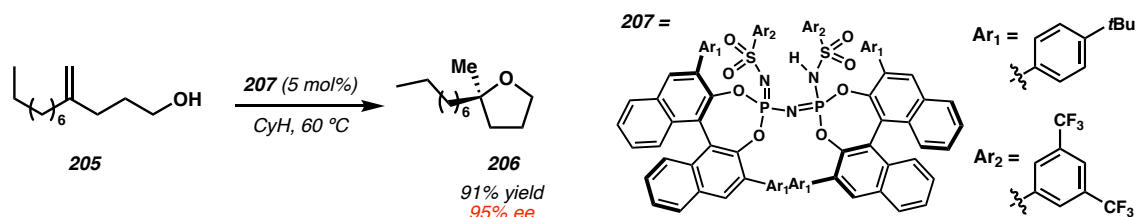


Jacobsen *et al.* reported the asymmetric reactions of tertiary carbocations with allyl silanes through the use of chiral hydrogen bond-donor catalysts (**204**) and stoichiometric TMS–OTf Lewis acids (Scheme 4.2).¹⁴ This system provides a means to construct enantioenriched all-carbon quaternary centers, and mechanistic experiments support the intermediacy of a carbocation intermediate. Notably, an early report by Braun highlights a similar enantioconvergent allylation reaction through use of chiral titanium catalysts, though no mechanistic support for a carbocation intermediate is provided in this report.¹⁵

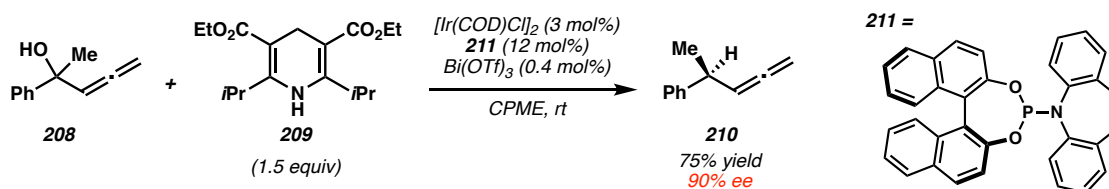
Scheme 4.2. Jacobsen's enantioselective allylation of a tertiary carbocation



List *et al.* have developed chiral strong acid catalysts comprised of an imidodiphosphorimidate (IDPi) acidic residue (**207**), which they have applied to enantioselective carbocation chemistry.¹⁶ In an early example, they reported the catalytic activation of olefins (**205**), which is proposed to undergo intramolecular cyclization *via* olefin protonation to deliver enantioenriched oxacycles (**206**) (Scheme 4.3).¹⁷ Their experimental and computational experiments support a concerted asynchronous process, wherein a carbocation-like transition state is intercepted by a pendant alcohol. Other related examples of carbocations not stabilized through π -resonance have been reported for this class of catalysts, including the non-classical norbornyl cation.¹⁸

Scheme 4.3. List's strong acid catalyzed olefin activation

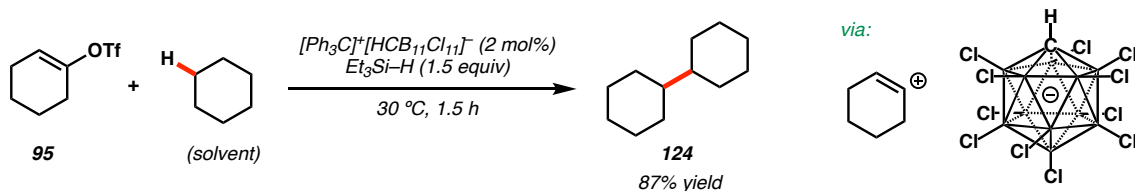
Carreira *et al.* reported an interesting strategy for inducing enantioselectivity on carbocation intermediates through coordination to chiral transition metal complexes. Specifically, they have shown that allenyl alcohols (**208**) can be engaged in S_N1-type reactions in the presence of catalytic Lewis acid and chiral iridium complexes (Scheme 4.4).^{19,20} Mechanistic studies support significant charge localization at the benzylic position, consistent with a tertiary carbocation intermediate. High enantioselectivities are achieved in trapping with Hantzsch ester derivatives (**209**) and organozinc nucleophiles.

Scheme 4.4. Carreira's coordination-induced enantioselective S_N1-type reactions**4.1.2 C–H Insertion Reactions of Vinyl Carbocations**

Unlike tricoordinated carbocations, dicoordinated carbocations, such as aryl and vinyl cations, have thus far been excluded from the field of asymmetric catalysis. This is likely due to the lack of catalytic methods for their generation and their high reactivity once

formed. Recent reports from our group and others highlight the ability of these intermediates to undergo insertion into unactivated sp^3 C–H bonds (Scheme 4.5).^{21–28} This is a fundamentally unique reactivity profile associated with this class of carbocations, and permits an untraditional approach towards C(sp^3)–H functionalization chemistry. In efforts to expand the synthetic utility of these C–H insertion reactions, we became interested in investigating the application of vinyl carbocations in asymmetric catalysis.

Scheme 4.5. Catalytic vinyl cation C–H insertion



Chiral catalysts necessary for such a reaction must be capable of generating a high energy carbocation while subsequently relaying stereochemical information to the reacting species through some means of highly-ordered interaction without directly trapping it. However, most catalytic C–H insertion reactions of dicoordinated carbocations have required the use of weakly coordinating anions (WCAs). These anions are notable in their weak basicity and nucleophilicity, which avoids deleterious E1 or S_N1 reactions.²⁹ However, the few chiral WCAs reported have not been successfully employed in asymmetric catalysis.^{30,31} As the name suggests, WCAs are characterized by their minimized coordinative interaction with cations. Moreover, previous studies on the C–H insertion reactions of dicoordinated cations have demonstrated very low energetic barriers for C–H insertion (in some cases computed to undergo almost barrierless insertion into

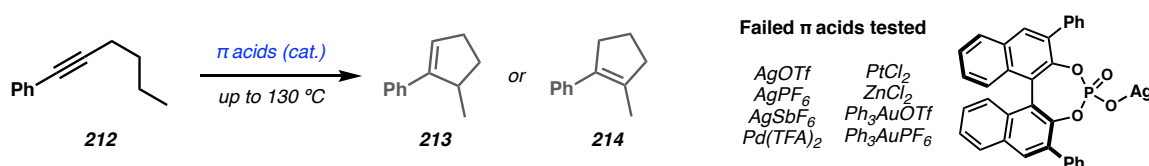
alkane C–H bonds^{23,25,26}), highlighting a fundamental energetic challenge associated with discriminating between diastereomeric transition states in an energetically facile process.

4.2 REACTION DEVELOPMENT

4.2.1 Catalyst Discovery

Given the challenges mentioned above, we spent considerable effort exploring chiral compounds that could catalyze the formation of a vinyl carbocation. Initial efforts to activate alkynes like **212** with π acids in a cycloisomerization reaction seemed promising given reports of such reactions in achiral systems (Scheme 4.6) and the potential to impart enantioselectivity through employment of chiral ligands.³² However, most tested π -acids were unsuccessful. Interestingly Ag^+ salts comprised of a weakly coordinating carborane ($\text{HCB}_{11}\text{Cl}_{11}$) counter anion did show low yields (<20%) of cyclized product **214**, though this was poorly reproducible and the addition of chiral ligands shut off this reactivity.

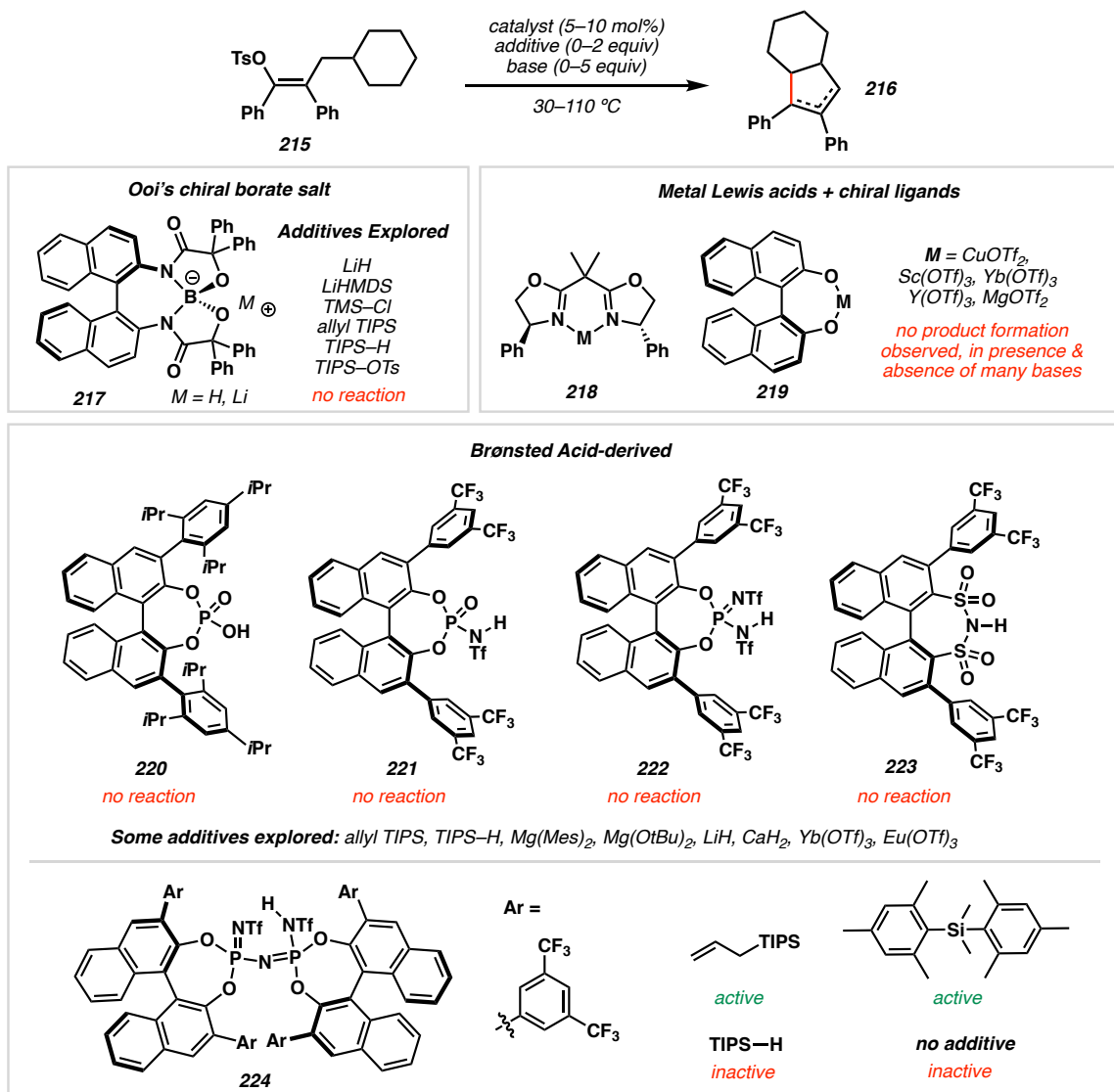
Scheme 4.6. Failed attempts at π -acid catalyzed cycloisomerization



We quickly shifted our focus to Lewis acid-mediated ionization of vinyl sulfonates per our previous studies.^{25,26} Exhaustive screening of a diverse range of chiral acids to screen for signs of catalysis or enantioinduction was undertaken. Scheme 4.7 highlights selected classes of compounds that were studied in the context of vinyl tosylate substrates

like **215**, including ligated metal-based Lewis acids (**218,219**) and organic acids (**217, 220–224**) While most tested additives yielded no signs of catalysis, we ultimately found that List's IDPi acid (**224**) are competent catalysts for these reactions in the presence of silanes, and demonstrated encouraging levels of enantioselectivity in initial experiments.^{16,33} We were also encouraged by reports by List utilizing these catalysts for highly enantioselective transformations of non-stabilized carbocation intermediates.^{17,18}

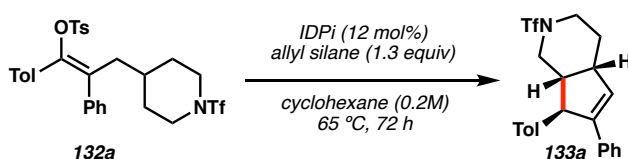
Scheme 4.7. Selected example of conditions tested for vinyl tosylate ionization



4.2.2 Reaction Optimization

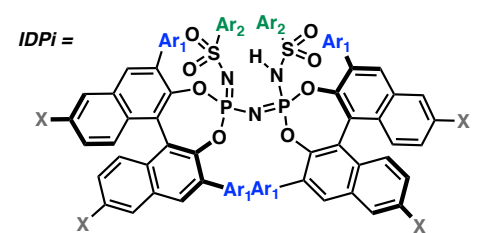
Our investigations focused on the desymmetrization of a piperidiny fragment *via* C–H insertion to generate bicyclic structures given the prevalence of nitrogen-containing polycyclic scaffolds in natural products.³⁴ Following extensive exploration of almost 50 IDPi variants, we found that IDPi **134** gave high enantioselectivity in the transformation of vinyl tosylate **132a** to **133b** (Table 4.1). This reaction forges three contiguous stereocenters with high diastereoselectivity, but incomplete conversion after 72 hours. In attempts to increase conversion, we explored different allyl silanes, given that the silylated IDPi is likely the active catalyst relevant to the presumed rate-limiting ionization. We were inspired by Lambert’s studies on the effects of steric bulk on silylium ion coordination, wherein $\text{Si}(\text{TMS})_3^+$ generated a near trivalent silylium cation, in contrast to trialkyl silylium cations which form tetravalent Si-centers by coordination to solvent or counter anion.³⁵ In our system we observed a positive correlation between silane size and activity, wherein bulky allyl $\text{Si}(\text{TES})_3$ (entry 4) resulted in full conversion and no influence on selectivity.

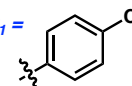
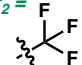
Table 4.1. Optimization of Silane and IDPi Catalyst



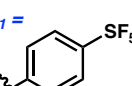
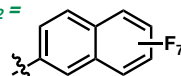
Entry	IDPi	Silane	Conv.	NMR Yield	%ee
1	225	allyl TIPS	70%	56%	52%
2	134	allyl TIPS	81%	72%	91%
3	134	allyl TMS	38%	34%	89%
4	134	allyl $\text{Si}(\text{TES})_3$	full	91%	91%
5	134	none	0%	0%	–

IDPi =



225 $\text{Ar}_1 =$  $\text{Ar}_2 =$ 

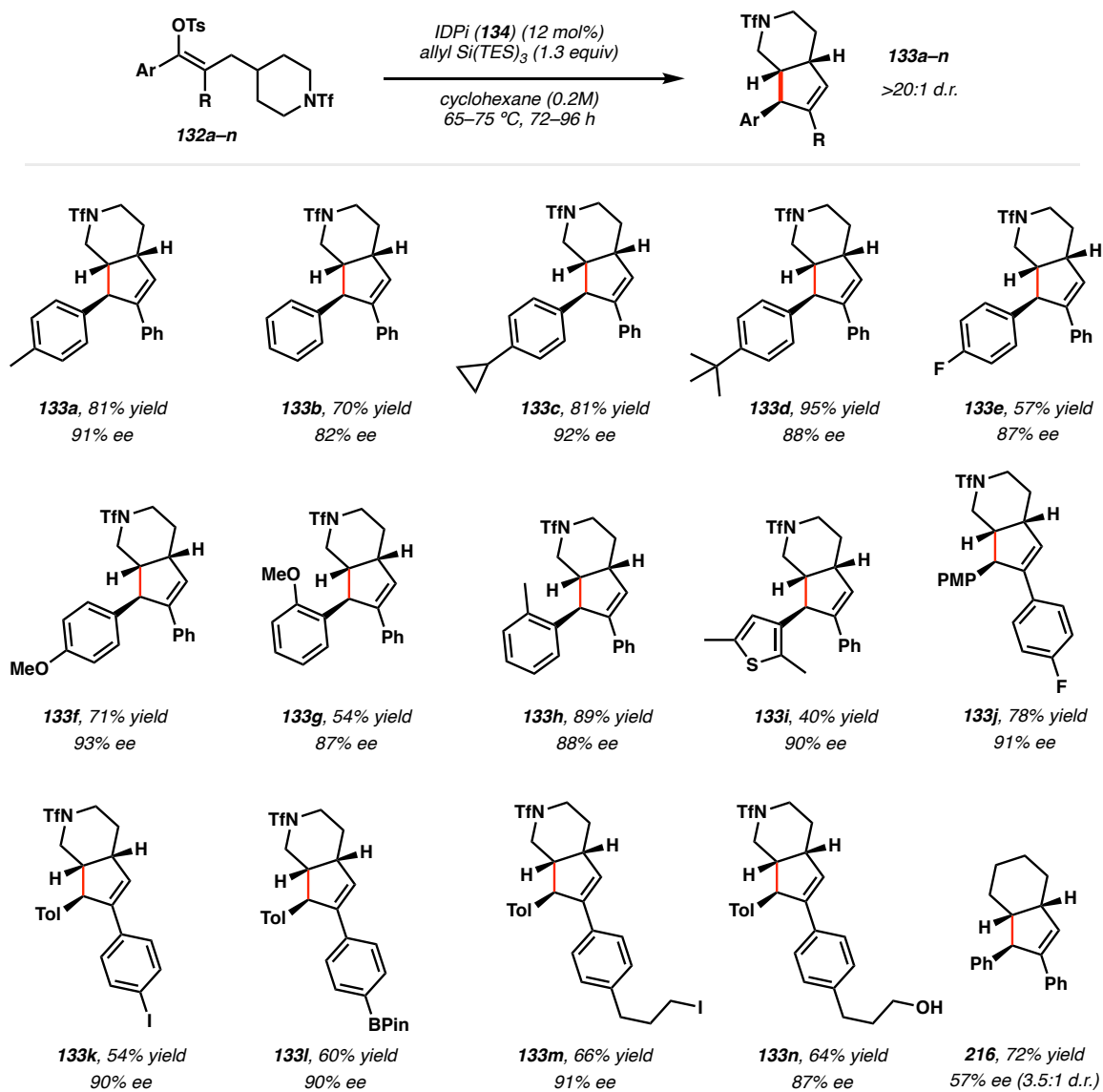
$\text{X} = \text{H}$

134 $\text{Ar}_1 =$  $\text{Ar}_2 =$ 

$\text{X} = \text{CF}_3$

4.2.3 Reaction Scope Studies

With this improved activity and encouraging enantioselectivity on our model substrate, we explored the scope of this reaction. The transformation proved compatible with substitution at both of the aryl rings on the substrate, delivering insertion products in moderate to good yield with excellent enantioselectivity (up to 93% *ee*) and diastereoselectivity (>20:1 *d.r.*). Select examples of the substrate scope studies are highlighted in Scheme 4.8. High levels of enantioselectivity were maintained with *ortho*-substitution near the insertion site (**133g** and **133h**), with electron-rich (**133f**), electron-deficient (**133e**, **133j**, and **133k**), and heterocyclic (**133i**) substrates also performing well. Moreover, functional groups labile in many transition metal-catalyzed processes such as alkyl iodides (**133m**), aryl iodides (**133k**), and boronic esters (**133l**) were compatible, highlighting this method's complementarity to transition metal-catalyzed C(*sp*³)–H functionalization platforms. Unprotected alcohols (**133n**) could be employed as substrates if an additional equivalent of silane is used, as rapid alcohol silylation precludes vinyl tosylate ionization. Upon completion of the reaction, addition of tetrabutylammonium fluoride (TBAF) desilylates the insertion product. The conversion of an all-hydrocarbon variant of the model substrate (**215**) to bicyclo[4.3.0]nonenes (**216**) occurred in modest stereoselectivity utilizing IDPi catalyst **225**. Notably, the enantiopurity of many of the piperidine insertion products could be readily upgraded *via* a single recrystallization to afford enantiopure material (>99% *ee*).

Scheme 4.8. Substrate scope studies of catalytic asymmetric C–H insertion

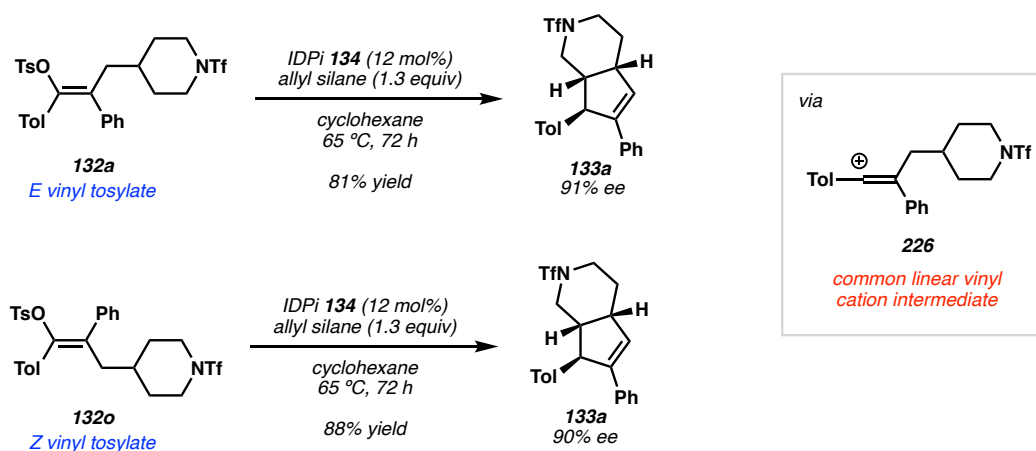
4.3 MECHANISTIC STUDIES

4.3.1 Evidence for Vinyl Carbocation Intermediate

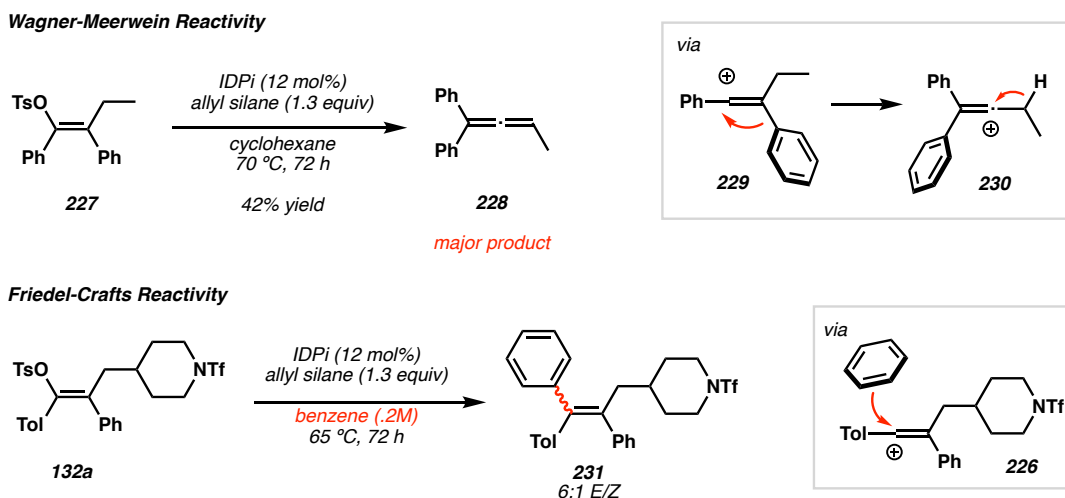
Although catalytic vinyl cation formation *via* sulfonate abstraction has been previously reported^{25,26}, we sought to further support its intermediacy in this system. To this end, we found that both the *Z*- and *E*- vinyl tosylate isomers (**132a** vs **132o**) afforded

the same insertion product with identical enantioselectivities, supporting the common intermediacy of a linear vinyl carbocation (**226**) in this reaction (Scheme 4.9).

Scheme 4.9. Influence of vinyl tosylate geometry on enantioselectivity



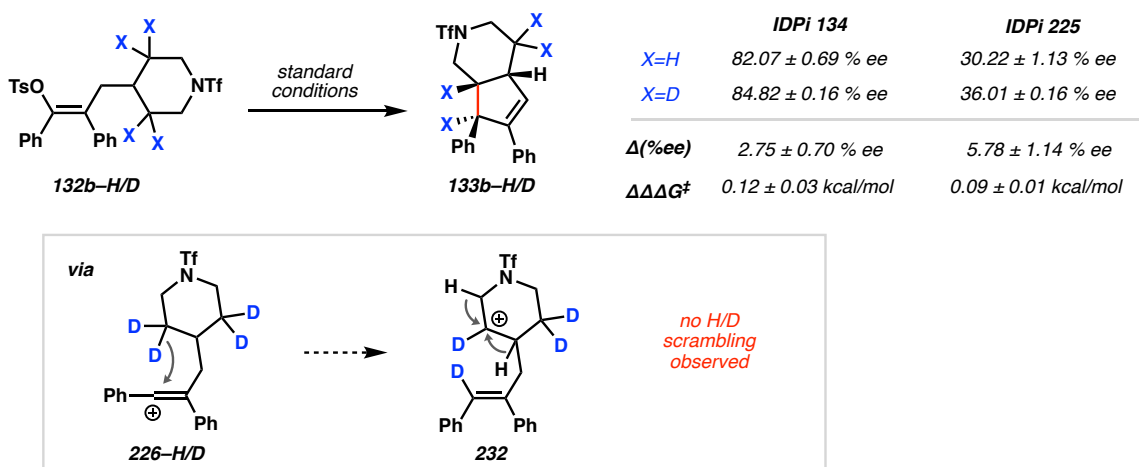
We also prepared tosylate **227** (which cannot undergo intramolecular C–H insertion) and found that allene **228** is produced as the major product under the reaction conditions, likely arising from a Wagner-Meerwein rearrangement of **229** – a known reactivity pathway of vinyl carbocations (Scheme 4.10).³⁶ Moreover, if the standard reaction is performed in benzene solvent instead of cyclohexane, we found that considerable amounts of the arylated product (**231**) is formed, consistent with the intermolecular Friedel-Crafts interception of a vinyl carbocation intermediate (**226**), which is apparently capable of competing with intramolecular C–H insertion.

Scheme 4.10. Side reactions consistent with vinyl cation intermediate**4.3.2 Origin of Stereoselectivity**

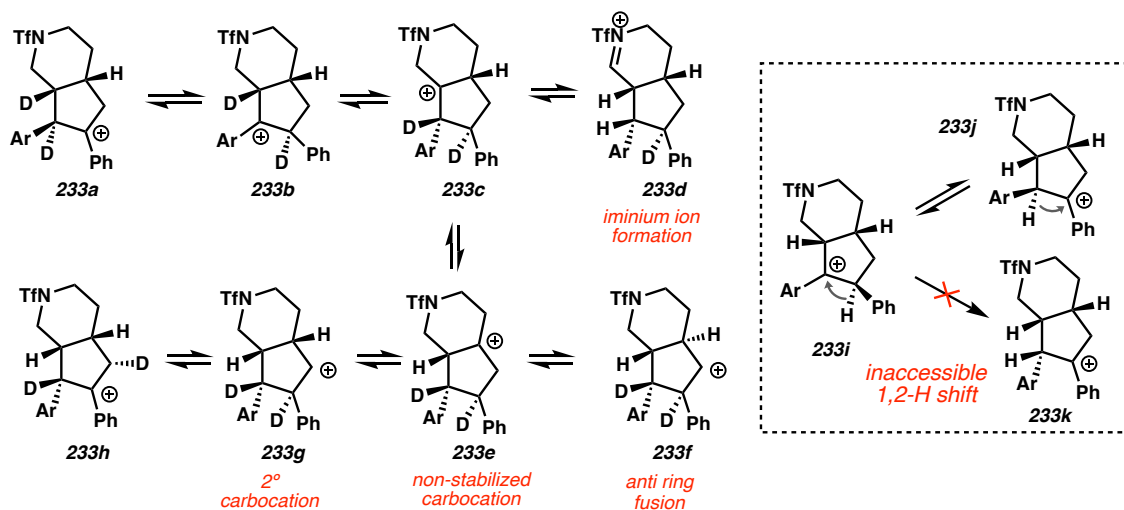
In the context of enantioselective insertion, the allyl silane did not influence the selectivity of the reaction, despite its profound influence on rate (Table 4.1). This result not only supports the proposed role of the Si-center in the ionization of the substrate, but also suggests that after ionization a discrete vinyl cation/IDPi ion pair is formed that undergoes the enantiodetermining C–H insertion step. Supporting this hypothesis, deuteration of the substrate's insertion sites resulted in an appreciable increase in %*ee* across two structurally distinct catalysts (Scheme 4.11), corresponding to up to a 0.12 ± 0.03 kcal/mol difference in $\Delta\Delta G^\ddagger$.³⁷ The presence of deuterium does not appear to influence the rate of reaction, consistent with a rate determining ionization prior to insertion. Moreover, no indication of deuterium incorporation adjacent to the CD₂ methylene was observed, which would be expected if a stepwise hydride rebound mechanism was operative²⁵, given that hydride shifts from **232** to more stabilized cations would result in H/D-scrambling (Scheme 4.11). While this observation supports either a concerted insertion or a rapid rebound mechanism,

wherein a putative 2° carbocation is trapped by olefin attack before 1,2-shifts can occur, we recognize that the mechanism likely resides on a continuum between these two extreme scenarios.

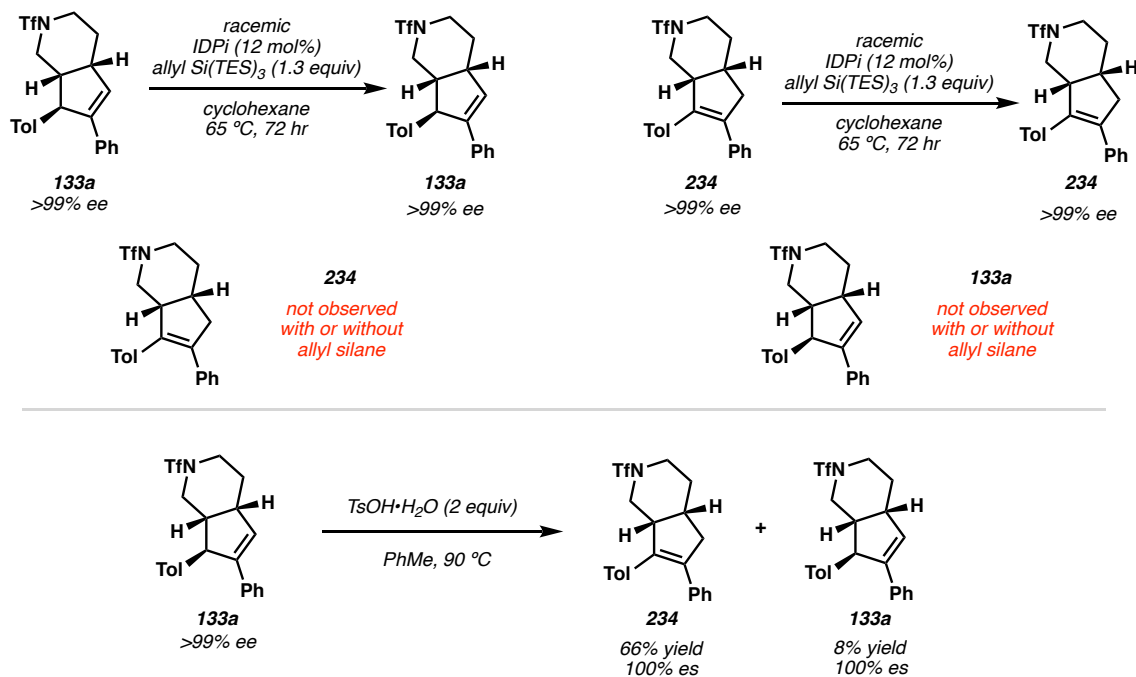
Scheme 4.11. Isotopic labeling experiments



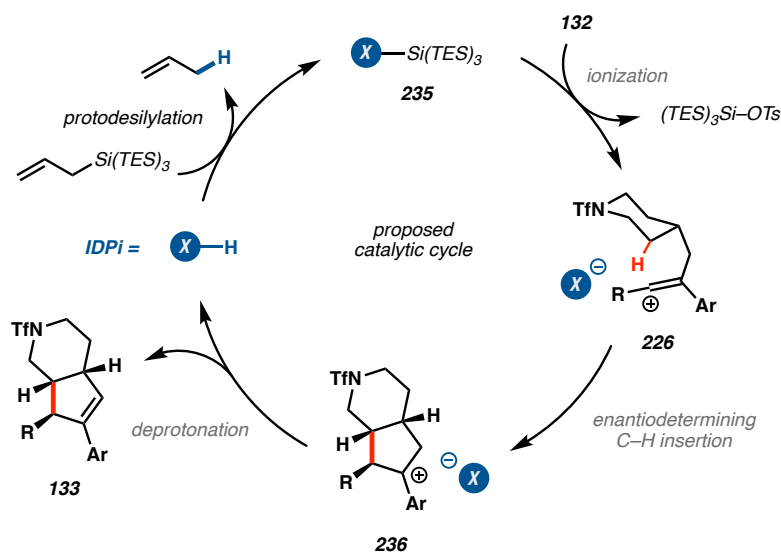
In the context of diastereoselectivity, we propose that all three stereocenters are set in a highly selective C–H insertion transition state. Although the observed diastereomer is predicted to be thermodynamic (calculated to be favored by 3.9 kcal/mol), it is not expected that the high diastereoselectivity observed is a result of thermodynamically-driven diastereomer formation *via* stereocenter epimerization. 1,2-hydride shifts are known to be stereospecific, ruling out hydride exchange between the neighboring benzylic centers (**233i** ⇌ **233k**) as a potential mechanism for epimerization (Scheme 4.12).³⁸ Hydride shifts through the ring fusion carbon (**233a–233h**) would result in higher energy cations, and this pathway is discounted given the lack of H/D scrambling observed in deuterated substrate **132b–D** (Scheme 4.11 and 4.12).

Scheme 4.12. Potential hydride shifts not operative

Another potential mechanism for benzylic stereocenter epimerization is *via* olefin transposition type mechanisms, wherein equilibration between the trisubstituted (**133a**) and tetrasubstituted (**234**) olefin isomer enables thermodynamic diastereomer formation (Scheme 4.13). However, exposure of enantioenriched trisubstituted (**133a**) or tetrasubstituted product (**234**) to racemic IDPi catalyst does not result in olefin isomerization, in the presence or absence of silane. The starting material is recovered quantitatively with no loss of enantioenrichment. However, heating enantioenriched trisubstituted product (**133a**) in the presence of stoichiometric *p*-toluenesulfonic acid (TsOH) furnishes a 9:1 ratio of tetrasubstituted product (**234**) to starting trisubstituted product (**133a**), resulting from acid-mediated olefin isomerization. Heating for longer periods of time, increasing the temperature, and increase the amount of TsOH does not lead to further conversion, suggesting that the 9:1 ratio is due to thermodynamic equilibrium. This is consistent with a kinetic deprotonation in the IDPi-catalyzed reaction.

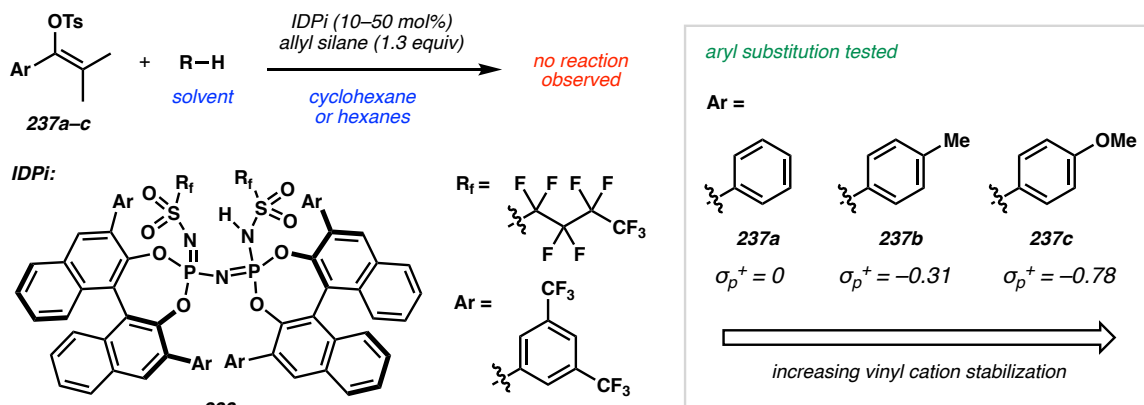
Scheme 4.13. Studies on IDPi and sulfonic acid-mediated isomerization

Based on the above discussion, we propose that the high diastereoselectivity observed in the reaction is a result of a stereoselective 1,1-insertion, wherein all three stereocenters are set selectively in a single transition state, and not a result of thermodynamically-driven equilibration after C–H insertion. A proposed mechanism is outlined in Scheme 4.14, wherein protodesilylation of the allylsilane by IDPi generates the active Lewis acid catalyst **235**. This is consistent with prior work by List *et al.*, which has demonstrated that IDPi can react with allyl silanes to generate silylated adducts that are Lewis acidic.³³ Subsequent ionization of the vinyl tosylate by **132** generates the reactive vinyl cation species (**226**), which we propose is confined within the IDPi anion as a contact ion pair. An enantiodetermining C–H insertion step followed by kinetic deprotonation delivers insertion product **133** and regenerates IDPi.

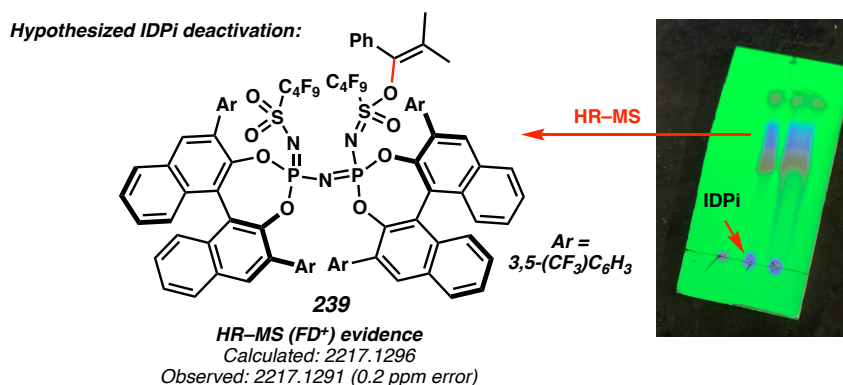
Scheme 4.14. Proposed mechanism

4.4 ATTEMPTS AT INTERMOLECULAR C–H INSERTION

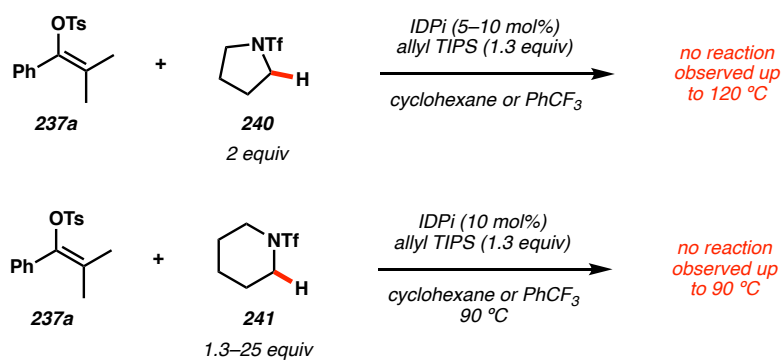
Upon completion of our studies on asymmetric intramolecular C–H insertion, we set out to determine whether intermolecular insertion chemistry could be carried out with IDPi catalysis. We conducted experiments with vinyl tosylates of type **237** in alkane solvent (cyclohexane and *n*-hexanes), with hopes of achieving alkylation of a vinyl carbocation intermediate derived from **237**, but found it difficult to observe starting material consumption employing some of the most active IDPi catalysts previously employed in our experiments (Scheme 4.15). This was true even at high loadings (50 mol%) of IDPi **238**. Attempts to stabilize the vinyl cation intermediate to impart the kinetic persistence needed to undergo an intermolecular reaction were also met with failure, as electron-donating groups (**237b** and **237c**) on the substrate did not promote reactivity.

Scheme 4.15. Attempts at intermolecular C–H insertion via IDPi catalysis

Careful inspection of the reaction mixture suggested that catalyst functionalization might be occurring. Higher R_f bright blue spots appeared on TLC under UV visualization (this color is characteristic of IDPi catalyst), however attempts to characterize these new species was difficult due to challenging purification (Scheme 4.16). However, HR–MS analysis is consistent with the IDPi adduct with the vinyl carbocation (**239** could be a potential adduct). It is possible that the greater kinetic persistence required for an intermolecular C–H insertion of the vinyl carbocation is outcompeted by the collapse of the carbocation-IDPi ion pair to form a covalent adduct (such as **239**). Although intermolecular Friedel-Crafts reactions with benzene are fast, and can even outcompete intramolecular insertion with IDPi catalysts (see Scheme 4.10), it appears that intermolecular C–H insertion is difficult to achieve with IDPi, likely due to relatively slow rate of insertion. These initial experiments suggest that stronger acid catalysts (i.e., more weakly coordinating conjugate base) may permit successful intermolecular insertion, as seen with weakly coordinating carborane anions.²⁵ Alternatively, additives to heterolyze this adduct could also be a feasible strategy to reverse this ion pair collapse.

Scheme 4.16. Evidence supporting catalyst deactivation

Attempts to employ substrates with more activated C–H bonds to potentially accelerate the C–H insertion were also met with failure (Scheme 4.17). While N-triflyl protected piperidines were shown to be competent nucleophiles in intramolecular C–H insertion, intermolecular insertion into protected pyrrolidine (**240**) or piperidines (**241**) (up to 25 equivalents, and up to 120 °C) resulted in no reaction.

Scheme 4.17. Attempts at intermolecular insertion into activated C–H bonds

4.5 CONCLUSION

In conclusion, we have demonstrated that vinyl cations can be generated *via* organocatalysis and engaged in highly stereoselective insertion into unactivated C(*sp*³)–H bonds. The confined IDPi catalysts employed in this study have resulted in unprecedented functional group tolerance compared to previously developed catalytic vinyl cation C–H insertion reactions, ultimately expanding the synthetic utility of this emerging transition metal-free C(*sp*³)–H functionalization platform. Mechanistic studies are consistent with an enantiodetermining C–H cleavage of the piperidine ring. These studies expand the scope of carbocation intermediates that can be utilized in asymmetric synthesis, and lay the conceptual foundation for further development of novel enantioselective reactions of dicoordinated carbocations.

4.6 EXPERIMENTAL SECTION

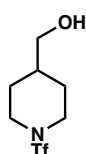
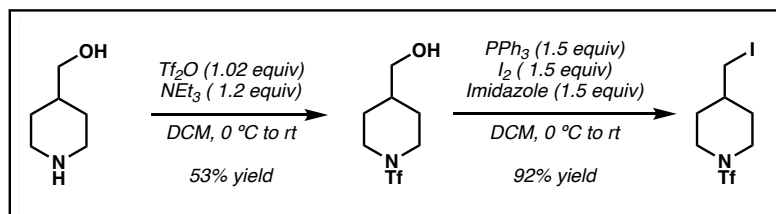
4.6.1 Materials & Methods

Unless otherwise stated, all reactions were performed in an MBraun glovebox under nitrogen atmosphere with ≤ 0.5 ppm O₂ levels. All glassware and stir-bars were dried in a 160 °C oven for at least 12 hours and cycled directly into the glovebox for use. Solid substrates were dried on high vacuum over P₂O₅ overnight. All solvents were rigorously dried before use. Cyclohexane was distilled over potassium. All other solvents used for substrate synthesis were dried in a JC Meyer solvent system. Silanes were dried by distillation over CaH₂ or dried on high vacuum over P₂O₅ overnight before being stored in a glovebox. Triethylamine and diisopropylamine were distilled over CaH₂ prior to use. Trifluoromethanesulfonic anhydride (Tf₂O) was purified by distillation over P₂O₅. Preparatory thin layer chromatography (TLC) was performed using Millipore silica gel 60 F₂₅₄ pre-coated plates (0.25 mm) and visualized by UV fluorescence quenching. SiliaFlash P60 silica gel (230-400 mesh) was used for flash chromatography. Purification by preparative HPLC was done on an Agilent 1200 series instrument with a reverse phase Alltima C₁₈ (5 μ , 25 cm length, 1 cm internal diameter) column. Measurements of enantiomeric excess (% *ee*) were performed using an Agilent 1260 infinity chiral HPLC using Daicel CHIRALPAK[®] or Daicel CHIRALCEL[®] columns (4.6 \times 250mm, 5 μ m particle size) and hexanes/isopropanol as the mobile phase. NMR spectra were recorded on a Bruker 400 MHz with Prodigy cryoprobe (¹H, ¹³C, ³¹P, ¹¹B), a Bruker 400 MHz (¹H, ¹³C, ¹⁹F) and a Varian 300 MHz (¹H, ¹⁹F). ¹H NMR spectra are reported relative to CDCl₃ (7.26 ppm), C₆D₆ (7.16 ppm), d₆-Acetone (2.05 ppm), or d₆-DMSO, (2.50 ppm) unless noted otherwise. Data for ¹H NMR spectra are as follows: chemical shift (ppm),

multiplicity, coupling constant (Hz), integration. Multiplicities are as follows: s = singlet, d = doublet, t = triplet, dd = doublet of doublet, dt = doublet of triplet, ddd = doublet of doublet of doublet, td = triplet of doublet, m = multiplet. ^{13}C NMR spectra are reported relative to CDCl_3 (77.1 ppm), C_6D_6 (128.0 ppm), d_6 -Acetone (29.8 ppm), or d_6 -DMSO (39.5 ppm) unless noted otherwise. IR Spectra were recorded on a Perkin Elmer Spectrum BXII FT-IR spectrometer and are reported in terms of frequency absorption (cm^{-1}). High resolution mass spectra (HR-MS) were recorded on an Agilent 6230 time-of-flight LC/MS (LC/TOF) using electrospray ionization (ESI) or acquired by the Caltech Mass Spectral Facility on a JEOL JMS-T2000 AccuTOF GC-Alpha time-of-flight mass spectrometer using Field Desorption (FD) ionization or an electron ionization source. Crystallographic data were obtained by the Beckman Institute Crystallography Facility and by the UCLA J.D. McCullough Laboratory of X-ray Crystallography. All commercial chemicals and reagents were used as received, unless otherwise noted. KOtBu , Ts_2O (97%), and 4-chloroboronic acid were purchased from Sigma-Aldrich and used as received. Bromomethyl methyl ether (MOM-Br) was ordered from Oakwood Chemicals and distilled before used. 1,1'-Bi-2-naphthol (R & S), EDCI, diiodine, 4-piperidinemethanol, trifluoromethanesulfonic anhydride (Tf_2O), imidazole, triphenylphosphine, 4-dimethylaminopyridine (DMAP), N,O-dimethylhydroxylamine hydrochloride, 2-phenylacetophenone, 1-bromo-4-pentafluorosulfanylbenzene, cyclohexylacetic acid, tert-butyl 4-(hydroxymethyl)piperidin-1-carboxylate, octafluoronaphthalene, pentachlorobenzenethiol, trifluoromethanesulfonamide, N-chlorosuccinimide, methyl 2,2-difluoro-2-(fluorosulfonyl)acetate, and sodium pentoxide were all ordered from Oakwood chemicals and used as received.

4.6.2 Preparation of Vinyl Tosylate Substrates

Figure 4.1: Representative scheme for the synthesis of *N*-Tf piperidinyl iodides



(1-((trifluoromethyl)sulfonyl)piperidin-4-yl)methanol (**242**)

To a flame-dried flask with a magnetic stir bar was added commercially available piperidin-4-ylmethanol (9.80 g, 1.0 equiv, 85.0 mmol) followed by 140 mL dry DCM and 14.2 mL of freshly distilled (over CaH_2) triethylamine (10.33 g, 1.2 equiv, 102.1 mmol). The solution was cooled to 0 °C and allowed to stir for 20 minutes at this temperature. Then, freshly dried and distilled (over P_2O_5) Tf_2O (24.48 mmol, 1.02 equiv, 86.79 mmol) was added dropwise very slowly over the course of ~20 minutes. The reaction was allowed to stir at 0 °C for 2 hours, then warmed to room temperature and allowed to stir overnight. The next morning, the reaction was cooled again to 0 °C and quenched with water and extracted with DCM (x3). The combined organics were dried over Na_2SO_4 , filtered, then concentrated *in vacuo*. The crude material was purified *via* silica flash column chromatography (20% diethyl ether in DCM, product stains with KMnO_4 TLC stain) to yield alcohol **242** as a white solid (11.2 g, 53% yield).

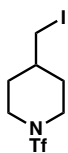
¹H NMR (400 MHz, CDCl₃) δ 3.99 (d, *J* = 13.1 Hz, 2H), 3.55 (d, *J* = 6.3 Hz, 2H), 3.04 (t, *J* = 12.7 Hz, 2H), 1.95 – 1.82 (m, 2H), 1.80 – 1.58 (m, 1H), 1.45 (br s, 1H), 1.41 – 1.27 (m, 2H).

¹³C NMR (101 MHz, CDCl₃) δ 120.2 (q, *J* = 323 Hz), 66.9, 46.8, 37.8, 28.6.

¹⁹F NMR (376 MHz, CDCl₃) δ -75.2 (br s).

FT-IR (neat film NaCl): 3333, 2927, 1447, 1385, 1227, 1184, 1150, 1124, 1049, 980, 939, 762, 708, 683 cm⁻¹.

HR-MS (FD) *m/z*: [M•]⁺ Calculated for C₇H₁₂F₃NO₃S: 247.0490; Measured: 247.0481.



4-(iodomethyl)-1-((trifluoromethyl)sulfonyl)piperidine (**243**)

To a flame-dried flask with a magnetic stir bar was added PPh₃ (18.1 g, 1.5 equiv, 69.2 mmol) and imidazole (4.7 g, 1.5 equiv, 69.2 mmol). The solids were dissolved in 145 mL dry DCM then cooled to 0 °C. After stirring at this temperature for 20 minutes, solid I₂ (17.6g, 1.5 equiv, 69.2 mmol) was added in three portions and allowed to stir for another 30 minutes at 0 °C under N₂. Then, a solution of alcohol **242** (11.4 g, 1.0 equiv, 46.1 mmol) in 30 mL dry DCM was added dropwise and the reaction was allowed to warm up to room temperature overnight. The next morning (SM consumed by TLC) saturated aqueous Na₂S₂O₃ was added and then subsequently extracted with DCM (x3). The combined organics were dried over Na₂SO₄, filtered, concentrated *in vacuo*, then purified *via* silica flash column chromatography (20% diethyl ether in hexanes) to yield pure iodide **243** as a white solid (15.2 g, 92% yield).

$^1\text{H NMR}$ (400 MHz, CDCl_3) δ 3.93 (dt, $J = 13.3, 2.5$ Hz, 2H), 3.11 (d, $J = 6.5$ Hz, 2H), 3.01 (t, $J = 12.8$ Hz, 2H), 2.30 – 1.81 (m, 2H), 1.63 (m, 1H), 1.39 – 1.24 (m, 2H).

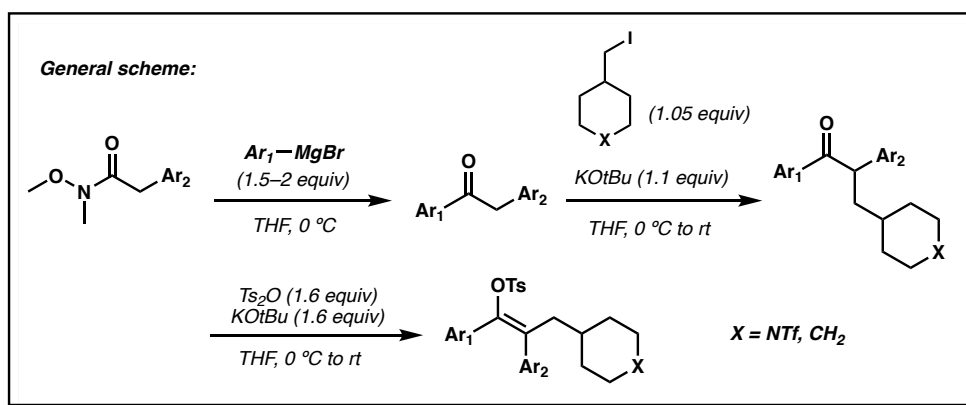
$^{13}\text{C NMR}$ (101 MHz, CDCl_3) δ 120.0 (q, $J = 323.4$ Hz), 46.4, 37.4, 32.2, 11.9.

$^{19}\text{F NMR}$ (376 MHz, CDCl_3): δ -75.3 (br s).

FT-IR (neat film NaCl): 2946, 2881, 1466, 1447, 1391, 1355, 1296, 1254, 1228, 1190, 1143, 1062, 1039, 993, 977, 945, 846, 810, 764, 709, 683, 668, 620 cm^{-1} .

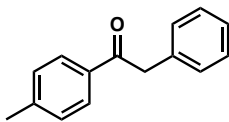
HR-MS (FD) m/z : $[\text{M}\cdot]^+$ Calculated for $\text{C}_7\text{H}_{11}\text{F}_3\text{INO}_2\text{S}$: 356.9507; Measured: 356.9493.

Figure 4.2: Representative scheme for the synthesis of vinyl tosylate substrates

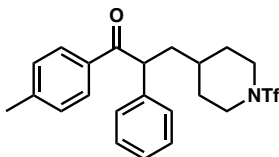


The general procedure outlined above was used to prepare *N*-Tf piperidinyl vinyl tosylate substrates from the corresponding aryl acetic acid-derived Weinreb amides, which were prepared according to published procedures.³⁹ The procedure for synthesis of aryl acetophenones was adopted from Schindler *et al.*⁴⁰ The tosylation step generates the *E* isomer shown as the major isomer, but some *Z* isomer is also produced, which is typically more polar in R_f and could be separated out via column chromatography. While both the *Z* and *E* isomer of the vinyl tosylate give similar results in C–H insertion reactions (activity and enantioselectivity), only the *E* isomer was used for experiments unless otherwise noted.

**If the vinyl tosylate is impure after column chromatography, pure material could be obtained via recrystallization from hexanes/ethyl acetate or hexanes/diethyl ether.*



2-phenyl-1-(p-tolyl)ethan-1-one (244) was prepared according to literature procedures and matched the NMR data in the literature.⁴¹



2-phenyl-1-(p-tolyl)-3-(1-((trifluoromethyl)sulfonyl)piperidin-4-yl)propan-1-one (245)

To a flamed-dried flask was added K₂OtBu (293 mg, 1.1 equiv, 2.6 mmol). This flask was evacuated under vacuum and backfilled with nitrogen three times. To this was added THF (8 mL), and the flask was cooled to 0 °C. To this flask was added ketone **244** (0.50 g, 1.0 equiv, 2.4 mmol) in THF (4 mL), and the solution was stirred at 0 °C for 20 minutes. To this was added a solution of iodide **243** (892 mg, 1.05 equiv, 2.50 mmol) in THF (4 mL). The reaction flask was allowed to warm up to room temperature overnight and quenched by addition of saturated aqueous NH₄Cl (10 mL). The aqueous layer was extracted with ethyl acetate (3x 15 mL), dried over Na₂SO₄, filtered, concentrated *in vacuo*, and purified by silica flash column chromatography (5% ethyl acetate in hexanes) to yield ketone **245** as a white solid (788 mg, 75% yield).

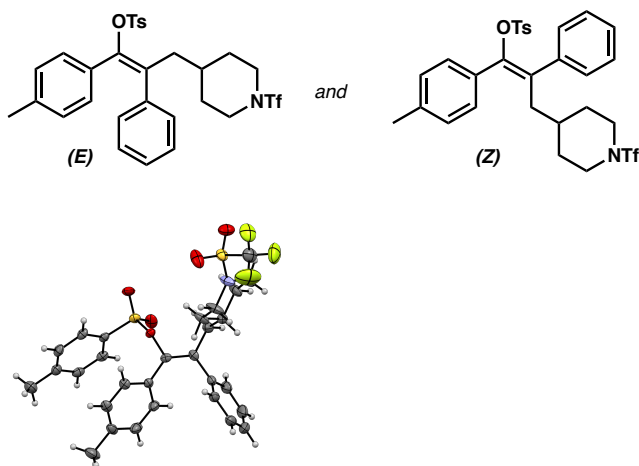
$^1\text{H NMR}$ (300 MHz, CDCl_3) δ 7.84 (d, $J = 8.1$ Hz, 2H), 7.28 – 7.23 (m, 5H), 7.17 (d, $J = 8.1$ Hz, 2H), 4.63 (t, $J = 7.5$ Hz, 1H), 4.09 – 3.66 (m, 2H), 2.90 (q, $J = 13.0$ Hz, 2H), 2.29 – 2.04 (m, 3H), 1.98 – 1.63 (m, 1H), 1.50 – 1.13 (m, 3H).

$^{13}\text{C NMR}$ (101 MHz, CDCl_3) δ 198.6, 144.1, 139.3, 133.9, 129.3, 129.0, 128.7, 127.9, 127.2, 120.0 (q, $J = 323.7$ Hz), 50.0, 46.7, 40.08, 32.82, 31.91, 21.57.

$^{19}\text{F NMR}$ (282 MHz, CDCl_3) δ -75.2.

FT-IR (neat film NaCl): 2919, 1675, 1604, 1460, 1387, 1182, 1149, 1118, 1047, 949, 937, 706 cm^{-1} .

HR-MS (ESI) m/z : $[\text{M}+\text{H}]^+$ Calculated for $\text{C}_{22}\text{H}_{25}\text{F}_3\text{NO}_3\text{S}$: 440.1507; Measured: 440.1509.



2-phenyl-1-(*p*-tolyl)-3-(1-((trifluoromethyl)sulfonyl)piperidin-4-yl)prop-1-en-1-yl 4-methylbenzenesulfonate (132a & 132o)

To a flame-dried flask was added KOTu (666 mg, 1.5 equiv, 5.94 mmol) and THF (15 mL). This solution was cooled to 0 °C and ketone **245** (1.74 g, 1.0 equiv, 3.9 mmol) was added dropwise as a solution in THF (10 mL). This solution was stirred at 0 °C for 1 hour. To this was added toluenesulfonic anhydride (1.94 g, 1.5 equiv, 5.94 mmol) as a fine

suspension in THF (15 mL). This solution was allowed to warm to room temperature and stirred for 1 hour. The reaction was diluted with ethyl acetate (30 mL) and 1M aqueous NaOH (10 mL). The organic layer was separated, and the aqueous layer was extracted with ethyl acetate (3 x 20 mL), dried over Na₂SO₄, filtered, concentrated *in vacuo*, and purified by flash column chromatography (1% → 20% ether in hexanes). Both new spots were collected (lower in R_f than starting ketone), which correspond to the *E* vinyl tosylate as the top compound (942 mg, 40% yield, white solid) and the *Z* vinyl tosylate as the bottom compound (minor). The *Z* isomer was further purified by recrystallization from hexanes to obtain pure white crystals (122 mg, 6% yield). The olefin isomer of the top spot is assigned to be *E* on the basis of NOESY NMR (observe NOE correlations between tosylate and piperidine fragments). Consistent with this assignment, the chemical shift of the allylic methylene protons (2.73 ppm) is congruent to similarly reported *E* diaryl vinyl tosylates (typically ~2.7 ppm for allylic methylene), which are distinct from the reported *Z* isomer chemical shift (typically ~2.3 ppm for allylic methylene of corresponding *Z* vinyl tosylate).⁴² Additionally, this product was crystallized in hexanes to yield X-ray quality crystals to definitively assign the olefin geometry. The lower R_f spot was assigned to be the *Z* isomer by process of elimination. Consistent with this assignment, the chemical shift of the allylic methylene protons (2.4 ppm) is congruent to similarly reported *Z* diaryl vinyl tosylates (typically ~2.3 ppm for allylic methylene).

132a (*E* isomer)

¹H NMR (400 MHz, CDCl₃) δ 7.45 (d, *J* = 8.3 Hz, 2H), 7.21 – 7.14 (m, 3H), 7.09 (d, *J* = 8.1 Hz, 1H), 7.02 (dd, *J* = 6.6, 2.9 Hz, 2H), 6.80 – 6.62 (m, 2H), 3.84 (d, *J* = 13.0 Hz, 2H),

2.89 (s, 1H), 2.69 (d, $J = 6.3$ Hz, 2H), 2.37 (s, 3H), 2.18 (s, 3H), 1.71 (d, $J = 11.8$ Hz, 2H), 1.44 – 1.17 (m, 3H).

^{13}C NMR (101 MHz, CDCl_3) δ 144.9, 144.4, 138.2, 137.9, 134.3, 131.6, 130.2, 129.8, 129.2, 129.2, 128.4, 128.1, 127.9, 127.3, 120.1 (q, $J = 323.3$ Hz), 46.6, 38.7, 33.0, 31.4, 21.5, 21.2.

^{19}F NMR (282 MHz, CDCl_3) δ -75.3 (br s).

FT-IR (neat film NaCl): 2927, 1598, 1386, 1226, 1188, 1150, 1049, 971, 941, 849 cm^{-1} .

HR-MS (EI-MS) m/z : $[\text{M}+\text{K}]^+$ Calculated for $\text{C}_{29}\text{H}_{30}\text{F}_3\text{NO}_5\text{S}_2\text{K}$: 632.1155; Measured: 632.1166.

132o (Z isomer)

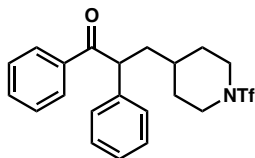
^1H NMR (400 MHz, CDCl_3) δ 7.36 – 7.28 (m, 3H), 7.25 – 7.20 (m, 4H), 7.18 – 7.04 (m, 4H), 6.96 (dd, $J = 8.7, 0.7$ Hz, 2H), 3.72 (d, $J = 12.9$ Hz, 2H), 3.01 – 2.60 (m, 2H), 2.40 (d, $J = 7.1$ Hz, 2H), 2.37 (s, 3H), 2.33 (s, 3H), 1.70 – 1.58 (m, 2H), 1.34 – 1.16 (m, 1H), 1.17 – 0.97 (m, 2H).

^{13}C NMR (101 MHz, CDCl_3) δ 143.8, 143.4, 139.0, 136.9, 133.9, 130.5, 129.8, 128.9, 128.9, 128.5, 128.2, 127.6, 127.3, 120.0 (q, $J = 323.8$ Hz), 46.5, 38.7, 33.1, 31.2, 21.5, 21.3.

^{19}F NMR (282 MHz, CDCl_3) δ -75.2 (br s).

FT-IR (neat film NaCl): 2919, 1597, 1386, 1226, 1176, 1150, 1116, 1051, 1005, 940, 831, 764, 707 cm^{-1} .

HR-MS (ESI) m/z : $[\text{M}+\text{K}]^+$ Calculated for $\text{C}_{29}\text{H}_{30}\text{F}_3\text{KNO}_5\text{S}_2$: 632.1155; Measured: 632.1155.

**1,2-diphenyl-3-(1-((trifluoromethyl)sulfonyl)piperidin-4-yl)propan-1-one (246)**

To a flame-dried flask was added commercially-available 2-diphenylethan-1-one (2.30 g, 1.0 equiv, 11.7 mmol) then dissolved in THF (25 mL) and cooled to 0 °C. In a separate flask, a fresh solution of KO^tBu (1.450 g, 1.10 equiv, 12.9 mmol) in THF (25 mL) was prepared and added dropwise to the ketone while at 0 °C. The yellow solution was allowed to stir at 0 °C for 20 minutes. Then, a solution of iodide **243** (4.39 g, 1.05 equiv, 12.3 mmol) in THF (10 mL) was added dropwise then allowed to warm to room temperature overnight. Once the reaction was completed by TLC analysis (15% ethyl acetate in hexanes), the reaction was quenched with saturated aqueous ammonium chloride and extracted with ethyl acetate (x3). The combined organics were washed once with brine, dried over Na₂SO₄, filtered, concentrated *in vacuo*, and purified by silica flash column chromatography (15% ethyl acetate in hexanes) to yield ketone **246** as an off-white solid (3.6 g, 72% yield).

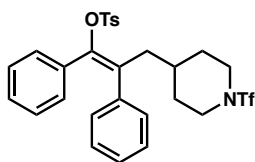
¹H NMR (400 MHz, CDCl₃) δ 8.03 – 7.93 (m, 2H), 7.55 – 7.46 (m, 1H), 7.46 – 7.35 (m, 2H), 7.34 – 7.27 (m, 4H), 7.25 – 7.17 (m, 1H), 4.72 – 4.64 (m, 1H), 3.90 (dddt, *J* = 17.5, 15.2, 4.4, 2.4 Hz, 2H), 3.01 – 2.85 (m, 2H), 2.28 – 2.16 (m, 1H), 1.90 (dt, *J* = 13.2, 2.6 Hz, 1H), 1.82 (dt, *J* = 13.8, 6.7 Hz, 1H), 1.74 (dt, *J* = 13.1, 2.6 Hz, 1H), 1.51 – 1.25 (m, 3H).

¹³C NMR (101 MHz, CDCl₃) δ 199.2, 139.2, 136.5, 133.2, 129.2, 128.7, 128.1, 127.4, 120.2 (q, *J* = 323.6 Hz), 50.3, 47.0 – 46.6 (m), 40.2, 32.9, 32.0 (d, *J* = 11.3 Hz).

¹⁹F NMR (282 MHz, CDCl₃) δ -75.0.

FT-IR (neat film NaCl): 3062, 3027, 2940, 2875, 1681, 1597, 1580, 1493, 1464, 1447, 1385, 1357, 1273, 1252, 1226, 1188, 1147, 1118, 1051, 1000, 950, 938, 911, 760, 736, 702 cm^{-1} .

HR-MS (ESI) m/z : $[\text{M}+\text{H}]^+$ Calculated for $\text{C}_{21}\text{H}_{23}\text{F}_3\text{NO}_3\text{S}$: 426.1345; Measured: 426.1344.



(E)-1,2-diphenyl-3-(1-((trifluoromethyl)sulfonyl)piperidin-4-yl)prop-1-en-1-yl 4-methylbenzenesulfonate (132b)

To a flame-dried flask was added ketone **246** (2.80 g, 1.0 equiv, 6.58 mmol) then dissolved in THF (20 mL) and cooled to 0 °C. In a separate flask, a fresh solution of KO^tBu (1.18 g, 1.60 equiv, 10.5 mmol) in THF (13 mL) was prepared and added dropwise to the ketone while at 0 °C. The yellow solution was allowed to stir at 0 °C for 90 minutes. Then, a solution of Ts_2O (3.44 g, 1.6 equiv, 10.6 mmol) in THF (10 mL, sonicated to dissolve as much as possible) was added dropwise to the enolate solution with vigorous stirring then allowed to warm to room temperature (solution turns thick). Once the reaction was completed by TLC analysis (20% ethyl acetate in hexanes), the reaction was quenched with water and extracted with ethyl acetate (x3). The combined organics were washed once with brine, dried over Na_2SO_4 , filtered, concentrated *in vacuo*, and purified by silica flash column chromatography (20% diethyl ether in hexanes) and recrystallized from ethyl acetate/hexanes to yield vinyl tosylate **132b** as a white crystalline solid (2.39 g, 60% yield). The olefin isomer is assigned to be *E* on the basis of NOESY NMR (observe NOE

correlations between tosylate and piperidine protons). Consistent with this assignment, the chemical shift of the allylic methylene protons (2.73 ppm in CDCl₃) is congruent to similarly reported *E* diaryl vinyl tosylates (typically ~2.7 ppm for allylic methylene in CDCl₃), which are distinct from the reported *Z* isomer chemical shift (typically ~2.3 ppm for allylic methylene of corresponding *Z* vinyl tosylate in CDCl₃).⁴²

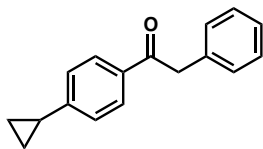
¹H NMR (400 MHz, CDCl₃) δ 7.48 – 7.40 (m, 2H), 7.23 – 7.12 (m, 3H), 7.12 – 6.96 (m, 5H), 6.94 – 6.82 (m, 4H), 3.86 (dd, *J* = 13.3, 3.9 Hz, 2H), 2.90 (app t, *J* = 11.9 Hz, 2H), 2.73 (d, *J* = 6.3 Hz, 2H), 2.35 (s, 3H), 1.72 (dt, *J* = 12.9, 2.6 Hz, 2H), 1.47 – 1.30 (m, 3H).

¹³C NMR (101 MHz, CDCl₃) δ 144.9, 144.7, 138.2, 134.4, 133.5, 132.5, 130.0, 129.4, 129.3, 128.6, 128.1, 128.0, 127.6, 127.5, 120.2 (q, *J* = 323 Hz), 46.7, 38.9, 33.2, 31.5, 21.7.

¹⁹F NMR (376 MHz, CDCl₃) δ -75.3 (br s).

FT-IR (neat film NaCl): 2927, 1598, 1445, 1386, 1226, 1189, 1177, 1149, 1115, 1084, 1049, 973, 942, 913, 847, 814, 780, 759, 730, 699, 679 cm⁻¹.

HR-MS (ESI) *m/z*: [M+Na]⁺ Calculated for C₂₈H₂₈F₃NNaO₅S₂: 602.1253; Measured: 602.1274.



1-(4-cyclopropylphenyl)-2-phenylethan-1-one (247)

Magnesium turnings (546 mg, 1.75 equiv, 22.5 mmol) were flame-dried under high vacuum in a round bottom flask (x3) then suspended in dry THF (64 mL). Commercially available 1-bromo-4-cyclopropylbenzene (5.06 g, 2.0 equiv, 25.7 mmol, 3.4 mL) was

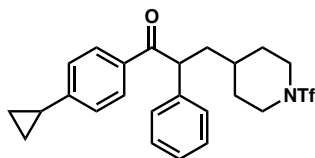
added followed by a small grain of I₂. The solution was allowed to stir with gentle heating *via* a heat gun until the purple-brown color of the I₂ disappears. The suspension was then stirred until all the magnesium turnings are visibly consumed. At this point, the reaction is cooled to 0 °C, and then a solution of *N*-methoxy-*N*-methyl-2-phenylacetamide (2.30 g, 1.0 equiv, 12.80 mmol) in 6.4 mL THF is added dropwise. The reaction is monitored closely by TLC to determine starting material consumption (usually 5–20 minutes), then quenched with 30 mL saturated aqueous ammonium chloride while at 0 °C. The reaction is extracted with diethyl ether (x3), then the combined organics are washed with brine, dried over MgSO₄, filtered through a short pad of silica (wash through with diethyl ether), and concentrated *in vacuo*. Pure material was obtained *via* silica flash column chromatography (7.5% ether/hexanes), furnishing ketone **247** as a white solid (2.6 g, 86%).

¹H NMR (400 MHz, CDCl₃) δ 7.91 – 7.84 (m, 2H), 7.31 – 7.25 (m, 2H), 7.25 – 7.17 (m, 3H), 7.11 – 7.05 (m, 2H), 4.21 (s, 2H), 1.90 (ddd, *J* = 8.4, 5.1, 3.4 Hz, 1H), 1.06 – 0.98 (m, 2H), 0.78 – 0.69 (m, 2H).

¹³C NMR (101 MHz, CDCl₃) δ 197.2, 150.6, 135.0, 134.1, 129.5, 129.0, 128.8, 126.9, 125.7, 45.5, 15.9, 10.5.

FT-IR (neat film NaCl): 1676, 1604, 1459, 1411, 1328, 1044, 812, 713 cm⁻¹.

HR-MS (ESI) *m/z*: [M+H]⁺ Calculated for C₁₇H₁₇O: 237.1274; Measured: 237.1275.



1-(4-cyclopropylphenyl)-2-phenyl-3-(1-((trifluoromethyl)sulfonyl)piperidin-4-yl)propan-1-one (248)

To a flamed-dried flask was added KOtBu (1.16 g, 1.1 equiv, 10.36 mmol). This flask was evacuated under vacuum and backfilled with nitrogen three times. To this was added THF (24 mL), and the flask was cooled to 0 °C. To this flask was added ketone **247** (2.22 g, 1.0 equiv, 9.4 mmol) in THF (20.5 mL), and the solution was stirred at 0 °C for 20 minutes. To this was added a solution of iodide **243** (3.53 g, 1.05 equiv, 9.89 mmol) in THF (16 mL). The reaction flask was allowed to warm up to room temperature overnight, and quenched by addition of saturated aqueous NH₄Cl (10 mL). The aqueous layer was extracted with ethyl acetate (3x 15 mL), dried over Na₂SO₄, filtered, concentrated *in vacuo*, and purified by silica flash column chromatography (15 → 20% diethyl ether in hexanes) to yield ketone **248** as a white solid (2.6 g, 59% yield).

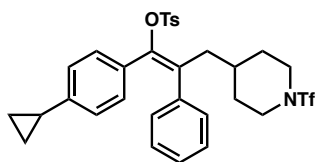
¹H NMR (400 MHz, CDCl₃) δ 7.84 (d, *J* = 8.5 Hz, 2H), 7.32 – 7.23 (m, 4H), 7.19 (tddd, *J* = 5.6, 4.9, 3.3, 2.6 Hz, 1H), 7.04 (d, *J* = 8.4 Hz, 2H), 4.62 (dd, *J* = 8.1, 6.7 Hz, 1H), 3.87 (tt, *J* = 12.8, 2.1 Hz, 2H), 2.90 (dt, *J* = 22.2, 12.7 Hz, 2H), 2.19 (ddd, *J* = 14.4, 8.1, 6.5 Hz, 1H), 1.94 – 1.81 (m, 2H), 1.81 – 1.65 (m, 2H), 1.48 – 1.23 (m, 3H), 1.07 – 0.96 (m, 2H), 0.71 (qd, *J* = 4.8, 2.6 Hz, 2H).

¹³C NMR (101 MHz, CDCl₃) δ 198.6, 150.7, 139.6, 133.9, 129.2, 129.0, 128.1, 127.4, 125.7, 120.2 (q, *J* = 323.4 Hz), 77.5, 77.2, 76.8, 50.2, 46.90, 46.88, 40.3, 33.0, 32.1, 15.8, 10.57, 10.55.

^{19}F NMR (376 MHz, CDCl_3) δ -75.2.

FT-IR (neat film NaCl): 3007, 2936, 1674, 1604, 1566, 1493, 1453, 1415, 1386, 1273, 1253, 1226, 1186, 1146, 1117, 1049, 998, 949, 910, 823, 728, 709, 610 cm^{-1} .

HR-MS (ESI) m/z : $[\text{M}+\text{Na}]^+$ Calculated for $\text{C}_{24}\text{H}_{26}\text{F}_3\text{NNaO}_3\text{S}$: 488.1478; Measured: 488.1471.



(*E*)-1-(4-cyclopropylphenyl)-2-phenyl-3-(1-((trifluoromethyl)sulfonyl)piperidin-4-yl)prop-1-en-1-yl 4-methylbenzenesulfonate (132c)

To a flame-dried flask was added ketone **248** (1.00 g, 1.0 equiv, 2.15 mmol) and dry THF (2.60 mL). A 1.0 M solution of LiOtBu in THF (3.2 mL) was added dropwise and stirred at room temperature for 30 minutes. Then, *p*-toluenesulfonic anhydride (1.05 g, 1.5 equiv, 3.22 mmol) in THF (5.6 mL) was added dropwise to the enolate solution with vigorous stirring, and then the solution was allowed to warm to room temperature (solution turns thick). This solution was then stirred for 1 hour. The reaction was quenched with NaHCO_3 (10 mL) and extracted with diethyl ether (3 x 15 mL). The combined organic layers were washed with brine, dried over Na_2SO_4 , filtered, concentrated *in vacuo*, and purified by silica flash chromatography (20% diethyl ether in hexanes) to give vinyl tosylate **132c** (300 mg, 23% yield). The olefin isomer is assigned to be *E* on the basis of NOESY NMR (observe NOE correlations between tosylate and piperidine fragments). Consistent with this assignment, the chemical shift of the allylic methylene protons (2.72 ppm in CDCl_3) is congruent to similarly reported *E* diaryl vinyl tosylates (typically ~2.7

ppm for allylic methylene in CDCl₃), which are distinct from the reported *Z* isomer chemical shift (typically ~2.3 ppm for allylic methylene of corresponding *Z* vinyl tosylate in CDCl₃).⁴²

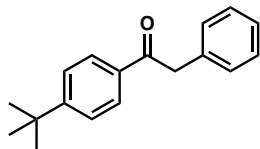
¹H NMR (400 MHz, CDCl₃) δ 7.47 – 7.36 (m, 2H), 7.22 – 7.13 (m, 3H), 7.13 – 6.99 (m, 4H), 6.70 (d, *J* = 8.4 Hz, 2H), 6.54 (d, *J* = 8.3 Hz, 2H), 3.85 (dd, *J* = 13.3, 4.0 Hz, 2H), 2.89 (s, 2H), 2.72 (d, *J* = 6.0 Hz, 2H), 2.36 (s, 3H), 1.71 (tdd, *J* = 8.4, 5.3, 2.8 Hz, 3H), 1.38 (dt, *J* = 11.9, 6.1 Hz, 3H), 0.95 – 0.85 (m, 2H), 0.53 (dt, *J* = 6.6, 4.6 Hz, 2H).

¹³C NMR (101 MHz, CDCl₃) δ 145.1, 144.4, 144.3, 138.4, 134.5, 131.7, 130.3, 129.9, 129.3, 129.3, 128.5, 128.0, 127.4, 124.6, 123.9 (*J* = 323.9 Hz), 46.7, 38.9, 33.2, 31.5, 31.5, 21.6, 15.2, 9.7.

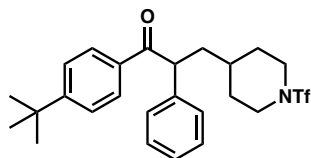
¹⁹F NMR (376 MHz, CDCl₃) δ -75.2.

FT-IR (neat film NaCl): 2924, 1598, 1444, 1387, 1226, 1188, 1177, 1149, 1116, 1049, 968, 941, 848, 830, 812, 777, 757, 707 cm⁻¹.

HR-MS (ESI) *m/z*: [M+Na]⁺ Calculated for C₃₁H₃₂F₃NNaO₅S₂: 642.1566; Measured: 642.1586.



1-(4-(*tert*-butyl)phenyl)-2-phenylethan-1-one (249) was prepared according to literature procedures and matched the NMR data in the literature.⁴¹



1-(4-(*tert*-butyl)phenyl)-2-phenyl-3-(1-((trifluoromethyl)sulfonyl)piperidin-4-yl)propan-1-one (250)

To a flamed-dried flask was added KOtBu (734 mg, 1.1 equiv, 6.54 mmol). This flask was evacuated under vacuum and backfilled with nitrogen three times. To this was added THF (15 mL), and the flask was cooled to 0 °C. To this flask was added ketone **249** (1.50 g, 1.0 equiv, 5.94 mmol) in THF (13 mL), and the solution was stirred at 0 °C for 20 minutes. To this was added a solution of iodide **243** (2.23 g, 1.05 equiv, 6.24 mmol) in THF (10 mL). The reaction flask was allowed to warm up to room temperature overnight, and quenched by addition of saturated aqueous NH₄Cl (10 mL). The aqueous layer was extracted with ethyl acetate (3x 15 mL), dried over Na₂SO₄, filtered, concentrated *in vacuo*, and purified by silica flash column chromatography (10% diethyl ether in hexanes) to yield ketone **250** as a white solid (2.0 g, 70% yield).

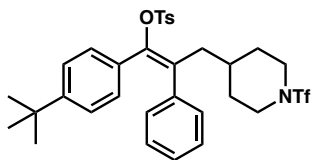
¹H NMR (400 MHz, CDCl₃) δ 7.94 – 7.88 (m, 2H), 7.44 – 7.39 (m, 2H), 7.30 (d, *J* = 4.9 Hz, 4H), 7.25 – 7.19 (m, 1H), 4.66 (dd, *J* = 8.2, 6.7 Hz, 1H), 3.89 (tdt, *J* = 13.0, 4.4, 2.4 Hz, 2H), 3.04 – 2.80 (m, 2H), 2.22 (ddd, *J* = 14.4, 8.2, 6.5 Hz, 1H), 1.89 (dp, *J* = 13.2, 2.7 Hz, 1H), 1.81 – 1.71 (m, 2H), 1.47 – 1.30 (m, 3H), 1.30 (s, 9H).

¹³C NMR (101 MHz, CDCl₃) δ 198.7, 157.1, 139.5, 134.0, 129.3, 128.8, 128.2, 127.4, 125.8, 120.2 (q, *J* = 323.9 Hz), 77.5, 77.2, 76.8, 50.3, 46.91, 46.88, 40.4, 35.2, 33.0, 32.08, 32.05, 31.2.

¹⁹F NMR (376 MHz, CDCl₃) δ -75.8.

FT-IR (neat film NaCl): 2963, 2870, 1676, 1603, 1387, 1268, 1226, 1186, 1147, 1117, 1051, 949, 709 cm^{-1} .

HR-MS (ESI) m/z : $[\text{M}+\text{H}]^+$ Calculated for $\text{C}_{25}\text{H}_{31}\text{F}_3\text{NO}_3\text{S}$: 482.1971; Measured: 482.1972.



(E)-1-(4-(*tert*-butyl)phenyl)-2-phenyl-3-(1-((trifluoromethyl)sulfonyl)piperidin-4-yl)prop-1-en-1-yl 4-methylbenzenesulfonate (132d)

To a flame-dried flask was added K_{OT}Bu (708 mg, 1.6 equiv, 6.31 mmol) and THF (9 mL). This solution was cooled to 0 °C and ketone **250** (1.90 g, 1.0 equiv, 3.95 mmol) was added dropwise as a solution in THF (14 mL). This solution was stirred at 0 °C for 2 hours. To this was quickly added solid toluenesulfonic anhydride (2.06 g, 1.6 equiv, 6.31 mmol) with vigorous stirring, and then the solution was allowed to warm to room temperature (solution turns thick). After 1.5 hours, the reaction was diluted with ethyl acetate (15 mL) and water (15 mL). The organic layer was separated, and the aqueous layer was extracted with ethyl acetate (3 x 10 mL), dried over Na₂SO₄, filtered, concentrated *in vacuo*, and purified by silica flash column chromatography (15% diethyl ether in hexanes) to give vinyl tosylate **132d** (1.0 g, 40% yield). The olefin isomer is assigned to be *E* on the basis of NOESY NMR (observe NOE correlations between tosylate and piperidine fragments). Consistent with this assignment, the chemical shift of the allylic methylene protons (2.77 ppm in CDCl₃) is congruent to similarly reported *E* diaryl vinyl tosylates (typically ~2.7 ppm for

allylic methylene in CDCl₃), which are distinct from the reported *Z* isomer chemical shift (typically ~2.3 ppm for allylic methylene of corresponding *Z* vinyl tosylate in CDCl₃).⁴²

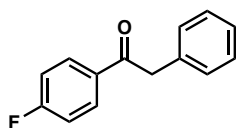
¹H NMR (400 MHz, CDCl₃) δ 7.38 (d, *J* = 8.4 Hz, 2H), 7.21 – 7.15 (m, 3H), 7.06 – 6.98 (m, 4H), 6.86 – 6.81 (m, 2H), 6.76 – 6.69 (m, 2H), 3.87 (dd, *J* = 13.3, 3.9 Hz, 2H), 2.90 (t, *J* = 10.8 Hz, 2H), 2.77 (d, *J* = 6.2 Hz, 2H), 2.31 (s, 3H), 1.79 – 1.68 (m, 2H), 1.46 – 1.32 (m, 3H), 1.17 (s, 9H).

¹³C NMR = (101 MHz, CDCl₃) δ 151.1, 145.1, 144.2, 138.4, 134.6, 132.0, 130.2, 129.7, 129.4, 129.3, 128.5, 128.1, 127.4, 124.40, 120.2 (app q, *J* = 323.5 Hz), 46.8, 39.0, 34.6, 33.30, 33.28, 33.26, 33.2, 31.6, 31.3, 21.7.

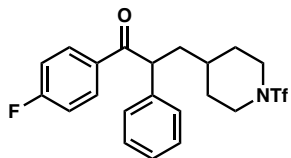
¹⁹F NMR (282 MHz, CDCl₃) δ -75.3.

FT-IR (neat film NaCl): 2960, 1598, 1444, 1389, 1227, 1177, 1150, 1116, 1065, 1049, 971, 942, 913, 852, 839, 812, 779, 760, 732, 707 cm⁻¹.

HR-MS (ESI) *m/z*: [M+K]⁺ Calculated for C₃₂H₃₆F₃KNO₅S₂: 674.1619; Measured: 674.1622.



1-(4-fluorophenyl)-2-phenylethan-1-one (251) was prepared according to literature procedures and matched the NMR data in the literature.⁴³



1-(4-fluorophenyl)-2-phenyl-3-(1-((trifluoromethyl)sulfonyl)piperidin-4-yl)propan-1-one (251)

To a flamed-dried flask was added KOtBu (576 mg, 1.1 equiv, 5.13 mmol). This flask was evacuated under vacuum and backfilled with nitrogen three times. To this was added THF (12 mL), and the flask was cooled to 0 °C. To this flask was added ketone **251** (1.00 g, 1.0 equiv, 4.67 mmol) in THF (10 mL), and the solution was stirred at 0 °C for 20 minutes. To this was added a solution of iodide **243** (1.75 g, 1.05 equiv, 4.90 mmol) in THF (8 mL). The reaction flask was allowed to warm up to room temperature overnight, and quenched by addition of saturated aqueous NH₄Cl (10 mL). The aqueous layer was extracted with ethyl acetate (3x 15 mL), dried over Na₂SO₄, filtered, concentrated *in vacuo*, and purified by silica flash column chromatography (10% diethyl ether in hexanes) to yield ketone **251** as a white solid (1.45 g, 70% yield).

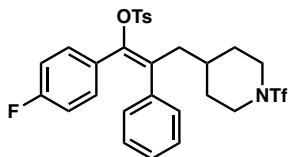
¹H NMR (400 MHz, CDCl₃) δ 8.02 – 7.88 (m, 2H), 7.32 – 7.19 (m, 5H), 7.11 – 6.98 (m, 2H), 4.58 (t, *J* = 7.4 Hz, 1H), 3.89 (ddt, *J* = 15.1, 12.8, 2.1 Hz, 2H), 2.92 (d, *J* = 15.3 Hz, 2H), 2.18 (ddd, *J* = 14.4, 7.8, 6.6 Hz, 1H), 1.88 (dt, *J* = 12.8, 2.5 Hz, 1H), 1.79 (dt, *J* = 13.7, 6.7 Hz, 1H), 1.71 (dt, *J* = 12.9, 2.6 Hz, 1H), 1.44 – 1.23 (m, 3H).

¹³C NMR (101 MHz, CDCl₃) δ 197.6, 165.8 d, *J* = 255.5 Hz), 139.1, 132.9 (d, *J* = 3.0 Hz), 131.5 (d, *J* = 9.2 Hz), 129.4, 128.1, 127.6, 120.2 (q, *J* = 323.9 Hz), 116.0, 115.8, 77.5, 77.2, 76.8, 50.5, 46.9, 40.2, 32.9, 32.1, 32.0.

¹⁹F NMR (376 MHz, CDCl₃) δ -75.8, -104.8.

FT-IR (neat film NaCl): 2929, 1680, 1597, 1505, 1448, 1386, 1275, 1226, 1187, 1155, 1118, 1052, 948, 741, 709 cm^{-1} .

HR-MS (ESI) m/z : $[\text{M}+\text{H}]^+$ Calculated for $\text{C}_{21}\text{H}_{22}\text{F}_4\text{NO}_3\text{S}$: 444.1251; Measured: 444.1252.



(E)-1-(4-fluorophenyl)-2-phenyl-3-(1-((trifluoromethyl)sulfonyl)piperidin-4-yl)prop-1-en-1-yl 4-methylbenzenesulfonate (132e)

To a flame-dried flask was added KOTu (555 mg, 1.6 equiv, 4.94 mmol) and THF (7 mL). This solution was cooled to 0 °C and ketone **252** (1.37 g, 1.0 equiv, 3.09 mmol) was added dropwise as a solution in THF (11 mL). This solution was stirred at 0 °C for 2 h. To this was quickly added solid toluenesulfonic anhydride (1.61 g, 1.6 equiv, 4.94 mmol). This solution was allowed to warm to room temperature and stirred for 1.5 hours. The reaction was diluted with ethyl acetate (15 mL) and water (15 mL). The organic layer was separated, and the aqueous layer was extracted with ethyl acetate (3 x 10 mL), dried over Na_2SO_4 , filtered, concentrated *in vacuo*, and purified by silica flash column chromatography (25% diethyl ether in hexanes) to give vinyl tosylate **132e** (700 mg, 38% yield) as a white solid. The olefin isomer is assigned to be *E* on the basis of NOESY NMR (observe NOE correlations between tosylate and piperidine fragment). Consistent with this assignment, the chemical shift of the allylic methylene protons (2.71 ppm in CDCl_3) is congruent to similarly reported *E* diaryl vinyl tosylates (typically ~2.7 ppm for allylic methylene in CDCl_3), which are distinct from the reported *Z* isomer (typically ~2.3 ppm).⁴²

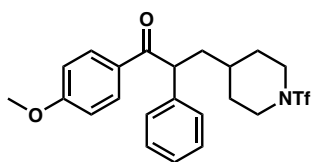
¹H NMR (400 MHz, CDCl₃) δ 7.55 – 7.36 (m, 2H), 7.24 – 7.16 (m, 3H), 7.13 (d, *J* = 8.1 Hz, 2H), 7.04 – 6.96 (m, 2H), 6.89 – 6.78 (m, 2H), 6.66 – 6.54 (m, 2H), 3.93 – 3.76 (m, 2H), 2.89 (t, *J* = 10.8 Hz, 2H), 2.71 (d, *J* = 6.0 Hz, 2H), 2.38 (s, 3H), 1.72 (dd, *J* = 12.8, 2.8 Hz, 2H), 1.46 – 1.28 (m, 3H).

¹³C NMR = (101 MHz, CDCl₃) δ 162.2 (d, *J* = 249.3 Hz) 145.0, 143.9, 138.0, 134.4, 132.8, 131.9 (d, *J* = 8.4 Hz), 129.8 (d, *J* = 3.5 Hz), 129.5, 129.3, 128.7, 128.0, 127.7, 120.2 (q, *J* = 323.5 Hz), 114.8, 114.6, 46.7, 38.9, 33.2, 31.6, 21.7.

¹⁹F NMR (282 MHz, CDCl₃) δ -75.3, -112.3.

FT-IR (neat film NaCl): 3052, 2927, 2874, 1649, 1600, 1508, 1493, 1445, 1385, 1334, 1306, 1276, 1227, 1189, 1178, 1150, 1116, 1080, 1065, 1049, 975, 942, 911, 852, 814, 776, 760, 735, 708, 673 cm⁻¹.

HR-MS (ESI) *m/z*: [M+Na]⁺ Calculated for C₂₈H₂₇F₄NNaO₅S₂: 620.1159; Measured: 620.1170.



1-(4-methoxyphenyl)-2-phenyl-3-(1-((trifluoromethyl)sulfonyl)piperidin-4-yl)propan-1-one (253)

To a flame-dried flask was added commercially-available 1-(4-methoxyphenyl)-2-phenylethan-1-one (1.30 g, 1.0 equiv, 5.74 mmol) then dissolved in THF (18 mL) and cooled to 0 °C. In a separate flask, a fresh solution of KO^{*t*}Bu (709 mg, 1.10 equiv, 6.3 mmol) in THF (18 mL) was prepared and added dropwise to the ketone while at 0 °C. The yellow solution was allowed to stir at 0 °C for 20 minutes. Then, a solution of iodide **243**

(2.15 g, 1.05 equiv, 6.0 mmol) in THF (10 mL) was added dropwise then allowed to warm to room temperature overnight. Once the reaction was completed by TLC analysis (15% ethyl acetate in hexanes), the reaction was quenched with saturated ammonium chloride and extracted with ethyl acetate (x3). The combined organics were washed once with brine, dried over Na₂SO₄, filtered, concentrated *in vacuo*, and purified by silica flash column chromatography (15% ethyl acetate in hexanes) to yield ketone **253** as a white solid (1.2 g, 46% yield).

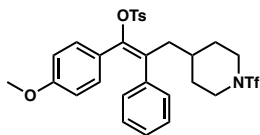
¹H NMR (400 MHz, CDCl₃) δ 8.01 – 7.91 (m, 2H), 7.29 (m, *J* = 3.3 Hz, 4H), 7.24 – 7.18 (m, 1H), 6.93 – 6.83 (m, 2H), 4.62 (dd, *J* = 8.1, 6.7 Hz, 1H), 3.90 (m, 2H), 3.82 (s, 3H), 3.01 – 2.85 (m, 2H), 2.21 (ddd, *J* = 14.4, 8.1, 6.5 Hz, 1H), 1.94 – 1.84 (m, 1H), 1.83 – 1.69 (m, 2H), 1.50 – 1.17 (m, 3H).

¹³C NMR (101 MHz, CDCl₃) δ 197.7, 163.6, 139.7, 131.0, 129.5, 129.2, 128.0, 127.3, 121.8, 120.2 (q, *J* = 323.6 Hz), 55.5, 50.0, 46.9, 40.3, 32.9, 32.0.

¹⁹F NMR (376 MHz, CDCl₃) δ -75.0 (br s).

FT-IR (neat film NaCl): 2939, 2844, 1672, 1600, 1574, 1510, 1493, 1453, 1419, 1386, 1356, 1312, 1253, 1226, 1182, 1146, 1117, 1050, 1029, 998, 950, 911, 833, 764, 734, 709 cm⁻¹.

HR-MS (ESI) *m/z*: [M+H]⁺ Calculated for C₂₂H₂₅F₃NO₄S: 456.1451; Measured: 456.1455.



(E)-1-(4-methoxyphenyl)-2-phenyl-3-(1-((trifluoromethyl)sulfonyl)piperidin-4-yl)prop-1-en-1-yl 4-methylbenzenesulfonate (132f)

To a flame-dried flask was added ketone **253** (1.05 g, 1.0 equiv, 2.30 mmol) then dissolved in THF (10.5 mL) and cooled to 0 °C. In a separate flask, a fresh solution of KO^tBu (413 mg, 1.60 equiv, 3.688 mmol) in THF (10.5 mL) was prepared and added dropwise to the ketone while at 0 °C. The yellow solution was allowed to stir at 0 °C for 90 minutes. Then, Ts₂O (1.20 g, 1.6 equiv, 3.688 mmol) was added as a solid in a single portion to the enolate solution with vigorous stirring then allowed to warm to room temperature (solution turns thick). Once the reaction was completed by TLC analysis (20% ethyl acetate in hexanes), the reaction was quenched with water and extracted with ethyl acetate (x3). The combined organics were washed once with brine, dried over Na₂SO₄, filtered, concentrated *in vacuo*, and purified by silica flash column chromatography (20% ethyl acetate in hexanes) and recrystallized from diethyl ether/hexanes to yield vinyl tosylate **132f** as a white crystalline solid (600 mg, 42% yield). The olefin isomer is assigned to be *E* on the basis of NOESY NMR (observe NOE correlations between tosylate and piperidine protons, as well as between the anisole and phenyl group protons). Consistent with this assignment, the chemical shift of the allylic methylene protons (2.69 ppm in CDCl₃) is congruent to similarly reported *E* diaryl vinyl tosylates (typically ~2.7 ppm for allylic methylene in CDCl₃), which are distinct from the reported *Z* isomer chemical shift (typically ~2.3 ppm for allylic methylene of corresponding *Z* vinyl tosylate in CDCl₃).⁴²

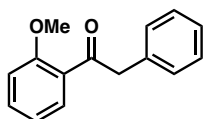
¹H NMR (400 MHz, CDCl₃) δ 7.50 – 7.42 (m, 2H), 7.22 – 7.14 (m, 3H), 7.13 – 7.08 (m, 2H), 7.07 – 6.98 (m, 2H), 6.82 – 6.74 (m, 2H), 6.46 – 6.38 (m, 2H), 3.89 – 3.80 (m, 2H), 3.68 (s, 3H), 2.89 (t, *J* = 12.1 Hz, 2H), 2.69 (d, *J* = 6.4 Hz, 2H), 2.37 (s, 3H), 1.71 (m, 2H), 1.39 – 1.23 (m, 3H).

¹³C NMR (101 MHz, CDCl₃) δ 159.3, 144.9, 144.5, 138.5, 134.6, 131.4, 131.2, 129.4, 128.6, 128.0, 127.4, 125.9, 120.2 (q, *J* = 323.7 Hz), 113.0, 55.2, 46.7, 38.8, 33.2, 31.5, 21.7

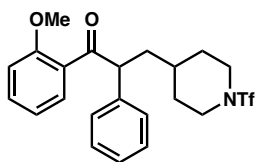
¹⁹F NMR (376 MHz, CDCl₃) δ -75.2 (br s).

FT-IR (neat film NaCl): 2927, 1607, 1509, 1443, 1386, 1294, 1250, 1226, 1176, 1150, 1115, 1048, 969, 942, 850, 836, 813, 774, 761, 733, 708, 674 cm⁻¹.

HR-MS (ESI) *m/z*: [M+Na]⁺ Calculated for C₂₉H₃₀F₃NNaO₆S₂: 632.1364; Measured: 632.1377.



1-(2-methoxyphenyl)-2-phenylethan-1-one (254) was prepared analogously to the reported literature procedures and matched the NMR data in the literature .⁴⁴



1-(2-methoxyphenyl)-2-phenyl-3-(1-((trifluoromethyl)sulfonyl)piperidin-4-yl)propan-1-one (255)

To a flame-dried flask was added ketone **254** (1.81 g, 1.0 equiv, 8.00 mmol) then dissolved in THF (12 mL) and cooled to 0 °C. In a separate flask, a fresh solution of KO^tBu (987 mg,

1.10 equiv, 8.80 mmol) in THF (12 mL) was prepared and added dropwise to the ketone while at 0 °C. The yellow solution was allowed to stir at 0 °C for 20 minutes. Then, a solution of iodide **243** (3.00 g, 1.05 equiv, 8.40 mmol) in THF (10 mL) was added dropwise then allowed to warm to room temperature overnight. Once the reaction was completed by TLC analysis (15% ethyl acetate in hexanes), the reaction was quenched with saturated ammonium chloride and extracted with ethyl acetate (x3). The combined organics were washed once with brine, dried over Na₂SO₄, filtered, concentrated *in vacuo*, and purified by silica flash column chromatography (15% diethyl ether in hexanes) then recrystallized from 3:1 hexanes/ethyl acetate to yield pure ketone **255** as a white crystals (1.95 g, 54% yield).

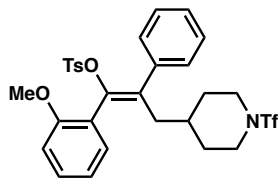
¹H NMR (400 MHz, CDCl₃) δ 7.30 (td, *J* = 7.3, 1.7 Hz, 2H), 7.23 – 7.07 (m, 5H), 6.86 – 6.77 (m, 2H), 4.70 (t, *J* = 7.5 Hz, 1H), 3.87 – 3.82 (m, 2H), 3.80 (s, 4H), 2.86 (q, *J* = 11.9 Hz, 2H), 2.13 (dt, *J* = 14.3, 7.2 Hz, 1H), 1.87 – 1.77 (m, 1H), 1.76 – 1.64 (m, 2H), 1.37 (m, 1H), 1.28 (m, 1H).

¹³C NMR (101 MHz, CDCl₃) δ 203.1, 157.6, 139.1, 133.2, 130.7, 128.9, 128.7, 128.6, 127.1, 120.9, 120.2 (q, *J* = 323.5 Hz), 111.5, 55.5, 54.3, 46.9, 39.6, 32.9, 32.1.

¹⁹F NMR (376 MHz, CDCl₃) δ -75.2 (br s)

FT-IR (neat film NaCl): 2940, 1674, 1597, 1485, 1465, 1437, 1386, 1287, 1246, 1226, 1184, 1147, 1119, 1051, 949, 761, 708 cm⁻¹.

HR-MS (ESI) *m/z*: [M+H]⁺ Calculated for C₂₂H₂₅F₃NO₄S: 456.1451; Measured: 456.1462.



(Z)-1-(2-methoxyphenyl)-2-phenyl-3-(1-((trifluoromethyl)sulfonyl)piperidin-4-yl)prop-1-en-1-yl 4-methylbenzenesulfonate (132g)

To a flame-dried flask was added ketone **255** (1.30 g, 1.0 equiv, 2.85 mmol) then dissolved in THF (8 mL) and cooled to 0 °C. In a separate flask, a fresh solution of KO^tBu (544 mg, 1.70 equiv, 4.85 mmol) in THF (8 mL) was prepared and added dropwise to the ketone while at 0 °C. The yellow solution was allowed to stir at 0 °C for 90 minutes. Then, Ts₂O (1.58 g, 1.7 equiv, 4.85 mmol) was added as a solid in a single portion to the enolate solution with vigorous stirring then allowed to warm to room temperature (solution turns thick). Once the reaction was completed by TLC analysis (20% ethyl acetate in hexanes), the reaction was quenched with water and extracted with ethyl acetate (x3). The combined organics were washed once with brine, dried over Na₂SO₄, filtered, concentrated *in vacuo*, and purified by silica flash column chromatography (20% ethyl acetate in hexanes) and recrystallized from diethyl ether/hexanes to yield pure vinyl tosylate **132g** as a white solid (700 mg, 40% yield). Note: typically, the higher R_f spot corresponds to the *E* olefin isomer (major), while the lower corresponds to the *Z* olefin isomer (minor). Due to difficulties in obtaining pure material of the higher R_f species, the lower R_f species was used instead, which was assigned to be *Z* by NOESY-NMR (observe NOE correlation between piperidine fragment and anisole arene, along with an NOE correlation between tosylate and phenyl ring). Note: NOESY experiments were conducted in C₆D₆ due to better resolution (CDCl₃ had many overlapping peaks). Both the CDCl₃ and C₆D₆ ¹H NMRs are reported. Consistent with this assignment, the chemical shift of the allylic methylene protons in

CDCl₃ (2.2–2.3 ppm) similar to reported *Z* diaryl vinyl tosylates (typically ~2.3 ppm for allylic methylene in CDCl₃), which are distinct from the reported *E* isomer chemical shift (typically ~2.7 ppm for allylic methylene of corresponding *Z* vinyl tosylate in CDCl₃).⁴²

¹H NMR (400 MHz, CDCl₃) δ 7.39 – 7.26 (m, 7H), 7.21 – 7.13 (m, 2H), 7.02 – 6.90 (m, 3H), 6.69 (dd, *J* = 8.3, 1.0 Hz, 1H), 3.69 (m, 5H), 2.78 (t, *J* = 12.4 Hz, 2H), 2.32 (m, 4H), 2.19 (dd, *J* = 14.0, 6.7 Hz, 1H), 1.71 – 1.58 (m, 2H), 1.31 – 1.16 (m, 1H), 1.08 (m, 1H), 0.99 – 0.83 (m, 1H).

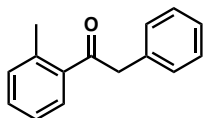
¹H NMR (400 MHz, C₆D₆) δ 7.53 (dd, *J* = 7.5, 1.7 Hz, 1H), 7.44 – 7.37 (m, 2H), 7.29 – 7.23 (m, 2H), 7.20 (dd, *J* = 8.4, 7.0 Hz, 2H), 7.13 – 7.06 (m, 1H), 7.00 (ddd, *J* = 8.3, 7.4, 1.8 Hz, 1H), 6.80 (td, *J* = 7.5, 1.1 Hz, 1H), 6.49 – 6.41 (m, 2H), 6.26 (dd, *J* = 8.3, 1.0 Hz, 1H), 3.37 (d, *J* = 10.0 Hz, 2H), 3.18 (s, 3H), 2.28 – 1.84 (m, 4H), 1.79 (s, 3H), 1.13 (d, *J* = 11.4 Hz, 2H), 0.99 – 0.81 (m, 1H), 0.70 – 0.44 (m, 2H).

¹³C NMR (101 MHz, CDCl₃) δ 157.6, 143.7, 140.5, 137.0, 134.1, 132.7, 131.9, 131.1, 128.9, 128.8, 128.3, 127.7, 127.5, 122.1, 120.2, 120.1 (app q, *J* = 323.4 Hz), 110.9, 55.4, 46.7, 39.0, 33.0, 31.5, 21.6.

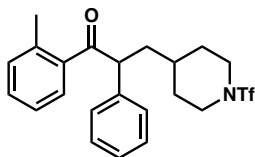
¹⁹F NMR (376 MHz, CDCl₃) δ -75.2 (br s).

FT-IR (neat film NaCl): 2942, 1598, 1494, 1459, 1386, 1367, 1226, 1180, 1177, 1149, 1116, 1050, 1007, 940, 837, 813, 781, 763, 733, 709, 681, 659 cm⁻¹.

HR-MS (ESI) *m/z*: [M+Na]⁺ Calculated for C₂₉H₃₀F₃NNaO₆S₂: 632.1364; Measured: 632.1375.

**2-phenyl-1-(*o*-tolyl)ethan-1-one (256)**

Prepared according to known procedures, and matched the reported NMR spectrum.⁴³

**2-phenyl-1-(*o*-tolyl)-3-(1-((trifluoromethyl)sulfonyl)piperidin-4-yl)propan-1-one (257)**

To a flamed-dried flask was added K₂OtBu (576 mg, 1.1 equiv, 5.1 mmol). This flask was evacuated under vacuum and backfilled with nitrogen three times. To this was added THF (15 mL), and the flask was cooled to 0 °C. To this flask was added ketone **256** (0.98 g, 1.0 equiv, 4.7 mmol) in THF (10 mL), and the solution was stirred at 0 °C for 20 minutes. To this was added a solution of iodide **243** (1.75 g, 1.05 equiv, 4.9 mmol) in THF (10 mL). The reaction flask was allowed to warm up to room temperature overnight, and quenched by addition of saturated aqueous NH₄Cl (10 mL). The aqueous layer was extracted with ethyl acetate (3x 20 mL), dried over Na₂SO₄, filtered, concentrated *in vacuo*, and purified by silica flash column chromatography (100% hexanes → 5% → 7% ethyl acetate in hexanes) to yield ketone **257** as a white solid (805 mg, 40% yield).

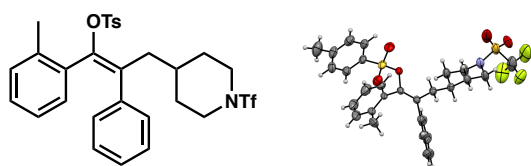
¹H NMR (300 MHz, CDCl₃) δ 7.61 – 7.47 (m, 1H), 7.38 – 7.27 (m, 2H), 7.24 – 7.01 (m, 5H), 4.49 (t, *J* = 7.5 Hz, 1H), 4.05 – 3.74 (m, 2H), 2.99 – 2.86 (m, 2H), 2.30 (s, 3H), 2.17 (dt, *J* = 14.0, 7.0 Hz, 1H), 1.99–1.80 (m, 2H), 1.75 (d, *J* = 11.8 Hz, 1H), 1.46–1.20 (m, 3H).

^{13}C NMR (101 MHz, CDCl_3) δ 203.1, 138.29, 138.26, 138.2, 131.8, 131.1, 129.0, 128.2, 127.7, 127.4, 125.5, 120.0 (q, $J = 323.6$ Hz), 53.3, 46.7, 39.2, 32.8, 32.1, 31.7, 20.8.

^{19}F NMR (282 MHz, CDCl_3) δ -75.2.

FT-IR (neat film NaCl): 2938, 2874, 1684, 1599, 1571, 1491, 1452, 1386, 1356, 1251, 1226, 1146, 1052, 997, 948, 761, 738, 708 cm^{-1} .

HR-MS (FD) m/z : $[\text{M}^+]$ Calculated for $\text{C}_{22}\text{H}_{24}\text{F}_3\text{NO}_3\text{S}$: 439.1419; Measured: 439.1412.



(E)-2-phenyl-1-(*o*-tolyl)-3-(1-((trifluoromethyl)sulfonyl)piperidin-4-yl)prop-1-en-1-yl 4-methylbenzenesulfonate (132h)

To a flame-dried flask was added KOtBu (308 mg, 1.5 equiv, 2.75 mmol) and THF (7 mL). This solution was cooled to 0 °C and ketone **257** (0.81 g, 1.0 equiv, 1.83 mmol) was added dropwise as a solution in THF (5 mL). This solution was stirred at 0 °C for 1 hour. To this was quickly added solid toluenesulfonic anhydride (0.90 g, 1.5 equiv, 2.75 mmol). This solution was allowed to warm to room temperature and stirred for 1 h. The reaction was diluted with ethyl acetate (15 mL) and 1M aqueous NaOH (5 mL). The organic layer was separated, and the aqueous layer was extracted with ethyl acetate (3 x 15 mL), dried over Na_2SO_4 , filtered, concentrated *in vacuo*, and purified by silica flash column chromatography (1% \rightarrow 20% ether in hexanes) to give vinyl tosylate **132h** (720 mg, 67% yield) as a white solid as single isomer, and was assigned to be the expected *E* isomer as determined by X-ray crystallography.

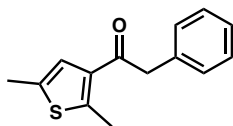
¹H NMR (300 MHz, CDCl₃) δ 7.31 (d, *J* = 8.4 Hz, 2H), 7.17 – 7.05 (m, 3H), 7.06 – 6.99 (m, 2H), 6.95 (dq, *J* = 6.9, 3.1, 2.3 Hz, 2H), 6.90 – 6.85 (m, 1H), 6.79 (t, *J* = 8.1 Hz, 2H), 3.88 (d, *J* = 12.9 Hz, 2H), 2.92 (dd, *J* = 13.7, 7.2 Hz, 3H), 2.74 (dd, *J* = 13.9, 4.8 Hz, 1H), 2.33 (s, 3H), 1.99 (s, 3H), 1.85 – 1.70 (m, 2H), 1.52 – 1.03 (m, 3H).

¹³C NMR (101 MHz, CDCl₃) δ 144.7, 144.2, 137.7, 137.4, 134.1, 133.0, 132.6, 132.1, 129.6, 129.0, 128.7, 128.6, 128.1, 127.5, 127.3, 125.0, 120.0 (q, *J* = 323.5 Hz), 46.6, 37.9, 33.3, 31.7, 31.1, 21.5, 19.8.

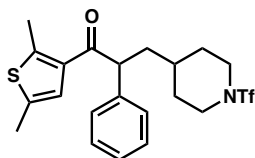
¹⁹F NMR (282 MHz, CDCl₃) δ -75.0.

FT-IR (neat film NaCl): 2927, 2875, 1598, 1494, 1387, 1226, 1138, 1150, 1117, 1050, 1006, 940, 837, 807, 789, 709 cm⁻¹.

HR-MS (ESI) *m/z*: [M+Na]⁺ Calculated for C₂₉H₃₀F₃NO₅S₂Na: 616.1415; Measured: 616.1416.



1-(2,5-dimethylthiophen-3-yl)-2-phenylethan-1-one (258) was prepared according to known procedures, and matched literature reported NMR spectra.⁴⁵



1-(2,5-dimethylthiophen-3-yl)-2-phenyl-3-(1-((trifluoromethyl)sulfonyl)piperidin-4-yl)propan-1-one (259)

To a flamed dried flask was added K₂OtBu (890 mg, 1.1 equiv, 7.9 mmol) then evacuated backfilled with nitrogen three times. To this was added THF (15 mL), and the flask was cooled to 0 °C. Ketone **258** (1.66 g, 1.0 equiv, 7.2 mmol) in THF (10 mL) was added, and the solution was stirred at 0 °C for 20 minutes. To this was added a solution of iodide **243** (2.7 g, 1.05 equiv, 7.6 mmol) in THF (10 mL). The reaction flask was allowed to warm up to room temperature overnight, and quenched by addition of saturated aqueous NH₄Cl (10 mL). The aqueous layer was extracted with ethyl acetate (3x 15 mL), dried over Na₂SO₄, filtered, concentrated *in vacuo*, and purified by silica flash column chromatography (0 → 5% ethyl acetate in hexanes) to yield ketone **259** as an off-white solid (1.81 g, 55% yield).

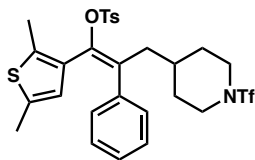
¹H NMR (400 MHz, CDCl₃) δ 7.34 – 7.28 (m, 2H), 7.27 – 7.18 (m, 3H), 6.95 (d, *J* = 1.3 Hz, 1H), 4.32 (dd, *J* = 7.9, 7.0 Hz, 1H), 3.90 (tdd, *J* = 11.4, 4.2, 2.2 Hz, 2H), 2.94 (q, *J* = 12.5 Hz, 2H), 2.64 (s, 3H), 2.35 (d, *J* = 1.0 Hz, 3H), 2.15 (ddd, *J* = 14.4, 8.0, 6.6 Hz, 1H), 1.87 (dt, *J* = 12.5, 2.5 Hz, 1H), 1.77 – 1.60 (m, 2H), 1.53 – 1.15 (m, 3H).

¹³C NMR (101 MHz, CDCl₃) δ 195.1, 149.1, 139.3, 135.1, 134.9, 129.0, 128.0, 127.1, 125.5, 120.0 (q, *J* = 323.7 Hz), 52.9, 46.7, 39.9, 32.8, 31.9, 31.8, 16.2, 15.0.

¹⁹F NMR (282 MHz, CDCl₃) δ -75.0.

FT-IR (neat film NaCl): 2921, 1668, 1476, 1450, 1387, 1361, 1186, 1149, 1114, 1052, 949, 937, 738, 709 cm⁻¹.

HR-MS (ESI) m/z : $[M+H]^+$ Calculated for $C_{21}H_{25}F_3NO_3S_2$: 460.1221; Measured: 460.1221.



(E)-1-(2,5-dimethylthiophen-3-yl)-2-phenyl-3-(1((trifluoromethyl)sulfonyl)piperidin-4-yl)prop-1-en-1-yl 4-methylbenzenesulfonate (132i)

To a flame dried flask was added KOtBu (366 mg, 1.5 equiv, 3.2 mmol) and THF (9 mL). This solution was cooled to 0°C and **259** (1.0 g, 1 equiv, 2.1 mmol) was added dropwise as a solution in THF (9 mL). This solution was stirred at 0°C for 1h. To this was quickly added solid toluenesulfonic anhydride (1.1 g, 1.5 equiv, 3.2 mmol). This solution was allowed to warm to room temperature and stirred for 3 hours. The reaction was diluted with ethyl acetate (15 mL) and 1M aqueous NaOH (5 mL). The organic layer was separated, and the aqueous layer was extracted with ethyl acetate (3 x 15 mL), dried over Na₂SO₄, filtered, concentrated *in vacuo*, and purified by silica flash column chromatography (2% → 20% ether in hexanes) to give vinyl tosylate **132i** (460 mg, 29% yield) as a single isomer. The olefin isomer is assigned to be *E* by NOESY-NMR (correlation between thiophene CH₃ group and adjacent phenyl arene).

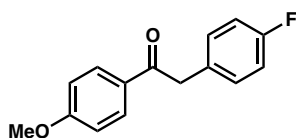
¹H NMR (300 MHz, CDCl₃) δ 7.40 (d, J = 8.1 Hz, 2H), 7.25 – 7.14 (m, 4H), 7.11 (d, J = 7.9 Hz, 2H), 7.04 – 6.95 (m, 2H), 5.98 (s, 1H), 3.86 (d, J = 12.9 Hz, 2H), 2.90 (s, 1H), 2.81 (s, 2H), 2.48 – 2.34 (m, 4H), 2.04 (s, 2H), 1.74 (d, J = 12.9 Hz, 2H), 1.69 (s, 3H), 1.50 – 1.14 (m, 3H).

^{13}C NMR (101 MHz, CDCl_3) δ 144.0, 140.5, 137.9, 137.7, 135.4, 134.4, 132.8, 129.5, 129.0, 128.6, 128.2, 127.5, 127.2, 126.3, 120.0 (q, $J = 323.6$ Hz), 46.6, 37.8, 33.5, 31.3, 21.5, 14.6, 13.8.

^{19}F NMR (282 MHz, CDCl_3) δ -75.2.

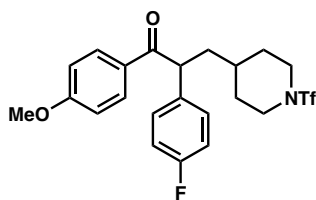
FT-IR (neat film NaCl): 2899, 1387, 1274, 1223, 1172, 1150, 1110, 1048, 958, 784, 753, 734 cm^{-1} .

HR-MS (ESI) m/z : $[\text{M}+\text{Na}]^+$ Calculated for $\text{C}_{28}\text{H}_{30}\text{F}_3\text{NO}_5\text{S}_3\text{Na}$: 636.1136; Measured: 636.1147.



2-(4-fluorophenyl)-1-(4-methoxyphenyl)ethan-1-one (260)

Prepared according to literature procedures and matched the NMR data in the literature.⁴⁵



2-(4-fluorophenyl)-1-(4-methoxyphenyl)-3-(1-((trifluoromethyl)sulfonyl)piperidin-4-yl)propan-1-one (261)

To a flamed-dried flask was added KOTBu (884 mg, 1.1 equiv, 7.88 mmol). This flask was evacuated under vacuum and backfilled with nitrogen three times. To this was added THF (18 mL), and the flask was cooled to 0 °C. To this flask was added ketone **260** (1.750 g, 1 equiv, 7.164 mmol) in THF (16 mL), and the solution was stirred at 0 °C for 20 minutes.

To this was added a solution of iodide **243** (2.69 g, 1.05 equiv, 7.52 mmol). The reaction flask was allowed to warm up to room temperature overnight, and quenched by addition of saturated aqueous NH₄Cl (10 mL). The aqueous layer was extracted with ethyl acetate (3x 15 mL), dried over Na₂SO₄, filtered, concentrated *in vacuo*, and purified by silica flash column chromatography (30% diethyl ether in hexanes) to yield ketone **261** as a white solid (2.00 g, 59% yield).

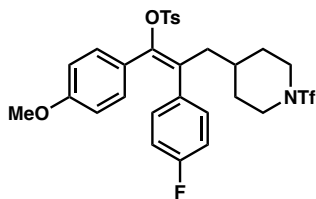
¹H NMR (400 MHz, CDCl₃) δ 7.98 – 7.90 (m, 2H), 7.30 – 7.23 (m, 2H), 7.04 – 6.95 (m, 2H), 6.93 – 6.85 (m, 2H), 4.63 (dd, *J* = 8.1, 6.8 Hz, 1H), 3.96 – 3.86 (m, 2H), 3.84 (s, 3H), 2.93 (q, *J* = 13.7 Hz, 2H), 2.24 – 2.16 (m, 1H), 1.88 (dt, *J* = 12.4, 2.6 Hz, 1H), 1.80 – 1.71 (m, 2H), 1.44 – 1.26 (m, 3H).

¹³C NMR (101 MHz, CDCl₃) δ 197.6, 163.8, 162.0 (d, *J* = 246.2 Hz), 135.4 (d, *J* = 3.3 Hz), 131.0, 129.6 (d, *J* = 8.0 Hz), 129.3, 120.2 (q, *J* = 323.5 Hz), 116.2, 116.0, 114.0, 55.6, 49.0, 46.9, 40.4, 33.0, 32.0.

¹⁹F NMR (376 MHz, CDCl₃) δ -75.2, -115.2.

FT-IR (neat film NaCl): 2941, 1672, 1600, 1575, 1508, 1460, 1421, 1385, 1313, 1252, 1226, 1172, 1151, 1117, 1049, 1030, 949, 836, 709 cm⁻¹.

HR-MS (ESI) *m/z*: [M+H]⁺ Calculated for C₂₂H₂₄F₄NO₄S: 474.1357; Measured: 474.1356.



(E)-2-(4-fluorophenyl)-1-(4-methoxyphenyl)-3-(1-((trifluoromethyl)sulfonyl)piperidin-4-yl)prop-1-en-1-yl 4-methylbenzenesulfonate (132j)

To a flame-dried flask was added KOtBu (728 mg, 1.6 equiv, 6.49 mmol) and THF (10.6 mL). This solution was cooled to 0 °C and ketone **261** (1.92 g, 1.0 equiv, 4.06 mmol) was added dropwise as a solution in THF (10.5 mL). This solution was stirred at 0 °C for 2 hours. To this was quickly added solid toluenesulfonic anhydride (2.12 g, 1.6 equiv, 6.49 mmol). This solution was allowed to warm to room temperature and stirred for 1.5 hours. The reaction was diluted with ethyl acetate (15 mL) and water (15 mL). The organic layer was separated, and the aqueous layer was extracted with ethyl acetate (3 x 10 mL), dried over Na₂SO₄, filtered, concentrated *in vacuo*, and purified by silica flash column chromatography (25% ether in hexanes) to give vinyl tosylate **132j** (1.0 g, 40% yield). The olefin isomer is assigned to be *E* on the basis of NOESY NMR (observe NOE correlations between tosylate and piperidine fragments). Consistent with this assignment, the chemical shift of the allylic methylene protons (2.68 ppm in CDCl₃) is congruent to similarly reported *E* diaryl vinyl tosylates (typically ~2.7 ppm for allylic methylene in CDCl₃), which are distinct from the reported *Z* isomer chemical shift (typically ~2.3 ppm for allylic methylene of corresponding *Z* vinyl tosylate in CDCl₃).⁴²

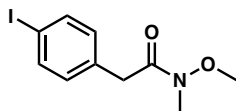
¹H NMR (400 MHz, CDCl₃) δ 7.44 (d, *J* = 8.4 Hz, 2H), 7.13 – 7.07 (m, 2H), 7.02 – 6.96 (m, 2H), 6.91 – 6.84 (m, 2H), 6.79 – 6.73 (m, 2H), 6.47 – 6.40 (m, 2H), 3.85 (dt, *J* = 12.2, 2.9 Hz, 2H), 3.69 (s, 3H), 2.90 (t, *J* = 12.0 Hz, 2H), 2.68 (d, *J* = 6.2 Hz, 2H), 2.37 (s, 3H), 1.74 – 1.66 (m, 2H), 1.37 (dt, *J* = 12.2, 6.1 Hz, 3H).

¹³C NMR = (101 MHz, CDCl₃) δ 161.9 (d, *J* = 247.4 Hz), 159.4, 145.2, 144.6, 134.5, 134.4 (d, *J* = 3.4 Hz), 131.4, 131.1 (d, *J* = 7.8 Hz), 130.2, 129.4, 128.0, 125.7, 120.2 (app q, *J* = 323.5 Hz), 115.8, 115.6, 113.2, 55.3, 46.7, 38.8, 33.3, 31.6, 21.7.

¹⁹F NMR (282 MHz, CDCl₃) δ -75.3, -114.2

FT-IR (neat film NaCl): 2941, 1604, 1509, 1464, 1446, 1385, 1295, 1251, 1226, 1189, 1177, 1151, 1115, 1095, 1067, 1049, 972, 943, 855, 839, 815, 784, 728, 709 cm⁻¹.

HR-MS (ESI) *m/z*: [M+Na]⁺ Calculated for C₂₉H₂₉F₄NNaO₆S₂: 650.1265; Measured: 650.1279.



2-(4-iodophenyl)-*N*-methoxy-*N*-methylacetamide (262)

Prepared according to similar published procedures³⁹, to a flame-dried flask was added commercially-available 2-(4-iodophenyl)acetic acid (5.0 g, 1.0 equiv, 19.1 mmol), *N*,*O*-dimethylhydroxylammonium chloride (2.8 g, 1.5 equiv, 28.6 mmol), and EDCI (5.5 g, 1.5 equiv, 28.6 mmol). While under N₂ atmosphere, 80 mL of dry DCM was then added. Then, DMAP (3.50 g, 1.5 equiv, 28.6 mmol) was added as a solid in one portion and the mixture was allowed stir overnight under N₂ at room temperature. The next morning, the reaction was quenched with water and extracted with DCM (x3). The combined organics were

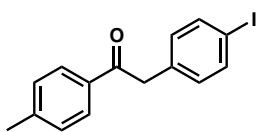
washed with 1M HCl twice, then washed with brine, then dried over Na₂SO₄ and filtered. Concentration afforded a tan solid that was pure by NMR, and was taken forward as is (5.4 g, 93% yield).

¹H NMR (400 MHz, CDCl₃) δ 7.69 – 7.58 (m, 2H), 7.09 – 6.99 (m, 2H), 3.71 (s, 2H), 3.63 (s, 3H), 3.19 (s, 3H).

¹³C NMR (101 MHz, CDCl₃) δ 171.8, 137.6, 134.6, 131.5, 92.3, 61.4, 38.9, 32.3.

FT-IR (neat film NaCl): 2932, 1670, 1400, 998, 682 cm⁻¹.

HR-MS (ESI) m/z: [M+H]⁺ Calculated for C₁₀H₁₃INO₂: 305.9985; Measured: 305.9988.



2-(4-iodophenyl)-1-(p-tolyl)ethan-1-one (263) was prepared according to similar reported procedure⁴⁰. Magnesium turnings (818 mg, 1.8 equiv, 33.63 mmol) were flame-dried under high vacuum in a round bottom flask (x3) then suspended in dry THF (144 mL). 1-Bromo-4-methylbenzene (6.66 g, 2.2 equiv, 38.9 mmol) was added followed by a small grain of I₂. The solution was allowed to stir with gentle heating *via* a heat gun until the purple-brown color of the I₂ disappears. The suspension was then stirred until all the magnesium chunks are visibly consumed. At this point, the reaction is cooled to 0 °C then Weinreb amide **262** (5.40 g, 1.0 equiv, 17.70 mmol) was added dropwise. The reaction is monitored closely by TLC to determine starting material consumption (usually 5–20 minutes), then quenched with 30 mL saturated ammonium chloride while at 0 °C. The reaction is extracted with diethyl ether (x3), then the combined organics are washed with

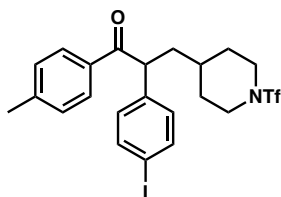
brine, dried over MgSO₄, filtered through a short pad of silica (wash through with diethyl ether), and concentrated *in vacuo*. Pure material was obtained *via* silica flash column chromatography (15% ethyl acetate/hexanes with 2% DCM to help with solubility), furnishing ketone **263** as a white solid (2.85 g, 48% yield).

¹H NMR (400 MHz, CDCl₃) δ 7.91 – 7.79 (m, 2H), 7.74 – 7.51 (m, 2H), 7.30 – 7.19 (m, 2H), 7.07 – 6.87 (m, 2H), 4.18 (s, 2H), 2.39 (s, 3H).

¹³C NMR (101 MHz, CDCl₃) δ 196.8, 144.4, 137.8, 134.5, 134.0, 131.7, 129.5, 128.8, 92.5, 44.9, 21.8.

FT-IR (neat film NaCl): 2933, 1677, 1606, 1482, 1444, 1385, 1252, 1183, 1146, 1049, 1006, 948, 815, 765, 709 cm⁻¹.

HR-MS (ESI) m/z: [M+H]⁺ Calculated for C₁₀H₁₃INO₂: 337.0084; Measured: 337.0084.



2-(4-iodophenyl)-1-(*p*-tolyl)-3-(1-((trifluoromethyl)sulfonyl)piperidin-4-yl)propan-1-one (264)

To a flamed-dried flask was added KOtBu (0.88 g, 1.1 equiv, 7.9 mmol). This flask was evacuated under vacuum and backfilled with nitrogen three times. To this was added THF (11 mL), and the flask was cooled to 0 °C. To this flask was added ketone **263** (2.4 g, 1.0 equiv, 7.1 mmol) in THF (15 mL), and the solution was stirred at 0 °C for 20 minutes. To this was added a solution of iodide **243** (2.7 g, 1.05 equiv, 7.5 mmol) in THF (10 mL). The

reaction flask was allowed to warm up to room temperature overnight, and quenched by addition of saturated aqueous NH_4Cl (10 mL). The aqueous layer was extracted with ethyl acetate (3x 15 mL), dried over Na_2SO_4 , filtered, concentrated *in vacuo*, and purified by silica flash column chromatography (15% ether in hexanes) to yield ketone **264** as a white solid (2.7 g, 67% yield).

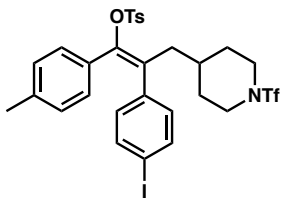
^1H NMR (400 MHz, CDCl_3) δ 7.83 (d, $J = 8.3$ Hz, 2H), 7.62 (d, $J = 8.3$ Hz, 2H), 7.25 – 7.17 (m, 2H), 7.04 (d, $J = 8.4$ Hz, 2H), 4.65 – 4.54 (m, 1H), 3.90 (tq, $J = 13.0, 2.0$ Hz, 2H), 2.93 (q, $J = 13.4$ Hz, 2H), 2.37 (s, 3H), 2.18 (ddd, $J = 14.4, 8.0, 6.6$ Hz, 1H), 1.87 (dt, $J = 12.7, 2.7$ Hz, 1H), 1.79 – 1.70 (m, 2H), 1.42 – 1.25 (m, 3H).

^{13}C NMR (101 MHz, CDCl_3) δ 198.4, 144.5, 139.2, 138.3, 133.8, 130.1, 129.6, 128.9, 120.2 (q, $J = 323.5$ Hz), 92.9, 49.6, 46.8, 40.1, 33.0, 32.1, 32.0, 21.8.

^{19}F NMR (376 MHz, CDCl_3) δ -75.1

FT-IR (neat film NaCl): 2933, 1677, 1606, 1482, 1444, 1385, 1226, 1183, 1146, 1049, 1006, 948 cm^{-1} .

HR-MS (ESI) m/z : $[\text{M}+\text{H}]^+$ Calculated for $\text{C}_{22}\text{H}_{24}\text{F}_3\text{INO}_3\text{S}$: 566.0468; Measured: 566.0466.



(*E*)-2-(4-iodophenyl)-1-(*p*-tolyl)-3-(1-((trifluoromethyl)sulfonyl)piperidin-4-yl)prop-1-en-1-yl 4-methylbenzenesulfonate (132k**)**

To a flame-dried flask was added KOtBu (302 mg, 1.6 equiv, 2.69 mmol) and THF (4.4 mL). This solution was cooled to 0°C and ketone **264** (0.950 g, 1.0 equiv, 1.68 mmol) was added dropwise as a solution in THF (4.4 mL). This solution was stirred at 0 °C for 2 hours. To this was quickly added solid toluenesulfonic anhydride (877 mg, 1.6 equiv, 2.69 mmol). This solution was allowed to warm to room temperature and stirred for 1.5 hours. The reaction was diluted with ethyl acetate (15 mL) and water (15 mL). The organic layer was separated, and the aqueous layer was extracted with ethyl acetate (3 x 10 mL), dried over Na₂SO₄, filtered, concentrated *in vacuo*, and purified by silica flash column chromatography (25% ether in hexanes) to deliver vinyl tosylate **132k** (475 mg, 39% yield). The olefin isomer is assigned to be *E* on the basis of NOESY NMR (observe NOE correlations between tosylate and piperidine fragments). Consistent with this assignment, the chemical shift of the allylic methylene protons (2.67 ppm in CDCl₃) is congruent to similarly reported *E* diaryl vinyl tosylates (typically ~2.7 ppm for allylic methylene in CDCl₃), which are distinct from the reported *Z* isomer chemical shift (typically ~2.3 ppm for allylic methylene of corresponding *Z* vinyl tosylate in CDCl₃)⁴²

¹H NMR (400 MHz, CDCl₃) δ 7.50 (d, J = 8.4 Hz, 2H), 7.43 (d, J = 8.4 Hz, 2H), 7.13 – 7.05 (m, 2H), 6.80 – 6.70 (m, 6H), 3.85 (dd, J = 13.2, 3.9 Hz, 2H), 3.05 – 2.79 (m, 2H),

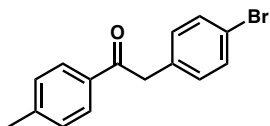
2.67 (d, $J = 5.9$ Hz, 2H), 2.37 (s, 3H), 2.20 (s, 3H), 1.74 – 1.64 (m, 2H), 1.42 – 1.24 (m, 5H).

^{13}C NMR = (101 MHz, CDCl_3) δ 145.5, 144.7, 138.5, 138.0, 137.7, 134.4, 131.3, 130.7, 130.2, 123.0, 129.4, 128.5, 128.0, 120.2 (app q, $J = 323.7$ Hz), 93.2, 46.7, 38.7, 33.3, 31.7, 31.5, 22.8, 21.7, 21.4, 14.3.

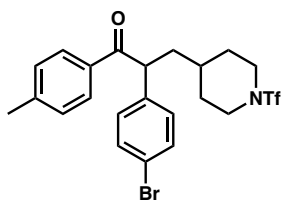
^{19}F NMR (282 MHz, CDCl_3) δ -75.2.

FT-IR (neat film NaCl): 2921, 1597, 1483, 1446, 1387, 1226, 1177, 1150, 1115, 1049, 973, 942, 849, 825, 763, 724, 708 cm^{-1} .

HR-MS (ESI) m/z : $[\text{M}+\text{Na}]^+$ Calculated for $\text{C}_{29}\text{H}_{29}\text{F}_3\text{INNaO}_5\text{S}_2$: 742.0376; Measured: 742.0385.



2-(4-bromophenyl)-1-(*p*-tolyl)ethan-1-one (265) was prepared according to known procedures, and the NMR spectrum matched reported literature spectra.⁴³



2-(4-bromophenyl)-1-(*p*-tolyl)-3-(1-((trifluoromethyl)sulfonyl)piperidin-4-yl)propan-1-one (266)

To a flamed-dried flask was added K₂CO₃ (615 mg, 1.1 equiv, 5.5 mmol). This flask was evacuated under vacuum and backfilled with nitrogen three times. To this was added THF

(15 mL), and the flask was cooled to 0 °C. To this flask was added ketone **265** (1.44 g, 1.0 equiv, 4.9 mmol) in THF (10 mL), and the solution was stirred at 0 °C for 20 minutes. To this was added a solution of iodide **243** (1.87 g, 1.05 equiv, 5.2 mmol) in THF (10 mL). The reaction flask was allowed to warm up to room temperature overnight, and quenched by addition of saturated aqueous NH₄Cl (10 mL). The aqueous layer was extracted with ethyl acetate (3x 15 mL), dried over Na₂SO₄, filtered, concentrated *in vacuo*, and purified by silica flash column chromatography (2% → 10% ethyl acetate in hexanes) to yield ketone **266** as a white solid (1.35 g, 52% yield).

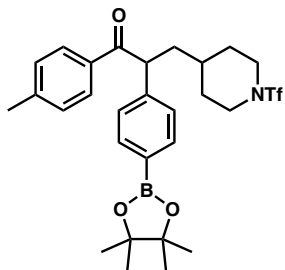
¹H NMR (400 MHz, CDCl₃) δ 7.83 (dd, *J* = 8.3, 2.6 Hz, 2H), 7.42 (dd, *J* = 8.5, 2.6 Hz, 2H), 7.29 – 7.03 (m, 4H), 4.62 (t, *J* = 7.8 Hz, 1H), 3.90 (t, *J* = 13.1 Hz, 2H), 2.93 (d, *J* = 14.7 Hz, 2H), 2.37 (s, 3H), 2.19 (dt, *J* = 14.9, 7.5 Hz, 1H), 1.87 (d, *J* = 13.2 Hz, 1H), 1.75 (dt, *J* = 13.3, 7.5 Hz, 2H), 1.35 (d, *J* = 16.5 Hz, 3H).

¹³C NMR (101 MHz, CDCl₃) δ 198.2, 144.3, 138.3, 133.6, 132.2, 129.7, 129.4, 128.7, 120.0 (q, *J* = 323.6 Hz), 49.3, 46.7, 39.9, 32.8, 31.9, 31.8, 21.6.

¹⁹F NMR (282 MHz, CDCl₃) δ -75.0.

FT-IR (neat film NaCl): 2942, 2870, 1677, 1606, 1486, 1386, 1362, 1227, 1149, 1048, 948, 708 cm⁻¹.

HR-MS (ESI) *m/z*: [M+H]⁺ Calculated for C₂₂H₂₄BrF₃NO₃S: 518.0612; Measured: 518.0587.



2-(4-(4,4,5,5-tetramethyl-1,3,2-dioxaborolan-2-yl)phenyl)-1-(*p*-tolyl)-3-(1-((trifluoromethyl)sulfonyl)piperidin-4-yl)propan-1-one (267)

To a 100 mL Schlenk flask was added ketone **266** (800 mg, 1.0 equiv, 1.5 mmol), potassium acetate (530 mg, 3.5 equiv, 5.4 mmol), bis(pinacolato)diboron (470 mg, 1.2 equiv, 1.8 mmol), and 1,4-dioxane (10 mL). This solution was degassed by freeze-pump-thaw (3 x cycles of 10 minutes under vacuum when frozen). To this degassed solution was added Pd(dppf)Cl₂ under a stream of N₂. The reaction was then sealed and heated to 80 °C for 15 hours. Saturated aqueous NH₄Cl (10 mL) was added and the solution was diluted with ethyl acetate (15 mL). The organic layer was separated and the aqueous layer was extracted with ethyl acetate (3 x 15 mL). The organics were washed with brine, dried over Na₂SO₄, concentrated, filtered, and purified by silica flash column chromatography (0%→20% ethyl acetate in hexanes) to give **267** as an orange oil (799 mg, 94% yield).

¹H NMR (400 MHz, CDCl₃) δ 7.83 (d, *J* = 8.3 Hz, 2H), 7.74 (d, *J* = 8.0 Hz, 2H), 7.28 (d, *J* = 7.8 Hz, 2H), 7.19 – 7.14 (m, 2H), 4.64 (t, *J* = 7.4 Hz, 1H), 4.01 – 3.75 (m, 2H), 2.91 (q, *J* = 13.3 Hz, 2H), 2.35 (s, 3H), 2.18 (dt, *J* = 14.3, 7.2 Hz, 1H), 1.95 – 1.85 (m, 1H), 1.80 (dt, *J* = 13.7, 6.6 Hz, 1H), 1.71 (dd, *J* = 12.8, 2.8 Hz, 1H), 1.31 (s, 12H).

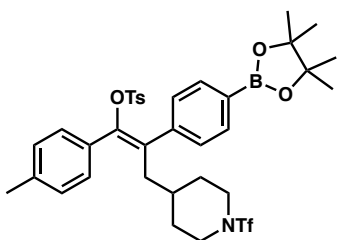
¹³C NMR (101 MHz, CDCl₃) δ 198.4, 144.0, 142.4, 135.5, 133.8, 129.3, 128.7, 127.4, 120.0 (q, *J* = 323.1 Hz), 83.8, 50.4, 46.7, 39.8, 32.7, 32.0, 31.8, 24.8 (d, *J* = 1.9 Hz), 21.5.

^{11}B NMR (128 MHz, CDCl_3) δ 30.1.

^{19}F NMR (282 MHz, CDCl_3) δ -75.8.

FT-IR (neat film NaCl): 2978, 2925, 1774, 1677, 1607, 1513, 1445, 1388, 1362, 1272, 1252, 1226, 1182, 1145, 1090, 1050, 948, 828, 709 cm^{-1} .

HR-MS (ESI) m/z : $[\text{M}+\text{H}]^+$ Calculated for $\text{C}_{28}\text{H}_{35}\text{BF}_3\text{NO}_5\text{S}$: 566.2359; Measured: 566.2355.



(Z)-2-(4-(4,4,5,5-tetramethyl-1,3,2-dioxaborolan-2-yl)phenyl)-1-(p-tolyl)-3-(1-((trifluoromethyl)sulfonyl)piperidin-4-yl)prop-1-en-1-yl 4-methylbenzenesulfonate (1321)

To a 50 mL Schlenk flask was added ketone **267** (435 mg, 1.0 equiv, 0.77 mmol) and THF (8 mL). To this solution was added KH (309 mg, 3.0 equiv, 2.3 mmol, 30% w/w). The flask was heated to 75 °C for 3 hours and cooled to room temperature. Toluenesulfonic anhydride (502 mg, 2.0 equiv, 1.5 mmol) was added under a stream of nitrogen and the reaction was allowed to stir at room temperature for 30 minutes. To this was added satd. aq. NH_4Cl (5 mL carefully!) and then diluted with ethyl acetate (10 mL). The organic layer was separated and the aqueous layer was extracted with ethyl acetate (3 x 10 mL). The combined organic layers were dried over Na_2SO_4 , filtered, concentrated *in vacuo*, and purified by silica flash column chromatography (0% \rightarrow 10% \rightarrow 20% \rightarrow 30% ether in hexanes) to yield vinyl tosylate **1321** (143 mg, 26% yield) as an off-white solid. The olefin isomer is assigned to be Z by NOESY-NMR (correlation of tolyl arene not on tosylate and

piperidine fragment). Consistent with this assignment, the chemical shift of the allylic methylene protons (2.33 ppm in CDCl₃) is congruent to similarly reported *Z* diaryl vinyl tosylates (typically ~2.3 ppm for allylic methylene in CDCl₃), which are distinct from the reported *E* isomer chemical shift (typically ~2.7 ppm for allylic methylene of corresponding *Z* vinyl tosylate in CDCl₃).⁴²

¹H NMR (400 MHz, CDCl₃) δ 7.64 (d, *J* = 8.1 Hz, 2H), 7.16 (dd, *J* = 9.5, 8.1 Hz, 4H), 7.05 (dd, *J* = 8.1, 4.0 Hz, 4H), 6.85 (d, *J* = 8.0 Hz, 2H), 3.63 (d, *J* = 12.9 Hz, 2H), 2.66 (t, *J* = 12.7 Hz, 2H), 2.33 (d, *J* = 7.1 Hz, 2H), 2.30 (s, 3H), 2.26 (s, 3H), 1.53 (dd, *J* = 13.8, 3.2 Hz, 2H), 1.31 (s, 12H), 1.17 – 1.06 (m, 2H), 1.04 – 0.81 (m, 2H).

¹³C NMR (101 MHz, CDCl₃) δ 143.8, 143.5, 139.8, 139.0, 134.5, 133.9, 130.6, 130.3, 129.7, 128.9, 128.8, 127.8, 127.5, 119.9 (q, *J* = 323.0 Hz), 83.8, 46.4, 38.6, 33.1, 31.2, 30.3, 24.9, 21.5, 21.3.

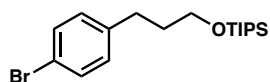
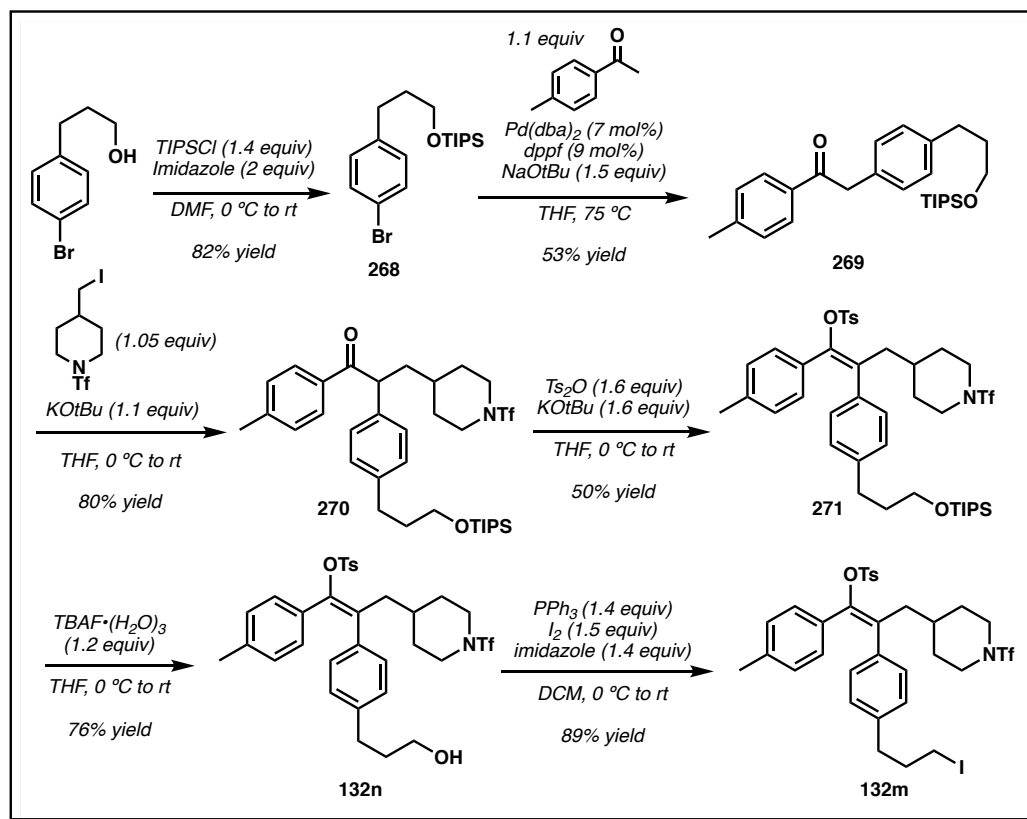
¹¹B NMR (128 MHz, CDCl₃) δ 29.1.

¹⁹F NMR (282 MHz, CDCl₃) δ -75.2.

FT-IR (neat film NaCl): 2943, 1398, 1225, 1177, 1144, 1092, 858, 829, 709 cm⁻¹.

HR-MS (ESI) *m/z*: [M+H]⁺ Calculated for C₃₅H₄₁BF₃NO₇S₂K: 758.2006; Measured:

758.2027.

Figure 4.3: Representative scheme for the synthesis of substrates **132n** and **132m****(3-(4-bromophenyl)propoxy)triisopropylsilane (268)**

To a flame-dried flask equipped with a stir bar was added imidazole (3.1 g, 2.0 equiv, 46.49 mmol), commercially available 3-(4-bromophenyl)propan-1-ol (5.0 g, 1.0 equiv, 23.25 mmol), and DMF (29 mL). The solution is then cooled to 0 °C and allowed to stir for 20 minutes before adding neat TIPS–Cl dropwise. The reaction was completed after 2 hours by TLC analysis (15% diethylether in hexanes). The reaction was quenched with saturated ammonium chloride, extracted with 1% diethyl ether in pentane (x3), and the combined organics were washed with water, then brine, then filtered through a pad of silica gel, then

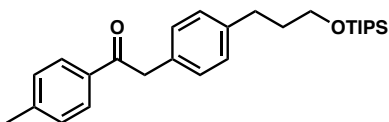
concentrated *in vacuo*. Further purification of the crude material was achieved *via* silica flash column chromatography (3% diethyl ether in hexanes) to afford aryl bromide **268** as a colorless oil (7.1 g, 82% yield).

$^1\text{H NMR}$ (400 MHz, CDCl_3) δ 7.43 – 7.35 (m, 2H), 7.12 – 7.04 (m, 2H), 3.70 (t, $J = 6.2$ Hz, 2H), 2.71 – 2.63 (m, 2H), 1.88 – 1.77 (m, 2H), 1.17 – 1.00 (m, 21H).

$^{13}\text{C NMR}$ (101 MHz, CDCl_3) δ 141.4, 131.4, 130.4, 119.5, 62.4, 34.6, 31.6, 18.1, 12.1.

FT-IR (neat film NaCl): 2942, 2865, 1488, 1461, 1387, 1247, 1107, 1072, 1011, 882, 809, 717, 67 cm^{-1} .

HR-MS (FD) m/z : $[\text{M}\cdot]^+$ Calculated for $\text{C}_{18}\text{H}_{31}\text{BrOSi}$: 370.1328; Measured: 370.1298.



1-(*p*-tolyl)-2-(4-(3-((triisopropylsilyl)oxy)propyl)phenyl)ethan-1-one (**269**)

Following a reported procedure⁴⁶, a flame-dried Schlenk flask was charged with NaOtBu (2.56 g, 1.5 equiv, 26.65 mmol) and dppf (886 mg, 0.09 equiv, 1.59 mmol). The flask was evacuated and back-filled with N_2 (x3). Then, degassed THF (36 mL) was added followed by aryl bromide **268** (6.60 g, 1.0 equiv, 17.77 mmol), followed by $\text{Pd}(\text{dba})_2$ (715 mg, 0.07 equiv, 1.24 mmol). After 5 minutes of stirring, commercially-available 1-(*p*-tolyl)ethan-1-one (2.62 g, 1.1 equiv, 19.55 mmol) was then added. The flask was then sealed with a glass stopper and heated to 75 $^\circ\text{C}$ overnight. The next morning, the reaction was quenched with water and extracted with diethyl ether (x3) and the combined organics were washed with brine, dried over Na_2SO_4 , filtered, and concentrated *in vacuo*. Silica flash chromatography

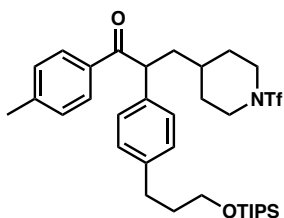
(4% diethyl ether in hexanes) afforded pure ketone **269** as a slightly-yellow oil (4.0 g, 53% yield).

¹H NMR (400 MHz, CDCl₃) δ 7.96 – 7.89 (m, 2H), 7.28 – 7.20 (m, 2H), 7.23 – 7.13 (m, 4H), 4.22 (s, 2H), 3.72 (t, *J* = 6.3 Hz, 2H), 2.74 – 2.65 (m, 2H), 2.39 (s, 3H), 1.91 – 1.80 (m, 2H), 1.18 – 1.01 (m, 21H).

¹³C NMR (101 MHz, CDCl₃) δ 197.4, 143.9, 140.9, 134.2, 132.0, 129.3, 129.2, 128.8, 62.6, 45.1, 34.6, 31.8, 21.7, 18.1, 12.1.

FT-IR (neat film NaCl): 3024, 2941, 2891, 2864, 2726, 1900, 1806, 1678, 1606, 1572, 1513, 1463, 1381, 1328, 1276, 1222, 1196, 1180, 1149, 1104, 1066, 1013, 996, 964, 918, 882, 809, 770, 721, 681, 658 cm⁻¹.

HR-MS (ESI) *m/z*: [M+K]⁺ Calculated for C₂₇H₄₀KO₂Si: 463.2429; Measured: 463.2428



1-(*p*-tolyl)-3-(1-((trifluoromethyl)sulfonyl)piperidin-4-yl)-2-(4-(3-((triisopropylsilyloxy)propyl)phenyl)propan-1-yl)propan-1-one (270)

To a flame-dried flask was added ketone **269** (3.95 g, 1.0 equiv, 9.3 mmol) then dissolved in THF (30 mL) and cooled to 0 °C. In a separate flask, a freshly-prepared solution of KO^{*t*}Bu (1.14 g, 1.1 equiv, 10.2 mmol) in THF (30 mL) was added dropwise to the ketone while at 0 °C. The yellow solution was allowed to stir at 0 °C for 20 minutes. Then, a solution of iodide **243** (3.48 g, 1.05 equiv, 9.7 mmol) in THF (10 mL) was added dropwise

then allowed to warm to room temperature overnight. The next morning, the reaction was quenched with saturated ammonium chloride and extracted with diethyl ether (x3). The combined organics were washed once with brine, dried over Na₂SO₄, filtered, concentrated *in vacuo*, and purified by silica flash column chromatography (10% diethyl ether in hexanes) to yield ketone **270** as a white solid (4.9 g, 81% yield).

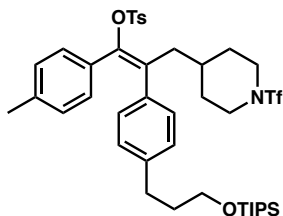
¹H NMR (400 MHz, CDCl₃) δ 7.91 – 7.84 (m, 2H), 7.23 – 7.16 (m, 4H), 7.13 (d, *J* = 8.1 Hz, 2H), 4.64 (t, *J* = 7.4 Hz, 1H), 3.97 – 3.83 (m, 2H), 3.67 (t, *J* = 6.3 Hz, 2H), 3.01 – 2.86 (m, 2H), 2.69 – 2.61 (m, 2H), 2.36 (s, 3H), 2.26 – 2.14 (m, 1H), 1.95 – 1.69 (m, 5H), 1.50 – 1.24 (m, 3H), 1.15 – 0.94 (m, 21H).

¹³C NMR (101 MHz, CDCl₃) δ 198.9, 144.0, 141.4, 136.6, 134.1, 129.4, 129.3, 128.9, 127.9, 120.2 (q, *J* = 323.6 Hz), 62.6, 49.8, 46.8, 40.1, 34.5, 32.9, 32.0 (d, *J* = 9.3 Hz), 31.7, 21.6, 18.1, 12.0.

¹⁹F NMR (376 MHz, CDCl₃) δ -75.1 (br s).

FT-IR (neat film NaCl): 2941, 2865, 1679, 1606, 1461, 1389, 1227, 1182, 1147, 1110, 1052, 997, 949, 882, 818, 763, 709, 680 cm⁻¹.

HR-MS (ESI) *m/z*: [M+H]⁺ Calculated for C₃₄H₅₁F₃NO₄SSi: 654.3254; Measured: 654.3266.



(*E*)-1-(*p*-tolyl)-3-(1-((trifluoromethyl)sulfonyl)piperidin-4-yl)-2-(4-(3-((triisopropylsilyl)oxy)propyl)phenyl)prop-1-en-1-yl 4-methylbenzenesulfonate (271)

To a flame-dried flask was added ketone **270** (4.70 g, 1.0 equiv, 7.20 mmol) then dissolved in THF (35 mL) and cooled to 0 °C. In a separate flask, a freshly-prepared solution of KO^tBu (1.29 g, 1.60 equiv, 11.52 mmol) in THF (25 mL) was added dropwise to the ketone while at 0 °C. The yellow solution was allowed to stir at 0 °C for 90 minutes. Then, Ts₂O (3.76 g, 1.6 equiv, 11.52 mmol) was added as a solid in one portion to the enolate solution with vigorous stirring then allowed to warm to room temperature (solution turns thick). After the reaction was completed by TLC analysis (20% diethyl ether in hexanes), the reaction was quenched with water and extracted with diethyl ether (x3). The combined organics were washed once with brine, dried over Na₂SO₄, filtered, concentrated *in vacuo*, and purified by silica flash column chromatography (15% diethyl ether in hexanes) to yield pure ketone **271** as a white solid (2.90 g, 50% yield). The olefin isomer is assigned to be *E* on the basis of NOESY NMR (observe NOE correlations between tosylate and piperidine protons, as well as between the two aryl rings). Consistent with this assignment, the chemical shift of the allylic methylene protons (2.68 ppm in CDCl₃) is congruent to similarly reported *E* diaryl vinyl tosylates (typically ~2.7 ppm for allylic methylene in CDCl₃), which are distinct from the reported *Z* isomer chemical shift (typically ~2.3 ppm for allylic methylene of corresponding *Z* vinyl tosylate in CDCl₃).⁴²

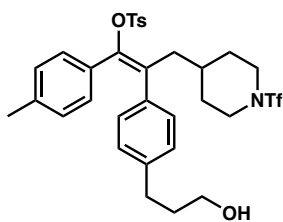
¹H NMR (400 MHz, CDCl₃) δ 7.49 – 7.41 (m, 2H), 7.09 (d, *J* = 8.1 Hz, 2H), 7.01 (d, *J* = 8.2 Hz, 2H), 6.96 – 6.89 (m, 2H), 6.75 (d, *J* = 8.3 Hz, 2H), 6.70 (d, *J* = 8.1 Hz, 2H), 3.85 (dd, *J* = 13.4, 3.8 Hz, 2H), 3.65 (t, *J* = 6.3 Hz, 2H), 2.95 – 2.85 (m, 2H), 2.71 – 2.60 (m, 4H), 2.37 (s, 3H), 2.18 (s, 3H), 1.87 – 1.67 (m, 4H), 1.47 – 1.29 (m, 3H), 1.15 – 0.98 (m, 21H).

¹³C NMR (101 MHz, CDCl₃) δ 144.7, 144.5, 141.5, 137.8, 135.4, 134.4, 131.6, 130.7, 129.8, 129.2, 129.1, 128.6, 128.2, 128.0, 120.2 (q, *J* = 323.8 Hz), 62.4, 46.7, 38.8, 34.2, 33.0, 31.7, 31.4, 21.5, 21.2, 17.7, 12.0.

¹⁹F NMR (376 MHz, CDCl₃) δ -75.3 (br s).

FT-IR (neat film NaCl): 3027, 2939, 2866, 1598, 1511, 1463, 1393, 1333, 1245, 1227, 1171, 1151, 1101, 1070, 1049, 972, 942, 910, 882, 850, 815, 781, 736, 708, 684 cm⁻¹.

HR-MS (ESI) *m/z*: [M+H]⁺ Calculated for C₄₁H₅₇F₃NO₆S₂Si: 808.3349; Measured: 808.3371.



(E)-2-(4-(3-hydroxypropyl)phenyl)-1-(*p*-tolyl)-3-(1-((trifluoromethyl)sulfonyl)piperidin-4-yl)prop-1-en-1-yl 4-methylbenzenesulfonate (132n)

To a scintillation vial equipped with a stir bar was added silyl ether **271** (2.20 g, 1.0 equiv, 2.72 mmol), followed by dry THF (5 mL). The solution was cooled to 0 °C then a freshly prepared solution of TBAF·(H₂O)₃ (1.03 g, 1.2 equiv, 3.26 mmol) in 5 mL of dry THF was

added dropwise then allowed to warm to room temperature. After 30 minutes, reaction was completed by TLC analysis. The reaction was quenched with saturated ammonium chloride and subsequently extracted with ethyl acetate (x3). The combined organics were dried over Na₂SO₄, filtered, concentrated *in vacuo*, then purified by silica flash chromatography (20% → 50% → 70% ethyl acetate in hexanes) to afford pure alcohol **132n** as a white solid (1.35 g, 76% yield). The olefin isomer is assigned to be *E* as it was directly derived from compound **271**, which was characterized to be the *E* vinyl tosylate. To further validate this, NOESY NMR was conducted and validated this assignment (observe NOE correlations between tosylate and piperidine protons, as well as between the two aryl rings).

¹H NMR (400 MHz, CDCl₃) δ 7.45 (app d, *J* = 8.4 Hz, 2H), 7.09 (app d, *J* = 8.5 Hz, 2H), 7.00 (app d, *J* = 8.2 Hz, 2H), 6.92 (app d, *J* = 8.2 Hz, 2H), 6.77 – 6.66 (m, 4H), 3.85 (dd, *J* = 13.1, 4.0 Hz, 2H), 3.63 (t, *J* = 6.4 Hz, 2H), 2.90 (t, *J* = 12.0 Hz, 2H), 2.70 – 2.59 (m, 4H), 2.37 (s, 3H), 2.18 (s, 3H), 1.90 – 1.79 (m, 2H), 1.75 – 1.67 (m, 2H), 1.45 – 1.27 (m, 4H).

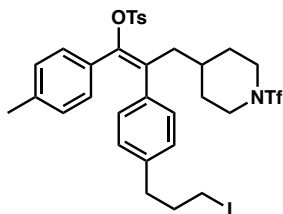
¹³C NMR (101 MHz, CDCl₃) δ 144.9, 144.6, 141.1, 138.0, 135.8, 134.5, 131.6, 130.7, 129.9, 129.4, 129.3, 128.6, 128.3, 128.0, 62.3, 46.7, 38.8, 34.0, 33.2, 31.8, 31.5, 21.7, 21.3.

*CF₃ quartet not apparent.

¹⁹F NMR (376 MHz, CDCl₃) δ -75.3 (br s).

FT-IR (neat film NaCl): 3300, 2931, 1386, 1226, 1176, 1151, 1050, 968, 942, 825 cm⁻¹.

HR-MS (ESI) *m/z*: [M+NH₄]⁺ Calculated for C₃₂H₄₀F₃N₂O₆S₂: 669.2280; Measured: 669.2287.



(E)-2-(4-(3-iodopropyl)phenyl)-1-(p-tolyl)-3-(1-((trifluoromethyl)sulfonyl)piperidin-4-yl)prop-1-en-1-yl 4-methylbenzenesulfonate (132m)

To a flame-dried flask with a magnetic stir bar was added PPh₃ (648 mg, 1.4 equiv, 2.47 mmol) and imidazole (168 mg, 1.4 equiv, 2.47 mmol). The solids were dissolved in 15 mL dry DCM then cooled to 0 °C. After stirring at this temperature for 20 minutes, solid I₂ (672 mg, 1.5 equiv, 2.65 mmol) was added in two portions and allowed to stir for another 30 minutes at 0 °C under N₂. Then, a solution of alcohol **132n** (1.15 g, 1.0 equiv, 1.76 mmol) in 10 mL dry DCM was added dropwise and the reaction was allowed to warm up to room temperature. After 30 minutes at room temperature, reaction was completed (SM consumed by TLC). Saturated aqueous Na₂S₂O₃ was added and then subsequently extracted with DCM (x3). The combined organics were dried over Na₂SO₄, filtered, concentrated *in vacuo*, then purified *via* silica flash column chromatography (5% → 20% diethyl ether in hexanes) to yield pure **132m** as a white solid (1.2 g, 89% yield). The olefin isomer is assigned to be *E* as it was directly derived from compounds **132n** and **271**, both of which were characterized by NOESY NMR to be the *E* vinyl tosylate isomer.

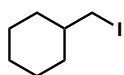
¹H NMR (400 MHz, CDCl₃) δ 7.38 (app d, *J* = 8.4 Hz, 2H), 7.06 – 6.97 (m, 2H), 6.93 (app d, *J* = 8.3 Hz, 2H), 6.86 (app d, *J* = 8.1 Hz, 2H), 6.68 – 6.61 (m, 4H), 3.78 (dd, *J* = 13.4, 3.9 Hz, 2H), 3.04 (t, *J* = 6.9 Hz, 2H), 2.89 – 2.78 (m, 2H), 2.63 – 2.54 (m, 4H), 2.30 (s, 3H), 2.11 (s, 3H), 2.07 – 1.95 (m, 2H), 1.69 – 1.60 (m, 2H), 1.40 – 1.20 (m, 3H).

^{13}C NMR (101 MHz, CDCl_3) δ 144.9, 144.6, 139.6, 138.0, 136.2, 134.5, 131.5, 130.7, 129.9, 129.4, 129.3, 128.7, 128.3, 128.0, 120.2 (app q, $J = 323.1$ Hz), 46.7, 38.8, 36.0, 34.7, 33.2, 31.5, 21.7, 21.3, 6.1.

^{19}F NMR (376 MHz, CDCl_3) δ -75.2 (br s).

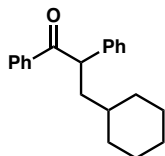
FT-IR (neat film NaCl): 2925, 2345, 1598, 1509, 1443, 1386, 1226, 1189, 1176, 1150, 1115, 1067, 1049, 972, 942, 853, 826, 763, 732, 708, 670 cm^{-1} .

HR-MS: (ESI) m/z : $[\text{M}+\text{Na}]^+$ Calculated for $\text{C}_{32}\text{H}_{35}\text{F}_3\text{INNaO}_5\text{S}_2$: 784.0846; Measured: 784.0853.



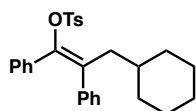
(iodomethyl)cyclohexane (272)

To a flame-dried flask with a magnetic stir bar was added PPh_3 (14.9 g, 1.3 equiv, 56.9 mmol) and imidazole (4.1 g, 1.4 equiv, 61.3 mmol). The solids were dissolved in 215 mL dry DCM then cooled to 0 °C. After stirring at this temperature for 20 minutes, solid I_2 (14.4 g, 1.3 equiv, 56.9 mmol) was added in three portions and allowed to stir for another 30 minutes at 0 °C under N_2 . Then, neat commercially-available cyclohexylmethanol (5.0 g, 1.0 equiv, 43.8 mmol, 5.45 mL) was added dropwise and the reaction was allowed to warm up to room temperature overnight. The next morning (SM consumed by TLC) saturated aqueous $\text{Na}_2\text{S}_2\text{O}_3$ was added and then subsequently extracted with DCM (x3). The combined organics were dried over MgSO_4 , filtered, concentrated *in vacuo*, then purified *via* flash column chromatography (100% hexanes) to yield pure alkyl iodide **272** as a colorless oil (7.3 g, 74% yield), which matches the reported NMR spectra.⁴⁷



3-cyclohexyl-1,2-diphenylpropan-1-one (273)

To a flame-dried flask was added commercially-available 1,2-diphenylethan-1-one (2.00 g, 1.0 equiv, 10.2 mmol) then dissolved in THF (15 mL) and cooled to 0 °C. In a separate flask, a fresh solution of KO^tBu (1.26 g, 1.1 equiv, 11.2 mmol) in THF (16 mL) was prepared and added dropwise to the ketone while at 0 °C. The yellow solution was allowed to stir at 0 °C for 20 minutes. Then, neat iodide **272** (2.74 g, 1.2 equiv, 12.2 mmol) was added dropwise then allowed to warm to room temperature overnight. Once the reaction was completed by TLC analysis (9% ethyl acetate in hexanes), the reaction was quenched with 1M HCl then water and extracted with ethyl acetate (x3). The combined organics were washed once with brine, dried over Na₂SO₄, filtered, concentrated *in vacuo*, and purified by flash column chromatography (5% ethyl acetate in hexanes) to yield ketone **273** as a white solid (2.35 g, 79% yield), which matches the reported NMR spectra.⁴⁸



(*E*)-3-cyclohexyl-1,2-diphenylprop-1-en-1-yl 4-methylbenzenesulfonate (215)

Following a reported procedure on similar *E*-vinyl tosylates⁴⁹, a solution of ketone **273** in dry toluene (10 mL) was added to a solution of LiHMDS and DMEA in toluene (20 mL) dropwise while at room temperature. Let stir for 20 minutes, then a solution of Ts₂O in DCM (sonicated to obtain fine suspension, then used immediately) was added to a vigorously stirring solution of the enolate (reaction solution thickens) and allowed to stir

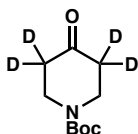
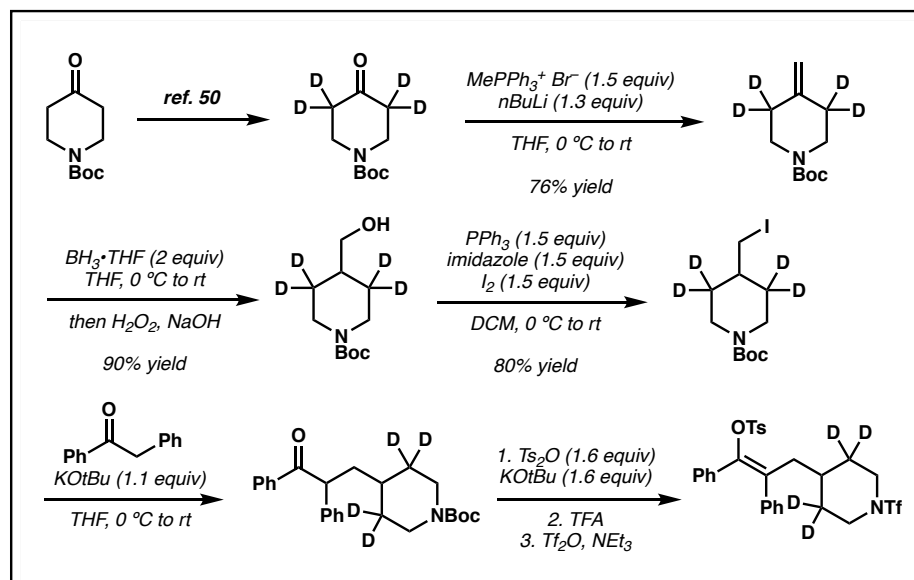
overnight. Once the reaction was completed by TLC analysis, the reaction was diluted with ethyl acetate then 10 mL of 1M NaOH was added, then 50 mL of water. The mixture was extracted with ethyl acetate (x3), and the combined organics were washed with water once, then brine, then dried over Na₂SO₄, then filtered and concentrated *in vacuo*. The crude material was purified by flash column chromatography (5% ethyl acetate in hexanes) to yield vinyl tosylate **215** as a white solid (1.97 g, 59% yield). The olefin isomer is assigned to be *E* on the basis of NOESY NMR (observe NOE correlations between tosylate and piperidine protons). Consistent with this assignment, the chemical shift of the allylic methylene protons (2.58 ppm in CDCl₃) is congruent to similarly reported *E* diaryl vinyl tosylates (typically ~2.7 ppm for allylic methylene in CDCl₃), which are distinct from the reported *Z* isomer chemical shift (typically ~2.3 ppm for allylic methylene of corresponding *Z* vinyl tosylate in CDCl₃). The procedure used to prepare this vinyl tosylate is used to obtain high *E*-selectivity on similar diaryl vinyl tosylates.⁴²

¹H NMR (400 MHz, CDCl₃) δ 7.50 – 7.42 (m, 2H), 7.20 – 7.10 (m, 3H), 7.09 – 7.04 (m, 2H), 7.02 (s, 3H), 6.93 – 6.80 (m, 4H), 2.58 (d, *J* = 7.0 Hz, 2H), 2.35 (s, 3H), 1.70 – 1.48 (m, 5H), 1.22 – 0.90 (m, 6H).

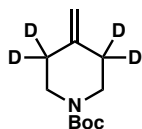
¹³C NMR (101 MHz, CDCl₃) δ 144.3, 143.9, 138.8, 134.5, 134.4, 134.1, 130.0, 129.4, 129.2, 128.2, 128.1, 127.6, 127.4, 127.0, 40.5, 35.6, 33.0, 26.5, 26.2, 21.6.

FT-IR (neat film NaCl): 3053, 3025, 2922, 2849, 1598, 1493, 1445, 1371, 1306, 1223, 1189, 1177, 1085, 1062, 977, 960, 910, 868, 827, 812, 778, 758, 733, 698, 679 cm⁻¹.

HR-MS (ESI) *m/z*: [M+NH₄]⁺ Calculated for C₂₈H₃₄NO₃S: 464.2259; Measured: 464.2270.

Figure 4.4: Representative scheme for the synthesis of deuterated variant***tert*-butyl 4-oxopiperidine-1-carboxylate-3,3,5,5-*d*₄ (274)**

Prepared according to known procedures, and the NMR spectrum matched reported literature spectra.⁵⁰ In order to obtain full deuterium incorporation (no H observable by ¹H NMR), the ketone was exposed to fresh deuterated solvent several times after workup to drive full conversion.

**tert-butyl 4-methylenepiperidine-1-carboxylate-3,3,5,5-*d*₄ (275)**

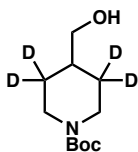
To a flame-dried flask equipped with a stir bar was added methyltriphenylphosphonium bromide (24.5 g, 1.5 equiv, 68.6 mmol) followed by 200 mL of dry THF. The suspension was cooled to $-78\text{ }^{\circ}\text{C}$ then *n*BuLi (27 mL, 1.3 equiv, 59.4 mmol, freshly titrated to be 2.2 M) was added dropwise to the reaction. After stirring for 1 hour at $-78\text{ }^{\circ}\text{C}$, the reaction was warmed to $0\text{ }^{\circ}\text{C}$ then allowed to stir for another 10 minutes. At this stage, a solution of tetradeuterated ketone **274** (9.3g, 1.0 equiv, 45.7 mmol) in 25 mL dry THF was added dropwise. After the addition is complete, the reaction is allowed to warm to room temperature and stirred further until starting ketone is consumed by TLC (3 hours). The reaction is then quenched with saturated aqueous ammonium chloride and extracted with diethyl ether three times. The combined organics were washed with brine, dried over Na_2SO_4 , filtered, concentrated *in vacuo*, then purified *via* flash chromatography (5% ether in hexanes) to obtain deuterated **275** as a colorless oil (7.0 g, 76% yield).

^1H NMR (400 MHz, CDCl_3) δ 4.72 (s, 2H), 3.39 (s, 4H), 1.45 (s, 9H).

^{13}C NMR (101 MHz, CDCl_3) δ 154.8, 145.4, 109.1, 79.6, 45.3, 34.4 – 33.4 (app quint), 28.5.

FT-IR (neat film NaCl): 3072, 2977, 2931, 2860, 2198, 2105, 1697, 1649, 1476, 1418, 1364, 1273, 1246, 1181, 1155, 1103, 1070, 1017, 944, 914, 886, 767 cm^{-1} .

HR-MS (ESI) *m/z*: $[\text{M}-\text{C}_4\text{H}_7]^+$ Calculated for $\text{C}_7\text{H}_8\text{D}_4\text{NO}_2$: 146.1114; Measured: 146.1114.



***tert*-butyl 4-(hydroxymethyl)piperidine-1-carboxylate-3,3,5,5-*d*₄ (276)**

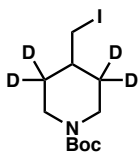
To a flame-dried flask equipped with a stir bar was added deuterated piperidine **275** (7.0 g, 1.0 equiv, 34.7 mmol) in dry THF (120 mL) then cooled to 0 °C. A commercial solution of BH₃•THF (69.5 mL, 2.0 equiv, 1.0 M, 69.5 mmol) was added dropwise to the reaction then allowed to warm to room temperature. After 1 hour at room temperature, TLC analysis indicated that starting material was consumed. The reaction was then cooled back down to 0 °C, then 2M aqueous NaOH (34.7 mL, 2 equiv, 69.5 mmol) was added followed by 30% aqueous H₂O₂ (21.3 mL, 6.0 equiv, 208.8 mmol) dropwise. The reaction was stirred for 10 minutes before allowing it to warm to room temperature overnight. The next morning, the reaction mixture was diluted with water and extracted with ethyl acetate three times. The combined organics were washed with Na₂S₂O₃ (saturated aqueous solution), then brine, then dried over Na₂SO₄, filtered, and concentrated *in vacuo* to obtain a white solid. The crude material was sufficiently pure to use in the next step, so no further purification was conducted (6.85 g, 90% yield).

¹H NMR (400 MHz, CDCl₃) δ 4.06 (d, *J* = 13.2 Hz, 2H), 3.44 (d, *J* = 6.5 Hz, 2H), 2.65 (d, *J* = 13.3 Hz, 2H), 2.26 (br s, 1H), 1.58 (t, *J* = 6.6 Hz, 1H), 1.41 (s, 9H).

¹³C NMR (101 MHz, CDCl₃) δ 155.0, 79.4, 67.4, 43.5, 38.4, 28.5, 28.31 – 27.32 (app quint).

FT-IR (neat film NaCl): 3436, 2975, 2905, 2865, 2197, 2111, 1693, 1671, 1467, 1428, 1364, 1277, 1254, 1166, 1128, 1089, 1053, 1041, 1014, 990, 932, 872, 767 cm⁻¹.

HR-MS (ESI) m/z : $[M-C_5H_7O_2]^+$ Calculated for $C_6H_{10}D_4NO$: 120.1321; Measured: 120.1323.



***tert*-butyl 4-(iodomethyl)piperidine-1-carboxylate-3,3,5,5- d_4 (277)**

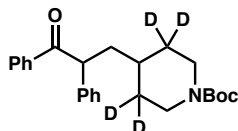
To a flame-dried flask with a magnetic stir bar was added PPh_3 (12.1 g, 1.5 equiv, 46.1 mmol) and imidazole (3.1 g, 1.5 equiv, 46.1 mmol). The solids were dissolved in 100 mL dry DCM then cooled to 0 °C. After stirring at this temperature for 20 minutes, solid I_2 (11.7 g, 1.5 equiv, 46.1 mmol) was added in three portions and allowed to stir for another 30 minutes at 0 °C under N_2 . Then, a solution of alcohol **276** (6.75 g, 1.0 equiv, 30.8 mmol) in dry DCM (30 mL) was added dropwise and the reaction was allowed to warm up to room temperature overnight. The next morning (SM consumed by TLC) saturated aqueous $Na_2S_2O_3$ was added and then subsequently extracted with DCM (x3). The combined organics were dried over $MgSO_4$, filtered, concentrated *in vacuo*, then purified *via* flash column chromatography (10% → 15% ethyl acetate in hexanes) to yield pure deuterated iodide **277** as a white solid (8.1 g, 80% yield).

1H NMR (400 MHz, $CDCl_3$) δ 4.06 (d, $J = 13.3$ Hz, 2H), 3.06 (d, $J = 6.6$ Hz, 2H), 2.63 (d, $J = 13.4$ Hz, 2H), 1.55 (t, $J = 7.2$ Hz, 1H), 1.41 (s, 9H).

^{13}C NMR (101 MHz, $CDCl_3$) δ 154.7, 79.5, 43.4, 38.3, 31.8 (app quint, $J = 19.4$ Hz), 28.5, 13.5.

FT-IR (neat film NaCl): 2974, 2928, 2855, 2203, 2114, 1687, 1464, 1419, 1391, 1363, 1274, 1254, 1158, 1110, 1091, 1053, 1014, 992, 969, 932, 875, 854, 796, 767, 616 cm^{-1} .

HR-MS (ESI) m/z : $[\text{M}-\text{C}_5\text{H}_7\text{O}_2]^+$ Calculated for $\text{C}_6\text{H}_9\text{D}_4\text{IN}$: 230.0338; Measured: 230.0342.



***tert*-butyl 4-(3-oxo-2,3-diphenylpropyl)piperidine-1-carboxylate-3,3,5,5-*d*₄ (278)**

To a flame-dried flask was added commercially-available 1,2-diphenylethan-1-one (1.25 g, 1.0 equiv, 6.3 mmol) then dissolved in THF (15 mL) and cooled to 0 °C. In a separate flask, a freshly-prepared solution of KO^tBu (786 mg, 1.1 equiv, 7.0 mmol) in THF (15 mL) was added dropwise to the ketone while at 0 °C. The yellow solution was allowed to stir at 0 °C for 20 minutes. Then, a solution of iodide **277** (2.2 g, 1.05 equiv, 6.6 mmol) was added in one portion as a solid, then allowed to warm to room temperature overnight. The next morning, the reaction was quenched with saturated ammonium chloride and extracted with ethyl acetate (x3). The combined organics were washed once with brine, dried over Na₂SO₄, filtered, concentrated *in vacuo*, and purified by silica flash column chromatography (10% ethyl acetate in hexanes) to yield ketone **278** as a white solid (1.98 g, 78% yield).

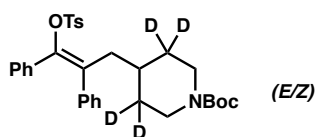
¹H NMR (400 MHz, CDCl₃) δ 8.00 – 7.93 (m, 2H), 7.54 – 7.45 (m, 1H), 7.44 – 7.35 (m, 2H), 7.33 – 7.28 (m, 4H), 7.24 – 7.15 (m, 1H), 4.69 (dd, $J = 7.8, 6.9$ Hz, 1H), 4.02 (t, $J =$

14.2 Hz, 2H), 2.64 – 2.51 (m, 2H), 2.23 – 2.11 (m, 1H), 1.75 (dt, $J = 13.8, 6.8$ Hz, 1H), 1.43 (s, 9H), 1.33 (t, $J = 6.9$ Hz, 1H).

^{13}C NMR (101 MHz, CDCl_3) δ 199.6, 154.9, 139.7, 136.8, 133.1, 129.1, 128.7, 128.6, 128.2, 127.2, 79.3, 50.5, 43.7 (br s), 40.7, 33.5, 28.6.

FT-IR (neat film NaCl): 2975, 1681, 1424, 1364, 1272, 1167, 1124, 935, 756, 700 cm^{-1} .

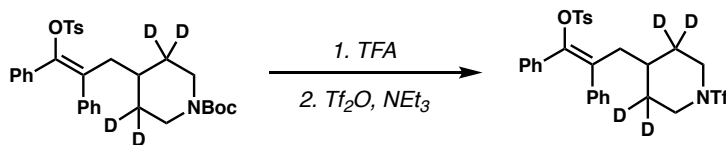
HR-MS (ESI) m/z : $[\text{M}-\text{C}_4\text{H}_7]^+$ Calculated for $\text{C}_{21}\text{H}_{20}\text{D}_4\text{NO}_3$: 342.2002; Measured: 342.2005.



tert-butyl (*E/Z*)-4-(2,3-diphenyl-3-(tosyloxy)allyl)piperidine-1-carboxylate-3,3,5,5- d_4
(279)

To a flame-dried flask was added ketone **278** (1.90 g, 1.0 equiv, 4.77 mmol) then dissolved in THF (25 mL) and cooled to 0 °C. In a separate flask, a fresh solution of KO^iBu (858 mg, 1.60 equiv, 7.64 mmol) in THF (25 mL) was prepared and added dropwise to the ketone while at 0 °C. The yellow solution was allowed to stir at 0 °C for 90 minutes. Then, Ts_2O (475 mg, 1.6 equiv, 1.45 mmol) in 15 mL THF (sonicated to promote solvation) was added dropwise to the enolate solution with vigorous stirring then allowed to warm to room temperature (solution turns thick). After 1 hour the reaction was completed by TLC analysis (20% ethyl acetate in hexanes), the reaction was quenched with water and extracted with ethyl acetate (x3). The combined organics were washed once with brine, dried over Na_2SO_4 , filtered through a short pad of silica gel (washing silica with 1:1 ethyl acetate/hexanes), and concentrated *in vacuo* to afford a white solid. This material appears

to be a mixture of E/Z vinyl tosylate isomers by NMR, but is carried forward to the next step without further purification/characterization.



(E)-1,2-diphenyl-3-(1-((trifluoromethyl)sulfonyl)piperidin-4-yl-3,3,5,5-*d*₄)prop-1-en-1-yl 4-methylbenzenesulfonate (132b-D)

Vinyl tosylate (crude mixture of isomers) from previous step (**279**) was dissolved in 45 mL DCM then cooled to 0 °C. Then 15 mL of a 1:1 TFA/DCM mixture was added slowly dropwise, and the reaction was allowed to stir further for another hour at 0 °C. The reaction was then quenched with saturated aqueous sodium bicarbonate dropwise while at 0 °C until aqueous layer is basic in pH. The mixture was then extracted with DCM x4, dried over Na₂SO₄, and concentrated *in vacuo*. The free amine was then dissolved in dry DCM in a flame-dried flask under N₂ and cooled to –40 °C. To this was added triethylamine (1.4 mL) followed by Tf₂O (800 uL) dropwise and allowed to warm up to room temperature overnight. The next morning, the reaction was quenched with saturated aqueous sodium bicarbonate dropwise. The mixture was then extracted with DCM x4, dried over Na₂SO₄, and concentrated *in vacuo*. Purification by silica flash column chromatography (20% diethyl ether in hexanes) followed by recrystallization from hexanes/ethyl acetate afforded pure deuterated vinyl tosylate **132b-D** which was assigned to be the *E* vinyl tosylate isomer given that the NMR spectra matches the non-deuterated analogue **132b** (905 mg, 32% yield over 3 steps from **278**)

¹H NMR (400 MHz, CDCl₃) δ 7.44 (d, *J* = 8.4 Hz, 2H), 7.21 – 7.14 (m, 3H), 7.12 – 6.97 (m, 5H), 6.94 – 6.82 (m, 4H), 3.85 (d, *J* = 13.0 Hz, 2H), 2.88 (d, *J* = 12.9 Hz, 2H), 2.72 (d, *J* = 7.3 Hz, 2H), 2.35 (s, 3H), 1.39 (t, *J* = 7.2 Hz, 1H).

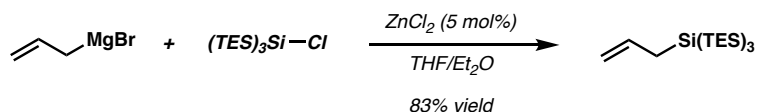
¹³C NMR (101 MHz, CDCl₃) δ 144.9, 144.7, 138.2, 134.4, 133.5, 132.5, 130.0, 129.4, 129.3, 128.5, 128.0, 128.0, 127.6, 127.5, 120.2 (q, *J* = 323.4 Hz), 46.6, 38.8, 32.8, 30.8 (m), 21.7.

¹⁹F NMR (376 MHz, CDCl₃) δ -75.2 (br s).

FT-IR (neat film NaCl): 2926, 1735, 1597, 1492, 1444, 1385, 1227, 1189, 1147, 1112, 1085, 1041, 987, 967, 842, 828, 780, 758, 699, 673 cm⁻¹.

HR-MS (ESI) *m/z*: [M+Na]⁺ Calculated for C₂₈H₂₄D₄F₃NNaO₅S₂: 606.1510; Measured: 606.1531.

4.6.3 Preparation of Allyl Silane

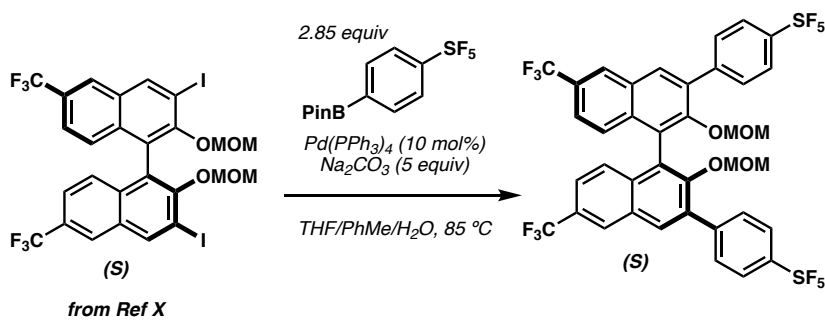


2-allyl-1,1,1,3,3,3-hexaethyl-2-(triethylsilyl)trisilane (135)

To a flame-dried flask was added dried ZnCl₂ (83.2 mg, 0.050 equiv, 0.61 mmol) and THF (18 mL). Commercially available chlorotris(triethylsilyl)silane (5.00 g, 1.0 equiv, 12.2 mmol) was then added. To this solution at room temperature was then added allylmagnesium bromide (30.5 mL, 3.0 equiv, 1.2 M). Upon addition of Grignard solution, reaction turned from homogeneous to cloudy with white precipitate. Once the reaction was completed by TLC analysis (100% hexanes), 3 mL of water was added *slowly*, followed

by 1M HCl. Pentanes was then added, and the organic layer was washed with water (x3), and then dried with MgSO₄ and concentrated *in vacuo*. The crude material was purified *via* silica flash column chromatography (100% pentane) to obtain allyl silane **135** as a colorless oil (4.2 g, 83% yield), and NMR characterization matched the reported literature spectra.⁵¹

4.6.4 Preparation of Catalysts



(S)-((2,2'-bis(methoxymethoxy)-6,6'-bis(trifluoromethyl)-[1,1'-binaphthalene]-3,3'-diyl)bis(4,1-phenylene))bis(pentafluoro- λ^6 -sulfane) (**280**)

Following a similar reported procedure⁵², MOM-protected (*S*)-3,3'-diiodo-6,6'-bis(trifluoromethyl)-binol (prepared according to published protocol⁵³) (5.0 g, 1.0 equiv, 6.56 mmol) was added to an oven-dried Schlenk flask, followed by Na₂CO₃ (3.5 g, 5 equiv, 32.80 mmol), and *p*-SF₅ aryl BPin (6.50 g, 3.0 equiv, 19.7 mmol). The flask was vac/backfilled with N₂ three times, then THF (112 mL), toluene (112 mL), and water (60 mL) were added. The mixture was degassed by sparging with nitrogen while vigorously stirring for 30 minutes. Then, under positive N₂ gas flow, solid Pd(PPh₃)₄ (758 mg, 0.1 equiv, 0.65 mmol) was added in one portion. The flask was then sealed and heated to 85 °C overnight. The next morning, starting material had been consumed by TLC. Water was

added to the reaction and extracted with ethyl acetate three times. The combined organics were washed with brine, dried over Na₂SO₄, filtered, and concentrated *in vacuo*. The crude material was purified *via* flash chromatography (4% diethyl ether in hexanes) to obtain MOM binol **280** mixed with the starting aryl Bpin, but was carried forward to the deprotection step as is (*see next step*).

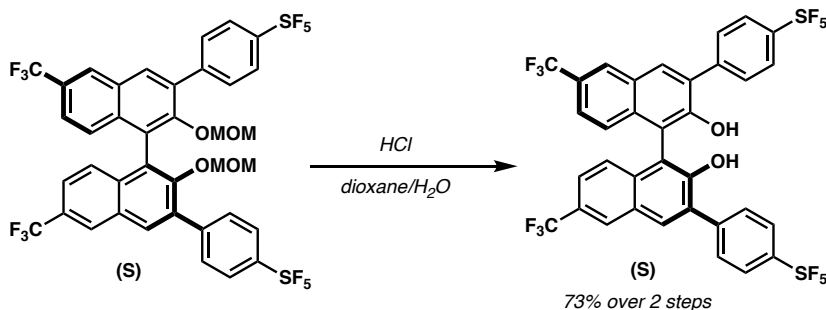
¹H NMR (400 MHz, CDCl₃) δ 8.26 (s, 2H), 8.10 (s, 2H), 7.94 – 7.82 (m, 8H), 7.52 (dd, *J* = 9.0, 1.9 Hz, 2H), 7.38 (d, *J* = 8.9 Hz, 2H), 4.40 (s, 4H), 2.36 (s, 6H).

¹³C NMR (101 MHz, CDCl₃) δ 155.2 – 152.1 (m), 141.7, 135.1, 135.0, 132.2, 129.9, 129.6, 128.1, 127.8, 127.4, 126.4, 126.3 (m), 126.0, 122.1, 99.3, 56.2. *CF₃ carbon (typically a quartet) difficult to see due to peak overlap, not included.

¹⁹F NMR (376 MHz, CDCl₃) δ 85.60 – 82.21 (m), 63.02 (d, *J* = 149.7 Hz), -62.44.

FT-IR (neat film NaCl): 2981, 1634, 1602, 1448, 1436, 1398, 1362, 1331, 1293, 1249, 1194, 1164, 1144, 1129, 1100, 1082, 1068, 1002, 963, 916, 836, 738, 654 cm⁻¹.

HR-MS (FD) *m/z*: [M•]⁺ Calculated for C₃₈H₂₆F₁₆O₄S₂: 914.1017; Measured: 914.1002.



(S)-3,3'-bis(4-(pentafluoro- λ^6 -sulfaneyl)phenyl)-6,6'-bis(trifluoromethyl)-[1,1'-binaphthalene]-2,2'-diol (281)

MOM-protected binol **280** was dissolved in 1,4-dioxane (42 mL). Then, 9 mL of 6 M aq. HCl was added dropwise. The reaction was then sealed and heated to 85 °C overnight, by which time starting material is consumed by TLC forming a more polar spot. Saturated aqueous bicarbonate solution was then added (~35 mL), and the mixture was extracted with DCM three times. The combined organics were washed with brine, dried over Na₂SO₄, filtered, concentrated, and purified *via* flash chromatography (10% ethyl acetate in hexanes) to obtain binol **281** as a white solid (4.0 g, 73% yield over two steps from diiodo precursor).

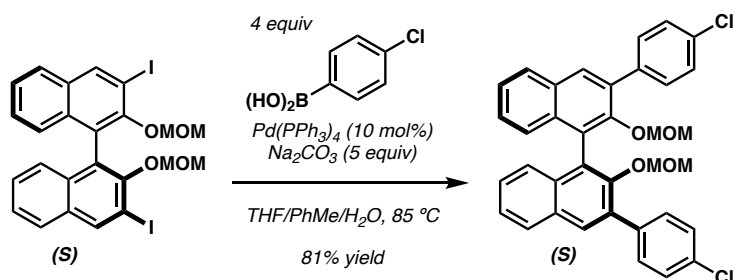
¹H NMR (400 MHz, CDCl₃) δ 8.31 – 8.26 (m, 2H), 8.18 (s, 2H), 7.99 – 7.87 (m, 4H), 7.83 (d, J = 8.6 Hz, 4H), 7.56 (dd, J = 8.9, 1.9 Hz, 2H), 7.33 – 7.24 (m, 2H), 5.44 (s, 2H).

¹³C NMR (101 MHz, CDCl₃) δ 155.1–152.9 (m), 151.9, 140.0, 134.6, 133.3, 130.3, 130.0, 128.4, 127.4, 127.1, 126.7 (m), 126.3 (m), 125.1, 124.2 (q, J = 272.1 Hz), 111.9.

¹⁹F NMR (376 MHz, CDCl₃) δ 84.1 (p, J = 150.3 Hz), 62.9 (d, J = 149.8 Hz), -62.3.

FT-IR (neat film NaCl): 3534, 2341, 1632, 1608, 1502, 1452, 1400, 1334, 1317, 1294, 1241, 1198, 1175, 1163, 1131, 1101, 1071, 945, 911, 836, 780, 739, 708, 667, 624, 604 cm⁻¹.

HR-MS (ESI) m/z : [M-H]⁻ Calculated for C₃₄H₁₇F₁₆O₂S₂: 825.0420; Measured: 825.0415.



(S)-3,3'-bis(4-chlorophenyl)-2,2'-bis(methoxymethoxy)-1,1'-binaphthalene (282)

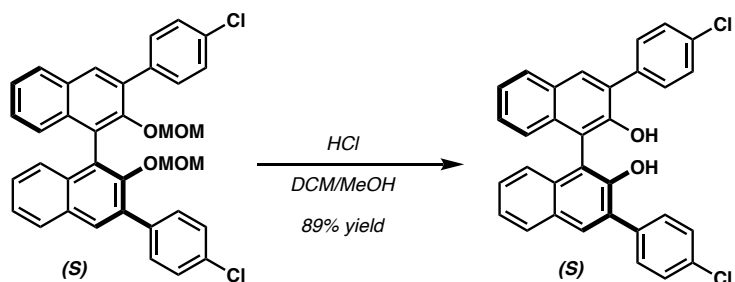
Following a similar procedure as above⁵², MOM-protected 3,3'-diiodo binol (1.40 g, 1 equiv, 2.24 mmol) was added to an oven-dried Schlenk flask, followed by Na₂CO₃ (1.18 g, 5 equiv, 11.2 mmol), and the aryl boronic acid (1.4 g, 4 equiv, 8.94 mmol). The flask was vac/backfilled with N₂ three times, then THF (38 mL), toluene (38 mL), and water (18 mL) were added. The mixture was degassed by sparging with nitrogen while vigorously stirring for 30 minutes. Then, under positive N₂ gas flow, solid Pd(PPh₃)₄ (258 mg, 0.1 equiv, 0.224 mmol) was added in one portion. The flask was then sealed and heated to 85 °C overnight. The next morning, starting material had been consumed by TLC. Water was added to the reaction and extracted with ethyl acetate three times. The combined organics were washed with brine, dried over Na₂SO₄, filtered, and concentrated *in vacuo*. The crude material was purified *via* flash chromatography (2.5% diethyl ether in hexanes) to obtain MOM binol **282** as a white solid (1.1 g, 81% yield).

¹H NMR (400 MHz, CDCl₃) δ 7.93 (s, 2H), 7.90 (d, *J* = 8.2 Hz, 2H), 7.75 – 7.68 (m, 4H), 7.49 – 7.41 (m, 6H), 7.33 – 7.26 (m, 4H), 4.40 (dd, *J* = 5.9, 0.6 Hz, 2H), 4.35 (dd, *J* = 5.9, 0.6 Hz, 2H), 2.37 (s, 6H).

¹³C NMR (101 MHz, CDCl₃) δ 151.3, 137.6, 134.4, 133.8, 133.6, 131.1, 130.9, 130.7, 128.7, 128.0, 126.7, 126.7, 126.5, 125.5, 98.8, 56.1.

FT-IR (neat film NaCl): 2930, 1590, 1492, 1427, 1387, 1352, 1246, 1157, 1091, 1015, 996, 967, 909, 830, 750, 731 cm⁻¹.

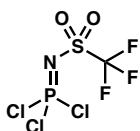
HR-MS (ESI) *m/z*: [M+Na]⁺ Calculated for C₃₆H₂₈Cl₂NaO₄: 617.1257; Measured: 617.1255.



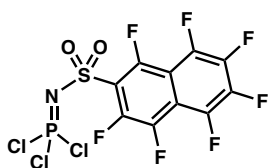
(S)-3,3'-bis(4-chlorophenyl)-[1,1'-binaphthalene]-2,2'-diol (**283**)

MOM-protected binol **282** was dissolved in 54 mL of DCM/MeOH (1:1) in an oven-dried flask equipped with a stir bar. Then, 2.7 mL of conc. HCl is added slowly dropwise. The mixture is allowed to stir at room temperature overnight, by which time starting material is consumed by TLC forming a more polar spot. Saturated aqueous bicarbonate solution was then added (~40 mL), and the mixture was extracted with DCM three times. The combined organics were washed with brine, dried over Na₂SO₄, filtered, concentrated, and purified *via* flash chromatography (10% diethyl ether in hexanes) to obtain binol **283** as a white solid (818 mg, 89% yield), which matched published NMR spectra.⁵⁴

Preparation of phosphorimidoyl trichloride: prepared according to procedures published by List from the corresponding sulfonamide:

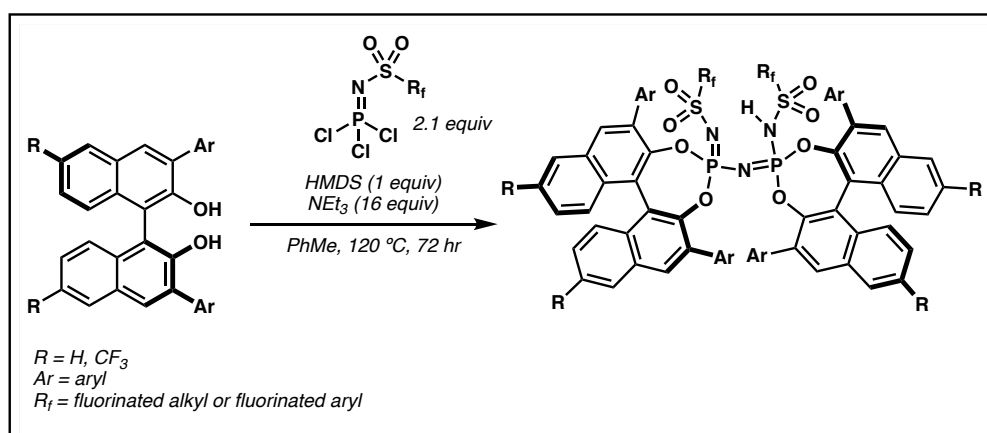


((trifluoromethyl)sulfonyl)phosphorimidoyl trichloride (284) was prepared according to published procedures.⁵⁵

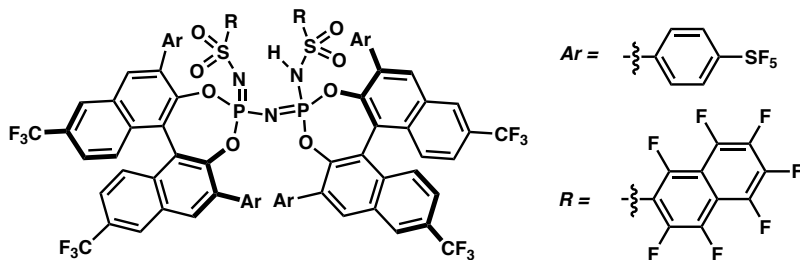


((perfluoronaphthalen-2-yl)sulfonyl)phosphorimidoyl trichloride (285) was prepared according to published procedures.³³

Figure 4.5: Representative scheme for the synthesis of IDPi catalysts



All IDPi catalysts were made in a similar manner as reported by List *et al.*⁵⁵ An oven-dried Schlenk flask was cycled into an inert atmosphere glovebox, and the corresponding phosphorimidoyl trichloride was weighed into it (2.1 equiv). The Schlenk flask was then sealed with a septa, brought out of the glovebox, and put under N₂ atmosphere. To the Schlenk flask was then added dry toluene solvent (to achieve 0.33 M in binol), followed by the binol under positive N₂ flow (2.1 equiv). In cases where the phosphorimidoyl trichloride reagent is a solid, the binol was added first followed by toluene. To the homogeneous solution was added freshly distilled (over CaH₂) triethylamine (16 equiv) and allowed to stir at room temperature. After 20 minutes of stirring at room temperature, dried HMDS (distilled over CaH₂) was added dropwise (1 equiv), then the Schlenk flask was sealed with a ground glass stopper and heated at 120 °C while sealed for 3 days. After this time, the reaction was cooled to room temperature, quenched with 1M HCl, and allowed to stir vigorously for 10 minutes before extracting the mixture with DCM (x3). The combined organics were dried over Na₂SO₄, filtered, and concentrated in vacuo. The crude material was purified by silica flash chromatography (0% → 10% ethyl acetate in benzene) to obtain pure IDPi after concentration *in vacuo*. This material was then dissolved in DCM and stirred vigorously with 6M aq. HCl for 10 minutes. The DCM layer is separated out and washed once more with 6M aq. HCl. The DCM layer was concentrated down, and azeotroped from dry toluene (x3), then dry benzene (x2), then dry DCM/Hex to obtain typically white or off-white solids which are further dried under high vacuum over P₂O₅ overnight before cycling into an inert atmosphere glovebox.

**IDPi 134**

¹H NMR (400 MHz, d₆-DMSO) δ 8.85 (s, 2H), 8.76 (s, 2H), 8.68 (s, 2H), 8.53 (s, 2H), 8.09 – 7.97 (m, 8H), 7.82 (dd, *J* = 9.2, 1.9 Hz, 2H), 7.41 – 7.32 (m, 2H), 7.21 (d, *J* = 8.6 Hz, 4H), 7.00 (t, *J* = 9.3 Hz, 4H), 6.59 (d, *J* = 8.6 Hz, 4H).

¹³C NMR (101 MHz, d₆-DMSO) δ 152.4 – 152.0 (m), 151.5 – 151.2 (m), 149.9 – 149.1 (m), 146.7 – 146.4 (m), 145.5 (t, *J* = 6.4 Hz), 145.0 (t, *J* = 4.9 Hz), 144.2 – 143.7 (m), 142.6 – 142.2 (m), 141.6 – 141.3 (m), 140.8 – 139.8 (m), 139.4 – 139.0 (m), 138.7, 138.5, 138.2 – 137.6, 136.9 – 136.5 (m), 133.1, 132.8, 132.4, 132.3, 131.9, 131.5, 130.5, 129.8, 129.5, 128.8, 128.3, 128.1, 128.0, 127.3, 126.9, 126.7, 126.5, 126.2, 125.9, 125.5, 125.3, 125.2, 124.0, 122.8 (m), 122.6, 122.2, 121.7, 120.1, 119.9, 110.0 – 109.6 (m), 106.9 – 106.3 (m).

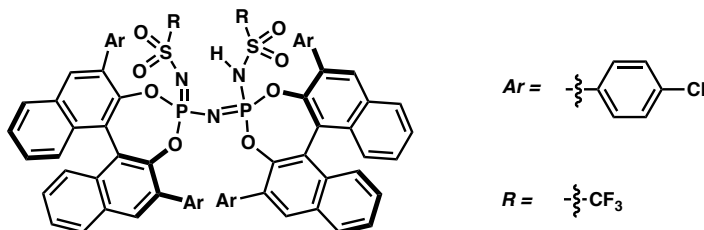
*other peaks not apparent.

¹⁹F NMR (376 MHz, d₆-DMSO) δ 87.0 (m), 64.3 (d, *J* = 255.0 Hz), 63.9 (d, *J* = 254.6 Hz), -61.0, -61.2 – -61.8 (m), -113.8 (dd, *J* = 77.4, 18.0 Hz), -133.9 (d, *J* = 20.1 Hz), -143.3 (dt, *J* = 76.3, 17.5 Hz), -146.6 (dd, *J* = 45.9, 28.5 Hz), -149.2 (dt, *J* = 56.5, 19.4 Hz), -152.0, -155.2 (q, *J* = 14.0 Hz).

³¹P NMR (161 MHz, d₆-DMSO) δ -1.39.

FT-IR (neat film NaCl): 1643, 1491, 1416, 1295, 1139, 1068, 960, 913, 851, 836 cm⁻¹.

HR-MS (ESI) *m/z*: [M-H]⁻ Calculated for C₈₈H₃₂F₄₆N₃O₈P₂S₆: 2385.9259; Measured 2385.9247.

**IDPi 225**

^1H NMR (400 MHz, CDCl_3) δ 8.01 (dd, $J = 8.3, 1.2$ Hz, 2H), 7.97 (s, 2H), 7.93 (dd, $J = 8.3, 1.1$ Hz, 2H), 7.71 (ddd, $J = 8.2, 6.6, 1.4$ Hz, 2H), 7.59 (dd, $J = 8.6, 1.3$ Hz, 2H), 7.56 – 7.51 (m, 2H), 7.46 (ddd, $J = 8.2, 6.3, 1.6$ Hz, 2H), 7.35 – 7.25 (m, 11H), 7.17 (d, $J = 4.7$ Hz, 3H), 6.90 – 6.80 (m, 4H), 6.39 – 6.29 (m, 4H).

^{13}C NMR (101 MHz, CDCl_3) δ 143.7 (t, $J = 5.1$ Hz), 143.4 (app t), 134.7, 134.1, 133.9, 133.8, 132.8, 132.6, 132.3, 132.0, 131.9, 131.8, 131.7, 131.3, 131.0, 130.4, 128.9, 128.8, 128.4, 127.8, 127.7, 127.2, 127.1, 127.0, 126.6, 123.7, 123.7, 123.6, 122.1, 119.5 (q, $J = 321.4$ Hz).

^{19}F NMR (376 MHz, CDCl_3) δ -78.4.

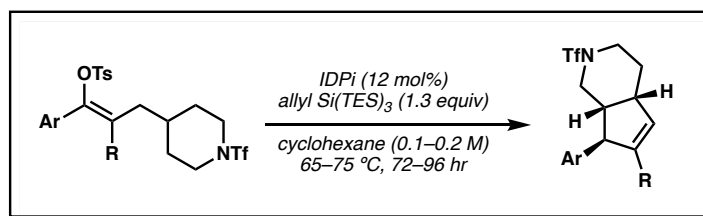
^{31}P NMR (162 MHz, CDCl_3) δ -13.5.

FT-IR (neat film NaCl): 2933, 1493, 1311, 1189, 1150, 1105, 990, 967, 900, 844, 829, 731 cm^{-1} .

HR-MS (ESI) m/z : $[\text{M}-\text{H}]^-$ - Calculated for $\text{C}_{66}\text{H}_{36}\text{Cl}_4\text{F}_6\text{N}_3\text{O}_8\text{P}_2\text{S}_2$: 1380.0053; Measured 1380.0050.

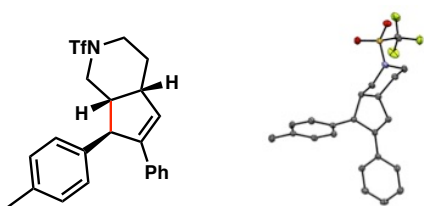
4.6.5 Catalytic Asymmetric C–H Insertion Reactions

Figure 4.6: Representative scheme for catalytic asymmetric C–H insertions



General Procedure: All C–H insertion reactions were conducted in a well-maintained glove box (O₂, H₂O <0.5 ppm) on 0.1 mmol scale unless otherwise noted. To a dram vial equipped with a magnetic stir bar was added IDPi catalyst followed by cyclohexane solvent (dried over potassium), followed by 2-allyl-1,1,1,3,3,3-hexaethyl-2-(triethylsilyl)trisilane. To this mixture was then added the corresponding vinyl tosylate in solid form in one portion. The reaction was then sealed with a Teflon cap and heated to 65 °C for 72 hours (unless otherwise noted). (*Note:* reaction mixture is typically heterogeneous at room temperature, but readily goes homogeneous once heated with stirring and typically remains homogeneous during the entire course of the reaction.) The reactions were monitored by TLC, typically using 5–15% ethyl acetate in hexanes for the mobile phase (C–H insertion products are typically higher in R_f than the starting vinyl tosylate). Once the reaction was completed, the vial was removed from the glovebox. A few drops of triethylamine were then added then diluted with DCM. The homogeneous solution was then plugged through silica gel (pushing through with 1:1 DCM/diethyl ether), concentrated *in vacuo*, and analyzed by ¹H NMR using nitromethane as an internal standard for qNMR analysis. The crude material was purified by flash column chromatography (typically 0–10% diethyl

ether or ethyl acetate in hexanes) then dried on high vacuum to obtain material that is pure by ^1H NMR. The enantiomeric excess of the material was then assessed by chiral HPLC. In cases where trace impurities (<5%) were observed on the chiral HPLC trace, further purification *via* reverse phase preparatory HPLC was performed to obtain analytical quantities of high-purity material to ensure accurate enantiomeric excess determination based on peak integration. Many of the products from this reaction could be recrystallized from hexanes to obtain highly enantioenriched material (typically >99% ee) by heating in hexanes solvent and allowing to cool to room temperature or to $-30\text{ }^\circ\text{C}$. **Note:** unless otherwise noted, characterization of all C–H insertion products by NMR required heating to $90\text{ }^\circ\text{C}$ in d_6 -DMSO which was necessary to prevent peak broadening of the N-Tf piperidine protons (due to the Perlin effect) and also to obtain accurate integration values.⁵⁶ Room temperature NMR in CDCl_3 could be used to obtain NMR yields, given that the diagnostic styrenyl olefin peak is sharp (only the N-Tf piperidine protons are broadened due to the Perlin effect).



(4aR,7R,7aR)-6-phenyl-7-(p-tolyl)-2-((trifluoromethyl)sulfonyl)-2,3,4,4a,7,7a-hexahydro-1H-cyclopenta[c]pyridine (133a)

To a dram vial equipped with a stir bar was added **IDPi 134** (28.7 mg, 0.12 equiv, 0.012 mmol), cyclohexane (0.5 mL), and 2-allyl-1,1,1,3,3,3-hexaethyl-2-(triethylsilyl)trisilane (53.9 mg, 1.3 equiv, 0.13 mmol). To this solution was added vinyl tosylate **132a** (59.4 mg,

1.0 equiv, 0.1 mmol). The reaction was sealed with a teflon cap and heated to 65 °C for 72 hours, the reaction was removed from the glovebox and a few drops of triethylamine were added to quench the reaction and diluted further with DCM. This homogeneous mixture was then plugged through silica gel with DCM/diethyl ether (1:1), concentrated *in vacuo*, and purified by flash column chromatography (4% diethyl ether in hexanes) to give insertion product **133a** as a white solid (34.1 mg, 81% yield). This solid was determined by chiral HPLC to be in 91% *ee*. Absolute stereochemistry was determined by X-ray crystallography by slow evaporation of the isolated material after column chromatography in cyclohexane, this material also determined to be >99% *ee*.

¹H NMR (400 MHz, d₆-DMSO, 90 °C) δ 7.39 – 7.31 (m, 2H), 7.28 – 7.21 (m, 2H), 7.21 – 7.15 (m, 1H), 7.14 – 7.07 (m, 4H), 6.40 (dd, *J* = 2.4, 1.5 Hz, 1H), 4.08 (d, *J* = 5.2 Hz, 1H), 3.73 (dd, *J* = 13.3, 5.4 Hz, 1H), 3.57 (ddd, *J* = 12.0, 7.6, 4.1 Hz, 1H), 3.47 (td, *J* = 13.1, 5.6 Hz, 2H), 3.29 – 3.11 (m, 1H), 2.39 (tt, *J* = 7.1, 5.3 Hz, 1H), 2.27 (s, 3H), 2.07 (dddd, *J* = 13.9, 7.6, 6.1, 4.1 Hz, 1H), 1.76 (dtd, *J* = 14.5, 7.5, 4.1 Hz, 1H).

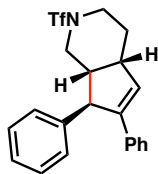
¹³C NMR (101 MHz, d₆-DMSO, 90 °C) δ 143.8, 138.6, 135.0, 134.9, 130.4, 128.6, 127.6, 126.9, 126.5, 125.7, 119.5 (q, *J* = 324.8 Hz), 52.9, 46.8, 45.6, 43.9, 26.4, 19.9.

¹⁹F NMR (376 MHz, d₆-DMSO, 90 °C) δ -75.3.

FT-IR (neat film NaCl): 2916, 1383, 1225, 1214, 1189, 1055, 1008, 764 cm⁻¹.

HR-MS (FD-MS) *m/z*: [M]⁺ Calculated for C₂₂H₂₂F₃NO₂S: 421.1323; Measured: 421.1317

HPLC (ChiralPak ADH column) 98:02 (hex/*i*PrOH) 1 mL/min; *t*_{major} (4.89 min), *t*_{minor} (6.09 min); 91% *ee*.



(4aR,7R,7aR)-6,7-diphenyl-2-((trifluoromethyl)sulfonyl)-2,3,4,4a,7,7a-hexahydro-1H-cyclopenta[c]pyridine (133b)

To a dram vial equipped with a stir bar was added **IDPi 134** (28.7 mg, 0.12 equiv, 0.012 mmol), cyclohexane (0.5 mL), and 2-allyl-1,1,1,3,3,3-hexaethyl-2-(triethylsilyl)trisilane (53.9 mg, 1.3 equiv, 0.13 mmol). To this solution was added vinyl tosylate **132b** (59.4 mg, 1.0 equiv, 0.1 mmol). The reaction was sealed with a Teflon cap and heated to 75 °C for 96 hours, then the reaction was removed from the glovebox and a few drops of triethylamine were added to quench the reaction and diluted further with DCM. This homogeneous mixture was then plugged through silica gel with DCM/diethyl ether (1:1), concentrated *in vacuo*, and purified by flash column chromatography (4% diethyl ether in hexanes) to give insertion product **133b** as a white solid (26.5 mg, 65% yield). This solid was determined by chiral HPLC to be in 82% ee.

¹H NMR (400 MHz, d₆-DMSO, 90 °C) δ 7.34 – 7.10 (m, 10H), 6.39 (dd, *J* = 2.5, 1.5 Hz, 1H), 4.09 (dt, *J* = 5.1, 1.7 Hz, 1H), 3.71 (dd, *J* = 13.3, 5.4 Hz, 1H), 3.58 – 3.37 (m, 3H), 3.18 (dtd, *J* = 9.4, 7.4, 2.2 Hz, 1H), 2.39 (tt, *J* = 7.1, 5.3 Hz, 1H), 2.04 (dddd, *J* = 13.9, 7.5, 6.1, 4.1 Hz, 1H), 1.74 (dtd, *J* = 14.5, 7.5, 4.1 Hz, 1H).

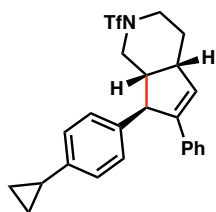
¹³C NMR (101 MHz, d₆-DMSO, 90 °C) 143.7, 141.8, 134.9, 130.6, 128.0, 127.6, 127.0, 126.6, 125.9, 125.7, 119.5 (q, *J* = 325.0 Hz), 46.8, 45.6, 43.9.

¹⁹F NMR (376 MHz, d₆-DMSO, 90 °C) δ -74.94.

FT-IR (neat film NaCl): 2926, 1601, 1493, 1446, 1385, 1226, 1185, 1147, 1098, 986, 951, 859, 835, 787, 761, 732, 700, 683, 668, 637, 616 cm^{-1} .

HR-MS (FD) m/z : $[\text{M}\cdot]^+$ Calculated for $\text{C}_{21}\text{H}_{20}\text{F}_3\text{NO}_2\text{S}$: 407.1167; Measured: 407.1161.

HPLC (ChiralPak ADH column) 98:02 (hex/*i*PrOH) 1mL/min; t_{major} (5.23 min), t_{minor} (6.26 min); 82% ee.



((4*aR*,7*R*,7*aR*)-7-(4-cyclopropylphenyl)-6-phenyl-2-((trifluoromethyl)sulfonyl)-2,3,4,4*a*,7,7*a*-hexahydro-1*H*-cyclopenta[*c*]pyridine (133c)

To a dram vial equipped with a stir bar was added **IDPi 134** (28.7 mg, 0.12 equiv, 0.012 mmol), cyclohexane (0.5 mL), and 2-allyl-1,1,1,3,3,3-hexaethyl-2-(triethylsilyl)trisilane (53.9 mg, 1.3 equiv, 0.13 mmol). To this solution was added vinyl tosylate **132c** (62.0 mg, 1.0 equiv, 0.1 mmol). The reaction was sealed with a Teflon cap and heated to 65 °C for 72 hours, then the reaction was removed from the glovebox and a few drops of triethylamine were added to quench the reaction and diluted further with DCM. This homogeneous mixture was then plugged through silica gel with DCM/diethyl ether (1:1), concentrated *in vacuo*, and purified by flash column chromatography (5% diethyl ether in hexanes) to give insertion product **133c** as a white solid (36.2 mg, 81% yield). This material was determined by chiral HPLC to be 92% ee.

¹H NMR (400 MHz, d₆-DMSO, 90 °C) δ 7.32 – 7.28 (m, 2H), 7.23 – 7.18 (m, 2H), 7.16 – 7.12 (m, 1H), 7.09 – 7.05 (m, 2H), 6.99 – 6.95 (m, 2H), 6.36 (dd, *J* = 2.4, 1.5 Hz, 1H), 4.03 (dt, *J* = 5.1, 1.7 Hz, 1H), 3.69 (dd, *J* = 13.3, 5.4 Hz, 1H), 3.57 – 3.34 (m, 3H), 3.18 – 3.13 (m, 1H), 2.34 (tt, *J* = 7.1, 5.2 Hz, 1H), 2.02 (dddd, *J* = 13.8, 7.6, 6.1, 4.2 Hz, 1H), 1.84 (tt, *J* = 8.4, 5.1 Hz, 1H), 1.72 (dtd, *J* = 14.4, 7.4, 4.1 Hz, 1H), 0.90 – 0.85 (m, 2H), 0.62 – 0.56 (m, 2H).

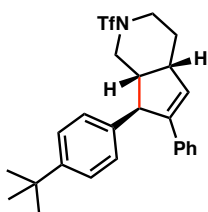
¹³C NMR (101 MHz, d₆-DMSO, 90 °C) δ 143.8, 141.2, 138.7, 135.0, 130.5, 127.6, 126.9, 126.6, 125.7, 125.4, 119.5 (q, *J* = 324.9 Hz), 52.9, 46.8, 45.6, 43.9, 26.4, 14.2, 8.1 (other signal not detected, likely under solvent peak).

¹⁹F NMR (376 MHz, d₆-DMSO, 90 °C) δ -75.0.

FT-IR (neat film NaCl): 2917, 1459, 1387, 1226, 1189, 1148, 952, 762 cm⁻¹.

HR-MS (ESI) *m/z*: [M+NH₄]⁺ Calculated for C₂₄H₂₈F₃N₂O₂S: 465.1818; Measured: 465.1816.

HPLC (ChiralPak ADH column) 98:02 (hex/*i*PrOH) 1mL/min; *t*_{major} (5.78 min), *t*_{minor} (7.01 min); 92% ee.



(4a*R*,7*R*,7a*R*)-7-(4-(*tert*-butyl)phenyl)-6-phenyl-2-((trifluoromethyl)sulfonyl)-2,3,4,4a,7,7a-hexahydro-1*H*-cyclopenta[*c*]pyridine (133d)

To a dram vial equipped with a stir bar was added **IDPi 134** (28.7 mg, 0.12 equiv, 0.012 mmol), cyclohexane (0.5 mL), and 2-allyl-1,1,1,3,3,3-hexaethyl-2-(triethylsilyl)trisilane

(53.9 mg, 1.3 equiv, 0.13 mmol). To this solution was added vinyl tosylate **132d** (63.7 mg, 1.0 equiv, 0.1 mmol). The reaction was sealed with a Teflon cap and heated to 65 °C for 72 hours, then the reaction was removed from the glovebox and a few drops of triethylamine were added to quench the reaction and diluted further with DCM. This homogeneous mixture was then plugged through silica gel with DCM/diethyl ether (1:1), concentrated *in vacuo*, and purified by flash column chromatography (4% diethyl ether in hexanes) to give insertion product **133d** as a white solid (44.5 mg, 96% yield). This material was determined by chiral HPLC to be 88% ee.

¹H NMR (400 MHz, d₆-DMSO, 90 °C) δ 7.34 – 7.30 (m, 2H), 7.30 – 7.26 (m, 2H), 7.21 (tt, *J* = 6.6, 1.0 Hz, 2H), 7.17 – 7.11 (m, 3H), 6.37 (dd, *J* = 2.4, 1.4 Hz, 1H), 4.05 (dt, *J* = 4.9, 1.7 Hz, 1H), 3.71 (dd, *J* = 13.2, 5.5 Hz, 1H), 3.48 (td, *J* = 8.0, 4.3 Hz, 2H), 3.39 (dd, *J* = 13.3, 7.3 Hz, 1H), 3.20 – 3.13 (m, 1H), 2.36 (tt, *J* = 7.3, 5.2 Hz, 1H), 2.06 – 1.98 (m, 1H), 1.74 (dtd, *J* = 14.2, 7.1, 4.4 Hz, 1H), 1.24 (s, 9H).

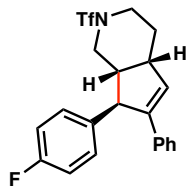
¹³C NMR (101 MHz, d₆-DMSO, 90 °C) δ 148.2, 143.9, 138.6, 135.1, 130.5, 127.7, 127.5, 127.3, 127.0, 126.7, 126.6, 125.8, 124.8, 119.6 (app q, *J* = 324.7 Hz), 53.0, 46.8, 45.8, 43.9, 39.4, 33.6, 30.7, 26.4.

¹⁹F NMR (376 MHz, d₆-DMSO, 90 °C) δ -75.0.

FT-IR (neat film NaCl): 2964, 1387, 1226, 1188, 1149, 762 cm⁻¹.

HR-MS (FD) *m/z*: [M•]⁺ Calculated for C₂₅H₂₈F₃NO₂S: 463.1793; Measured: 463.1797.

HPLC (ChiralPak ADH column) 98:02 (hex/*i*PrOH) 1 mL/min; *t*_{major} (4.05 min), *t*_{minor} (4.95 min); 88% ee.



(4aR,7R,7aR)-7-(4-fluorophenyl)-6-phenyl-2-((trifluoromethyl)sulfonyl)-2,3,4,4a,7,7a-hexahydro-1H-cyclopenta[*c*]pyridine (133e)

To a dram vial equipped with a stir bar was added **IDPi 134** (28.7 mg, 0.12 equiv, 0.012 mmol), cyclohexane (0.5 mL), and 2-allyl-1,1,1,3,3,3-hexaethyl-2-(triethylsilyl)trisilane (53.9 mg, 1.3 equiv, 0.13 mmol). To this solution was added vinyl tosylate **132e** (59.76 mg, 1.0 equiv, 0.1 mmol). The reaction was sealed with a Teflon cap and heated to 75 °C for 96 hours, then the reaction was removed from the glovebox and a few drops of triethylamine were added to quench the reaction and diluted further with DCM. This homogeneous mixture was then plugged through silica gel with DCM/diethyl ether (1:1), concentrated *in vacuo*, and purified by flash column chromatography (5% diethyl ether in hexanes) to give insertion product **133e** as a white solid (24.3 mg, 57% yield). This material was determined by chiral HPLC to be 87% ee.

¹H NMR (400 MHz, *d*₆-DMSO, 90 °C) δ 7.33 – 7.28 (m, 2H), 7.22 (dddd, *J* = 8.1, 6.5, 2.4, 1.2 Hz, 4H), 7.18 – 7.13 (m, 1H), 7.11 – 7.00 (m, 2H), 6.39 (dd, *J* = 2.5, 1.5 Hz, 1H), 4.11 (dt, *J* = 5.1, 1.7 Hz, 1H), 3.72 (dd, *J* = 13.3, 5.4 Hz, 1H), 3.57 – 3.37 (m, 3H), 3.21 – 3.14 (m, 1H), 2.37 (tt, *J* = 7.1, 5.2 Hz, 1H), 2.03 (dddd, *J* = 13.9, 7.6, 6.0, 4.2 Hz, 1H), 1.74 (dtd, *J* = 14.5, 7.4, 4.2 Hz, 1H).

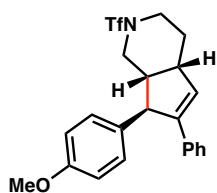
^{13}C NMR (101 MHz, d_6 -DMSO, 90 °C) δ 160.6 (d, $J = 242.6$ Hz), 143.7, 137.8 (d, $J = 3.1$ Hz), 134.8, 130.8, 128.9 (d, $J = 8.0$ Hz), 127.7, 126.7, 125.8, 119.5 (app q, $J = 324.7$ Hz), 114.9, 114.6, 52.5, 46.7, 45.6, 43.9, 26.4 (other signal not detected, likely under solvent peak).

^{19}F NMR (376 MHz, d_6 -DMSO, 90 °C) δ -75.0, -116.7

FT-IR (neat film NaCl): 2921, 1508, 1386, 1224, 1189, 1147, 1068, 758 cm^{-1} .

HR-MS (FD) m/z : $[\text{M}\cdot]^+$ Calculated for $\text{C}_{21}\text{H}_{19}\text{F}_4\text{NO}_2\text{S}$: 425.1073; Measured: 425.1062

HPLC (ChiralPak ADH column) 98:02 (hex/*i*PrOH) 1 mL/min; t_{major} (6.42 min), t_{minor} (7.21 min); 87% ee.



(4aR,7R,7aR)-7-(4-methoxyphenyl)-6-phenyl-2-((trifluoromethyl)sulfonyl)-2,3,4,4a,7,7a-hexahydro-1H-cyclopenta[*c*]pyridine (133f)

To a dram vial equipped with a stir bar was added **IDPi 134** (28.7 mg, 0.12 equiv, 0.012 mmol), cyclohexane (1.0 mL), and 2-allyl-1,1,1,3,3,3-hexaethyl-2-(triethylsilyl)trisilane (53.9 mg, 1.3 equiv, 0.13 mmol). To this solution was added **132f** (60.9 mg, 1.0 equiv, 0.1 mmol). The reaction was sealed with a Teflon cap and heated to 65 °C for 72 hours, then the reaction was removed from the glovebox and a few drops of triethylamine were added to quench the reaction and diluted further with DCM. This homogeneous mixture was then plugged through silica gel with DCM/diethyl ether (1:1), concentrated *in vacuo*, and purified by flash column chromatography (5% diethyl ether in hexanes) to give insertion

product **133f** as a white solid (31 mg, 71% yield). This solid was determined by chiral HPLC to be in 93% ee.

¹H NMR (400 MHz, d₆-DMSO, 90 °C) δ 7.34 – 7.26 (m, 2H), 7.24 – 7.18 (m, 2H), 7.18 – 7.05 (m, 3H), 6.88 – 6.77 (m, 2H), 6.36 (dd, *J* = 2.4, 1.5 Hz, 1H), 4.03 (dt, *J* = 5.2, 1.7 Hz, 1H), 3.71 (s, 3H), 3.67 (d, *J* = 5.4 Hz, 1H), 3.59 – 3.35 (m, 3H), 3.20 – 3.11 (m, 1H), 2.34 (tt, *J* = 7.1, 5.2 Hz, 1H), 2.03 (dddd, *J* = 13.8, 7.5, 6.0, 4.1 Hz, 1H), 1.72 (dtd, *J* = 14.5, 7.6, 4.1 Hz, 1H).

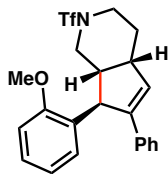
¹³C NMR (101 MHz, d₆-DMSO, 90 °C) δ 157.6, 143.9, 135.0, 133.6, 130.3, 128.0, 127.6, 126.5, 125.7, 119.5 (app q, *J* = 324.8 Hz), 113.8, 54.6, 52.5, 46.8, 45.6, 43.9, 39.2, 26.4.

¹⁹F NMR (376 MHz, d₆-DMSO, 90 °C) δ -74.9.

FT-IR (neat film NaCl): 2923, 1611, 1512, 1463, 1385, 1302, 1226, 1181, 1148, 1115, 1066, 1037, 985, 950, 826, 802, 754, 732 cm⁻¹.

HR-MS (ESI) *m/z*: [M+NH₄]⁺ Calculated for C₂₂H₂₆F₃N₂O₃S: 455.1611; Measured: 455.1614.

HPLC (CHIRALCEL ODH column) 95:05 (hex/*i*PrOH) 1mL/min; *t*_{major} (11.00 min), *t*_{minor} (6.49 min); 93% ee.



**(4aR,7S,7aR)-7-(2-methoxyphenyl)-6-phenyl-2-((trifluoromethyl)sulfonyl)-
2,3,4,4a,7,7a-hexahydro-1H-cyclopenta[c]pyridine (133g)**

To a dram vial equipped with a stir bar was added **IDPi 134** (28.7 mg, 0.12 equiv, 0.012 mmol), cyclohexane (1.0 mL), and 2-allyl-1,1,1,3,3,3-hexaethyl-2-(triethylsilyl)trisilane (53.9 mg, 1.3 equiv, 0.13 mmol). To this solution was added vinyl tosylate **132g** (60.9 mg, 1.0 equiv, 0.1 mmol). The reaction was sealed with a Teflon cap and heated to 65 °C for 72 hours, then the reaction was removed from the glovebox and a few drops of triethylamine were added to quench the reaction and diluted further with DCM. This homogeneous mixture was then plugged through silica gel with DCM/diethyl ether (1:1), concentrated *in vacuo*, and purified by flash column chromatography (7.5% diethyl ether in hexanes) to give vinyl tosylate **133g** as a colorless film (23.7 mg, 54% yield). This material was determined by chiral HPLC to be in 87% ee.

¹H NMR (400 MHz, d₆-DMSO, 90 °C) δ 7.38 – 7.27 (m, 2H), 7.26 – 7.19 (m, 2H), 7.16 (ddt, *J* = 8.2, 7.3, 1.5 Hz, 2H), 7.00 (dd, *J* = 8.2, 1.1 Hz, 1H), 6.89 (dd, *J* = 7.5, 1.8 Hz, 1H), 6.76 (td, *J* = 7.4, 1.1 Hz, 1H), 6.38 (dd, *J* = 2.3, 1.3 Hz, 1H), 4.34 (dt, *J* = 3.4, 1.6 Hz, 1H), 3.86 (s, 3H), 3.78 – 3.69 (m, 1H), 3.60 – 3.35 (m, 3H), 3.14 (tdd, *J* = 8.3, 6.1, 2.2 Hz, 1H), 2.39 (dddd, *J* = 8.4, 7.4, 5.7, 3.7 Hz, 1H), 2.01 (dddd, *J* = 14.5, 8.6, 6.1, 4.7 Hz, 1H), 1.84 (dtd, *J* = 14.2, 6.4, 4.1 Hz, 1H).

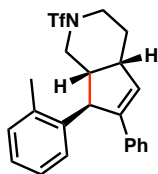
^{13}C NMR (101 MHz, d_6 -DMSO, 90 °C) δ 156.6, 143.2, 134.8, 130.2, 129.4, 127.7, 127.1, 126.8, 126.7, 125.5, 119.9, 119.5 (q, $J = 325.1$ Hz), 110.9, 55.2, 47.4, 46.0, 45.2, 43.5, 25.6.

^{19}F NMR (376 MHz, d_6 -DMSO, 90 °C) δ -74.9.

FT-IR (neat film NaCl): 2928, 1599, 1492, 1461, 1386, 1226, 1184, 1150, 1109, 1047, 955, 755, 728, 695, 666 cm^{-1} .

HR-MS (ESI) m/z : $[\text{M}+\text{NH}_4]^+$ Calculated for $\text{C}_{22}\text{H}_{26}\text{F}_3\text{N}_2\text{O}_3\text{S}$: 455.1611; Measured: 455.1618.

HPLC (ChiralPak ADH column) 98:02 (hex/*i*PrOH) 1 mL/min; t_{major} (5.39 min), t_{minor} (4.89 min); 87% ee.



(4aR,7R,7aR)-6-phenyl-7-(*o*-tolyl)-2-((trifluoromethyl)sulfonyl)-2,3,4,4a,7,7a-hexahydro-1H-cyclopenta[*c*]pyridine (133h)

To a dram vial equipped with a stir bar was added **IDPi 134** (28.7 mg, 0.12 equiv, 0.012 mmol), cyclohexane (0.5 mL), and 2-allyl-1,1,1,3,3,3-hexaethyl-2-(triethylsilyl)trisilane (53.9 mg, 1.3 equiv, 0.13 mmol). To this solution was added vinyl tosylate **132h** (59.4 mg, 1.0 equiv, 0.1 mmol). The reaction was sealed with a Teflon cap and heated to 65 °C for 72 hours, the reaction was removed from the glovebox and a few drops of triethylamine were added to quench the reaction. This mixture was then plugged through silica gel with diethyl ether, concentrated *in vacuo*, and purified by flash column chromatography (5% ethyl acetate in hexanes) to give insertion product **133h** as a colorless low-melting point

solid (37.4 mg, 89% yield). This solid material was analyzed by chiral HPLC and determined to be in 88% *ee*.

¹H NMR (400 MHz, d₆-DMSO, 90 °C) δ 7.33 (dt, *J* = 8.1, 1.8 Hz, 2H), 7.30 – 7.16 (m, 4H), 7.15 – 6.95 (m, 3H), 6.46 (dd, *J* = 2.4, 1.3 Hz, 1H), 4.26 (d, *J* = 1.7 Hz, 1H), 3.81 (dd, *J* = 13.2, 5.6 Hz, 1H), 3.65 – 3.32 (m, 3H), 3.28 – 3.14 (m, 1H), 2.46 (s, 3H), 2.42 (ddd, *J* = 6.6, 3.1, 1.5 Hz, 1H), 2.04 (dddd, *J* = 13.9, 10.8, 5.3, 3.3 Hz, 1H), 1.92 (dtd, *J* = 14.2, 5.9, 3.9 Hz, 1H).

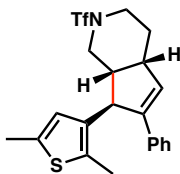
¹³C NMR (101 MHz, d₆-DMSO, 90 °C) δ 143.9, 138.9, 135.1, 134.8, 130.2, 130.1, 127.7, 126.7, 126.1, 125.8, 125.5, 125.6, 119.5 (q, *J* = 324.9 Hz), 50.5, 46.2, 45.2, 43.6, 25.6, 18.6.

¹⁹F NMR (376 MHz, d₆-DMSO) δ -75.2 (br s).

FT-IR (neat film NaCl): 2955, 1383, 1357, 1269, 1222, 1194, 1153, 1040, 827, 758 cm⁻¹.

HR-MS (ESI) *m/z*: [M+H]⁺ Calculated for C₂₂H₂₃F₃NO₂S: 422.1401; Measured: 422.1409.

HPLC (CHIRALCEL ODH column) 90:10 (hex/*i*PrOH) 1 mL/min; *t*_{major} (11.04 min), *t*_{minor} (4.63 min); 88% *ee*.



(4a*R*,7*S*,7a*R*)-7-(2,5-dimethylthiophen-3-yl)-6-phenyl-2-((trifluoromethyl)sulfonyl)-2,3,4,4a,7,7a-hexahydro-1*H*-cyclopenta[*c*]pyridine (133i)

To a dram vial equipped with a stir bar was added **IDPi 134** (14.3 mg, 0.12 equiv, 0.006 mmol), cyclohexane (0.5 mL), and 2-allyl-1,1,1,3,3,3-hexaethyl-2-(triethylsilyl)trisilane (27.0 mg, 1.3 equiv, 0.065 mmol). To this solution was added vinyl tosylate **132i** (31.0 mg, 1.0 equiv, 0.05 mmol). The reaction was sealed with a teflon cap and heated to 70 °C for 72 hours, the reaction was removed from the glovebox and a few drops of triethylamine were added to quench the reaction. This mixture was then plugged through silica gel with diethyl ether, concentrated *in vacuo*, and purified by flash column chromatography (0% → 2% ether in hexanes) to give insertion product **133i** as a colorless semi-solid (9.0 mg, 40% yield). This solid was determined by chiral HPLC to be in 90% ee.

¹H NMR (400 MHz, d₆-DMSO, 90 °C) δ 7.35 – 7.31 (m, 2H), 7.32 – 7.24 (m, 2H), 7.24 – 7.17 (m, 1H), 6.36 (d, *J* = 1.3 Hz, 1H), 6.32 (dd, *J* = 2.4, 1.6 Hz, 1H), 4.10 (dt, *J* = 5.2, 1.8 Hz, 1H), 3.70 (dd, *J* = 13.2, 5.4 Hz, 1H), 3.56 (ddd, *J* = 12.1, 7.7, 4.1 Hz, 1H), 3.53 – 3.34 (m, 2H), 3.22 (dtd, *J* = 9.6, 7.6, 2.2 Hz, 1H), 2.46 (tt, *J* = 7.0, 5.3 Hz, 1H), 2.41 (s, 3H), 2.27 (s, 3H), 2.08 (dddd, *J* = 13.9, 7.7, 6.0, 4.1 Hz, 1H), 1.76 (dtd, *J* = 14.5, 7.4, 4.1 Hz, 1H).

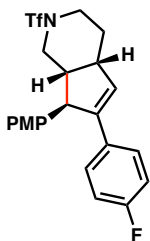
¹³C NMR (101 MHz, d₆-DMSO, 90 °C) δ 144.2, 137.1, 135.1, 134.2, 130.0, 129.7, 127.6, 126.5, 125.4, 125.0, 119.5 (q, *J* = 325.0 Hz), 46.7, 45.6, 45.1, 43.8, 26.2, 14.1, 11.9.

¹⁹F NMR (376 MHz, CDCl₃) δ -75.2 (br s).

FT-IR (neat film NaCl): 2890, 1371, 1265, 1052, 942, 763 cm^{-1} .

HR-MS (ESI) m/z : $[M+H]^+$ Calculated for $\text{C}_{21}\text{H}_{23}\text{F}_3\text{NO}_2\text{S}_2$: 441.1044; Measured: 441.1039.

HPLC (ChiralPak ADH column) 98:02 (hex/*i*PrOH) 1mL/min; t_{major} (4.21 min), t_{minor} (4.68 min); 90% ee.



(4*a*R,7*R*,7*a*R)-6-(4-fluorophenyl)-7-(4-methoxyphenyl)-2-((trifluoromethyl)sulfonyl)-2,3,4,4*a*,7,7*a*-hexahydro-1*H*-cyclopenta[*c*]pyridine (133j)

To a dram vial equipped with a stir bar was added **IDPi 134** (28.7 mg, 0.12 equiv, 0.012 mmol), cyclohexane (1.0 mL), and 2-allyl-1,1,1,3,3,3-hexaethyl-2-(triethylsilyl)trisilane (53.9 mg, 1.3 equiv, 0.13 mmol). To this solution was added vinyl tosylate **132j** (63.0 mg, 1.0 equiv, 0.1 mmol). The reaction was sealed with a Teflon cap and heated to 65 °C for 72 hours, then the reaction was removed from the glovebox and a few drops of triethylamine were added to quench the reaction and diluted further with DCM. This homogeneous mixture was then plugged through silica gel with DCM/diethyl ether (1:1), concentrated *in vacuo*, and purified by flash column chromatography (10% diethyl ether in hexanes) to give insertion product **133j** as a sticky opaque solid (35.6 mg, 78% yield).

$^1\text{H NMR}$ (400 MHz, d_6 -DMSO, 90 °C) δ 7.36 – 7.30 (m, 2H), 7.12 – 7.08 (m, 2H), 7.03 – 6.98 (m, 2H), 6.85 – 6.80 (m, 2H), 6.33 (dd, $J = 2.4, 1.5$ Hz, 1H), 4.01 (dt, $J = 5.3, 1.7$ Hz,

1H), 3.71 (s, 3H), 3.70–3.65 (m, 1H), 3.53 (ddt, $J = 11.7, 7.6, 4.1$ Hz, 1H), 3.42 (td, $J = 12.8, 5.6$ Hz, 2H), 3.17–3.10 (m, 1H), 2.34 (tt, $J = 7.0, 5.3$ Hz, 1H), 2.02 (dddd, $J = 13.8, 7.5, 6.0, 4.0$ Hz, 1H), 1.71 (dtd, $J = 14.1, 7.6, 4.1$ Hz, 1H).

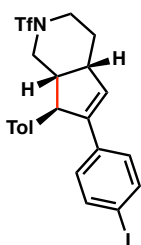
^{13}C NMR (101 MHz, d_6 -DMSO, 90 °C) δ 160.9 (d, $J = 244.6$ Hz), 157.7, 142.9, 133.4, 131.6 (d, $J = 3.2$ Hz), 130.37, 130.36, 128.1, 127.7 (d, $J = 8.0$ Hz), 119.5 (q, $J = 324.8$ Hz), 114.5, 114.3, 113.8, 54.6, 52.6, 46.9, 45.6, 43.9, 26.5 (other signal not detected, likely under solvent peak).

^{19}F NMR (376 MHz, d_6 -DMSO, 90 °C) δ -75.0, -115.0.

FT-IR (neat film NaCl): 2929, 1736, 1609, 1509, 1459, 1387, 1303, 1226, 1185, 1149, 1098, 1037, 987, 952, 831, 806 cm^{-1} .

HR-MS (FD) m/z : $[\text{M}\cdot]^+$ Calculated for $\text{C}_{22}\text{H}_{21}\text{F}_4\text{NO}_3\text{S}$: 455.1178; Measured: 455.1200.

HPLC (ChiralPak ADH column) 95:05 (hex/*i*PrOH) 1 mL/min; t_{major} (6.74 min), t_{minor} (7.95 min); 91% ee.



(4aR,7R,7aR)-6-(4-iodophenyl)-7-(*p*-tolyl)-2-((trifluoromethyl)sulfonyl)-2,3,4,4a,7,7a-hexahydro-1H-cyclopenta[*c*]pyridine (133k)

To a dram vial equipped with a stir bar was added **IDPi 134** (28.7 mg, 0.12 equiv, 0.012 mmol), cyclohexane (0.5 mL), and 2-allyl-1,1,1,3,3,3-hexaethyl-2-(triethylsilyl)trisilane (53.9 mg, 1.3 equiv, 0.13 mmol). To this solution was added vinyl tosylate **132k** (72.0 mg, 1.0 equiv, 0.1 mmol). The reaction was sealed with a Teflon cap and heated to 65 °C for

72 hours, then the reaction was removed from the glovebox and a few drops of triethylamine were added to quench the reaction and diluted further with DCM. This homogeneous mixture was then plugged through silica gel with DCM/diethyl ether (1:1), concentrated *in vacuo*, and purified by flash column chromatography (5% diethyl ether in hexanes) to give insertion product **133k** as a clear oil (29.8 mg, 54% yield). This material was determined by chiral HPLC to be 90% ee.

¹H NMR (400 MHz, d₆-DMSO, 90 °C) δ 7.64 – 7.47 (m, 2H), 7.12 – 7.08 (m, 2H), 7.06 (s, 4H), 6.42 (dd, *J* = 2.5, 1.5 Hz, 1H), 4.02 (dt, *J* = 5.4, 1.7 Hz, 1H), 3.67 (dd, *J* = 13.3, 5.3 Hz, 1H), 3.53 (ddd, *J* = 11.9, 7.4, 4.2 Hz, 1H), 3.47 – 3.36 (m, 2H), 3.16 – 3.10 (m, 1H), 2.34 (tt, *J* = 7.0, 5.3 Hz, 1H), 2.24 (s, 3H), 2.02 (dddd, *J* = 13.8, 7.4, 6.0, 4.0 Hz, 1H), 1.70 (dtd, *J* = 14.1, 7.8, 4.1 Hz, 1H).

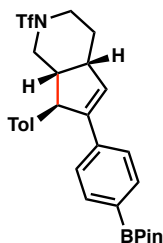
¹³C NMR (101 MHz, d₆-DMSO, 90 °C) δ 142.9, 138.4, 136.5, 135.1, 134.7, 131.7, 128.7, 127.9, 127.0, 119.5 (app q, *J* = 324.7 Hz), 92.1, 52.7, 46.9, 45.5, 43.9, 39.45, 26.4, 20.0.

¹⁹F NMR (376 MHz, d₆-DMSO, 90 °C) δ -74.9

FT-IR (neat film NaCl): 2932, 1738, 1514, 1486, 1385, 1225, 1187, 1002, 952, 814 cm⁻¹

HR-MS (ESI) *m/z*: [M+Na]⁺ Calculated for C₂₂H₂₁F₃INNaO₂S: 570.0182; Measured: 570.0191.

HPLC (ChiralPak ADH column) 98:02 (hex/*i*PrOH) 1mL/min; *t*_{major} (6.94 min), *t*_{minor} (9.92 min); 90% ee.



(4aR,7R,7aR)-6-(4-(4,4,5,5-tetramethyl-1,3,2-dioxaborolan-2-yl)phenyl)-7-(p-tolyl)-2-((trifluoromethyl)sulfonyl)-2,3,4,4a,7,7a-hexahydro-1H-cyclopenta[*c*]pyridine (133I)

To a dram vial equipped with a stir bar was added **IDPi 134** (14.3 mg, 0.12 equiv, 0.006 mmol), cyclohexane (0.5 mL), and 2-allyl-1,1,1,3,3,3-hexaethyl-2-(triethylsilyl)trisilane (27.0 mg, 1.3 equiv, 0.065 mmol). To this solution was added vinyl tosylate **132I** (36.0 mg, 1.0 equiv, 0.05 mmol). The reaction was sealed with a Teflon cap and heated to 70 °C for 72 hours, the reaction was removed from the glovebox and a few drops of triethylamine were added to quench the reaction. This mixture was then plugged through silica gel with diethyl ether, concentrated *in vacuo*, and purified by flash column chromatography (5% → 10% ethyl acetate in hexanes) to give insertion product **133I** as a white solid (16.1 mg, 60% yield). This solid was determined by chiral HPLC to be 90% ee.

¹H NMR (400 MHz, d₆-DMSO, 90 °C) δ 7.55 (d, *J* = 8.3 Hz, 2H), 7.34 (d, *J* = 8.2 Hz, 2H), 7.10 (d, *J* = 1.0 Hz, 4H), 6.47 (dd, *J* = 2.5, 1.5 Hz, 1H), 4.10 (dt, *J* = 5.4, 1.7 Hz, 1H), 3.82 – 3.66 (m, 1H), 3.57 (ddd, *J* = 12.0, 6.0, 3.1 Hz, 1H), 3.47 (dt, *J* = 12.9, 5.7 Hz, 2H), 3.32 – 3.11 (m, 1H), 2.40 (tt, *J* = 6.8, 5.3 Hz, 1H), 2.27 (s, 3H), 2.07 (dddd, *J* = 13.7, 7.3, 6.0, 4.0 Hz, 1H), 1.75 (dtd, *J* = 14.1, 7.7, 4.0 Hz, 1H), 1.31 (s, 12H).

¹³C NMR (101 MHz, d₆-DMSO, 90 °C) δ 143.8, 138.5, 137.8, 134.9, 133.7, 131.8, 128.6, 126.9, 125.1, 119.5 (q, *J* = 325.0 Hz), 83.1, 52.7, 46.8, 45.5, 43.9, 26.4, 24.1 (d, *J* = 3.5 Hz), 19.9.

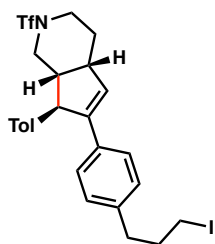
^{19}F NMR (376 MHz, CDCl_3) δ -75.2 (br s).

^{11}B NMR (128 MHz, CDCl_3) δ 32.2.

FT-IR (neat film NaCl): 2875, 1458, 1383, 1363, 1223, 1190, 1169, 1142, 1045, 824, 763 cm^{-1} .

HR-MS (ESI) m/z : $[\text{M}+\text{K}]^+$ Calculated for $\text{C}_{28}\text{H}_{33}\text{BF}_3\text{NO}_4\text{SK}$: 586.1812; Measured: 586.1815.

HPLC (ChiralPak IC column) 90:10 (hex/*i*PrOH) 1mL/min; t_{major} (6.72 min), t_{minor} (4.22 min); 90% ee.



(4a*R*,7*R*,7a*R*)-6-(4-(3-iodopropyl)phenyl)-7-(*p*-tolyl)-2-((trifluoromethyl)sulfonyl)-2,3,4,4a,7,7a-hexahydro-1*H*-cyclopenta[*c*]pyridine (133m)

Following a slightly modified version of the general procedure: To a dram vial equipped with a stir bar was added **IDPi 134** (28.7 mg, 0.12 equiv, 0.012 mmol), cyclohexane (0.5 mL), and 2-allyl-1,1,1,3,3,3-hexaethyl-2-(triethylsilyl)trisilane (53.9 mg, 1.3 equiv, 0.13 mmol). To this solution was added vinyl tosylate **132m** (76.2 mg, 1.0 equiv, 0.1 mmol). The reaction was sealed with a Teflon cap and heated to 65 °C for 72 hours, then the reaction was removed from the glovebox and loaded directly onto a silica gel column for purification (5% diethyl ether in hexanes) to give insertion product **133m** as a colorless oil (39 mg, 66% yield). This material was determined by chiral HPLC to be in 91% ee.

¹H NMR (400 MHz, C₆D₆, 70 °C) δ 7.19 – 7.11 (m, 5H), 7.07 – 6.99 (m, 2H), 6.94 – 6.87 (m, 2H), 6.83 – 6.75 (m, 2H), 5.86 (dd, *J* = 2.4, 1.6 Hz, 1H), 3.85 (d, *J* = 5.7 Hz, 1H), 3.32 (dd, *J* = 13.7, 5.8 Hz, 1H), 3.18 (s, 2H), 2.87 (d, *J* = 11.9 Hz, 1H), 2.65 (t, *J* = 6.9 Hz, 2H), 2.55 – 2.46 (m, 1H), 2.30 (t, *J* = 7.3 Hz, 2H), 2.12 – 2.00 (m, 4H), 1.72 – 1.60 (m, 2H), 1.47 – 1.33 (m, 1H), 1.19 (dtd, *J* = 14.2, 7.8, 3.9 Hz, 1H).

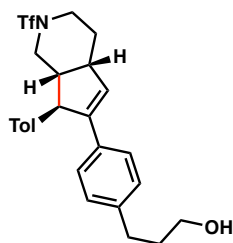
¹³C NMR (101 MHz, C₆D₆, 70 °C) 45.1, 139.5, 138.6, 135.9, 133.5, 129.4, 129.3, 128.2, 126.5, 120.6 (app q, *J* = 324.2 Hz), 53.5, 47.8, 46.1, 44.2, 39.8, 35.6, 34.4, 27.6, 20.4, 4.8.

¹⁹F NMR (376 MHz, C₆D₆, 70 °C) δ -75.5.

FT-IR (neat film NaCl): 2920, 1511, 1387, 1225, 1184, 1147, 984, 951, 815, 725, 682 cm⁻¹.

HR-MS (ESI) *m/z*: [M+H]⁺ Calculated for C₂₅H₂₈F₃INO₂S: 590.0832; Measured: 590.0816.

HPLC (ChiralPak ADH column) 98:02 (hex/*i*PrOH) 1mL/min; *t*_{major} (7.16 min), *t*_{minor} (9.65 min); 91% ee.



3-(4-((4aR,7R,7aR)-7-(*p*-tolyl)-2-((trifluoromethyl)sulfonyl)-2,3,4,4a,7,7a-hexahydro-1H-cyclopenta[*c*]pyridin-6-yl)phenyl)propan-1-ol (133n)

Following a slightly modified version of the general procedure: To a dram vial equipped with a stir bar was added **IDPi 134** (28.7 mg, 0.12 equiv, 0.012 mmol), cyclohexane (0.5 mL), and 2-allyl-1,1,1,3,3,3-hexaethyl-2-(triethylsilyl)trisilane (95.4 mg, 2.3 equiv, 0.23

mmol). To this solution was added vinyl tosylate **132n** (65.2 mg, 1.0 equiv, 0.1 mmol). The reaction was sealed with a Teflon cap and heated to 65 °C for 72 hours. After this time, the reaction was removed from the glovebox and to the reaction vial was added 1 mL of a freshly prepared solution of TBAF•(H₂O)₃ in THF (0.05M) at room temperature and allowed to stir overnight. The next morning, saturated aqueous ammonium chloride was added to the reaction vial (~2 mL) then the mixture was extracted with ethyl acetate three times. The combined organics were dried over Na₂SO₄, filtered, concentrated *in vacuo*, then purified *via* flash chromatography (1% → 2% diethyl ether in DCM) to obtain free alcohol **133n** as a white solid (30.7 mg, 64% yield). This material was determined by chiral HPLC to be in 87% ee.

¹H NMR (400 MHz, d₆-DMSO, 90 °C) δ 7.25 – 7.15 (m, 2H), 7.12 – 6.98 (m, 6H), 6.30 (dd, *J* = 2.4, 1.5 Hz, 1H), 4.00 (dt, *J* = 5.0, 1.7 Hz, 1H), 3.69 (dd, *J* = 13.3, 5.4 Hz, 1H), 3.56 – 3.32 (m, 5H), 3.15 (q, *J* = 6.9 Hz, 1H), 2.57 – 2.52 (m, 2H), 2.33 (tt, *J* = 7.2, 5.2 Hz, 1H), 2.24 (s, 3H), 2.02 (dddd, *J* = 13.9, 7.6, 6.0, 4.2 Hz, 1H), 1.79 – 1.62 (m, 3H).

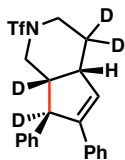
¹³C NMR (101 MHz, d₆-DMSO, 90 °C) δ 143.7, 140.8, 138.8, 134.9, 132.3, 129.4, 128.6, 127.5, 126.9, 125.6, 119.5 (q, *J* = 324.8 Hz), 59.7, 53.0, 46.8, 45.6, 43.8, 33.4, 30.8, 26.4, 19.9.

¹⁹F NMR (376 MHz, d₆-DMSO, 90 °C) δ -74.9.

FT-IR (neat film NaCl): 3366 (br s), 2919, 2859, 1732, 1653, 1561, 1512, 1447, 1386, 1269, 1226, 1186, 1148, 1065, 1045, 984, 952, 819, 735, 606.

HR-MS (ESI) *m/z*: [M+H]⁺ Calculated for C₂₅H₂₉F₃NO₃S: 480.1815; Measured: 480.1809.

HPLC (ChiralPak ADH column) 90:10 (hex/*i*PrOH) 1 mL/min; t_{major} (7.86 min), t_{minor} (9.69 min); 87% ee.



(4aR,7R,7aR)-6,7-diphenyl-2-((trifluoromethyl)sulfonyl)-2,3,4,4a,7,7a-hexahydro-1H-cyclopenta[*c*]pyridine-4,4,7,7a-*d*4 (133b-D)

Following General Procedure A: To a dram vial equipped with a stir bar was added **IDPi 134** (28.7 mg, 0.12 equiv, 0.012 mmol), cyclohexane (0.5 mL), and 2-allyl-1,1,1,3,3,3-hexaethyl-2-(triethylsilyl)trisilane (53.9 mg, 1.3 equiv, 0.13 mmol). To this solution was added tetradeuterated vinyl tosylate **132b-D** (58.4 mg, 1.0 equiv, 0.1 mmol). The reaction was sealed with a Teflon cap and heated to 75 °C for 96 hours, then the reaction was removed from the glovebox and a few drops of triethylamine were added to quench the reaction and diluted further with DCM. This homogeneous mixture was then plugged through silica gel with DCM/diethyl ether (1:1), concentrated *in vacuo*, and purified by flash column chromatography (4% diethyl ether in hexanes) to give insertion product **133b-D** as a white solid (29.9 mg, 73% yield). This solid was determined by chiral HPLC to be in 85% ee.

$^1\text{H NMR}$ (400 MHz, d_6 -DMSO, 90 °C) δ 7.34 – 7.10 (m, 10H), 6.39 (d, $J = 2.4$ Hz, 1H), 3.71 (d, $J = 13.2$ Hz, 1H), 3.52 (d, $J = 12.5$ Hz, 1H), 3.48 – 3.37 (m, 2H), 3.16 (d, $J = 2.4$ Hz, 1H).

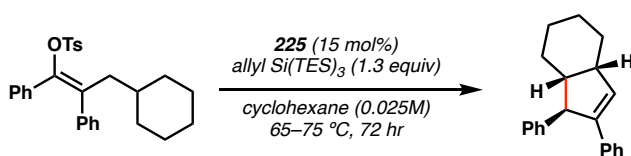
^{13}C NMR (101 MHz, d_6 -DMSO, 90 °C) δ 143.6, 141.7, 134.9, 130.6, 128.0, 127.6, 127.0, 126.6, 125.8, 125.7, 119.5 (q, $J = 324.8, 189.0$ Hz), 45.5, 43.7. *other peaks not apparent.

^{19}F NMR (376 MHz, d_6 -DMSO, 90 °C) δ -74.9.

FT-IR (neat film NaCl): 3025, 2926, 1492, 1386, 1227, 1189, 1173, 1137, 1115, 1051, 995, 760, 694, 683 cm^{-1} .

HR-MS (FD) m/z : $[\text{M}\cdot]^+$ Calculated for $\text{C}_{21}\text{H}_{16}\text{D}_4\text{F}_3\text{NO}_2\text{S}$: 411.1418; Measured: 411.1417.

HPLC (ChiralPak ADH column) 98:02 (hex/*i*PrOH) 1mL/min; t_{major} (5.25 min), t_{minor} (6.28 min); 85% ee.



1,2-diphenyl-3a,4,5,6,7,7a-hexahydro-1H-indene (216)

To a dram vial equipped with a stir bar was added **IDPi 225** (31.1 mg, 0.15 equiv, 0.0225 mmol), cyclohexane (6.0 mL), and 2-allyl-1,1,1,3,3,3-hexaethyl-2-(triethylsilyl)trisilane (80.9 mg, 1.3 equiv, 0.195 mmol). To this solution was added vinyl tosylate **215** (67 mg, 1.0 equiv, 0.15 mmol). The reaction was sealed with a Teflon cap and heated to 75 °C for 72 hours, then the reaction was removed from the glovebox and a few drops of triethylamine were added to quench the reaction and diluted further with DCM. This homogeneous mixture was then plugged through silica gel with DCM then concentrated *in vacuo*. The crude material was purified by flash column chromatography (3% benzene in hexanes) to give **216** as a mixture of diastereomers (3.5:1) as a colorless oil (29.5 mg, 72%

yield). The diastereomers were separated by reverse phase HPLC. The major isomer was determined by chiral HPLC to be 57% ee.

¹H NMR (400 MHz, CDCl₃) δ 7.33 – 7.07 (m, 10H), 6.38 (dd, $J = 2.4, 1.3$ Hz, 1H), 3.91 (dt, $J = 4.8, 1.5$ Hz, 1H), 2.92 (qt, $J = 6.3, 1.9$ Hz, 1H), 2.22 – 2.12 (m, 1H), 1.75 – 1.29 (m, 8H).

¹³C NMR (101 MHz, CDCl₃) δ 143.8, 143.3, 136.6, 134.2, 128.4, 128.2, 127.9, 126.7, 126.2, 126.0, 57.0, 49.1, 42.6, 28.6, 27.9, 23.7, 23.4.

FT-IR (neat film NaCl): 3025, 2923, 2849, 1599, 1492, 1445, 754, 696 cm⁻¹.

HR-MS (FD) m/z : [M•]⁺ Calculated for C₂₁H₂₂: 274.1722; Measured: 274.1734.

HPLC (CHIRALCEL OJH column) 99:1 (hex/*i*PrOH) 1mL/min; t_{major} (6.62 min), t_{minor} (4.92 min); 57% ee.

4.6.6 Isotopic labeling studies

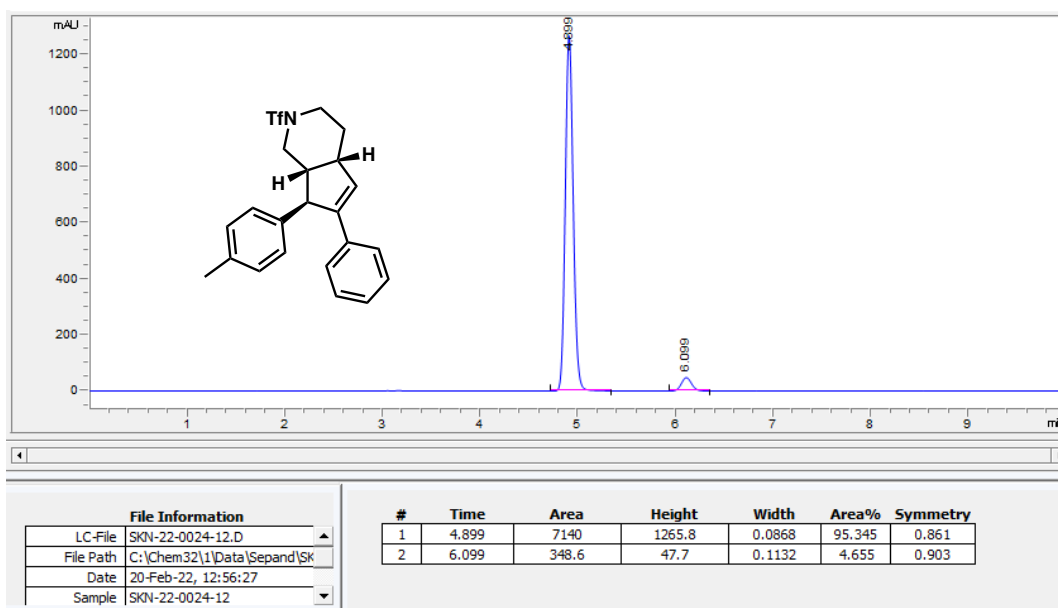
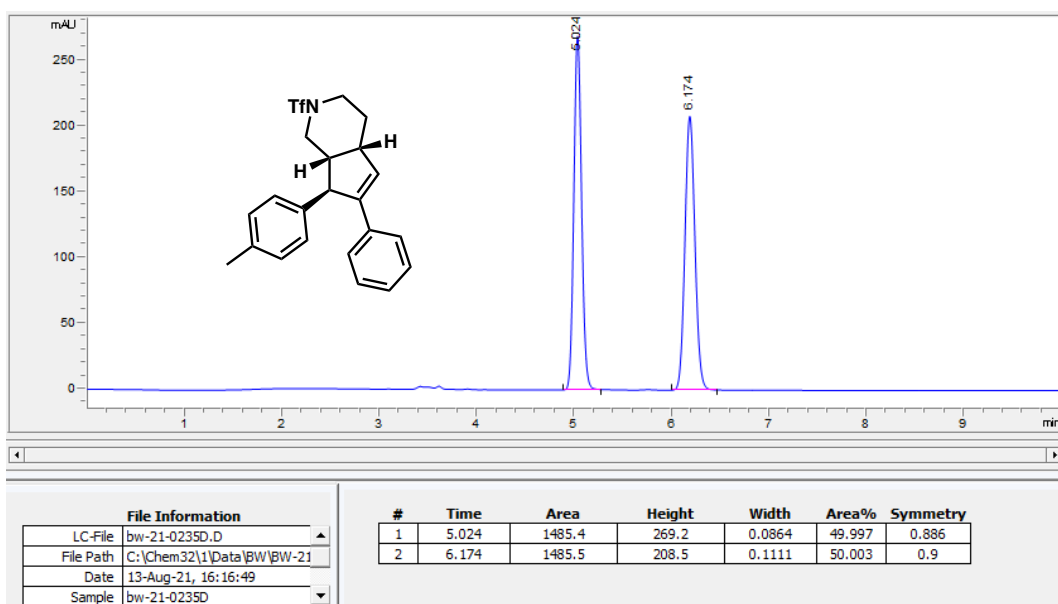
Reactions of deuterated (**132b-D**) and non-deuterated (**132b**) substrates we run in triplicate with two structurally distinct catalyst, **IDPi-1** and **IDPi-2**, and their %ee's were averaged to assess differences in enantioselectivity resulting from isotopic labeling. Error from differences (Δ) in %ee and $\Delta\Delta G^\ddagger$ were determined through standard error propagation. For difference in $\Delta\Delta G^\ddagger$, enantiomeric ratios (e.r.) were averaged and the associated errors were propagated through calculation using $\Delta\Delta G^\ddagger = -RT \cdot \ln(\text{e.r.})$ for $T = 75$ °C. The increased %ee from deuteration of the C–H insertion sites are consistent with an enantiodetermining C–H cleavage step, and while the increases in %ee are small (2.754–5.788% ee), they

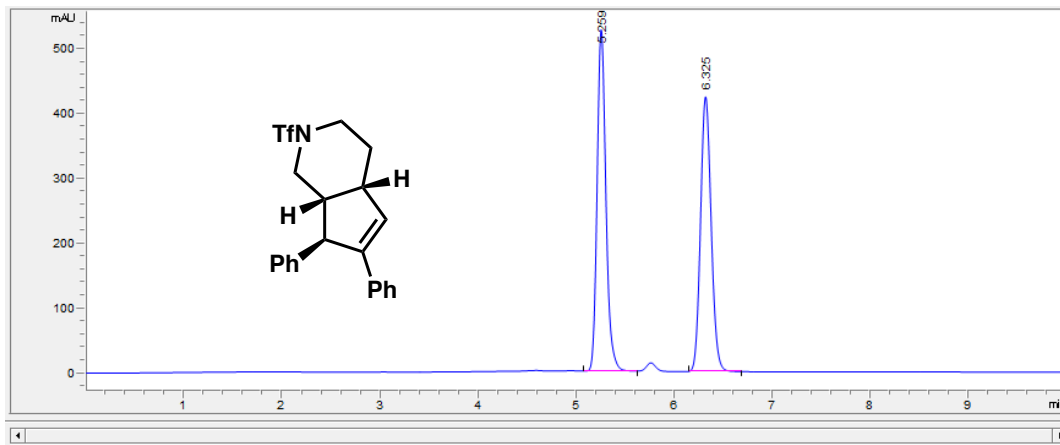
correspond to a considerable difference in $\Delta\Delta G^\ddagger$ (0.089–0.125 kcal/mol) using two structural unique catalyst in this experiment.

Table 4.2. Triplicated reactions of deuterated and non-deuterated substrates

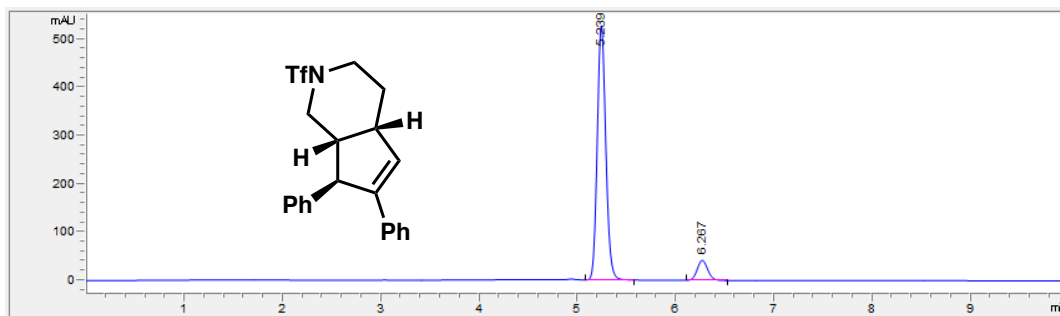
	Substrate 132b (H ₄) (% ee)	Substrate 132b-D (D ₄) (% ee)	Δ (% ee)	$\Delta\Delta G^\ddagger$ (kcal/mol)
IDPi 134	Run 1: 81.150%	Run 1: 84.852%	2.754 ±	0.125 ± 0.030
	Run 2: 82.232%	Run 2: 84.622%	0.160%	
	Run 3: 82.842%	Run 3: 85.012%		
	<u>AVG: 82.074 ± 0.160%</u>	<u>AVG: 84.828 ± 0.160%</u>		
IDPi 225	Run 1: 30.620%	Run 1: 36.228%	5.788 ±	0.089 ± 0.017
	Run 2: 31.380%	Run 2: 35.832%	1.147%	
	Run 3: 28.682%	Run 3: 35.986%		
	<u>AVG: 30.227 ± 1.135%</u>	<u>AVG = 36.015 ± 0.163%</u>		

4.6.7 Chiral HPLC Traces of Racemic and Enantioenriched Products

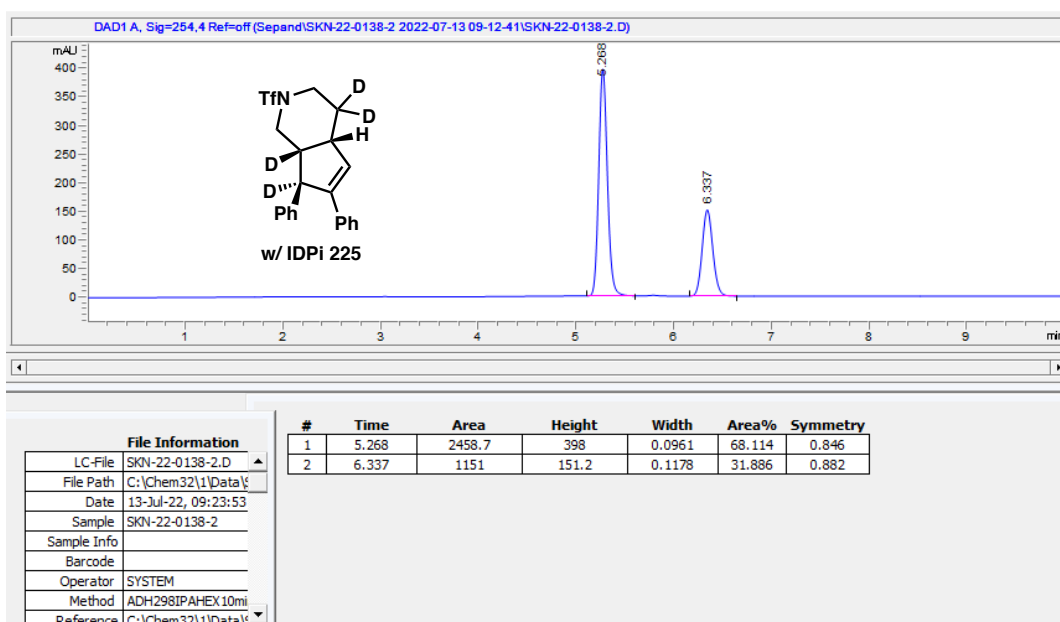
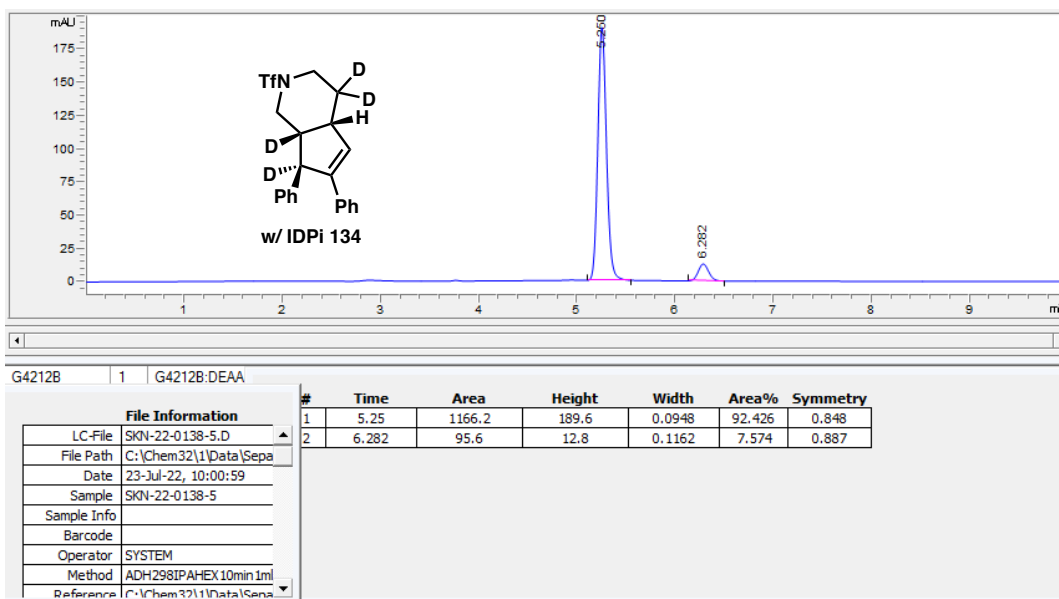


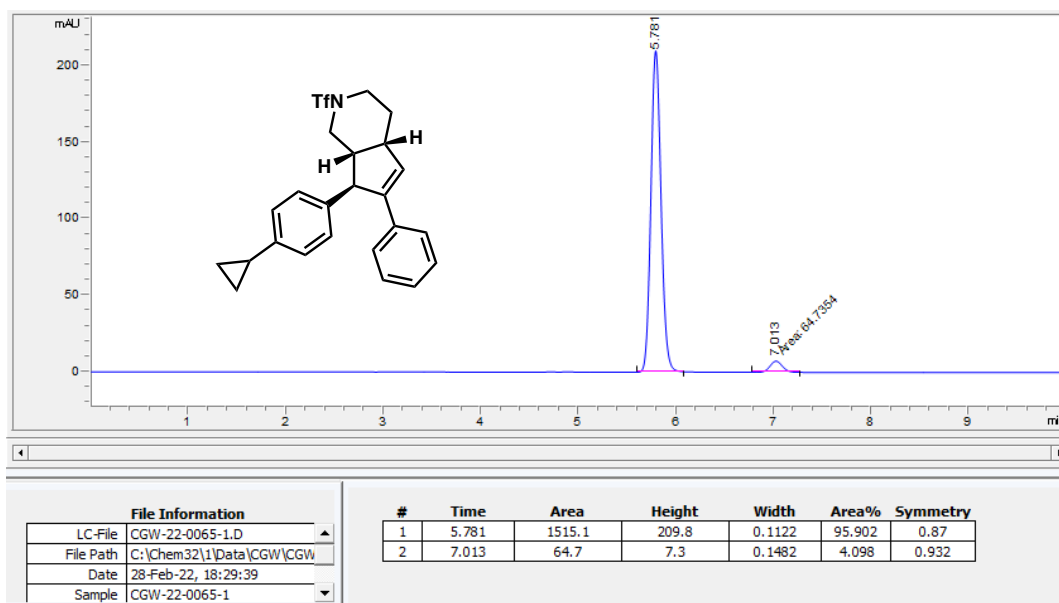
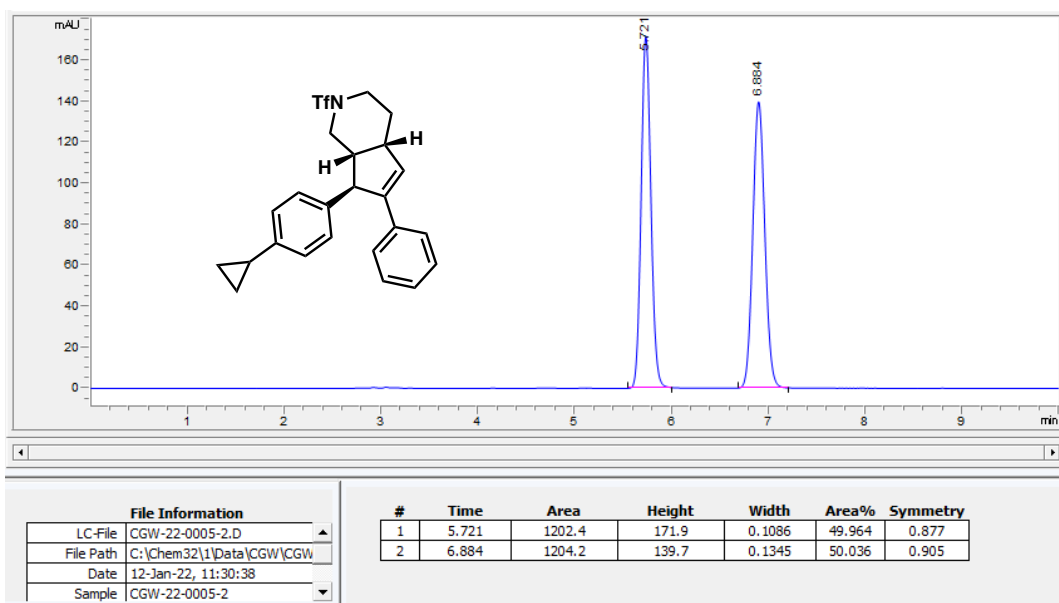


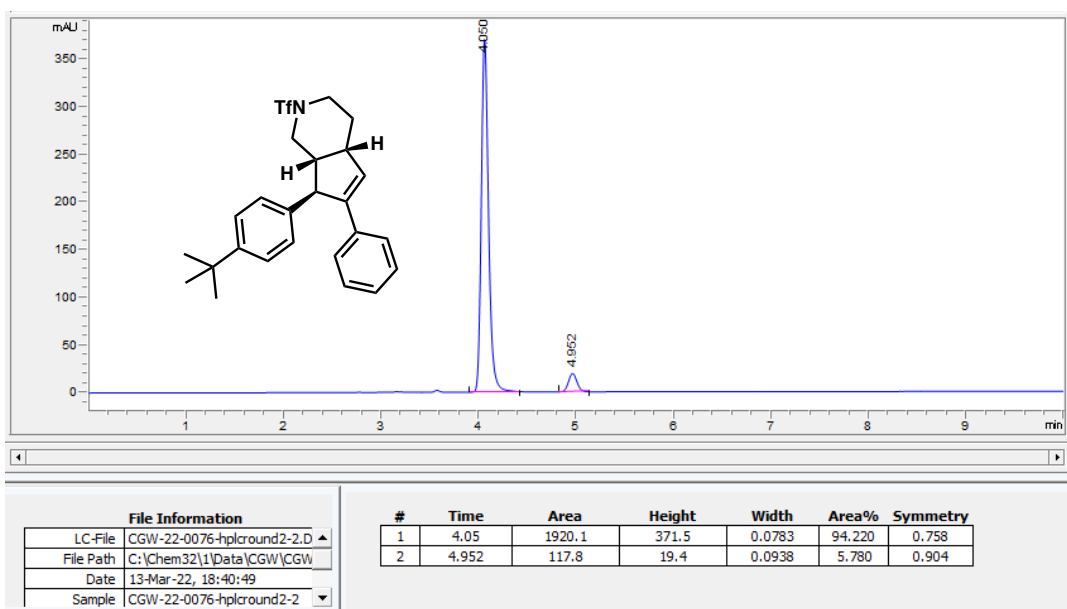
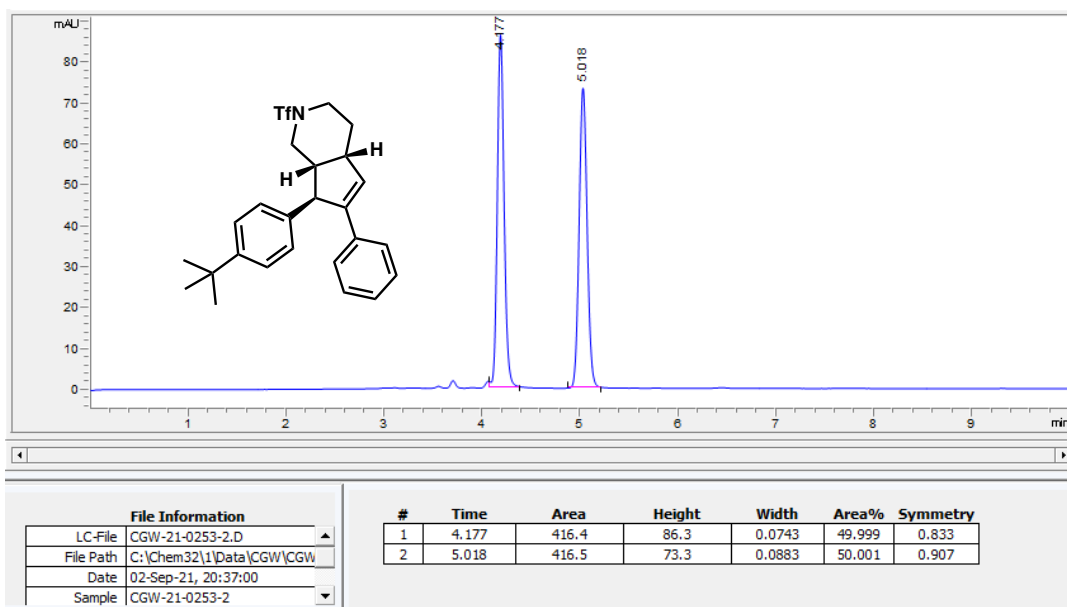
File Information		#	Time	Area	Height	Width	Area%	Symmetry
LC-File	CGW-22-0134-1.D	1	5.259	3312.8	527.9	0.0962	50.799	0.814
File Path	C:\Chem32\1\Data\CGW\CGW-	2	6.325	3208.5	424.7	0.1171	49.201	0.869
Date	29-May-22, 12:12:21							
Sample	CGW-22-0134-1							

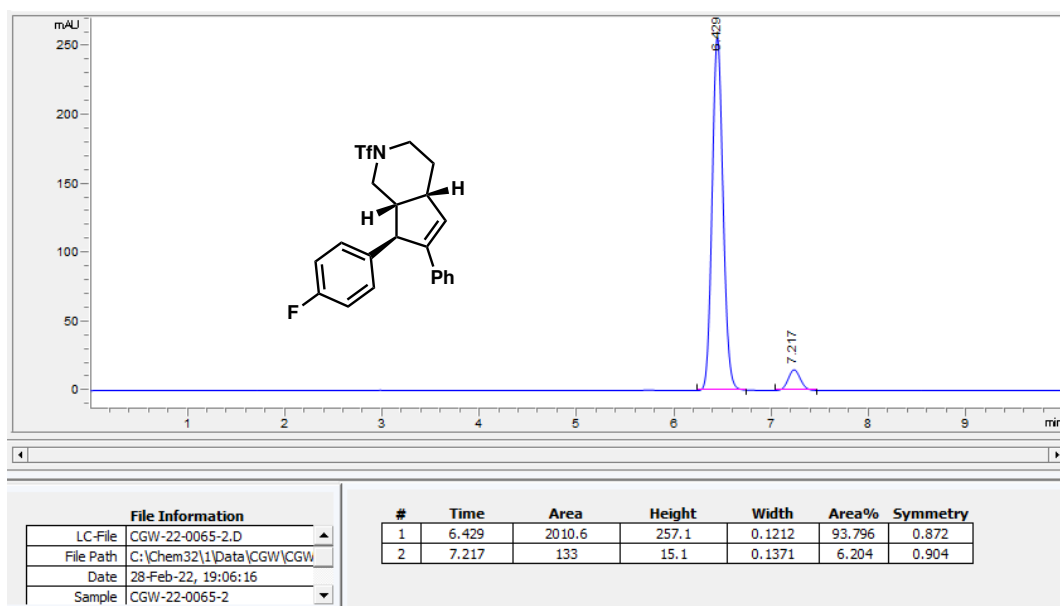
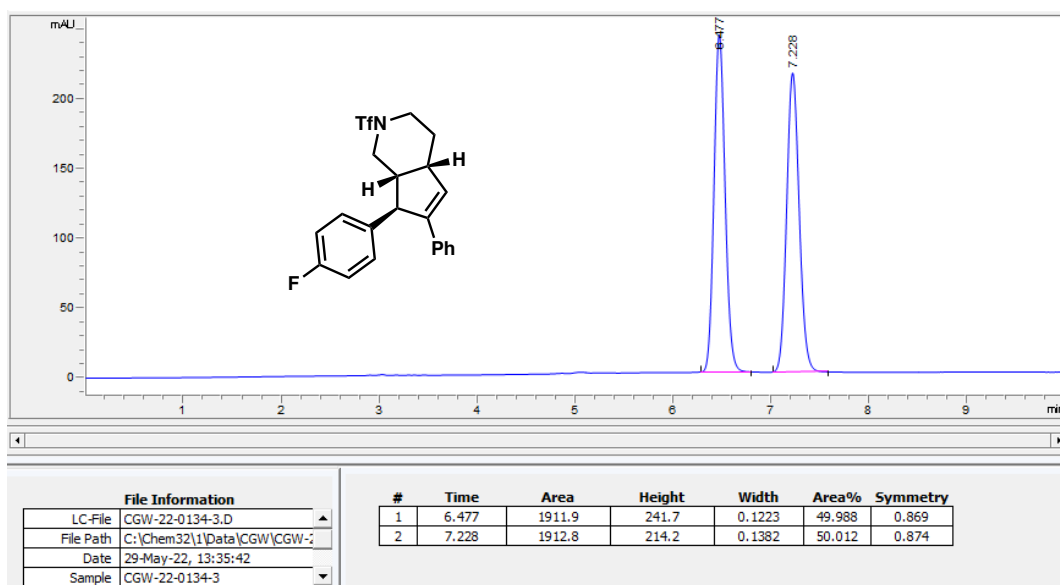


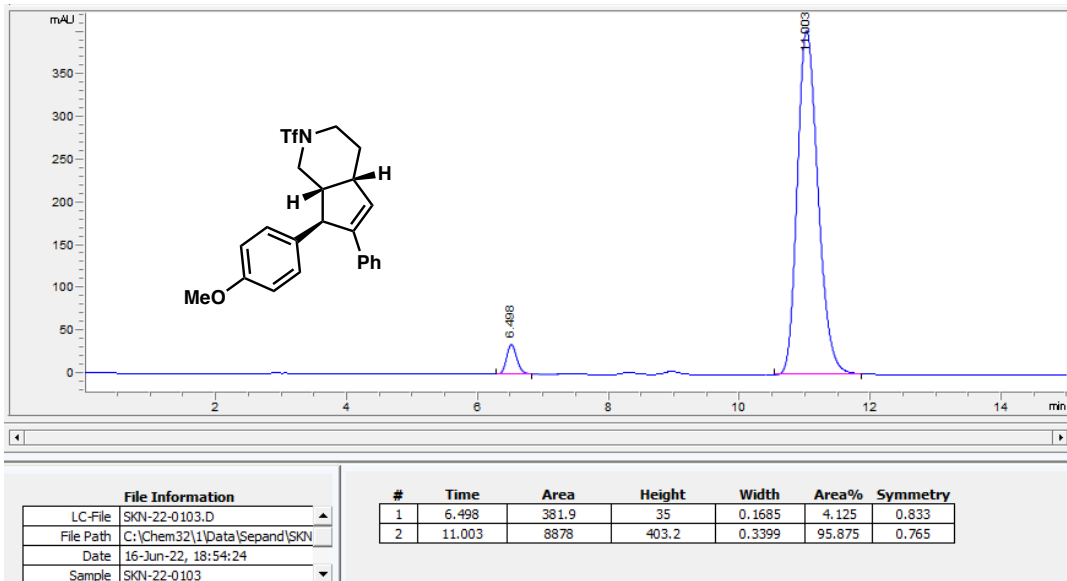
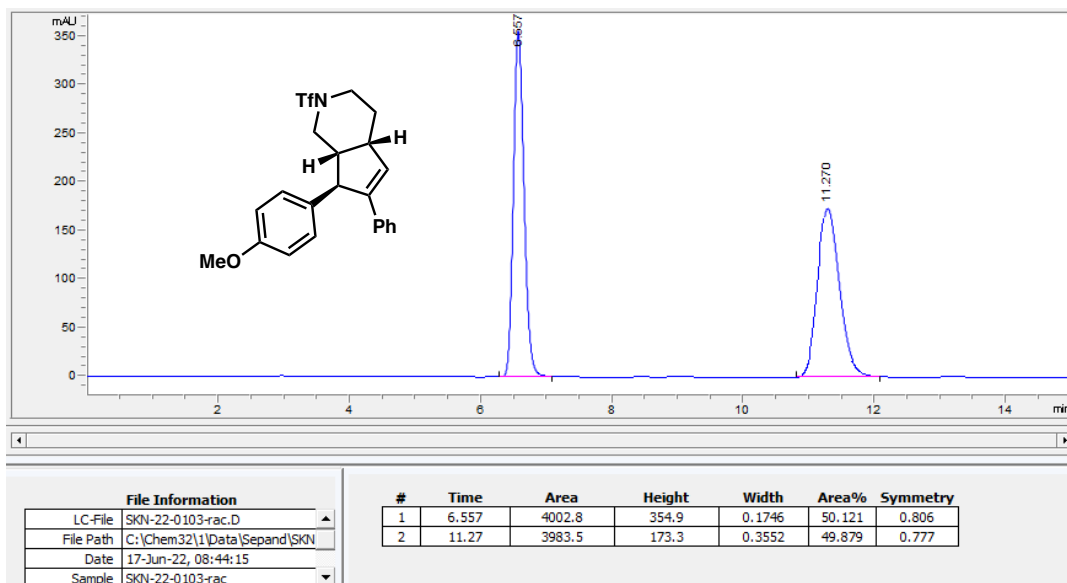
File Information		#	Time	Area	Height	Width	Area%	Symmetry
LC-File	SKN-22-0058-1.D	1	5.239	3178.3	525.1	0.0936	91.116	0.853
File Path	C:\Chem32\1\Data\Sepa	2	6.267	309.9	41.4	0.1162	8.884	0.887
Date	01-Aug-22, 12:41:53							
Sample	SKN-22-0058-1							
Sample Info								
Barcode								
Operator	SYSTEM							
Method	ADH298IPAHEX10min1ml							
Reference	C:\Chem32\1\Data\Sepa							

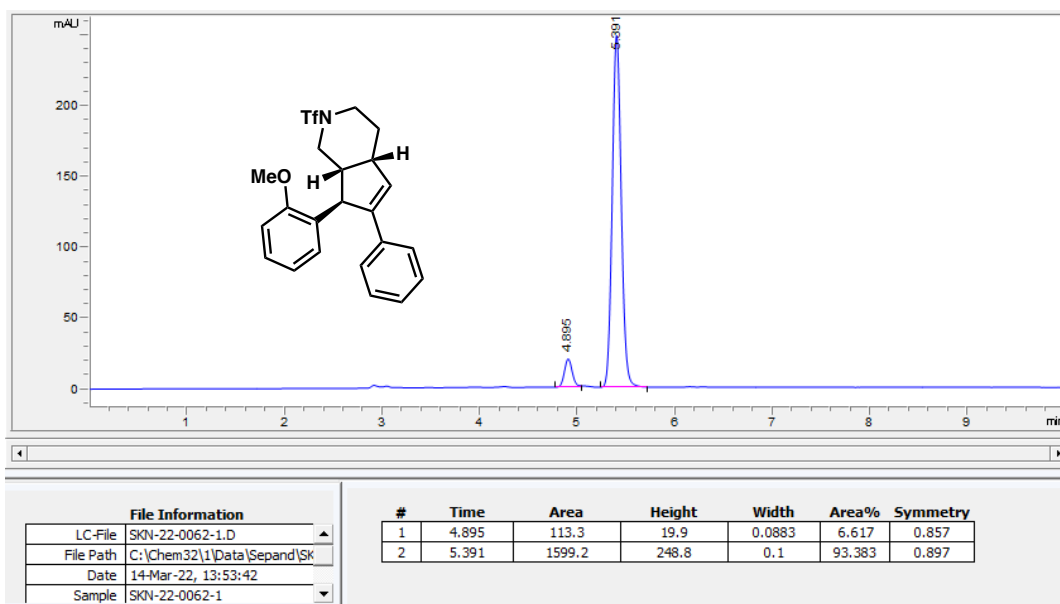
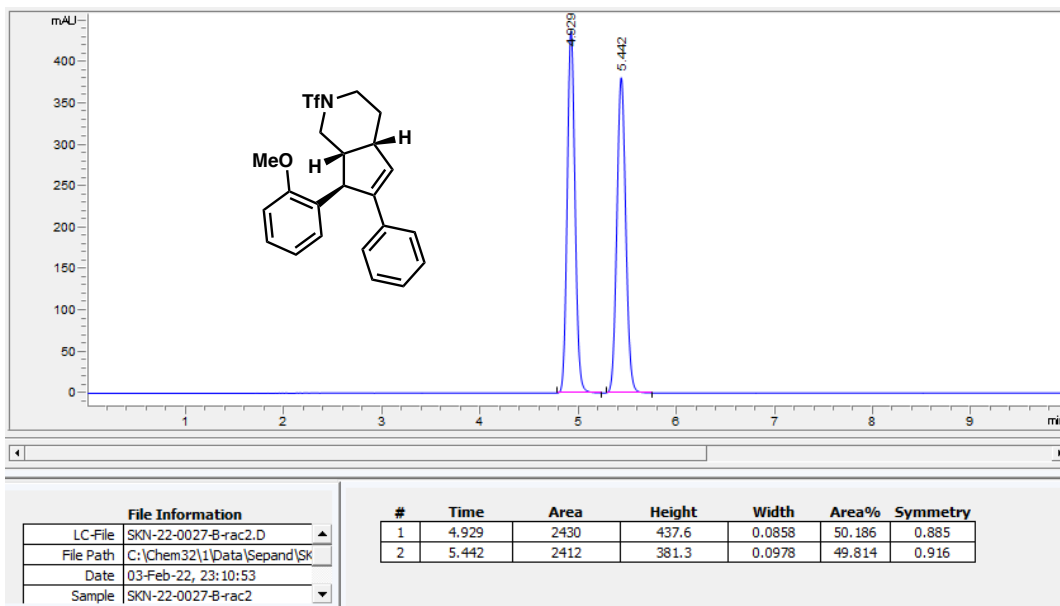


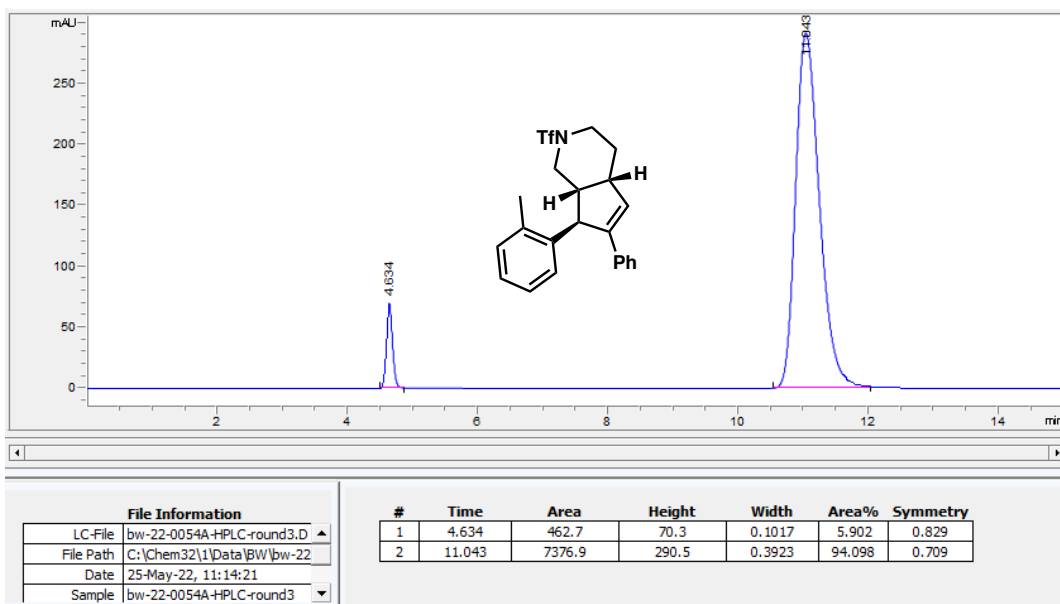
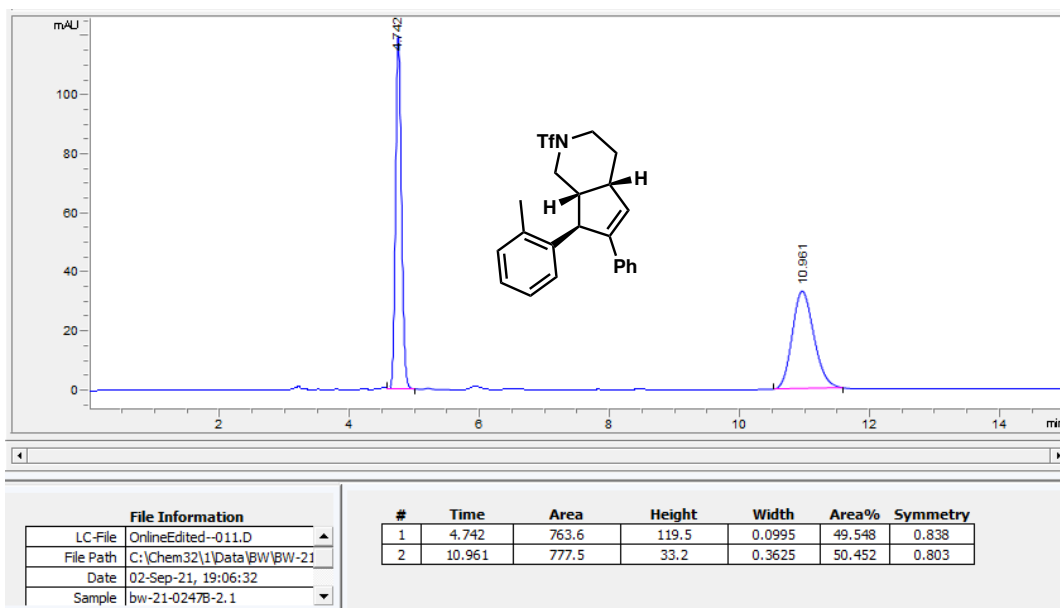


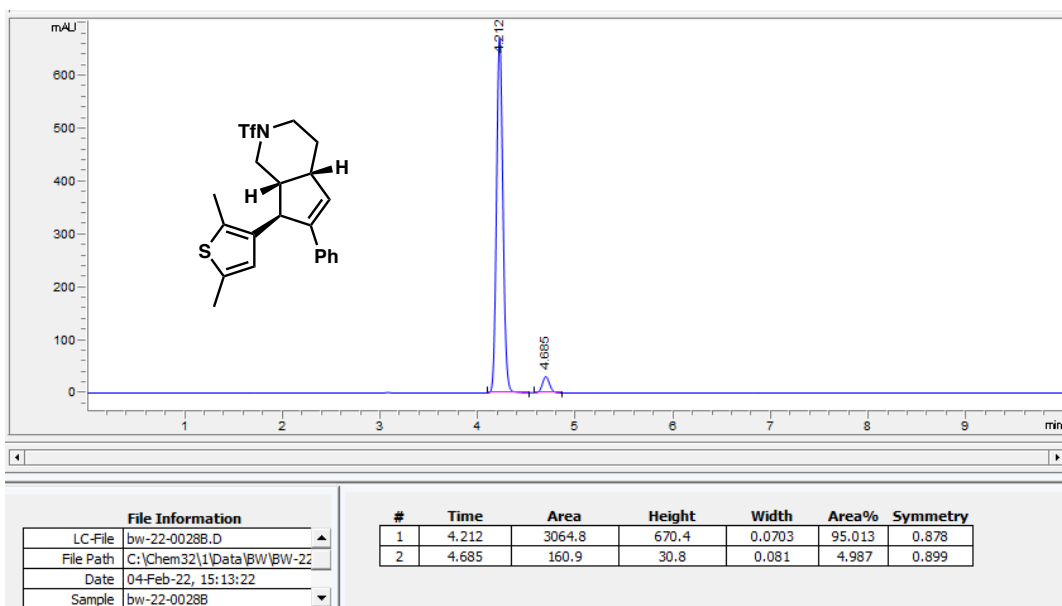
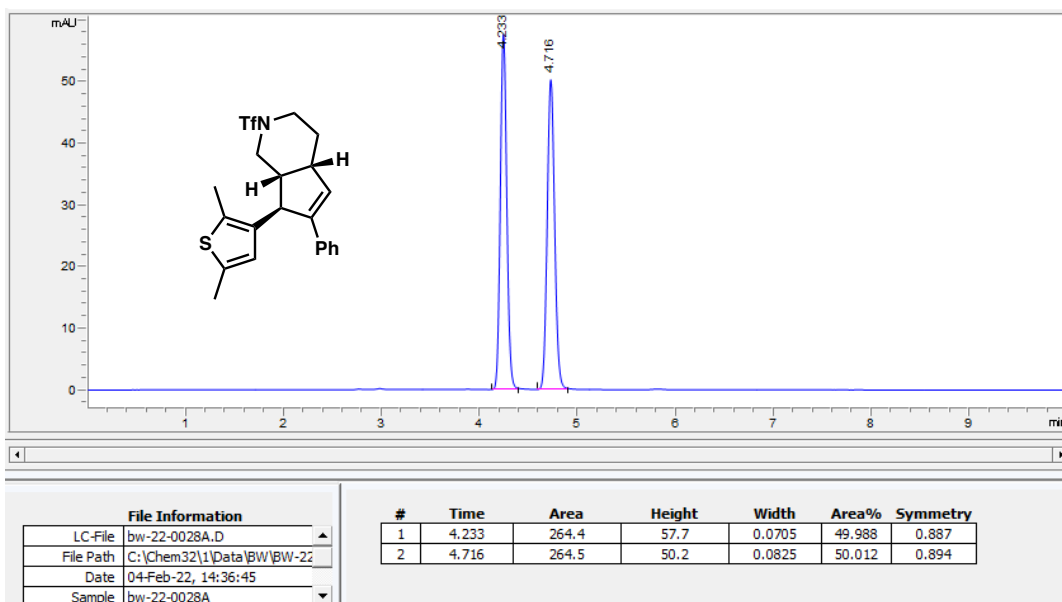


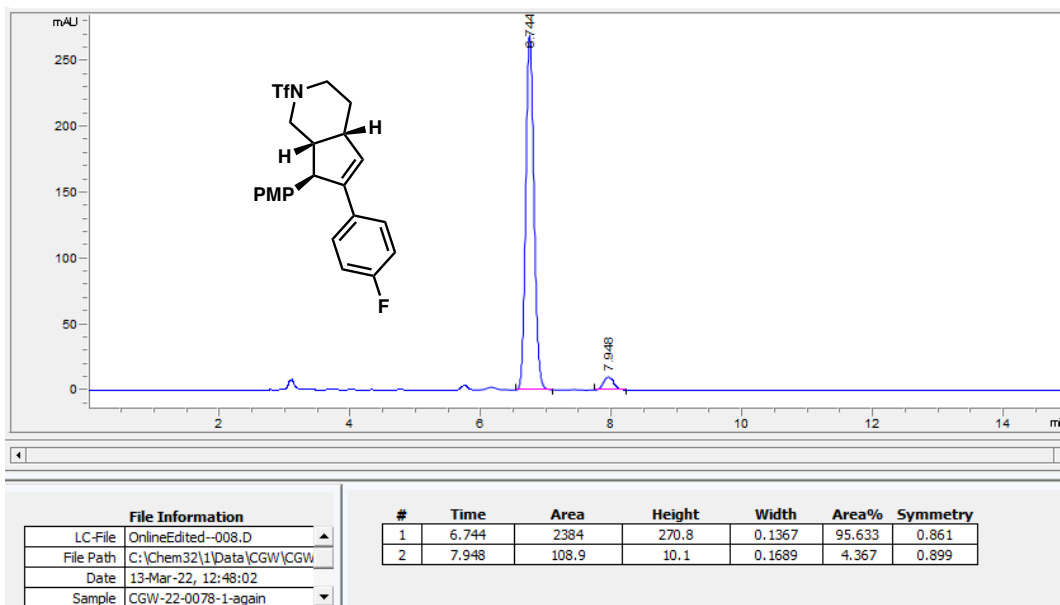
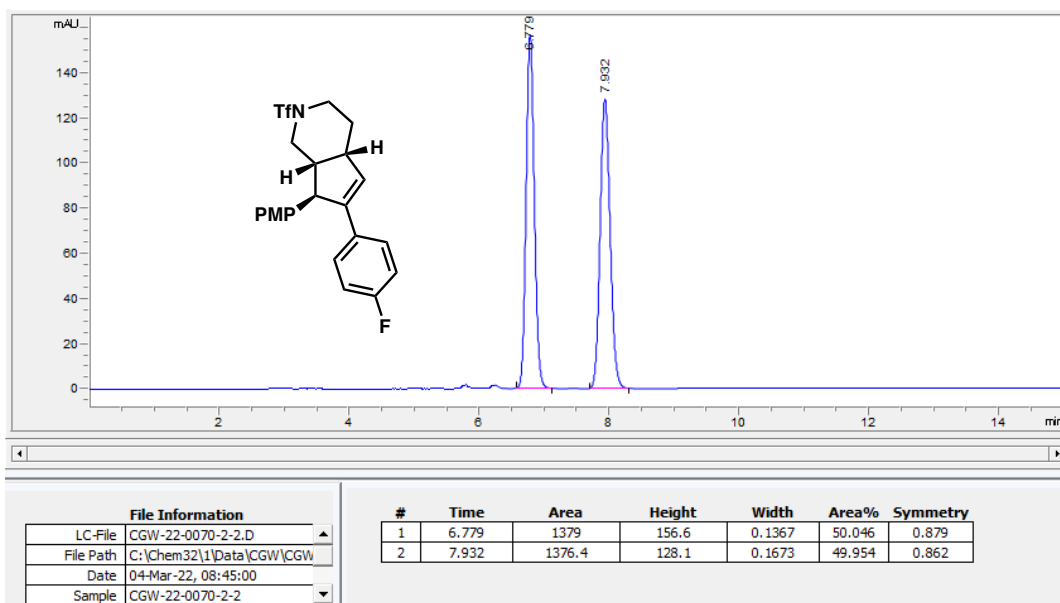


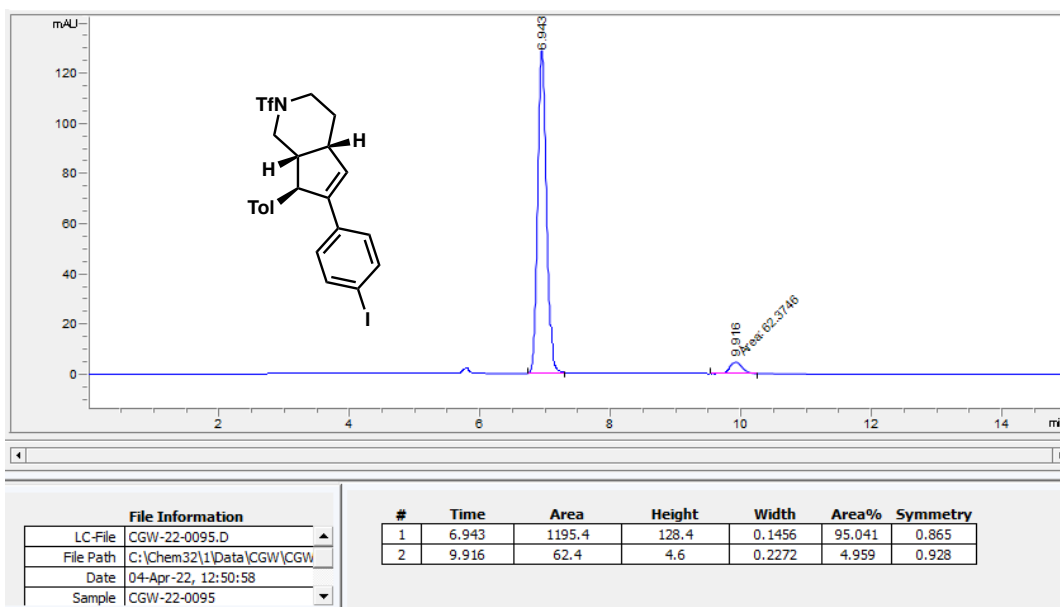
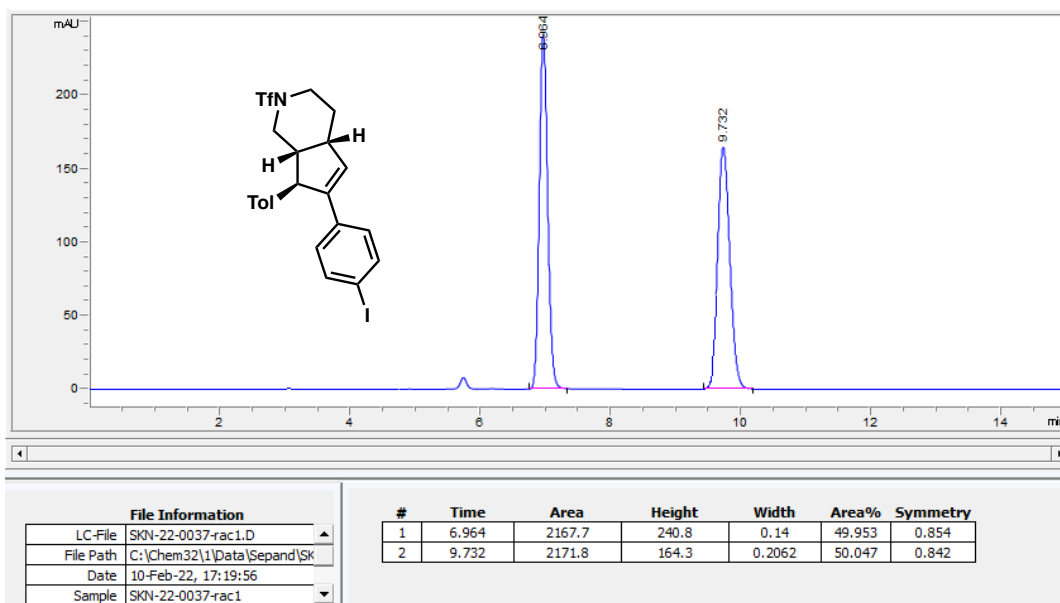


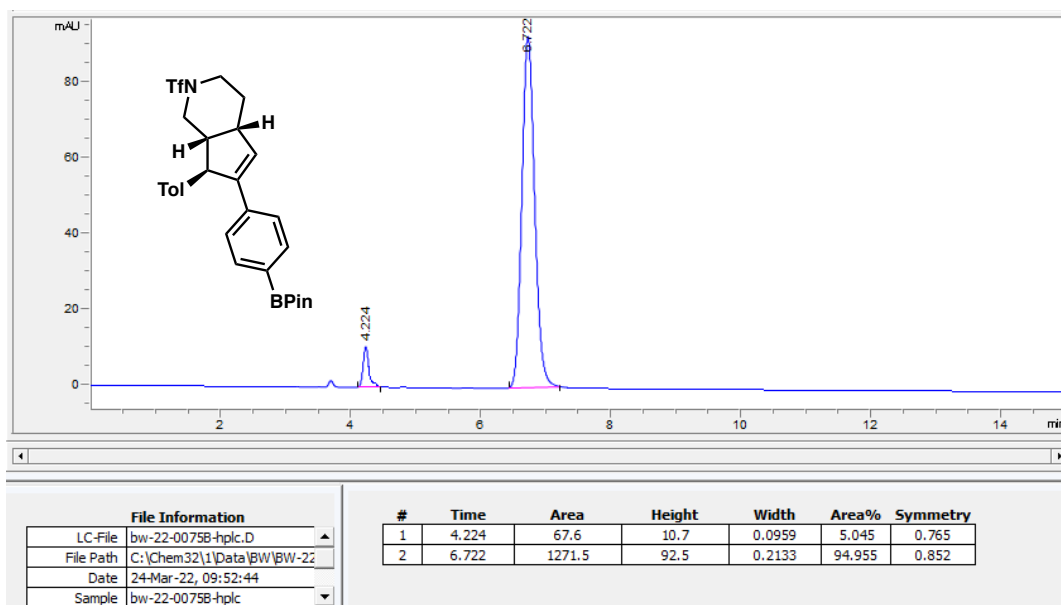
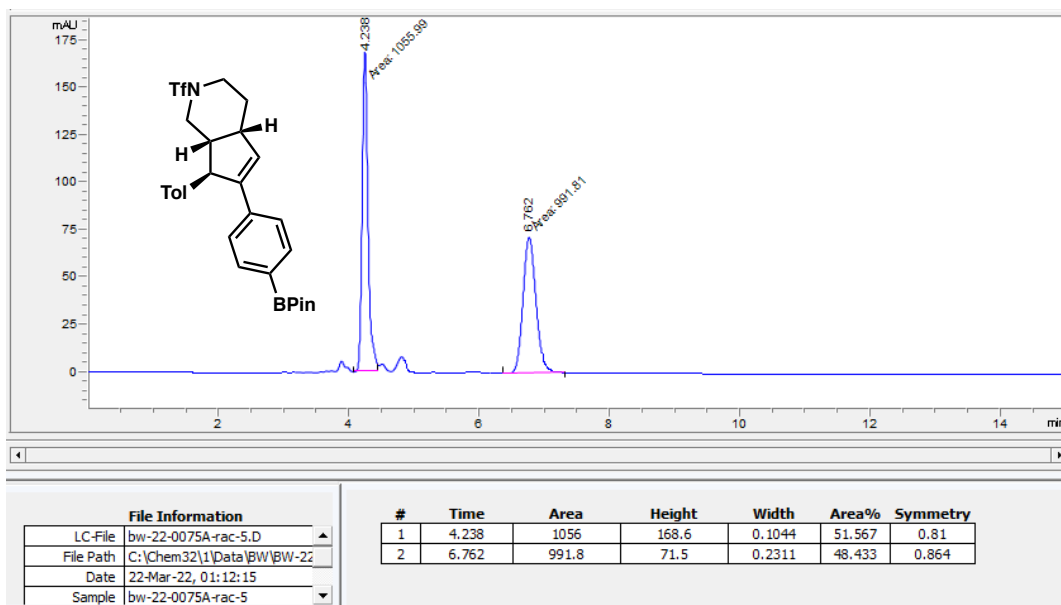


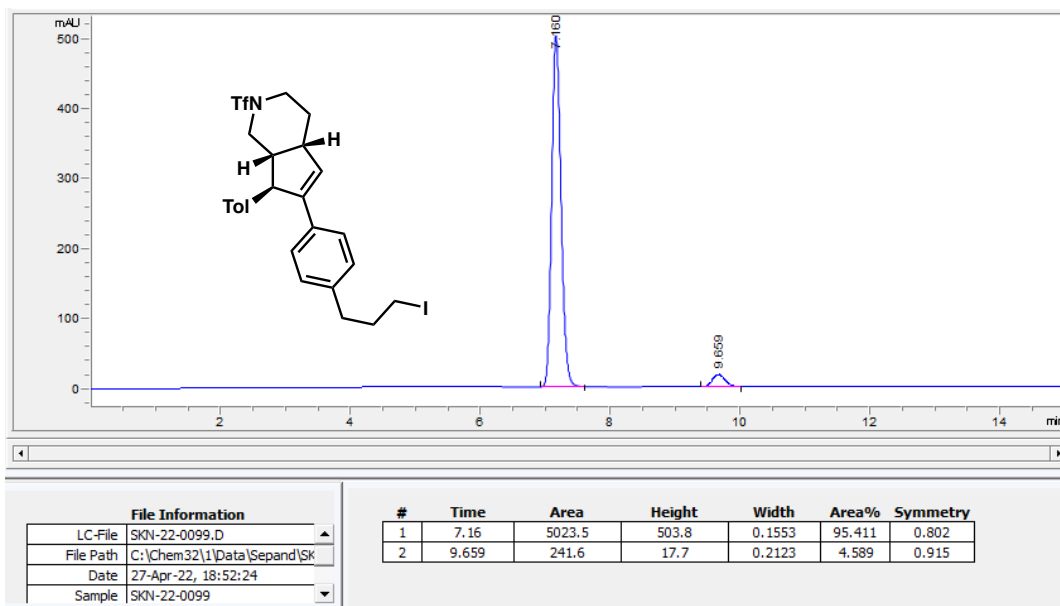
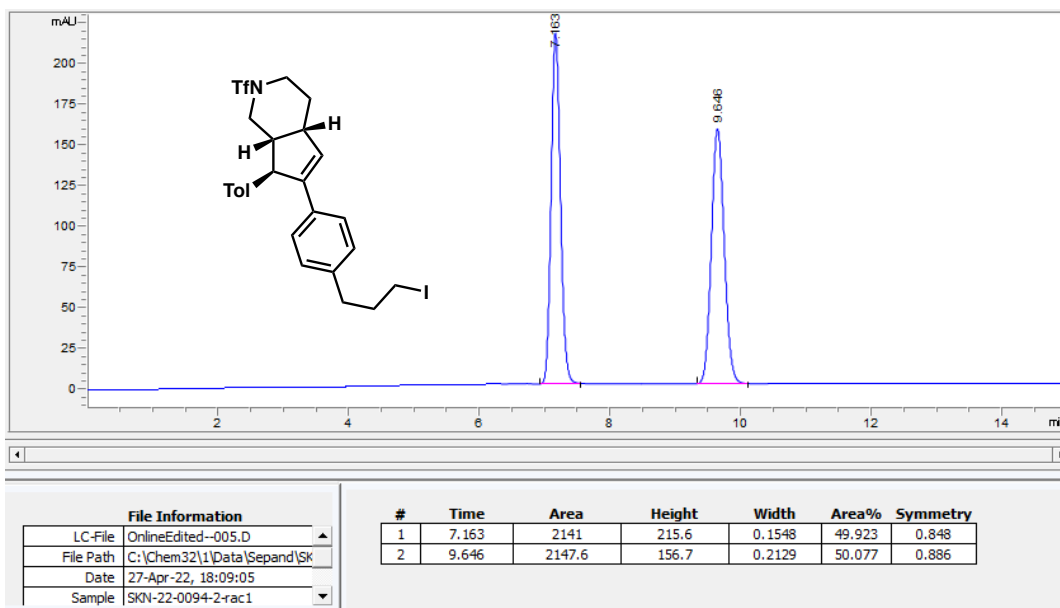


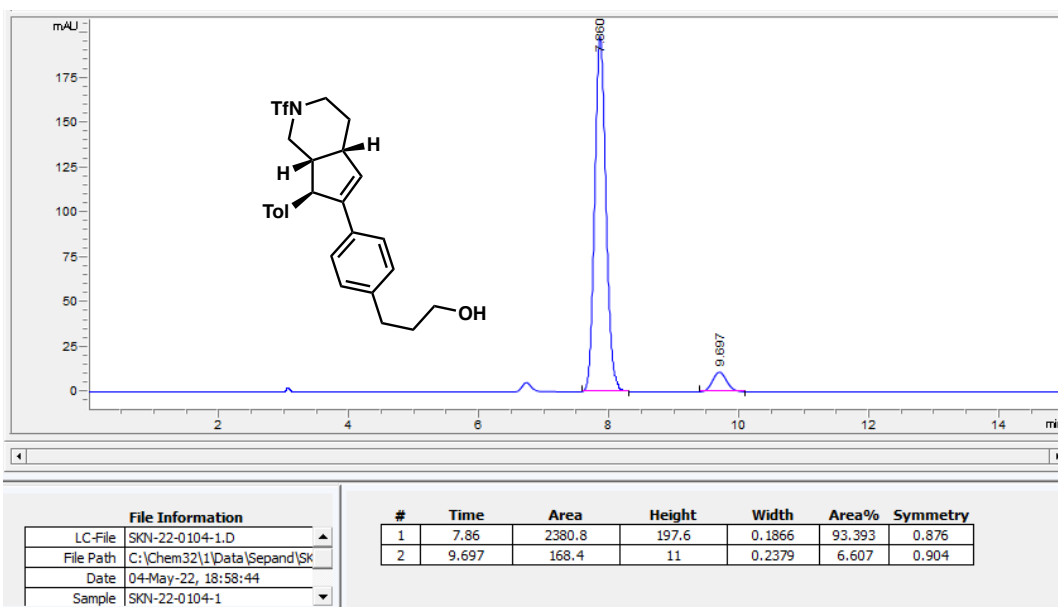
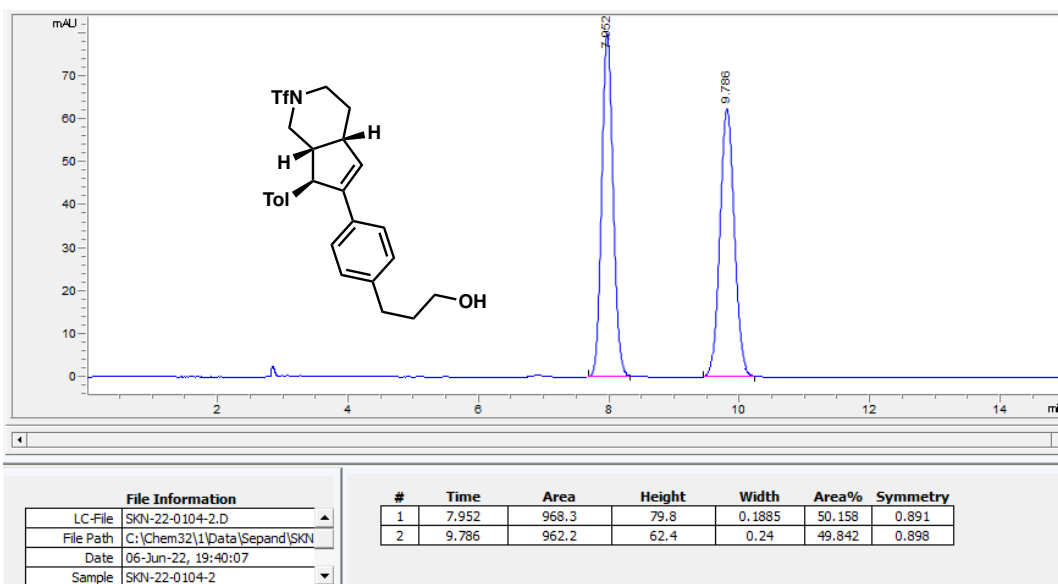


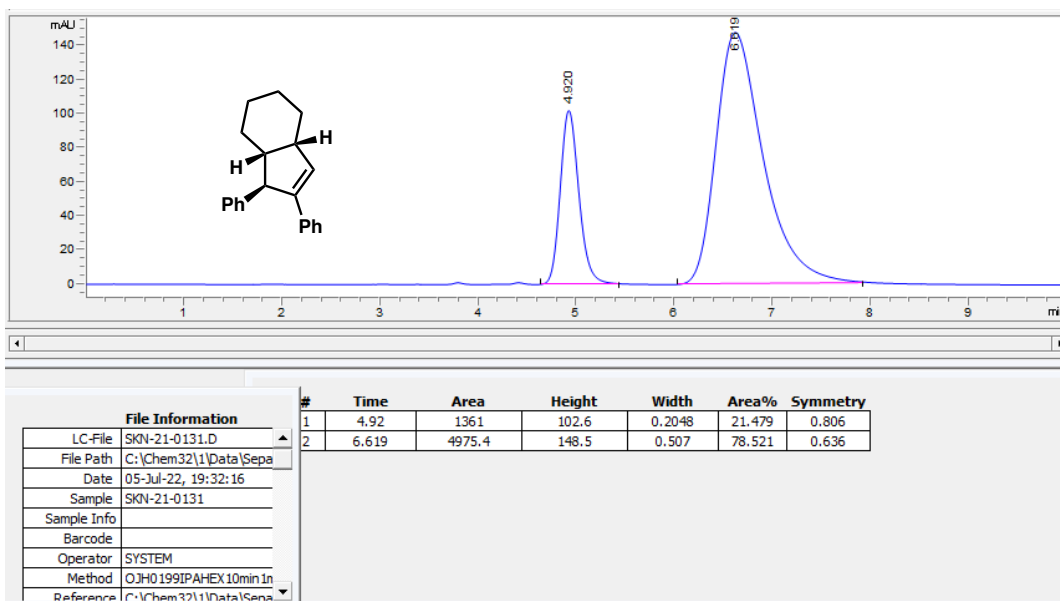
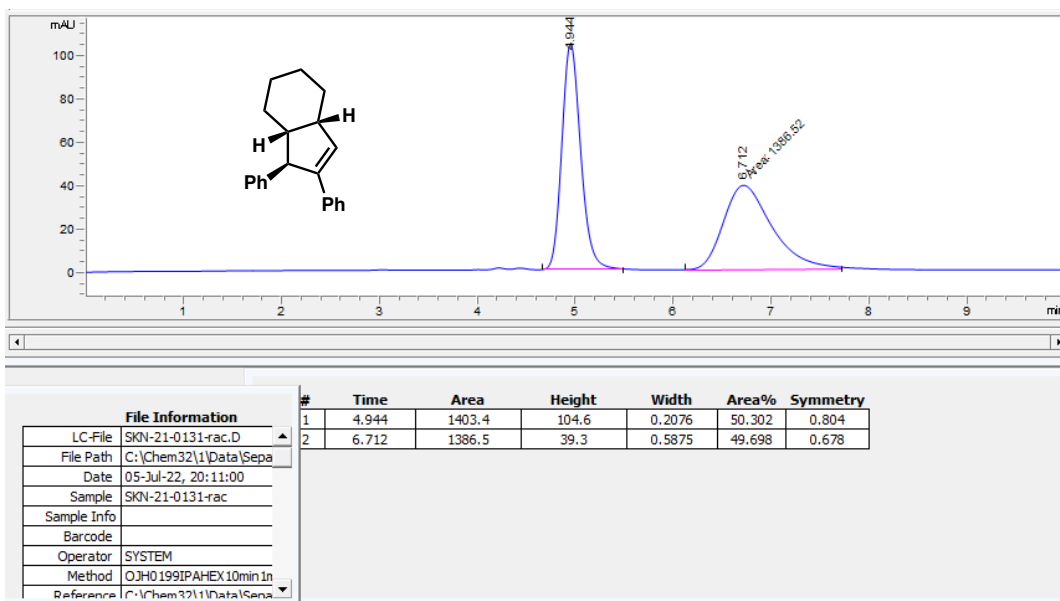












4.7 REFERENCES

- (1) Olah, G. A. 100 Years of Carbocations and Their Significance in Chemistry ¹. *J. Org. Chem.* **2001**, *66*, 5943–5957.
- (2) Naredla, R. R.; Klumpp, D. A. Contemporary Carbocation Chemistry: Applications in Organic Synthesis. *Chem. Rev.* **2013**, *113*, 6905–6948.
- (3) Eschenmoser, A.; Ruzicka, L.; Jeger, O.; Arigoni, D. Zur Kenntnis der Triterpene. 190. Mitteilung. Eine stereochemische Interpretation der biogenetischen Isoprenregel bei den Triterpenen. *Helv. Chim. Acta* **1955**, *38*, 1890–1904.
- (4) Tantillo, D. J. Biosynthesis via Carbocations: Theoretical Studies on Terpene Formation. *Nat. Prod. Rep.* **2011**, *28*, 1035.
- (5) Terada, M. Binaphthol-Derived Phosphoric Acid as a Versatile Catalyst for Enantioselective Carbon–Carbon Bond Forming Reactions. *Chem. Commun.* **2008**, *35*, 4097.
- (6) Brak, K.; Jacobsen, E. N. Asymmetric Ion-Pairing Catalysis. *Angew. Chem. Int. Ed.* **2013**, *52*, 534–561.
- (7) Lee, S.; Kaib, P. S. J.; List, B. Asymmetric Catalysis via Cyclic, Aliphatic Oxocarbenium Ions. *J. Am. Chem. Soc.* **2017**, *139*, 2156–2159.
- (8) Trifonidou, M.; Kokotos, C. G. Enantioselective Organocatalytic α -Alkylation of Ketones by SN1-Type Reaction of Alcohols. *Eur. J. Org. Chem.* **2012**, *2012*, 1563–
- (9) Brown, A. R.; Kuo, W.-H.; Jacobsen, E. N. Enantioselective Catalytic α -Alkylation of Aldehydes via an S_N1 Pathway. *J. Am. Chem. Soc.* **2010**, *132*, 9286–9288.

- (10) Bergonzini, G.; Vera, S.; Melchiorre, P. Cooperative Organocatalysis for the Asymmetric γ Alkylation of α -Branched Enals. *Angew. Chem. Int. Ed.* **2010**, *49*, 9685–9688.
- (11) Rueping, M.; Uria, U.; Lin, M.-Y.; Atodiresei, I. Chiral Organic Contact Ion Pairs in Metal-Free Catalytic Asymmetric Allylic Substitutions. *J. Am. Chem. Soc.* **2011**, *133*, 3732–3735.
- (12) Capdevila, M. G.; Benfatti, F.; Zoli, L.; Stenta, M.; Cozzi, P. G. Merging Organocatalysis with an Indium(III)-Mediated Process: A Stereoselective α -Alkylation of Aldehydes with Allylic Alcohols. *Chem. - Eur. J.* **2010**, *16*, 11237–11241.
- (13) Wang, P.-S.; Zhou, X.-L.; Gong, L.-Z. An Organocatalytic Asymmetric Allylic Alkylation Allows Enantioselective Total Synthesis of Hydroxymetasequirin-A and Metasequirin-B Tetramethyl Ether Diacetates. *Org. Lett.* **2014**, *16*, 976–979.
- (14) Wendlandt, A. E.; Vangal, P.; Jacobsen, E. N. Quaternary Stereocentres via an Enantioconvergent Catalytic SN1 Reaction. *Nature* **2018**, *556*, 447–451.
- (15) Braun, M.; Kotter, W. Titanium(IV)-Catalyzed Dynamic Kinetic Asymmetric Transformation of Alcohols, Silyl Ethers, and Acetals under Carbon Allylation. *Angew. Chem. Int. Ed.* **2004**, *43*, 514–517.
- (16) Schreyer, L.; Properzi, R.; List, B. IDPi Catalysis. *Angew. Chem. Int. Ed.* **2019**, *58*, 12761–12777.
- (17) Tsuji, N.; Kennemur, J. L.; Buyck, T.; Lee, S.; Prévost, S.; Kaib, P. S. J.; Bykov, D.; Farès, C.; List, B. Activation of Olefins via Asymmetric Brønsted Acid Catalysis. *Science* **2018**, *359*, 1501–1505.

- (18) Properzi, R.; Kaib, P. S. J.; Leutzsch, M.; Pupo, G.; Mitra, R.; De, C. K.; Song, L.; Schreiner, P. R.; List, B. Catalytic Enantiocontrol over a Non-Classical Carbocation. *Nat. Chem.* **2020**, *12*, 1174–1179.
- (19) Isomura, M.; Petrone, D. A.; Carreira, E. M. Coordination-Induced Stereocontrol over Carbocations: Asymmetric Reductive Deoxygenation of Racemic Tertiary Alcohols. *J. Am. Chem. Soc.* **2019**, *141*, 4738–4748.
- (20) Petrone, D. A.; Isomura, M.; Franzoni, I.; Rössler, S. L.; Carreira, E. M. Allenylic Carbonates in Enantioselective Iridium-Catalyzed Alkylations. *J. Am. Chem. Soc.* **2018**, *140*, 4697–4704.
- (21) Jin, T.; Himuro, M.; Yamamoto, Y. Brønsted Acid-Catalyzed Cascade Cycloisomerization of Enynes via Acetylene Cations and sp^3 -Hybridized C–H Bond Activation. *J. Am. Chem. Soc.* **2010**, *132*, 5590–5591.
- (22) Cleary, S. E.; Hensinger, M. J.; Brewer, M. Remote C–H Insertion of Vinyl Cations Leading to Cyclopentenones. *Chem. Sci.* **2017**, *8*, 6810–6814.
- (23) Cleary, S. E.; Li, X.; Yang, L.-C.; Houk, K. N.; Hong, X.; Brewer, M. Reactivity Profiles of Diazo Amides, Esters, and Ketones in Transition-Metal-Free C–H Insertion Reactions. *J. Am. Chem. Soc.* **2019**, *141*, 3558–3565.
- (24) Biermann, U.; Koch, R.; Metzger, J. O. Intramolecular Concerted Insertion of Vinyl Cations into C–H Bonds: Hydroalkylating Cyclization of Alkynes with Alkyl Chloroformates To Give Cyclopentanes. *Angew. Chem. Int. Ed.* **2006**, *45*, 3076–3079.
- (25) Popov, S.; Shao, B.; Bagdasarian, A. L.; Benton, T. R.; Zou, L.; Yang, Z.; Houk, K. N.; Nelson, H. M. Teaching an Old Carbocation New Tricks: Intermolecular C–H Insertion Reactions of Vinyl Cations. *Science* **2018**, *361*, 381–387.

- (26) Wigman, B.; Popov, S.; Bagdasarian, A. L.; Shao, B.; Benton, T. R.; Williams, C. G.; Fisher, S. P.; Lavallo, V.; Houk, K. N.; Nelson, H. M. Vinyl Carbocations Generated under Basic Conditions and Their Intramolecular C–H Insertion Reactions. *J. Am. Chem. Soc.* **2019**, *141*, 9140–9144.
- (27) Shao, B.; Bagdasarian, A. L.; Popov, S.; Nelson, H. M. Arylation of Hydrocarbons Enabled by Organosilicon Reagents and Weakly Coordinating Anions. *Science* **2017**, *355*, 1403–1407.
- (28) Zhang, F.; Das, S.; Walkinshaw, A. J.; Casitas, A.; Taylor, M.; Suero, M. G.; Gaunt, M. J. Cu-Catalyzed Cascades to Carbocycles: Union of Diaryliodonium Salts with Alkenes or Alkynes Exploiting Remote Carbocations. *J. Am. Chem. Soc.* **2014**, *136*, 8851–8854.
- (29) Riddlestone, I. M.; Kraft, A.; Schaefer, J.; Krossing, I. Taming the Cationic Beast: Novel Developments in the Synthesis and Application of Weakly Coordinating Anions. *Angew. Chem. Int. Ed.* **2018**, *57*, 13982–14024.
- (30) De, C.; Mitra, R.; List, B. Design and Synthesis of Enantiopure Tetrakis(Pentafluorophenyl) Borate Analogues for Asymmetric Counteranion Directed Catalysis. *Synlett* **2017**, *28*, 2435–2438.
- (31) Pommerening, P.; Oestreich, M. Chiral Modification of the Tetrakis(Pentafluorophenyl)Borate Anion with Myrtanyl Groups. *Eur. J. Org. Chem.* **2019**, *2019*, 7240–7246.
- (32) Bae, H. J.; Baskar, B.; An, S. E.; Cheong, J. Y.; Thangadurai, D. T.; Hwang, I.-C.; Rhee, Y. H. Gold(I)-Catalyzed Cycloisomerization of 3-Methoxy-1,6-Enynes Featuring

Tandem Cyclization and [3,3]-Sigmatropic Rearrangement. *Angew. Chem. Int. Ed.* **2008**, *47*, 2263–2266.

(33) Kaib, P. S. J.; Schreyer, L.; Lee, S.; Properzi, R.; List, B. Extremely Active Organocatalysts Enable a Highly Enantioselective Addition of Allyltrimethylsilane to Aldehydes. *Angew. Chem. Int. Ed.* **2016**, *55*, 13200–13203.

(34) Fattorusso, E.; Tagliatalata-Scafati, O. *Modern Alkaloids: Structure, Isolation, Synthesis and Biology*; Wiley-VCH: Weinheim, 2008.

(35) Lambert, J. B.; Zhang, S.; Ciro, S. M. Silyl Cations in the Solid and in Solution. *Organometallics* **1994**, *13*, 2430–2443.

(36) Rappoport, Z.; Stang, P. J. *Dicoordinated Carbocations*; Wiley: Chichester; New York, **1997**.

(37) Neel, A. J.; Milo, A.; Sigman, M. S.; Toste, F. D. Enantiodivergent Fluorination of Allylic Alcohols: Data Set Design Reveals Structural Interplay between Achiral Directing Group and Chiral Anion. *J. Am. Chem. Soc.* **2016**, *138*, 3863–3875.

(38) Dickschat, J. S. Bacterial Terpene Cyclases. *Nat. Prod. Rep.* **2016**, *33*, 87–110.

(39) Tan, Y.; Yuan, W.; Gong, L.; Meggers, E. Aerobic Asymmetric Dehydrogenative Cross-Coupling between Two Csp³–H Groups Catalyzed by a Chiral-at-Metal Rhodium Complex. *Angew. Chem.* **2015**, *127*, 13237–13240.

(40) Watson, R. B.; Schindler, C. S. Iron-Catalyzed Synthesis of Tetrahydronaphthalenes via 3,4-Dihydro-2 H -Pyran Intermediates. *Org. Lett.* **2018**, *20*, 68–71.

- (41) Su, Y.; Sun, X.; Wu, G.; Jiao, N. Catalyst-Controlled Highly Selective Coupling and Oxygenation of Olefins: A Direct Approach to Alcohols, Ketones, and Diketones. *Angew. Chem. Int. Ed.* **2013**, *52*, 9808–9812.
- (42) Zell, D.; Kingston, C.; Jermaks, J.; Smith, S. R.; Seeger, N.; Wassmer, J.; Sirois, L. E.; Han, C.; Zhang, H.; Sigman, M. S.; Gosselin, F. Stereoconvergent and -Divergent Synthesis of Tetrasubstituted Alkenes by Nickel-Catalyzed Cross-Couplings. *J. Am. Chem. Soc.* **2021**, *143*, 19078–19090.
- (43) Majhi, B.; Kundu, D.; Ranu, B. C. Ascorbic Acid Promoted Oxidative Arylation of Vinyl Arenes to 2-Aryl Acetophenones without Irradiation at Room Temperature under Aerobic Conditions. *J. Org. Chem.* **2015**, *80*, 7739–7745.
- (44) Mehta, V. P.; García-López, J.-A.; Greaney, M. F. Ruthenium-Catalyzed Cascade C–H Functionalization of Phenylacetophenones. *Angew. Chem. Int. Ed.* **2014**, *53*, 1529–1533.
- (45) Kang, Y.; Hou, R.; Min, X.; Wang, T.; Liang, Y.; Zhang, Z. An Oxidant- and Catalyst-Free Synthesis of Dibenzo[a,c]Carbazoles via UV Light Irradiation of 2,3-Diphenyl-1H-Indoles. *Synthesis* **2022**, *54*, 1621–1632.
- (46) Wang, H.-Y.; Mueller, D. S.; Sachwani, R. M.; Kapadia, R.; Londino, H. N.; Anderson, L. L. Regioselective Synthesis of 2,3,4- or 2,3,5-Trisubstituted Pyrroles via [3,3] or [1,3] Rearrangements of *O*-Vinyl Oximes. *J. Org. Chem.* **2011**, *76*, 3203–3221.
- (47) Brouder, T. A.; Slattery, C. N.; Ford, A.; Khandavilli, U. B. R.; Skořepová, E.; Eccles, K. S.; Lusi, M.; Lawrence, S. E.; Maguire, A. R. Desymmetrization by Asymmetric Copper-Catalyzed Intramolecular C–H Insertion Reactions of α -Diazo- β -Oxosulfones. *J. Org. Chem.* **2019**, *84*, 7543–7563.

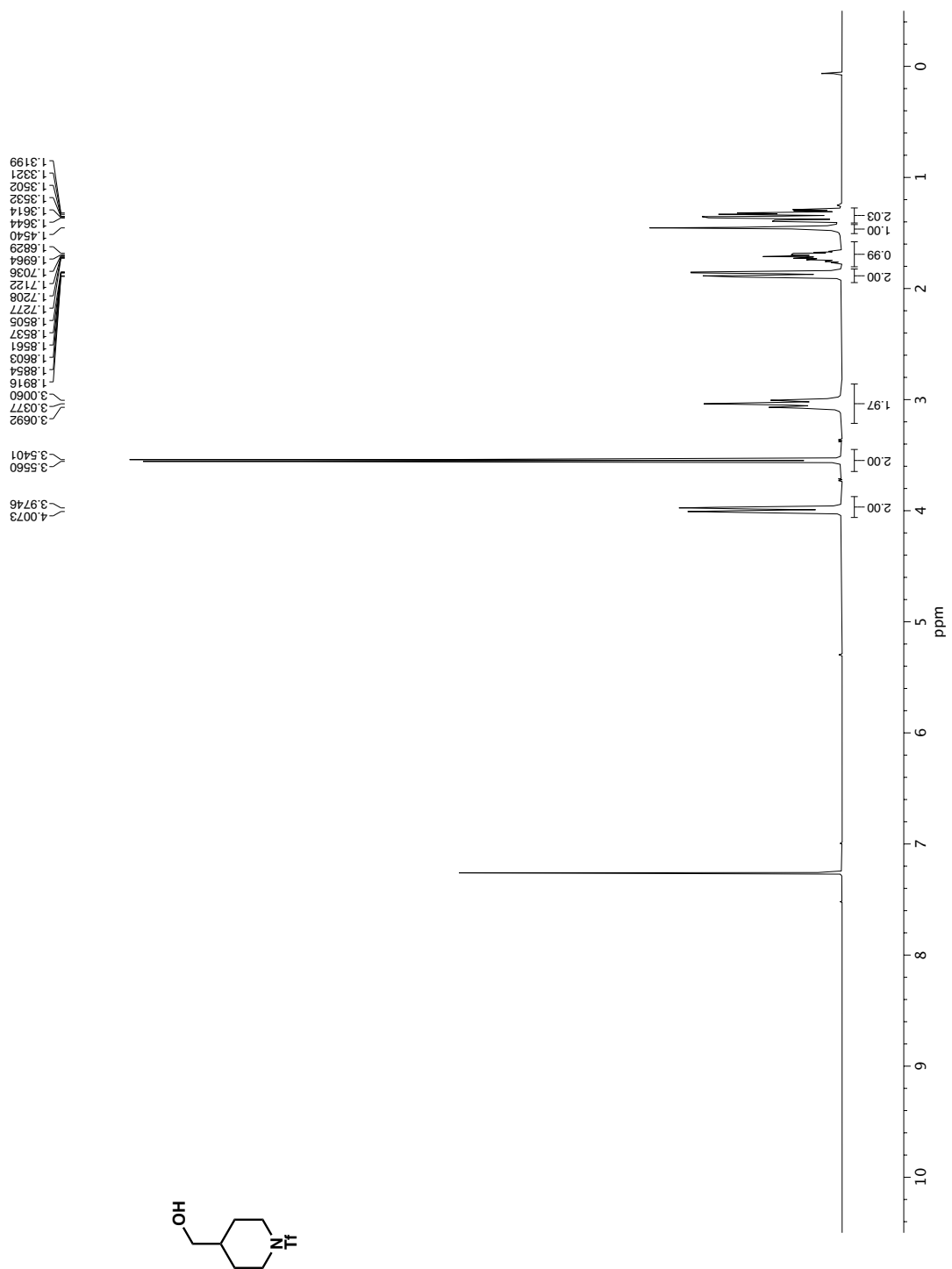
- (48) Cao, X.-N.; Wan, X.-M.; Yang, F.-L.; Li, K.; Hao, X.-Q.; Shao, T.; Zhu, X.; Song, M.-P. NNN Pincer Ru(II)-Complex-Catalyzed α -Alkylation of Ketones with Alcohols. *J. Org. Chem.* **2018**, *83*, 3657–3668.
- (49) Li, B. X.; Le, D. N.; Mack, K. A.; McClory, A.; Lim, N.-K.; Cravillion, T.; Savage, S.; Han, C.; Collum, D. B.; Zhang, H.; Gosselin, F. Highly Stereoselective Synthesis of Tetrasubstituted Acyclic All-Carbon Olefins via Enol Tosylation and Suzuki–Miyaura Coupling. *J. Am. Chem. Soc.* **2017**, *139*, 10777–10783.
- (50) Beutner, G. L.; Simmons, E. M.; Ayers, S.; Bemis, C. Y.; Goldfogel, M. J.; Joe, C. L.; Marshall, J.; Wisniewski, S. R. A Process Chemistry Benchmark for Sp^2 – Sp^3 Cross Couplings. *J. Org. Chem.* **2021**, *86*, 10380–10396.
- (51) Sai, M.; Akakura, M.; Yamamoto, H. Chemoselective Silyl Transfer in the Mukaiyama Aldol Reaction Promoted by Super Silyl Lewis Acid. *Chem Commun* **2014**, *50*, 15206–15208.
- (52) Narute, S.; Parnes, R.; Toste, F. D.; Pappo, D. Enantioselective Oxidative Homocoupling and Cross-Coupling of 2-Naphthols Catalyzed by Chiral Iron Phosphate Complexes. *J. Am. Chem. Soc.* **2016**, *138*, 16553–16560.
- (53) Jiang, Y.; Diagne, A. B.; Thomson, R. J.; Schaus, S. E. Enantioselective Synthesis of Allenes by Catalytic Traceless Petasis Reactions. *J. Am. Chem. Soc.* **2017**, *139*, 1998–2005.
- (54) Xiao, B.; Fu, Y.; Xu, J.; Gong, T.-J.; Dai, J.-J.; Yi, J.; Liu, L. Pd(II)-Catalyzed C–H Activation/Aryl–Aryl Coupling of Phenol Esters. *J. Am. Chem. Soc.* **2010**, *132*, 468–469.

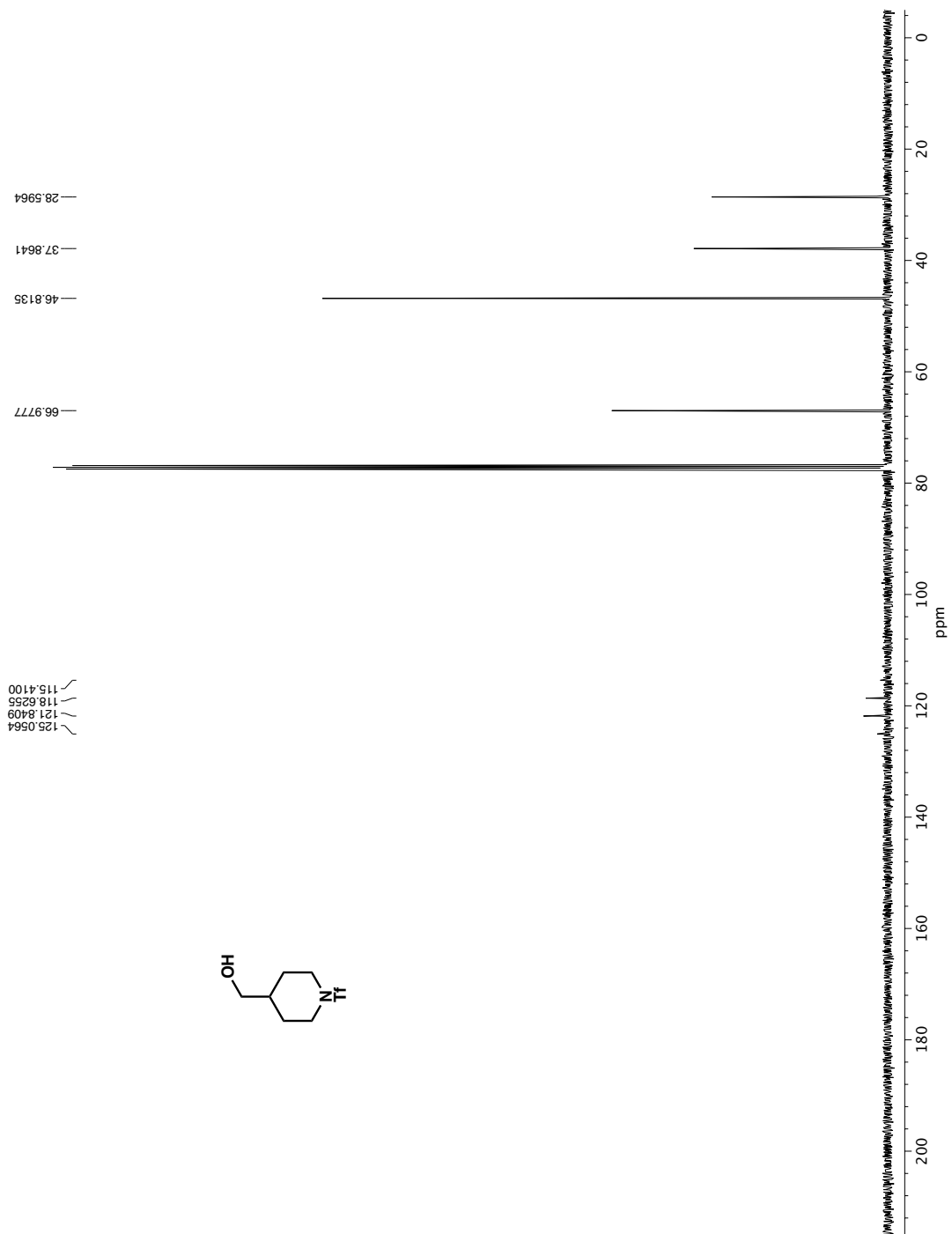
- (55) Gatzenmeier, T.; Turberg, M.; Yepes, D.; Xie, Y.; Neese, F.; Bistoni, G.; List, B. Scalable and Highly Diastereo- and Enantioselective Catalytic Diels–Alder Reaction of α,β -Unsaturated Methyl Esters. *J. Am. Chem. Soc.* **2018**, *140*, 12671–12676.
- (56) Shainyan, B. A.; Ushakov, I. A.; Tolstikova, L. L.; Koch, A.; Kleinpeter, E. N-Triflyl Substituted 1,4-Diheterocyclohexanes—Stereodynamics and the Perlin Effect. *Tetrahedron* **2008**, *64*, 5208–5216.

Appendix 4

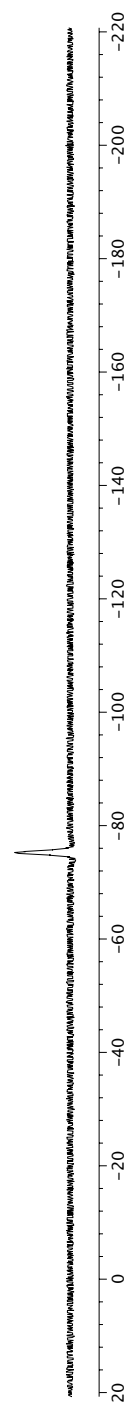
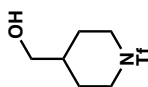
Spectra Relevant to Chapter 4: Catalytic Asymmetric C–H Insertion

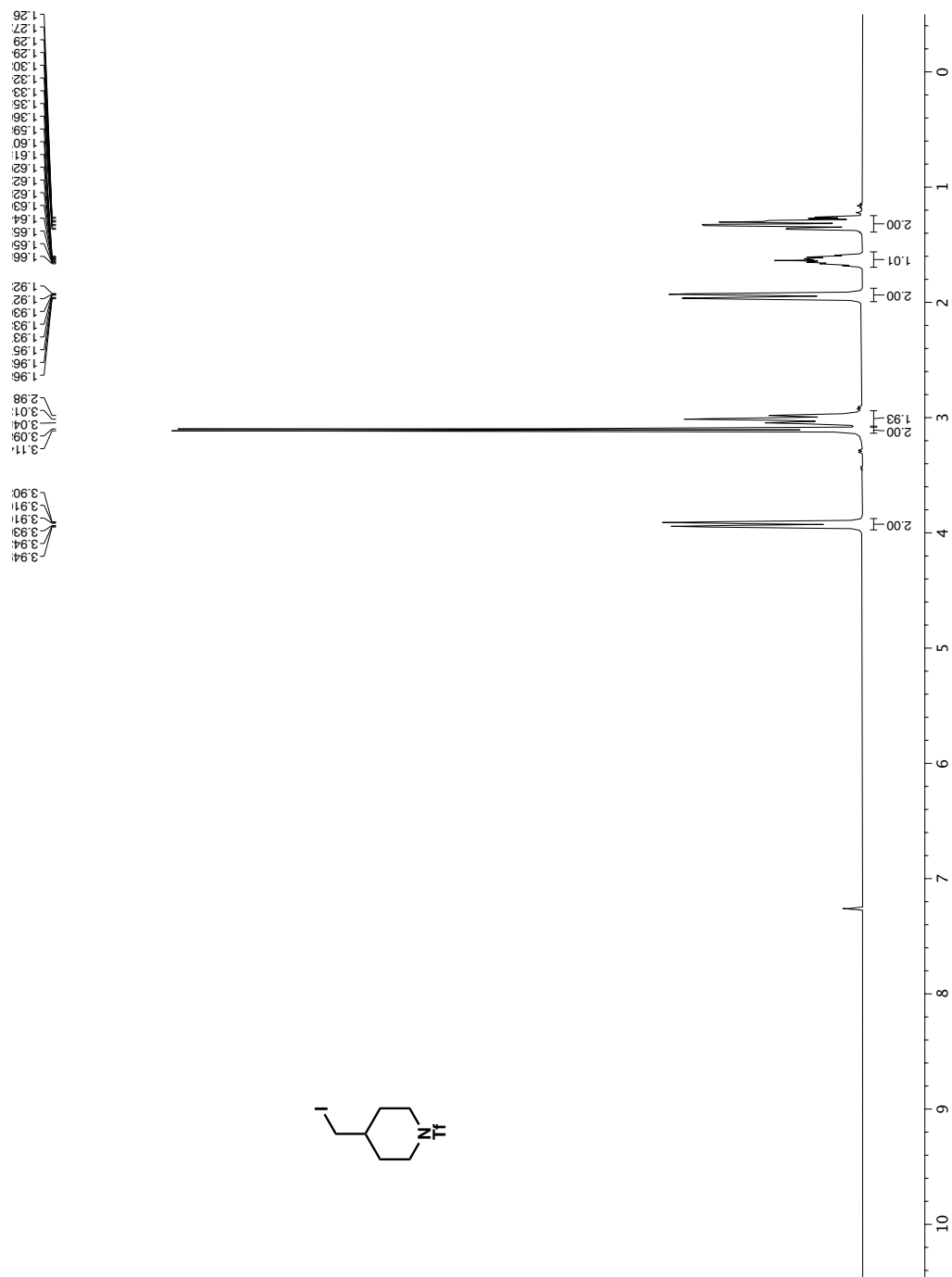
Reactions of Vinyl Carbocations

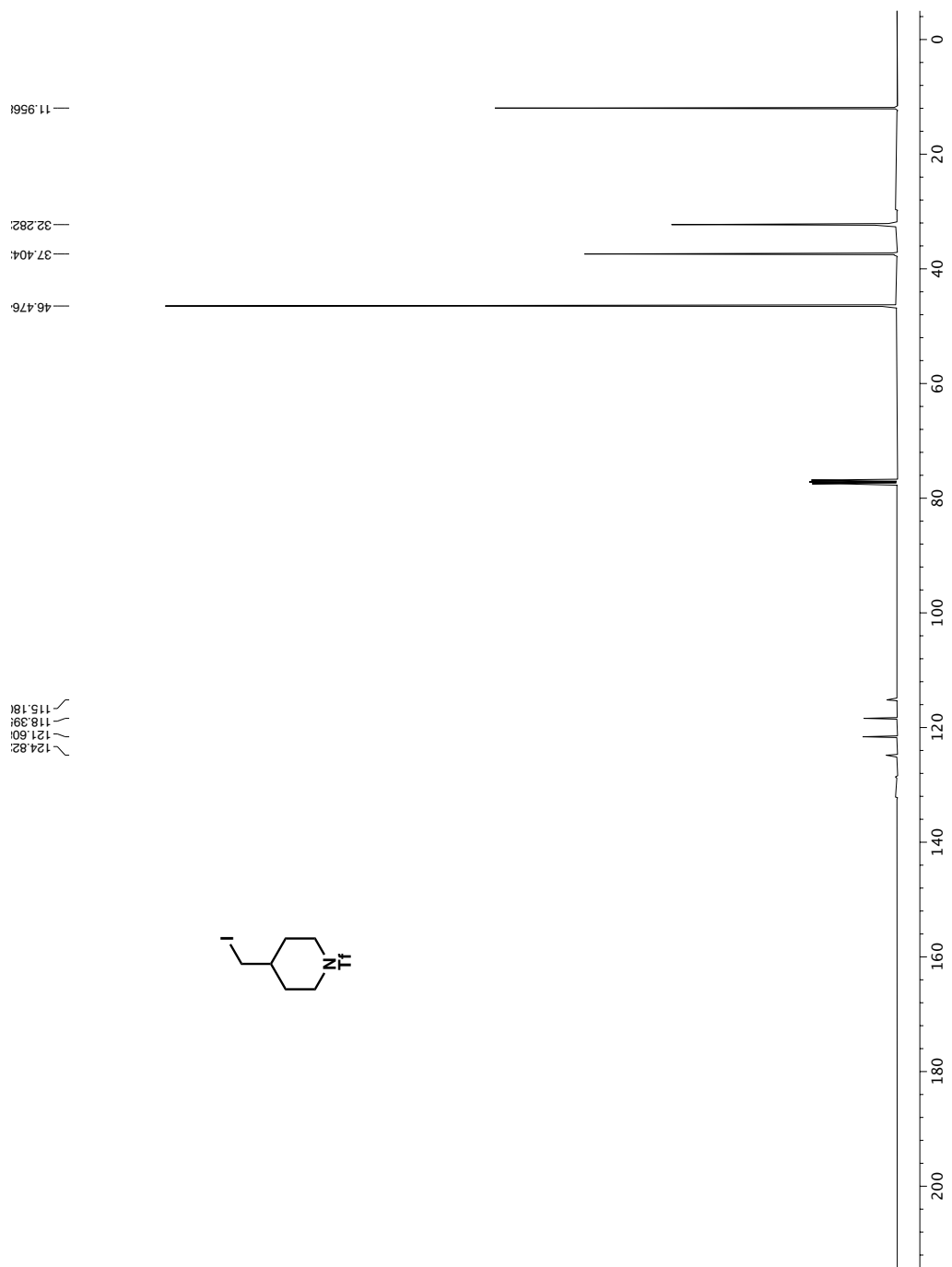




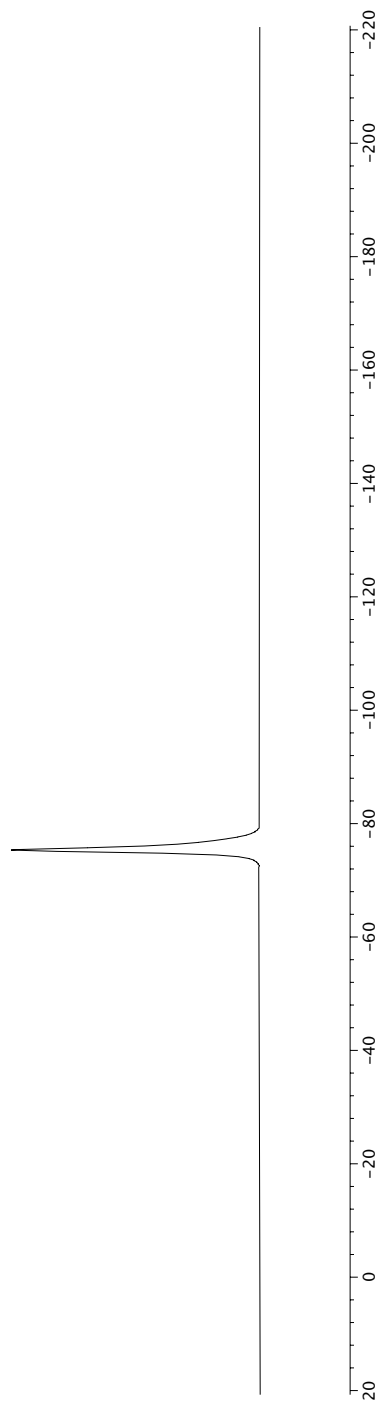
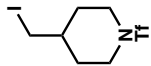
— 75.22

 ^{19}F NMR (376 MHz, CDCl_3) of **242**.

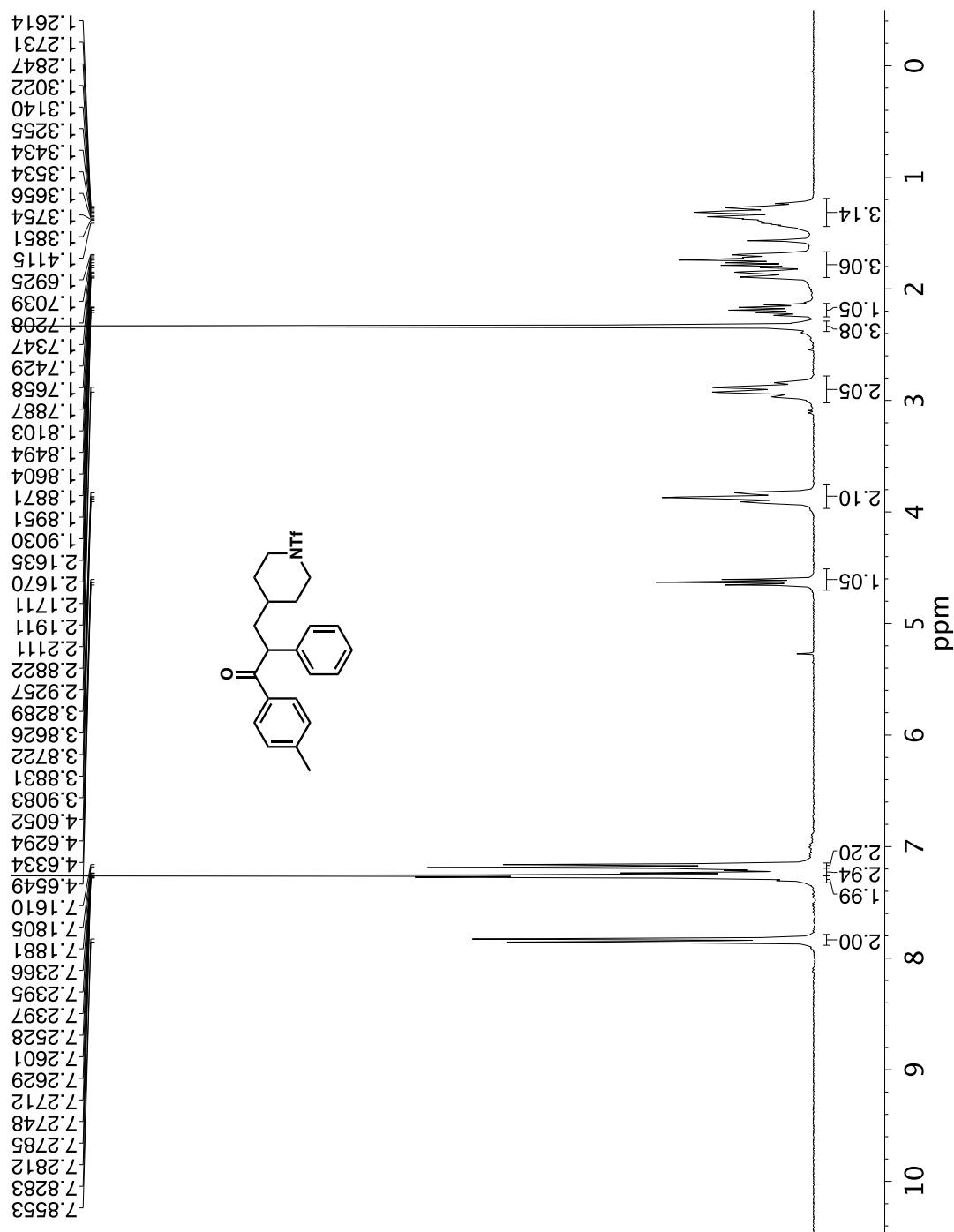
¹H NMR (400 MHz, CDCl₃) of **243**.

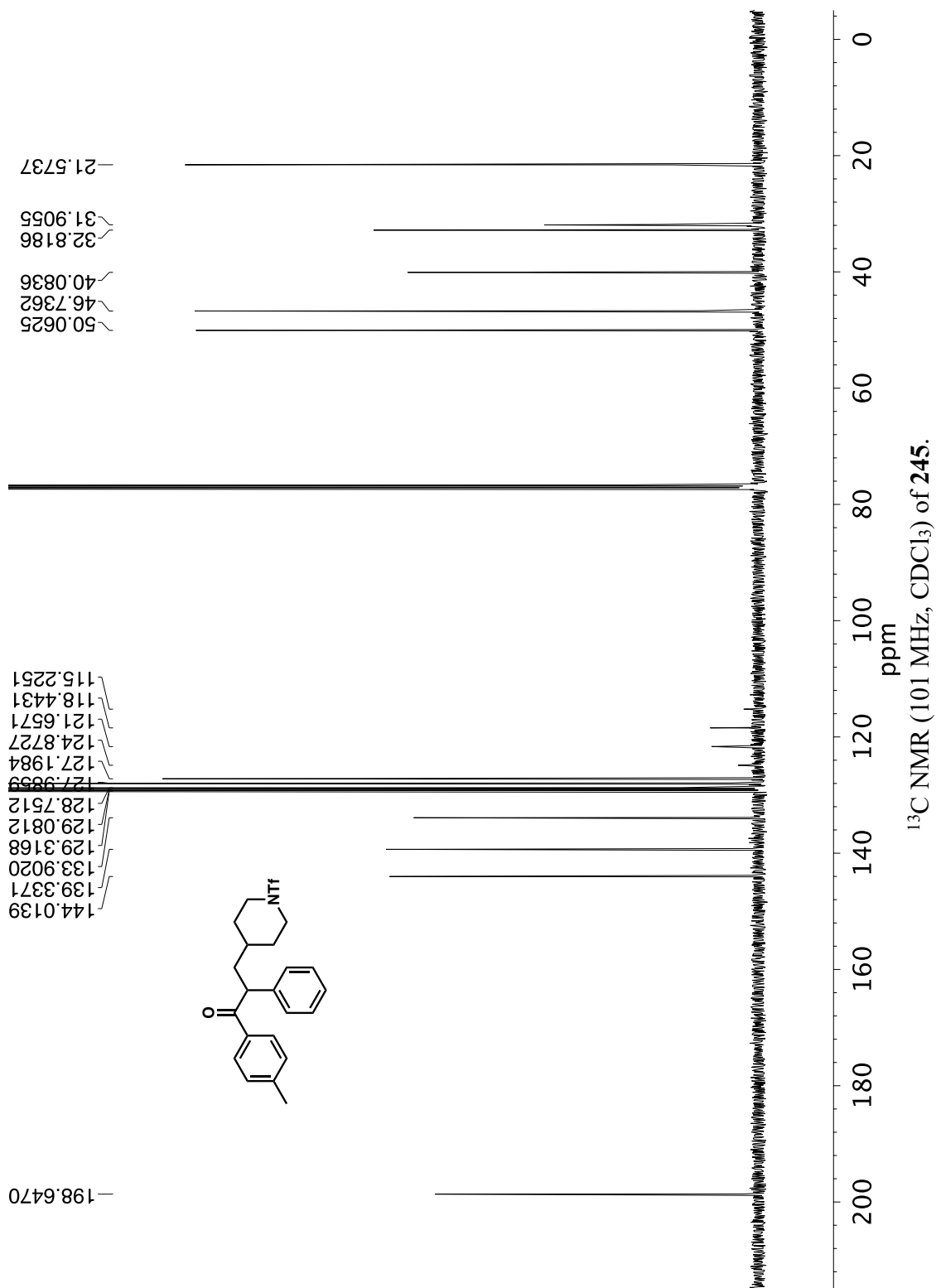


—75.34

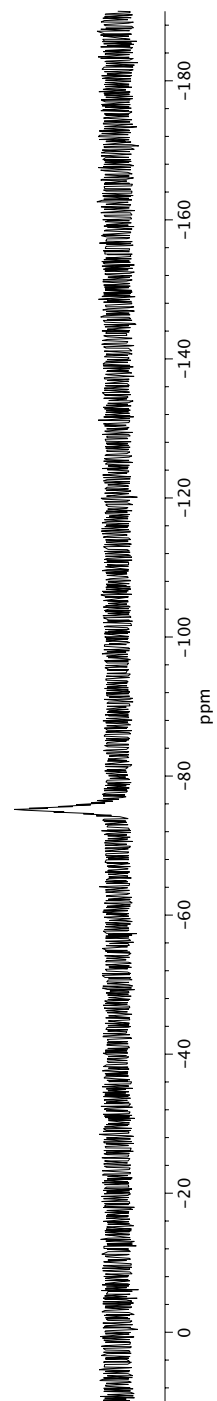
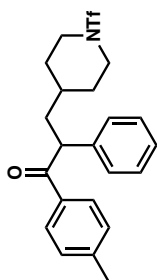


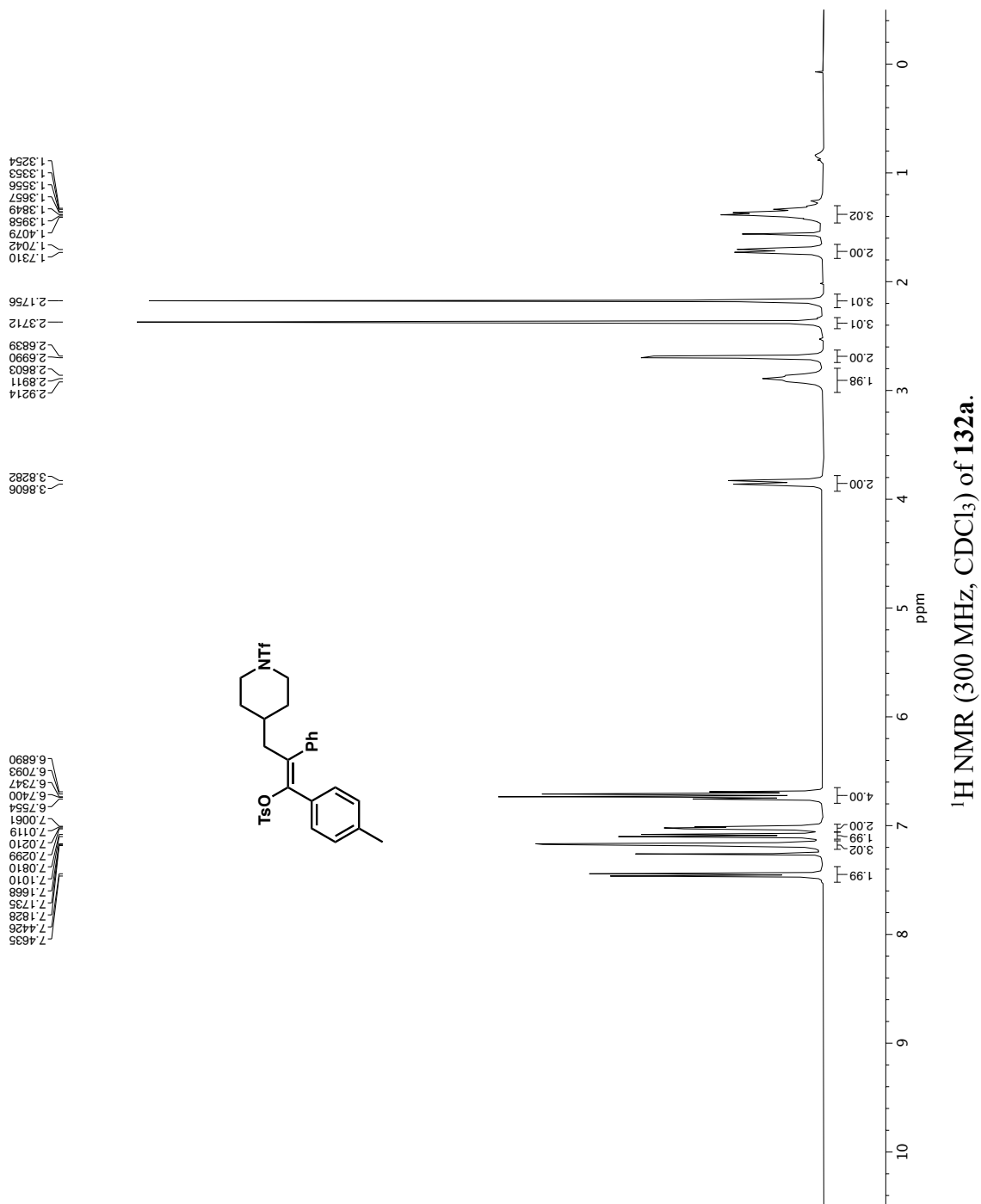
¹⁹F NMR (376 MHz, CDCl₃) of **243**.

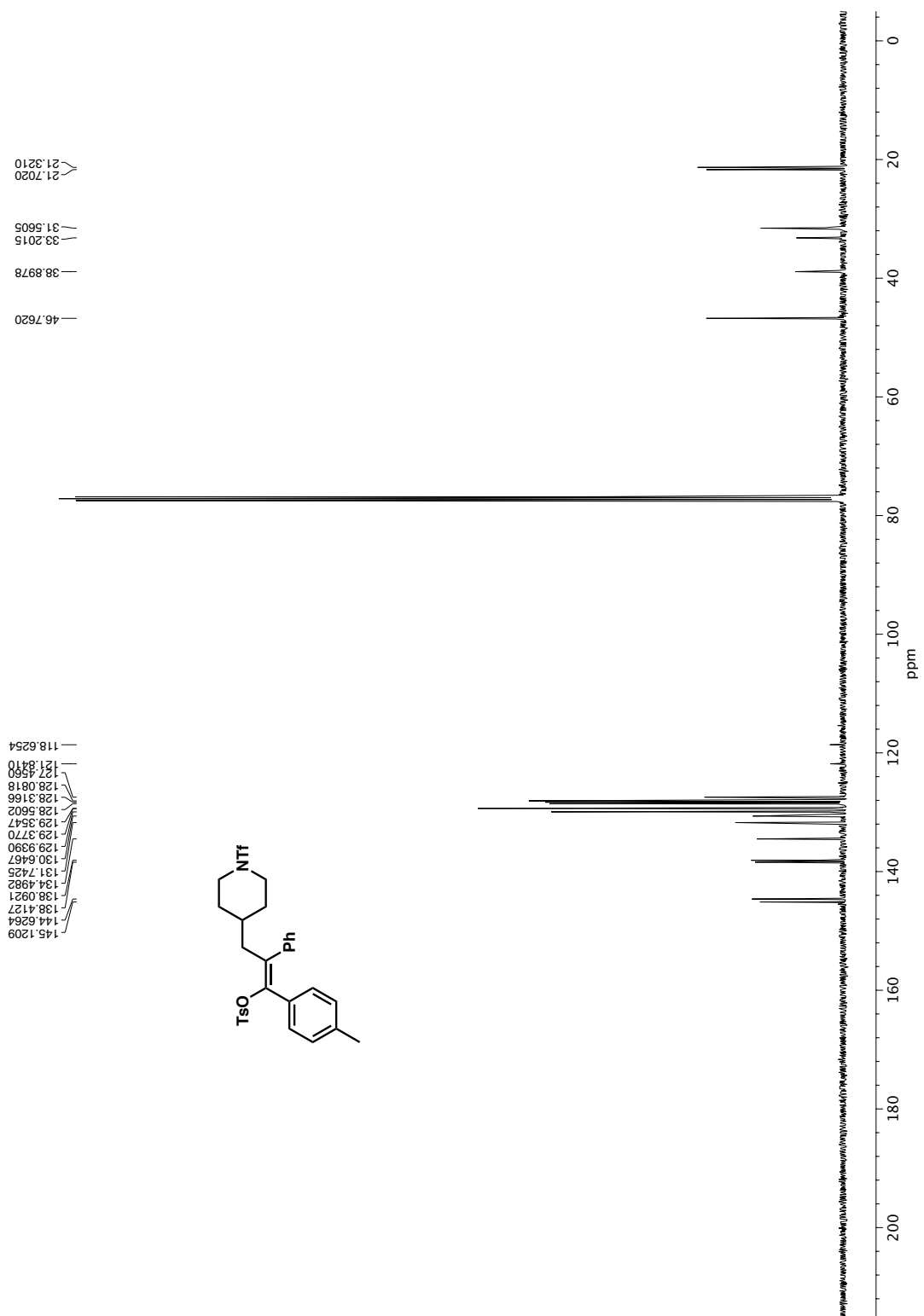




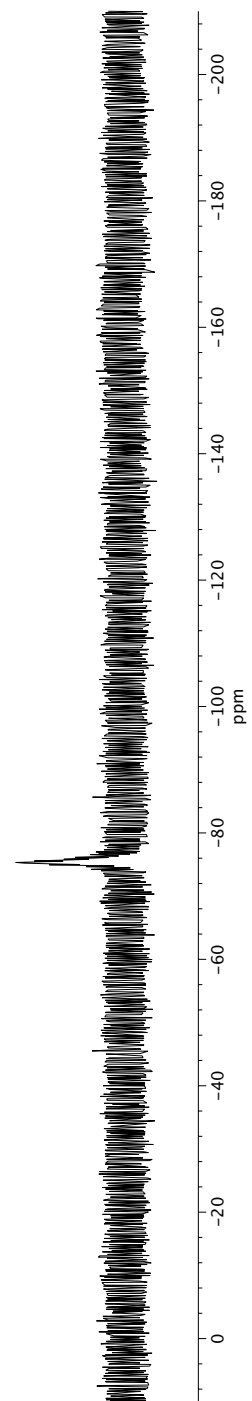
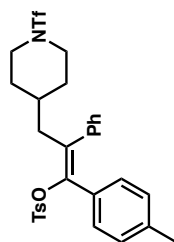
—75.1554

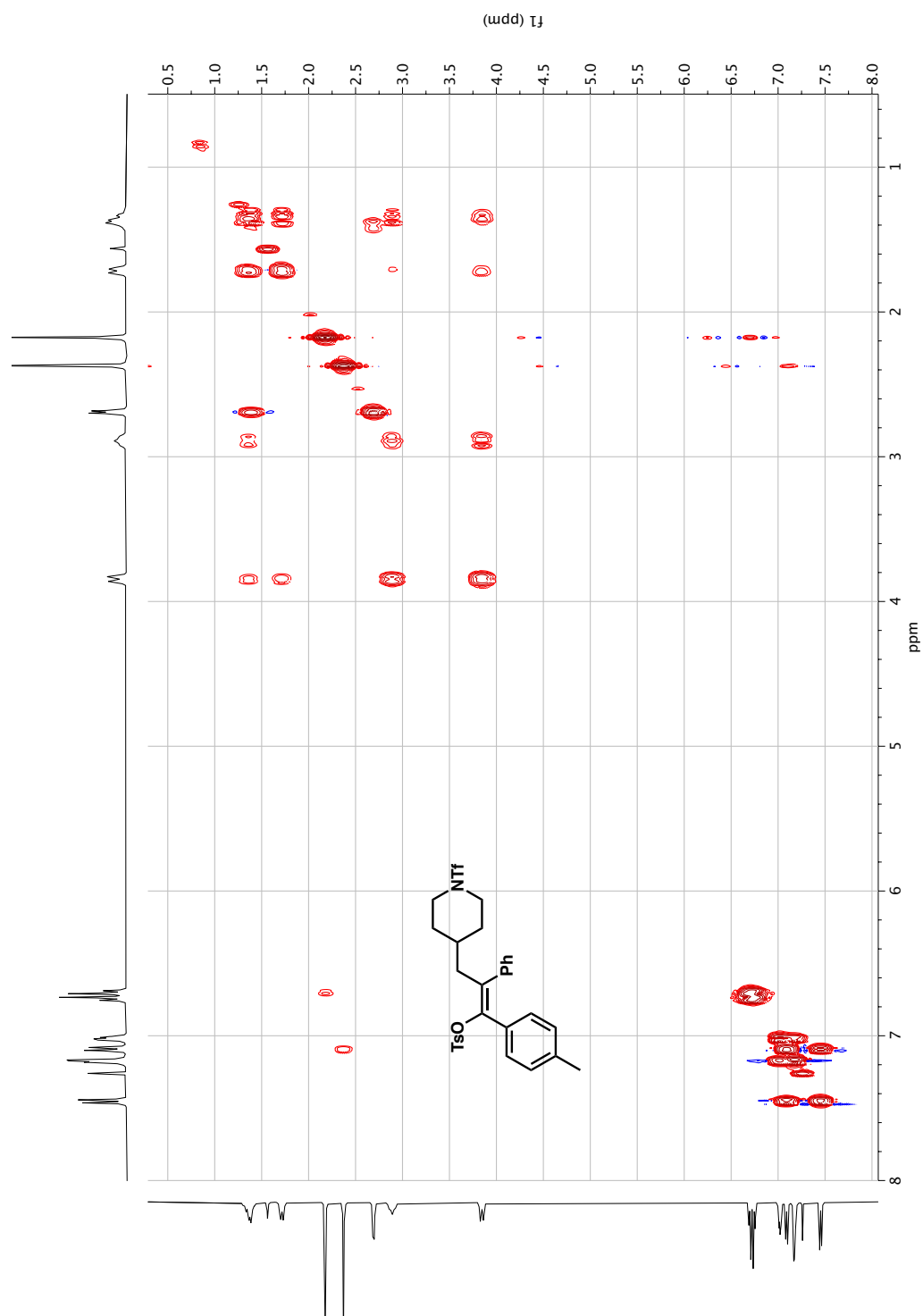
 ^{19}F NMR (282 MHz, CDCl_3) of **245**.

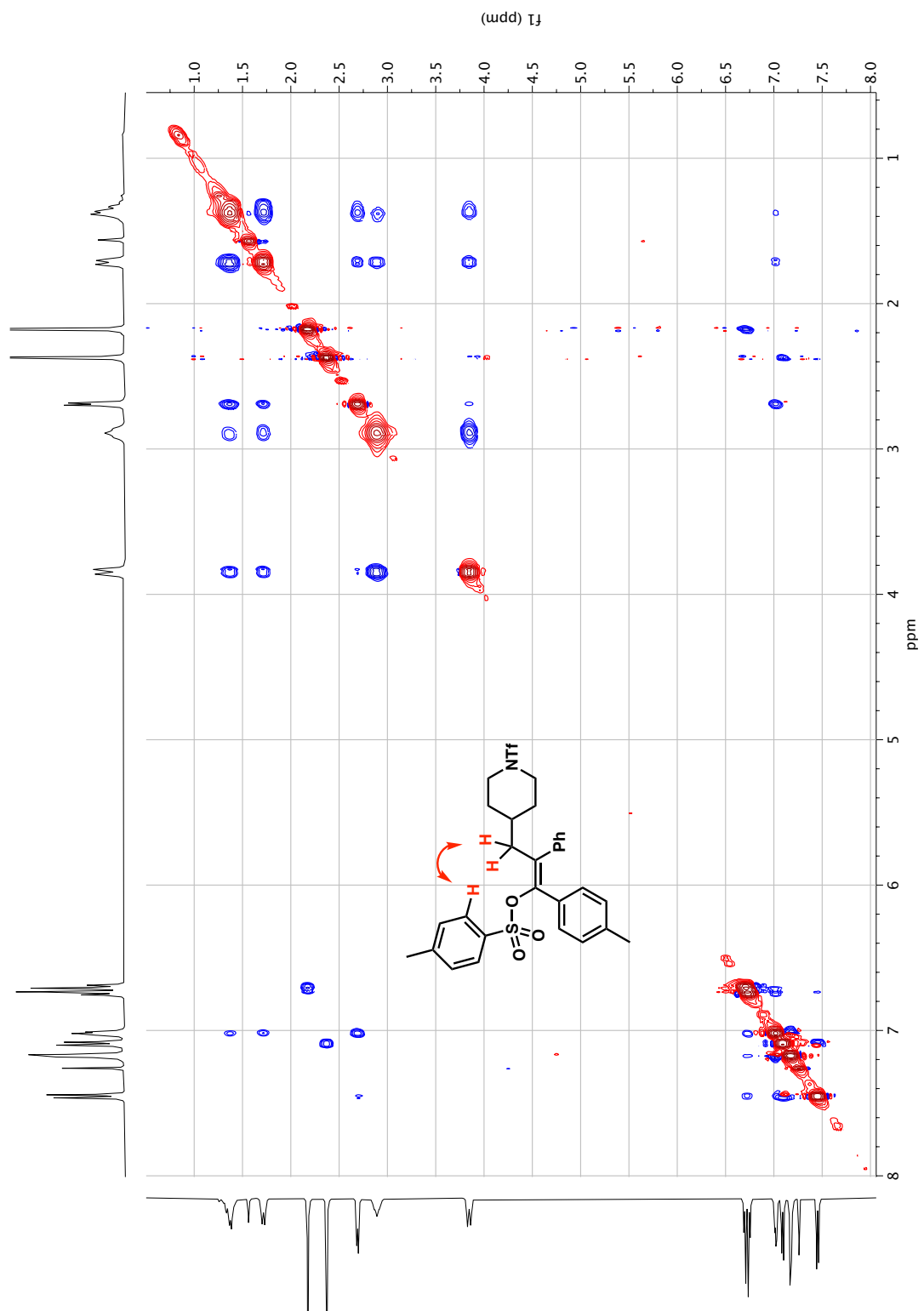


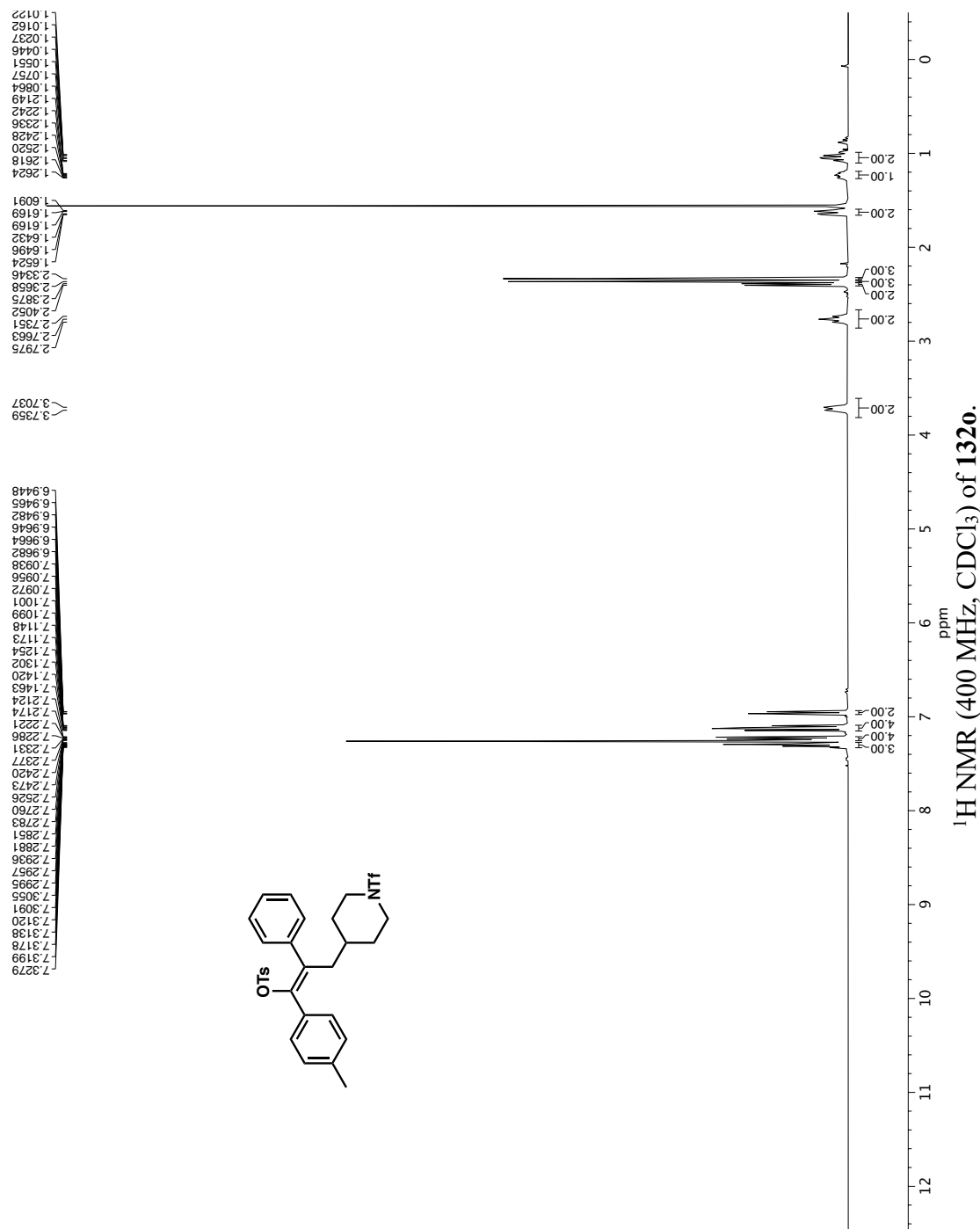


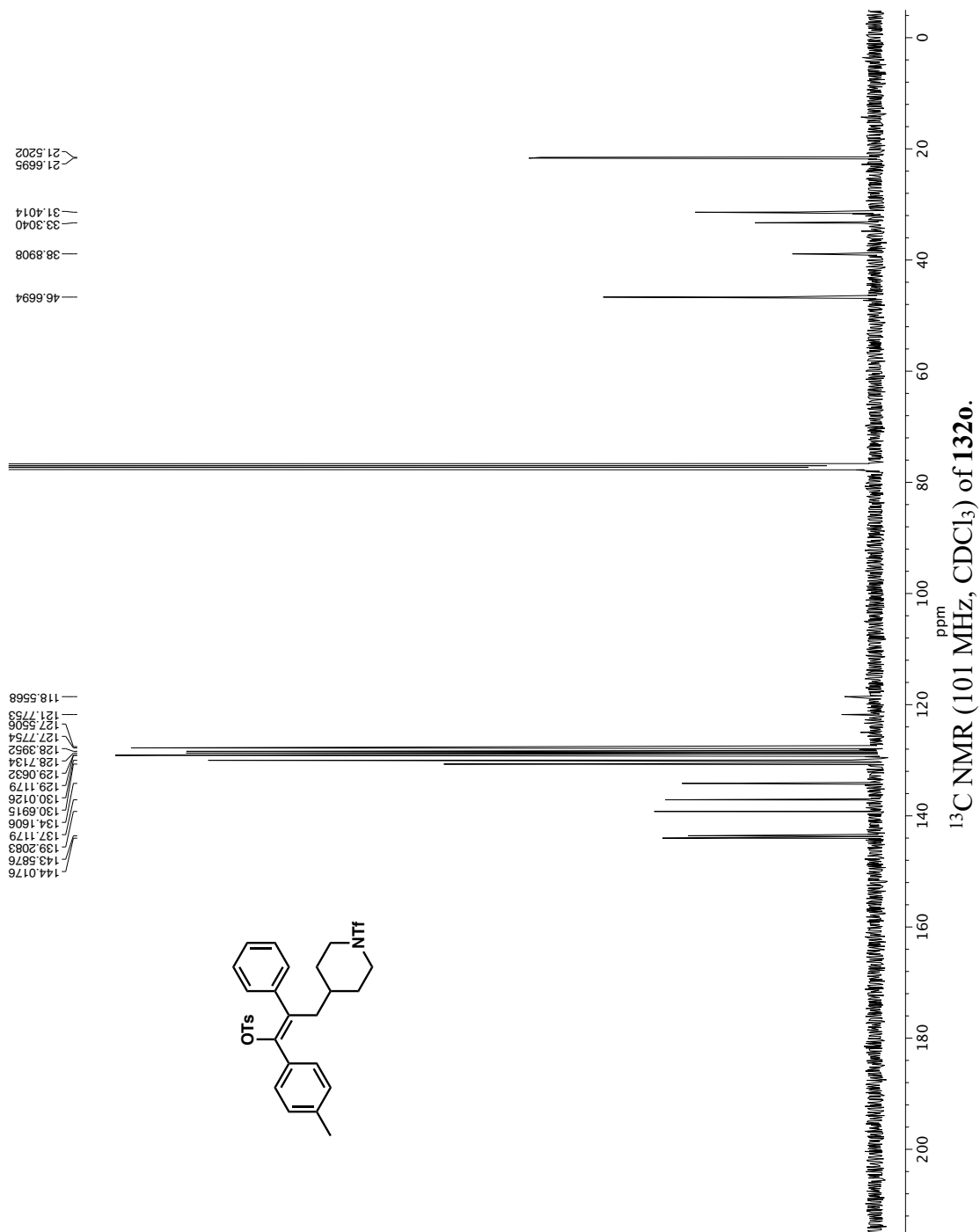
—75.3398

 ^{19}F NMR (282 MHz, CDCl_3) of **132a**.

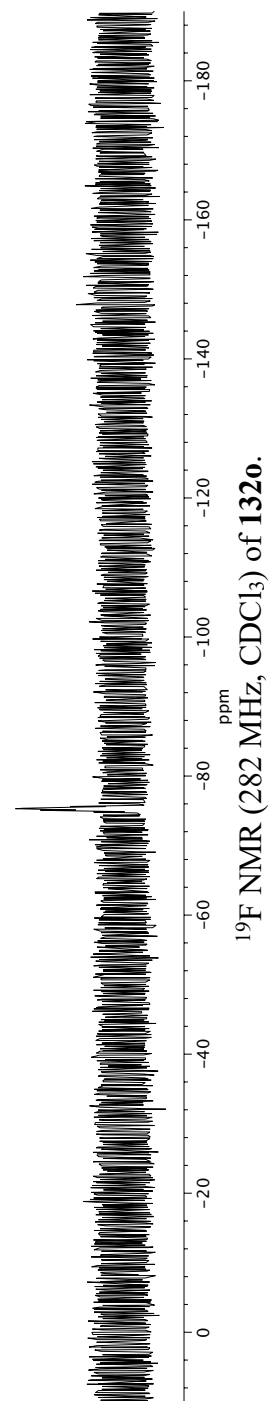
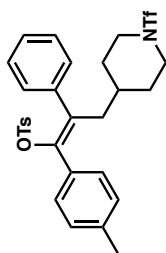
COSY NMR (400 MHz, CDCl₃) of **132a**.

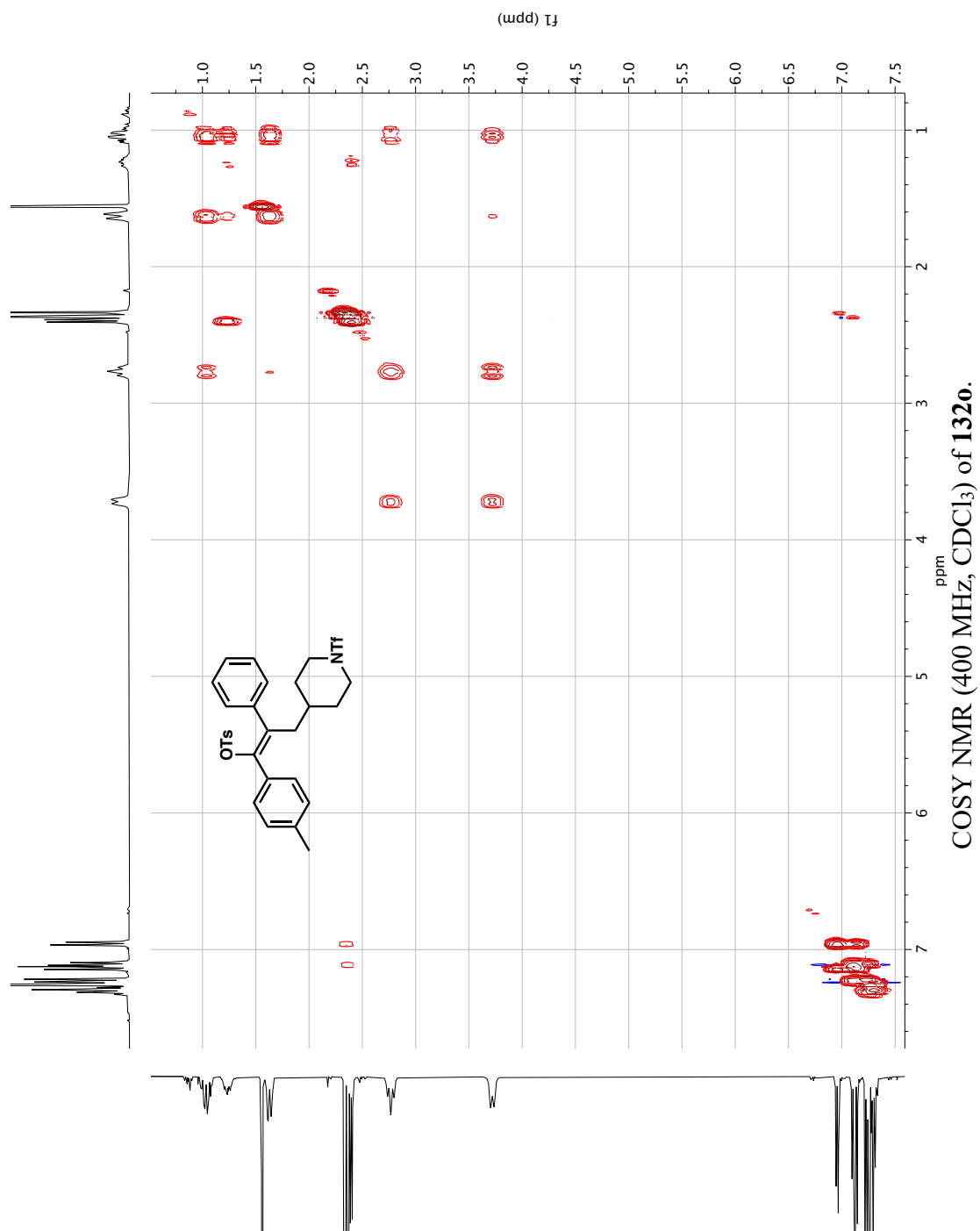


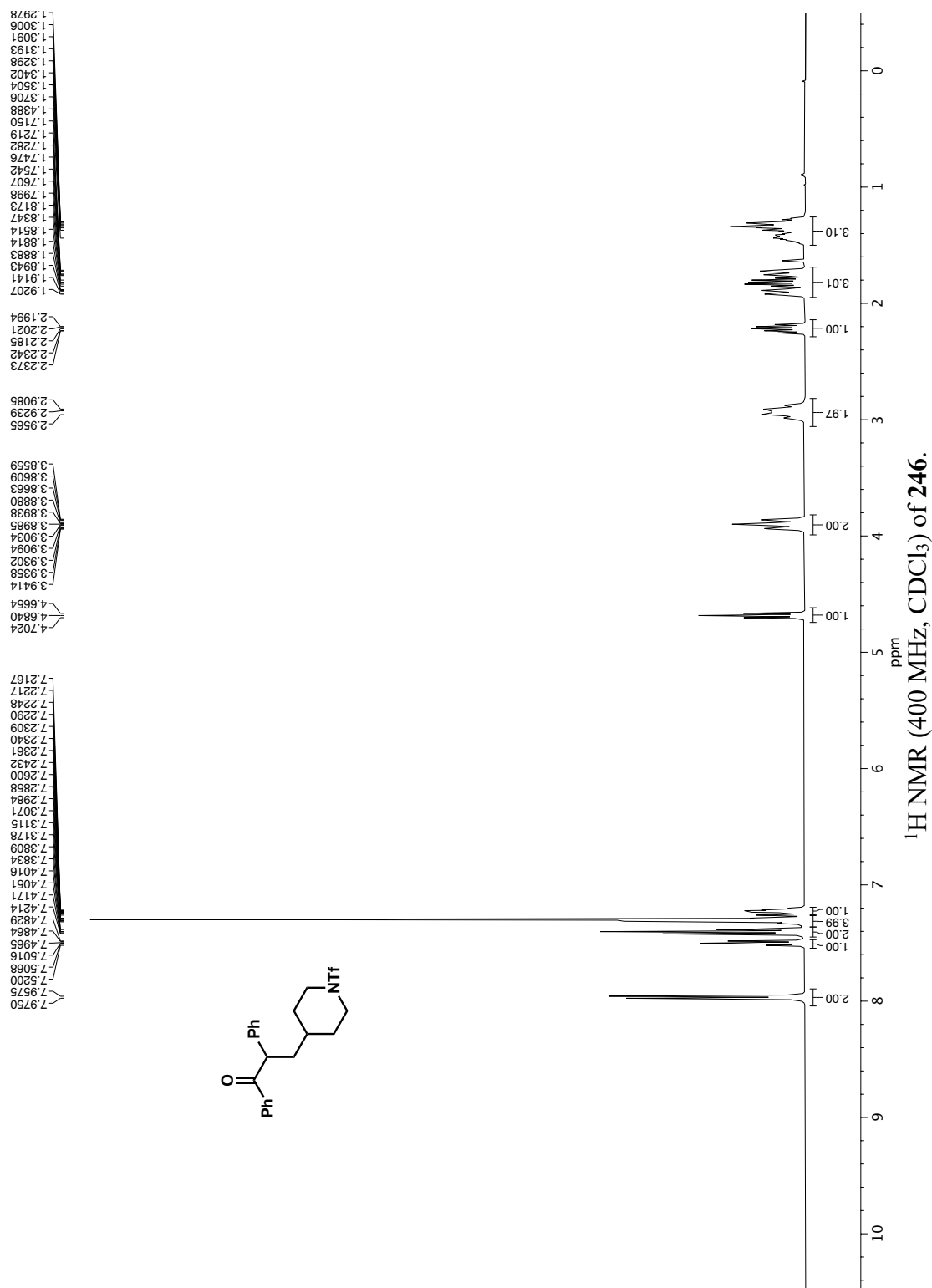


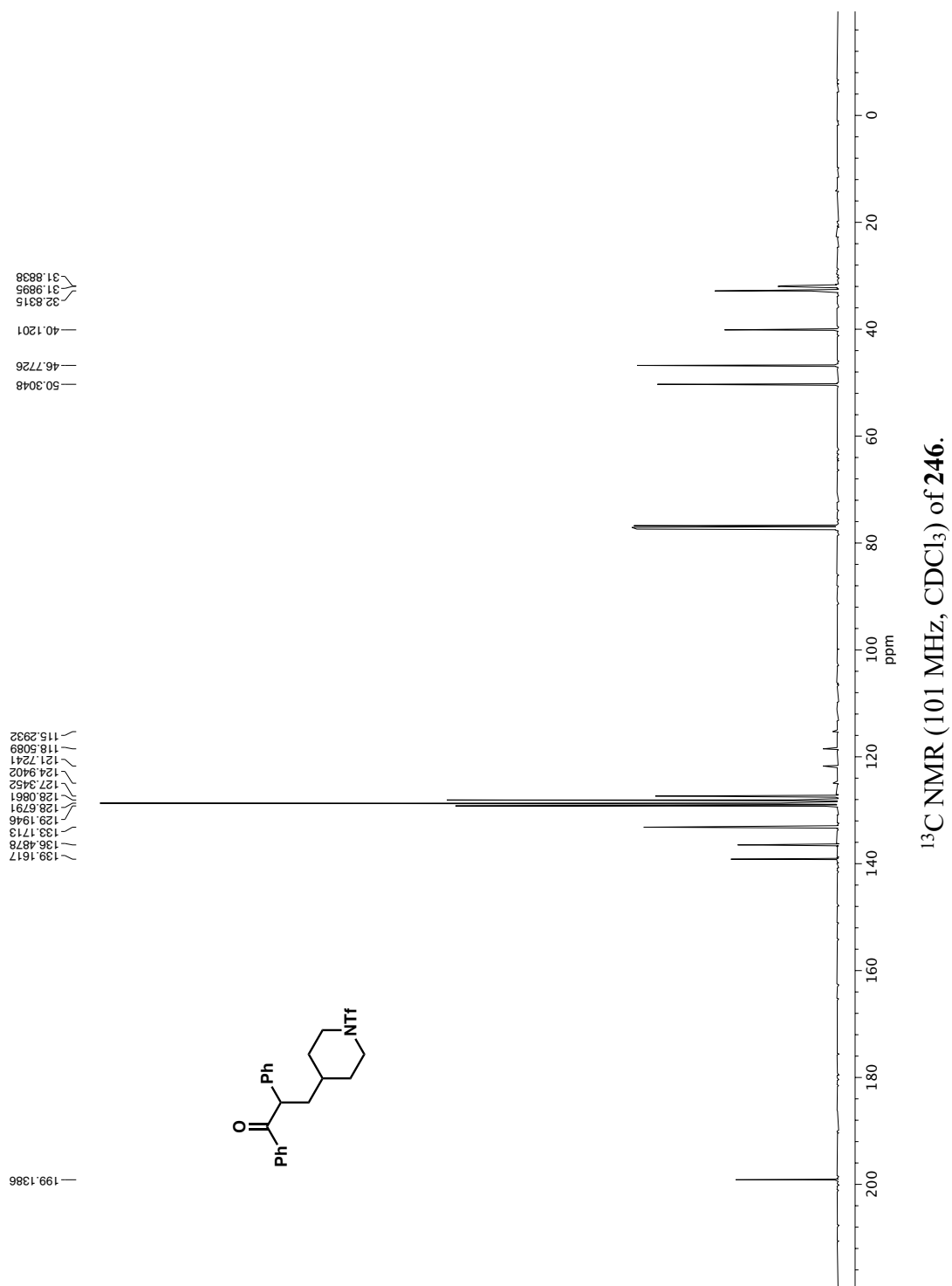


-75.3046

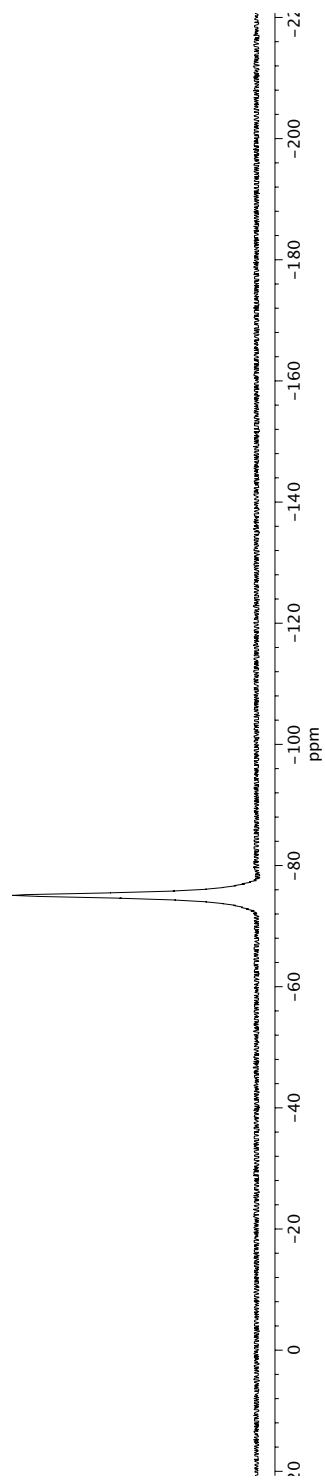
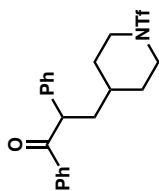




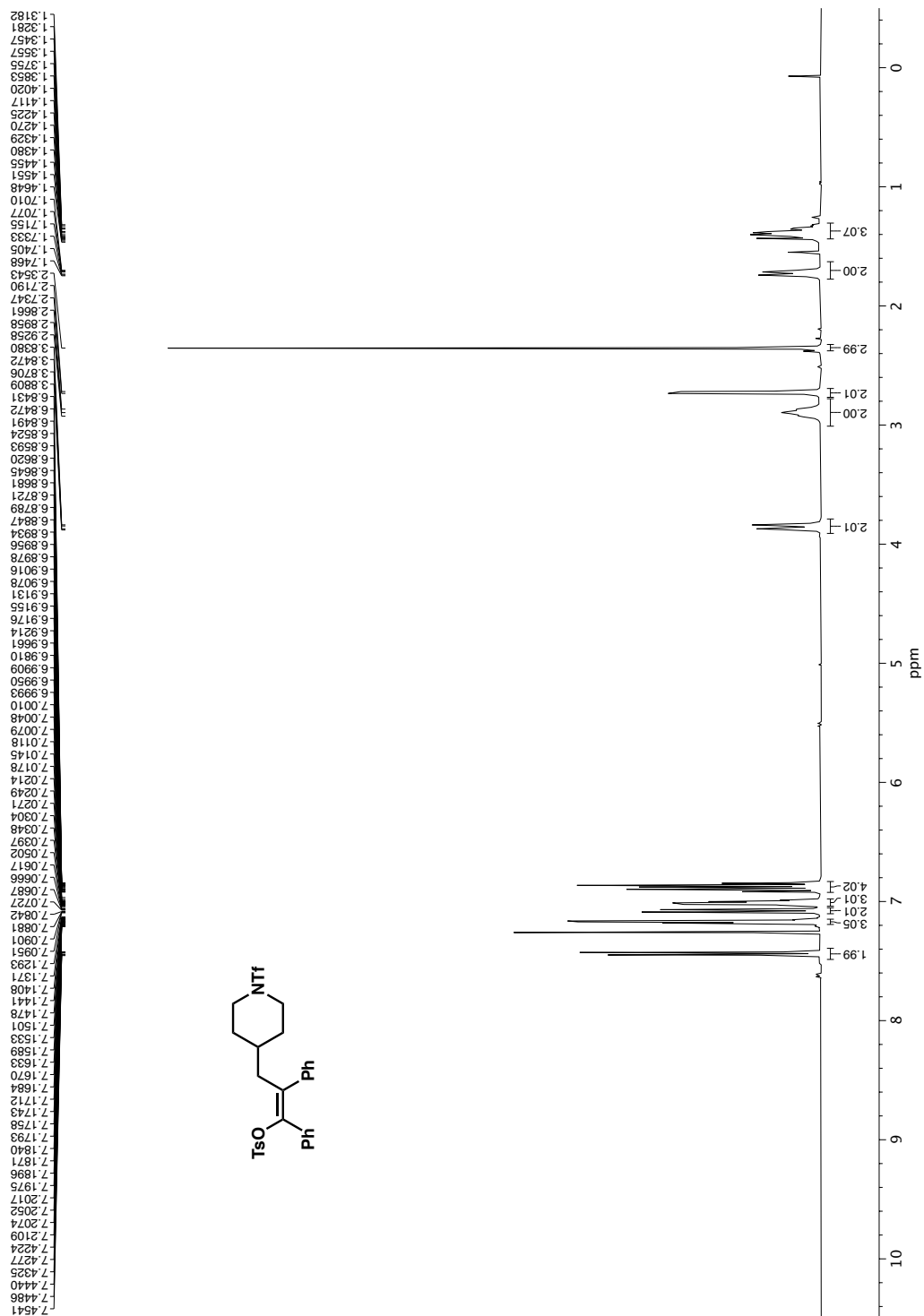


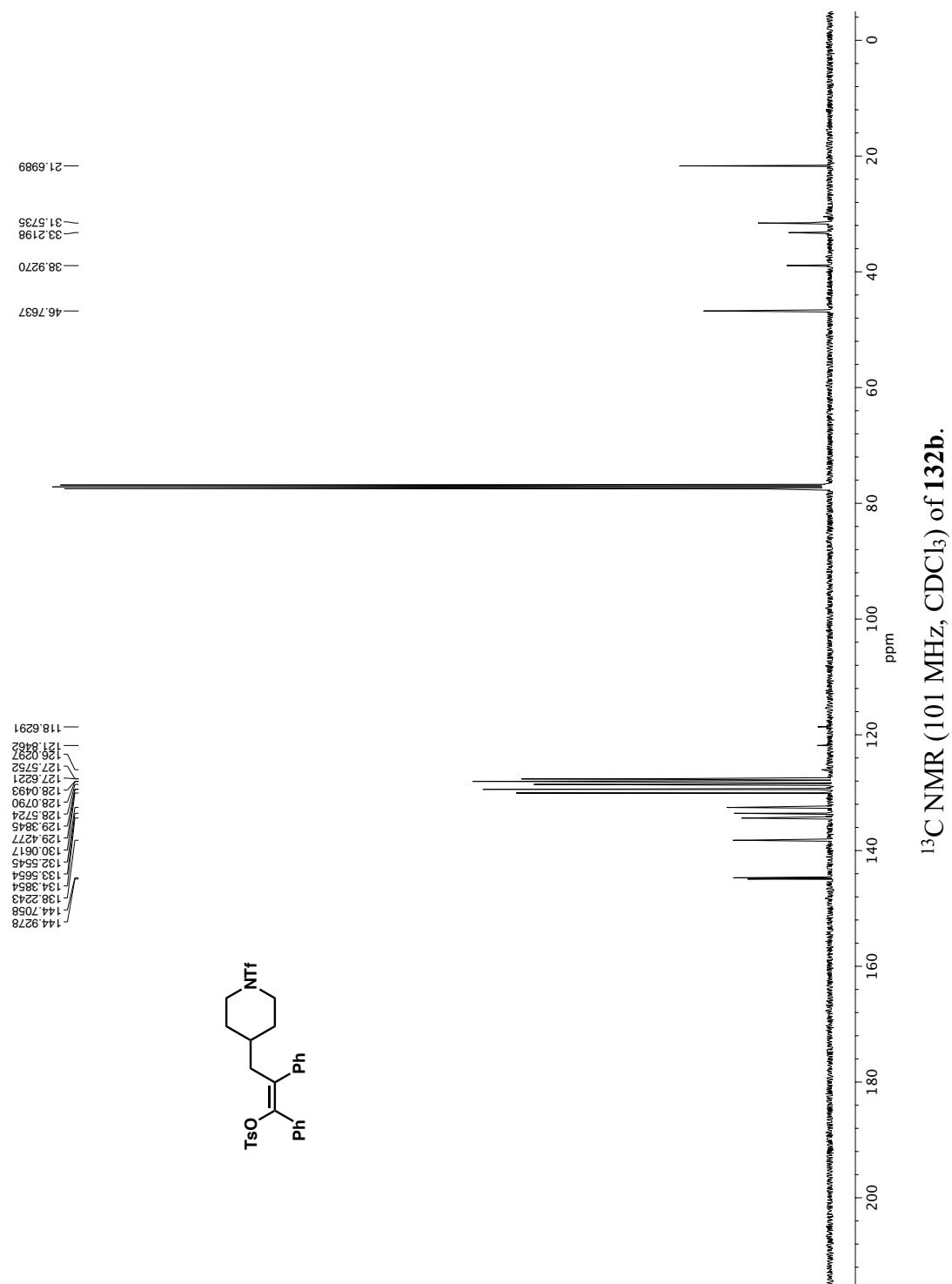


-75.0748

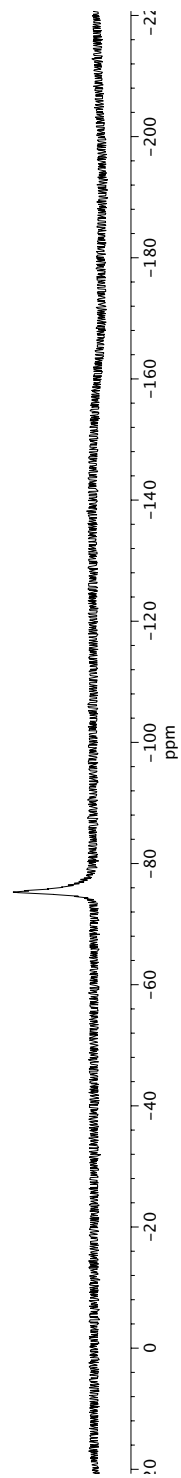
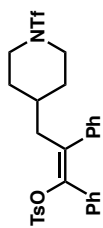


¹⁹F NMR (376 MHz, CDCl₃) of **246**.

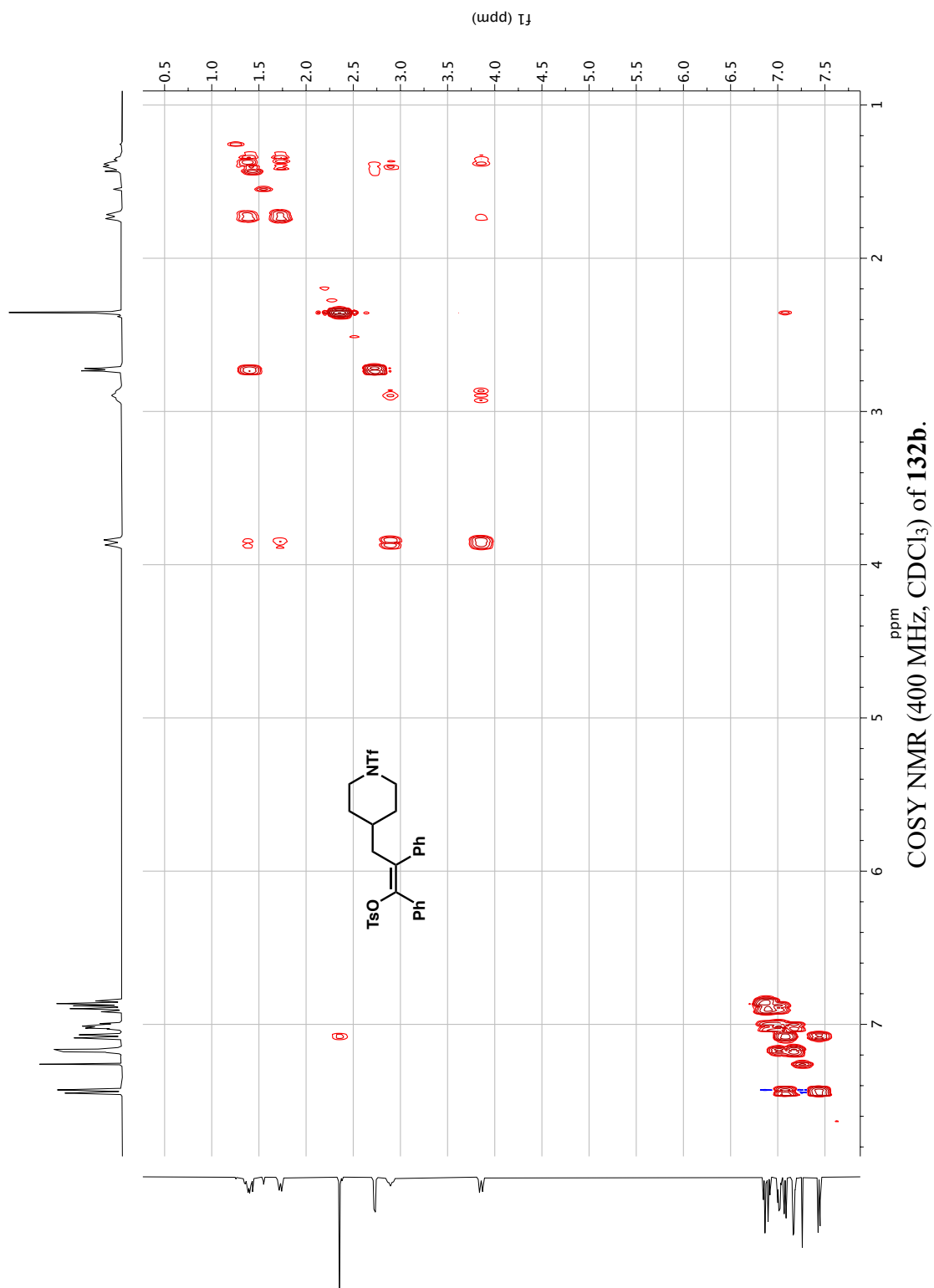


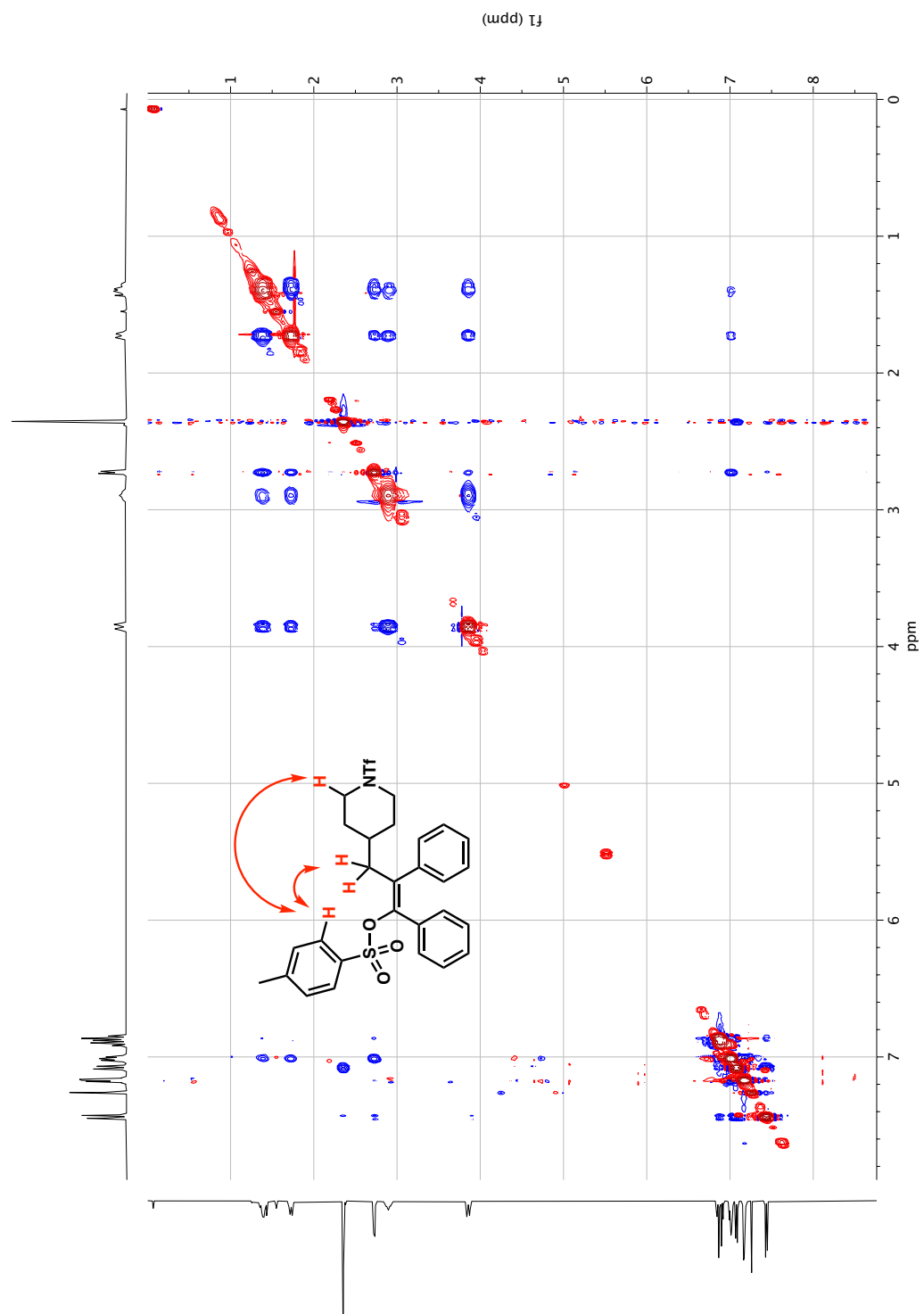


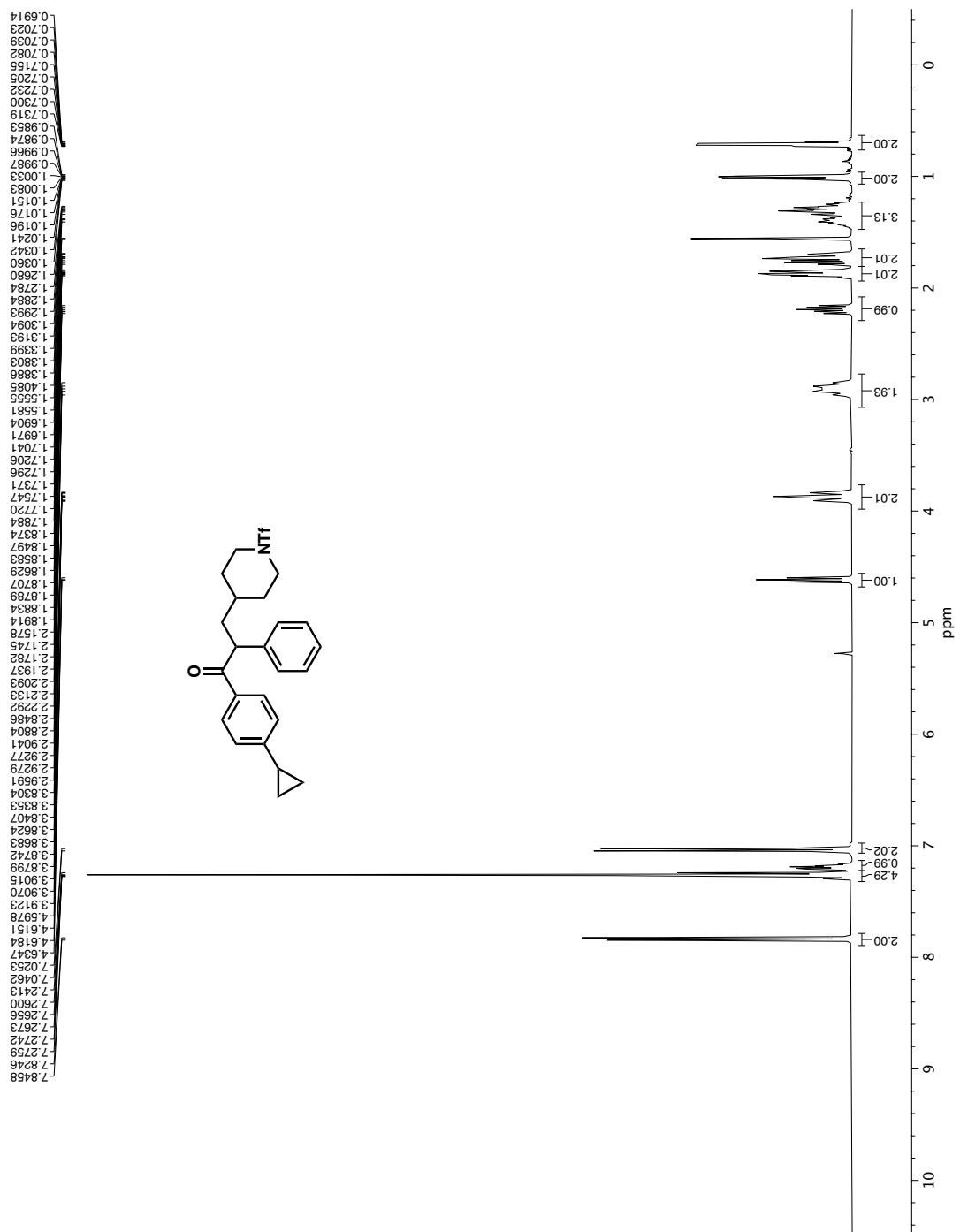
-75.3081

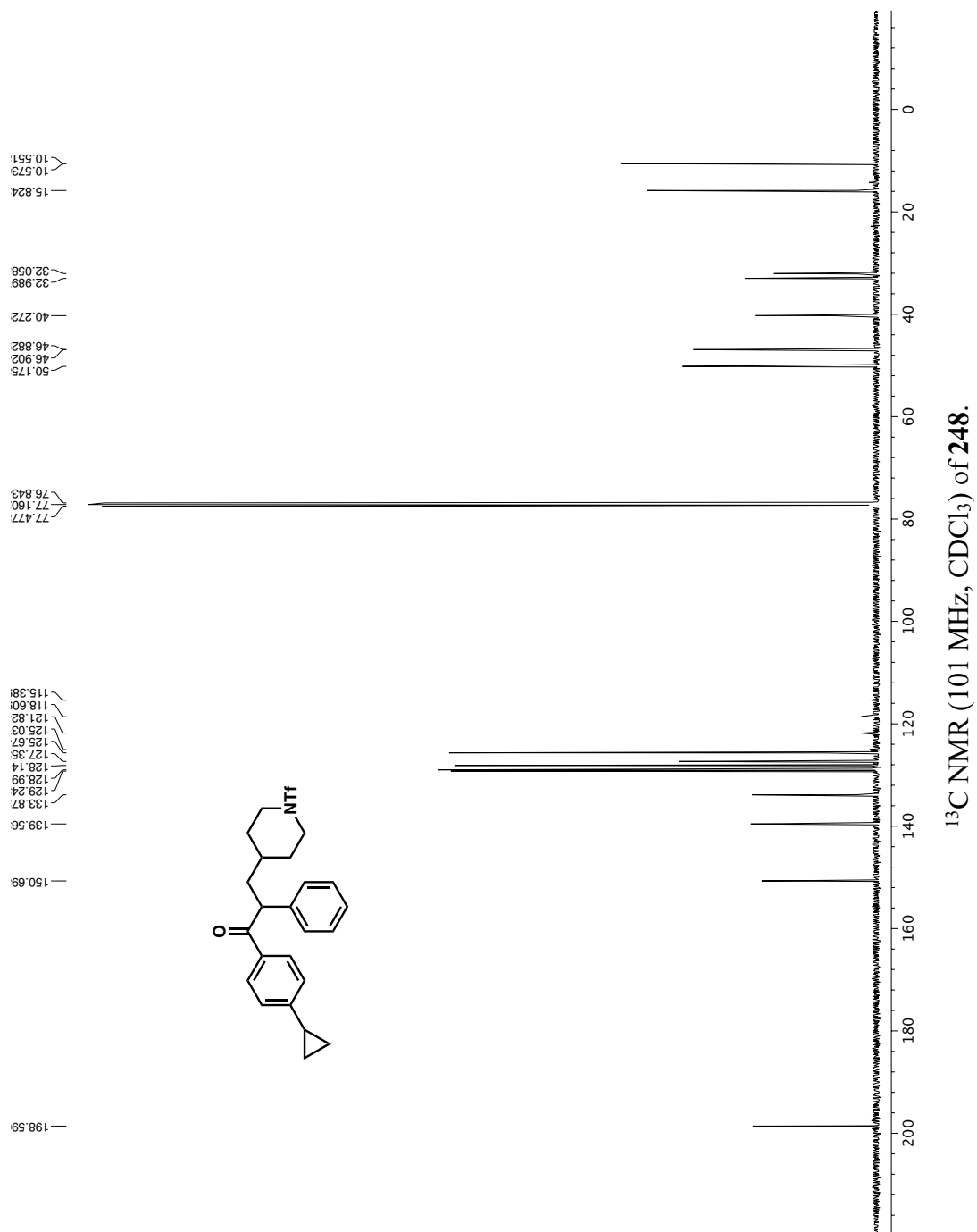


¹⁹F NMR (376 MHz, CDCl₃) of **132b**.

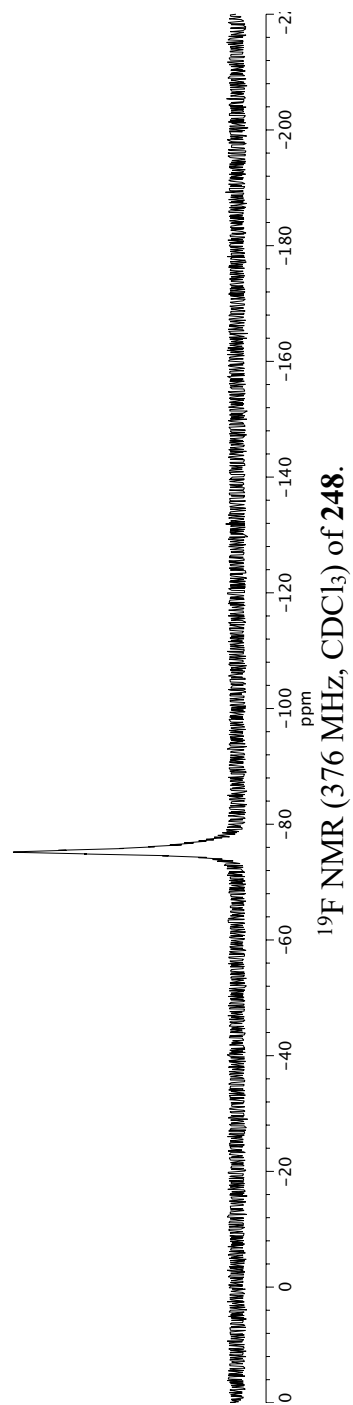
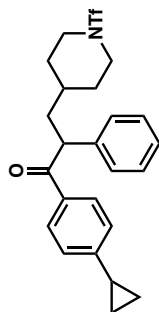


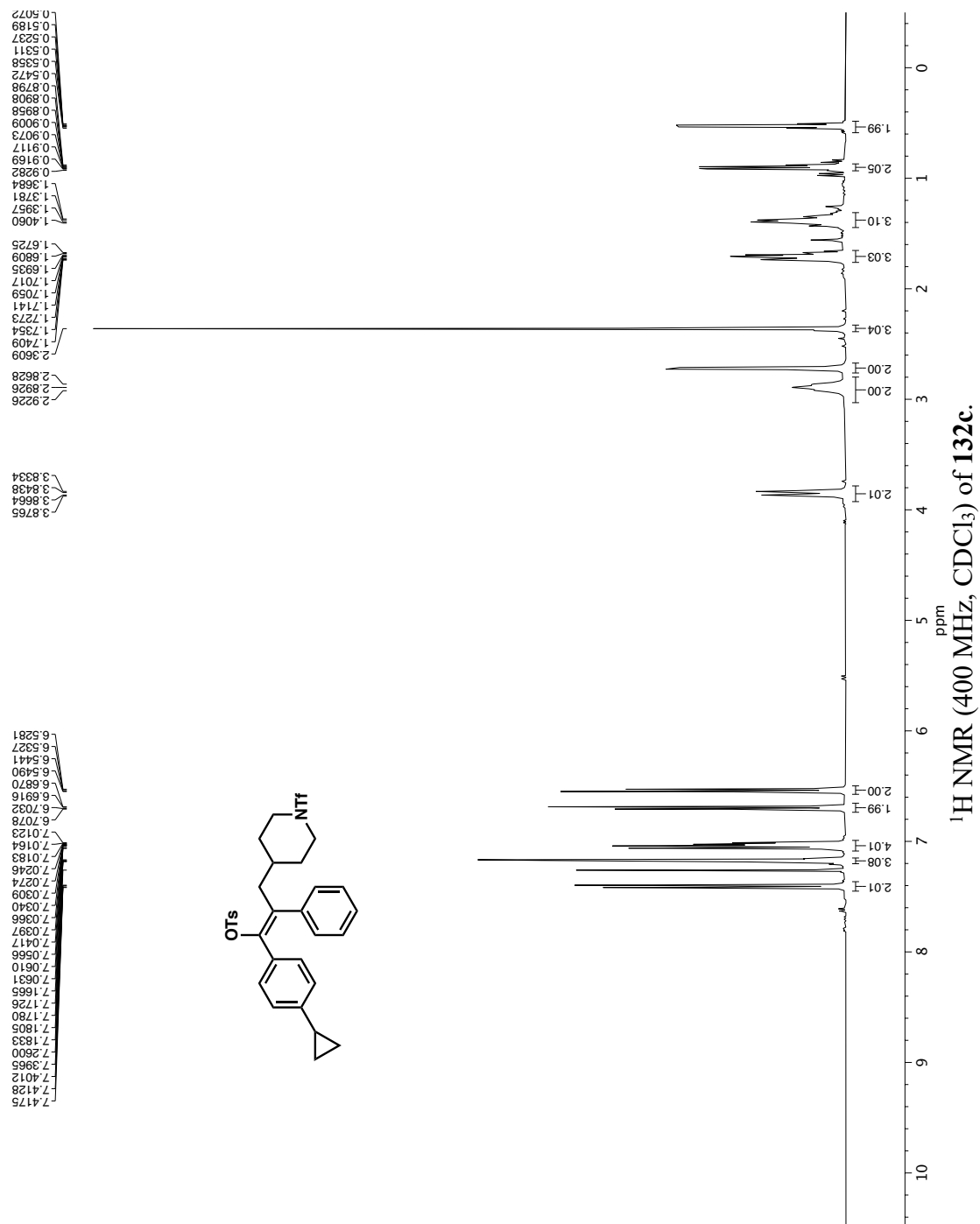


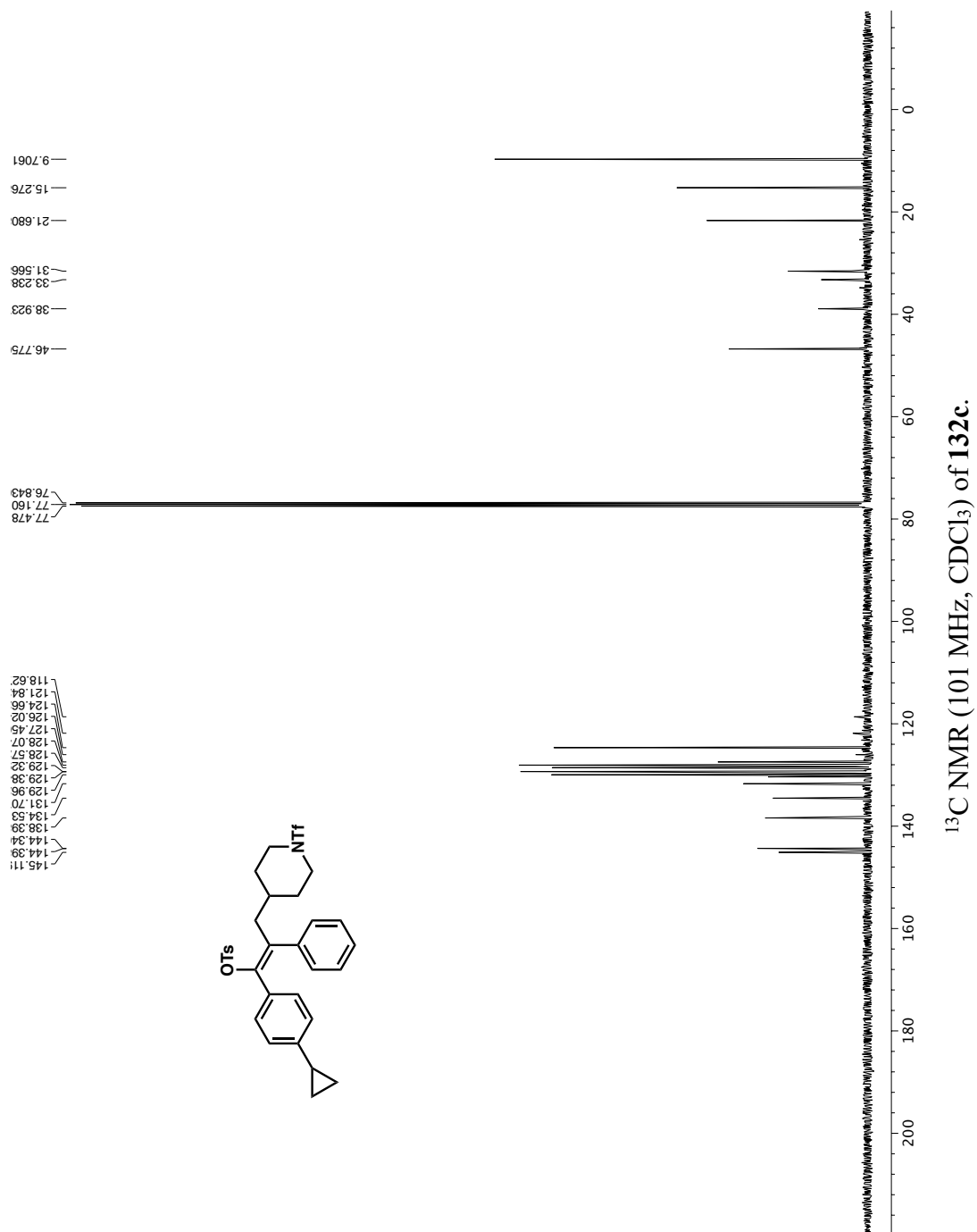




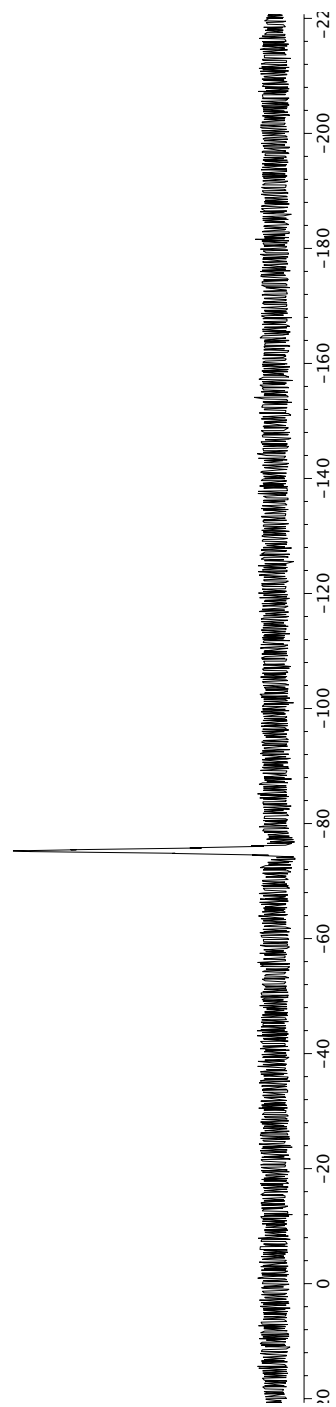
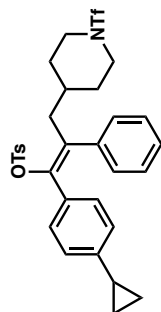
—75.1593

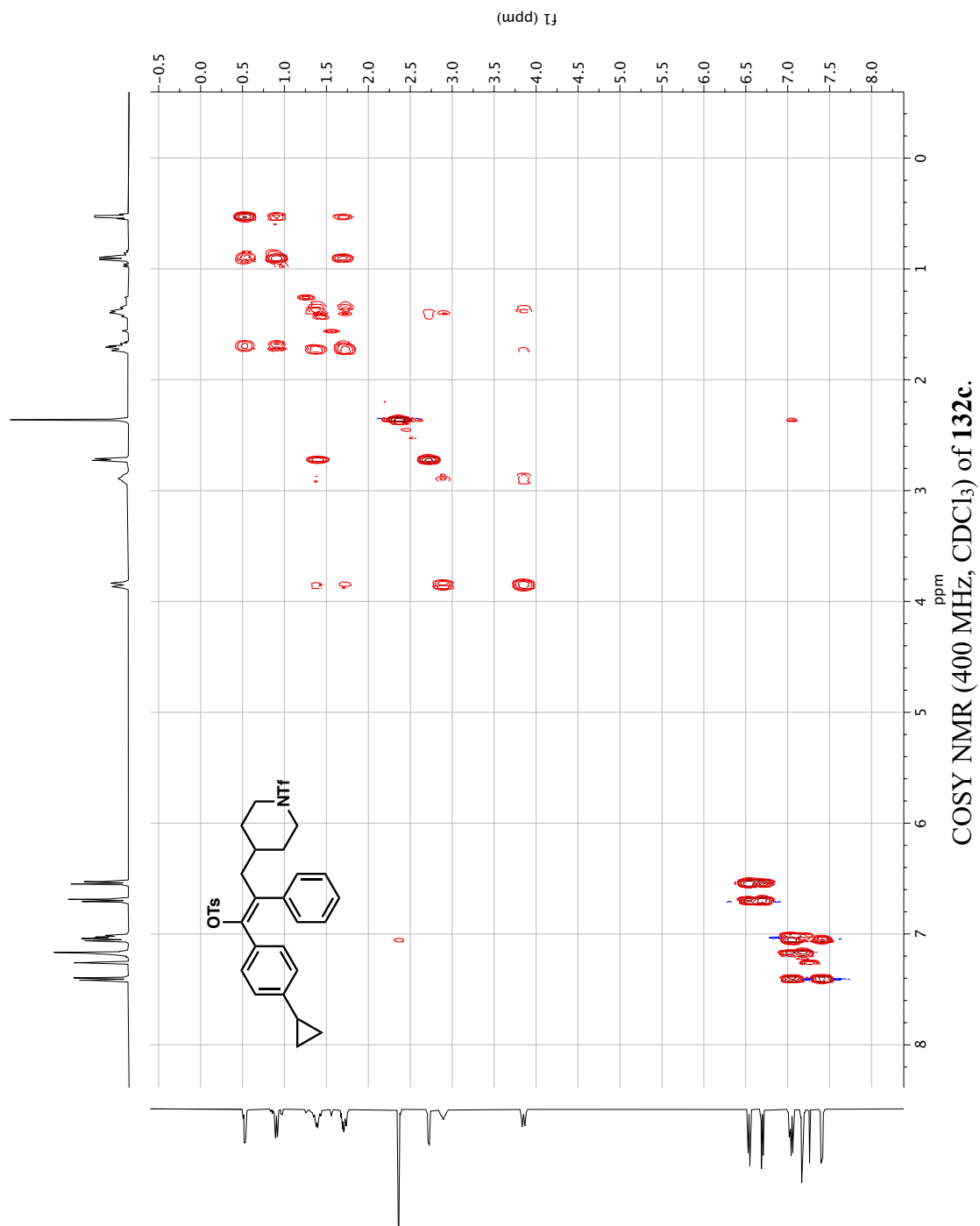


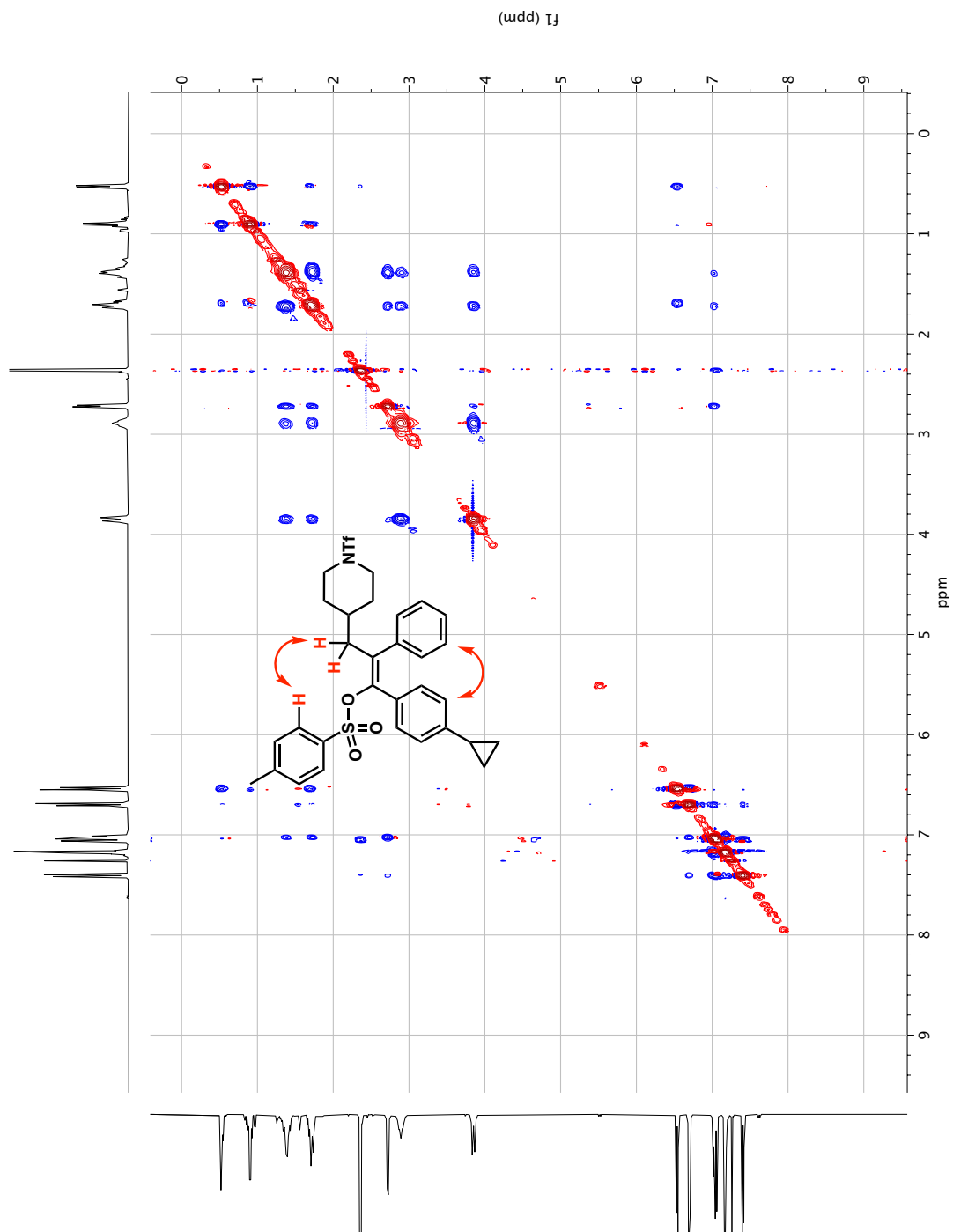




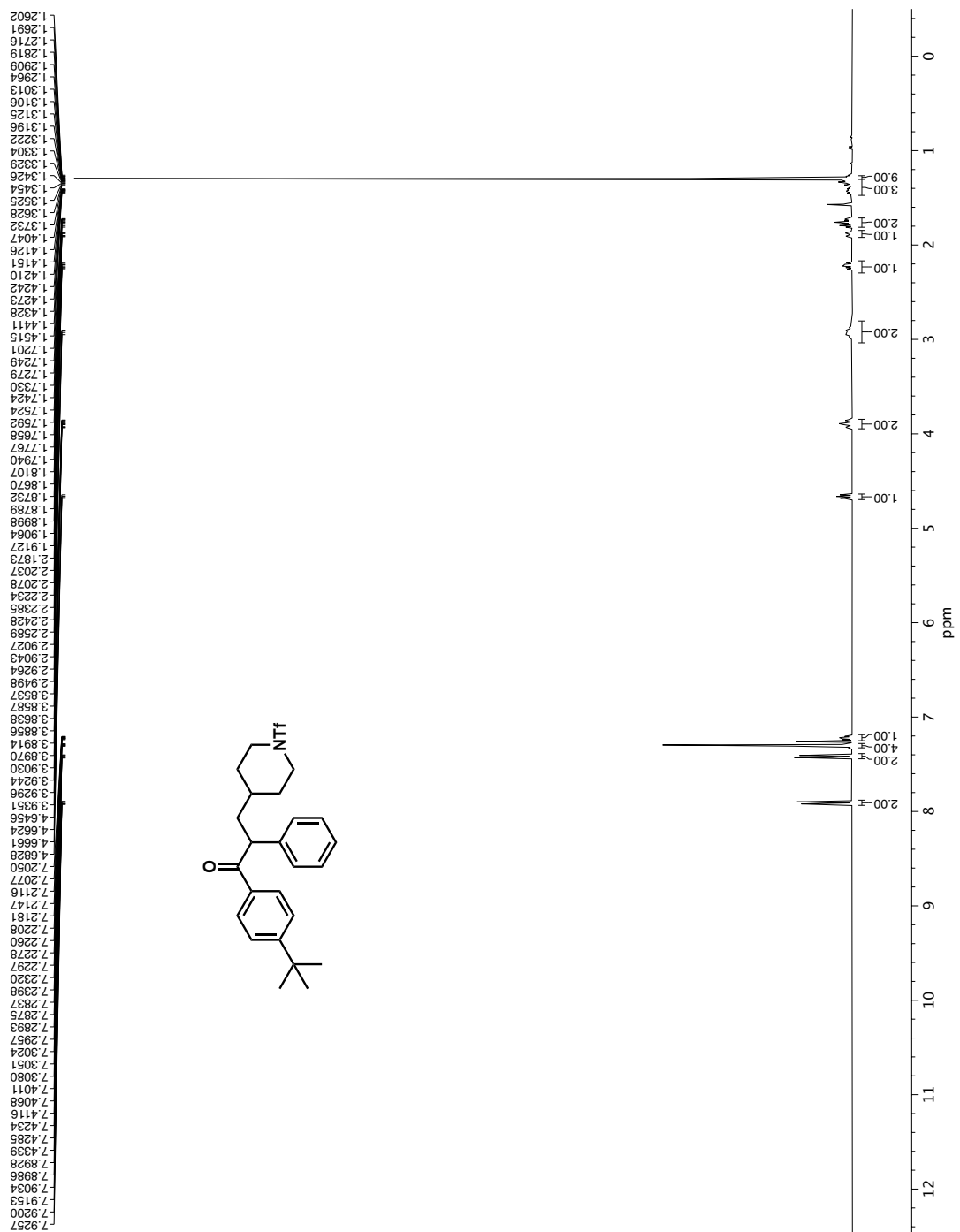
-75.2164

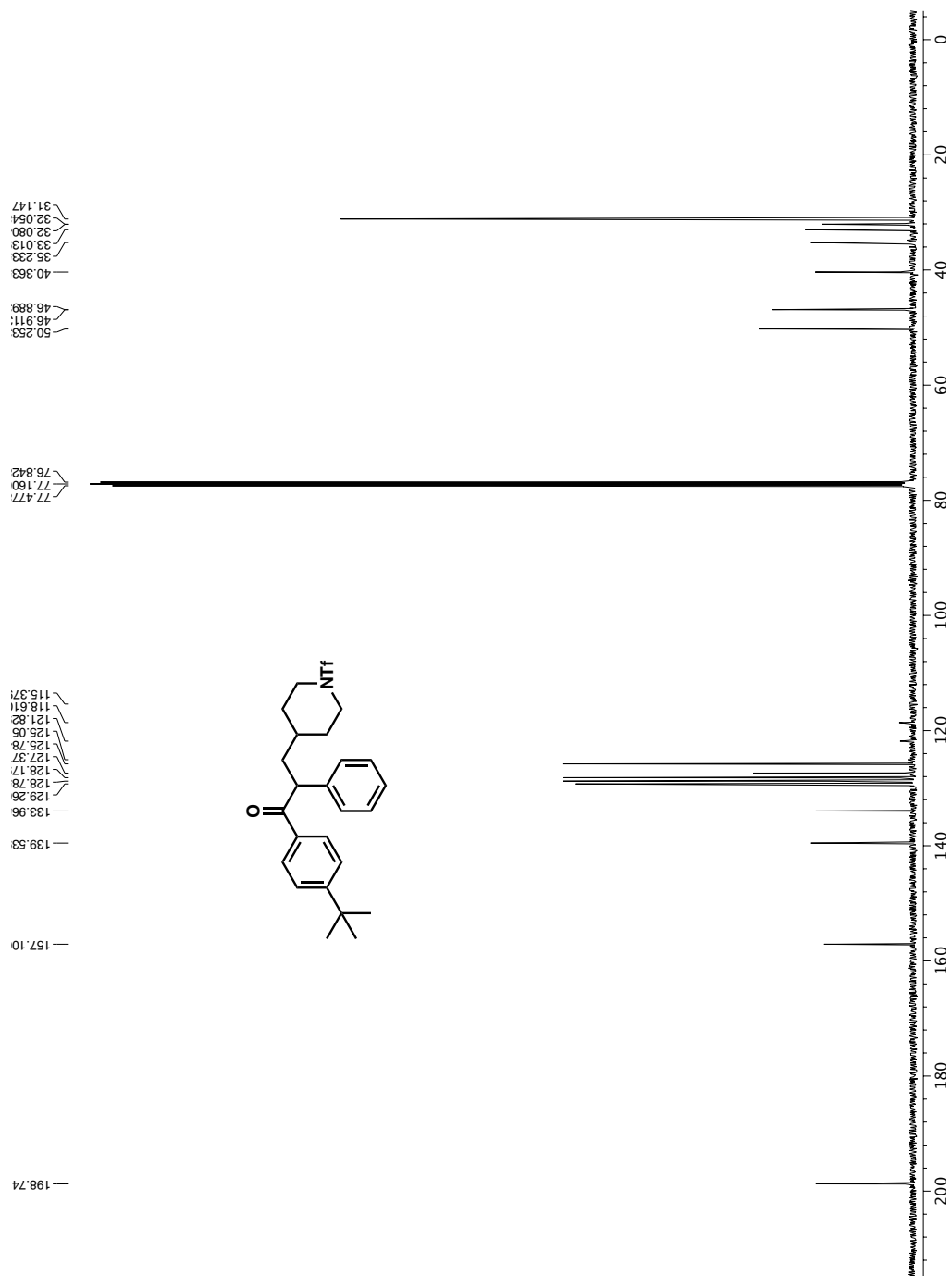
 ^{19}F NMR (376 MHz, CDCl_3) of **132c**.



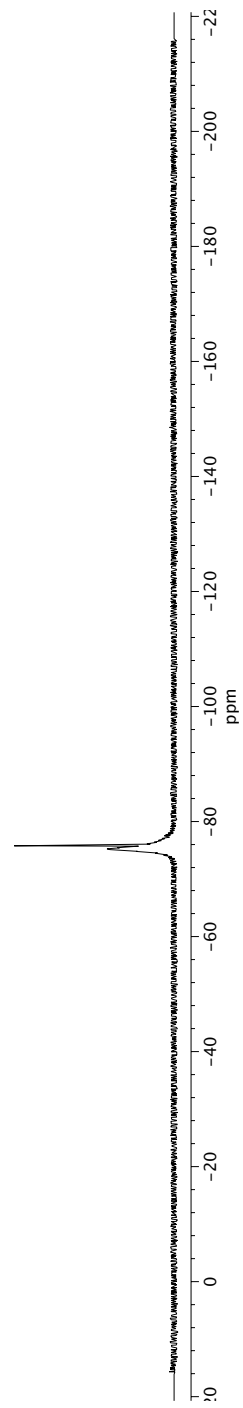
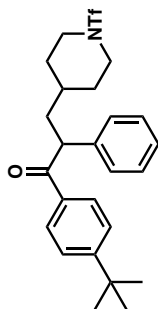


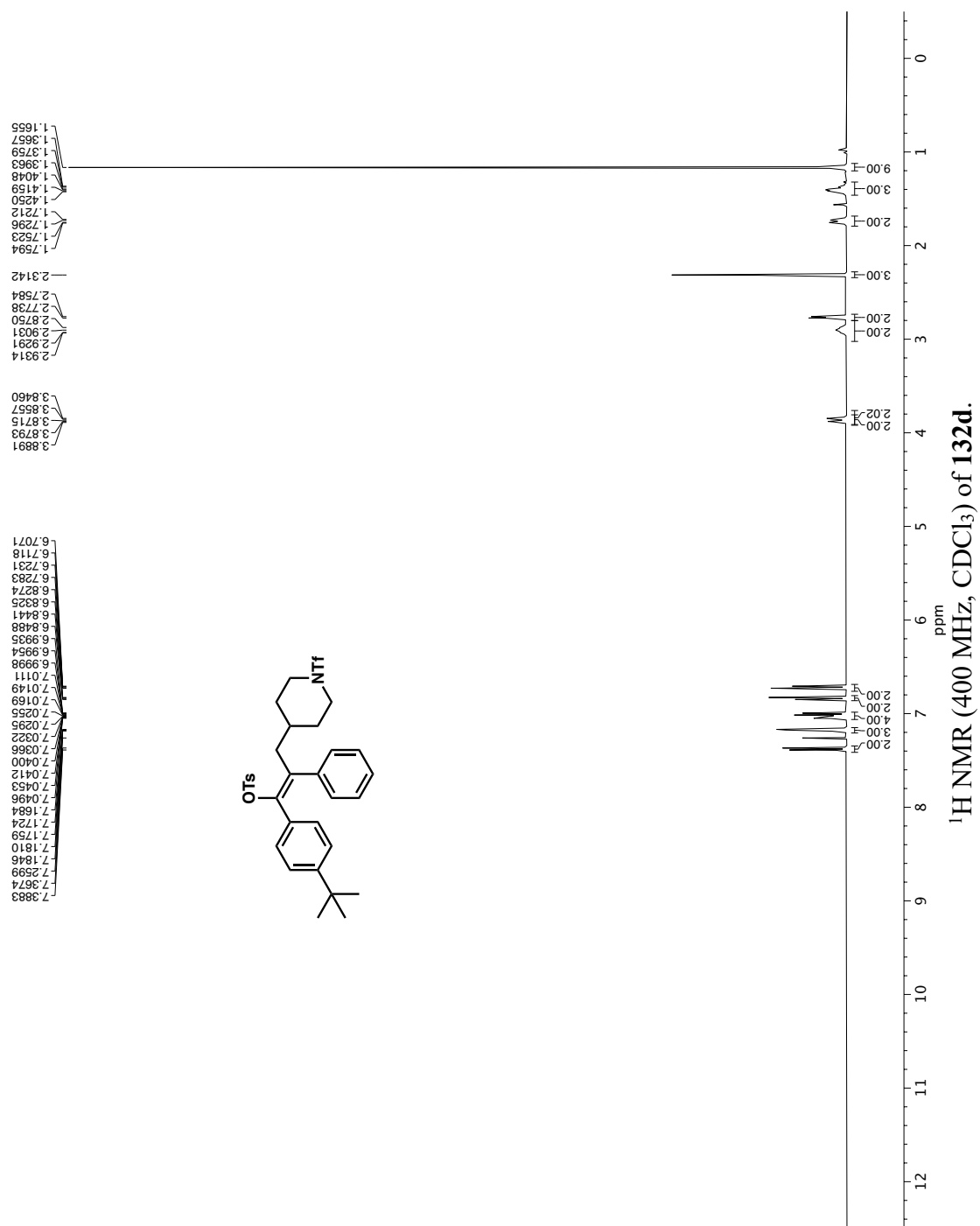
NOESY NMR (400 MHz, CDCl₃) of **132c**.

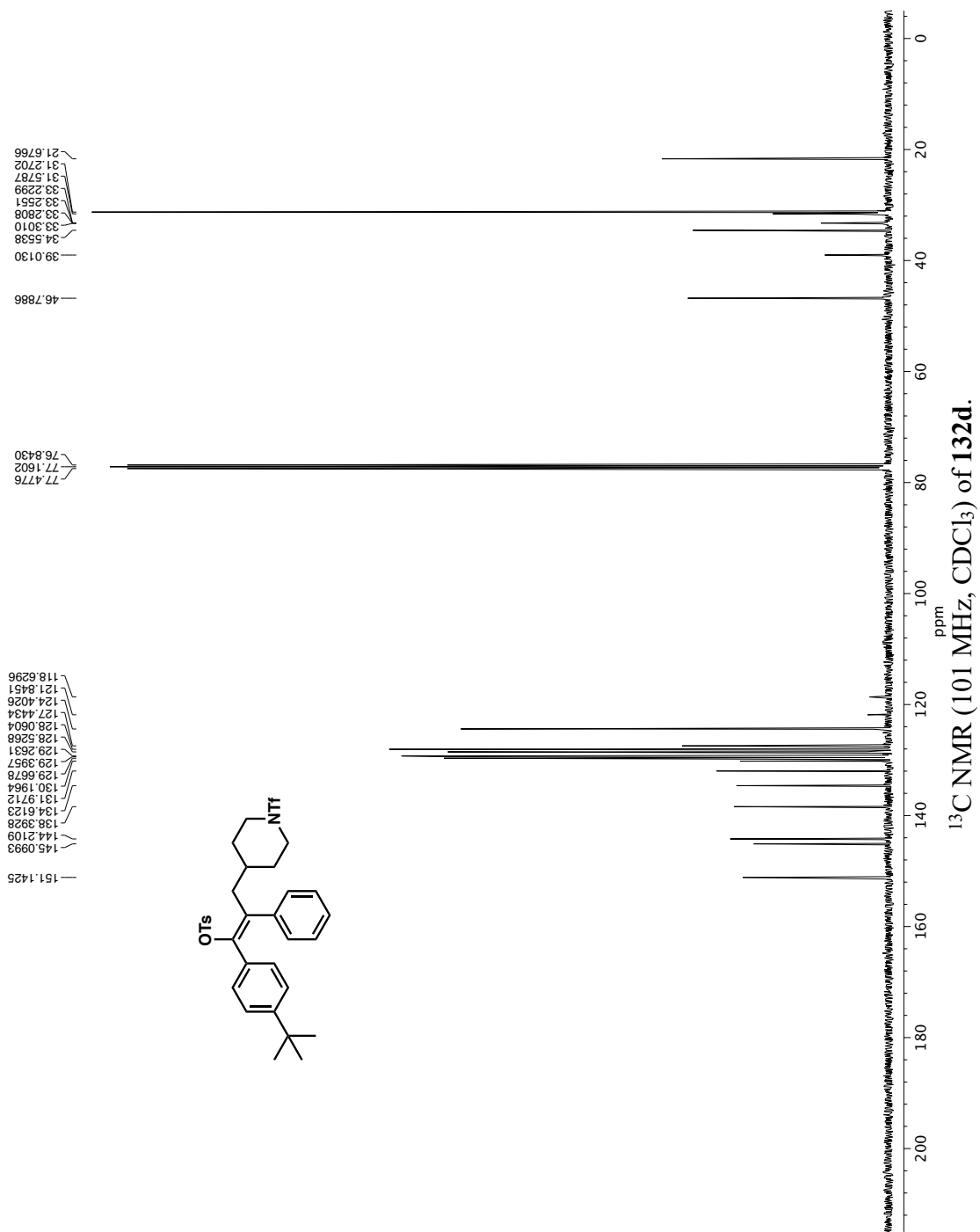




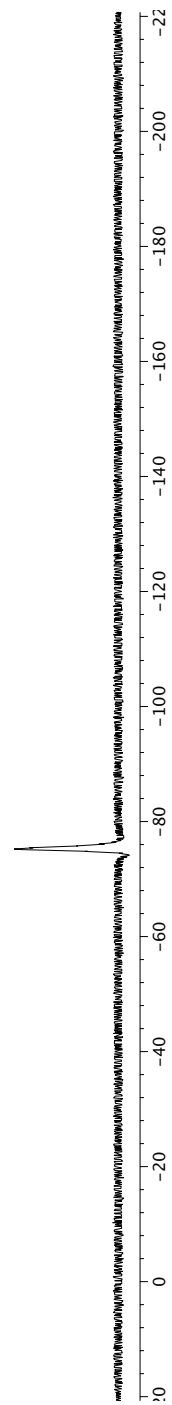
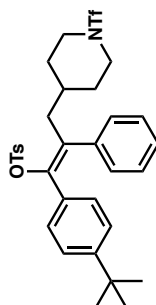
—75.7806

 ^{19}F NMR (376 MHz, CDCl_3) of **250**.

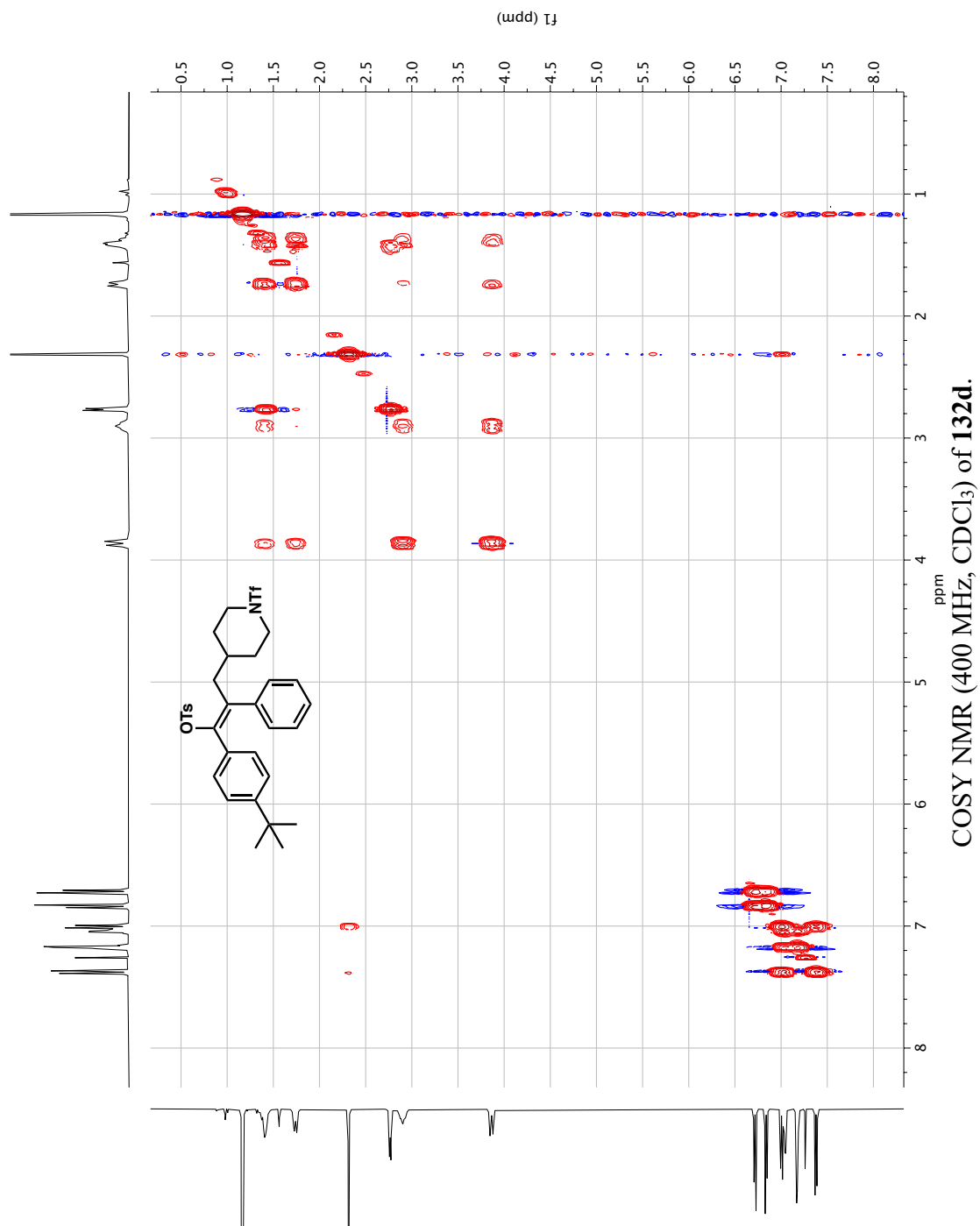


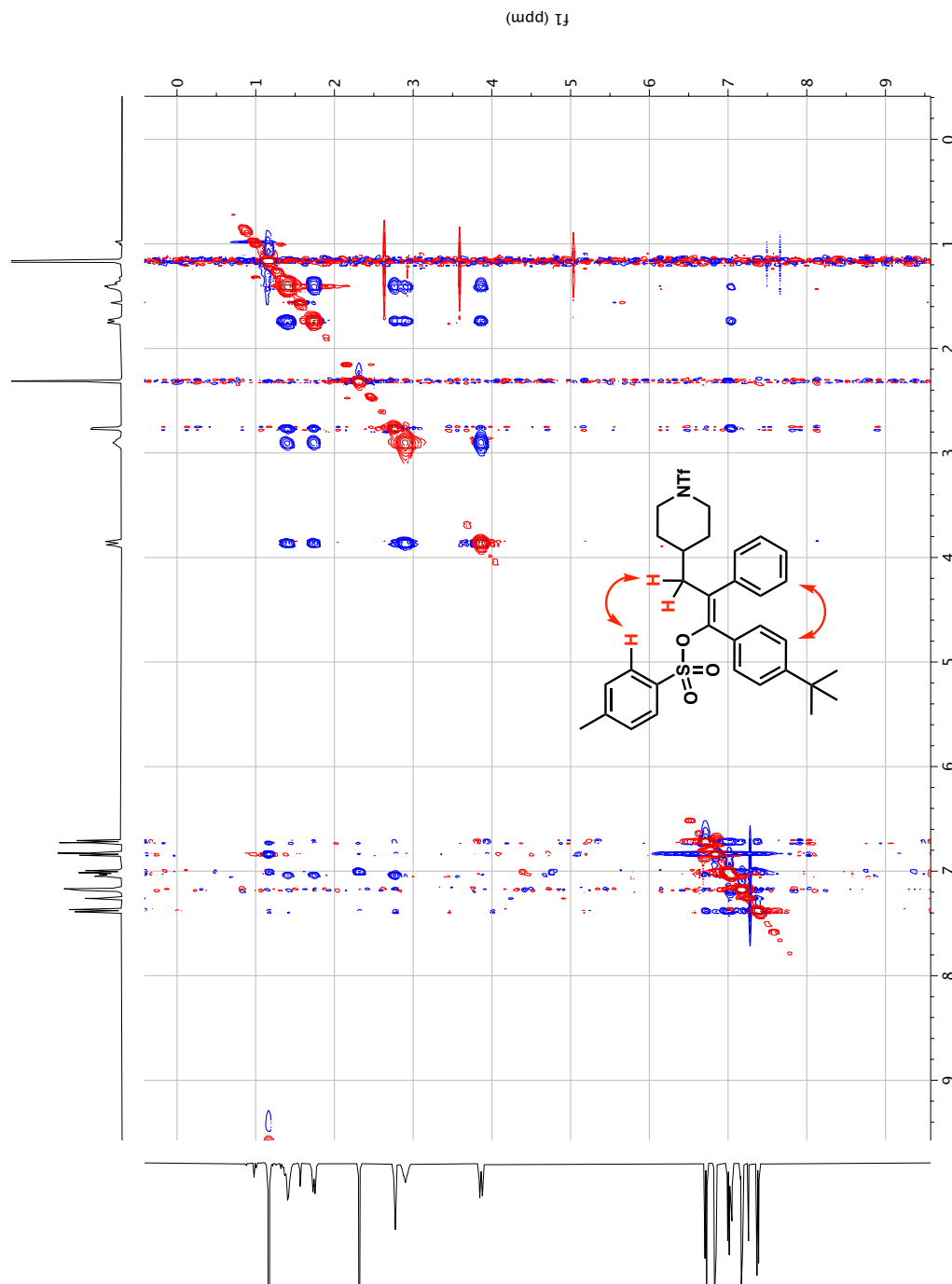


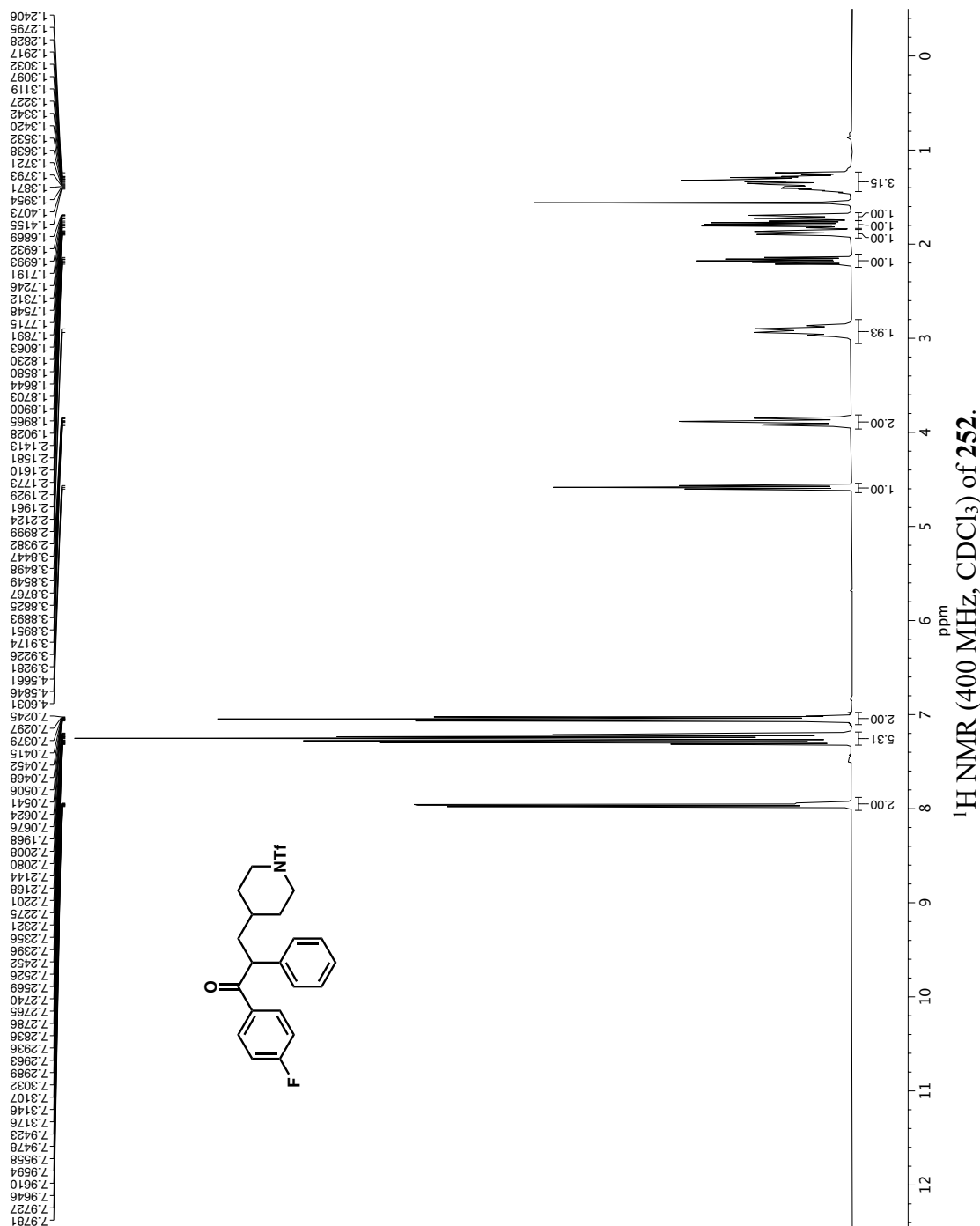
— -75.2664

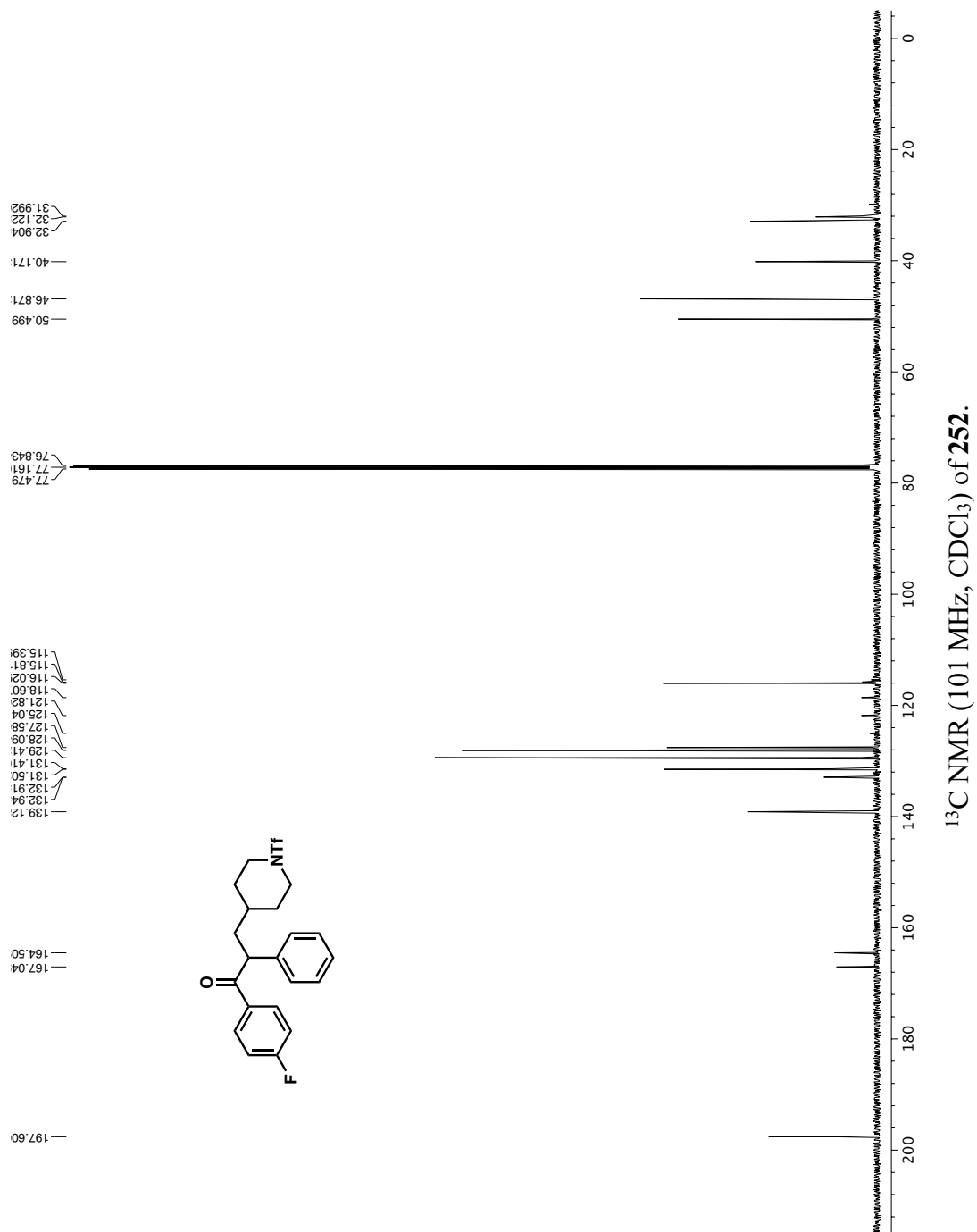


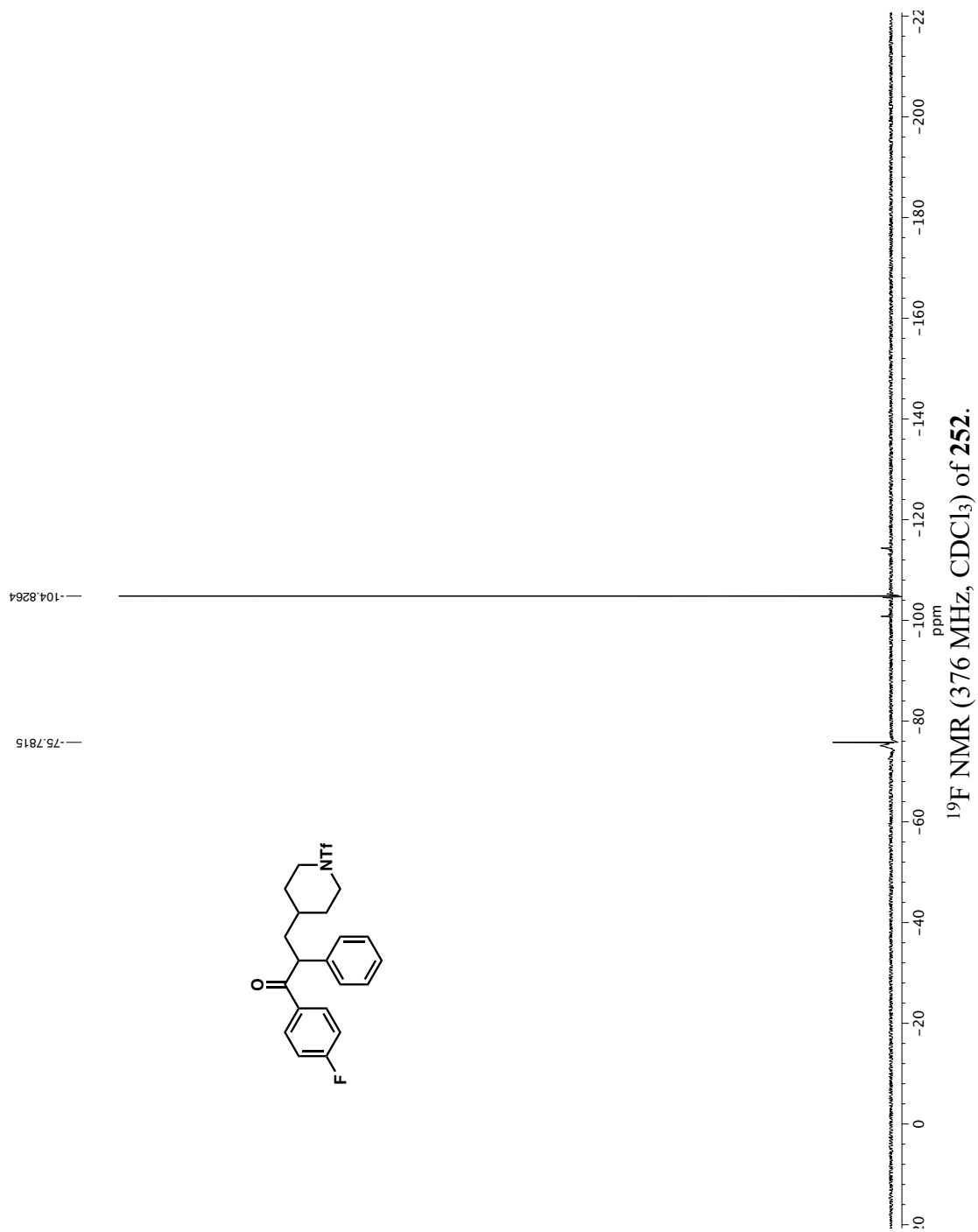
¹⁹F NMR (376 MHz, CDCl₃) of **132d**.

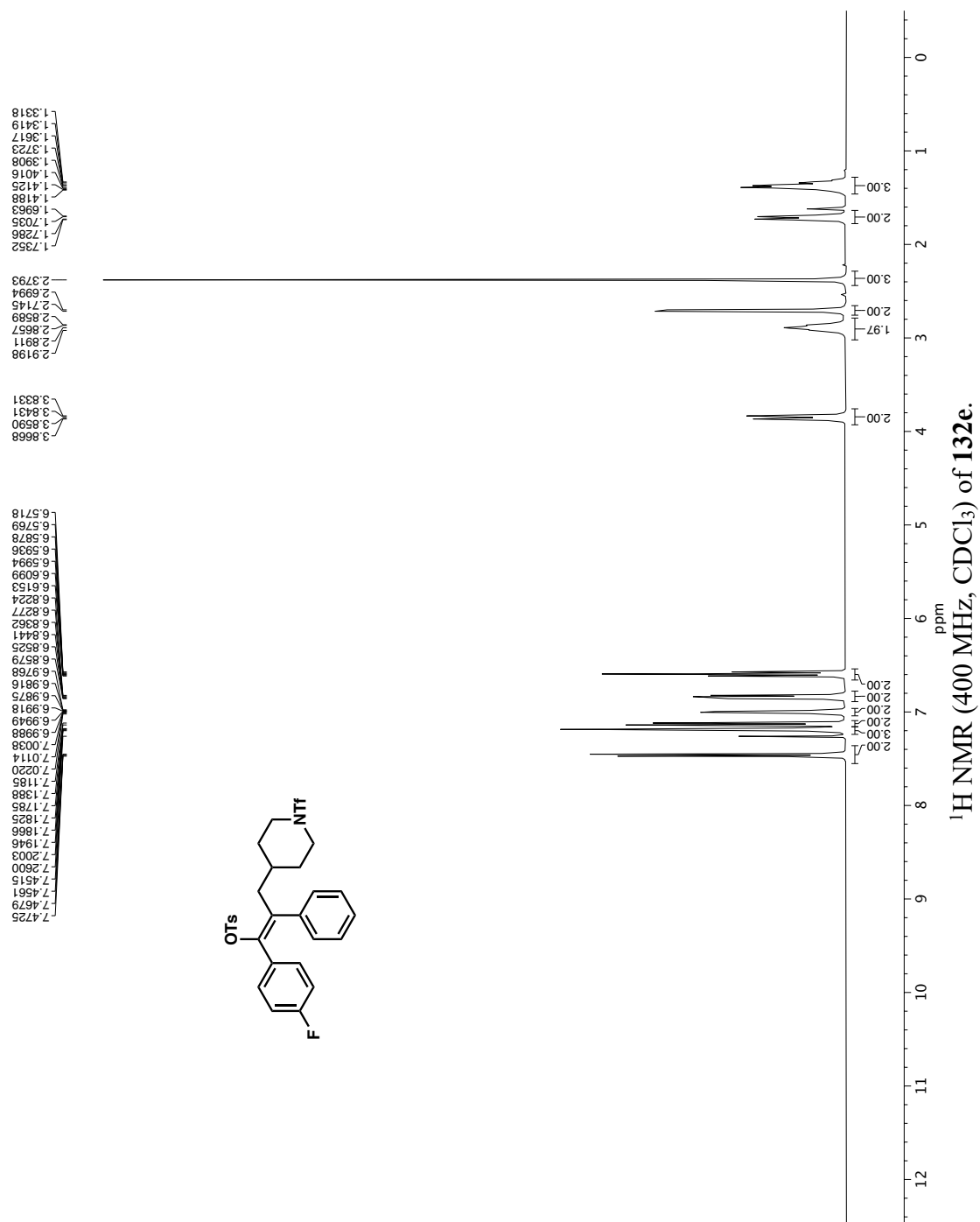


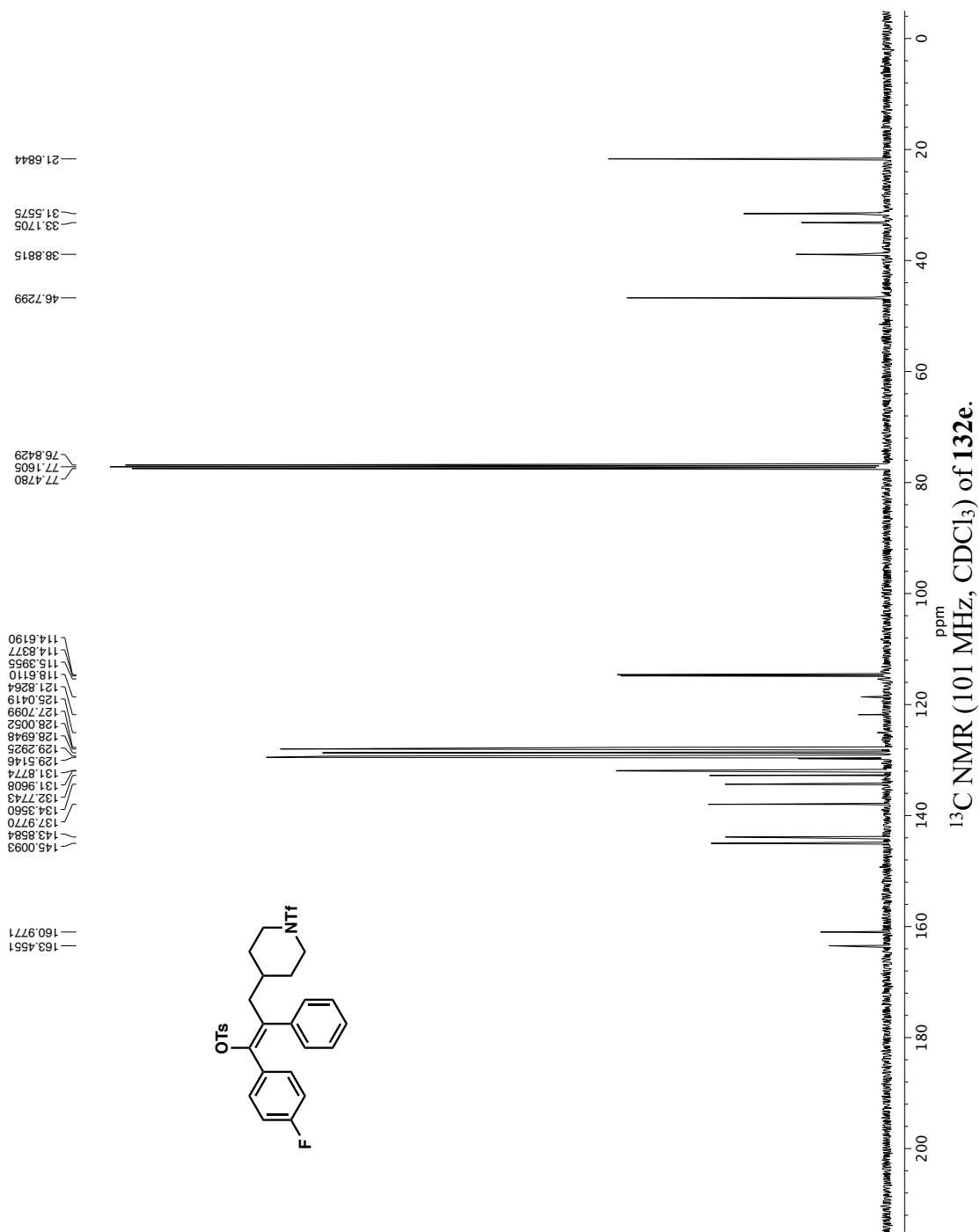


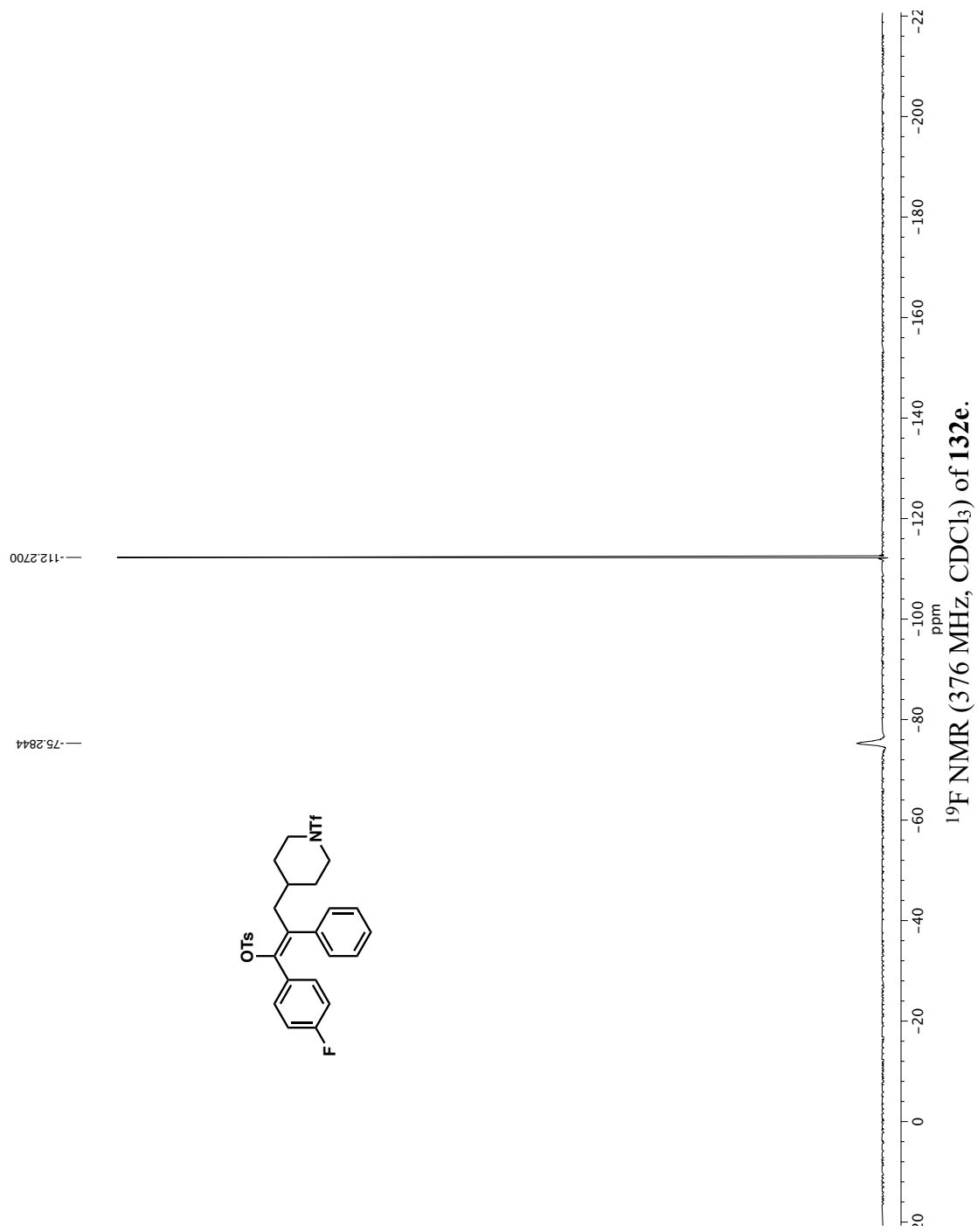


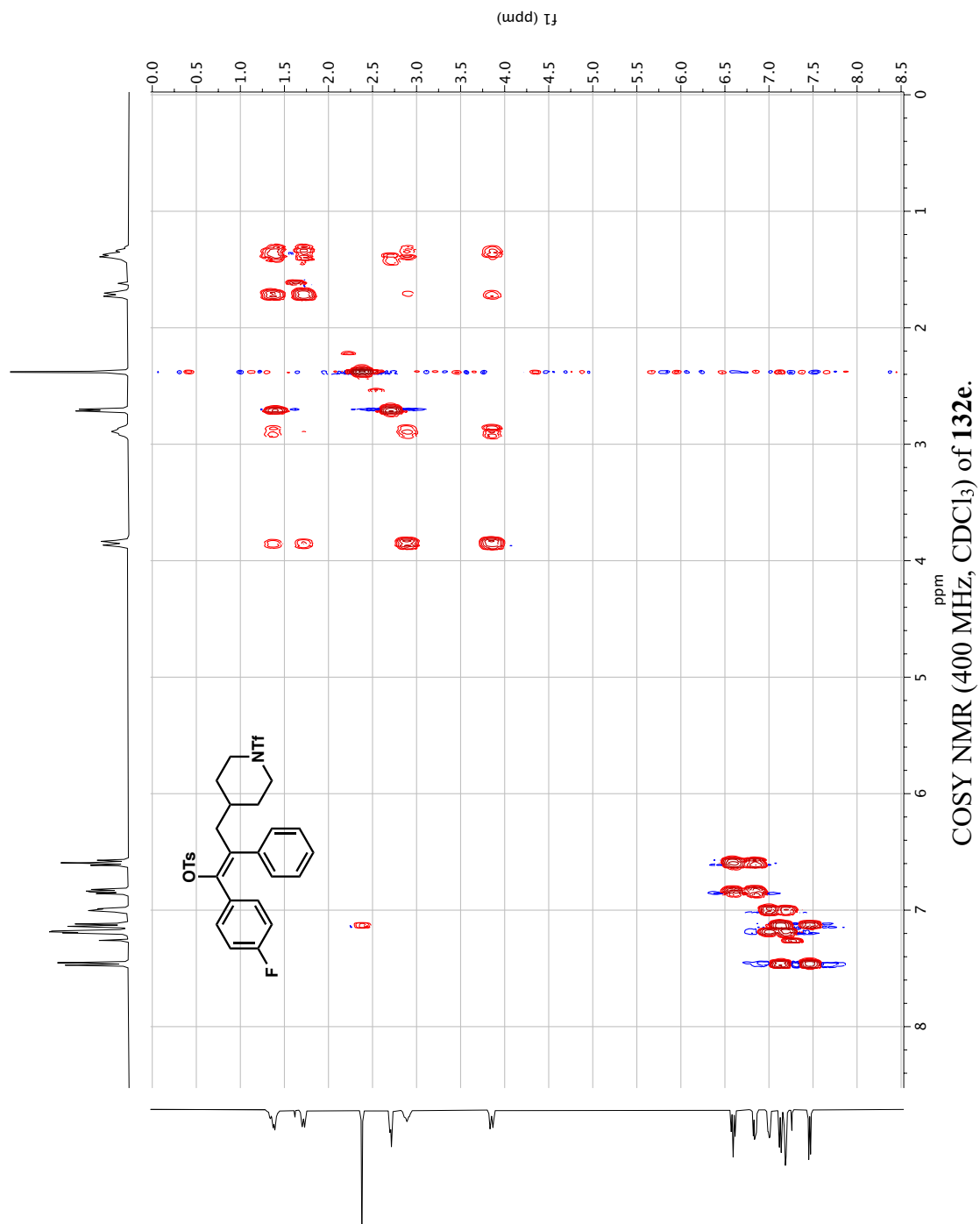


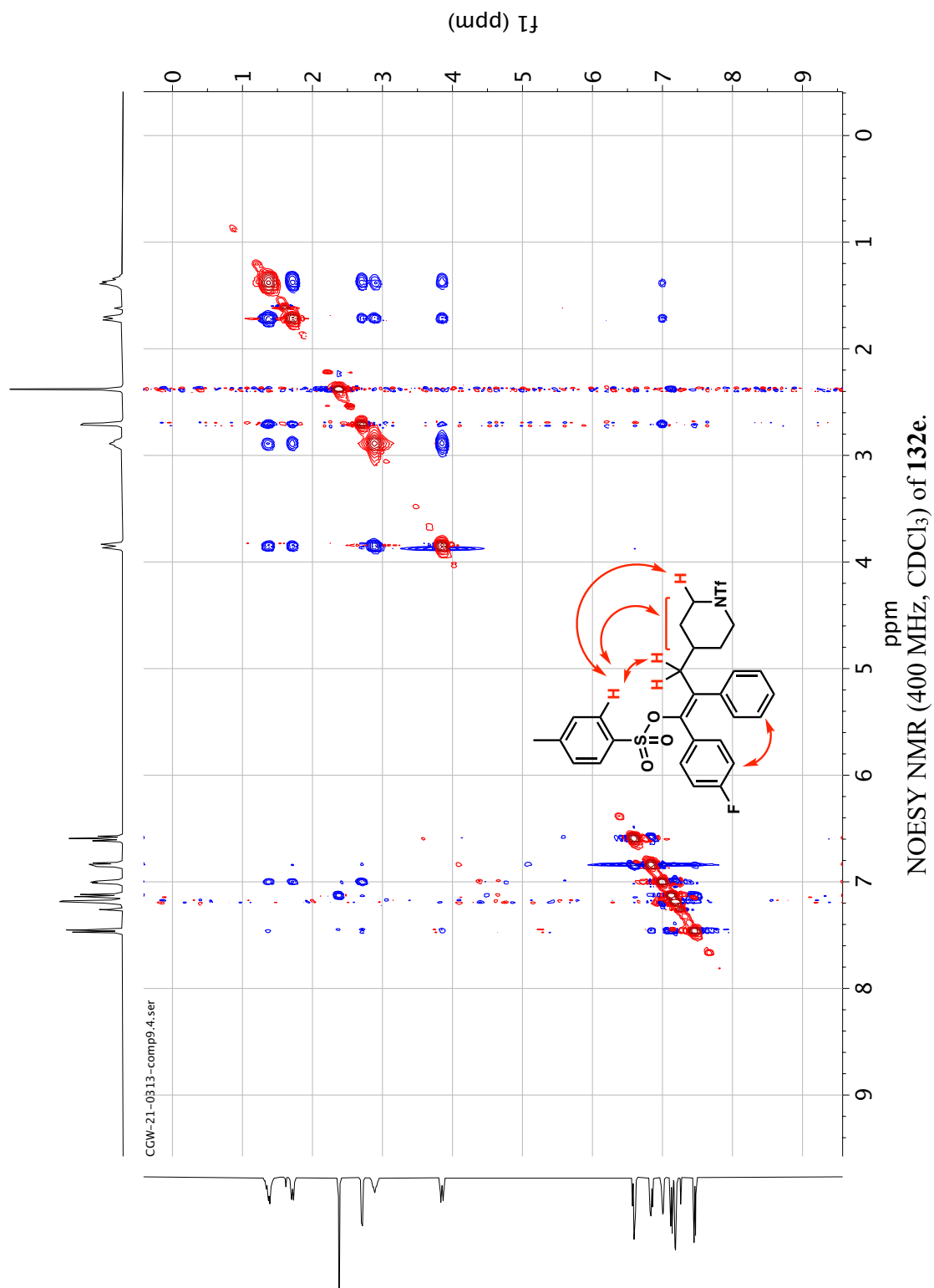


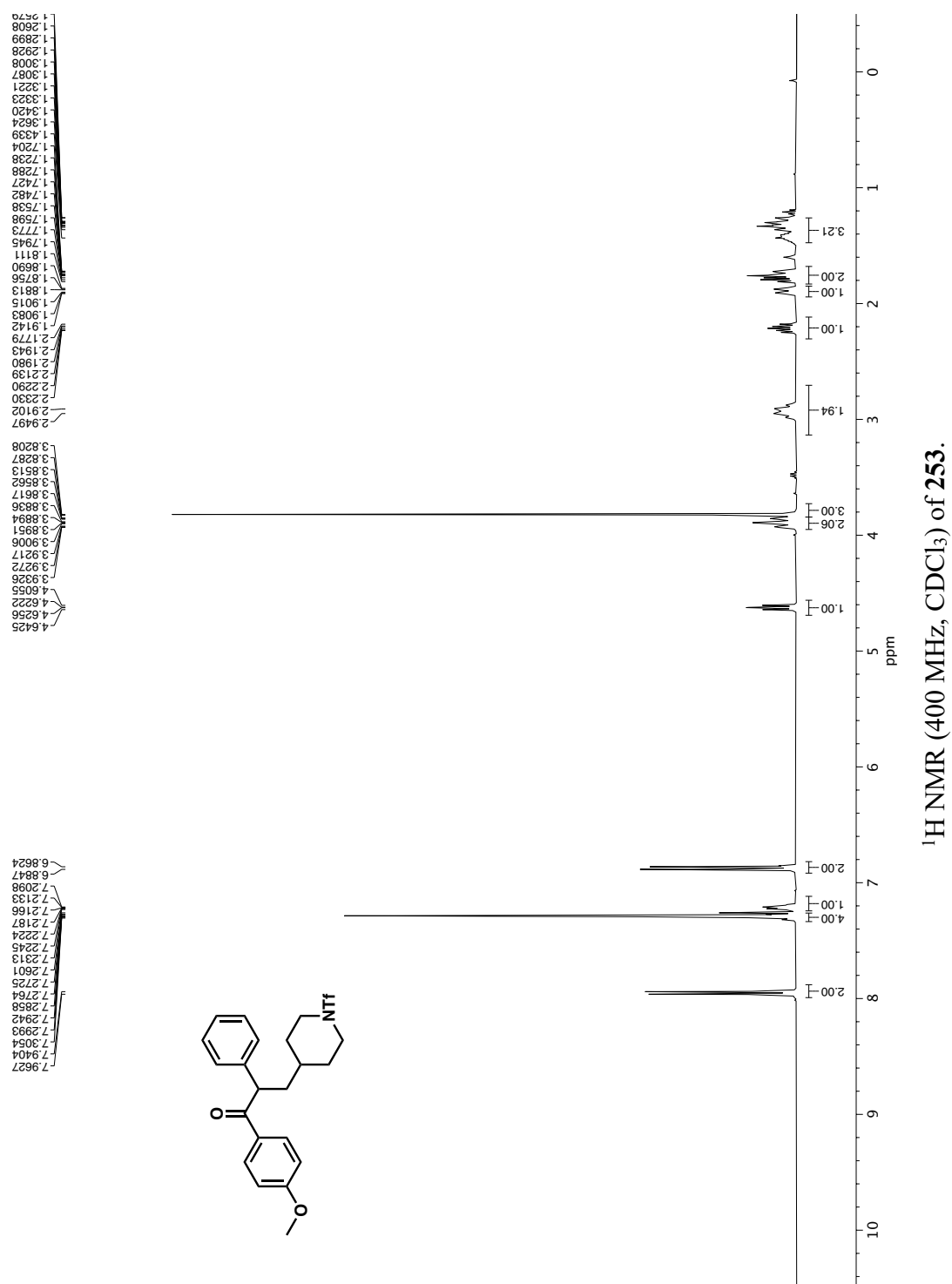


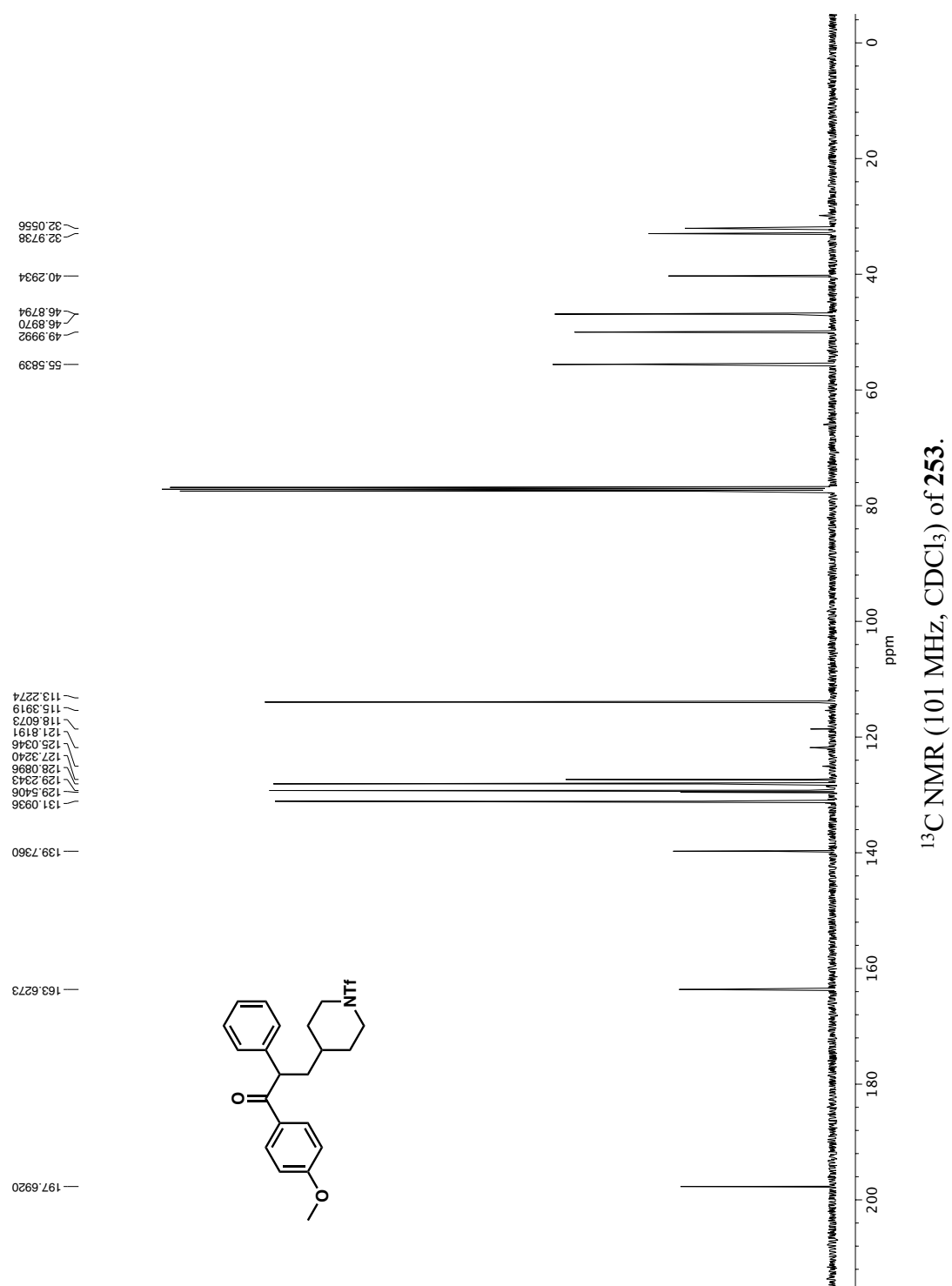




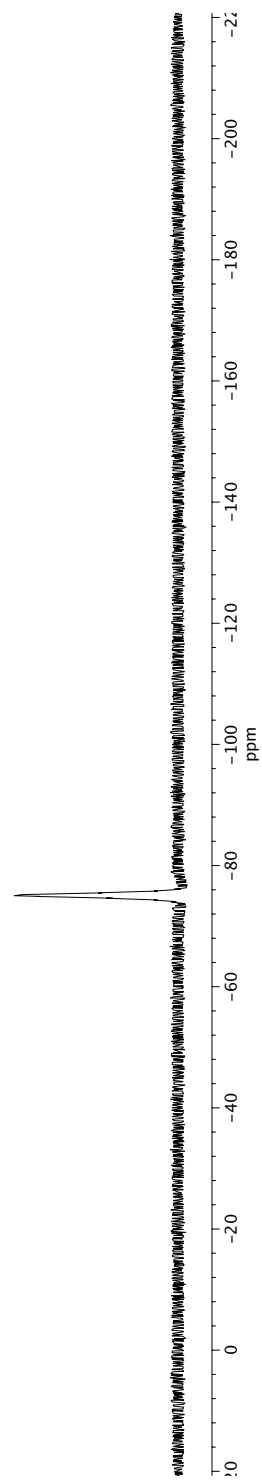
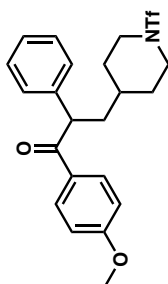


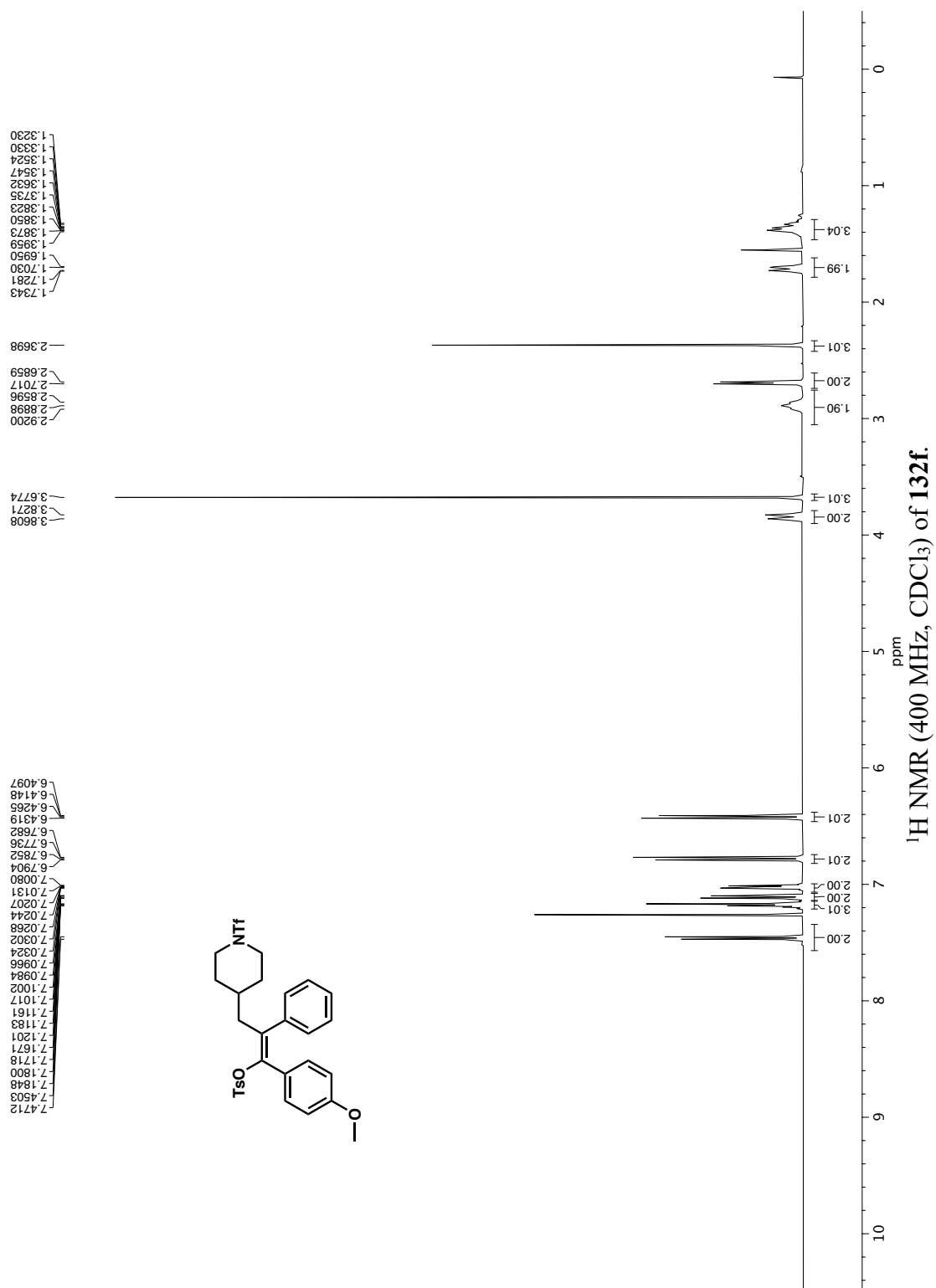


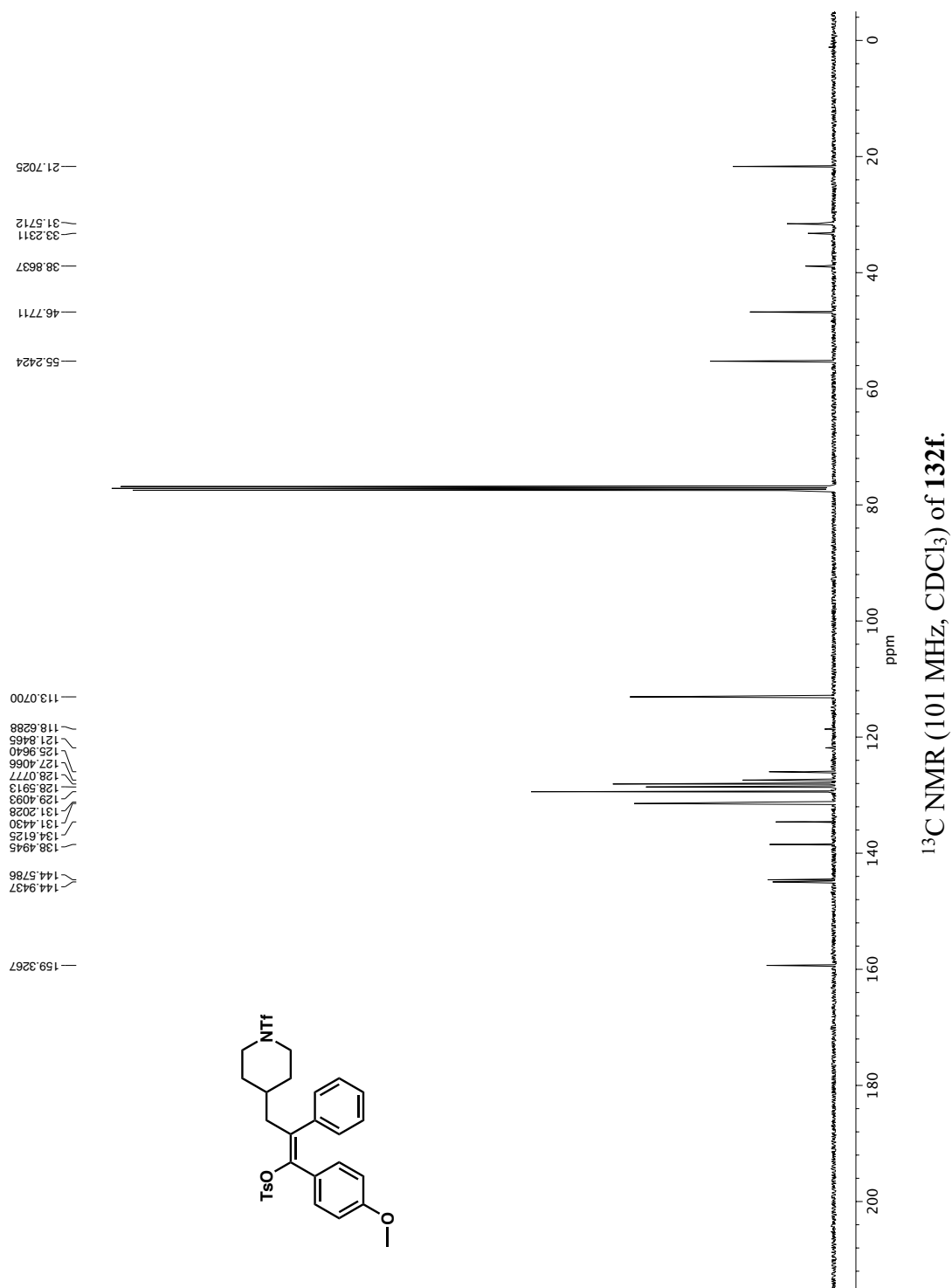




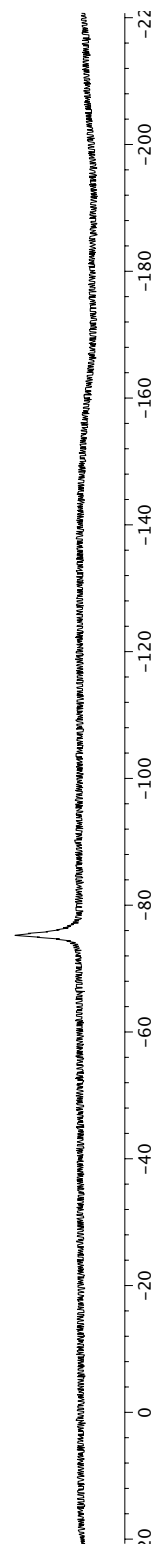
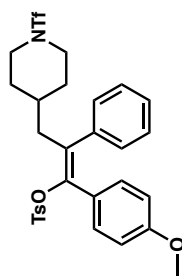
—75.0772

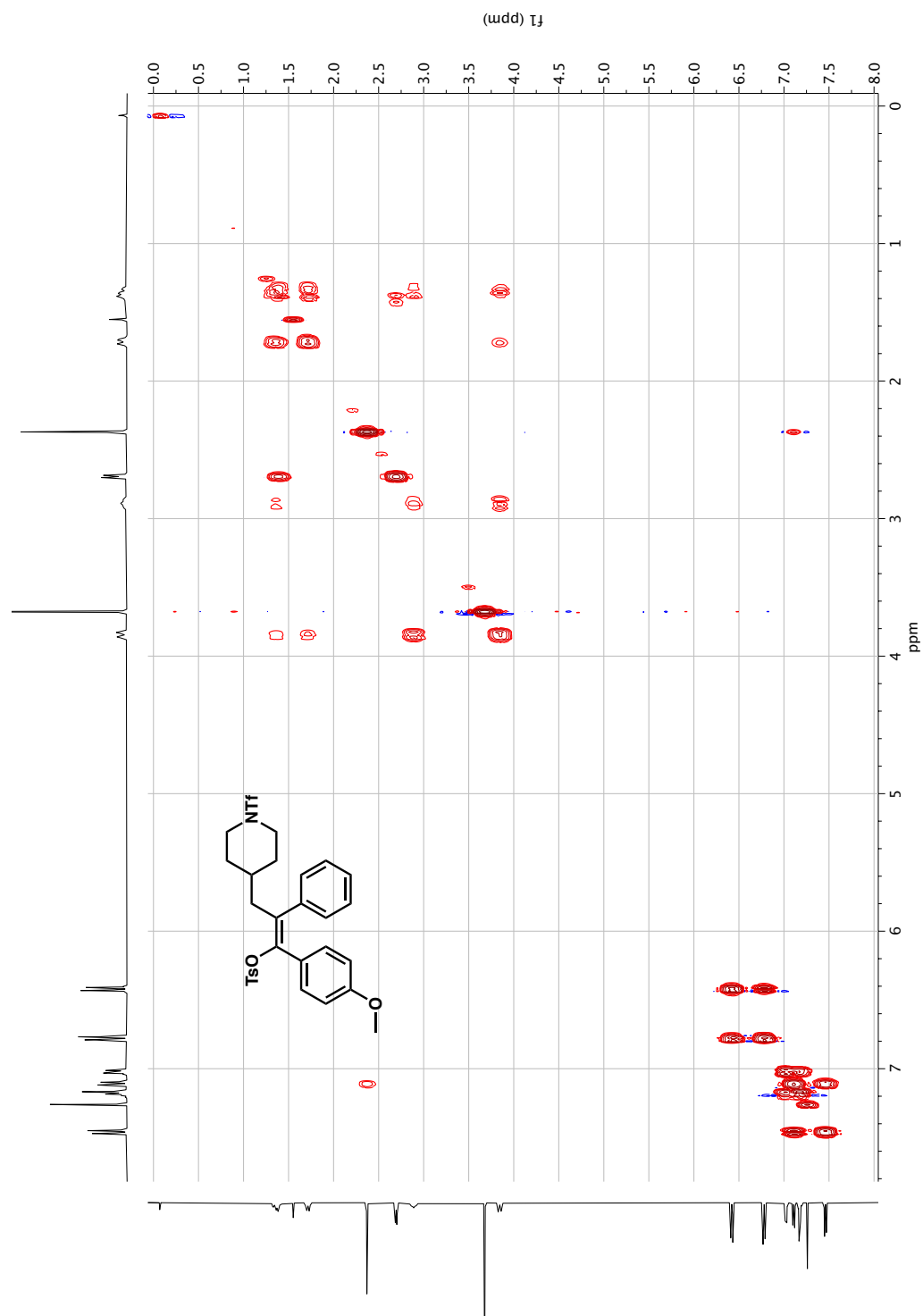
 ^{19}F NMR (376 MHz, CDCl_3) of **253**.

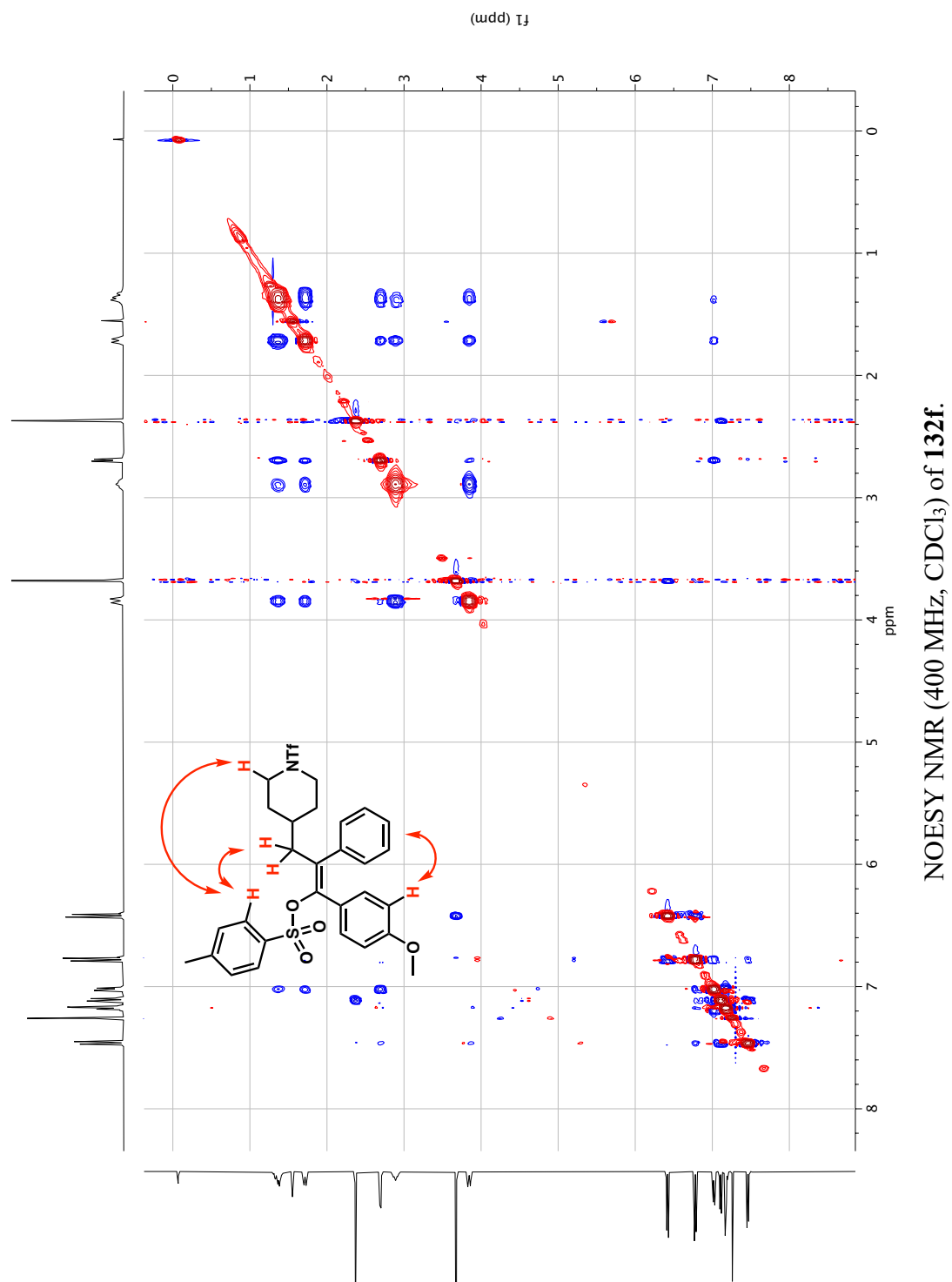


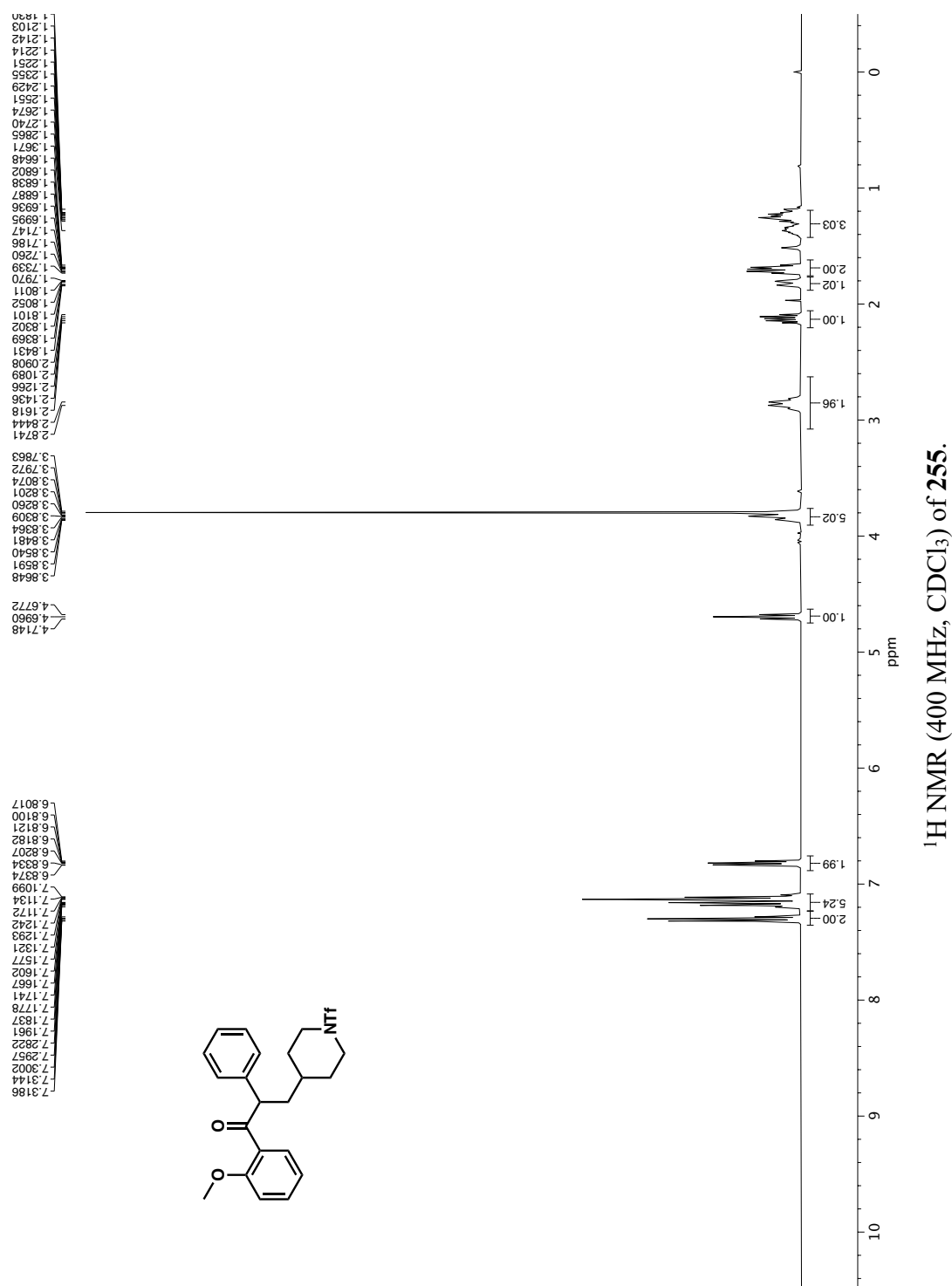


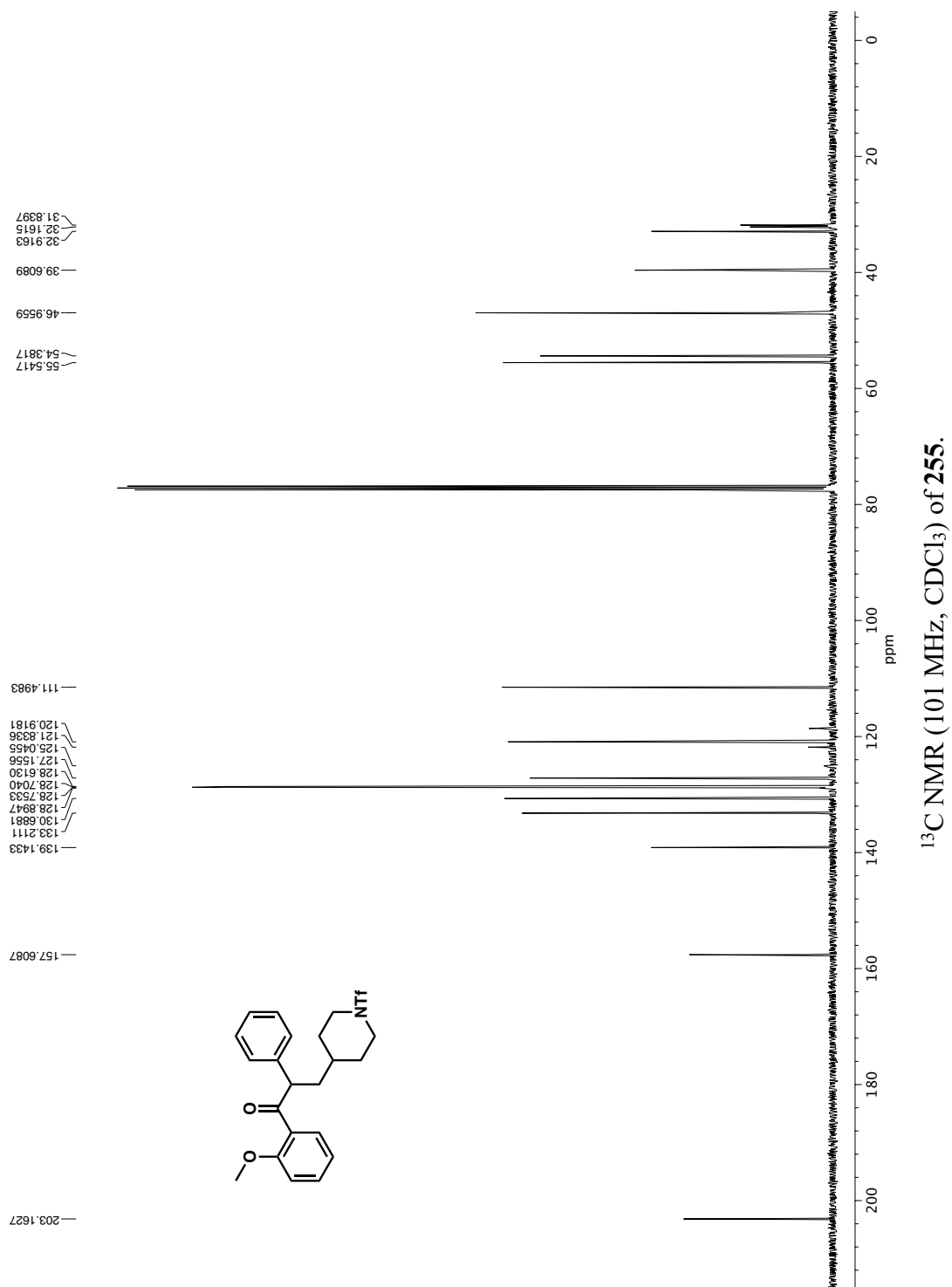
—75.2514

 ^{19}F NMR (376 MHz, CDCl_3) of **132f**.

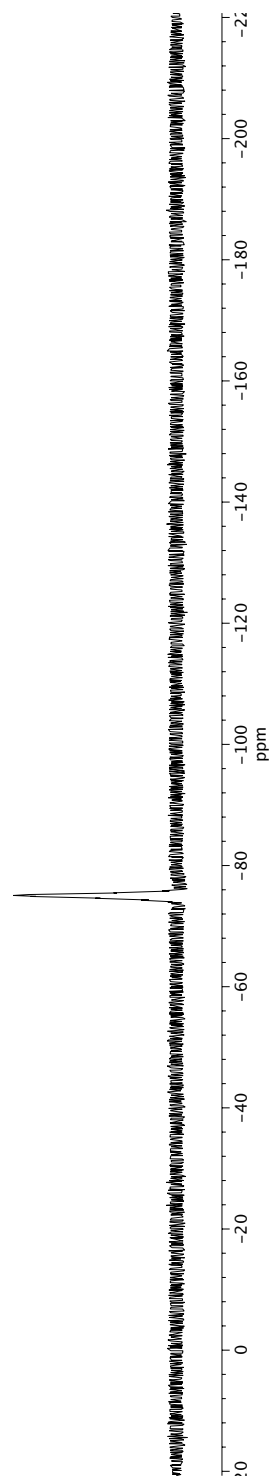
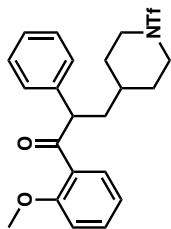


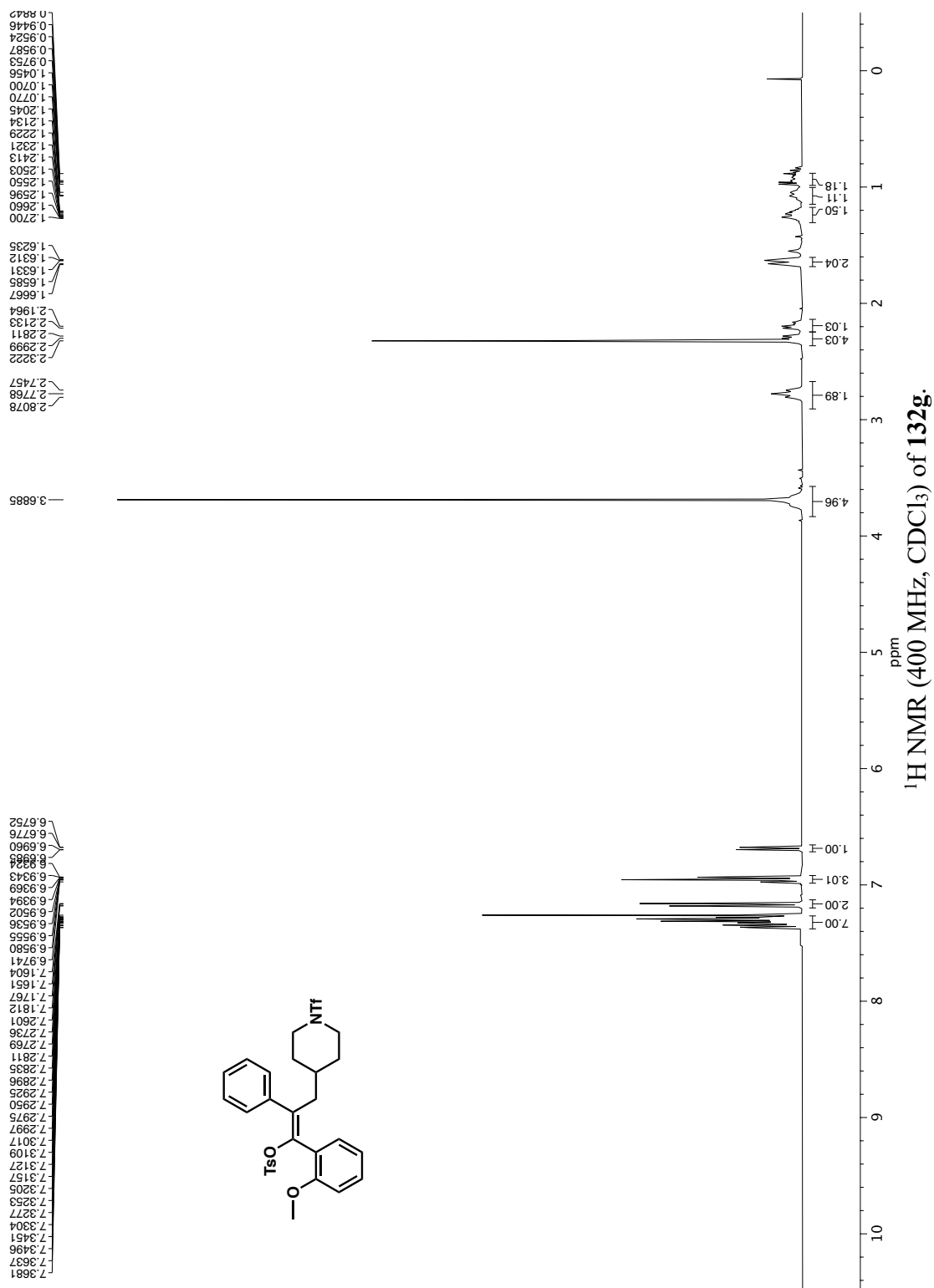


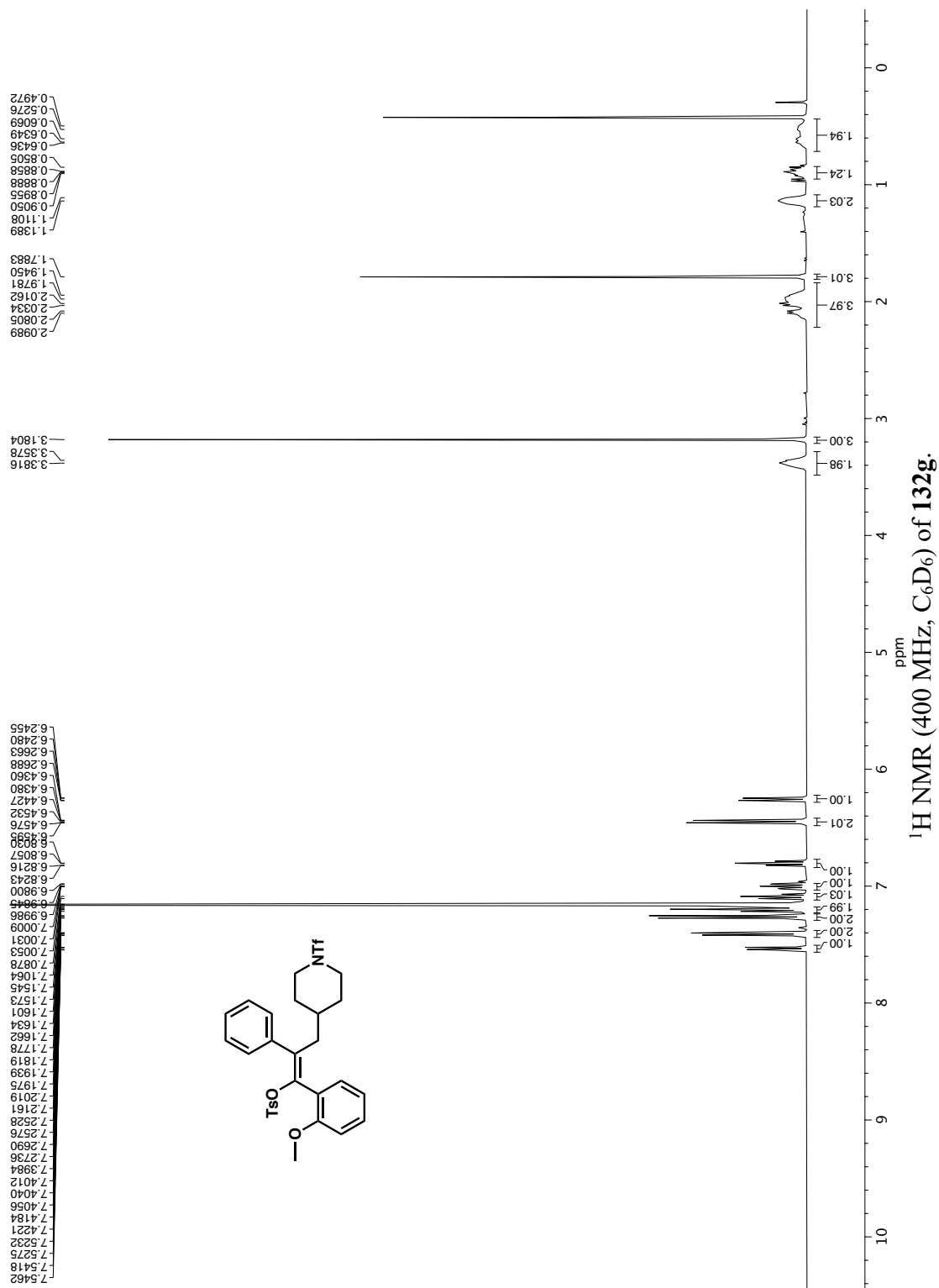


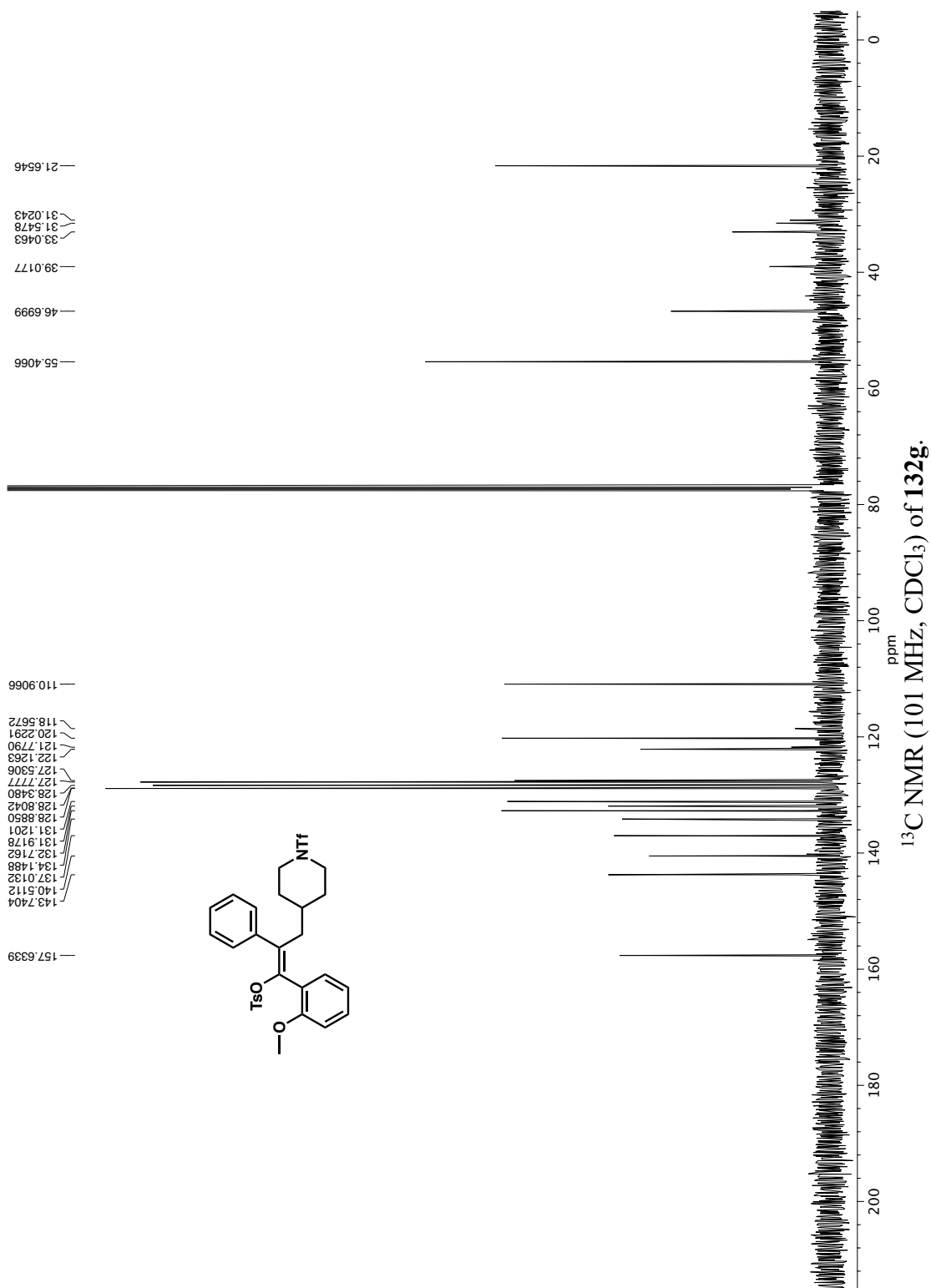


— 75.2269

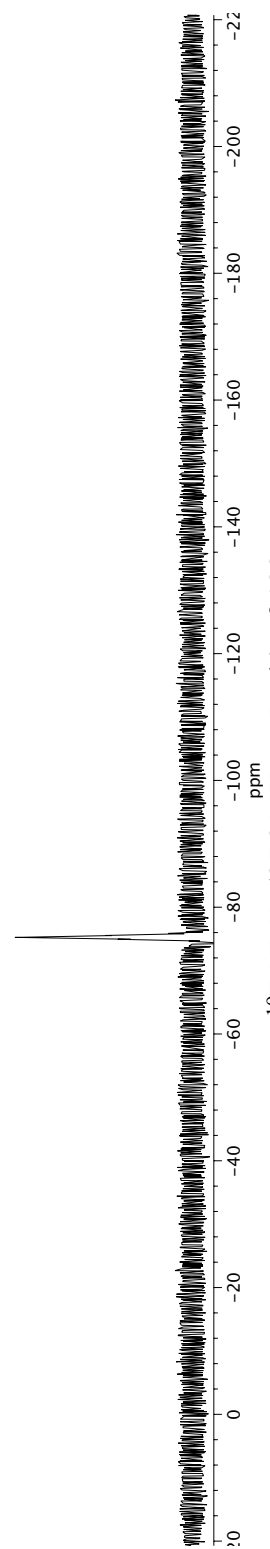
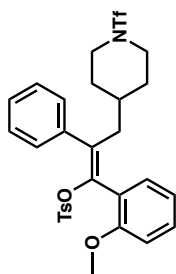
 ^{19}F NMR (376 MHz, CDCl_3) of **255**.

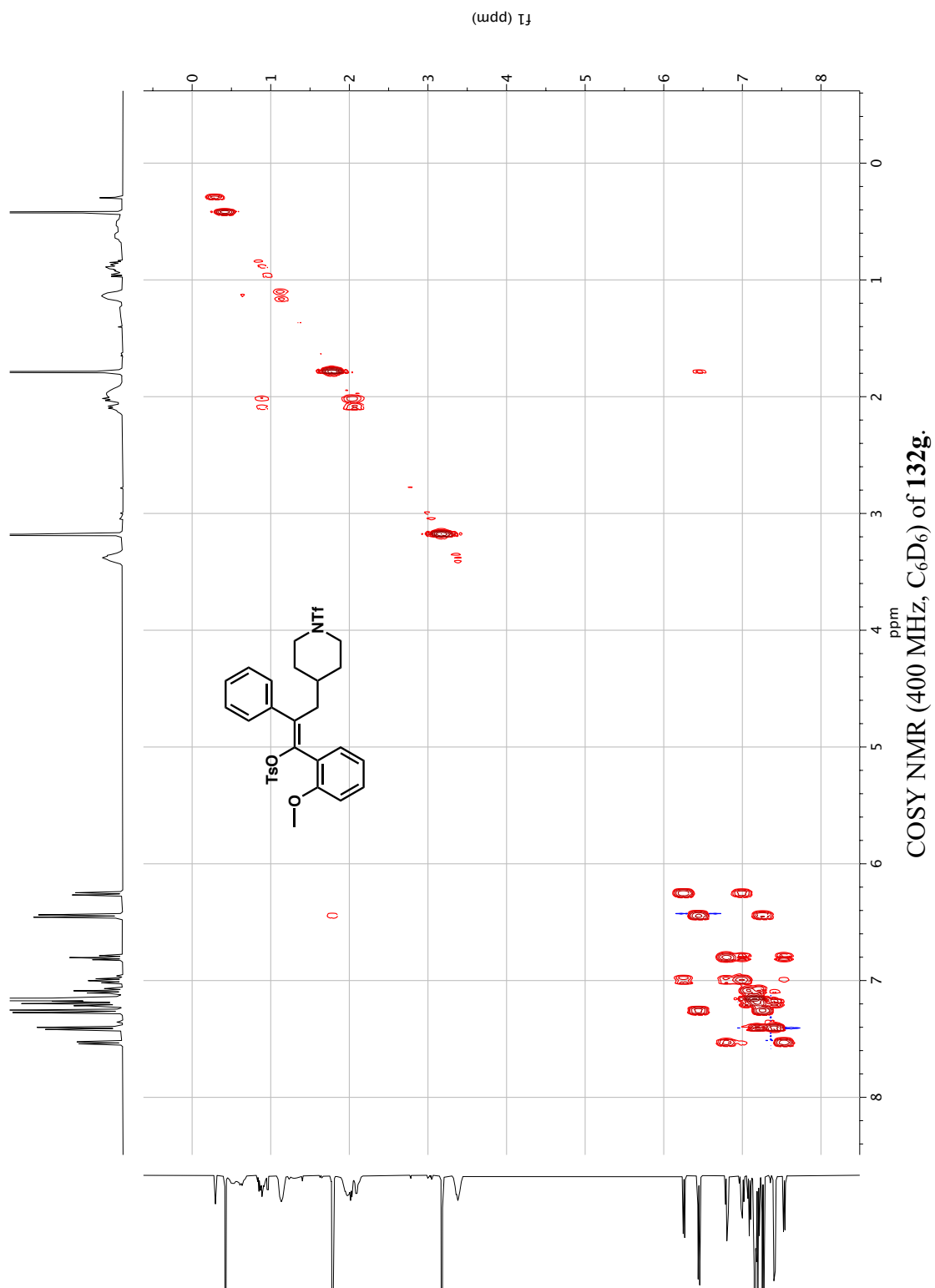


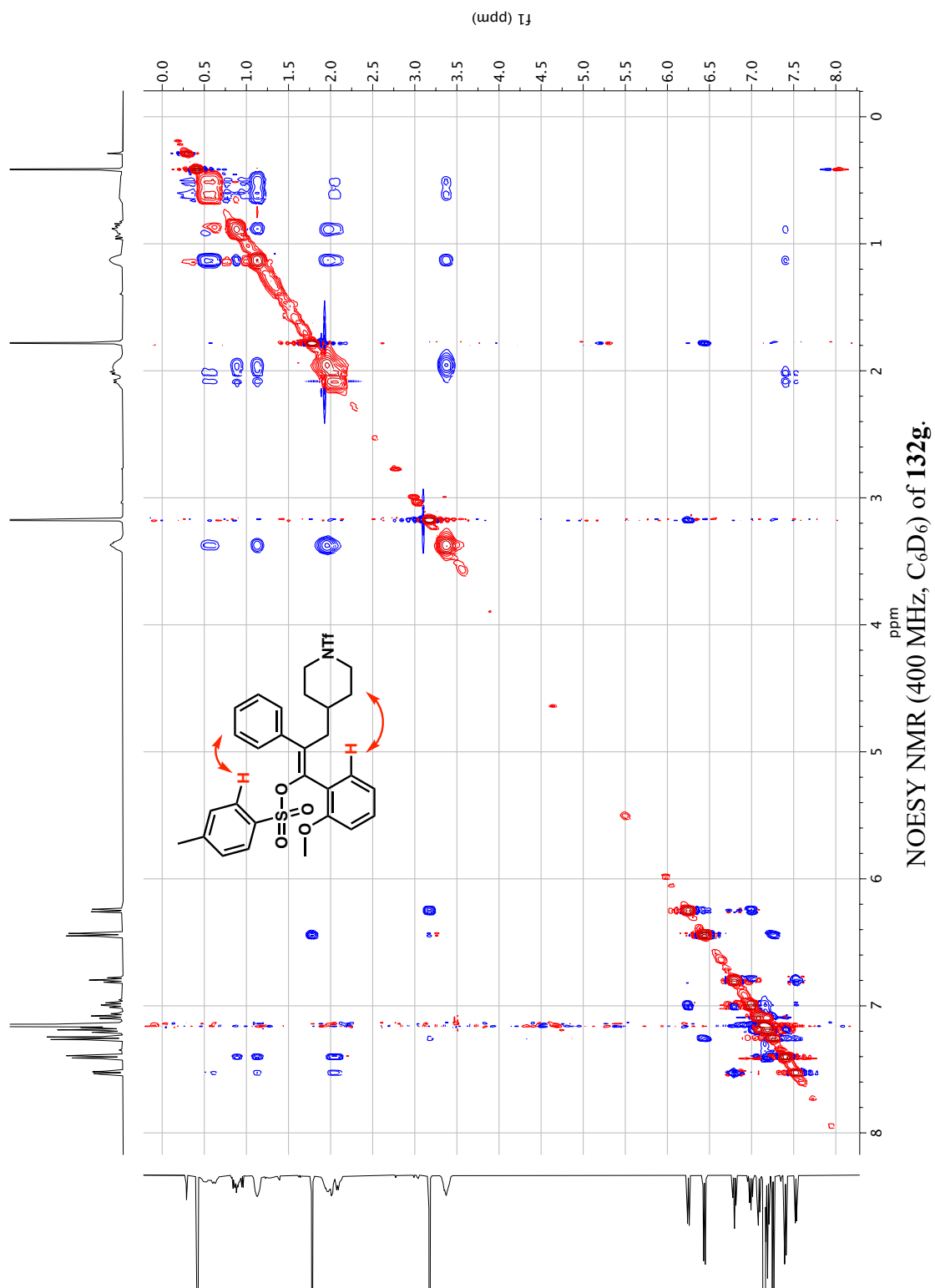


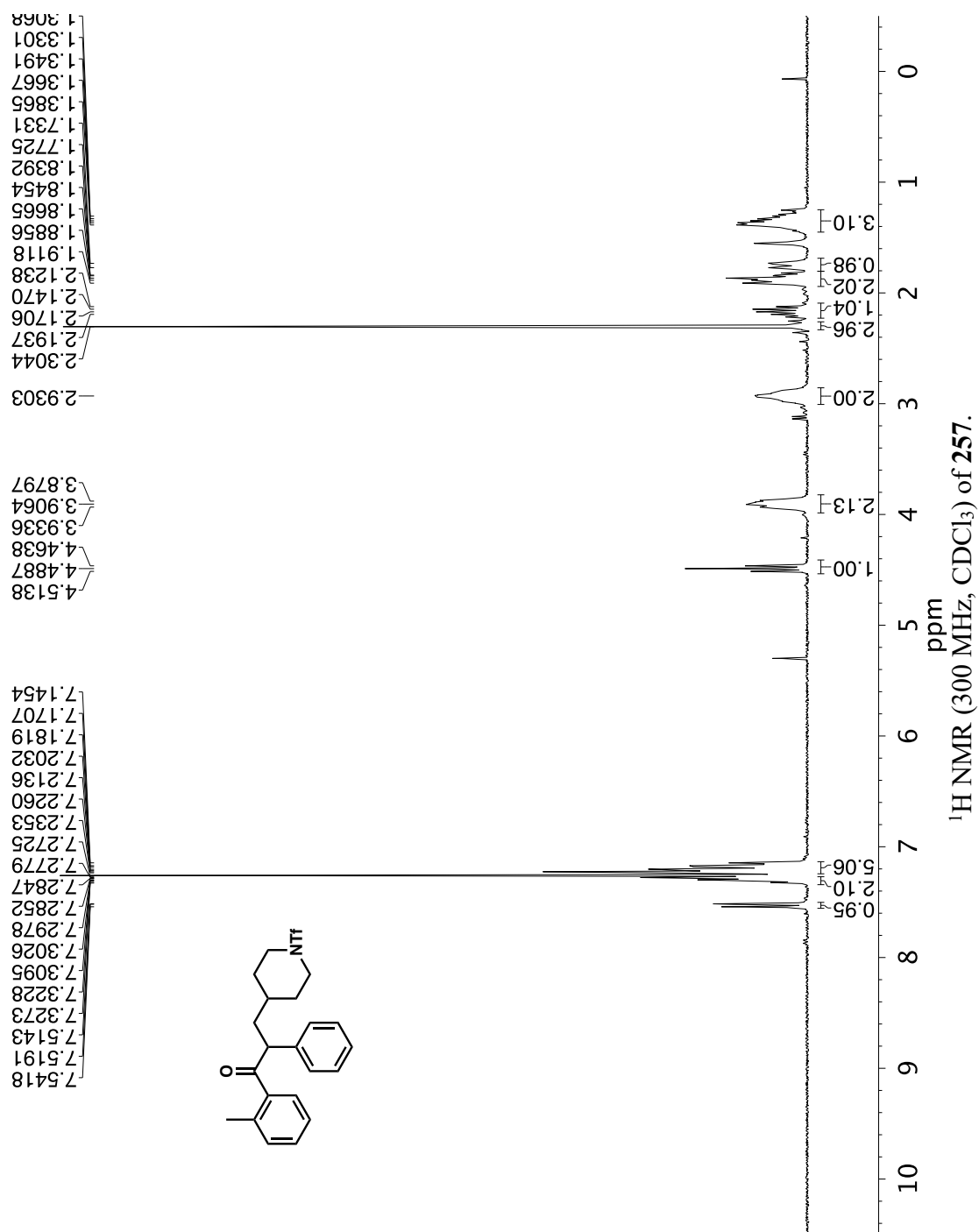


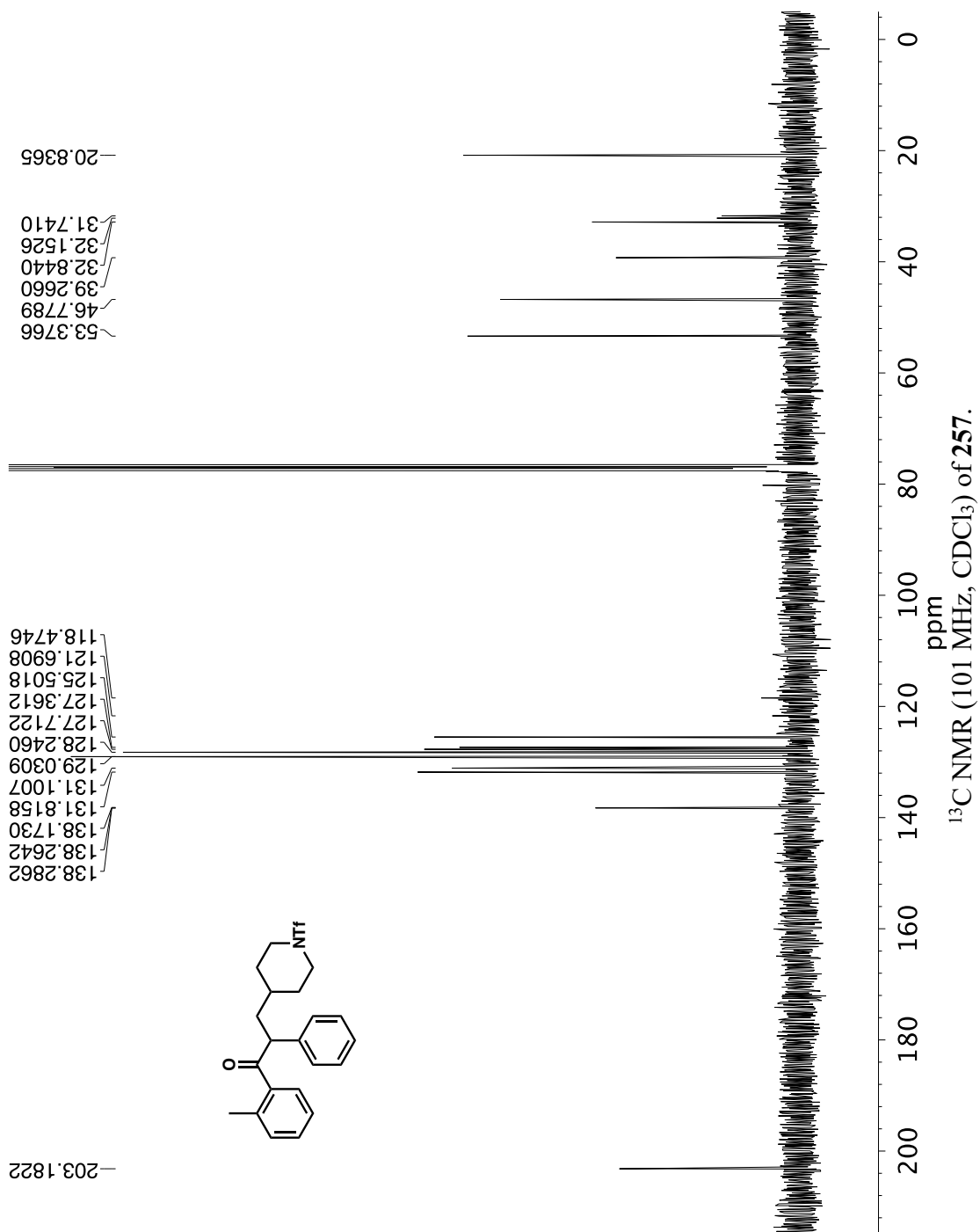
—75.2455

**¹⁹F NMR (376 MHz, CDCl₃) of 132g.**

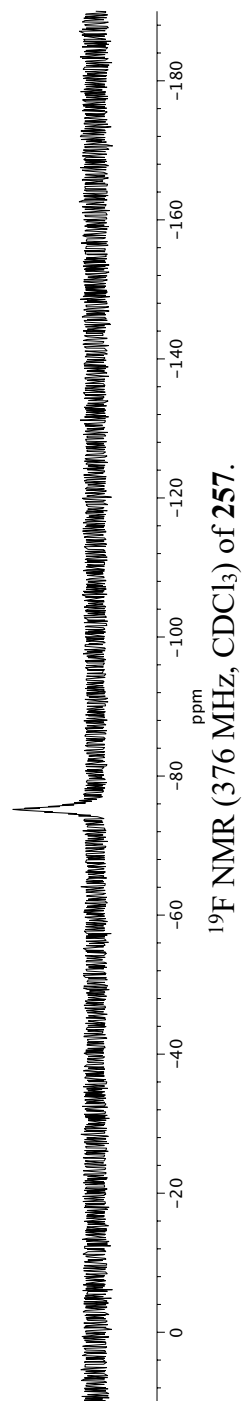
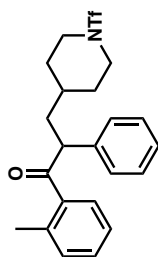


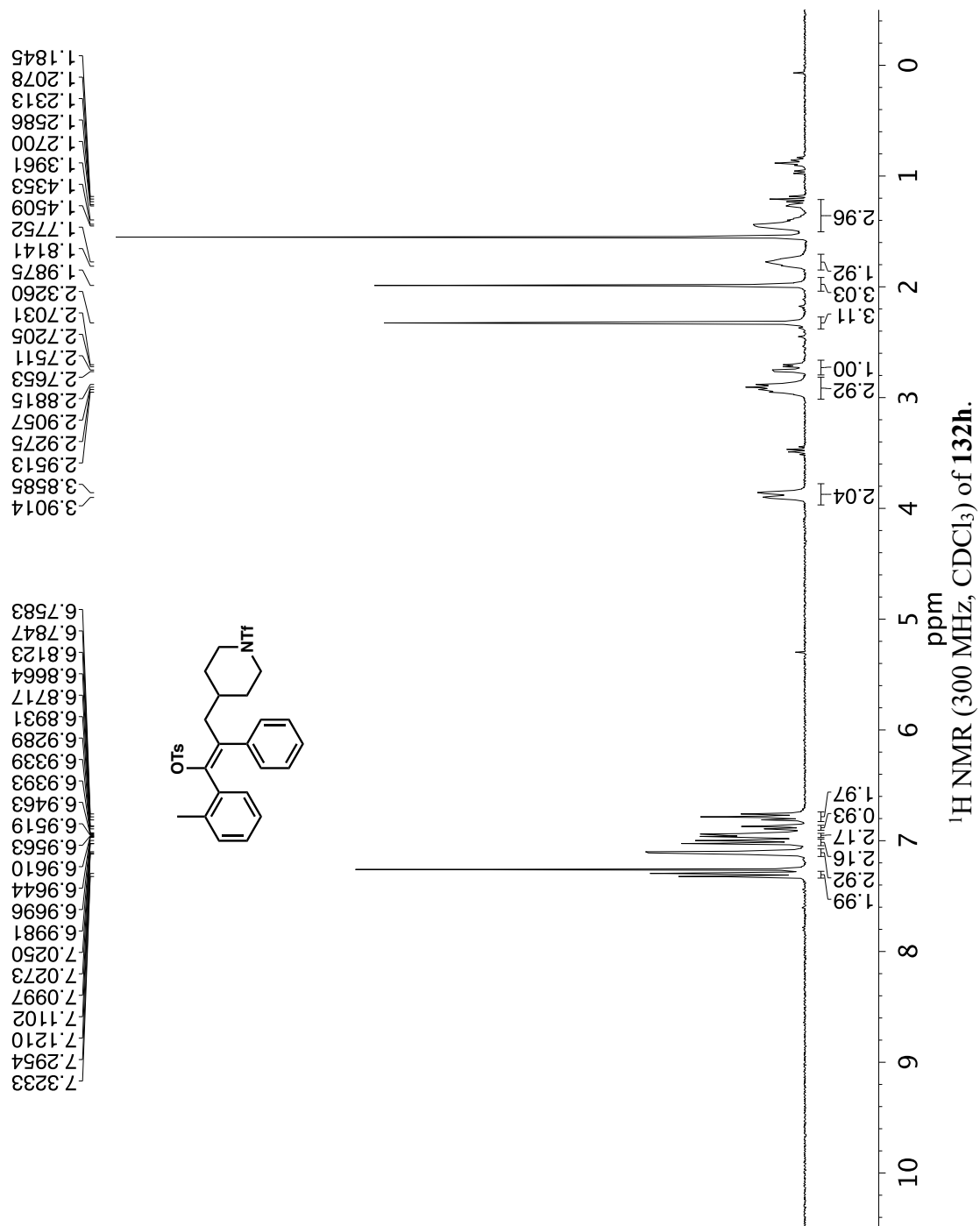


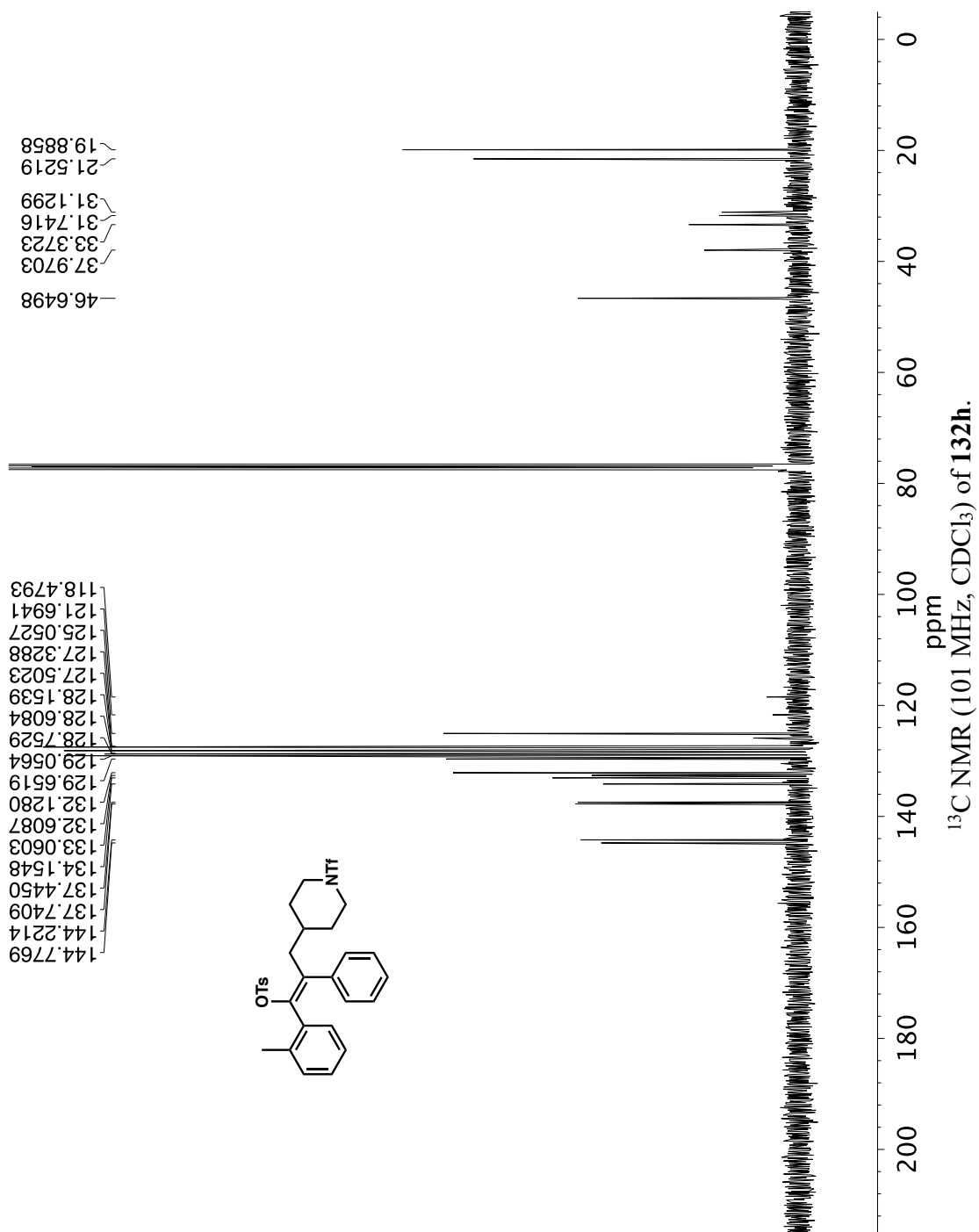


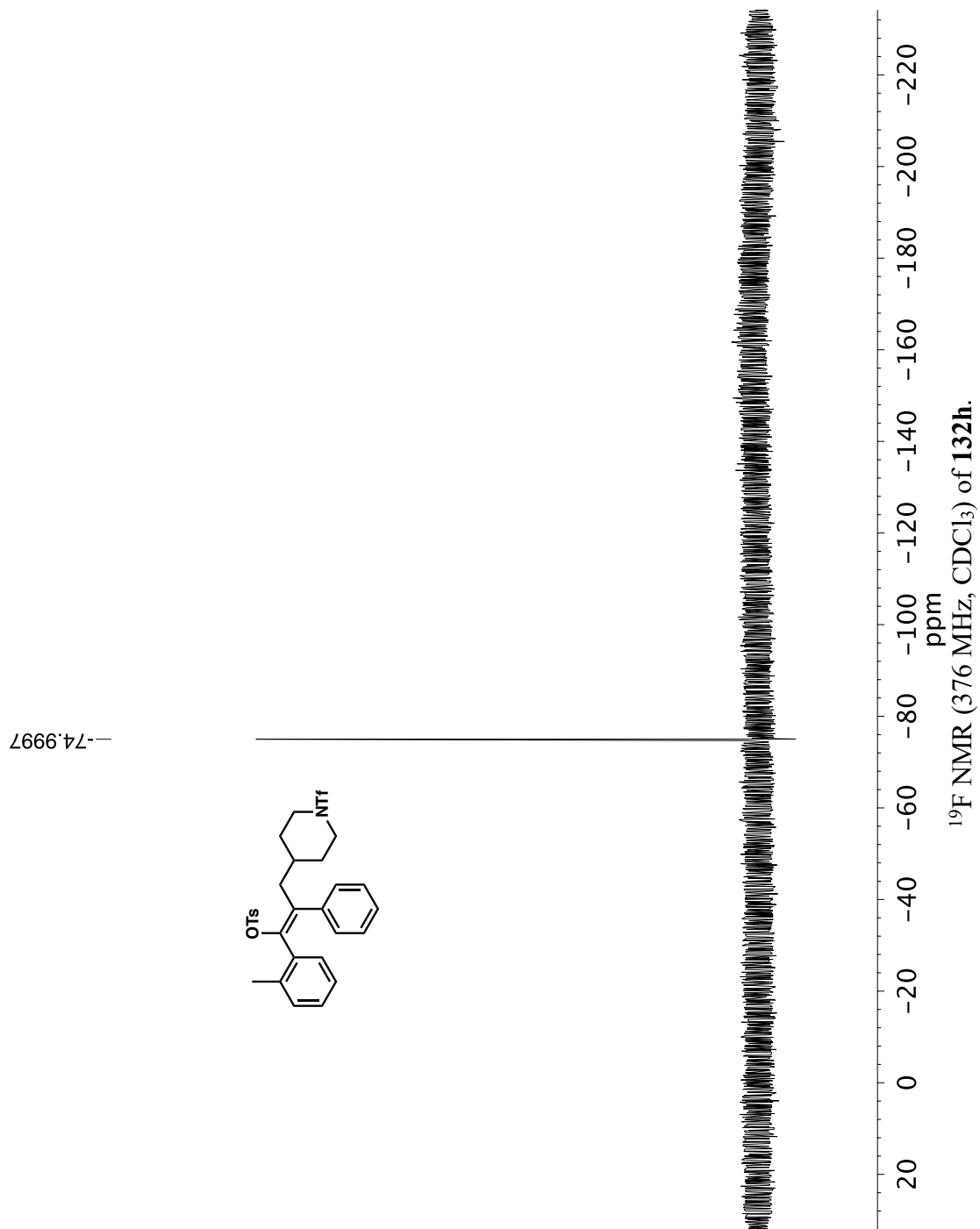


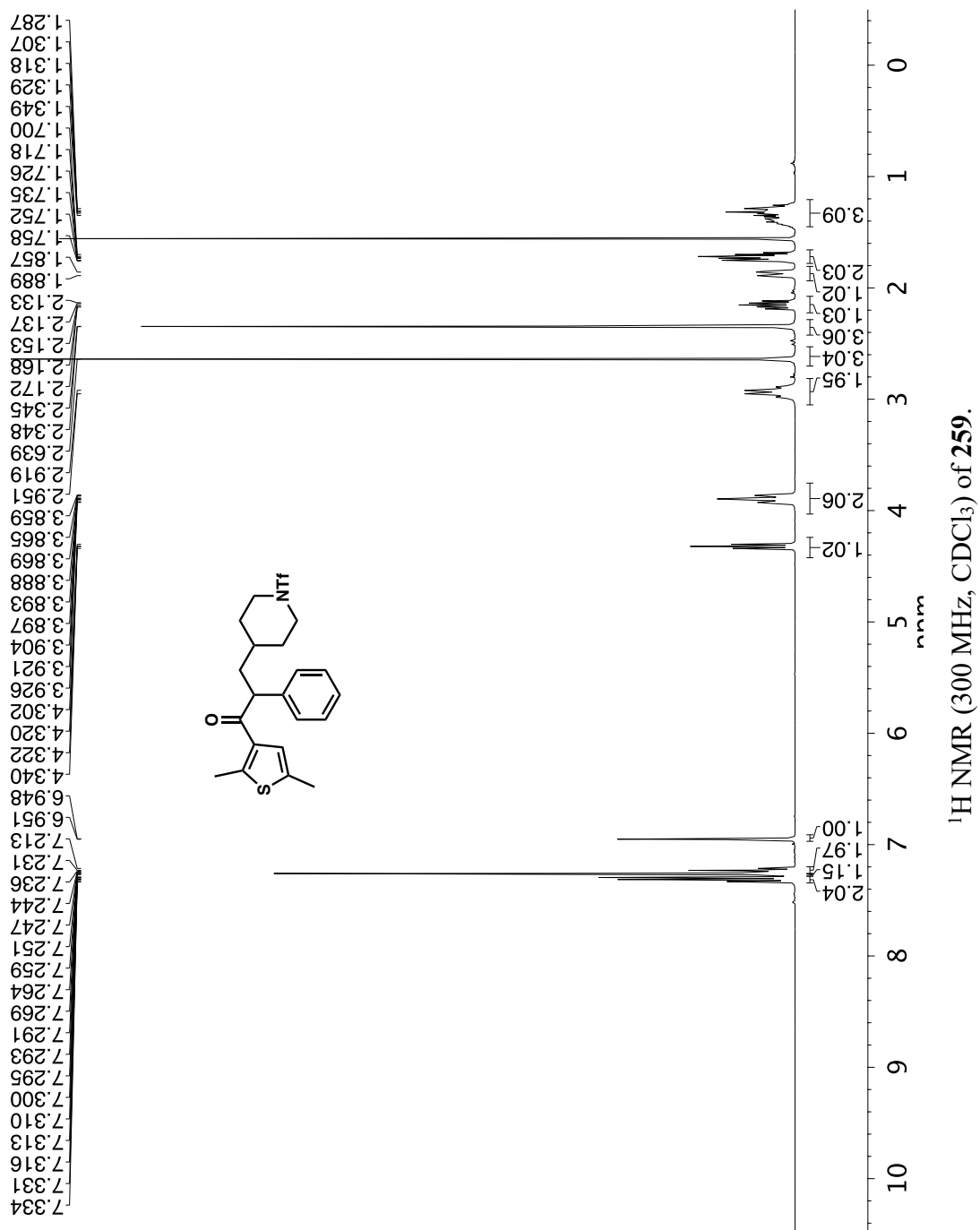
-75.1712

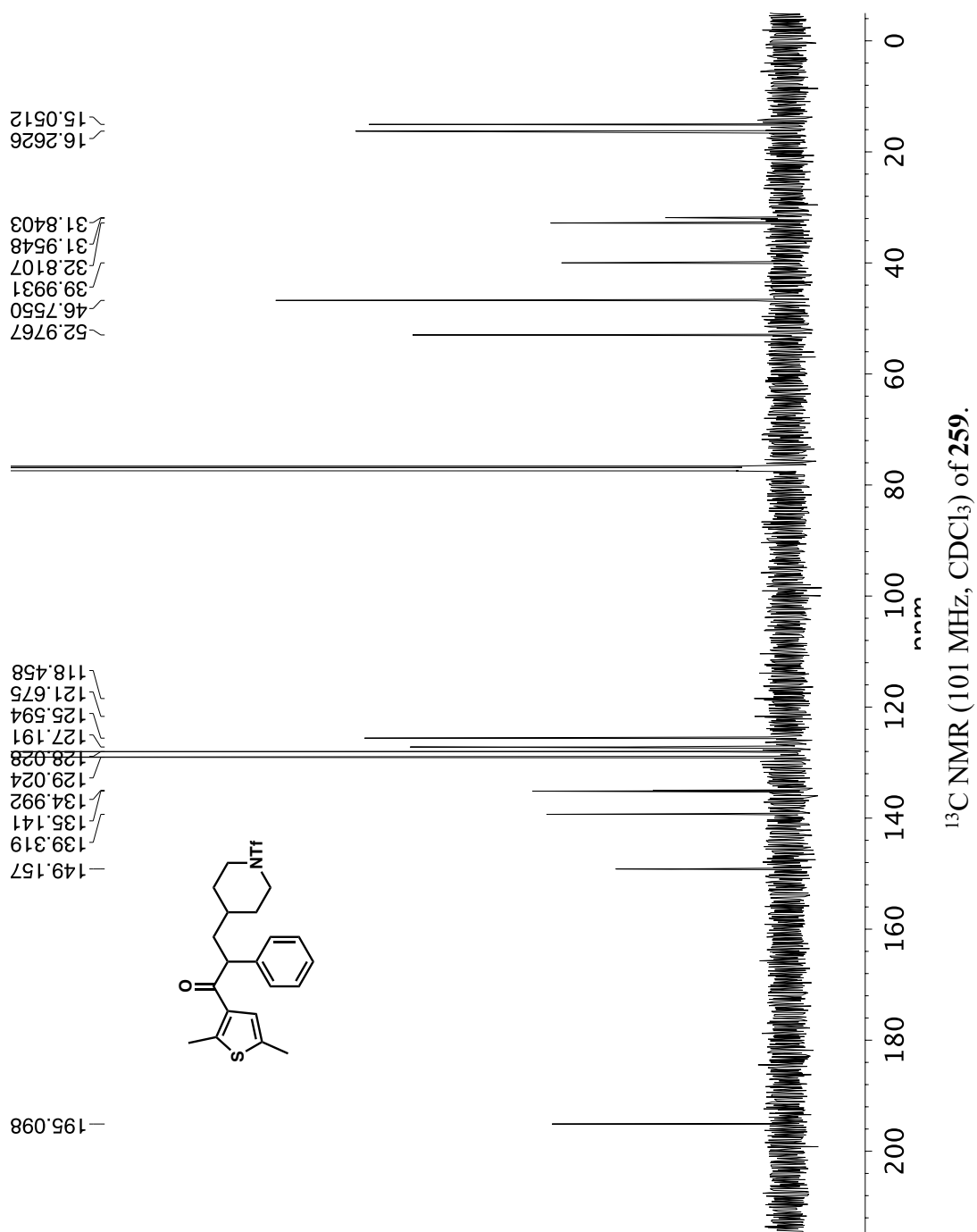




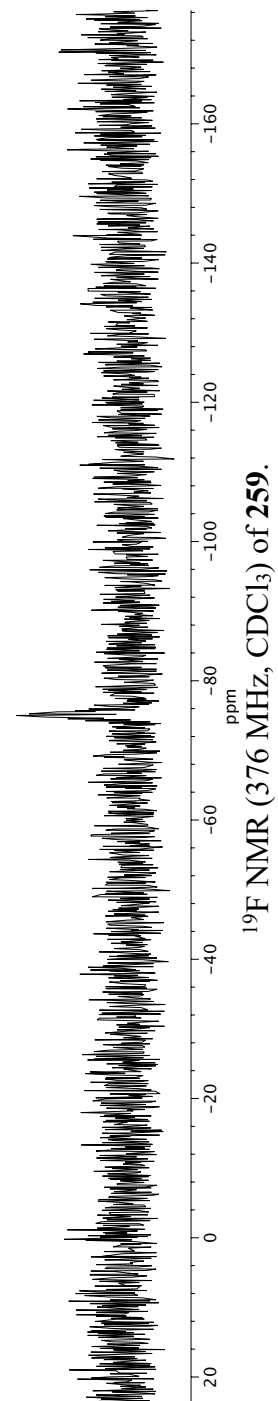
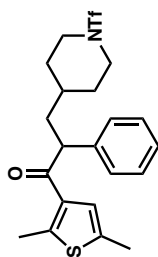


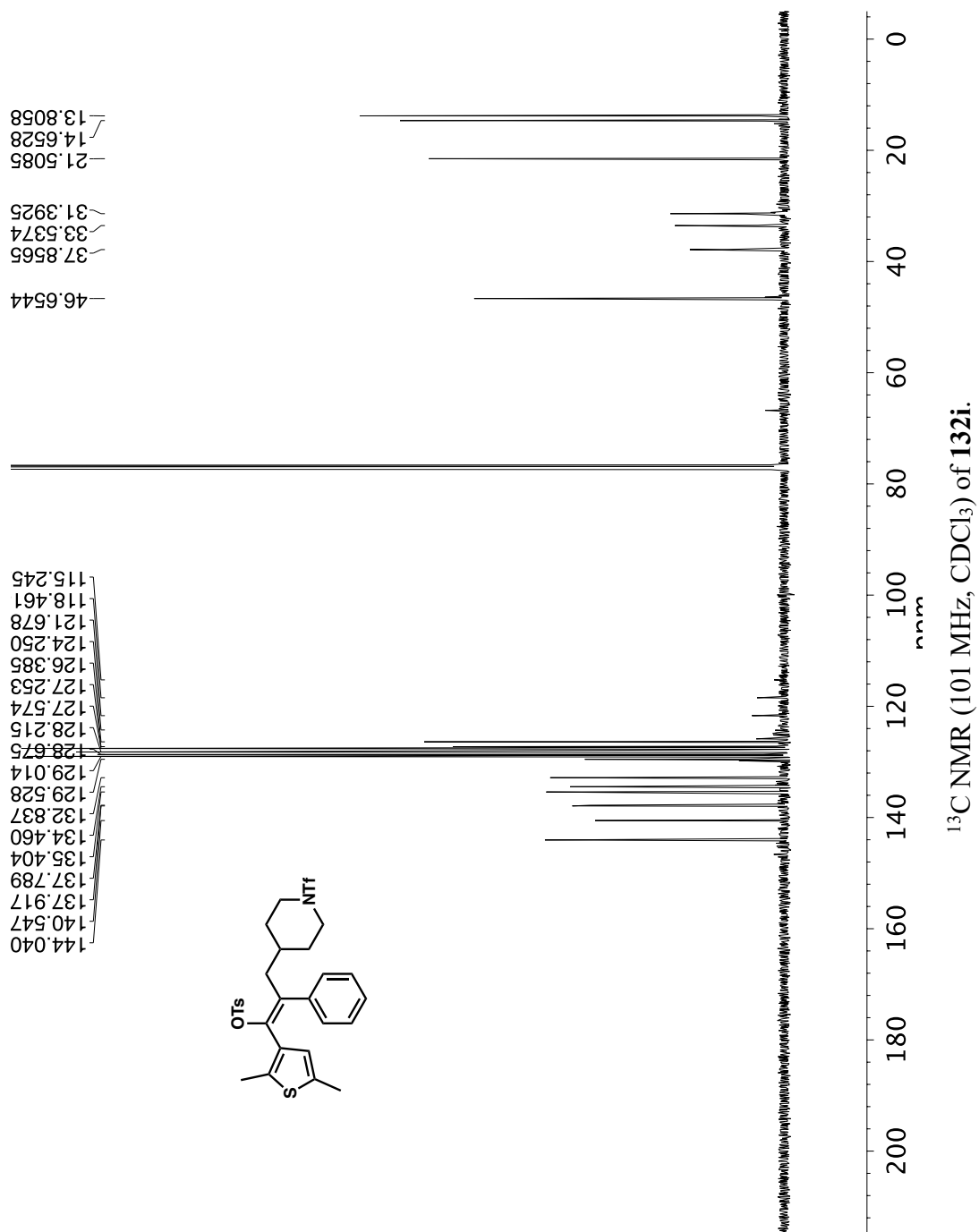




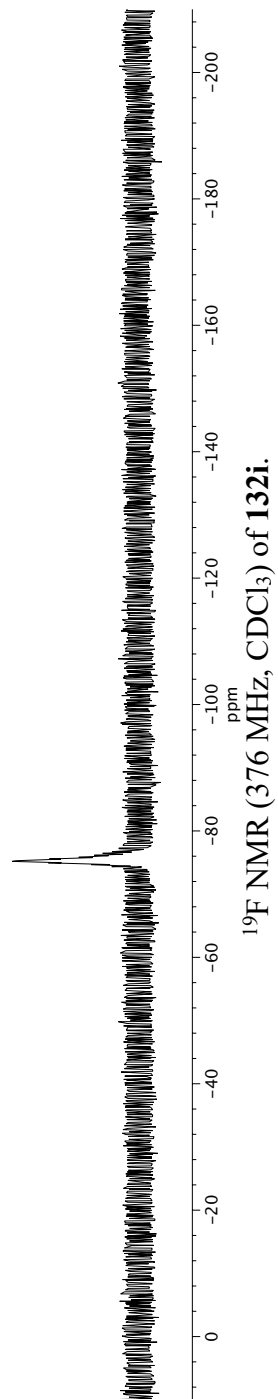
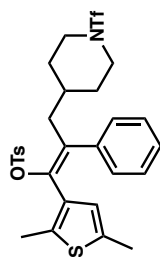


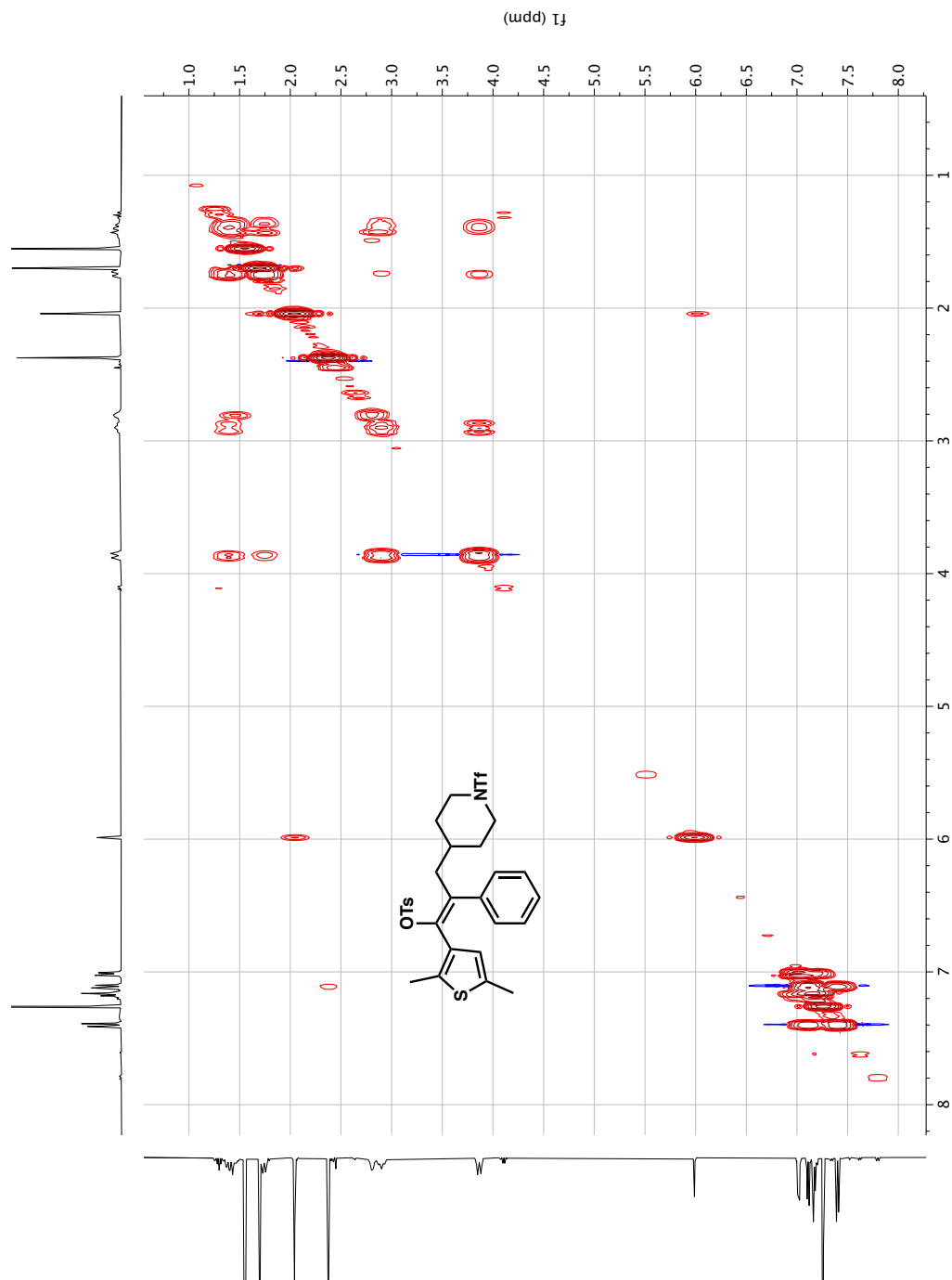
—74.9789



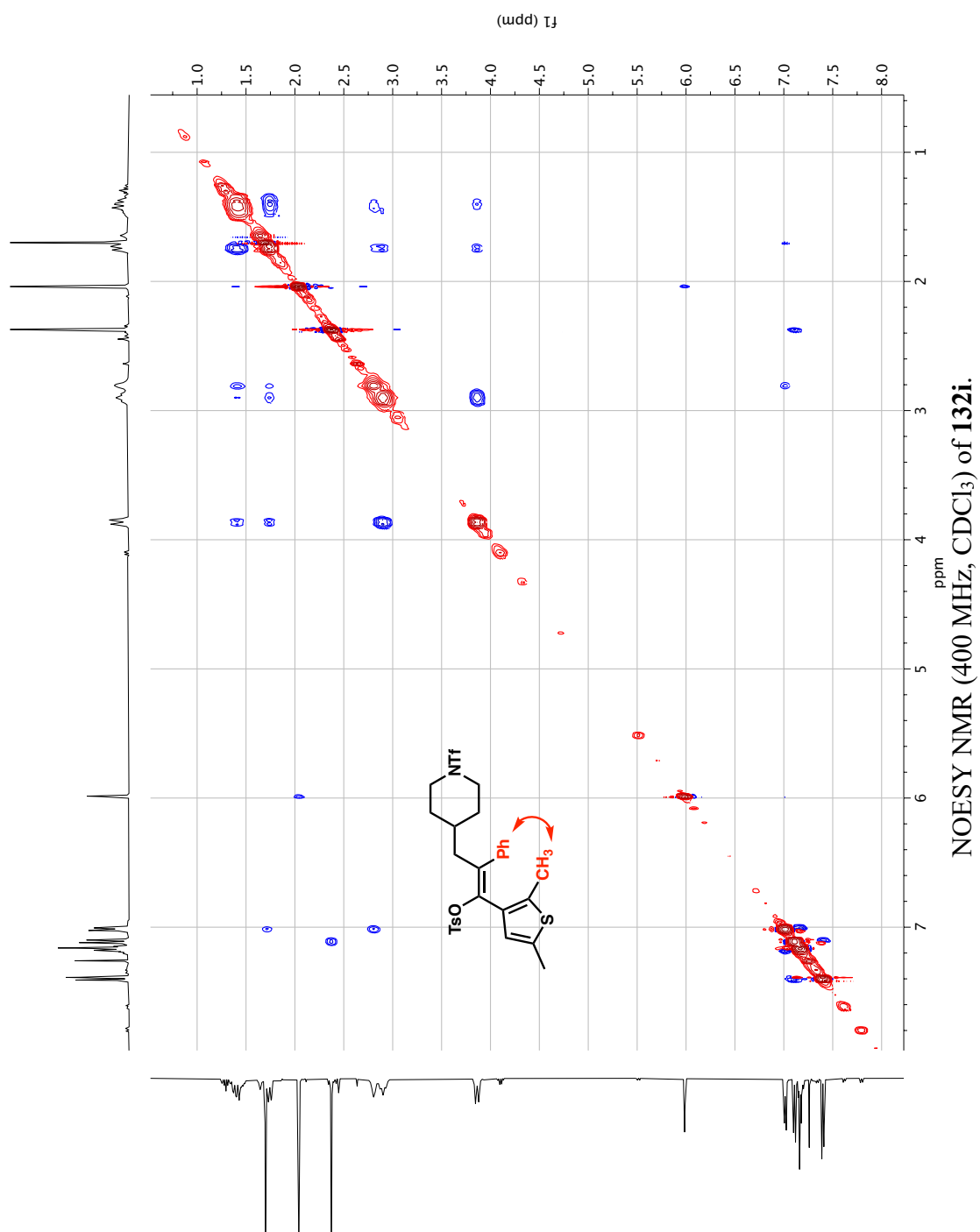


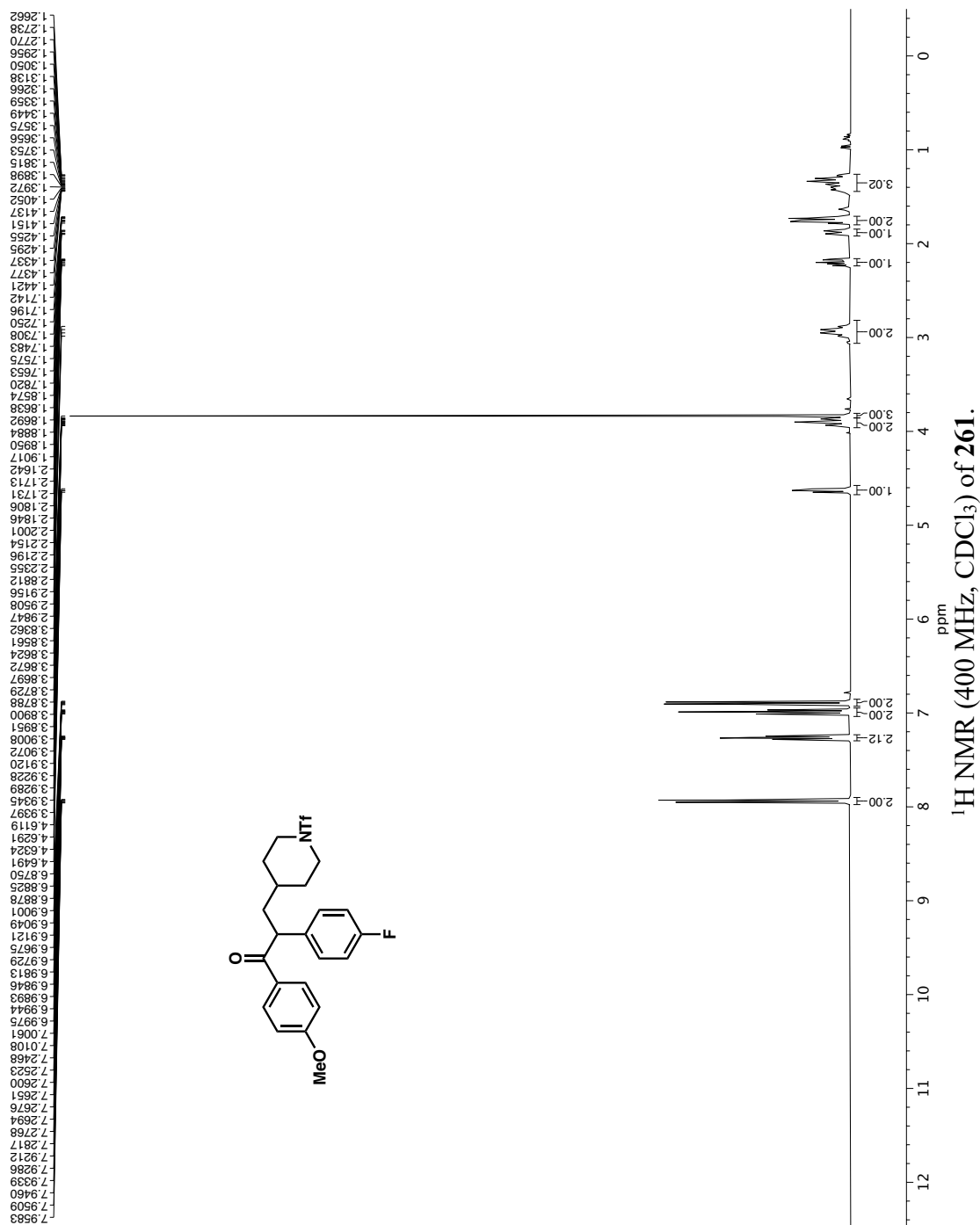
—75.2367

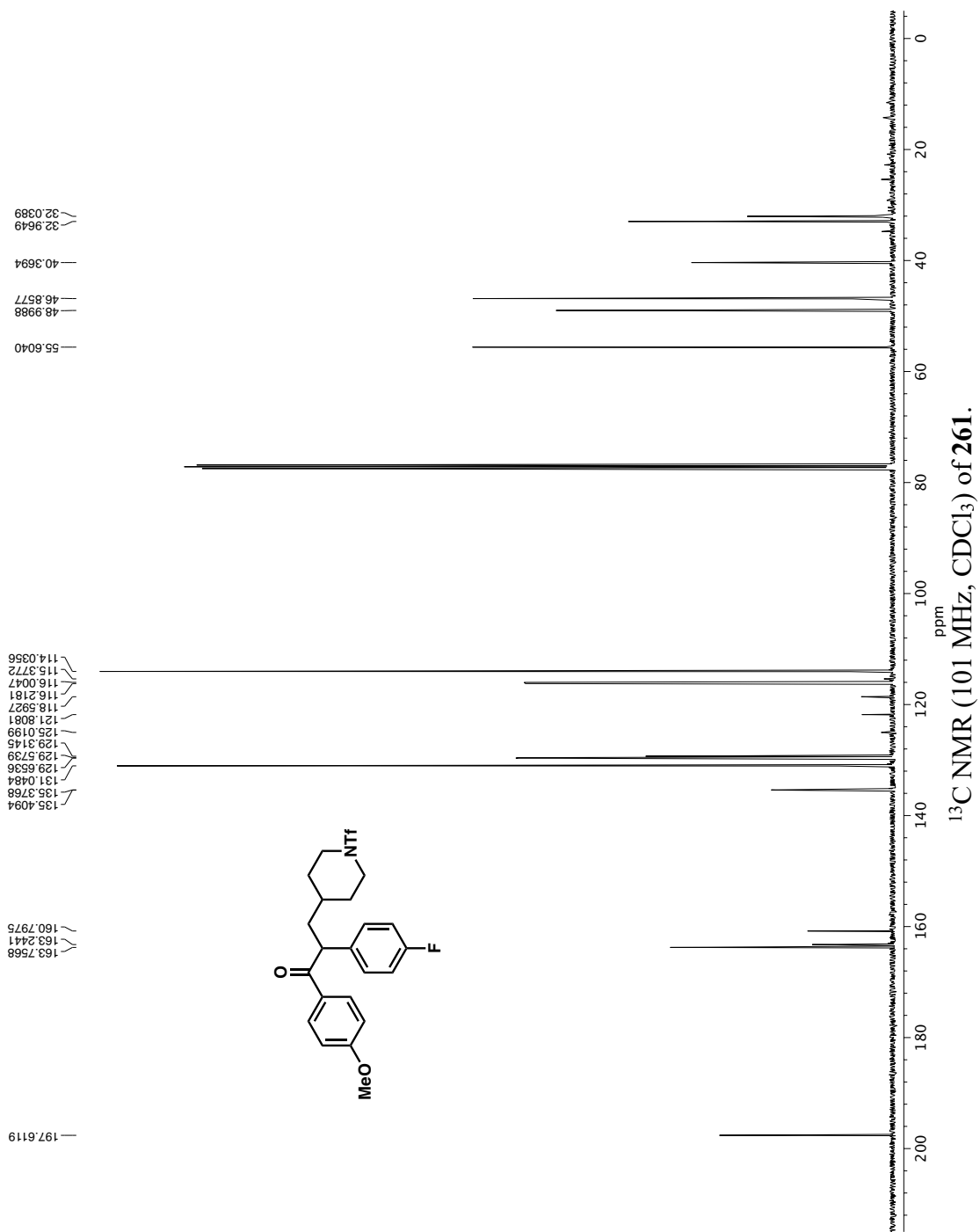


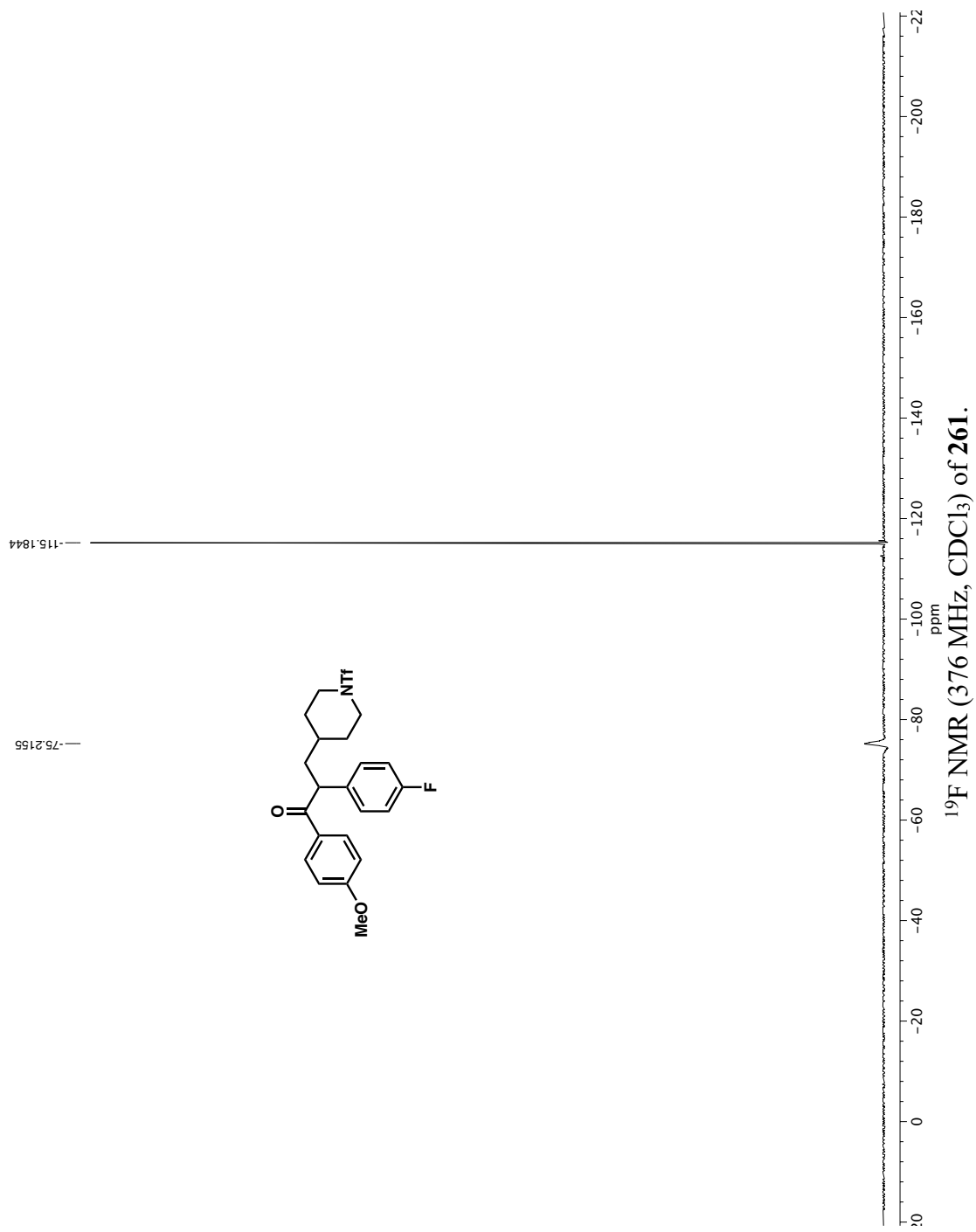


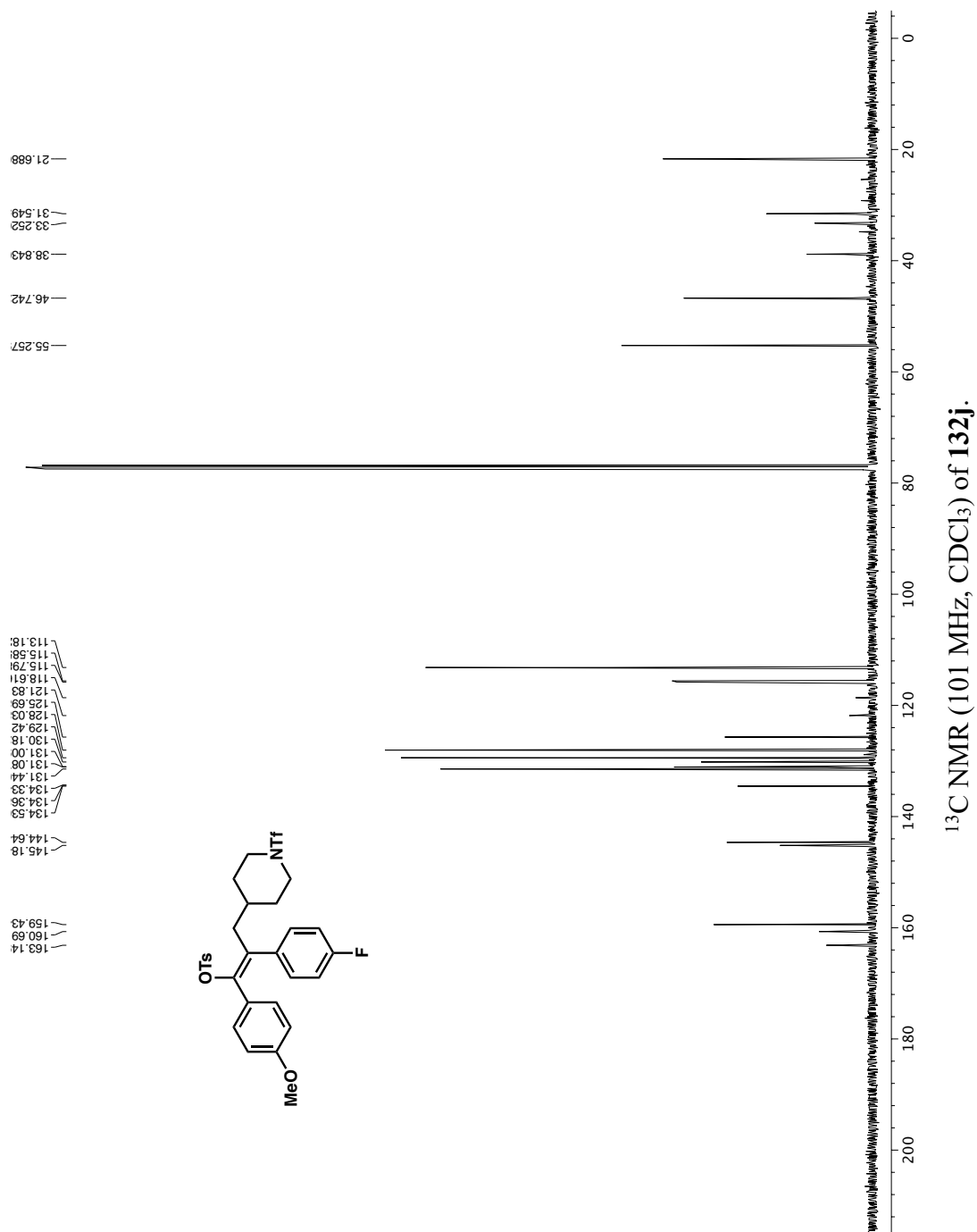
COSY NMR (400 MHz, CDCl₃) of **132i**.

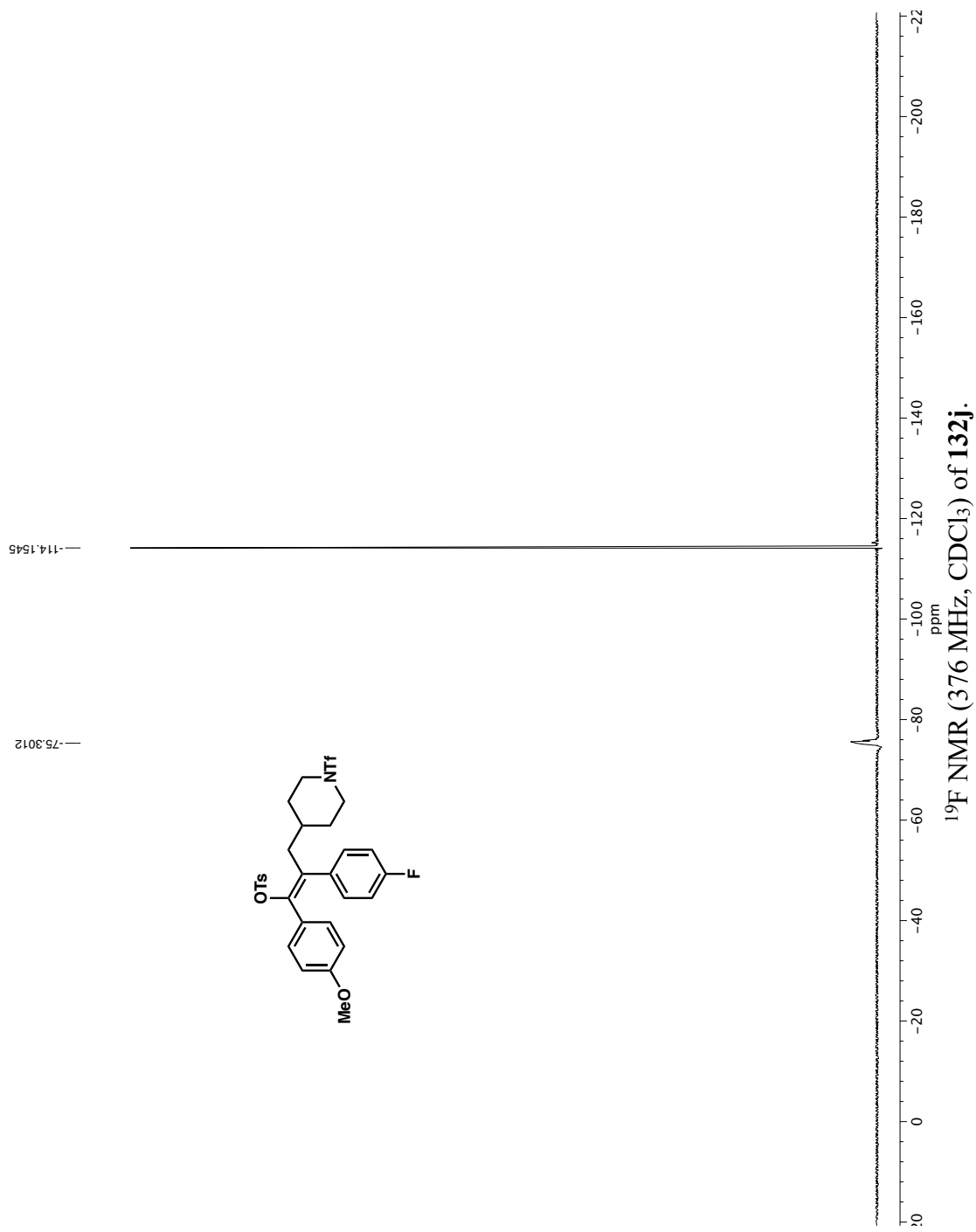


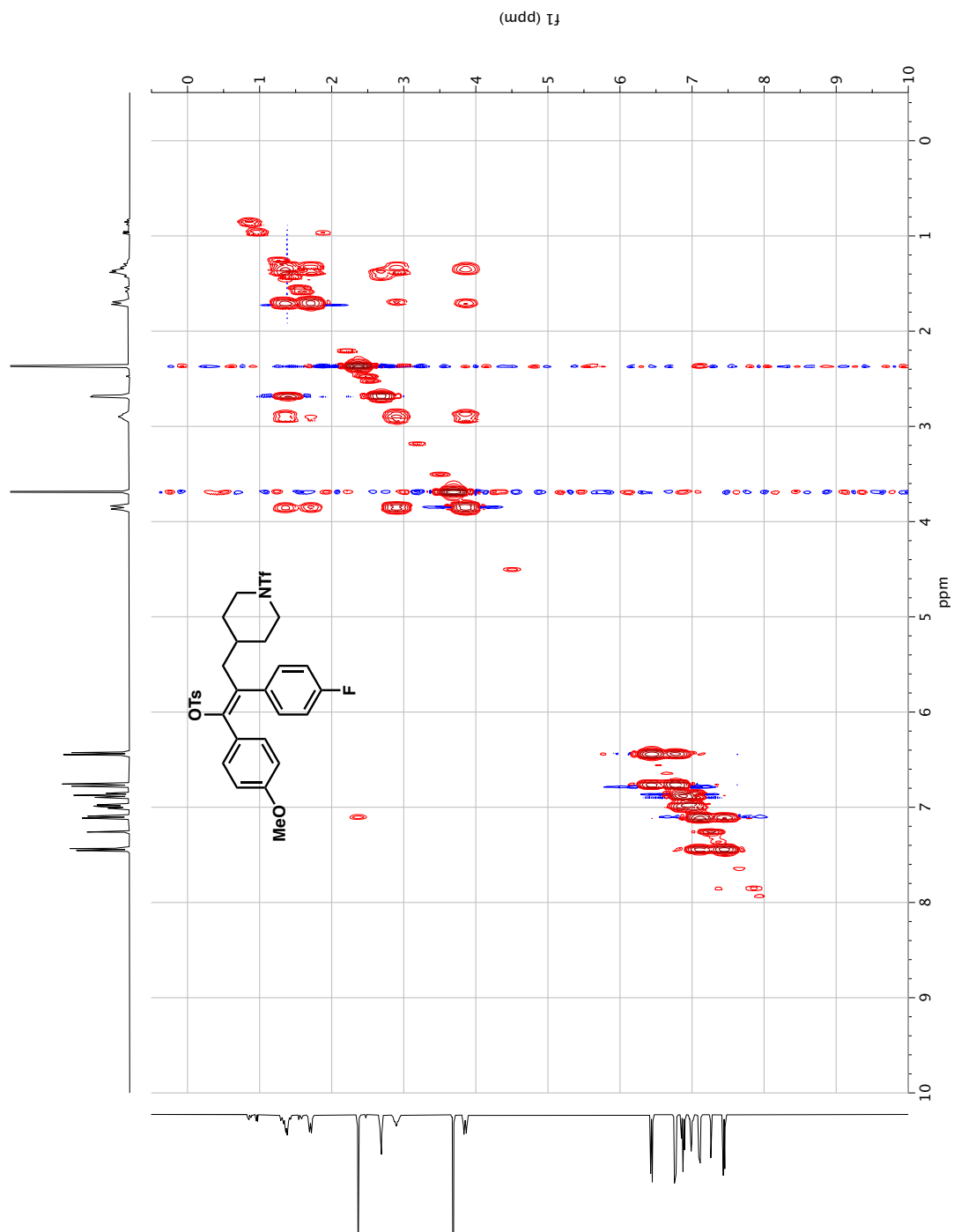




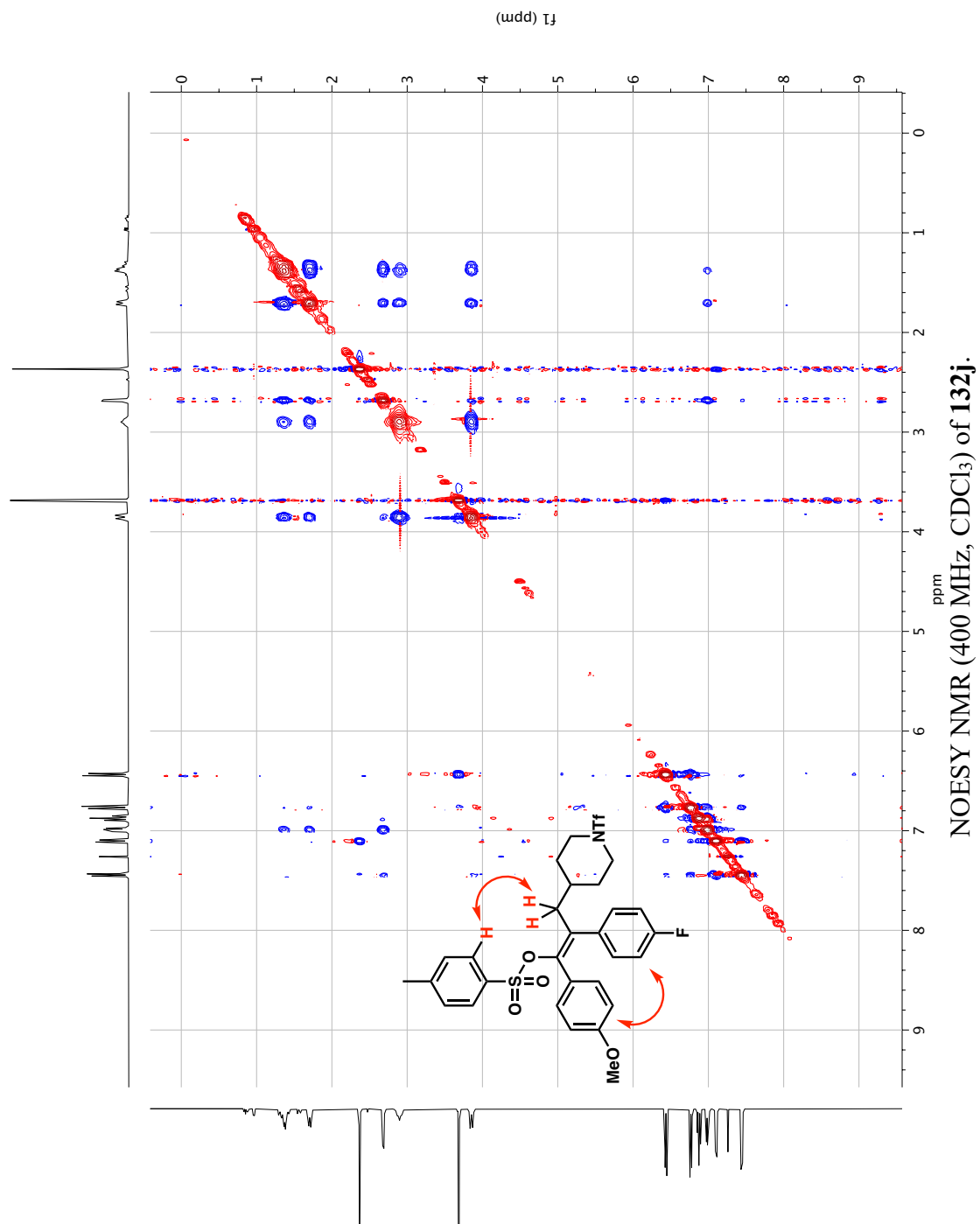


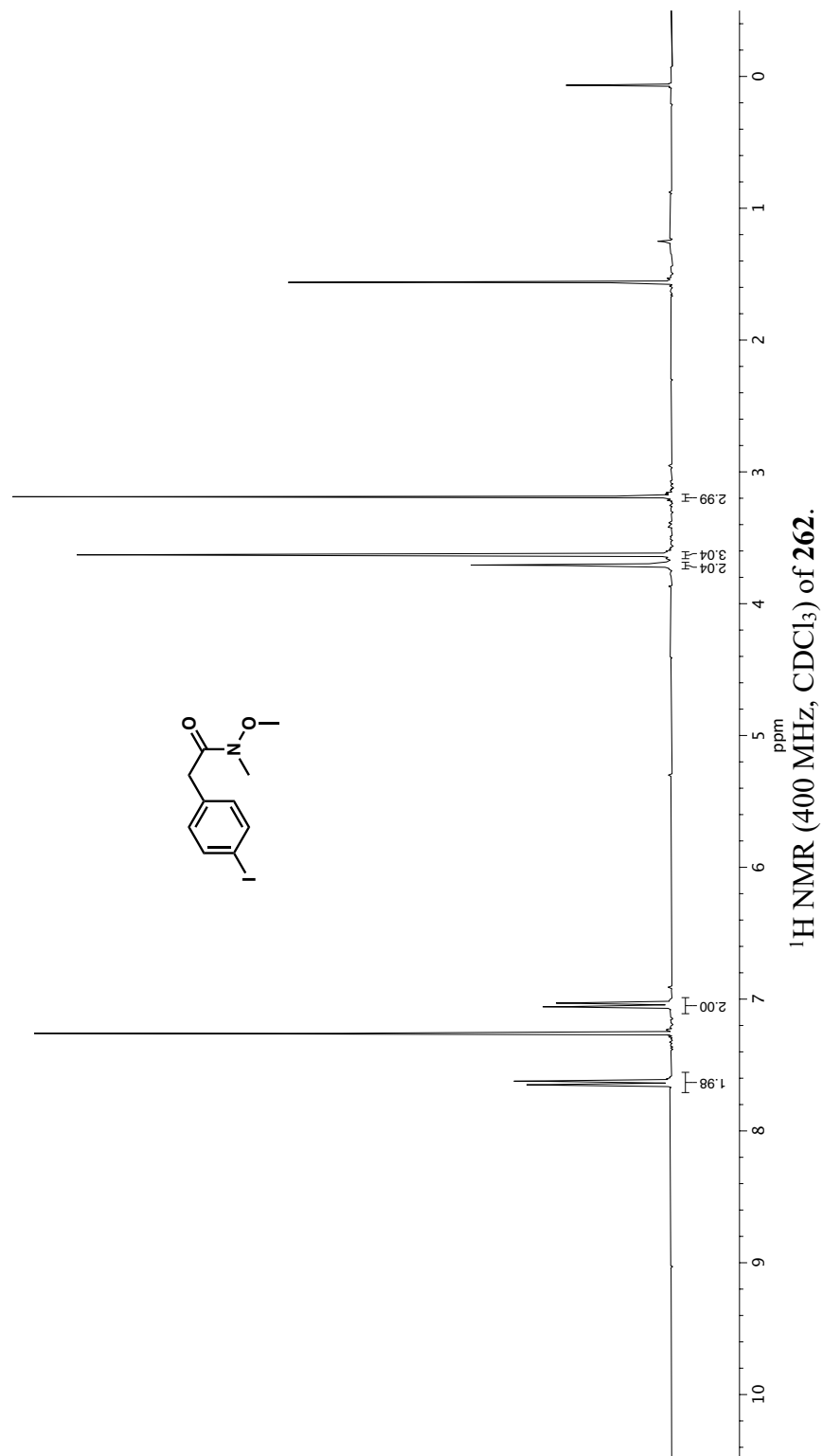


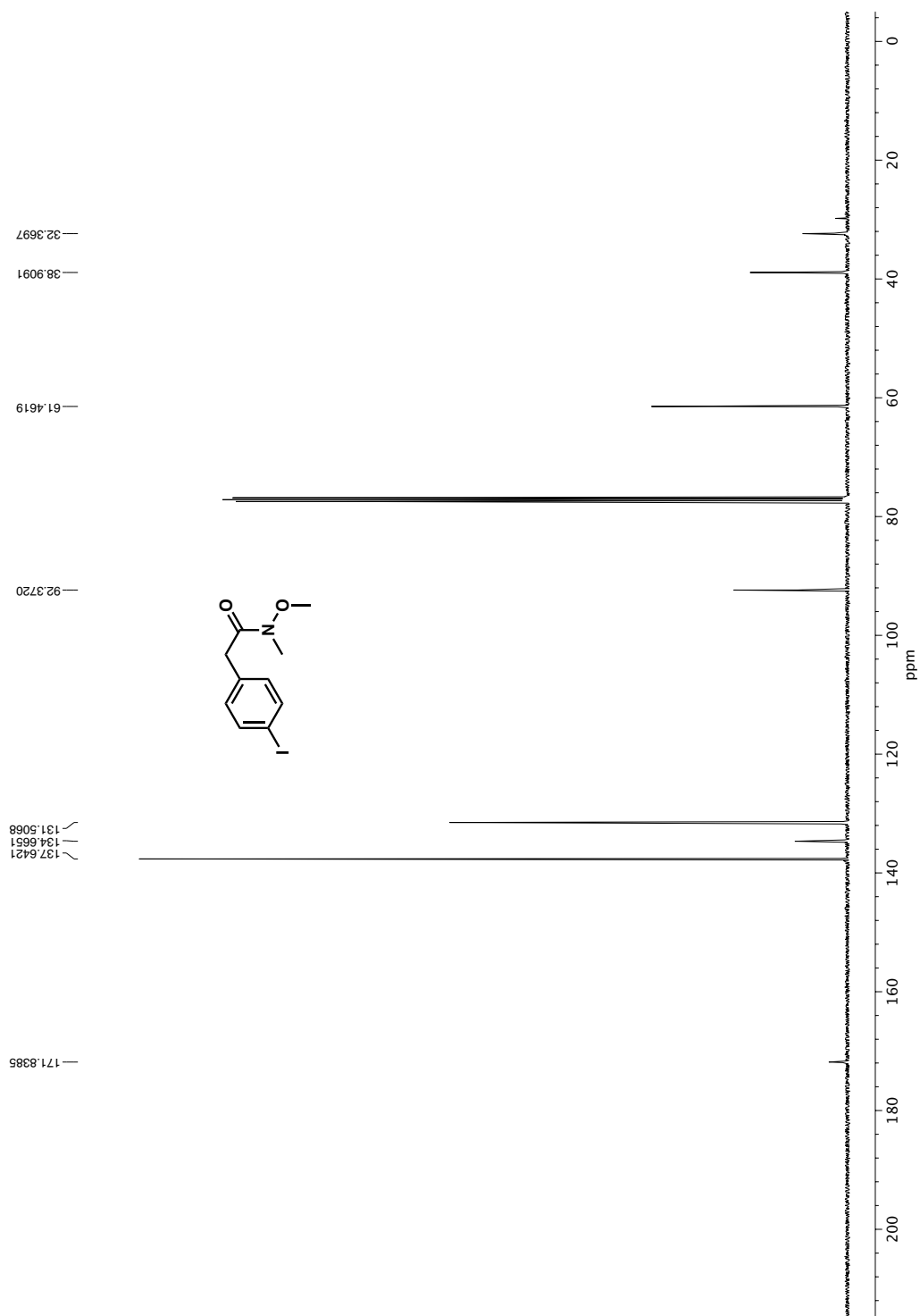


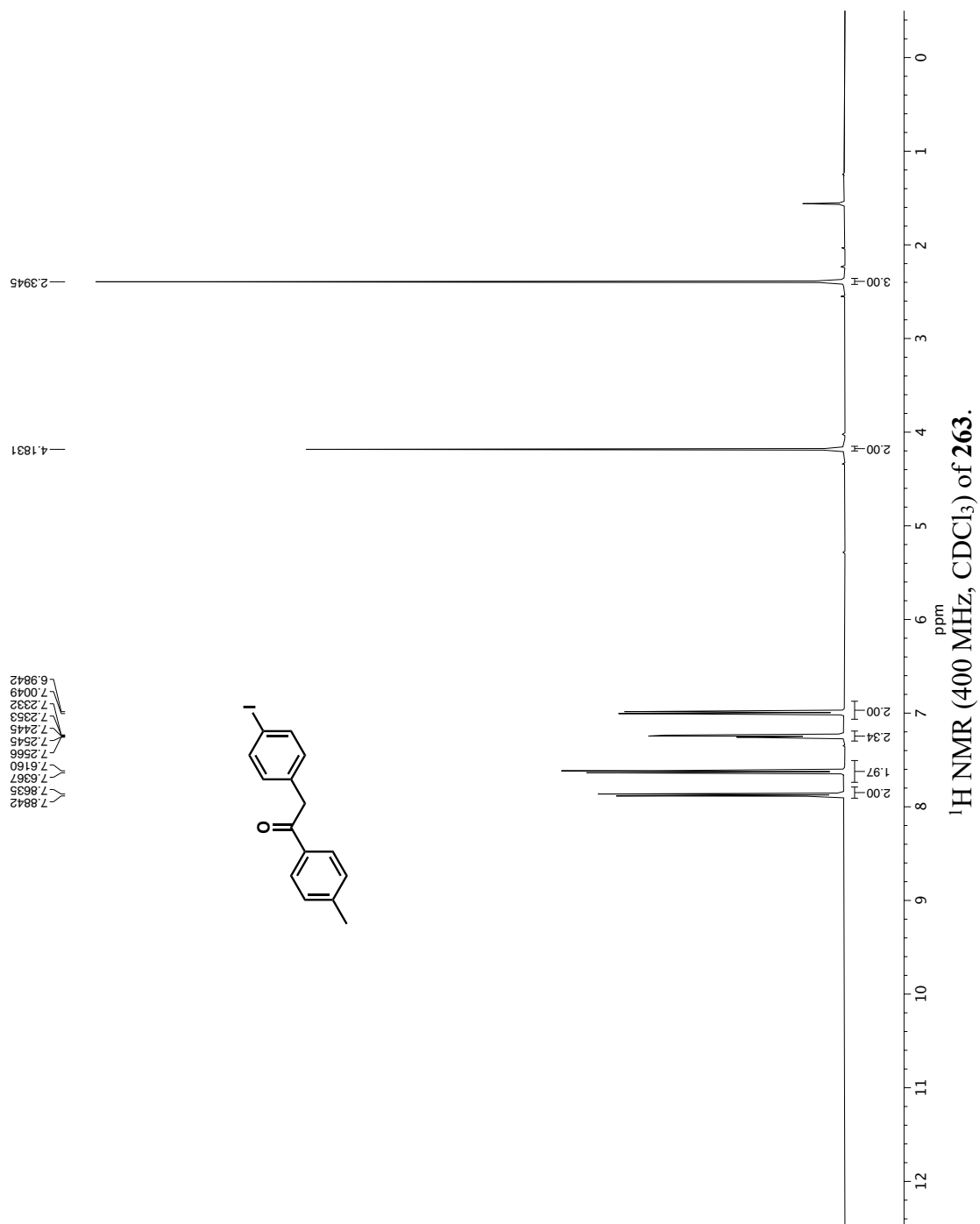


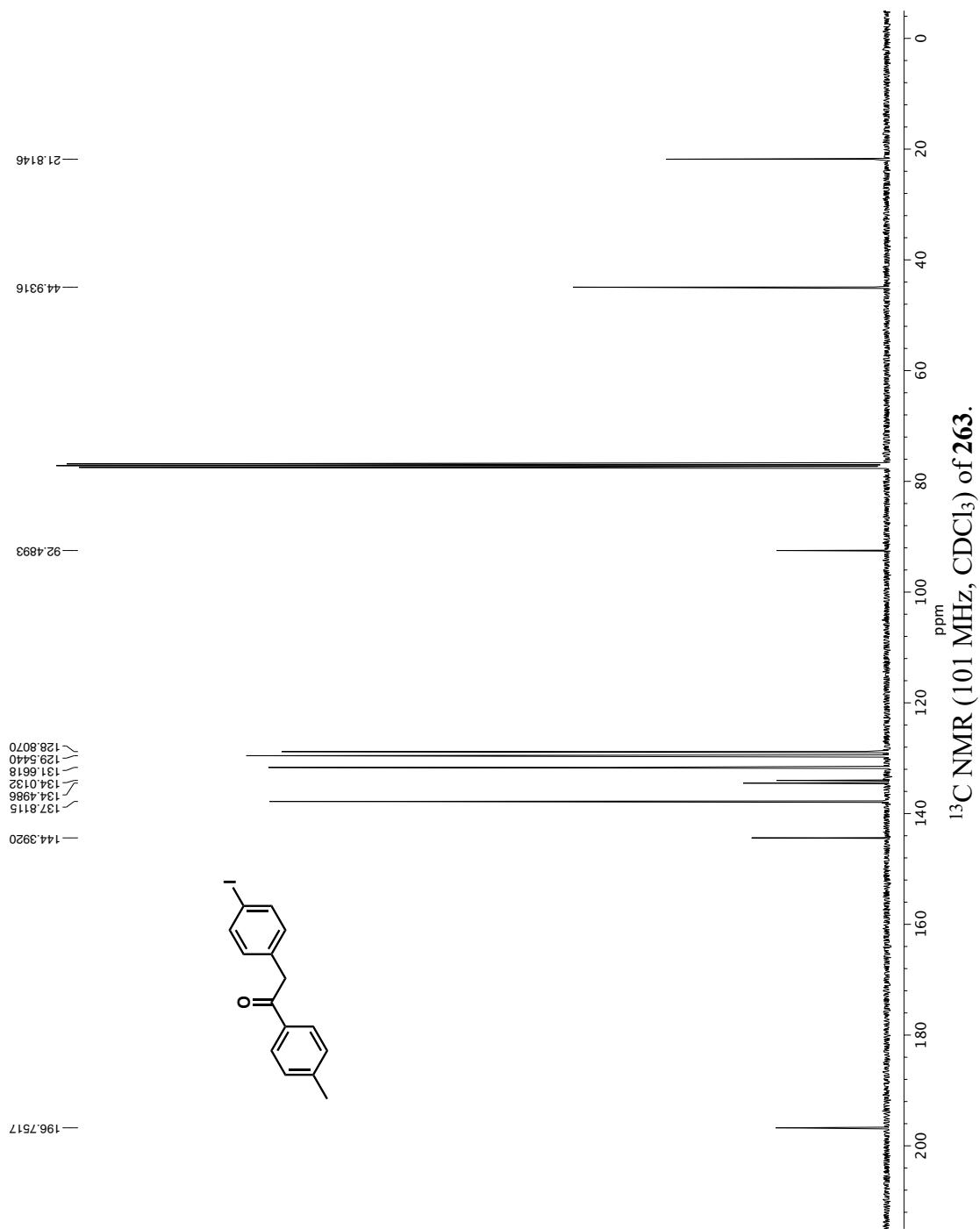
COSY NMR (400 MHz, CDCl₃) of **132j**.

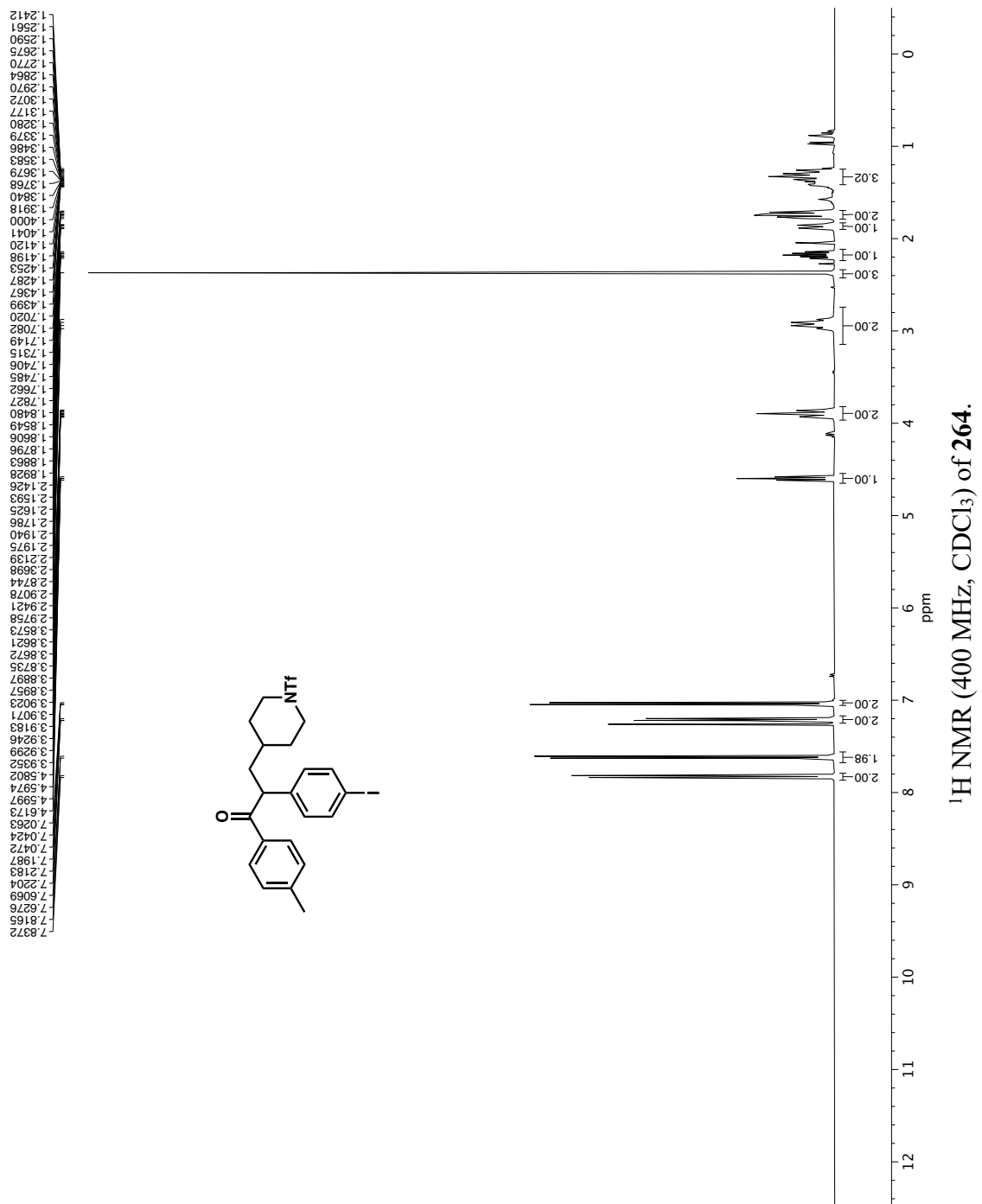


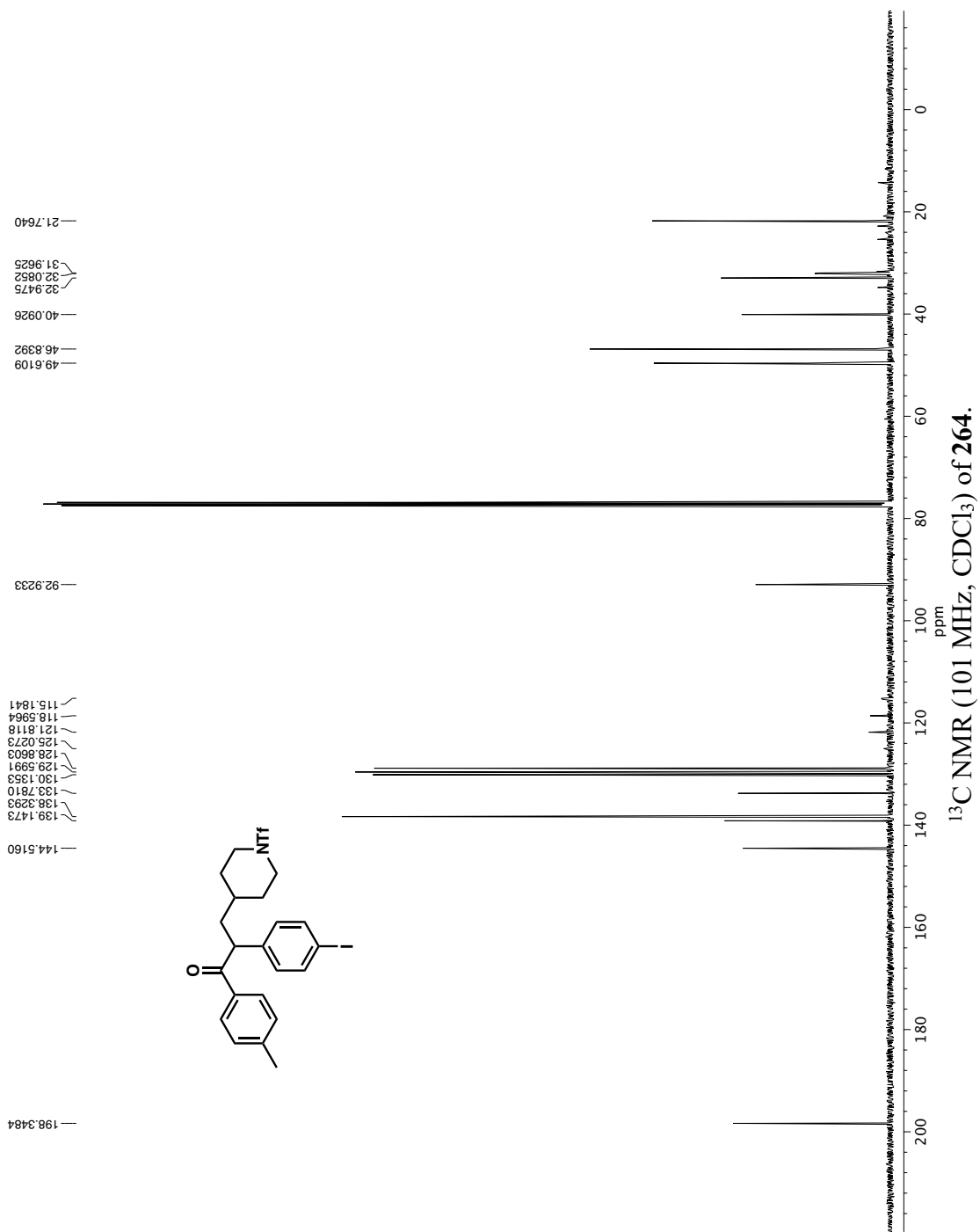


 ^{13}C NMR (101 MHz, CDCl_3) of **262**.

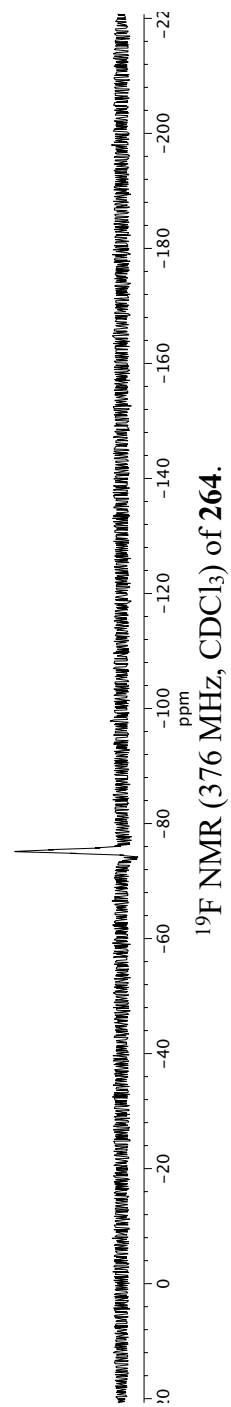
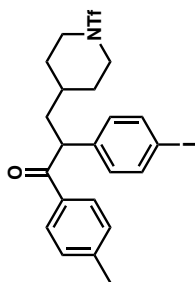


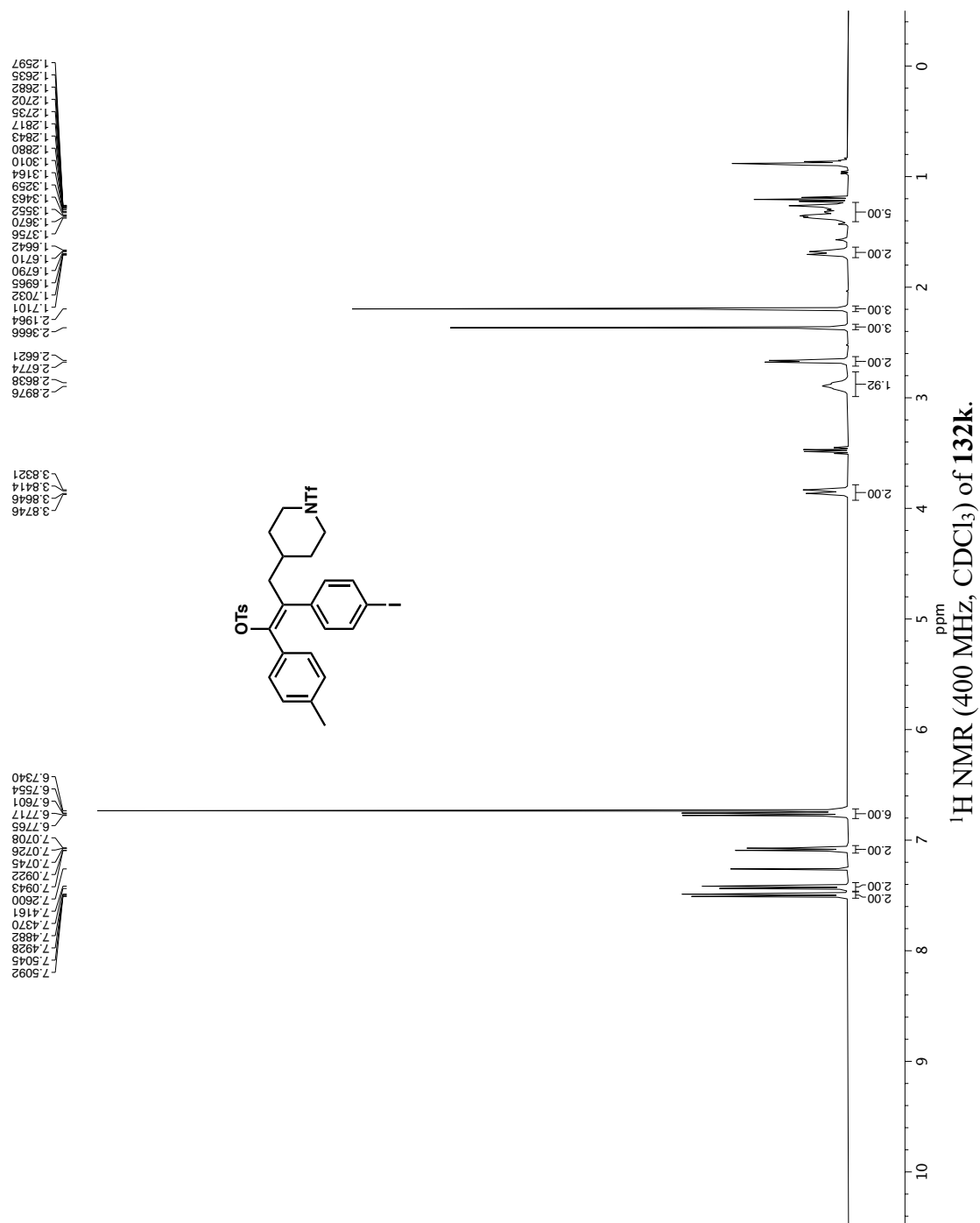


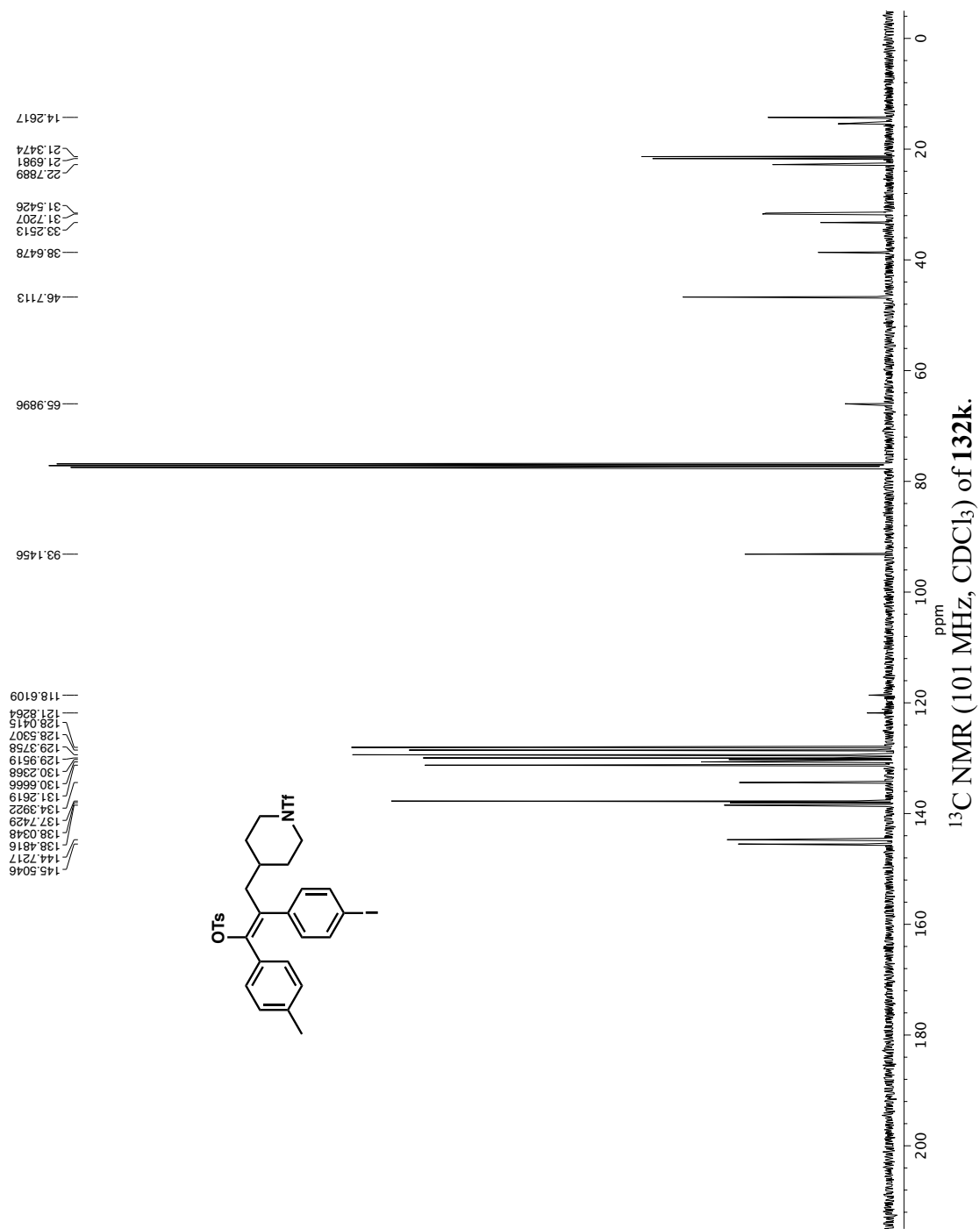




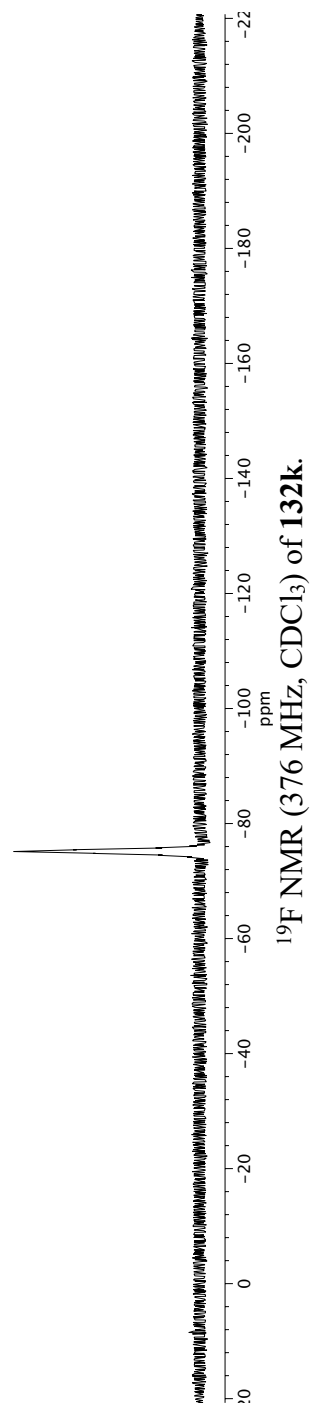
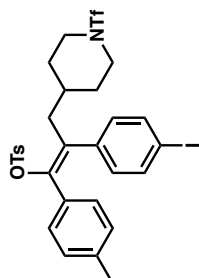
—75.1059

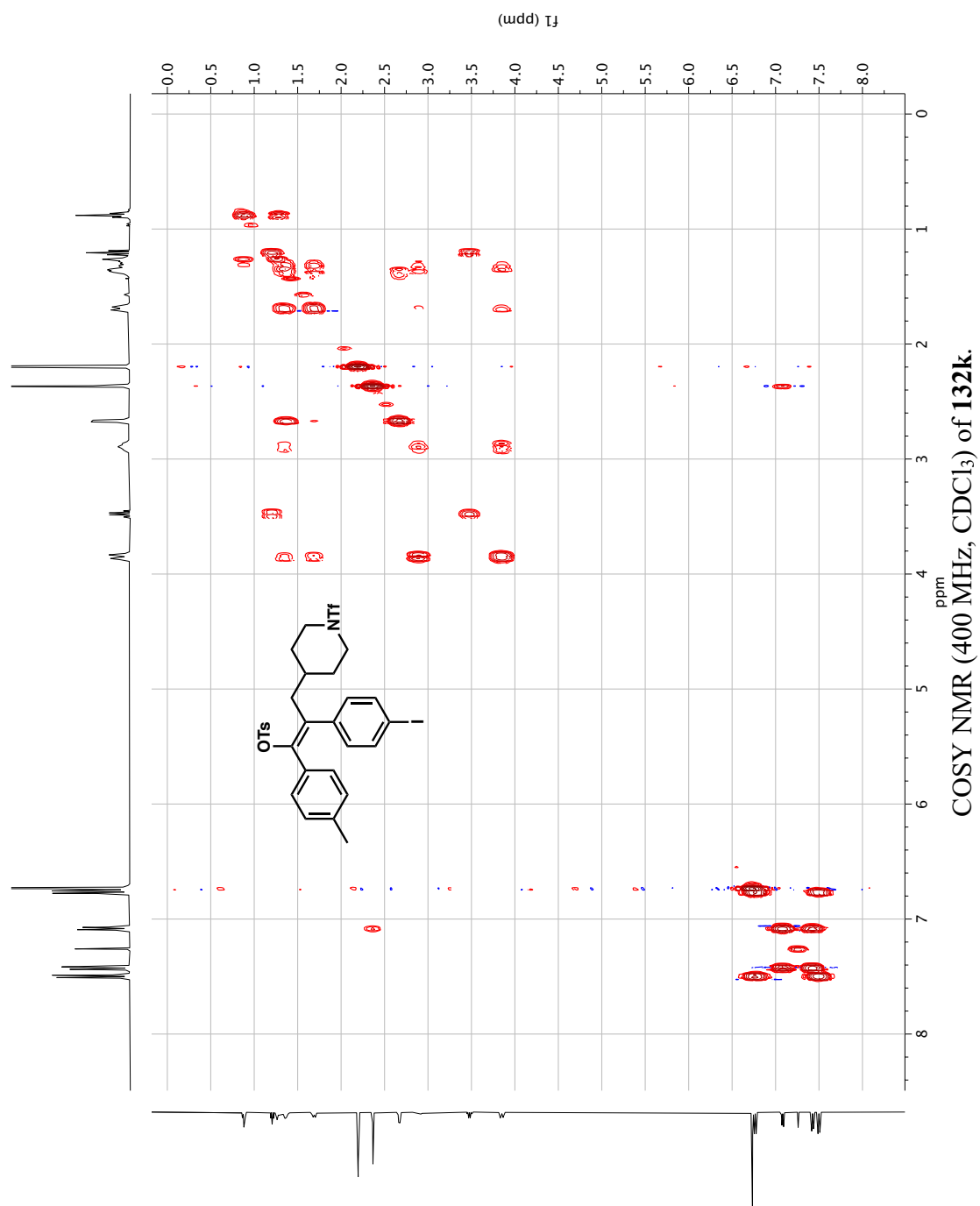


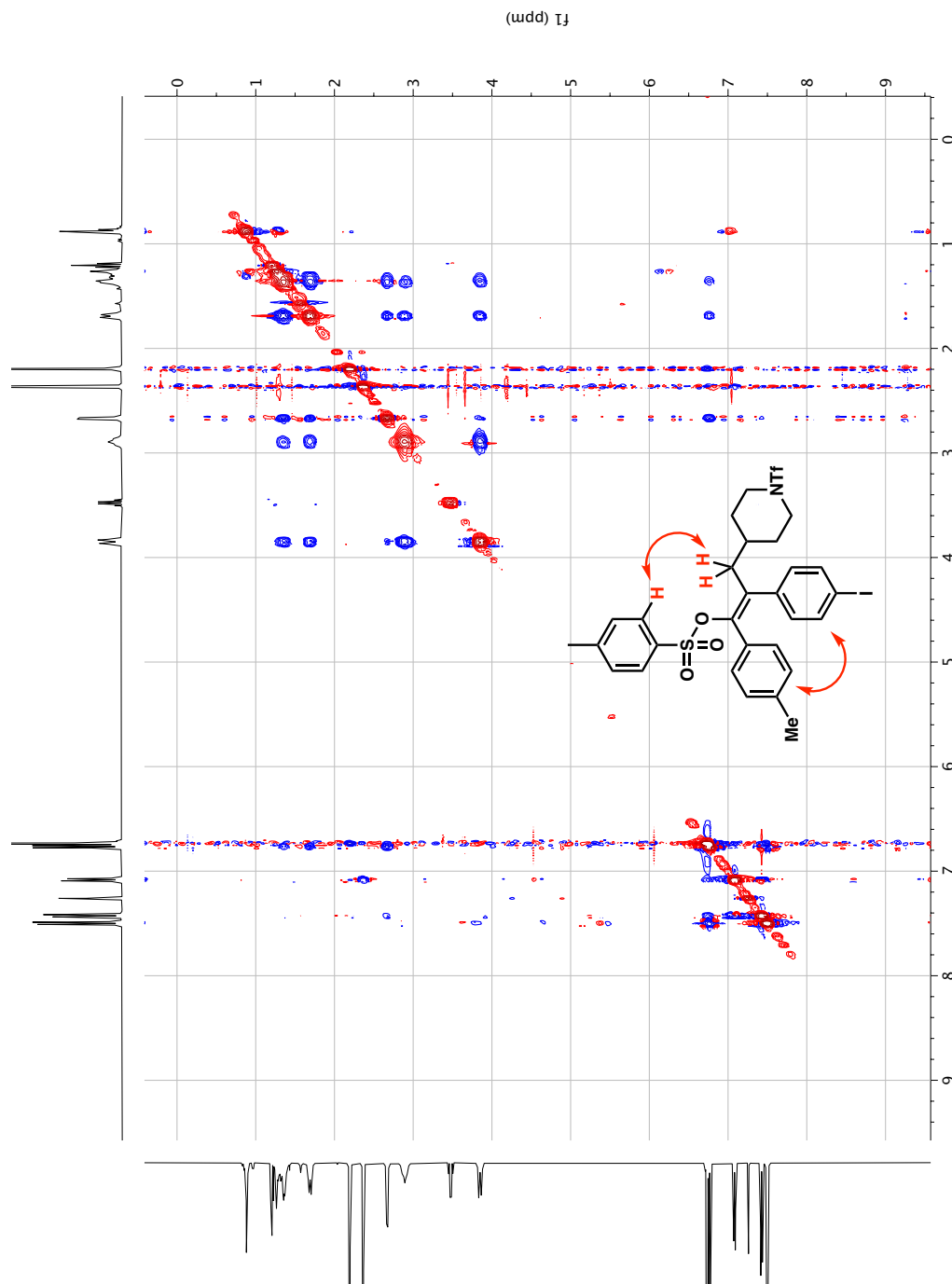


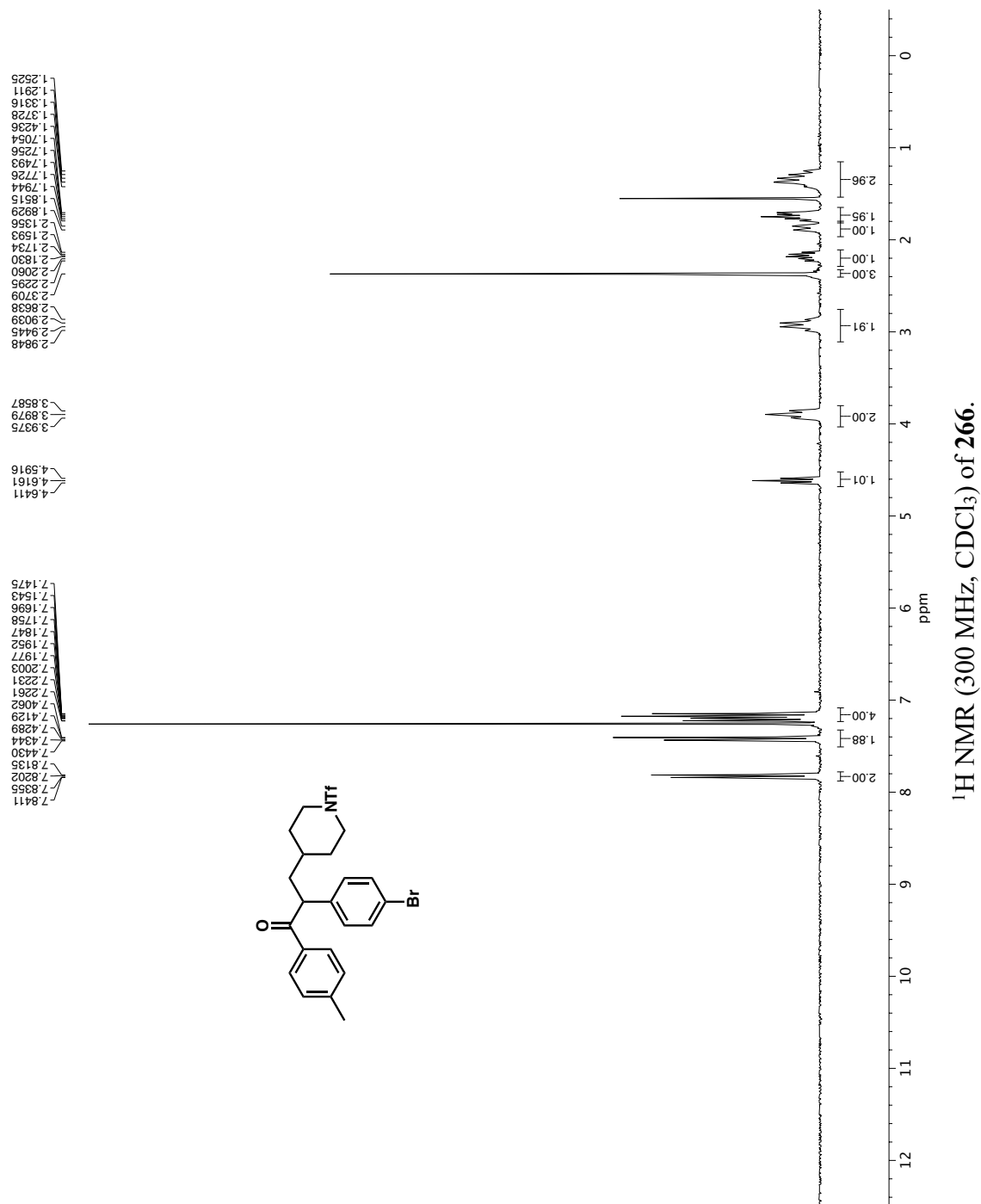


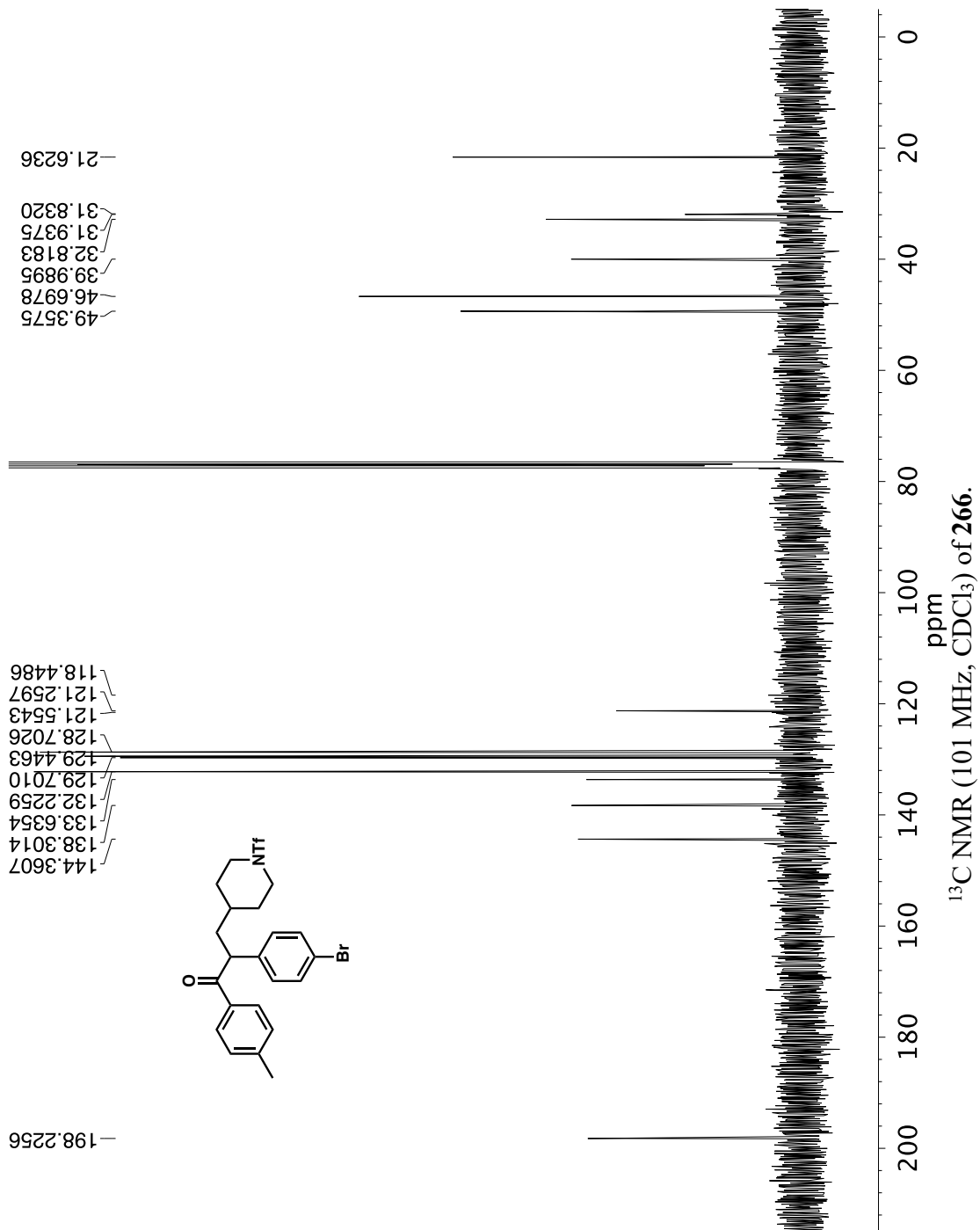
—75.1595



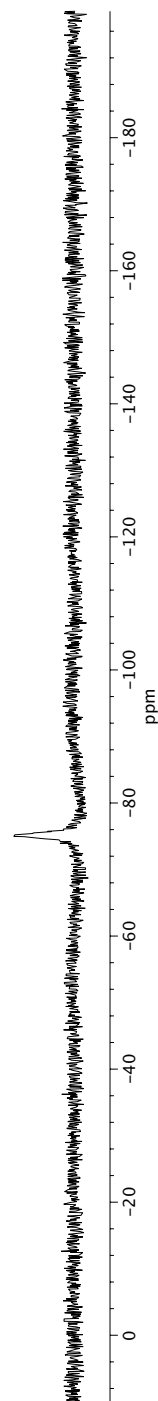
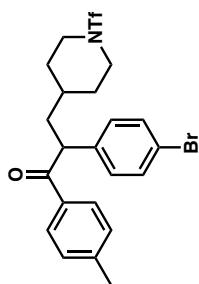




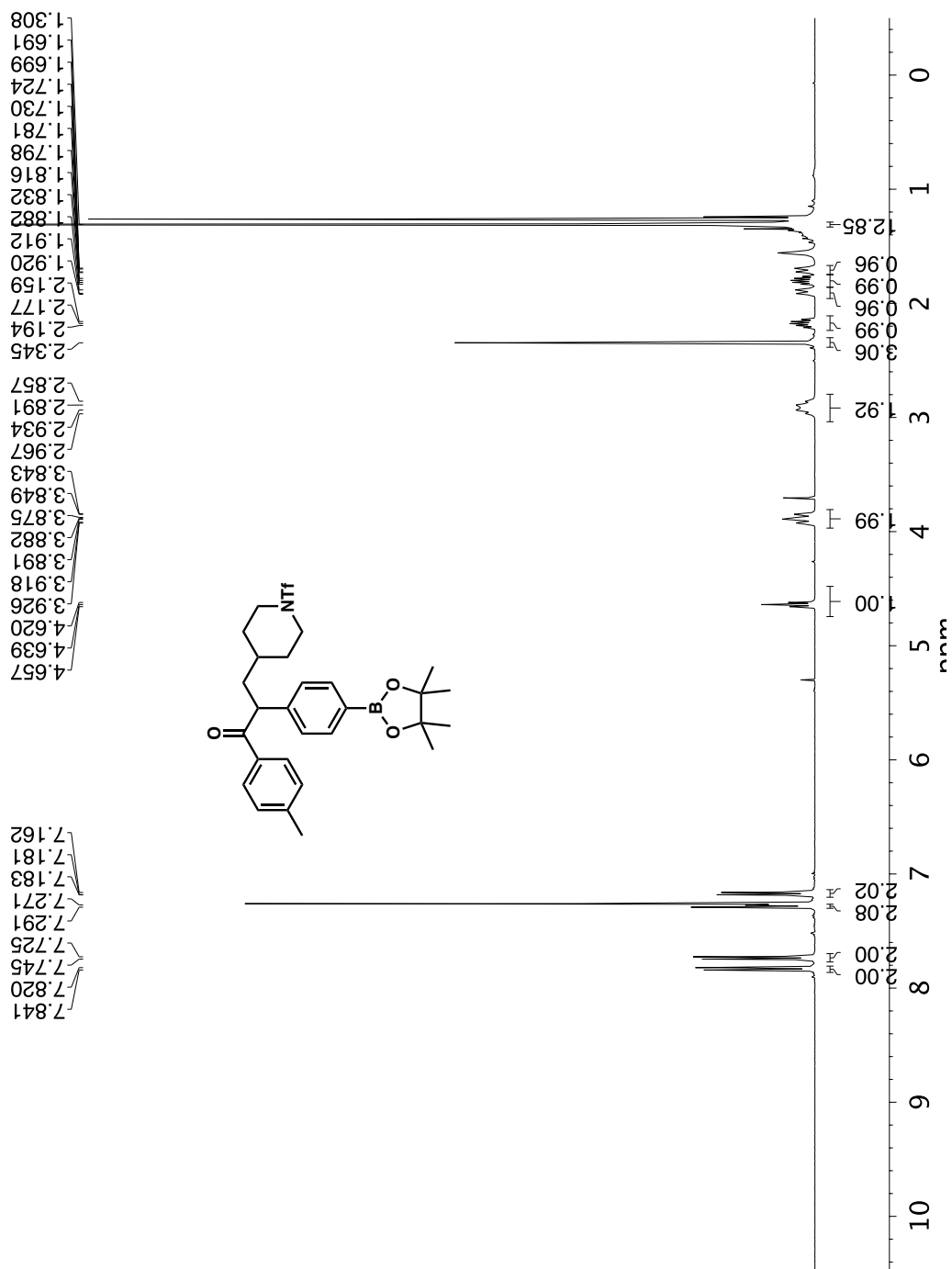


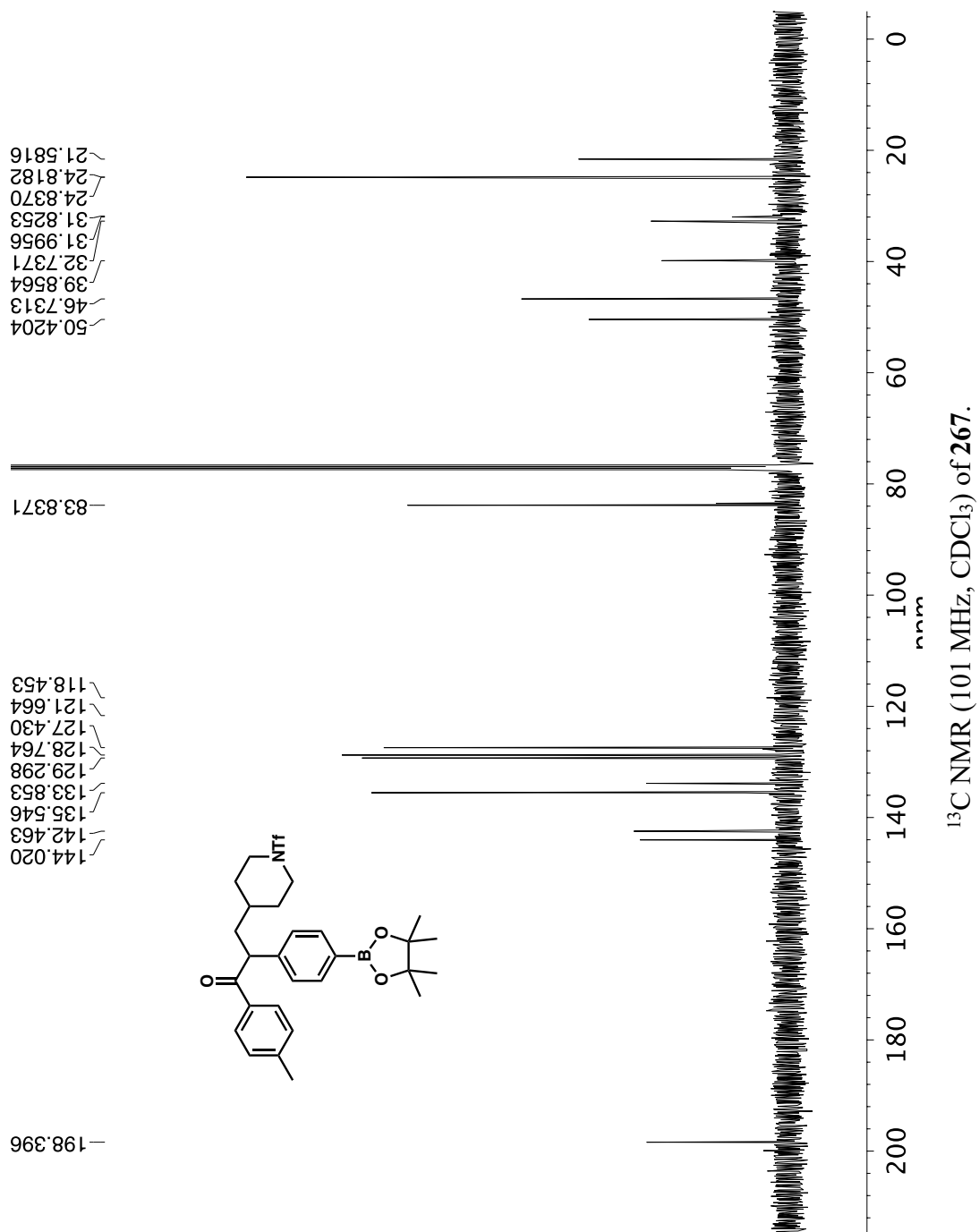


—75.0989

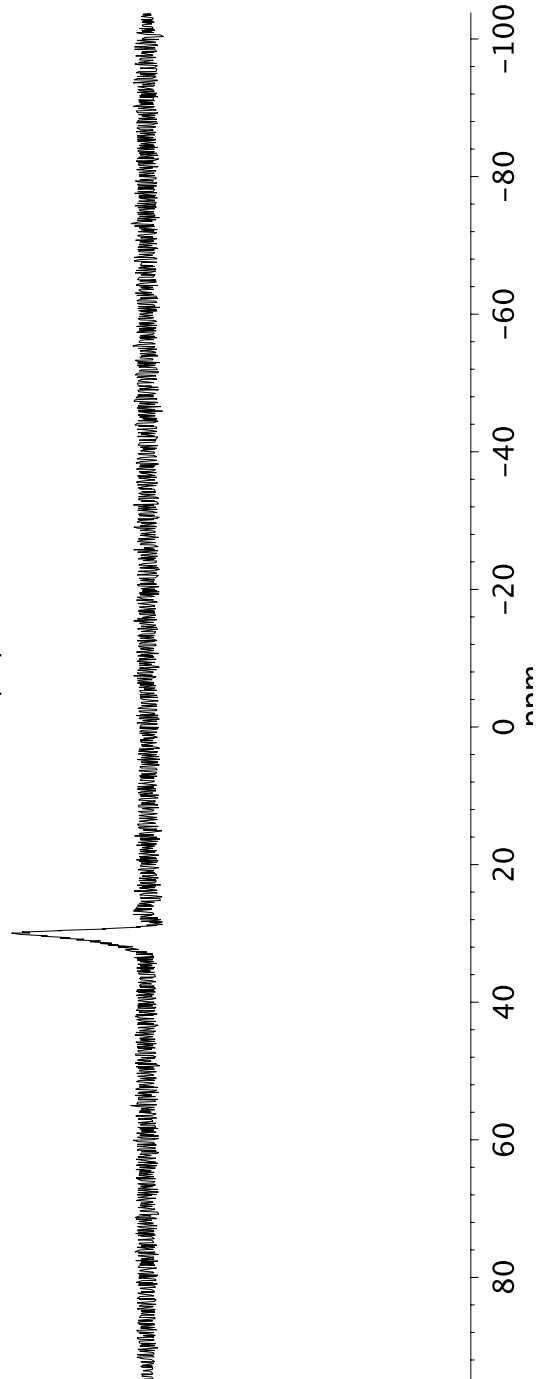
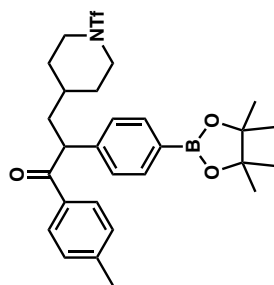


¹⁹F NMR (376 MHz, CDCl₃) of **266**.

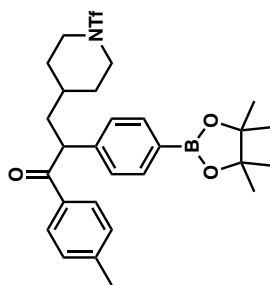


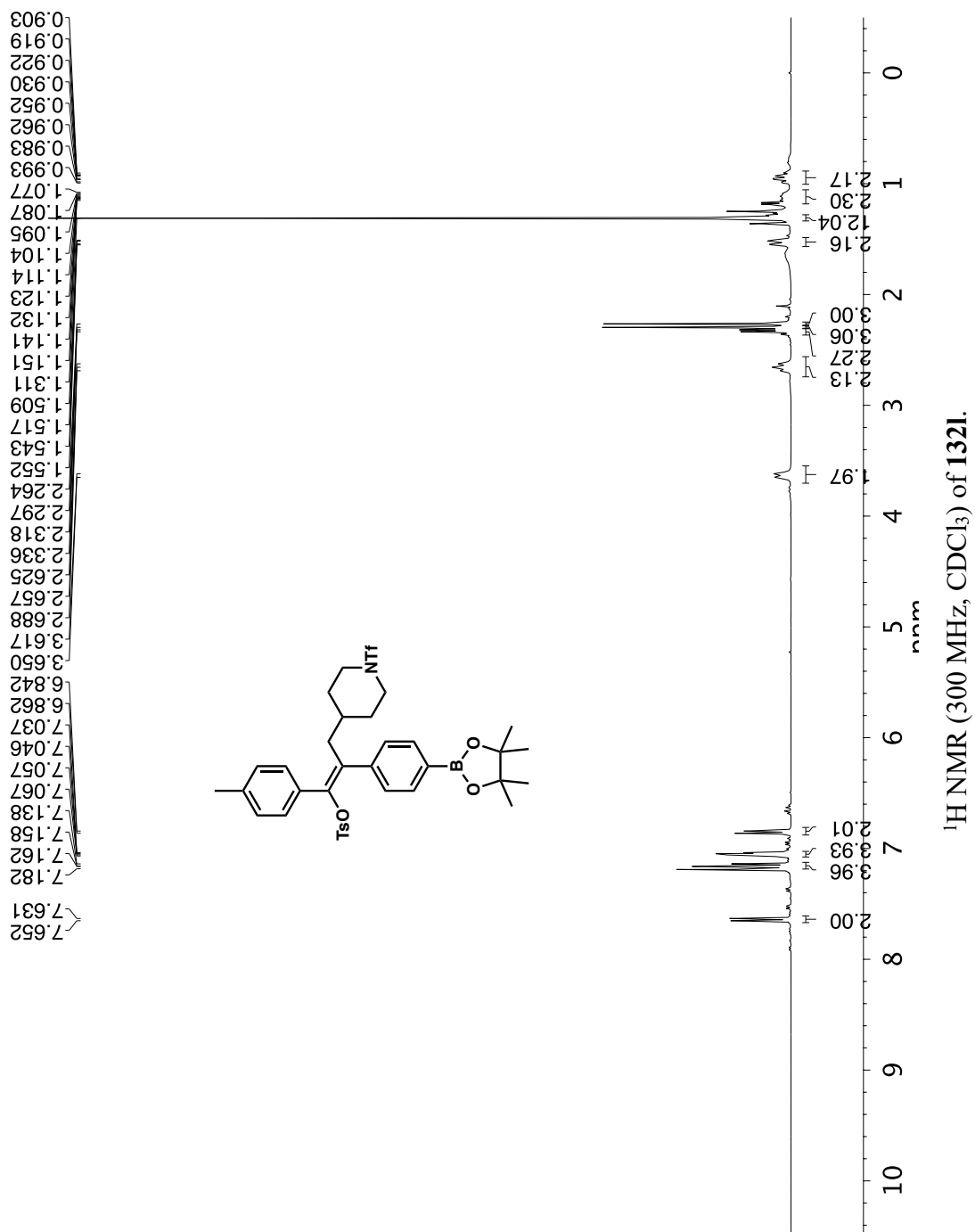


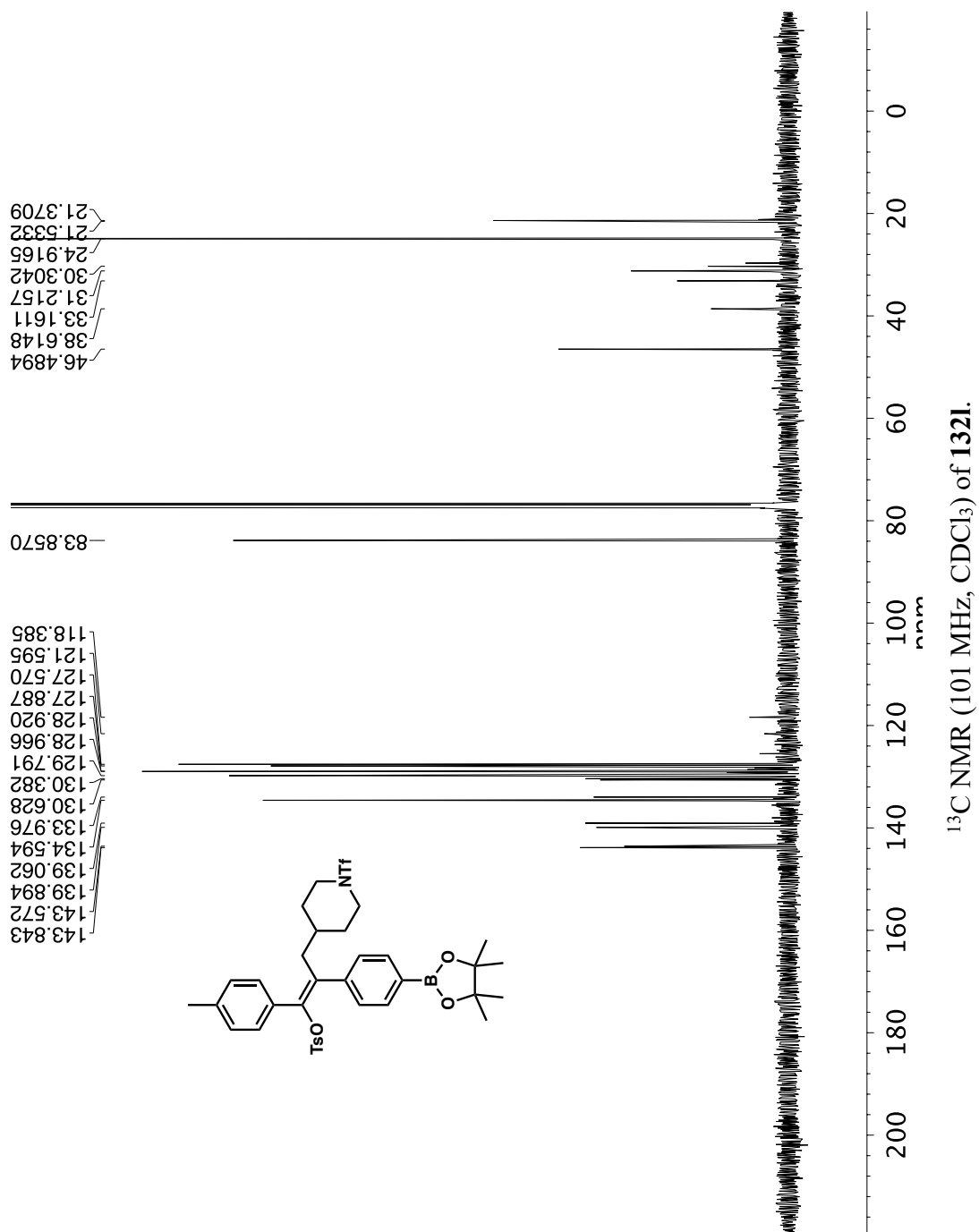
-30.126

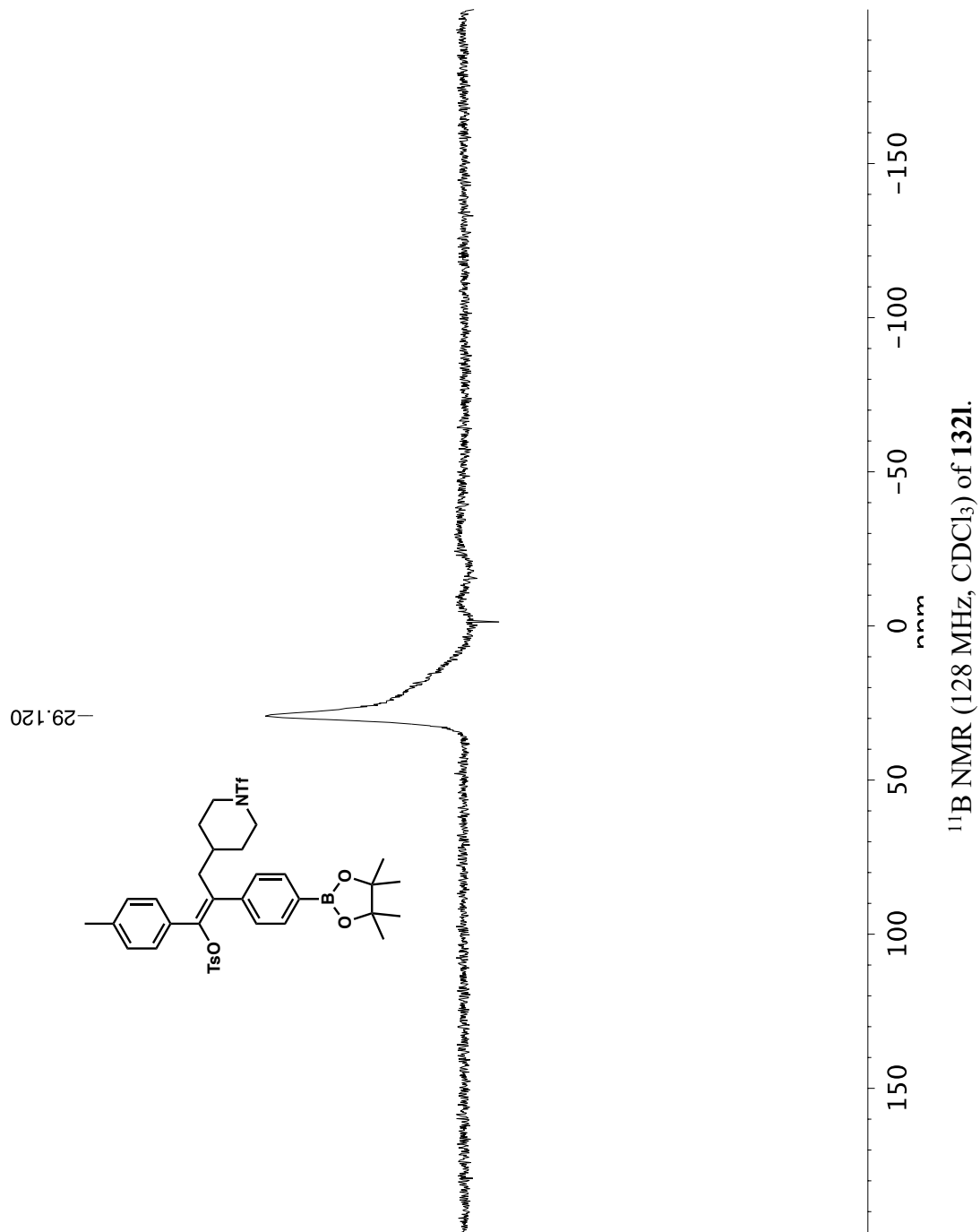
 ^{11}B NMR (128 MHz, CDCl_3) of **267**.

—75.7783

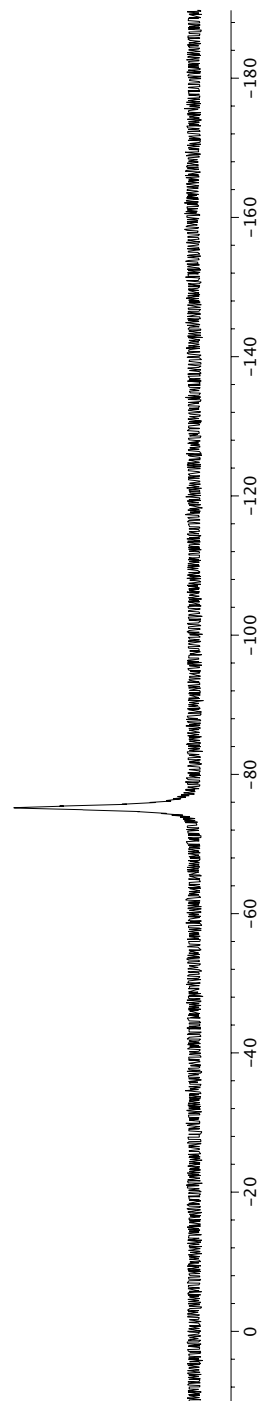
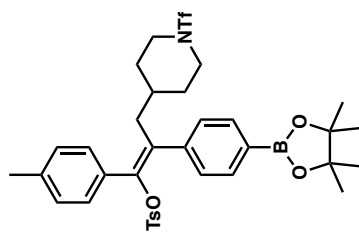




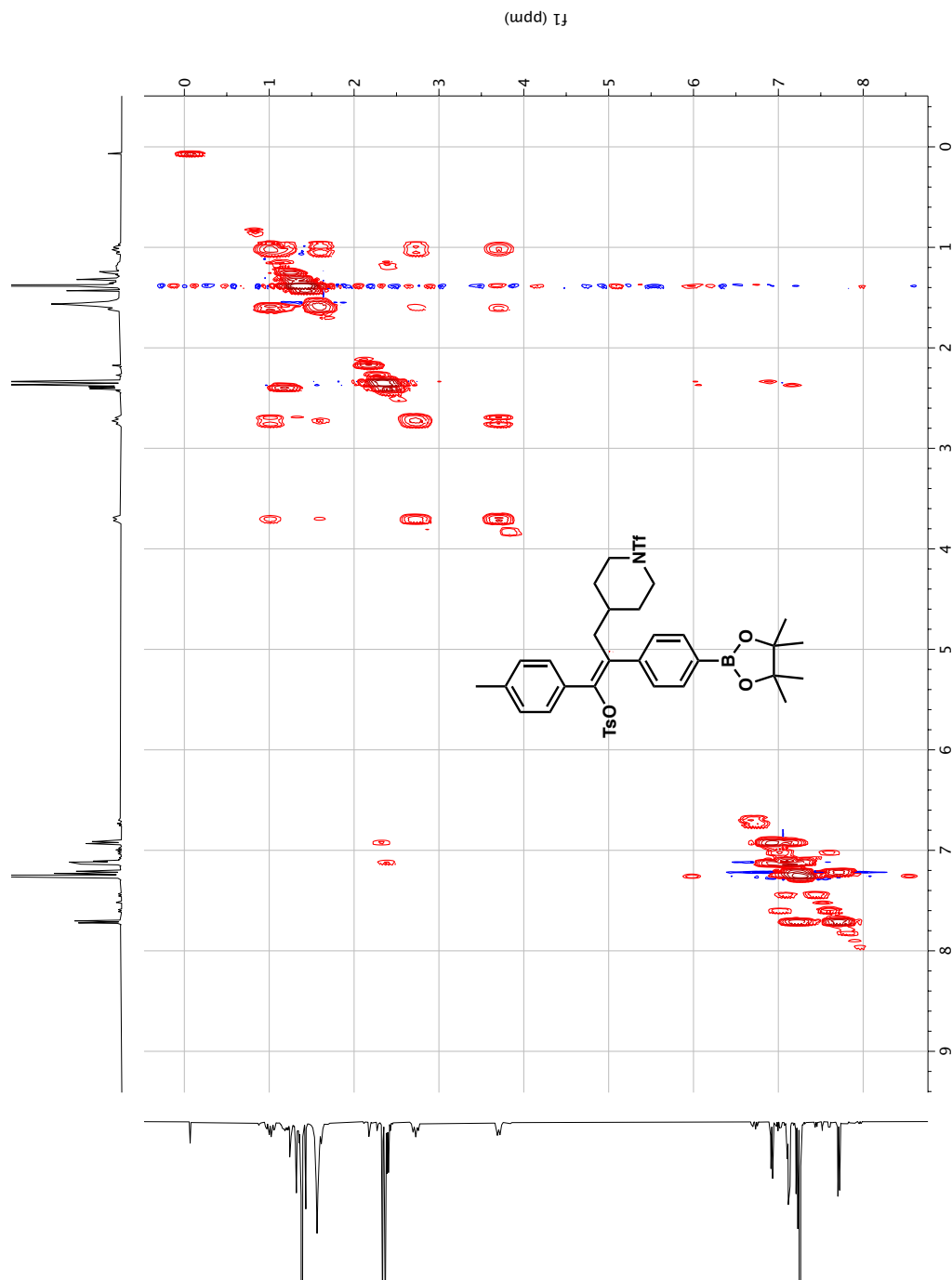


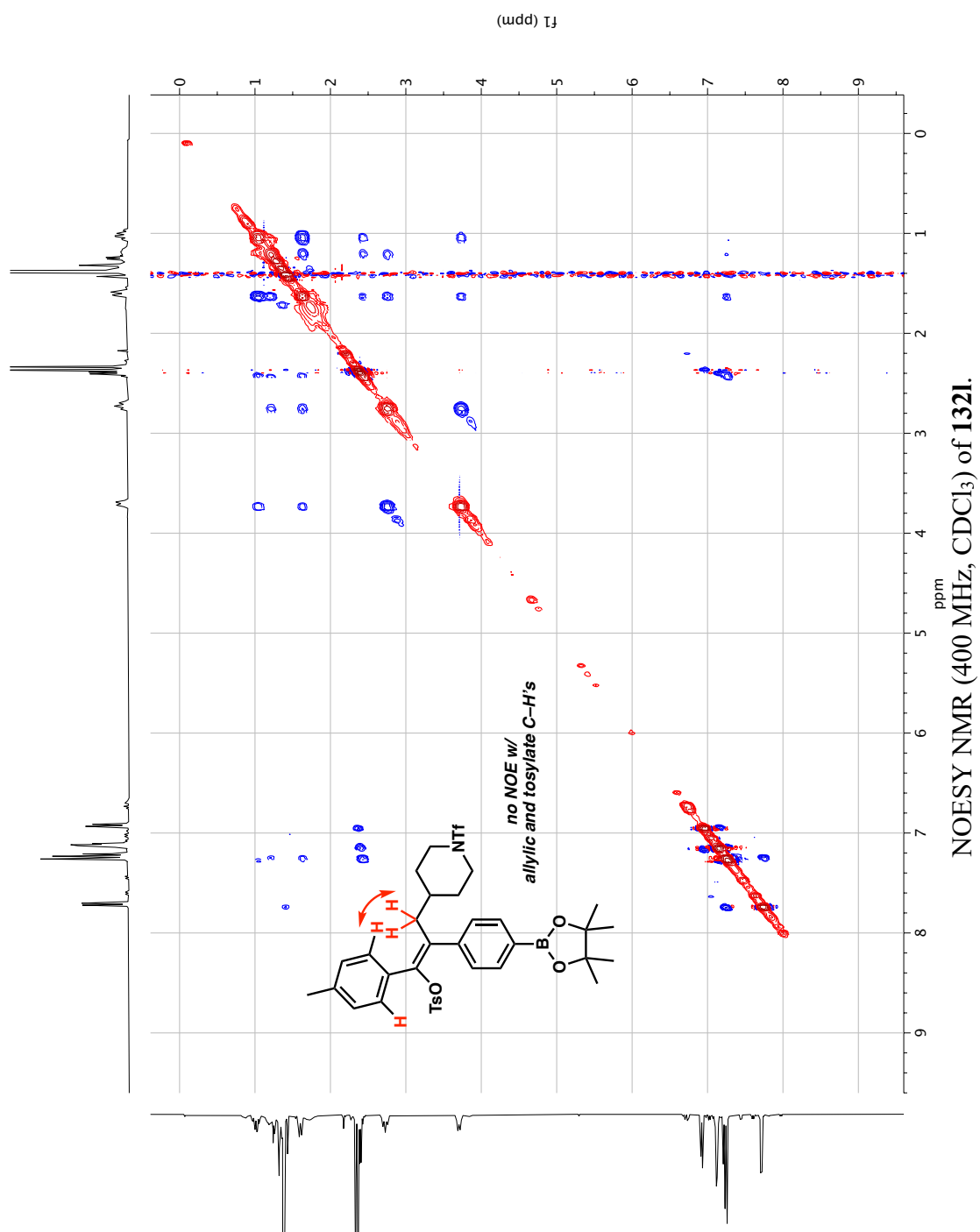


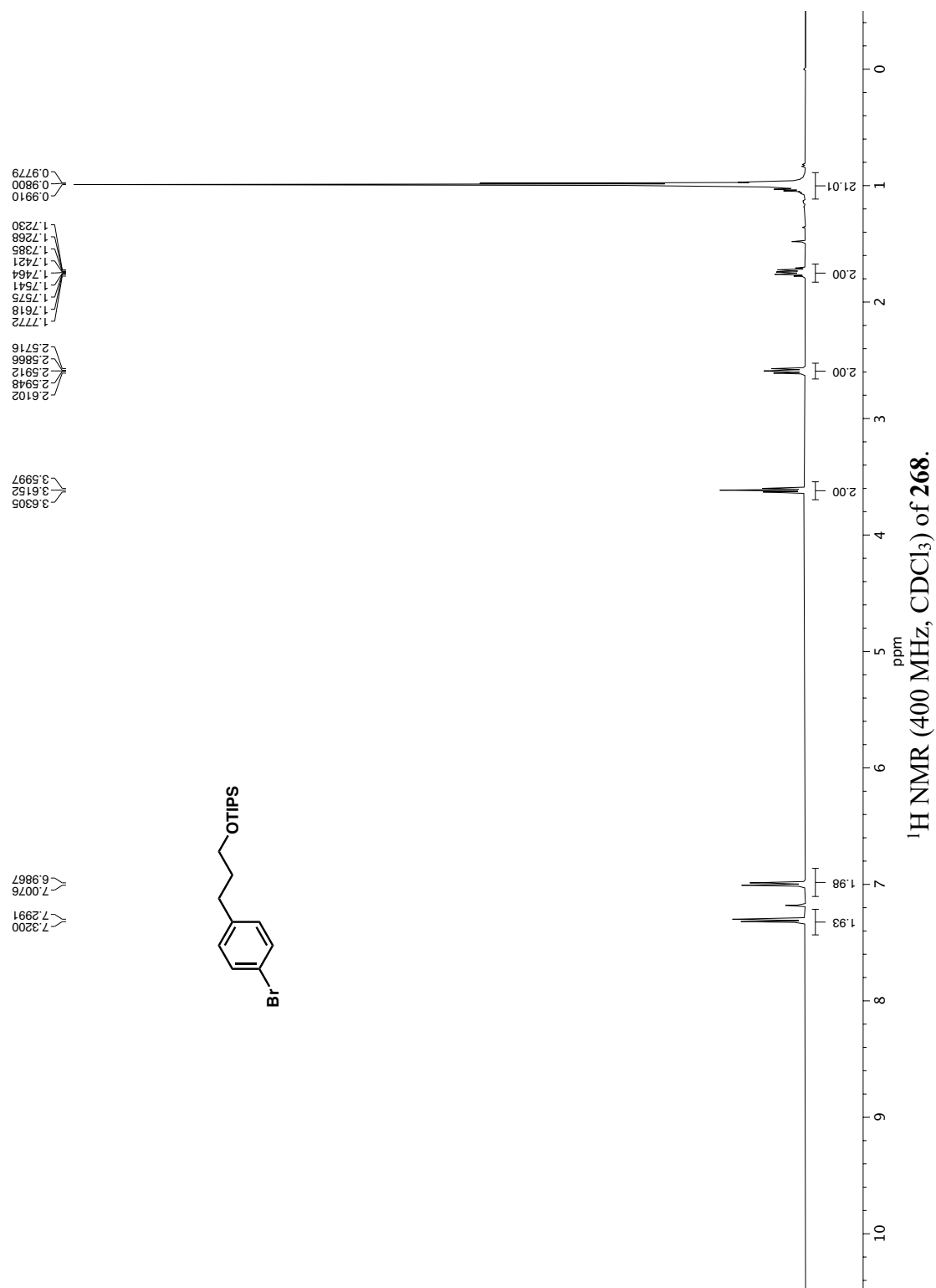
—75.2348

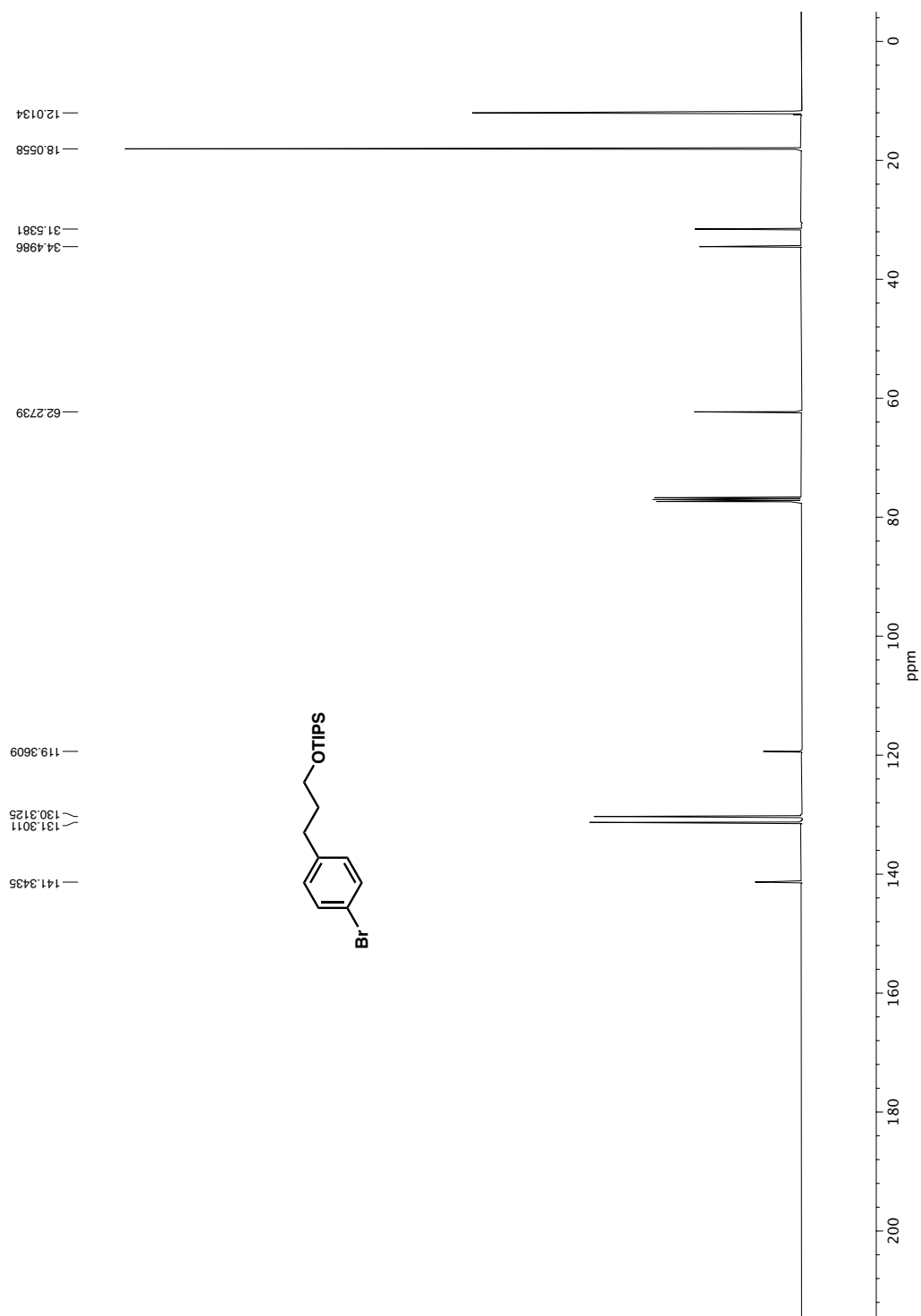


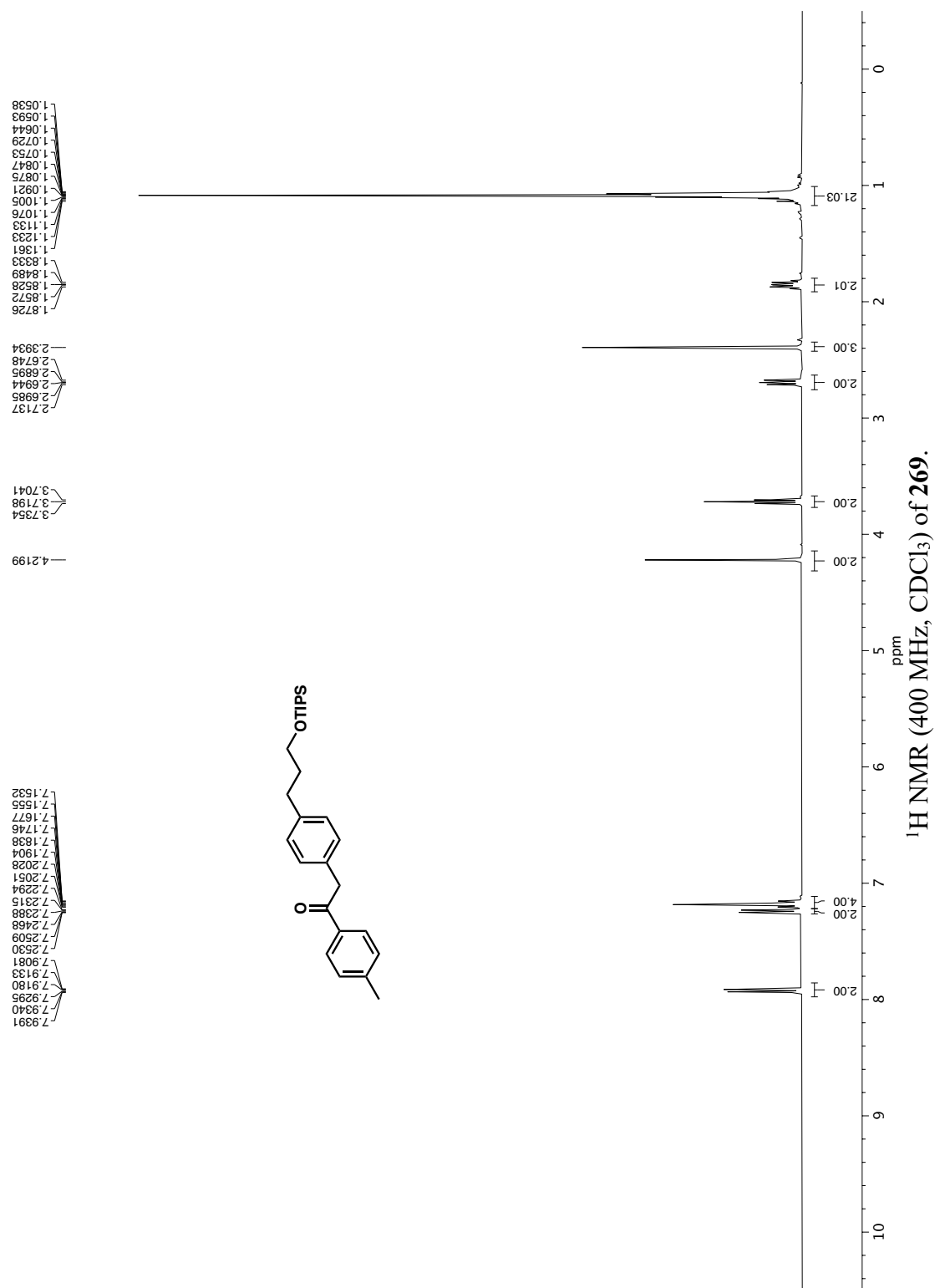
^{19}F NMR (376 MHz, CDCl_3) of **132i**.

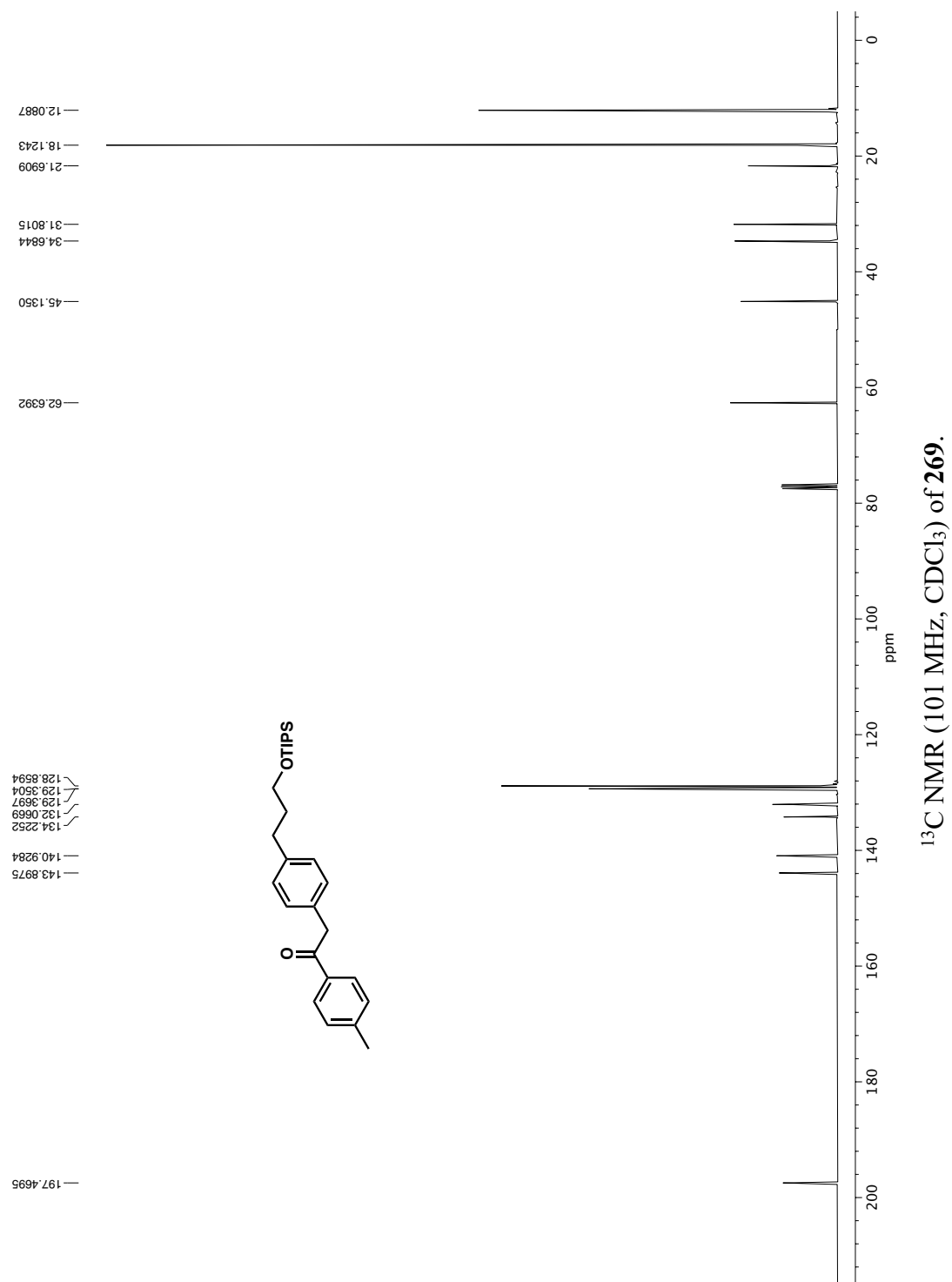


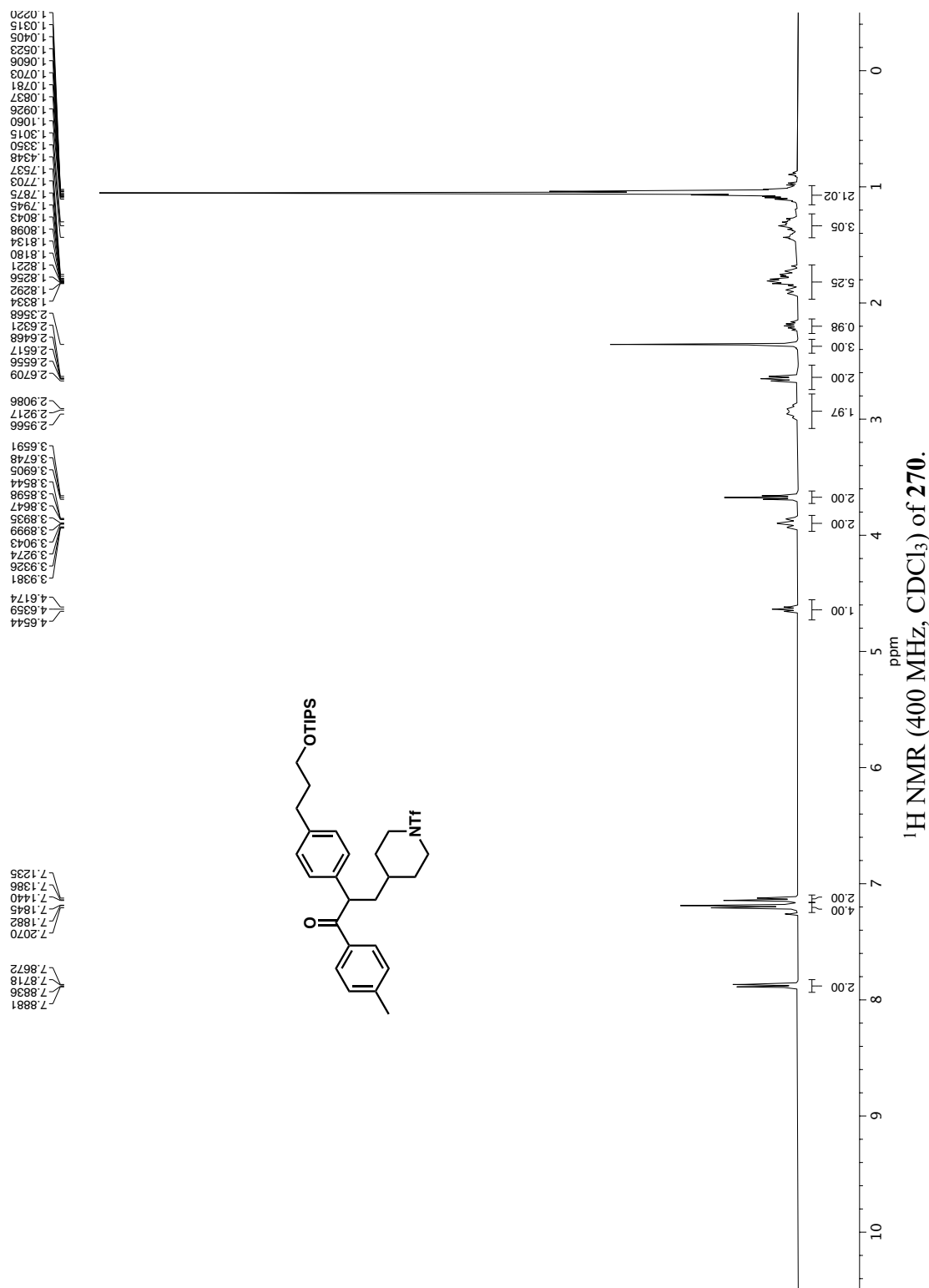


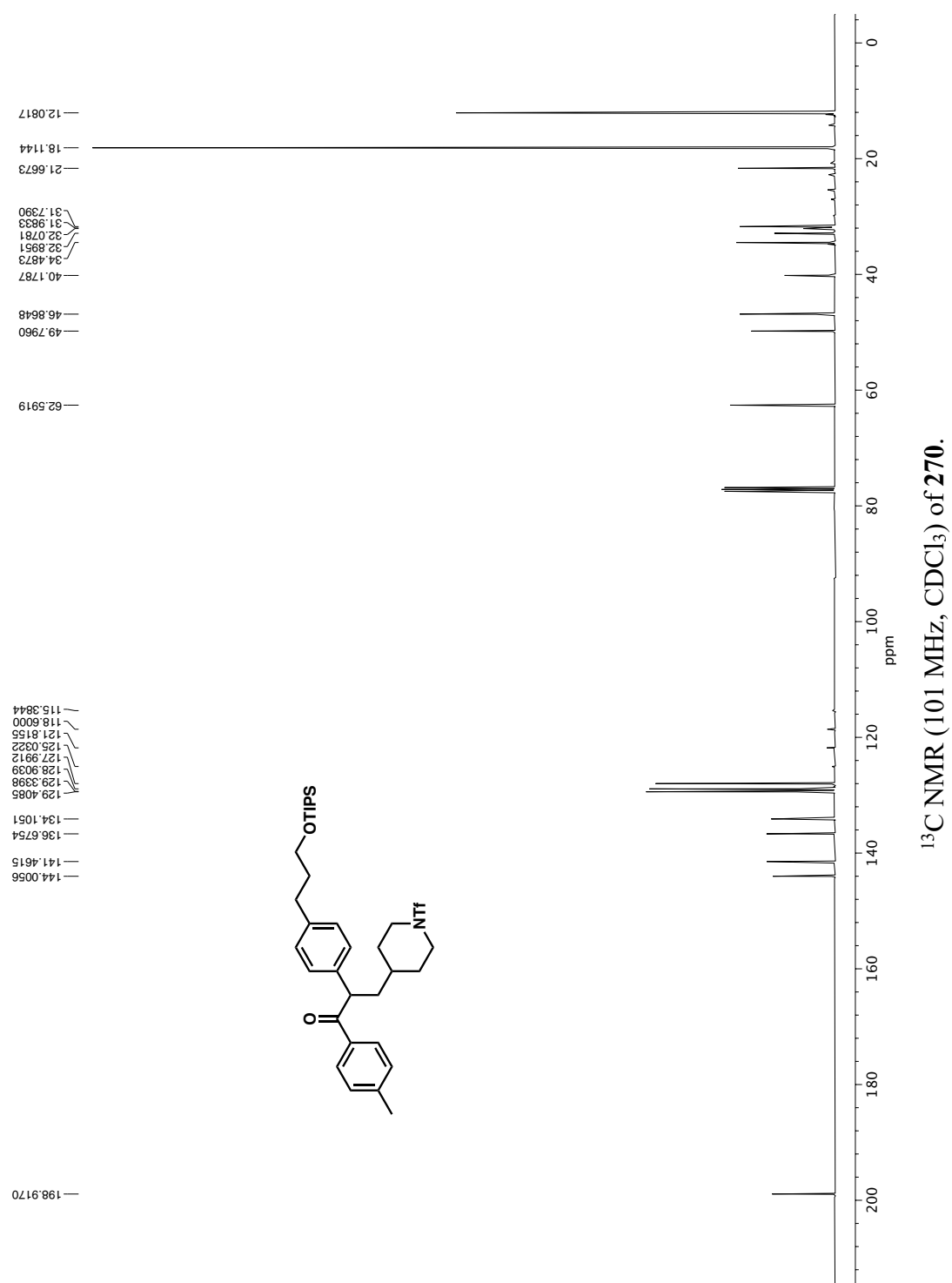




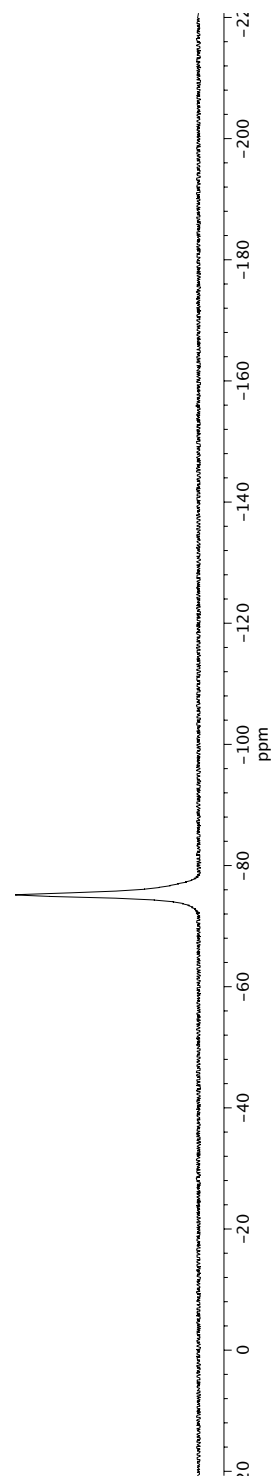
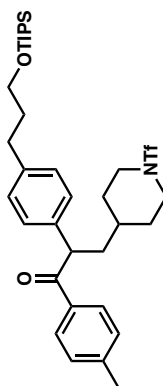


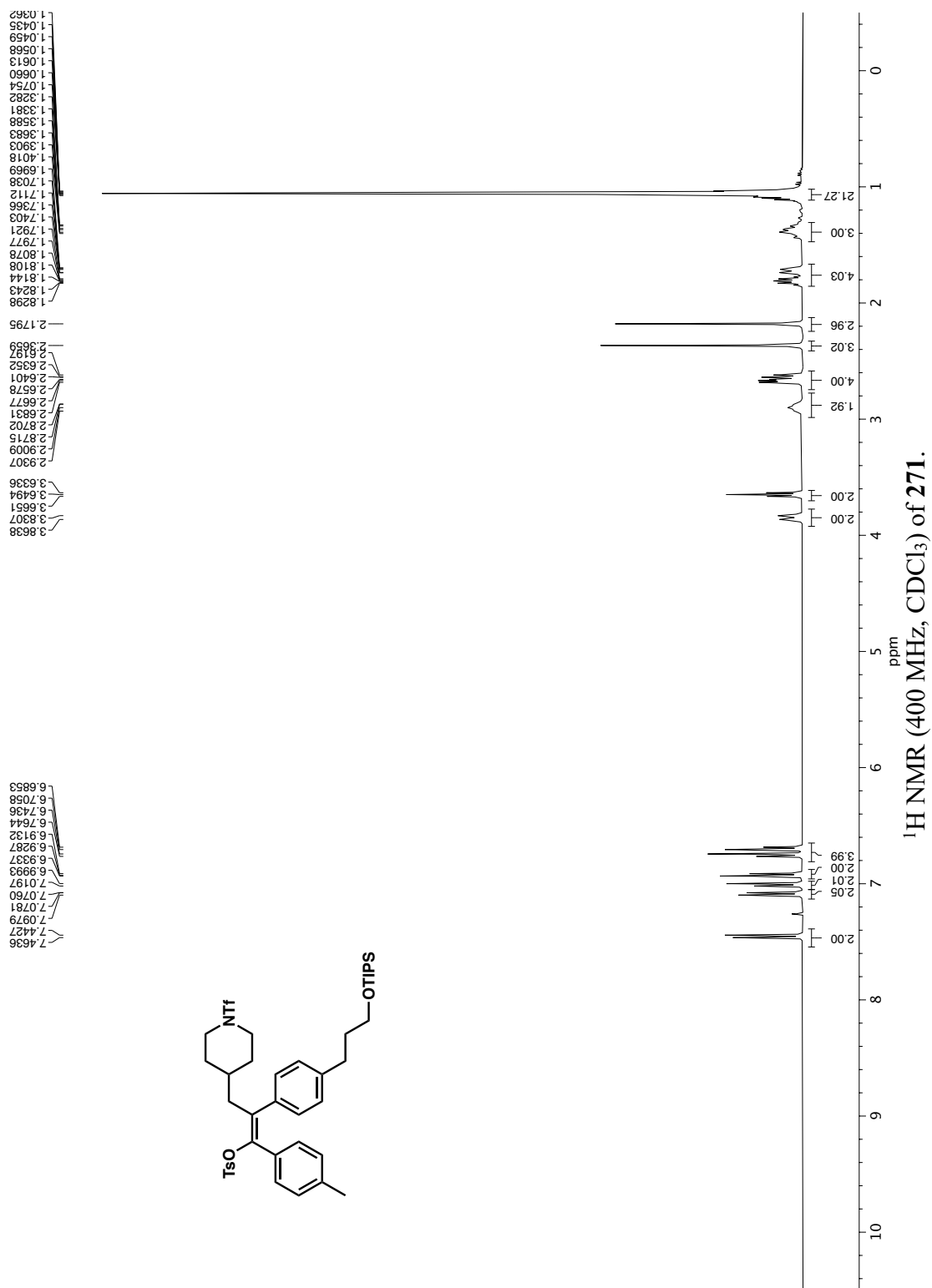


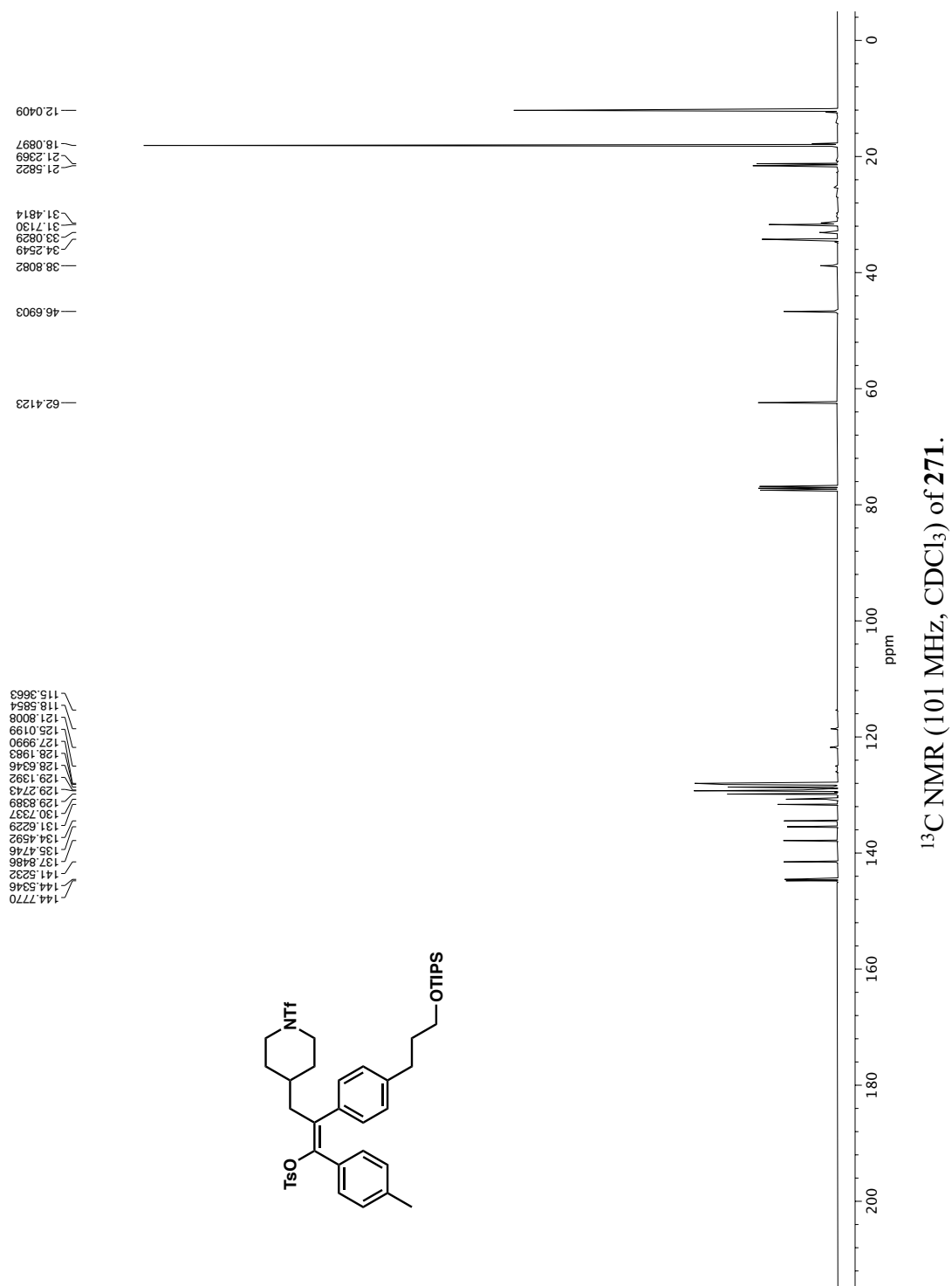




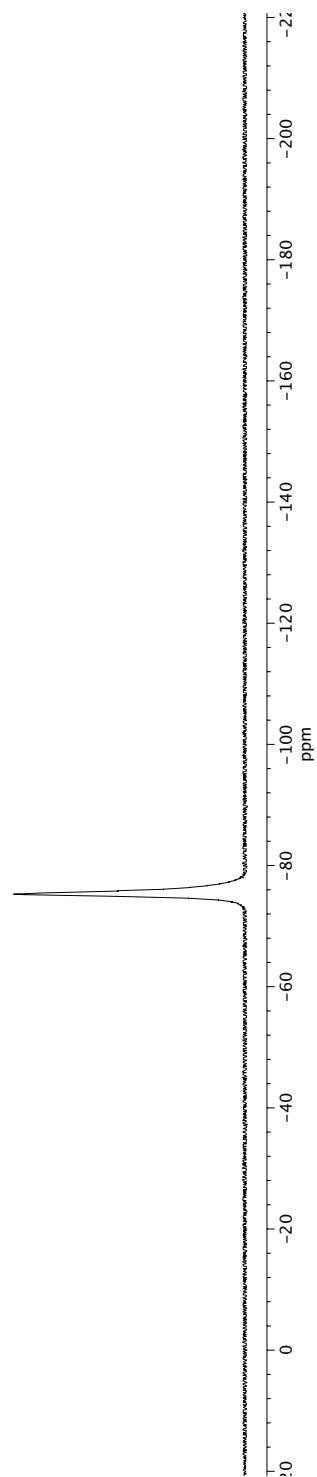
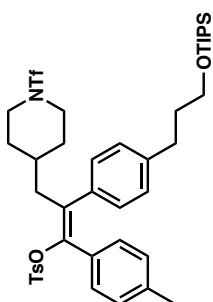
-75.1513

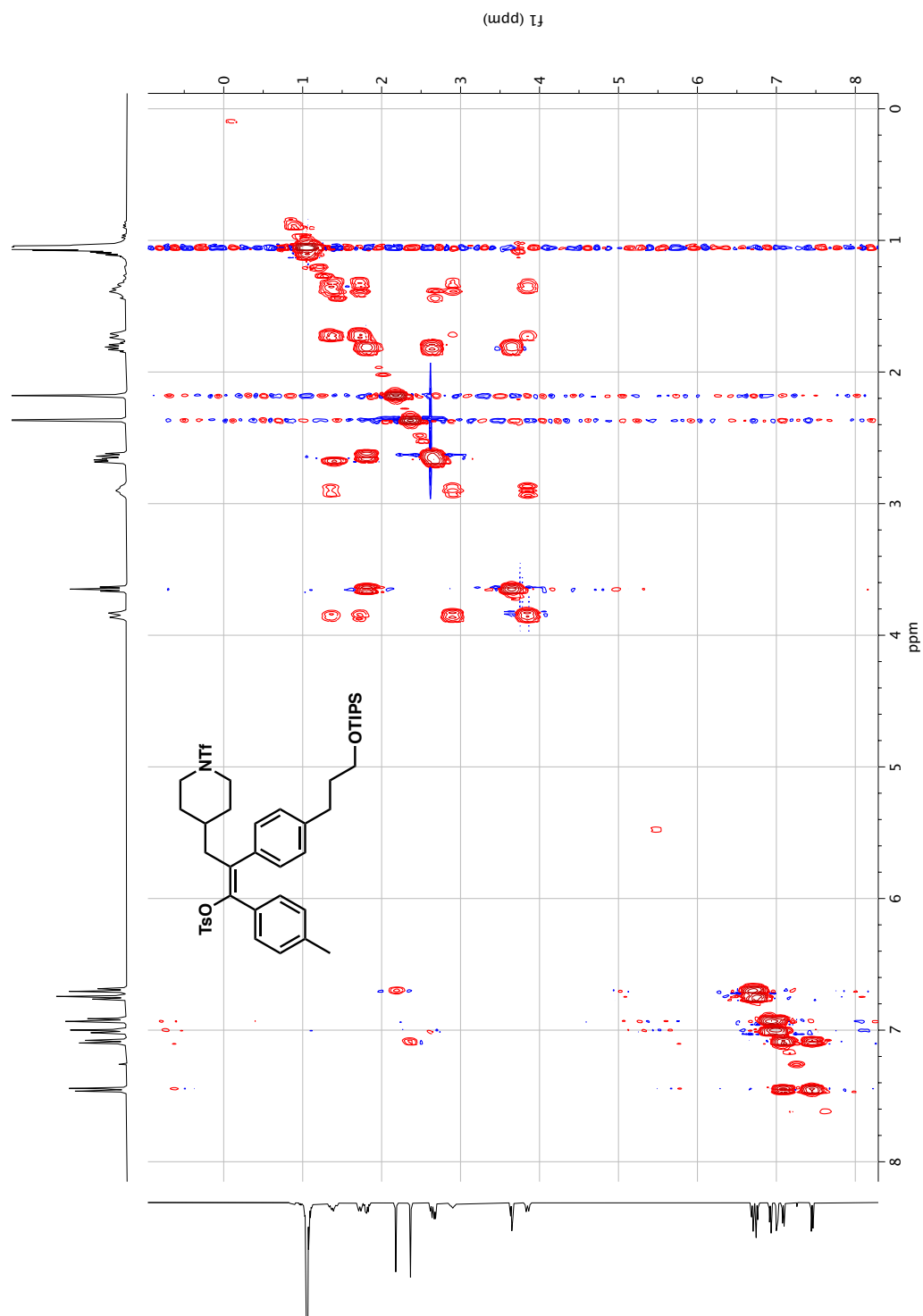
 ^{19}F NMR (376 MHz, CDCl_3) of **270**.

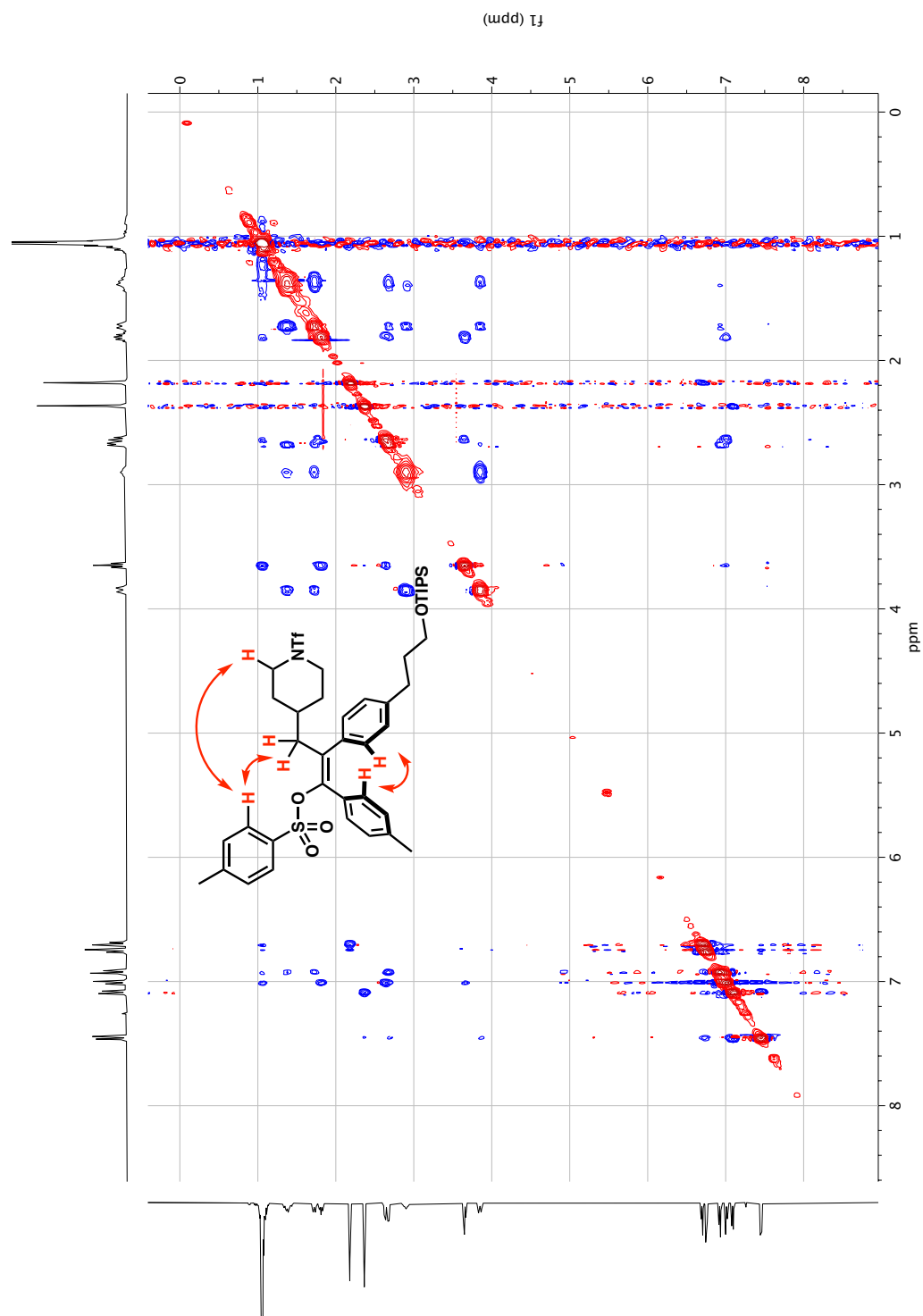


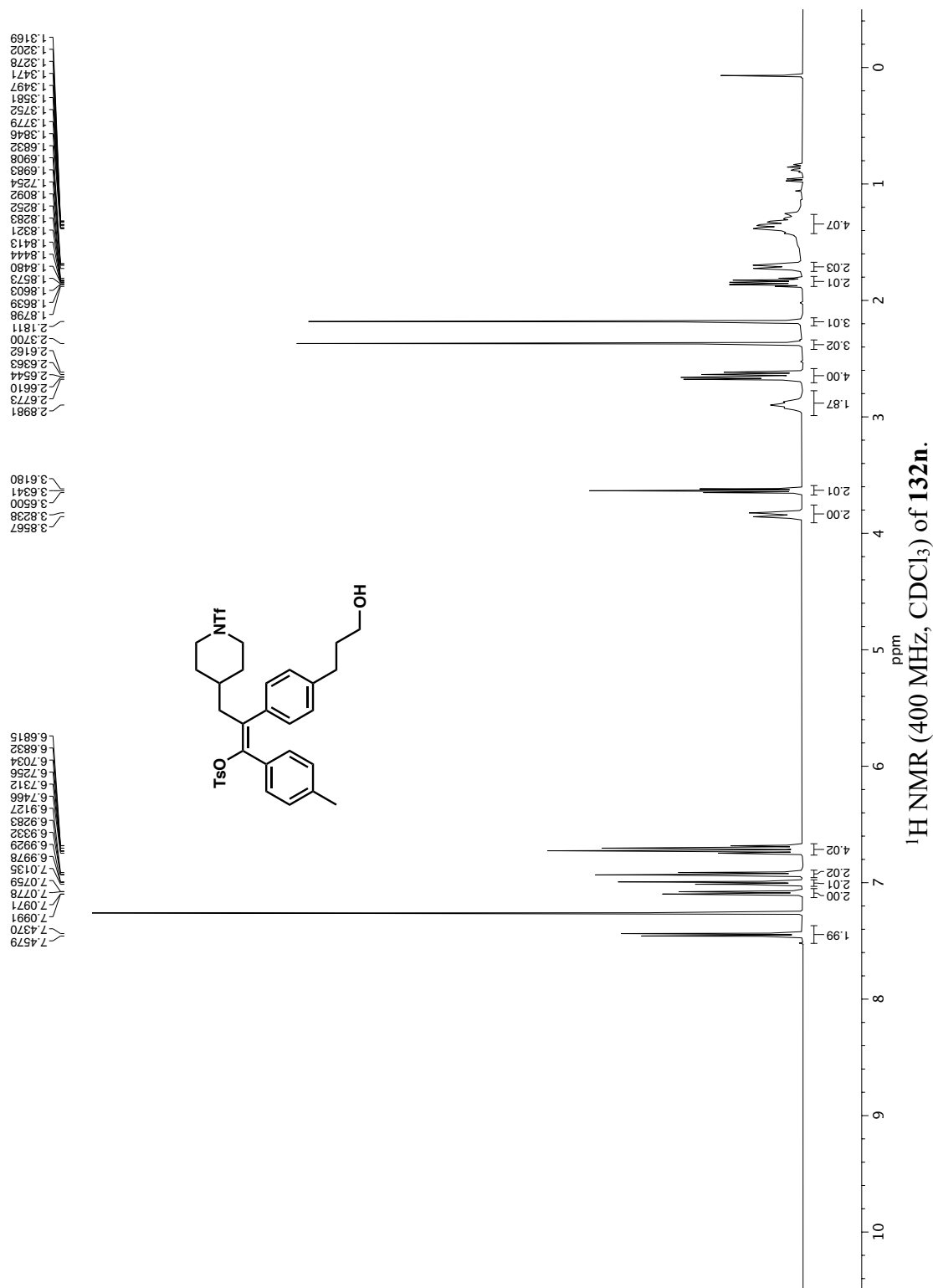


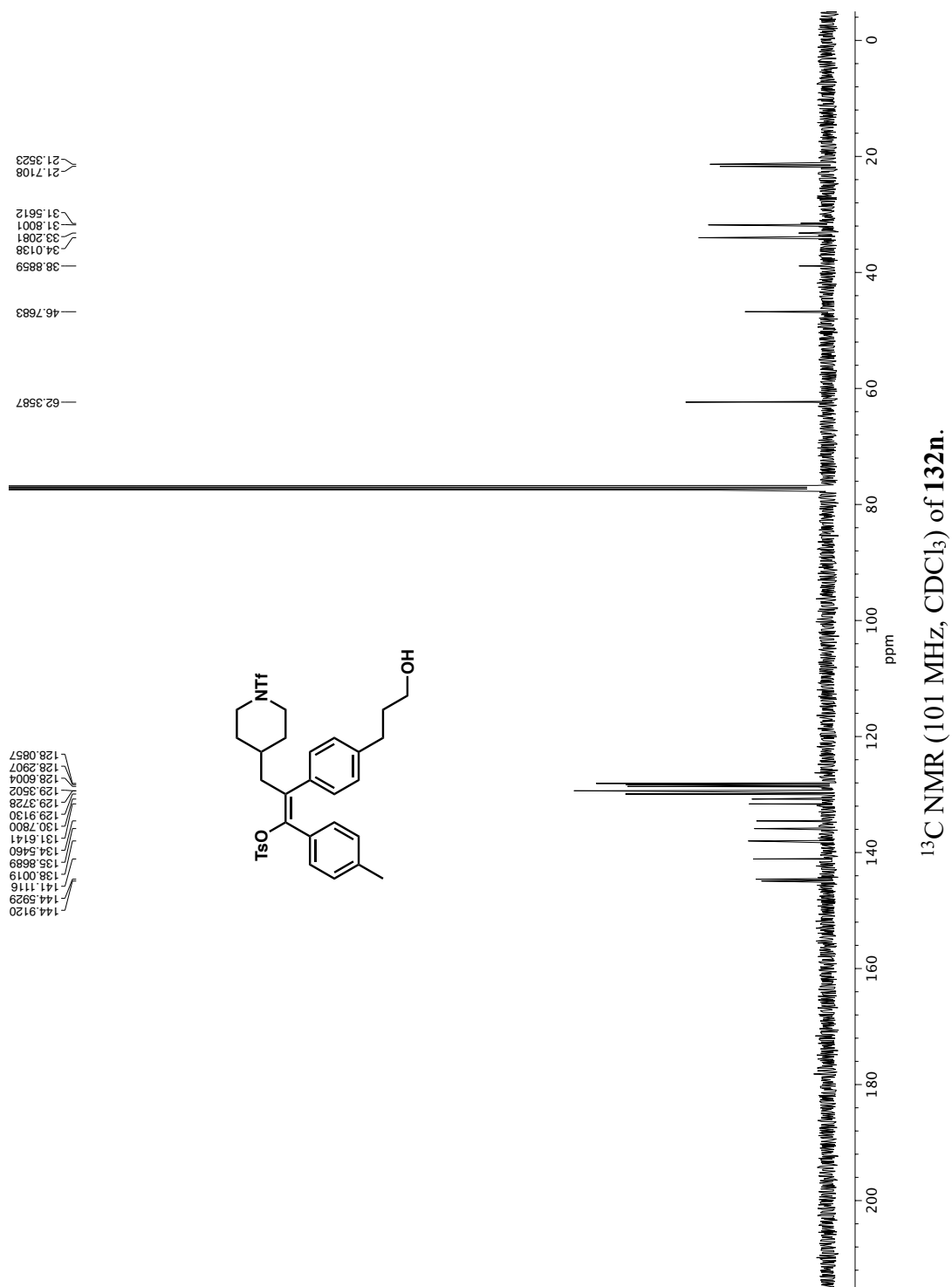
-75.3212

 ^{19}F NMR (376 MHz, CDCl_3) of **271**.

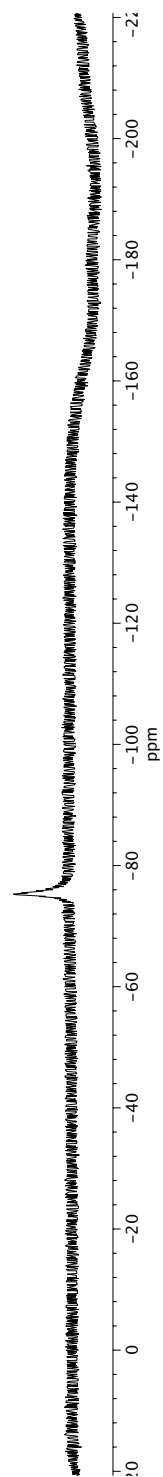
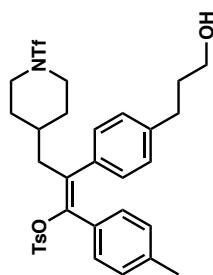


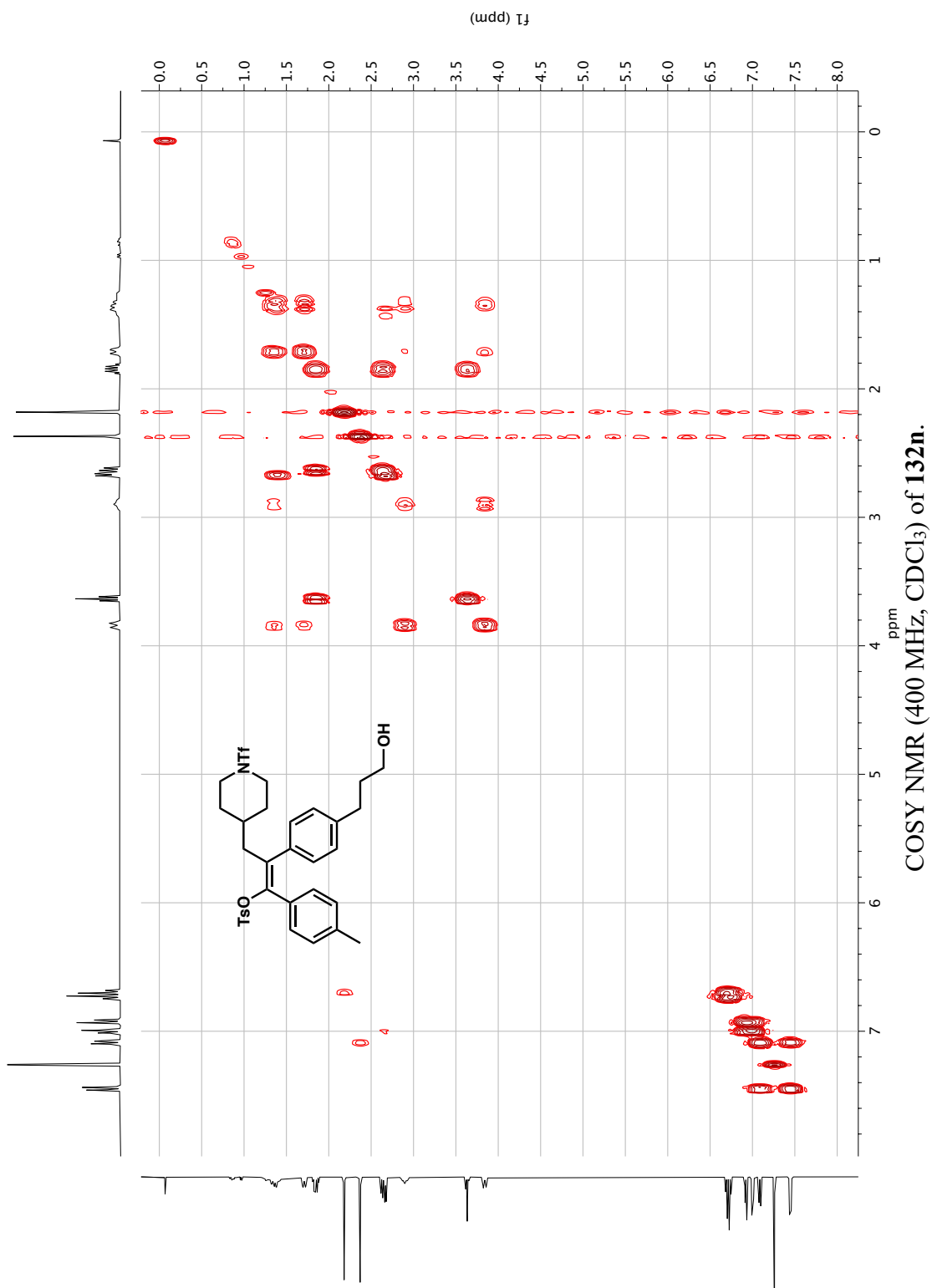


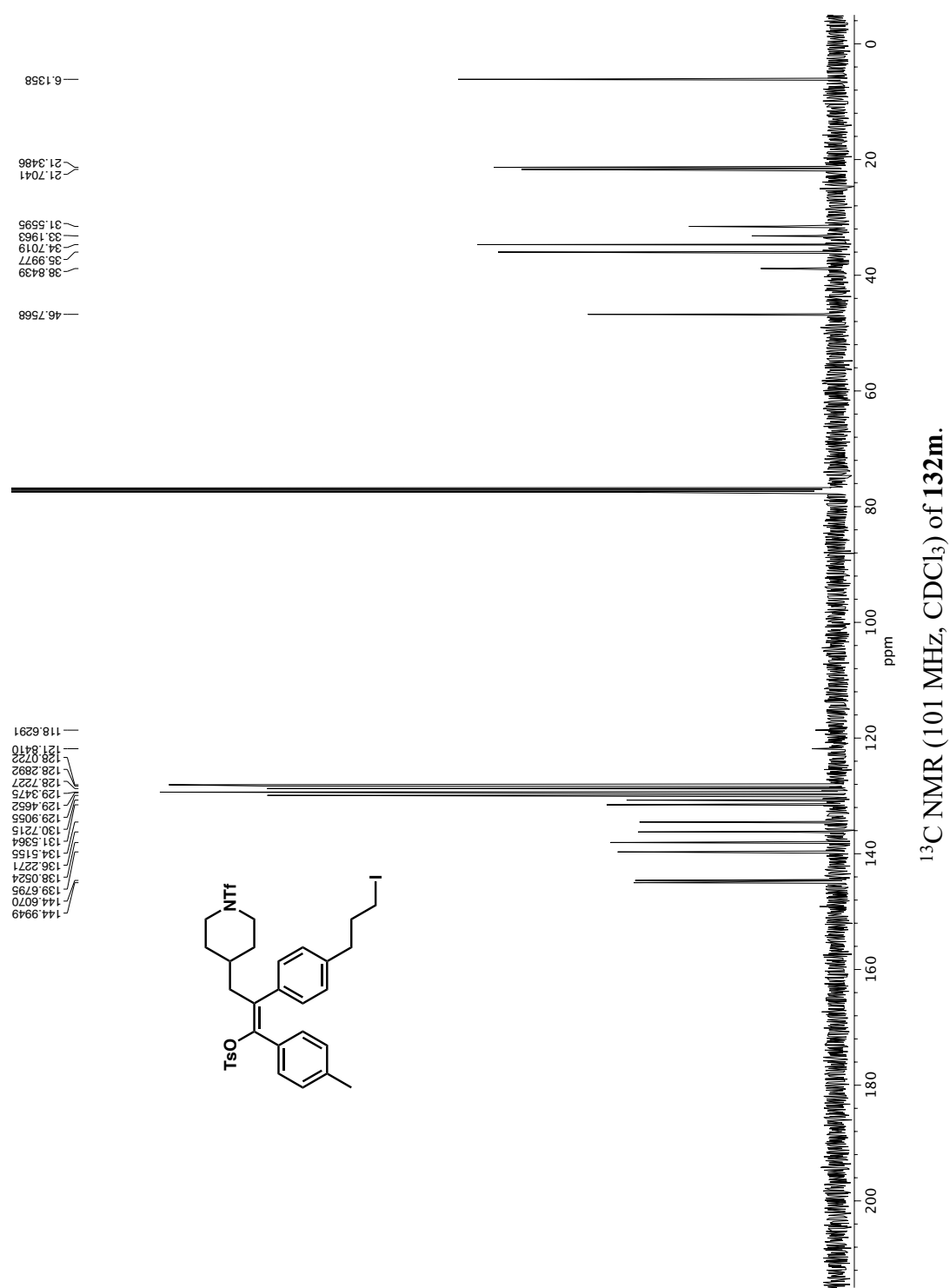




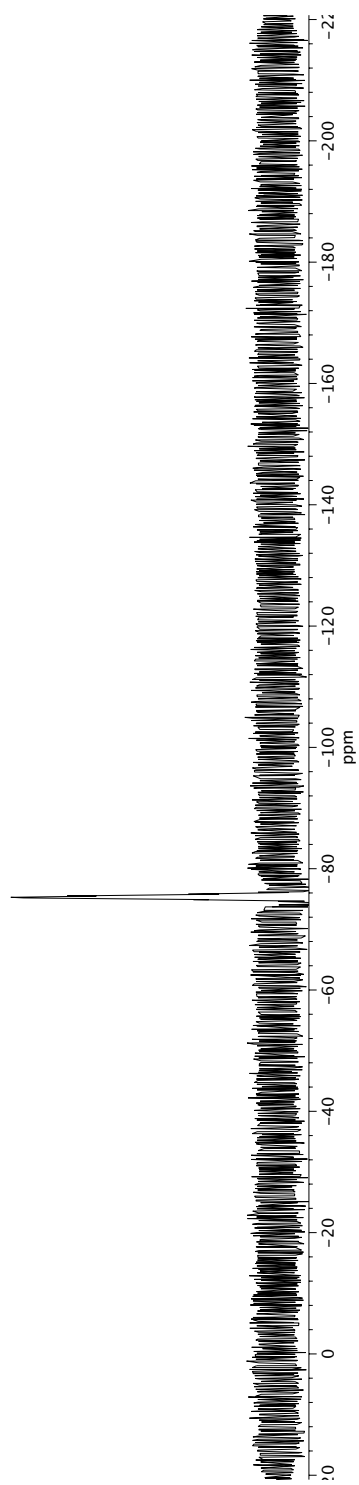
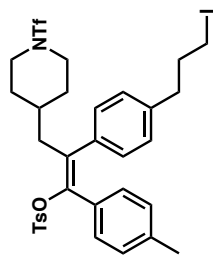
-75.3252

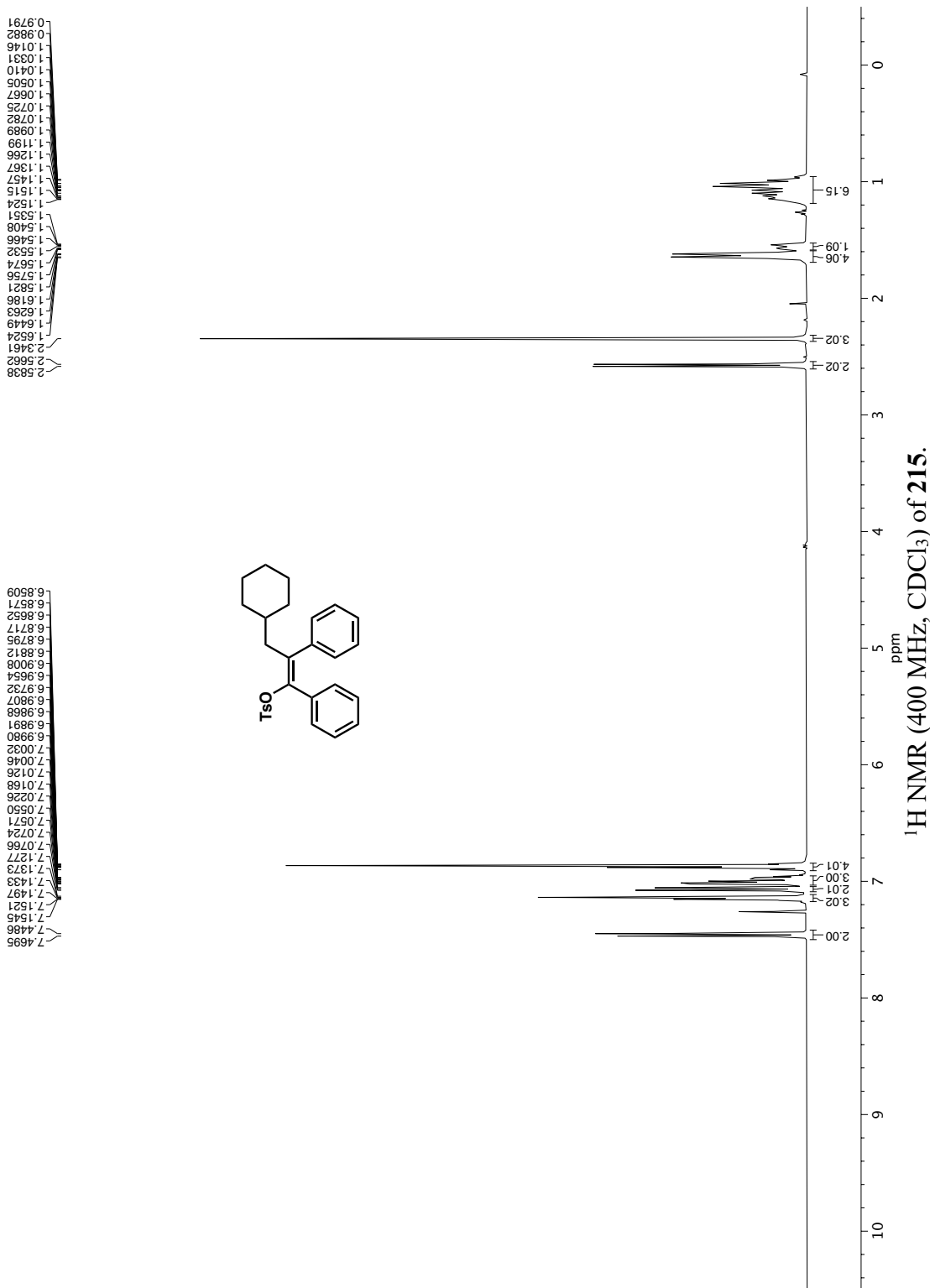
 ^{19}F NMR (376 MHz, CDCl_3) of **132n**.

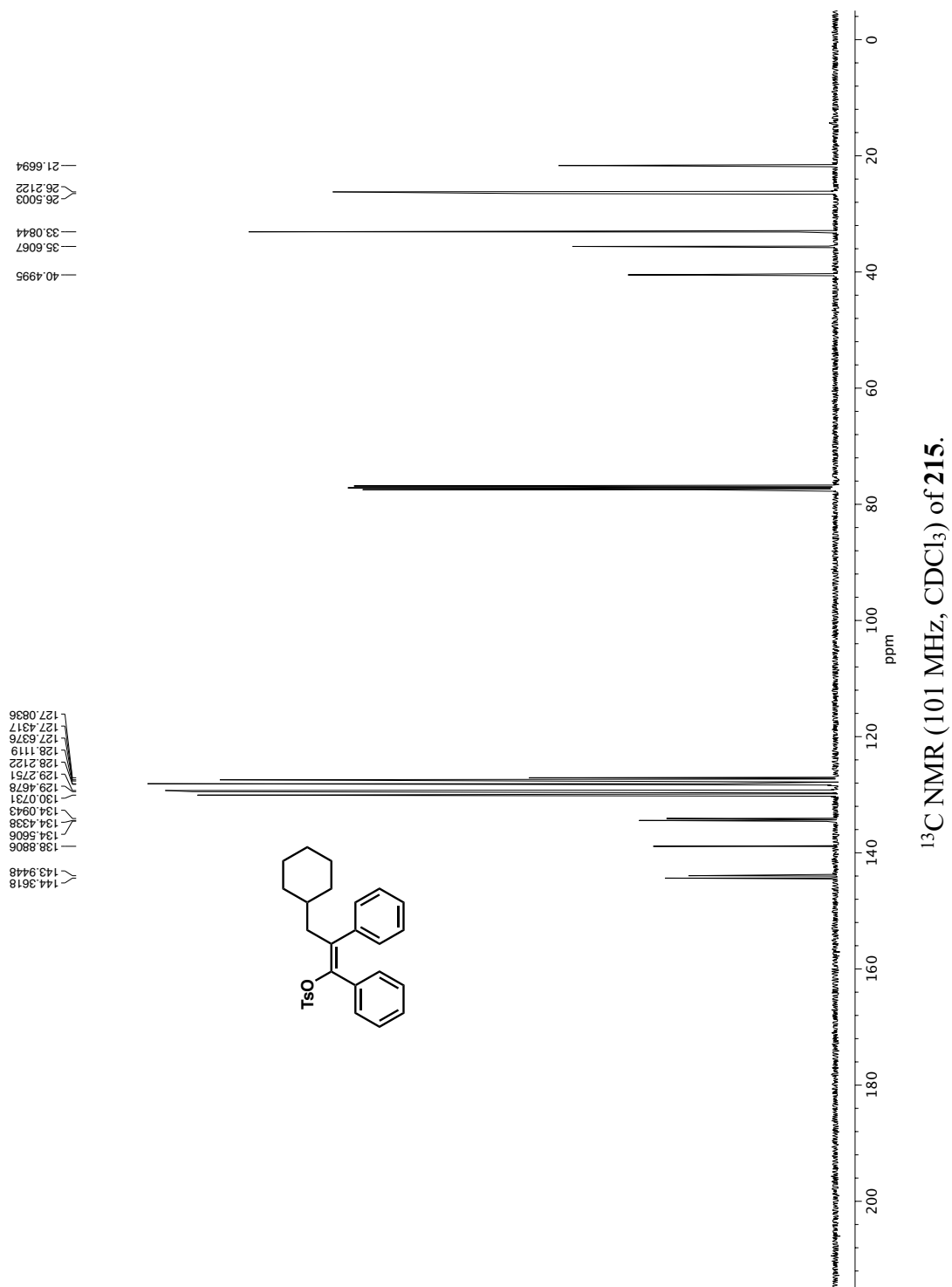


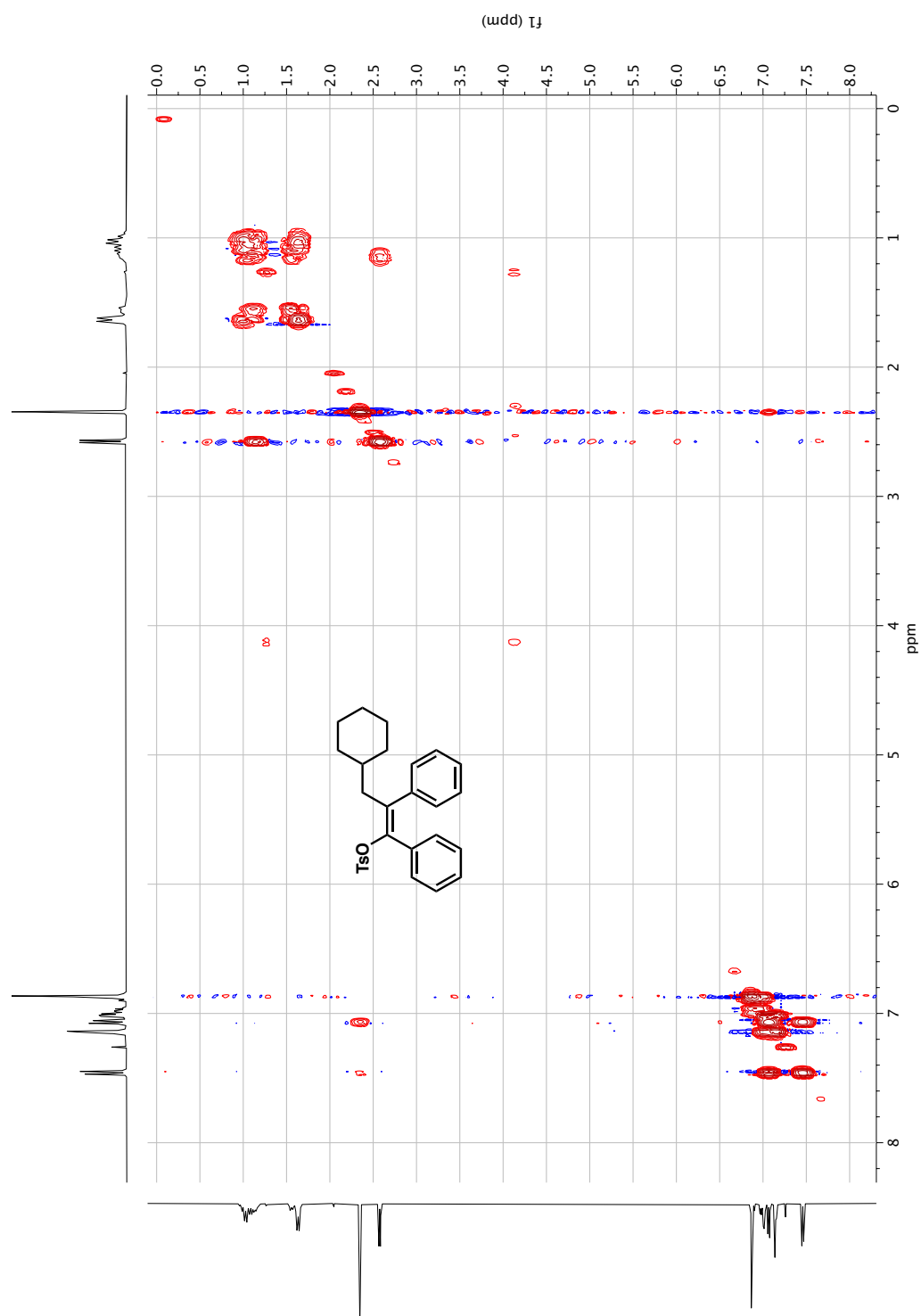


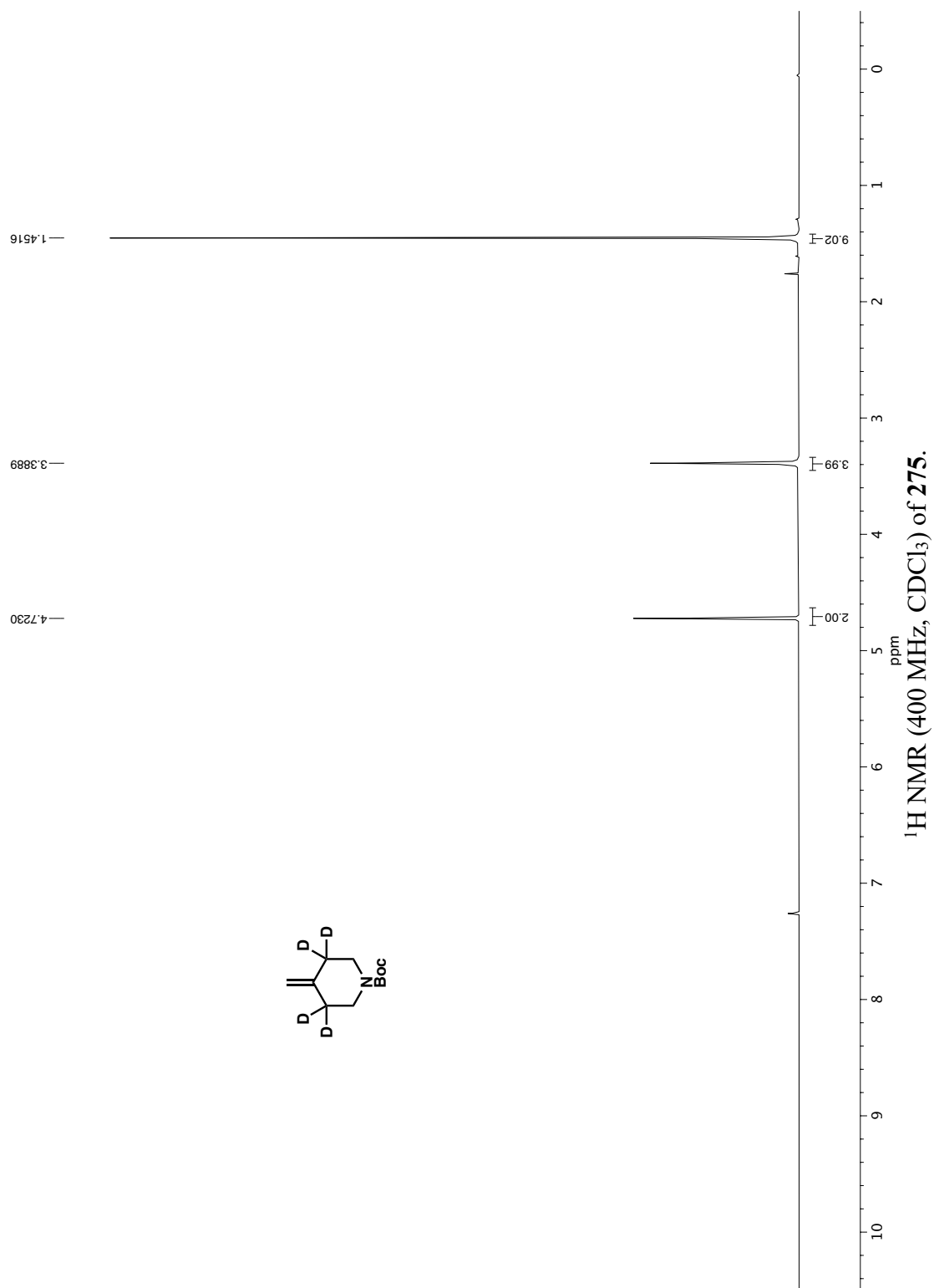
—75.2846

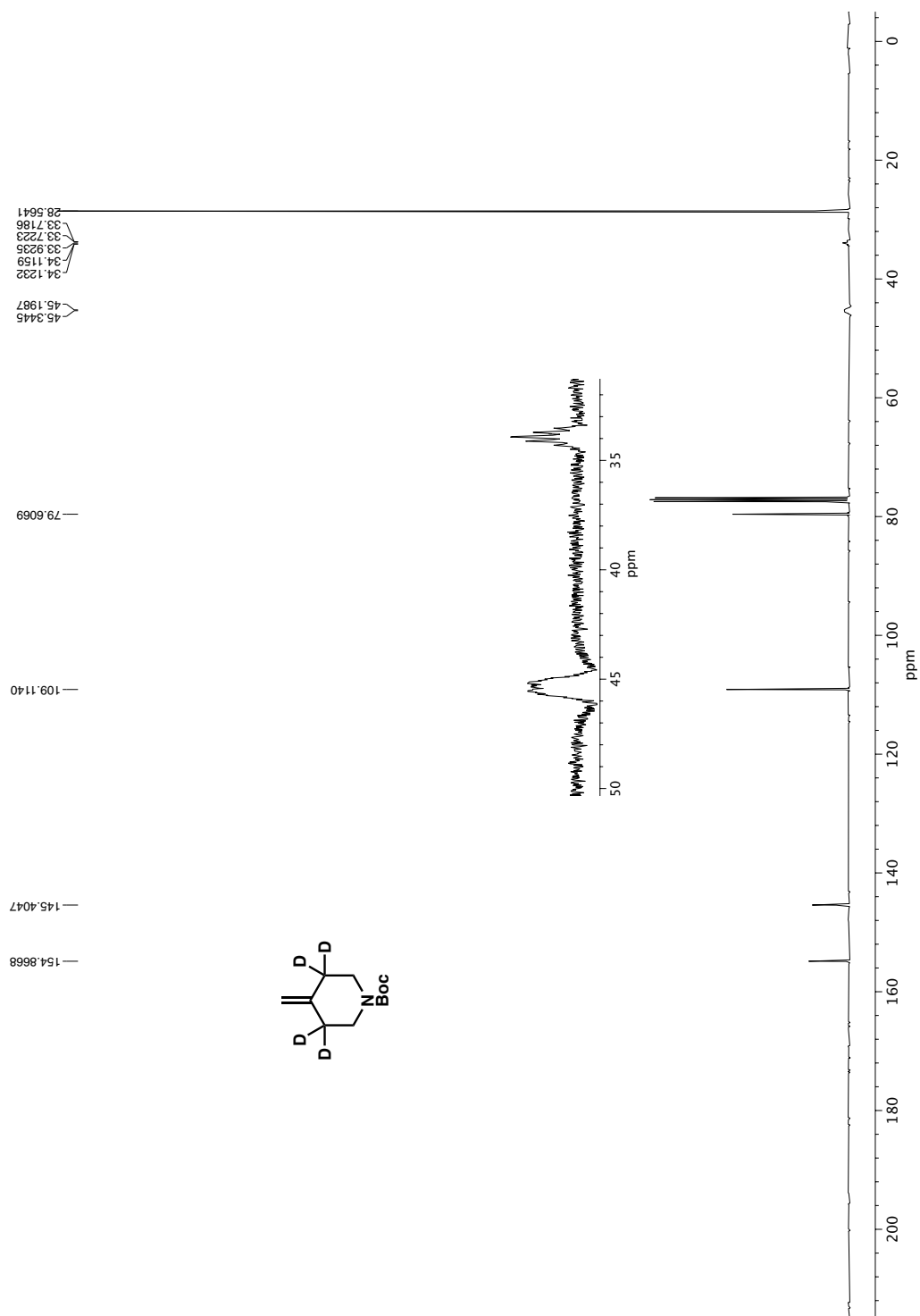
 ^{19}F NMR (376 MHz, CDCl_3) of **132m**.

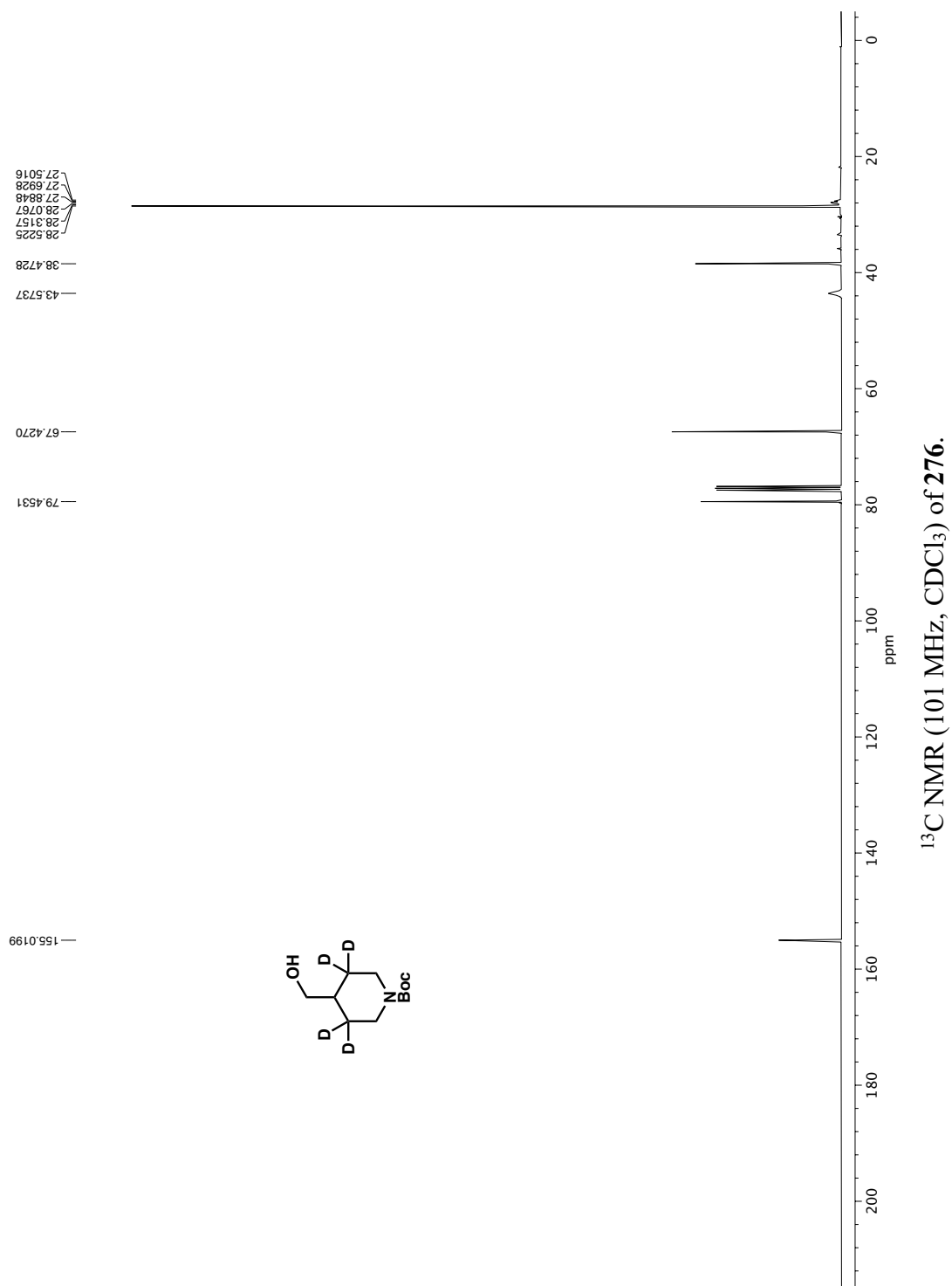


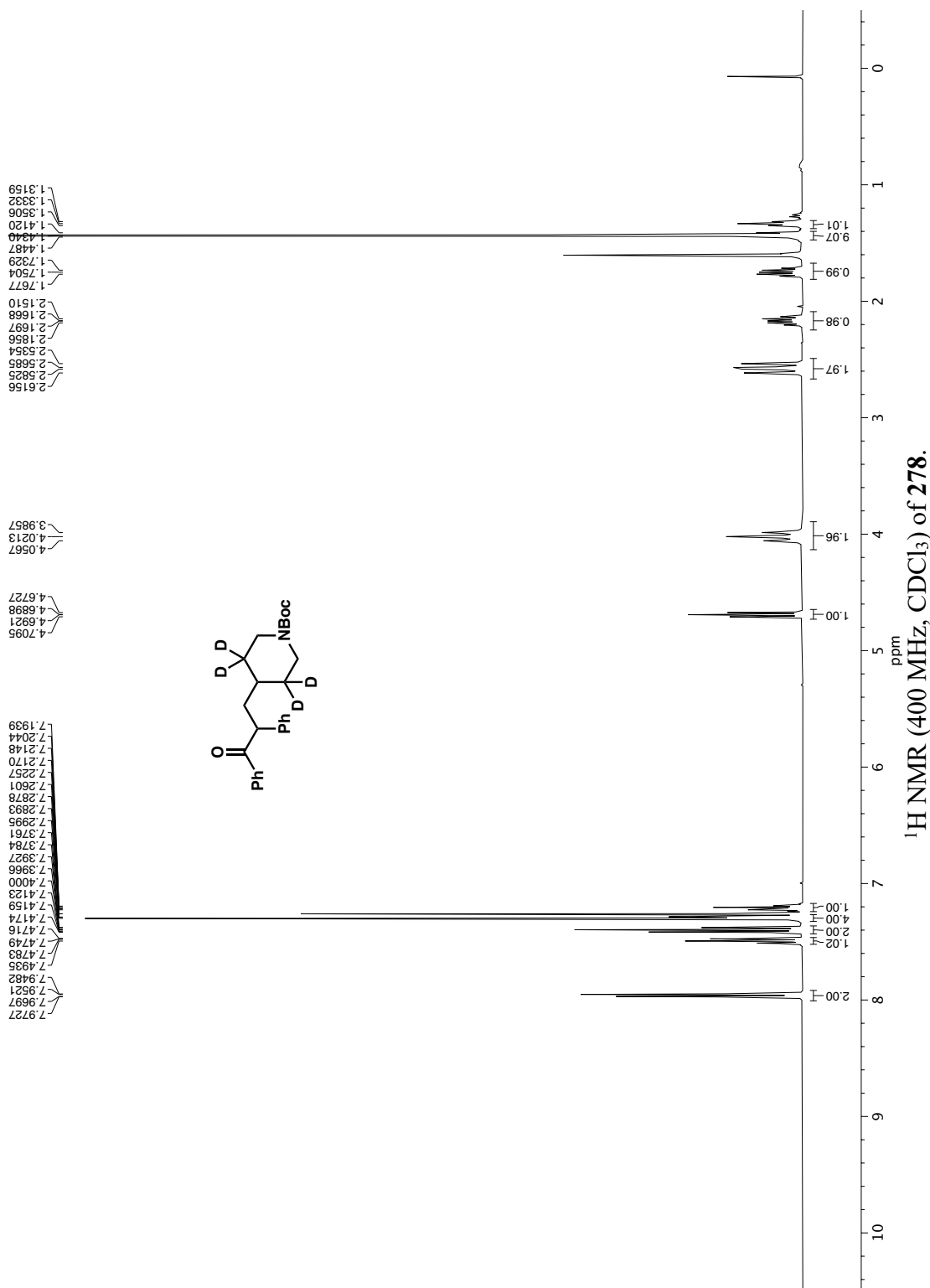


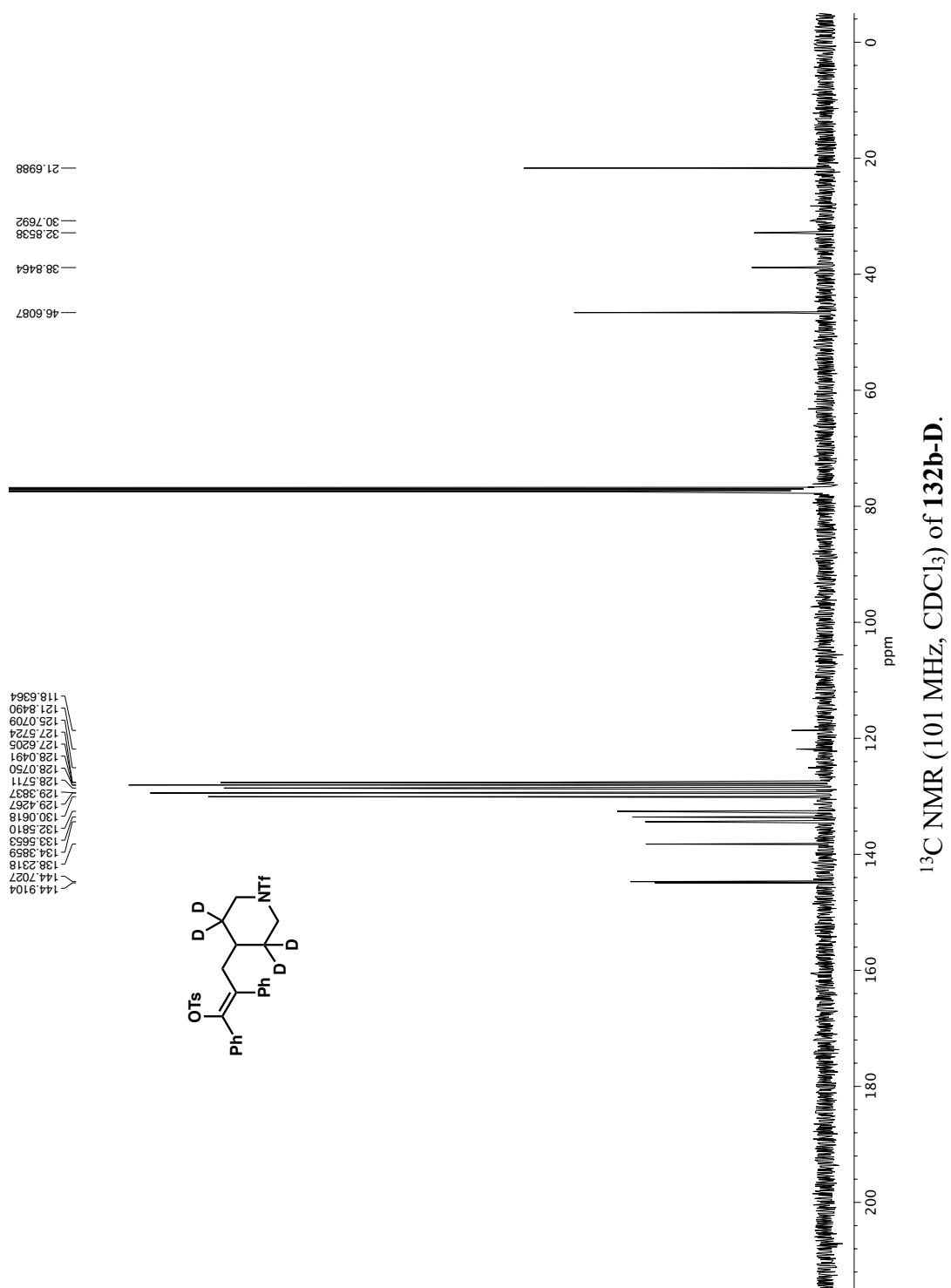




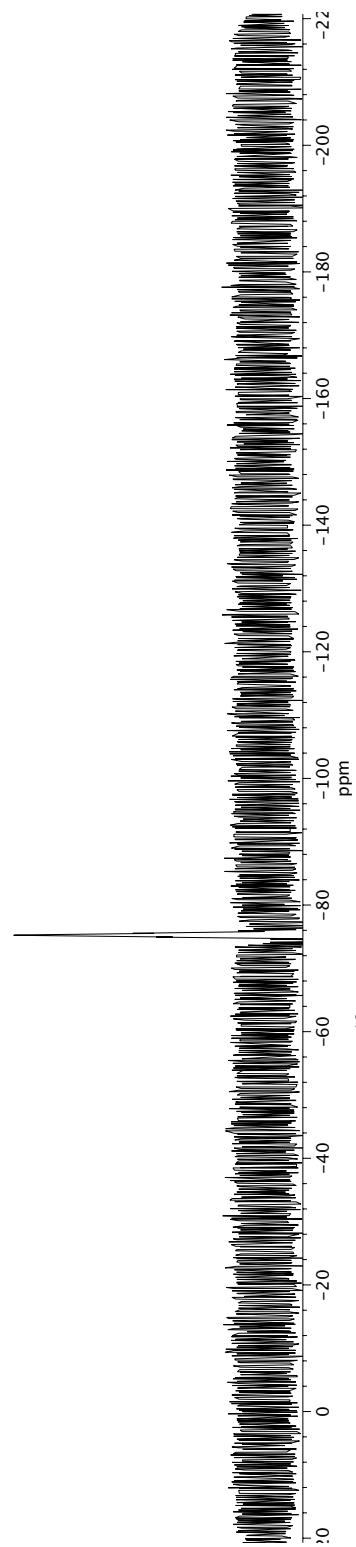
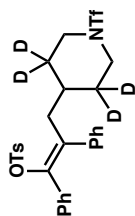


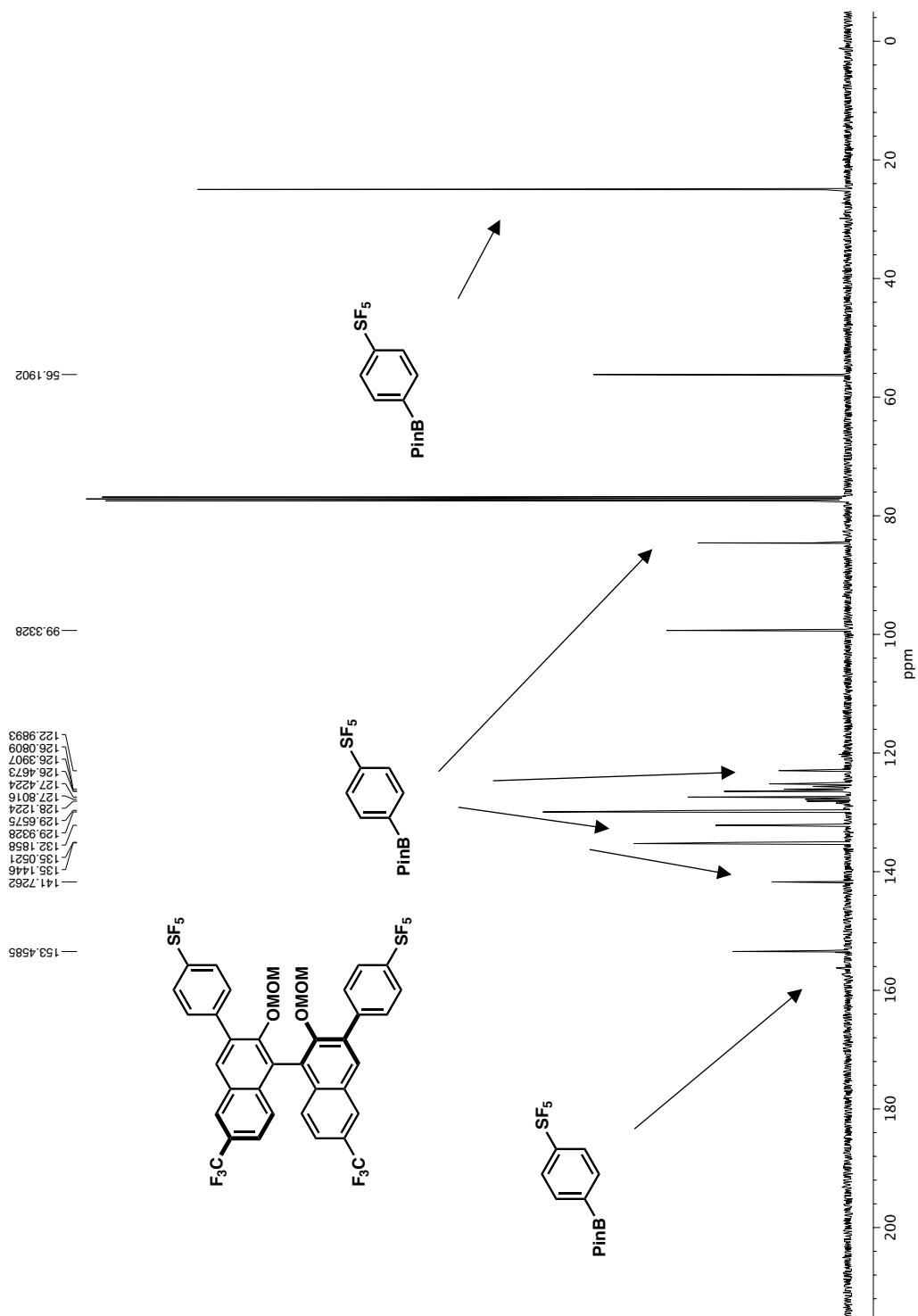


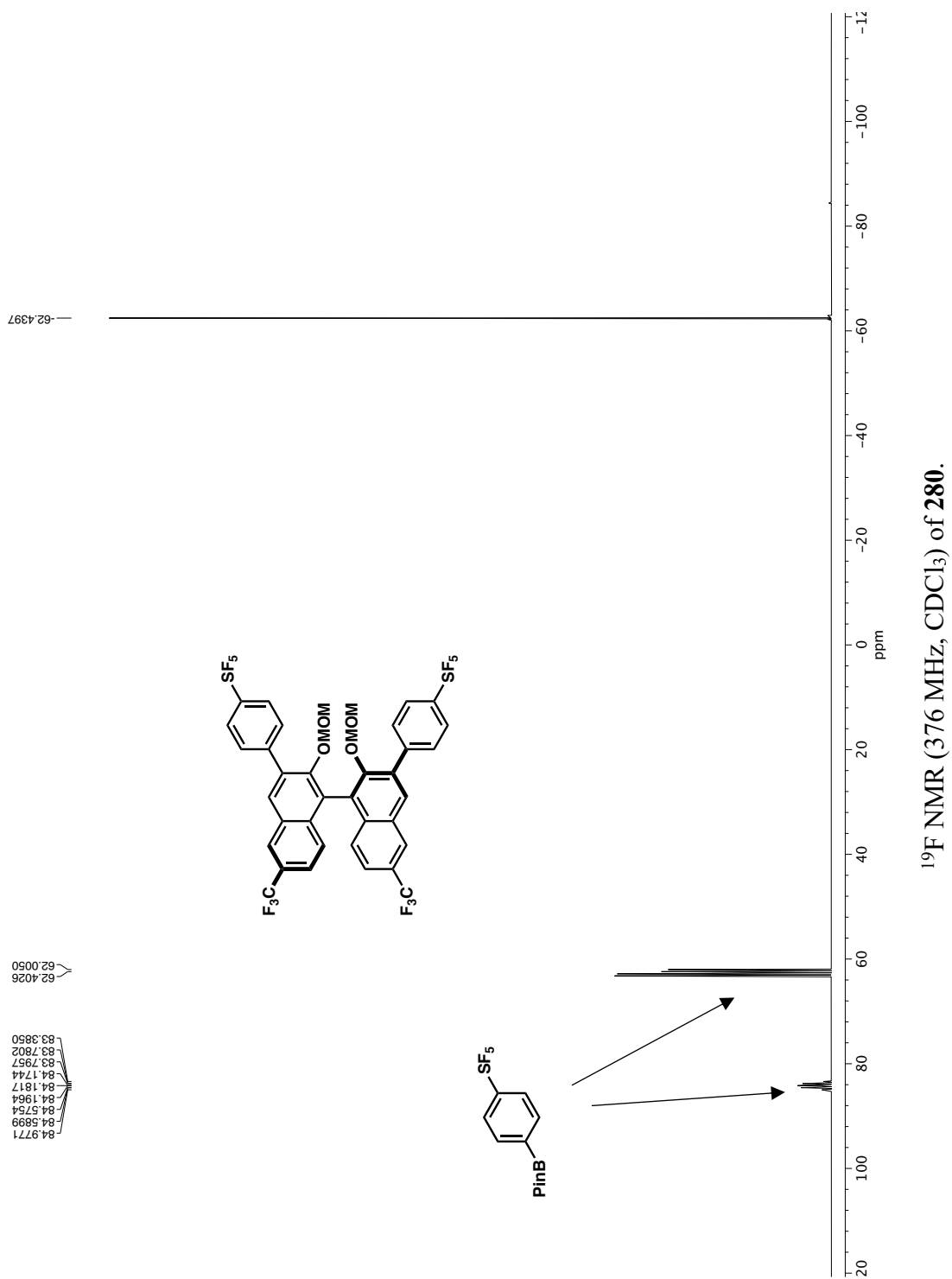


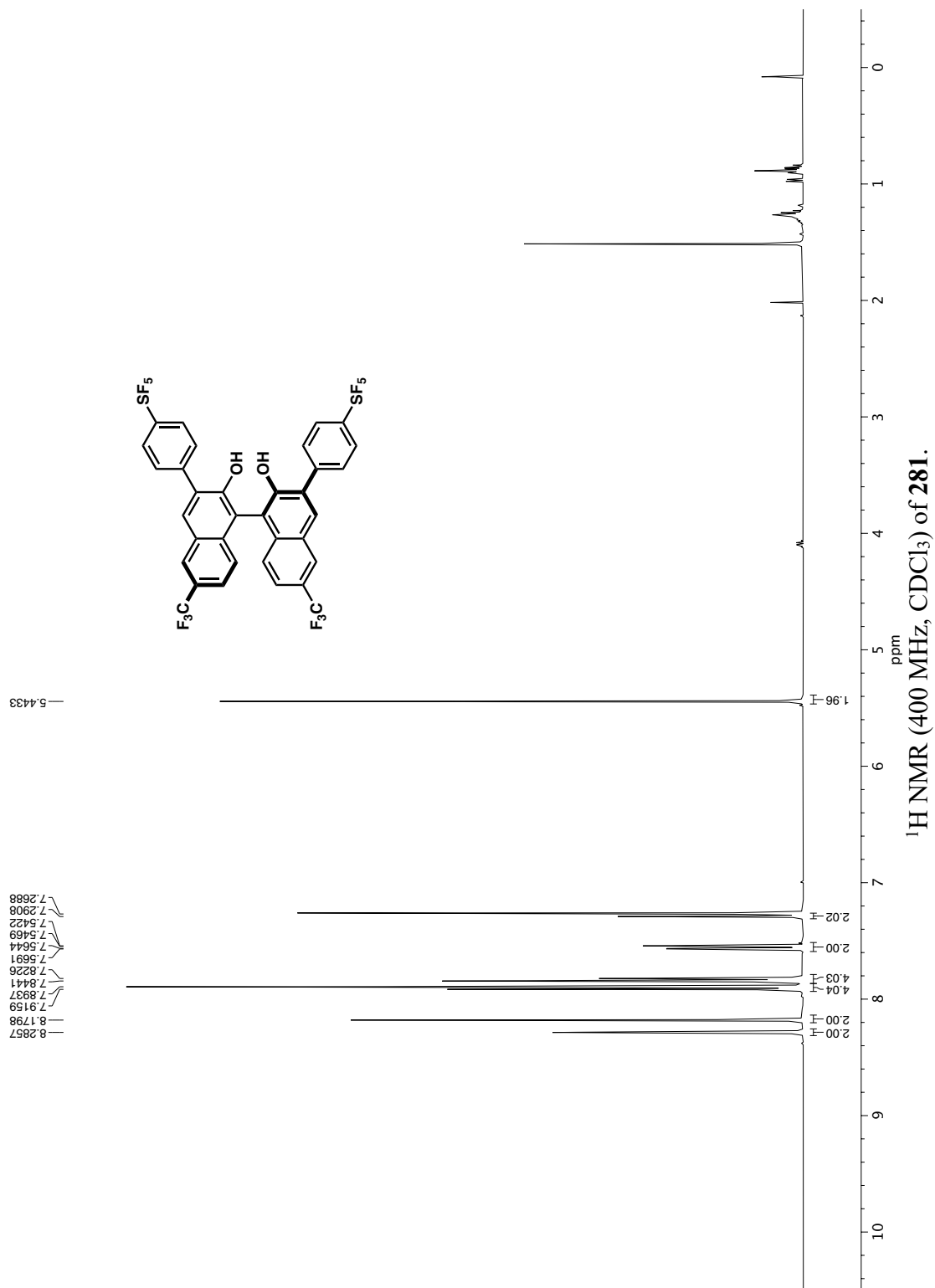


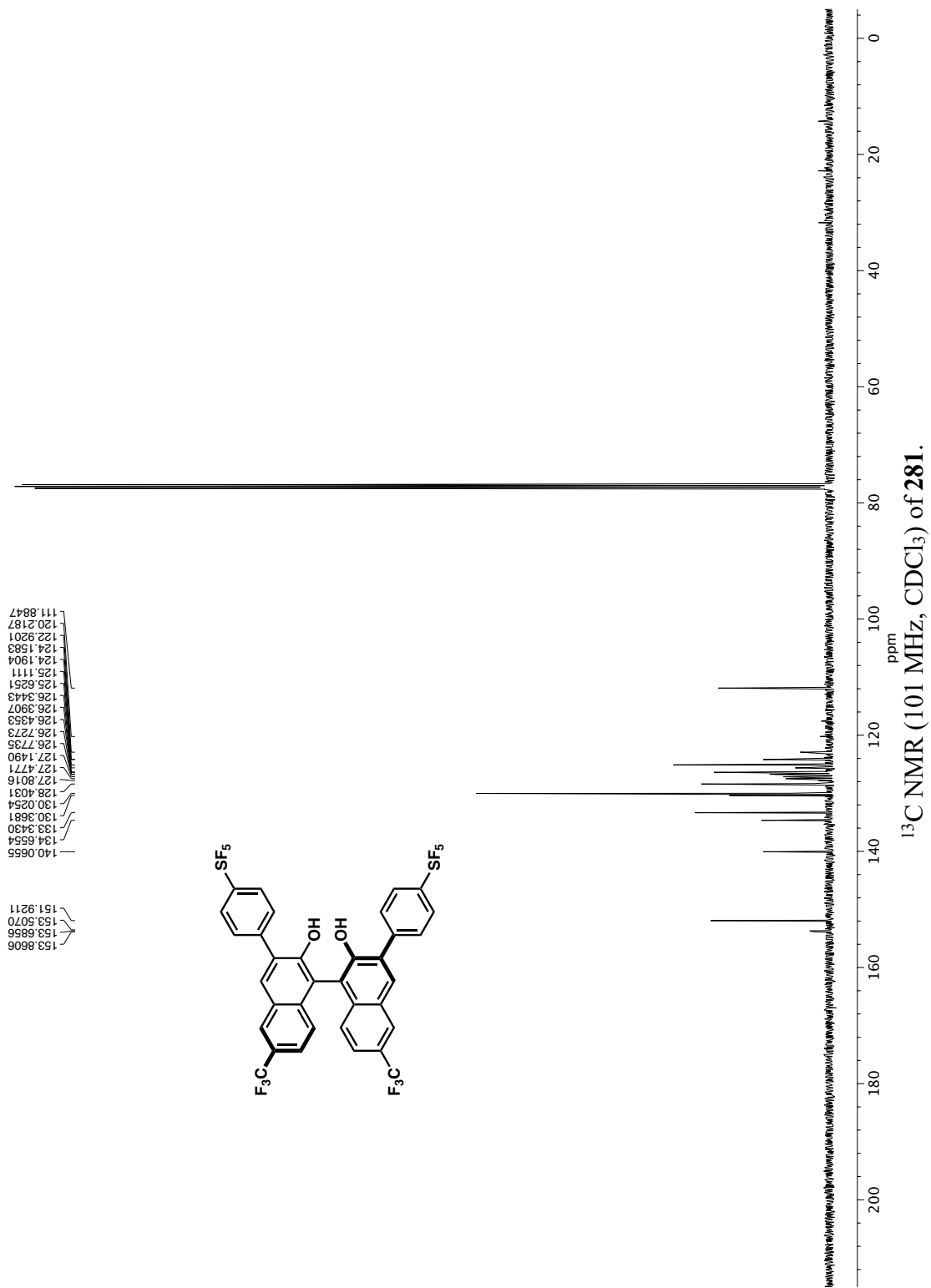
—75.2146

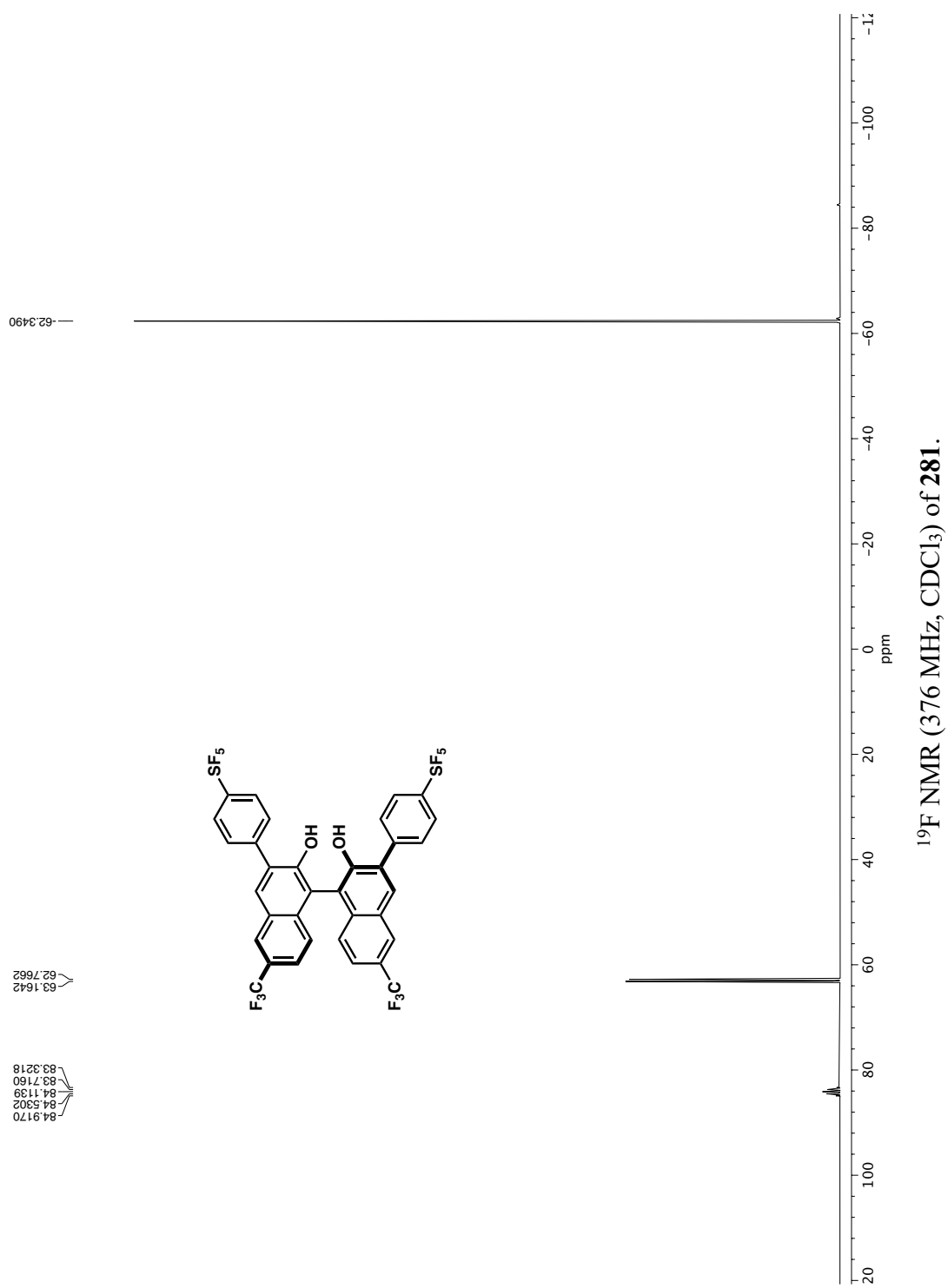


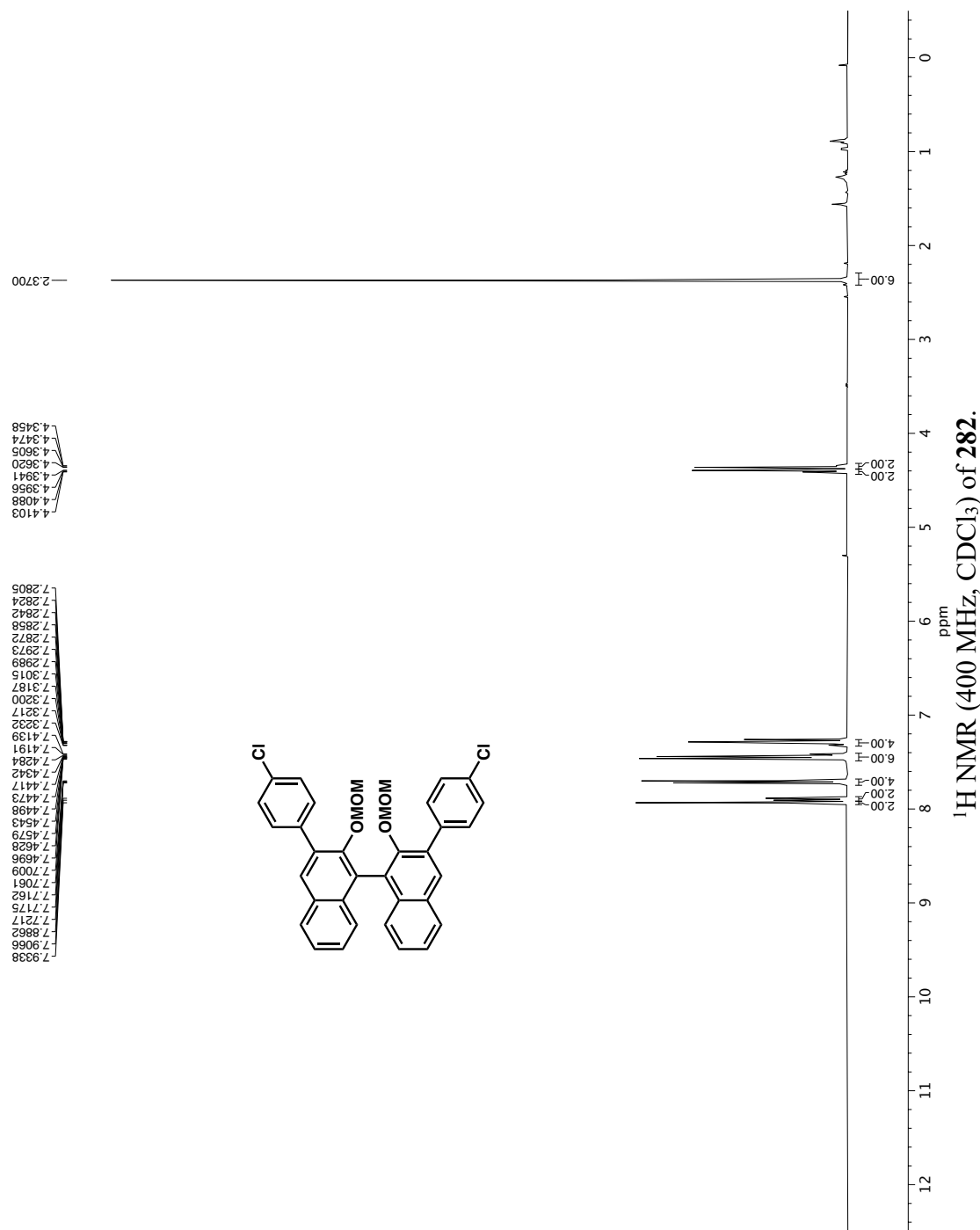


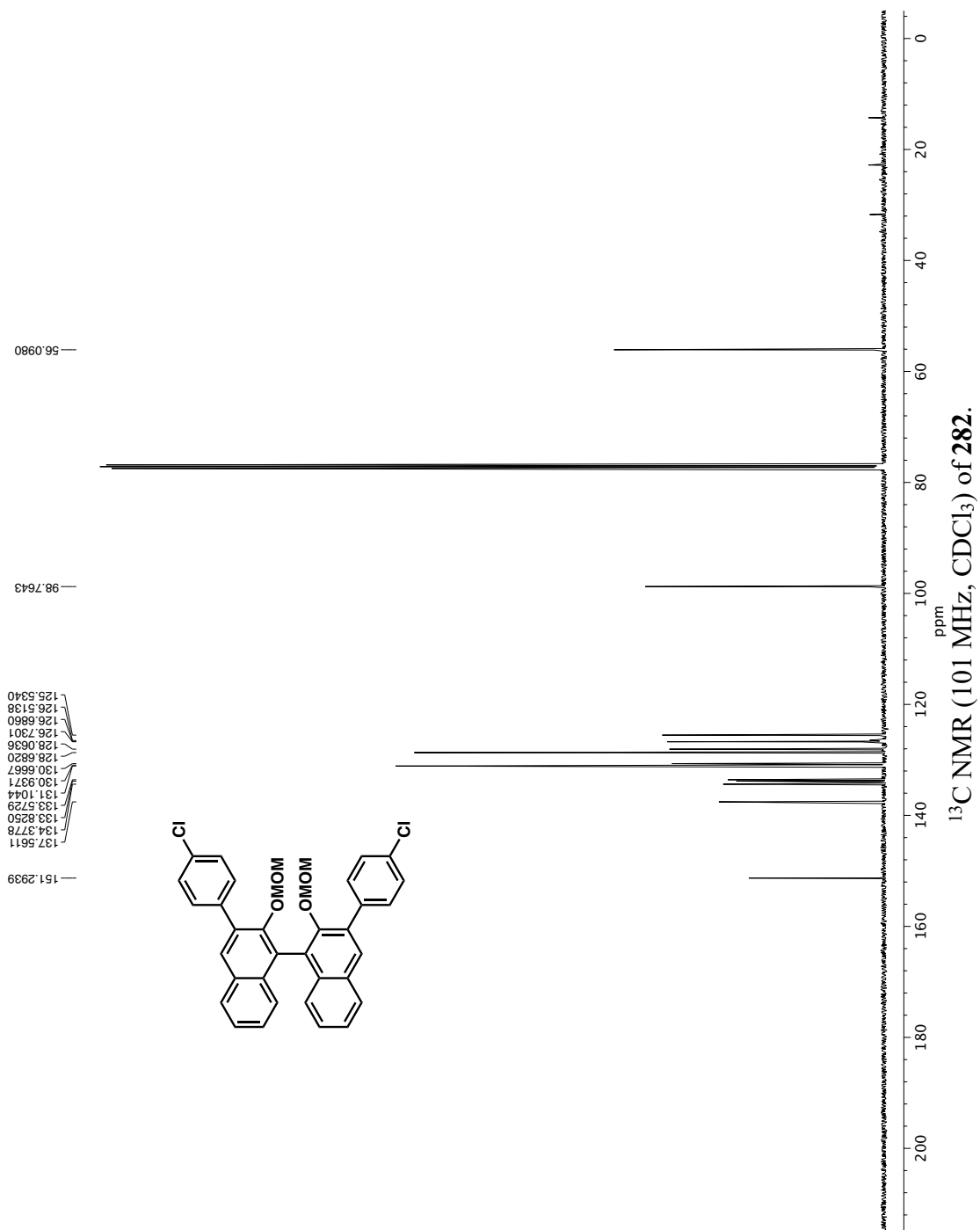


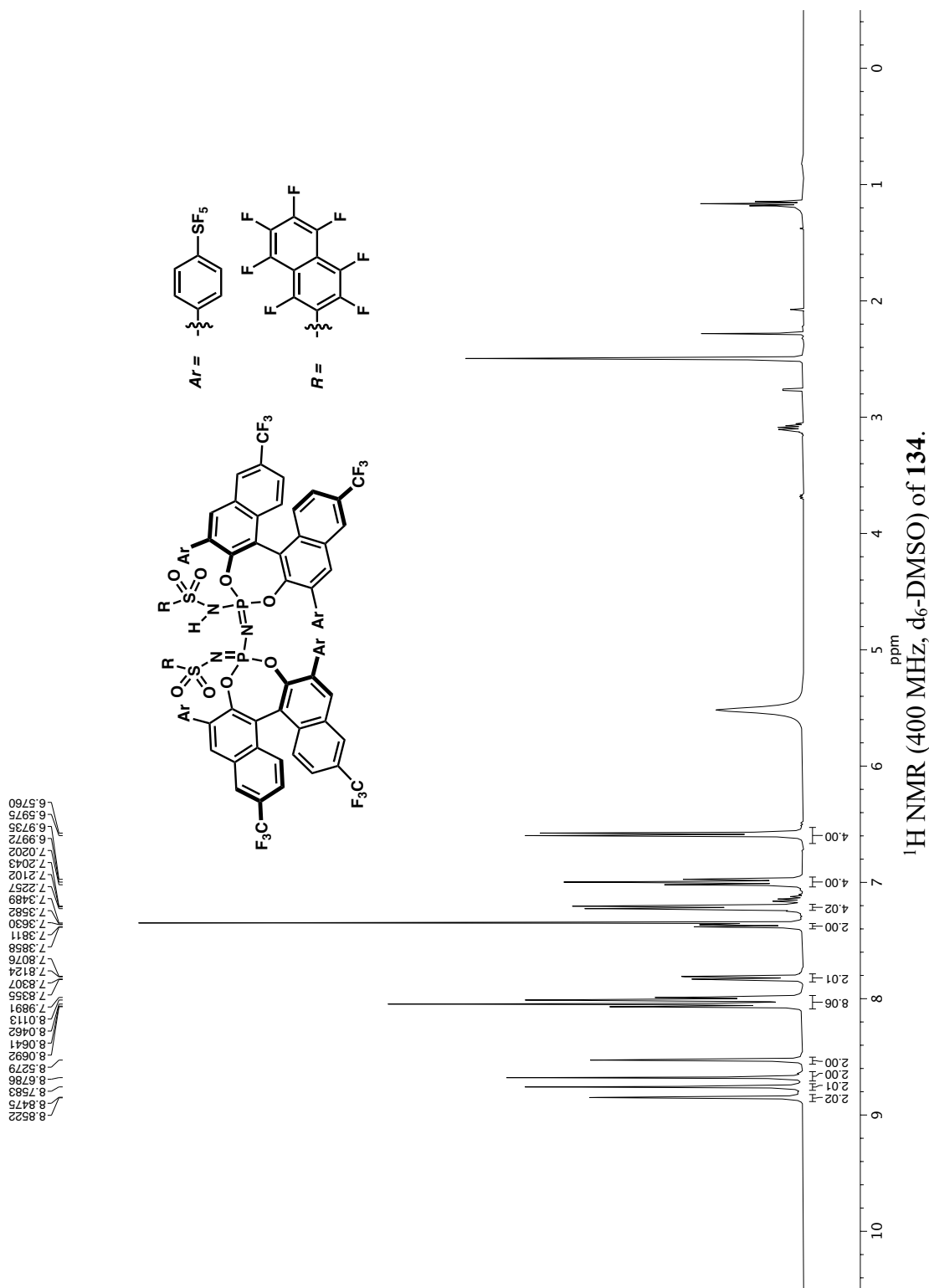


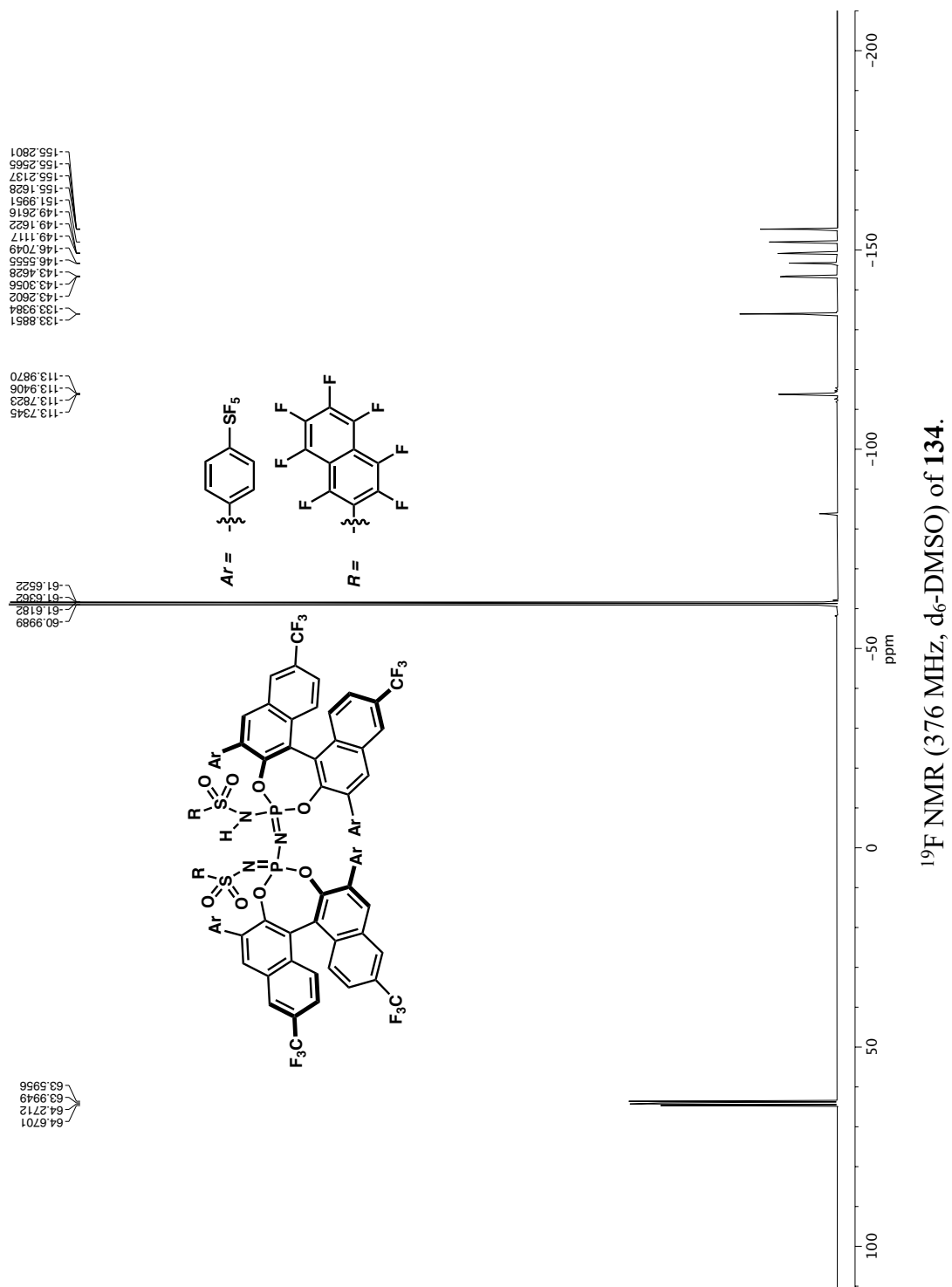




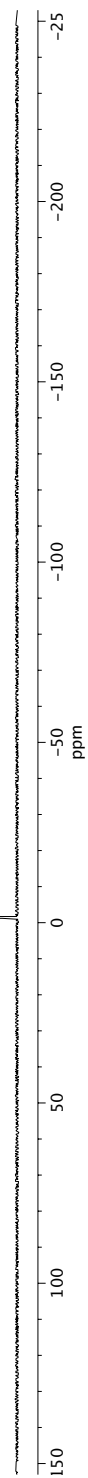
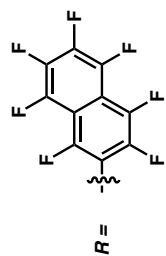
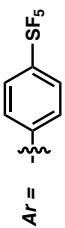
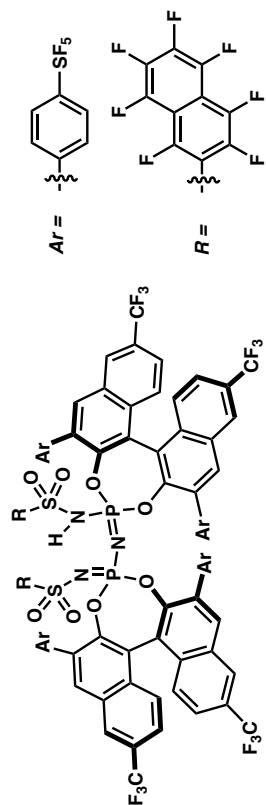




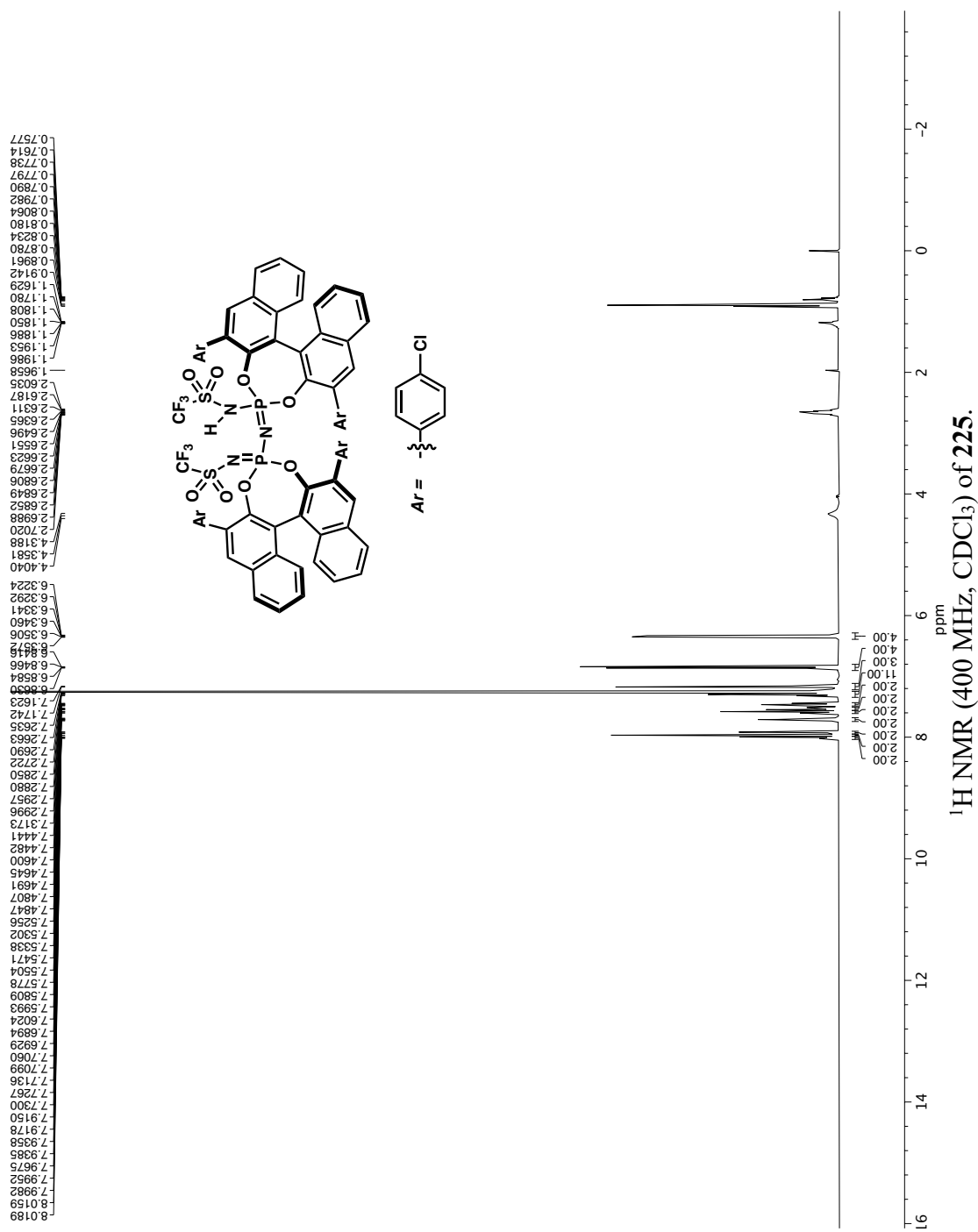


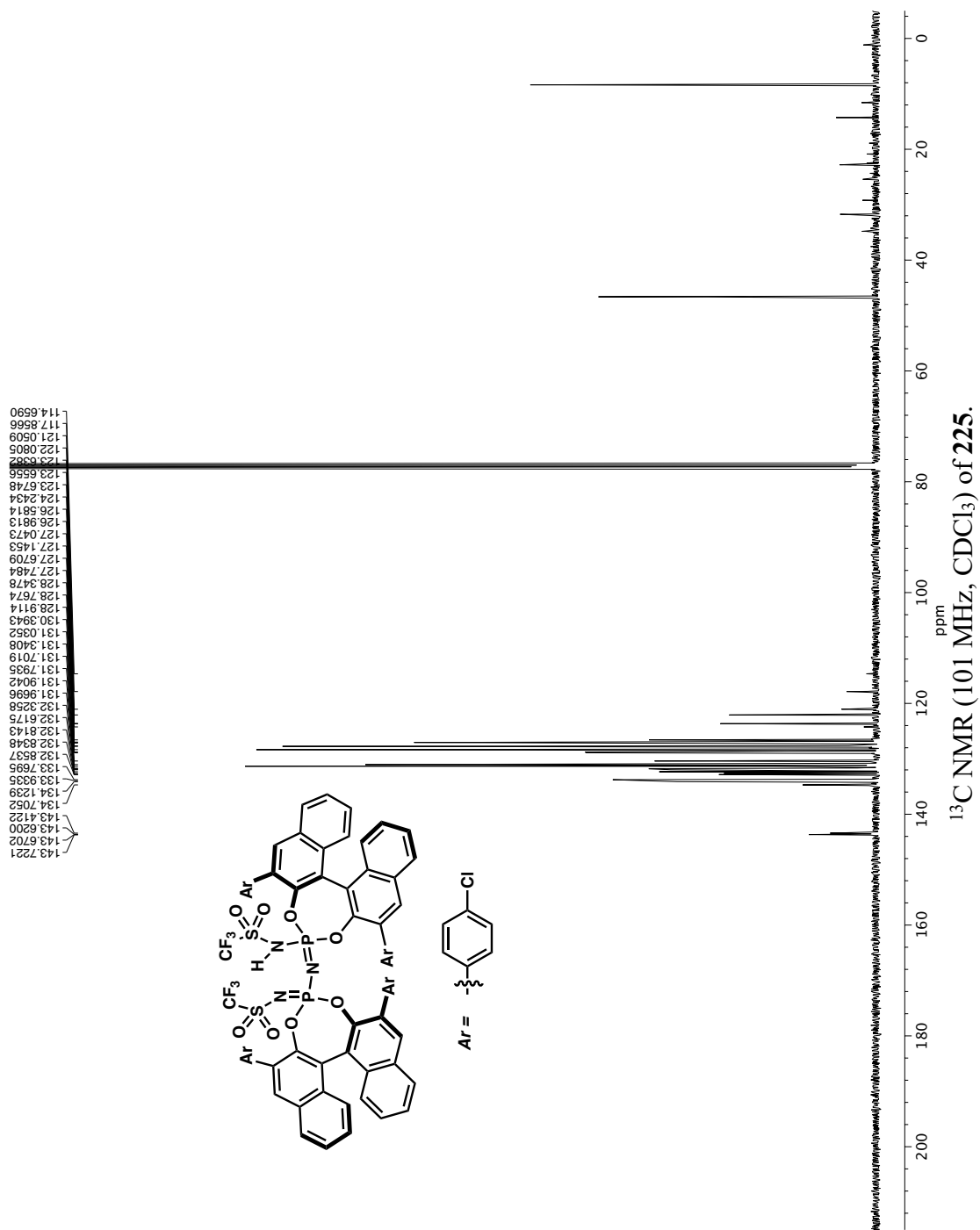


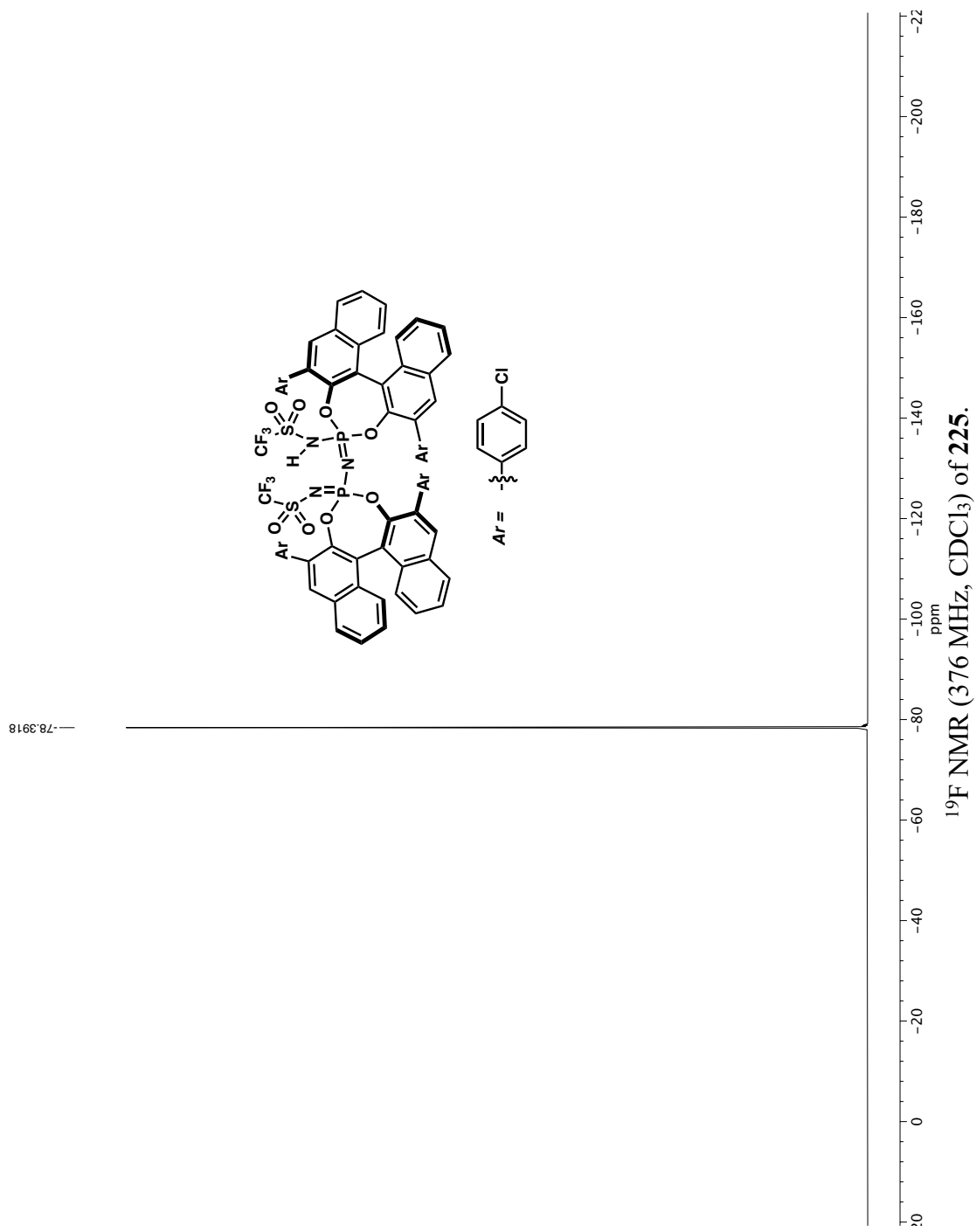
— -1.3941



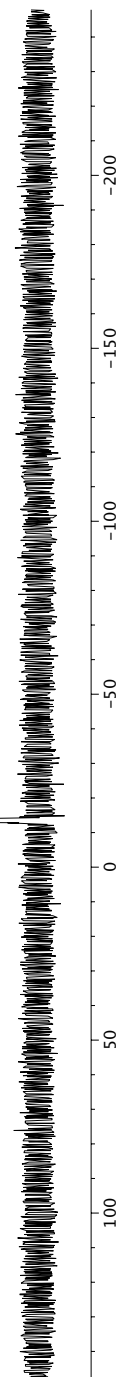
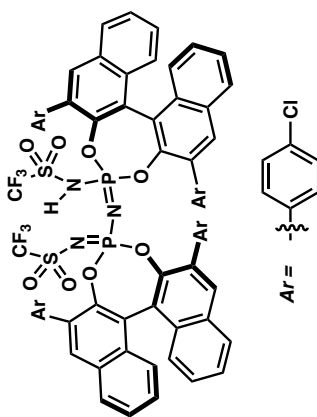
^{31}P NMR (161 MHz, d_6 -DMSO) of **134**.

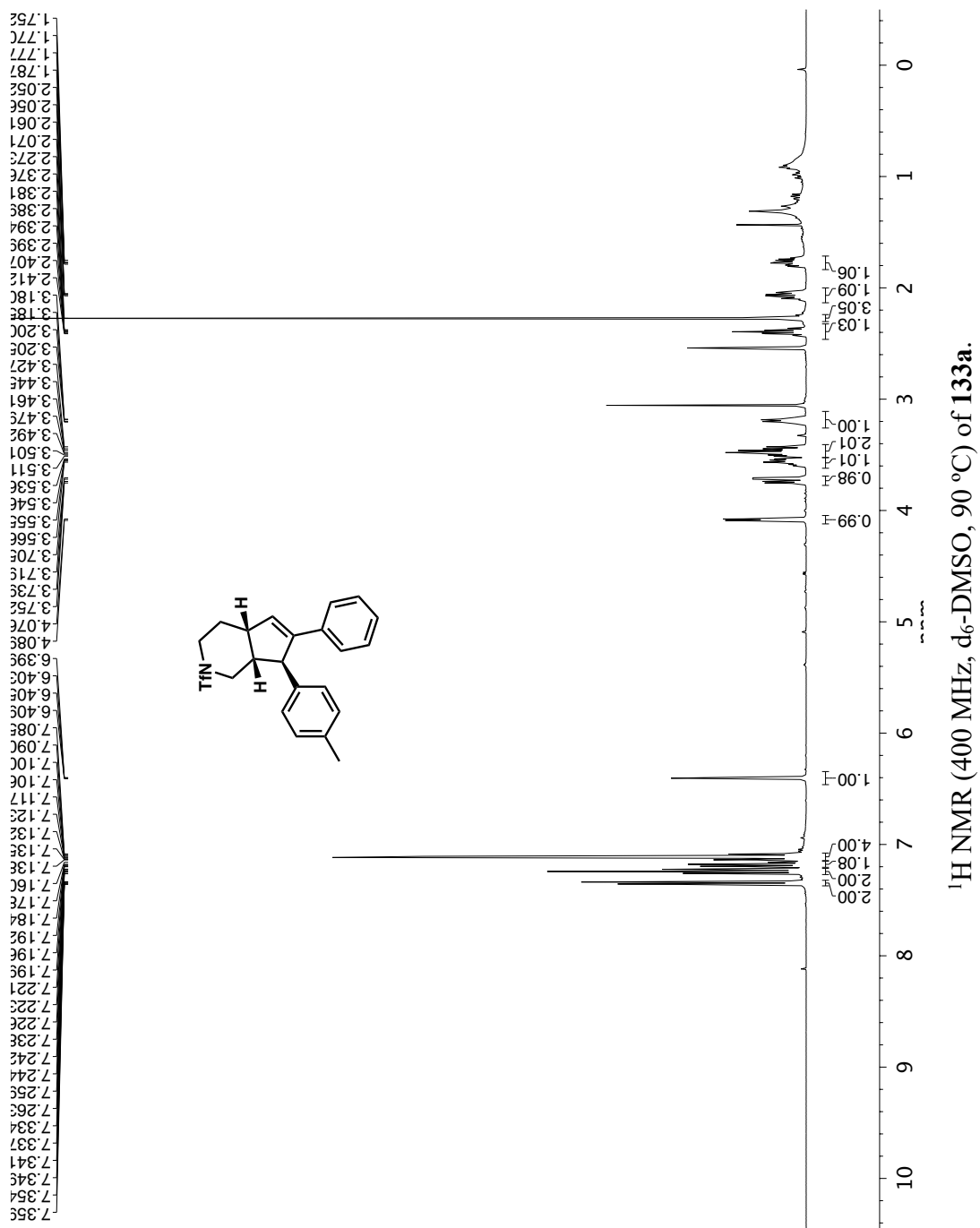


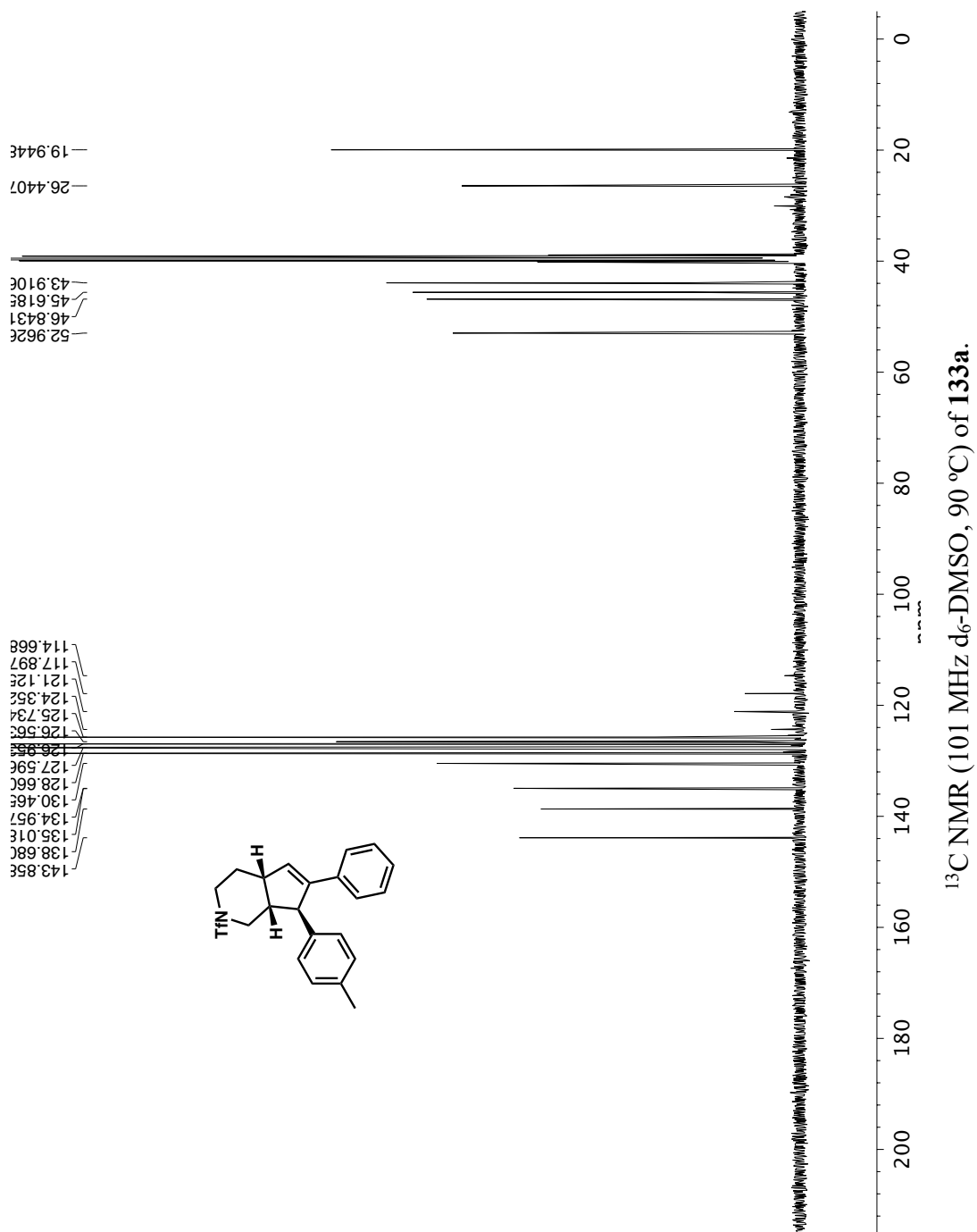




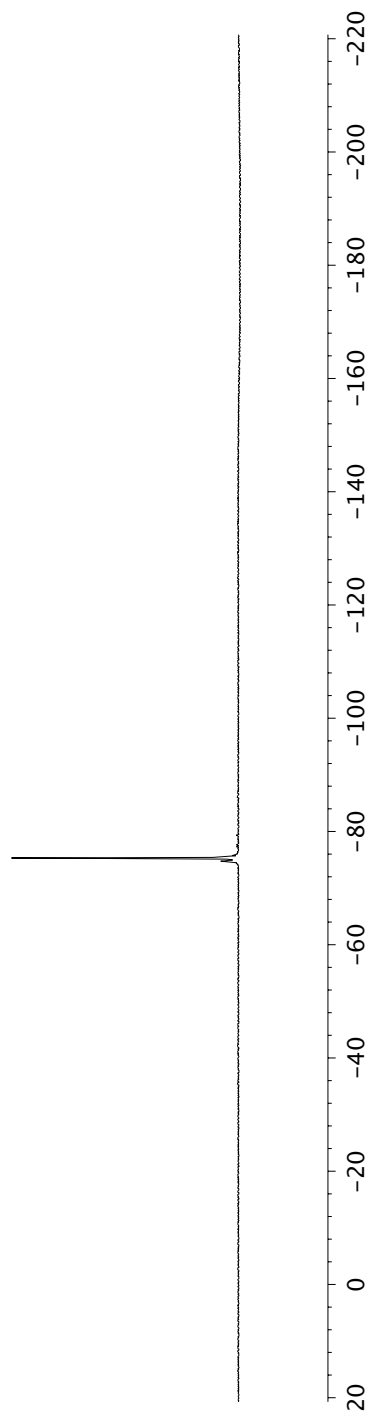
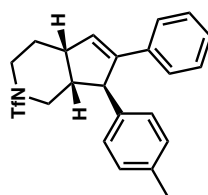
—13.49

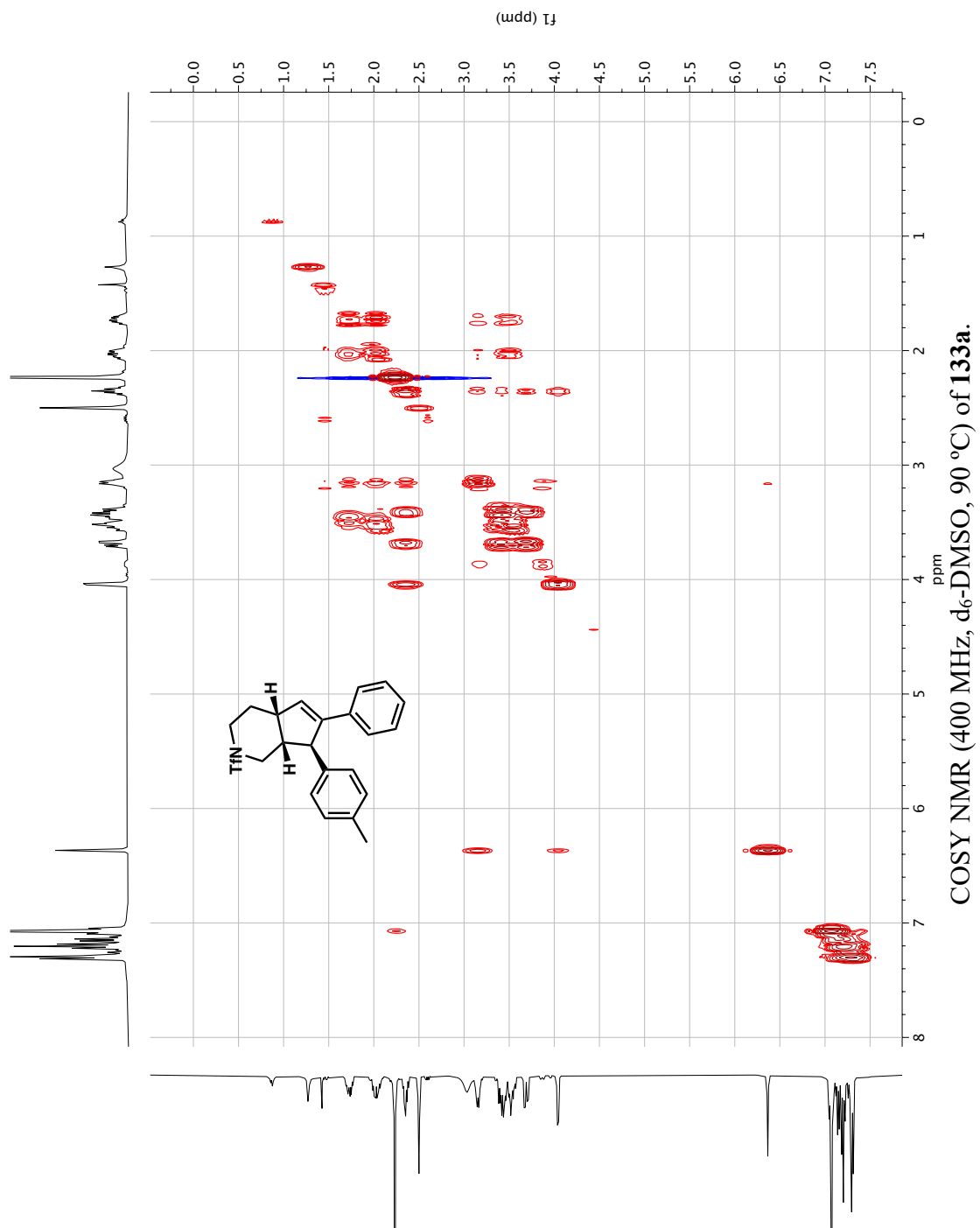
 ^{31}P NMR (162 MHz, CDCl_3) of **225**.

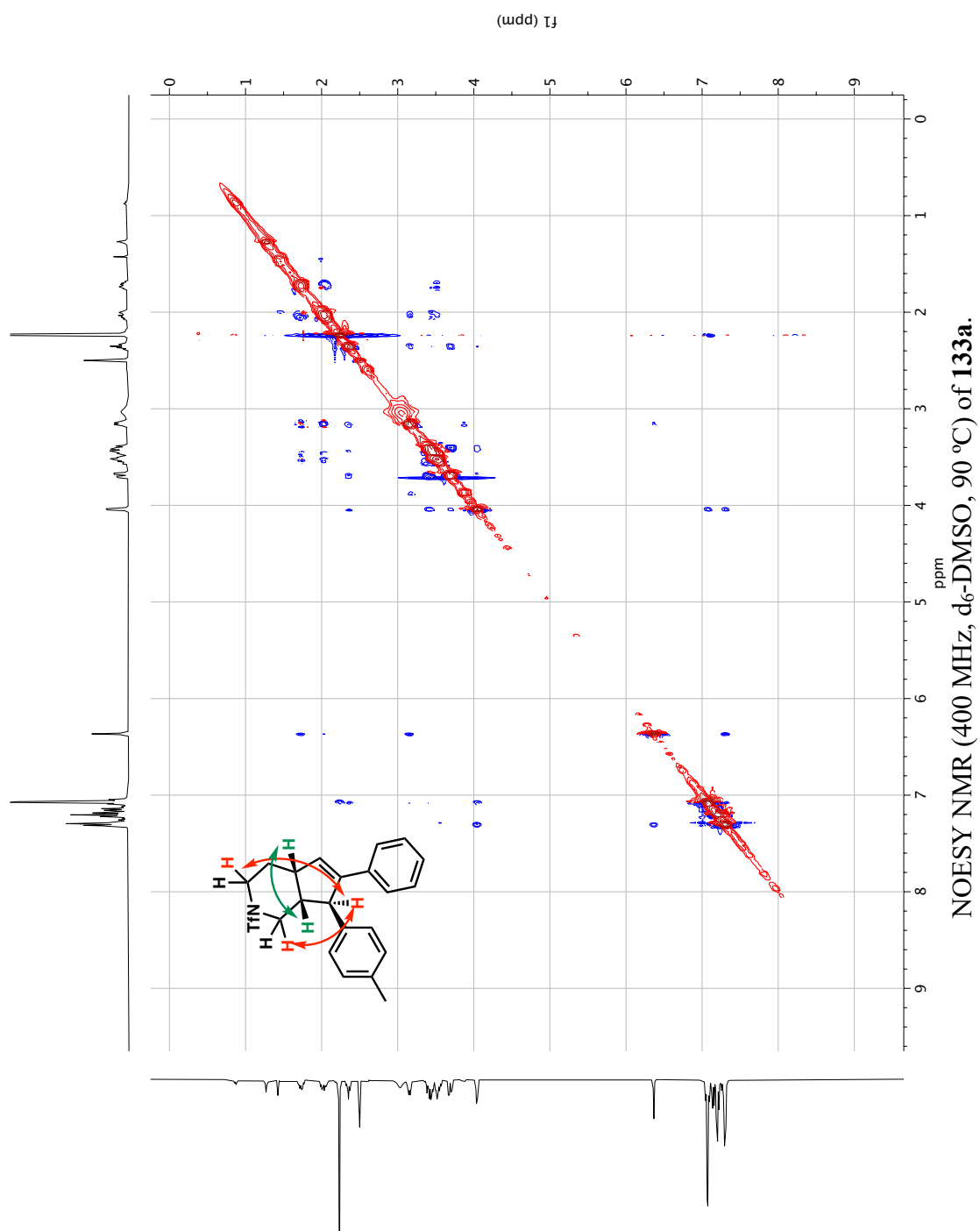


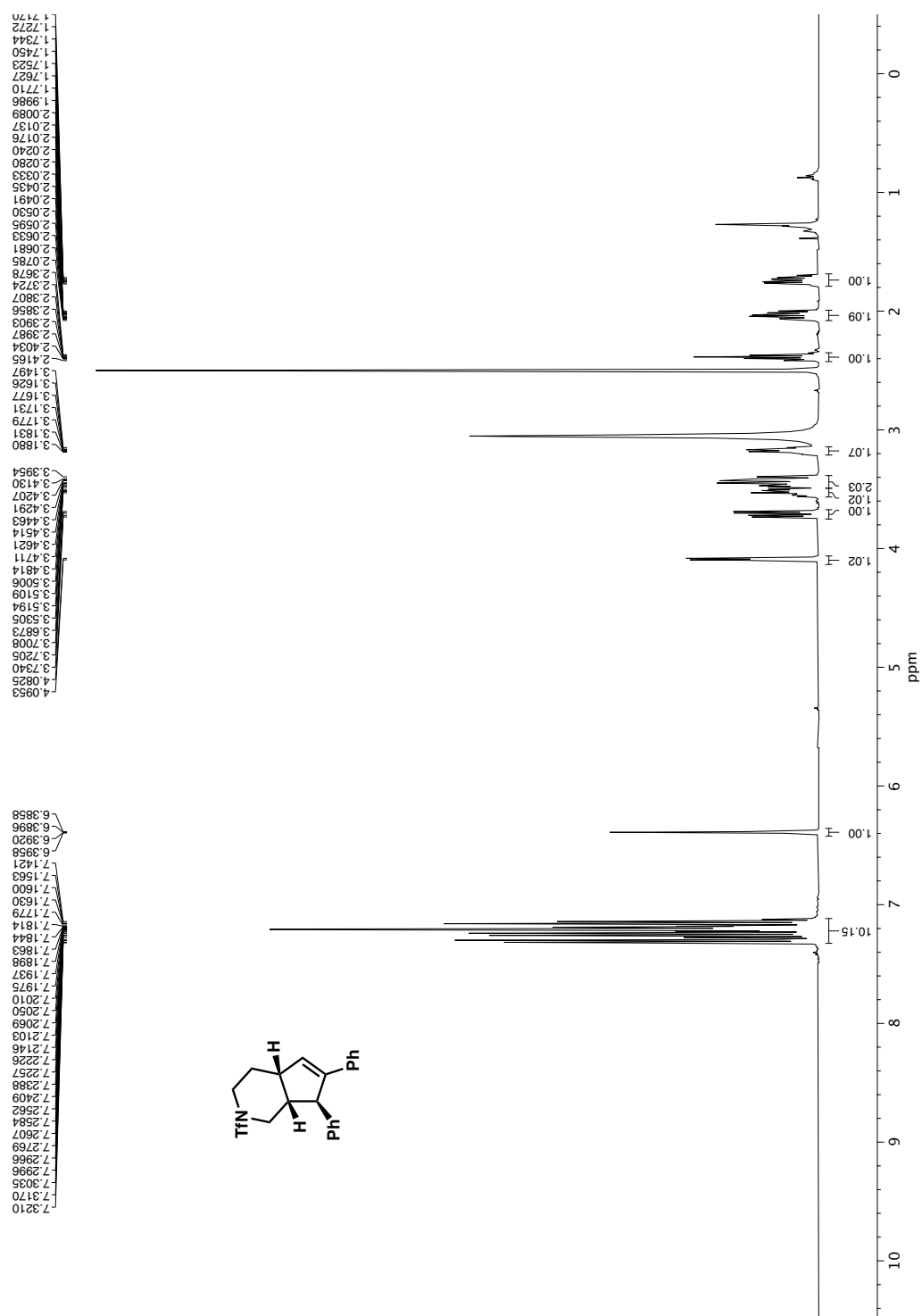


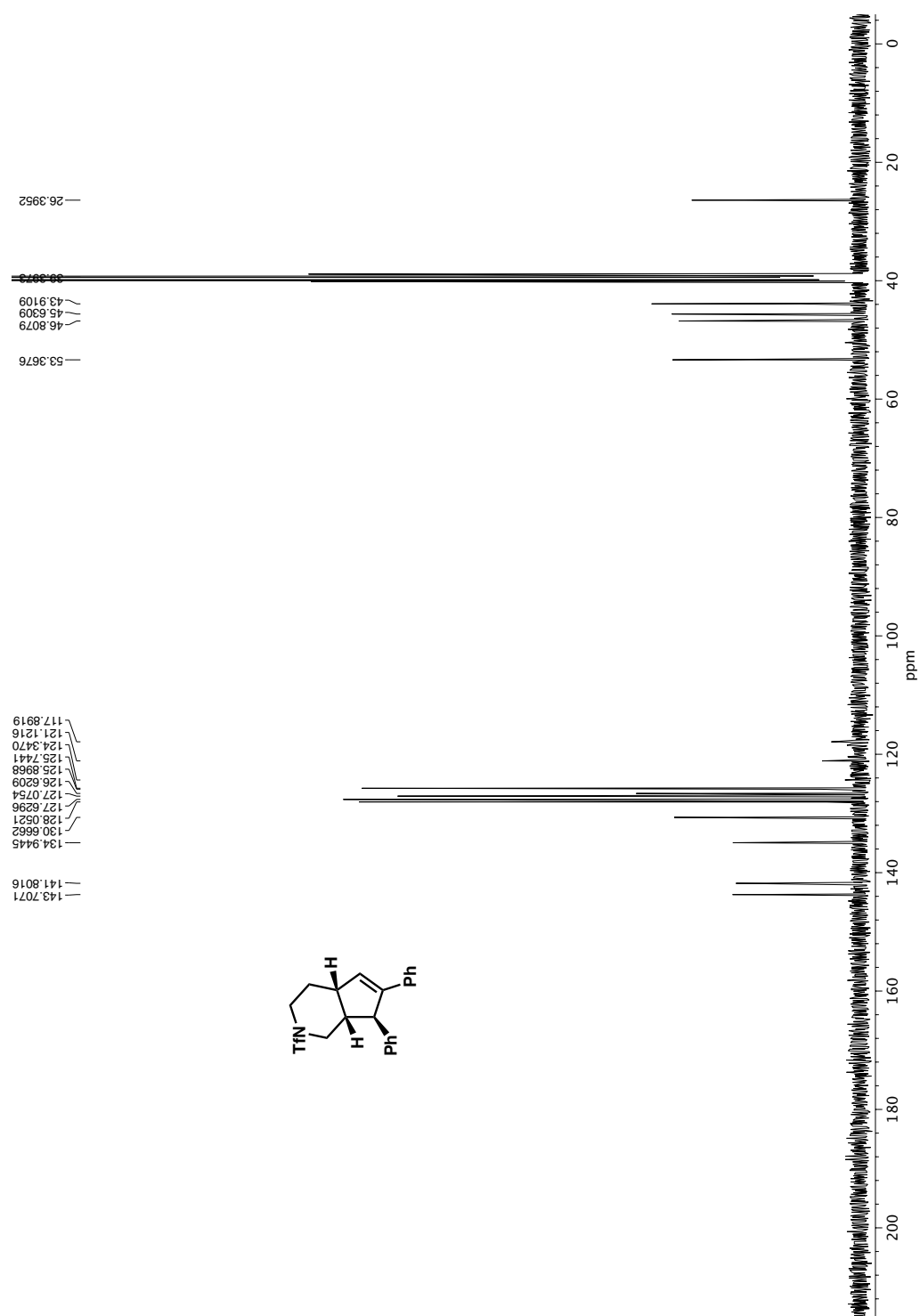
-75.314

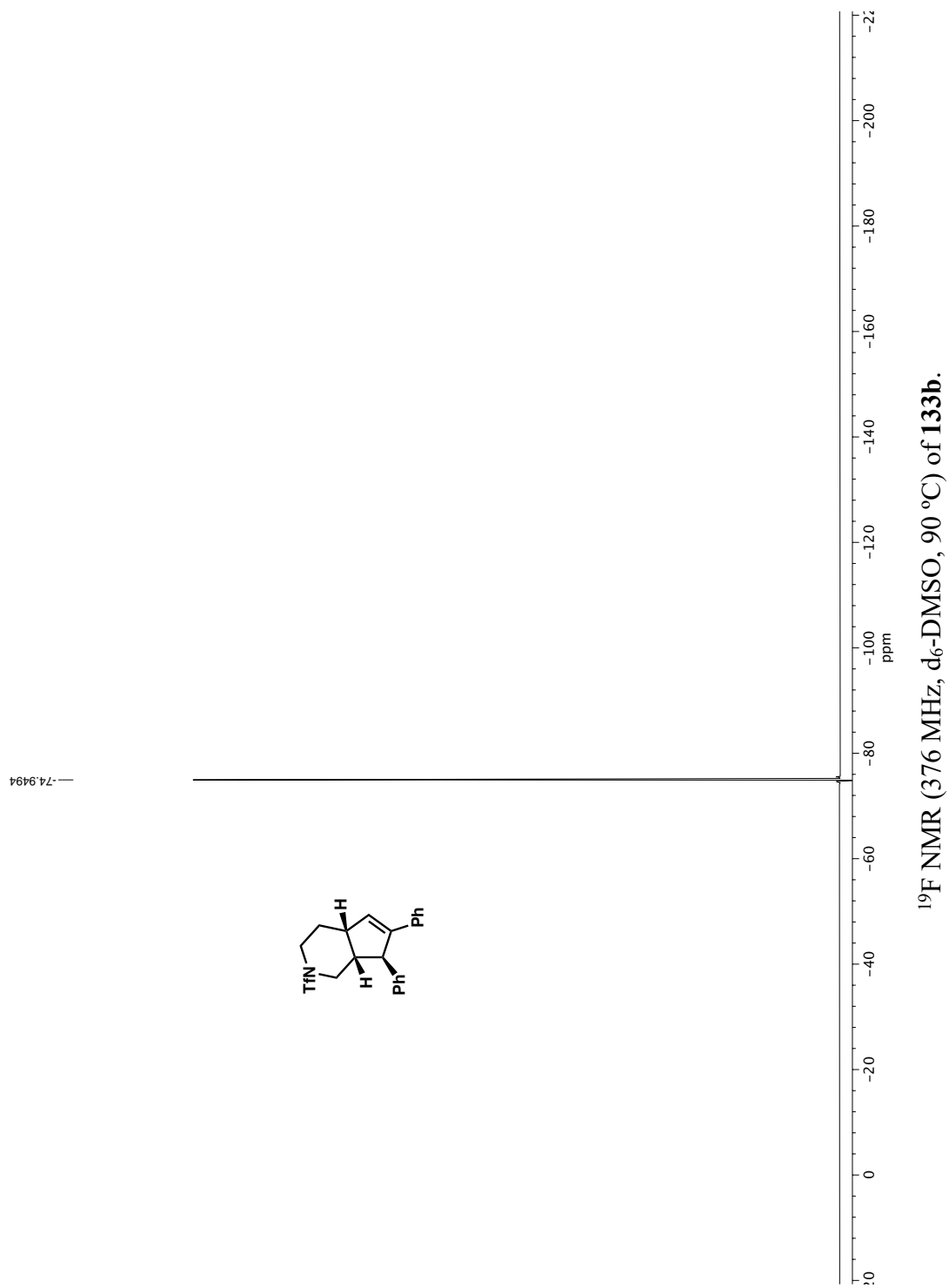
 ^{19}F NMR (376 MHz, $\text{d}_6\text{-DMSO}$, 90°C) of **133a**.

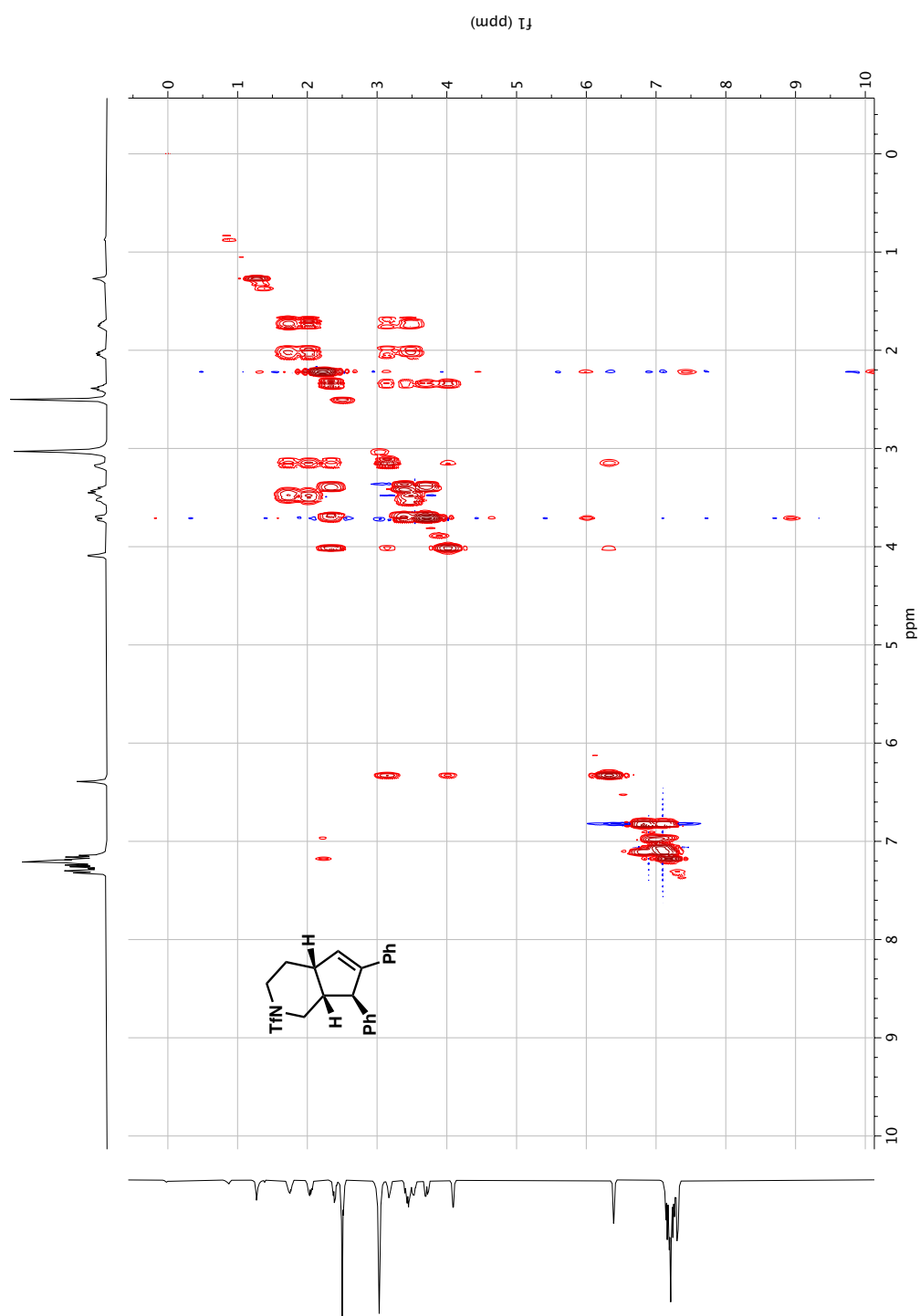


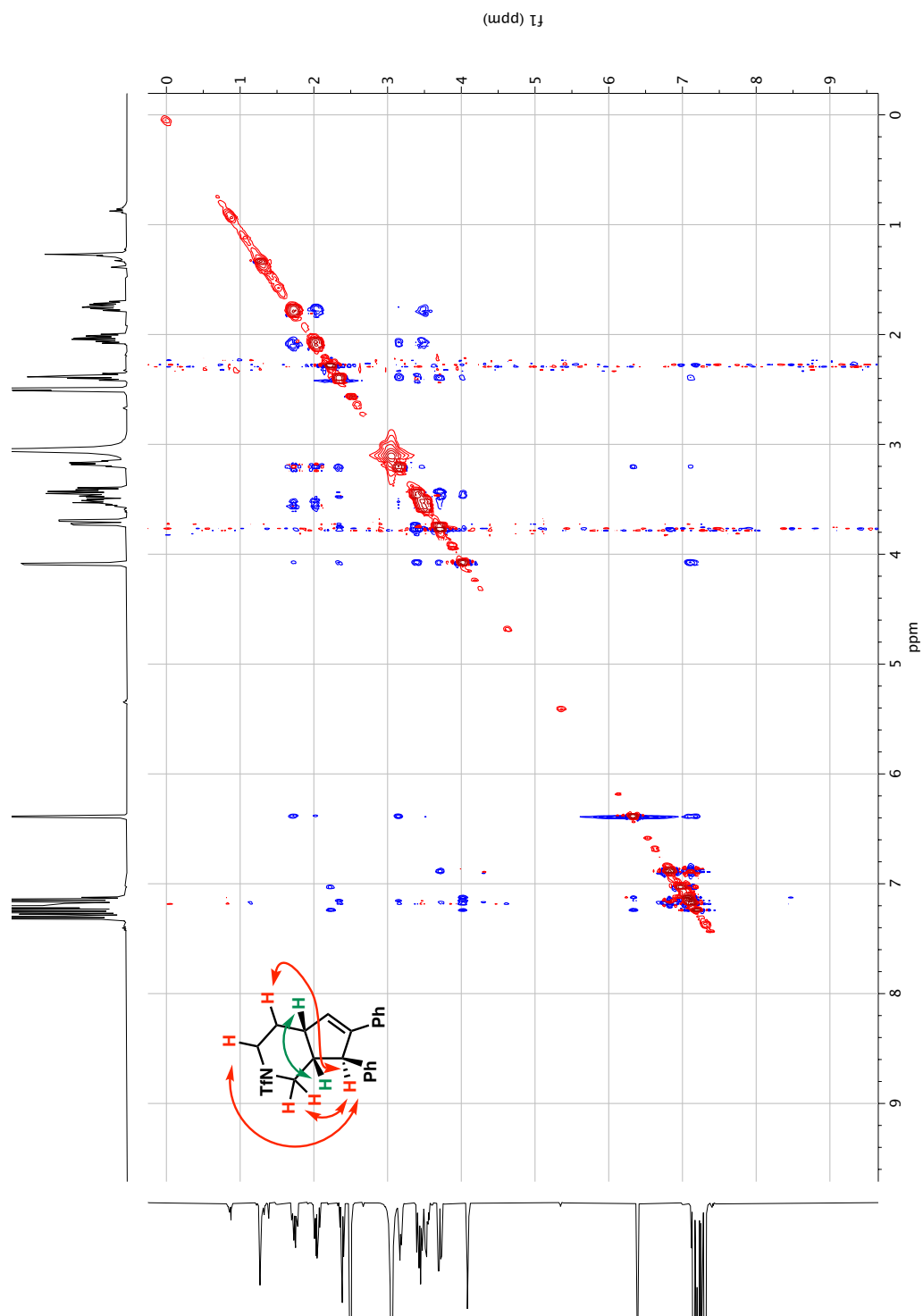


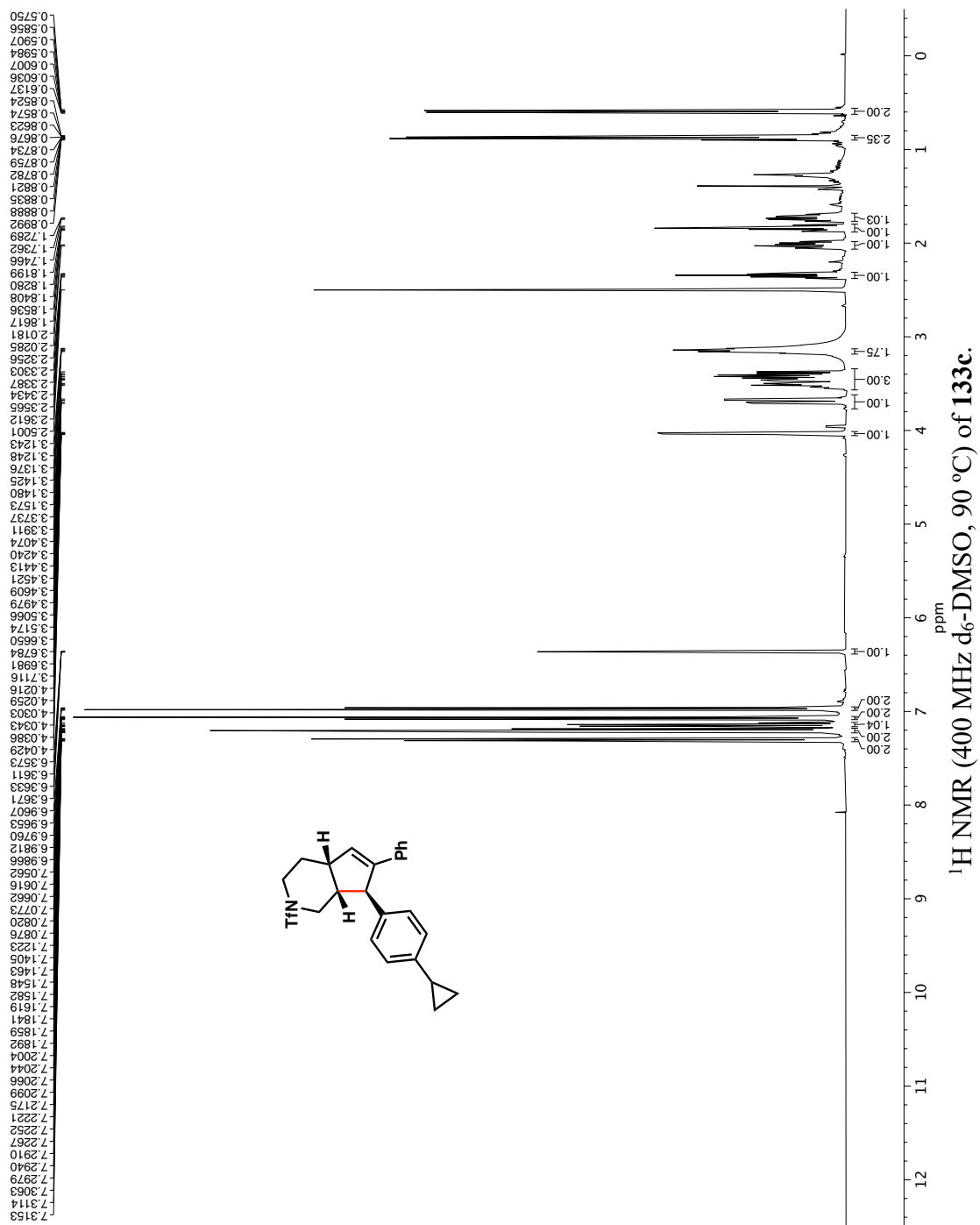


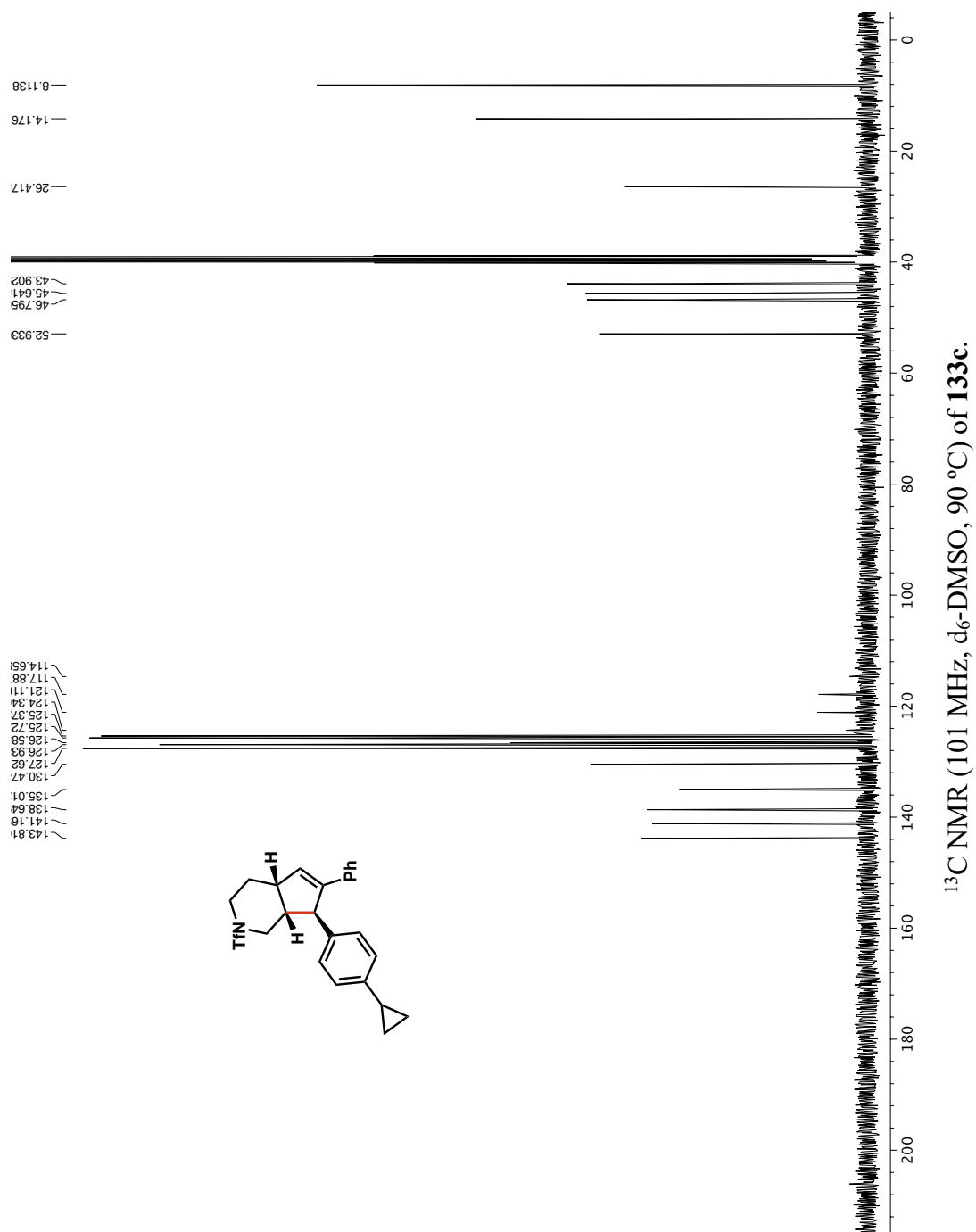


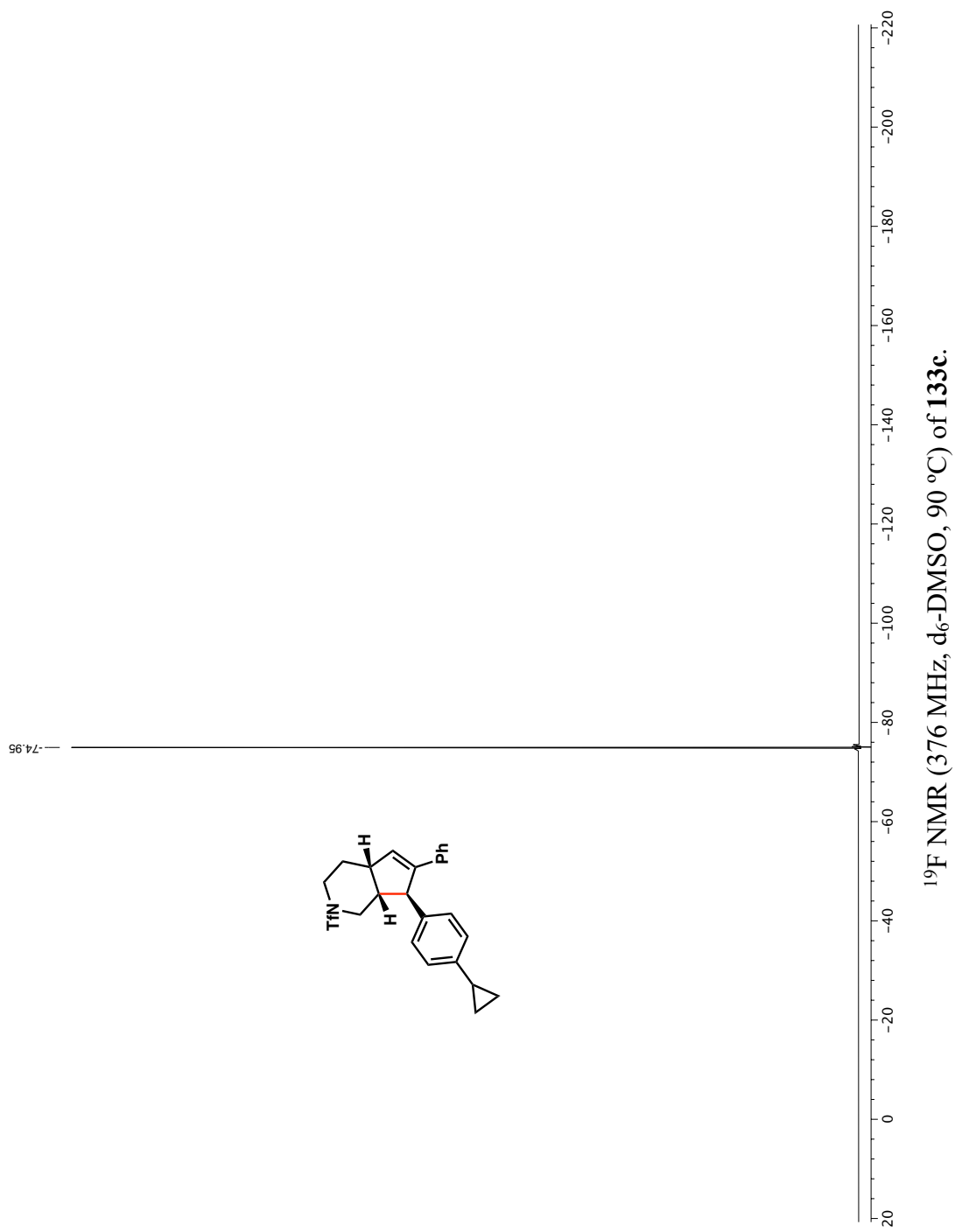


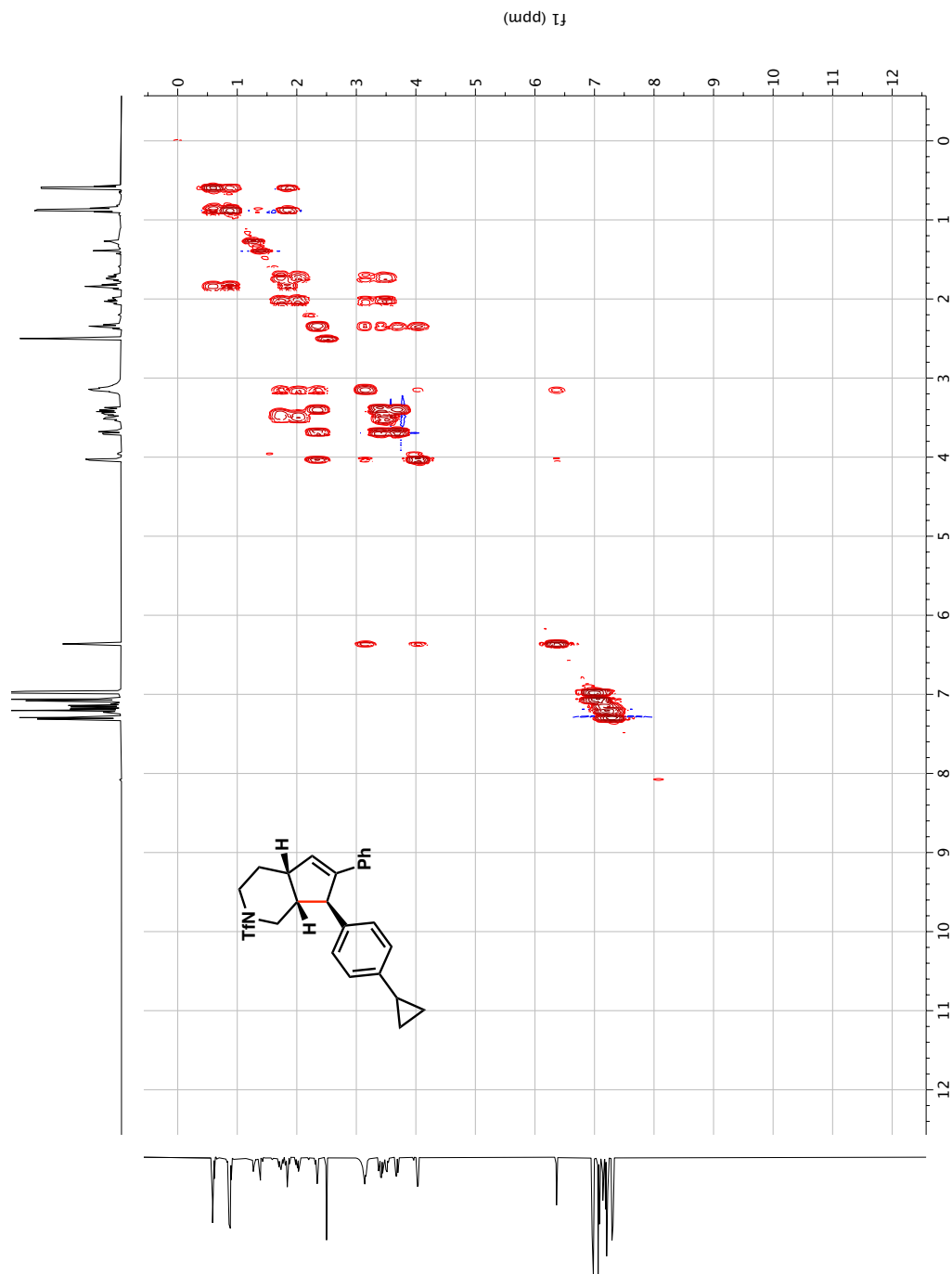


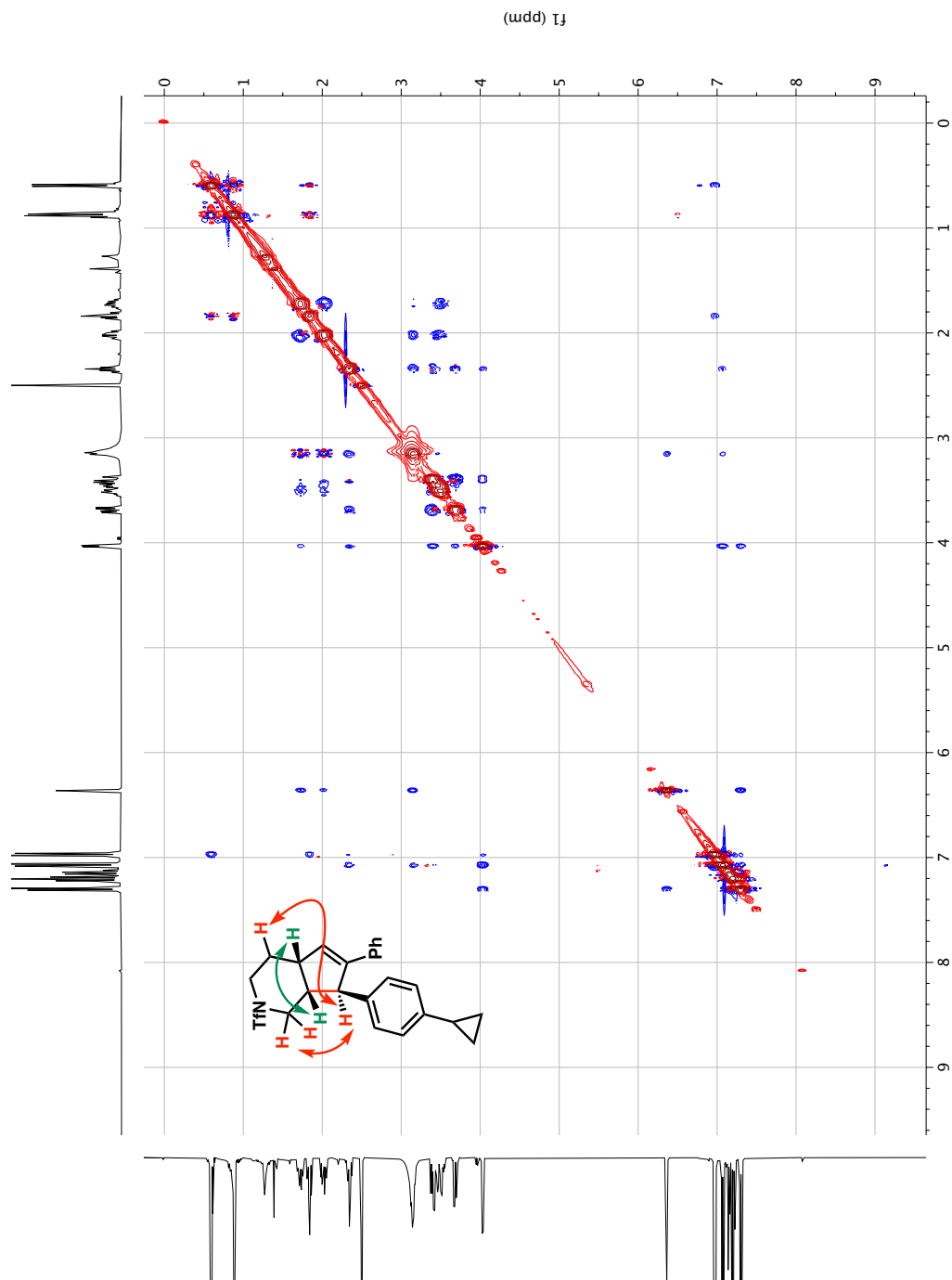


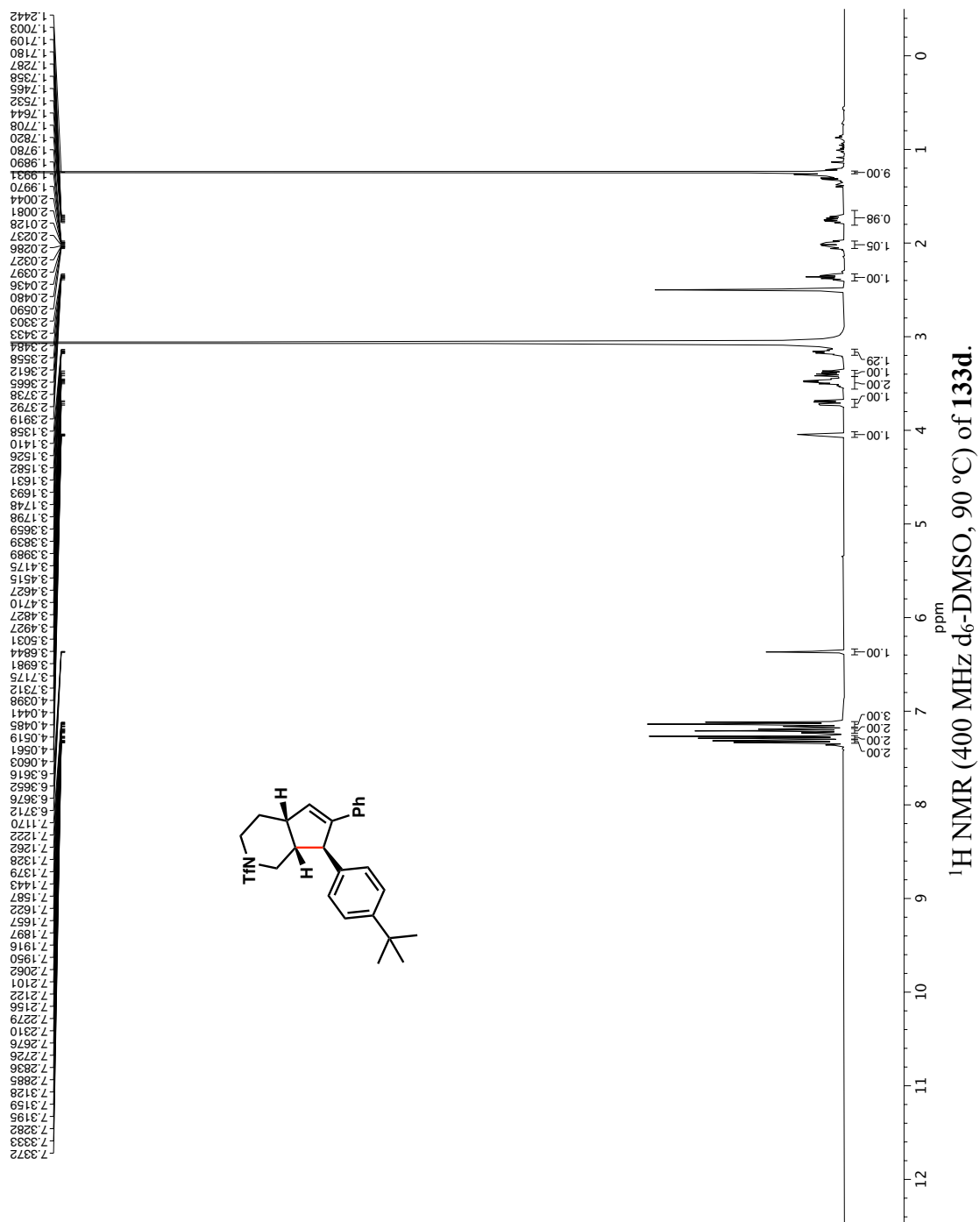


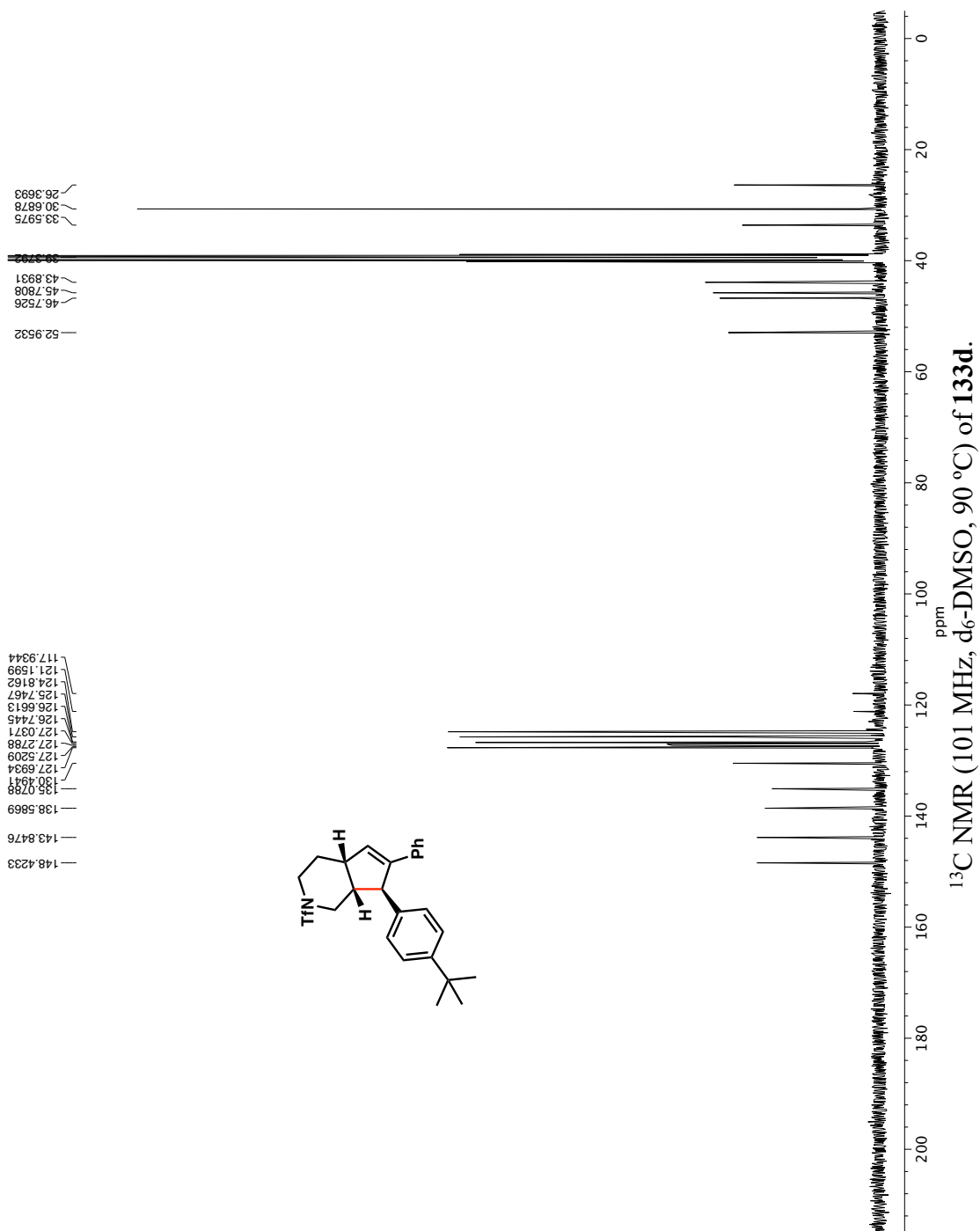


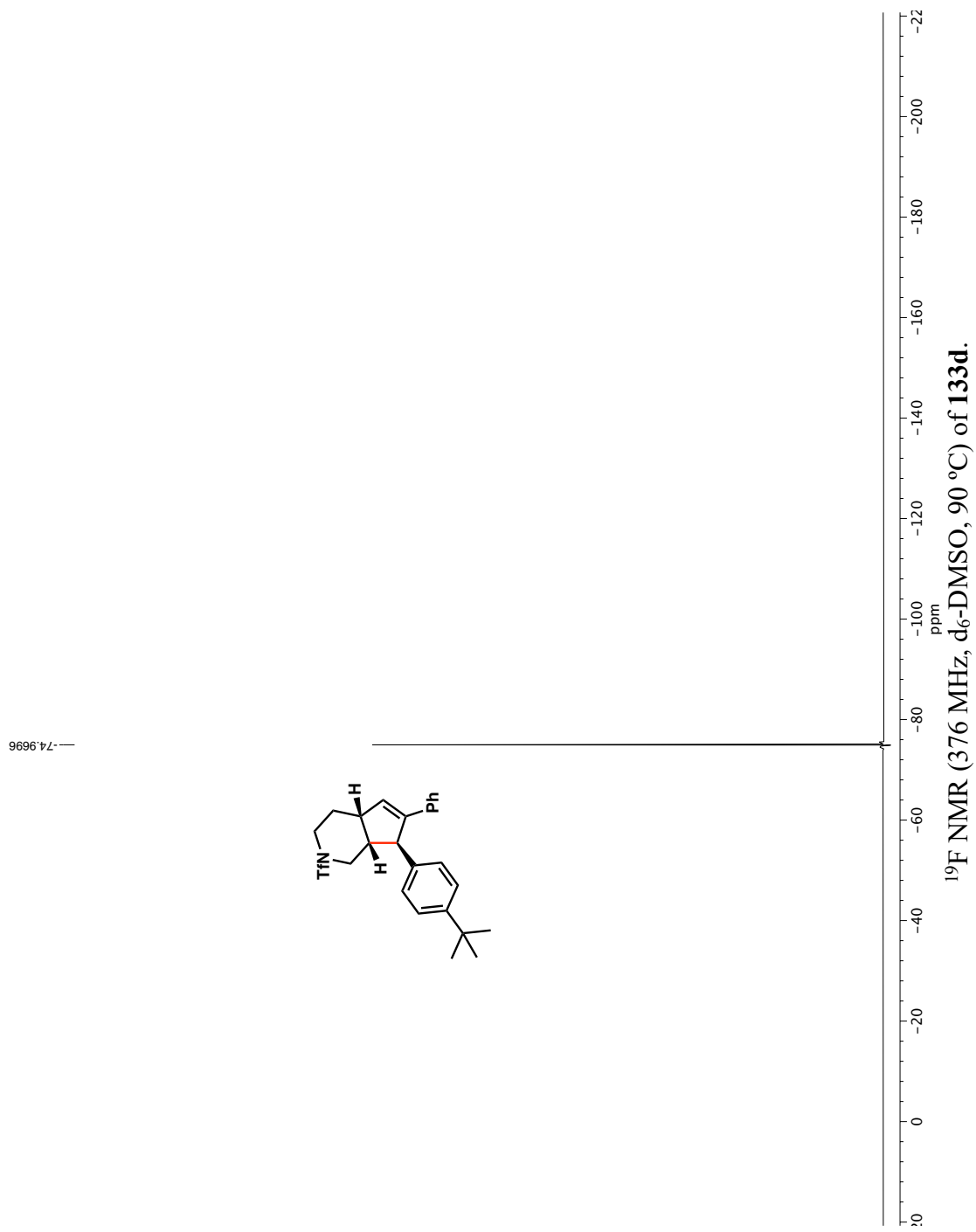


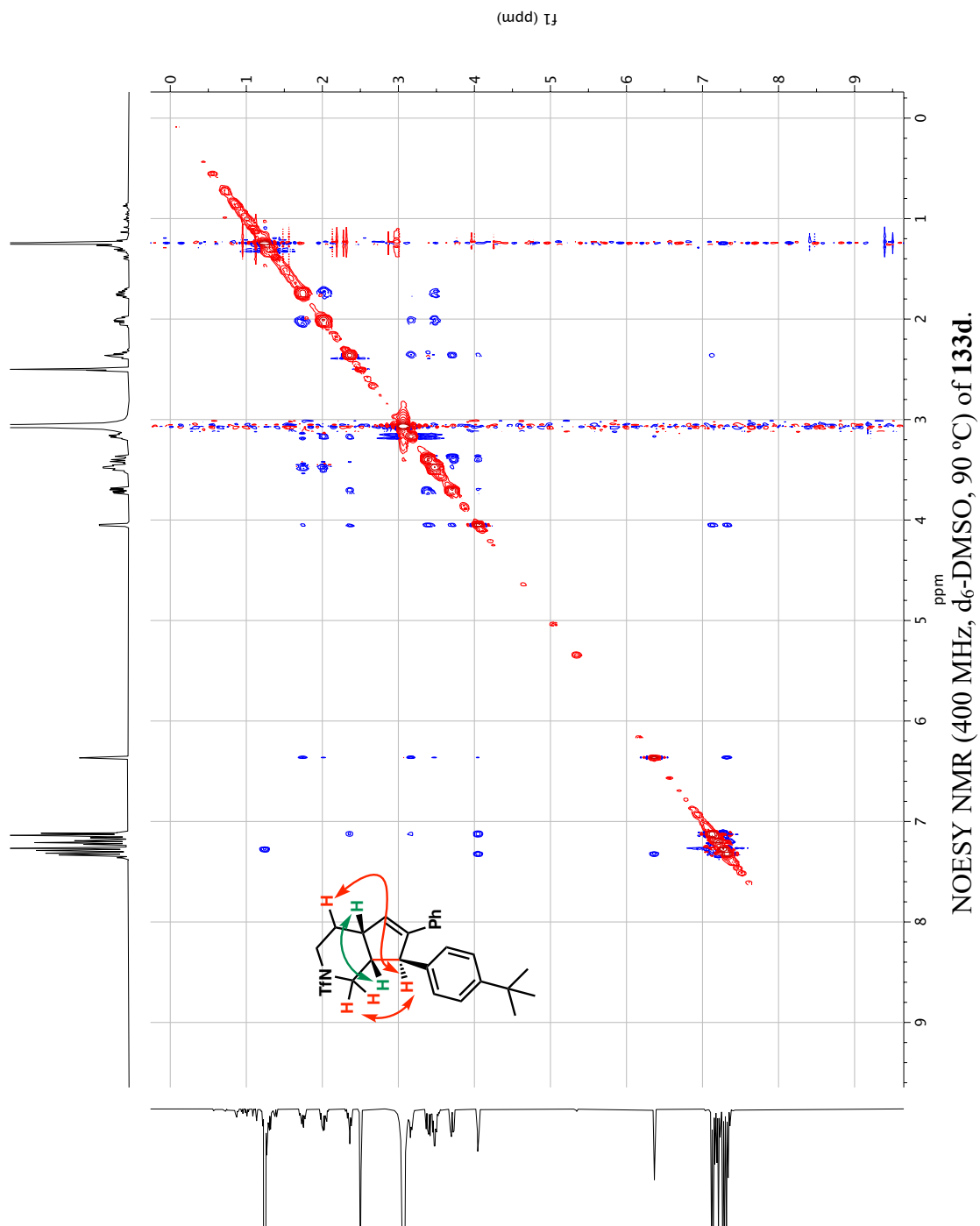


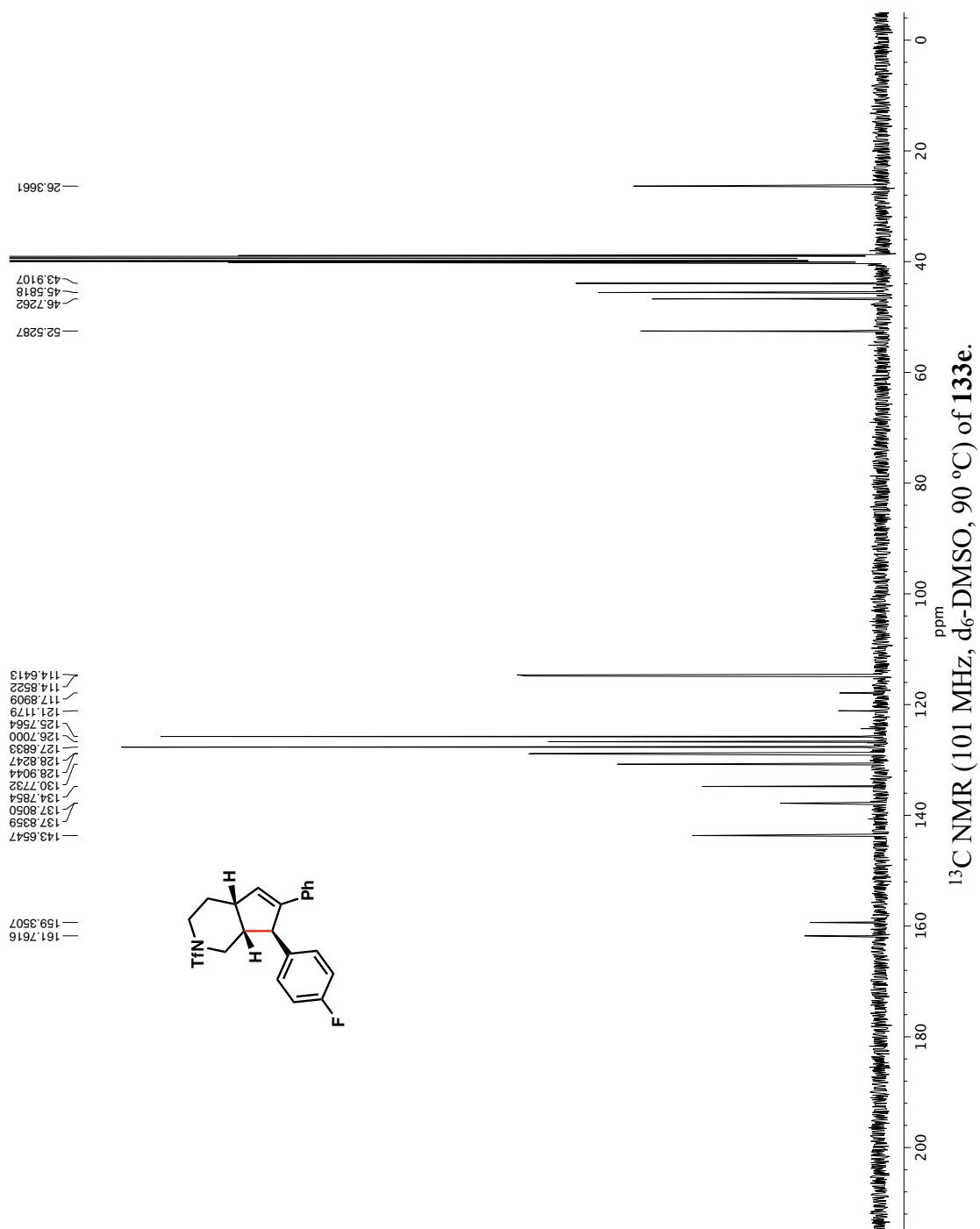


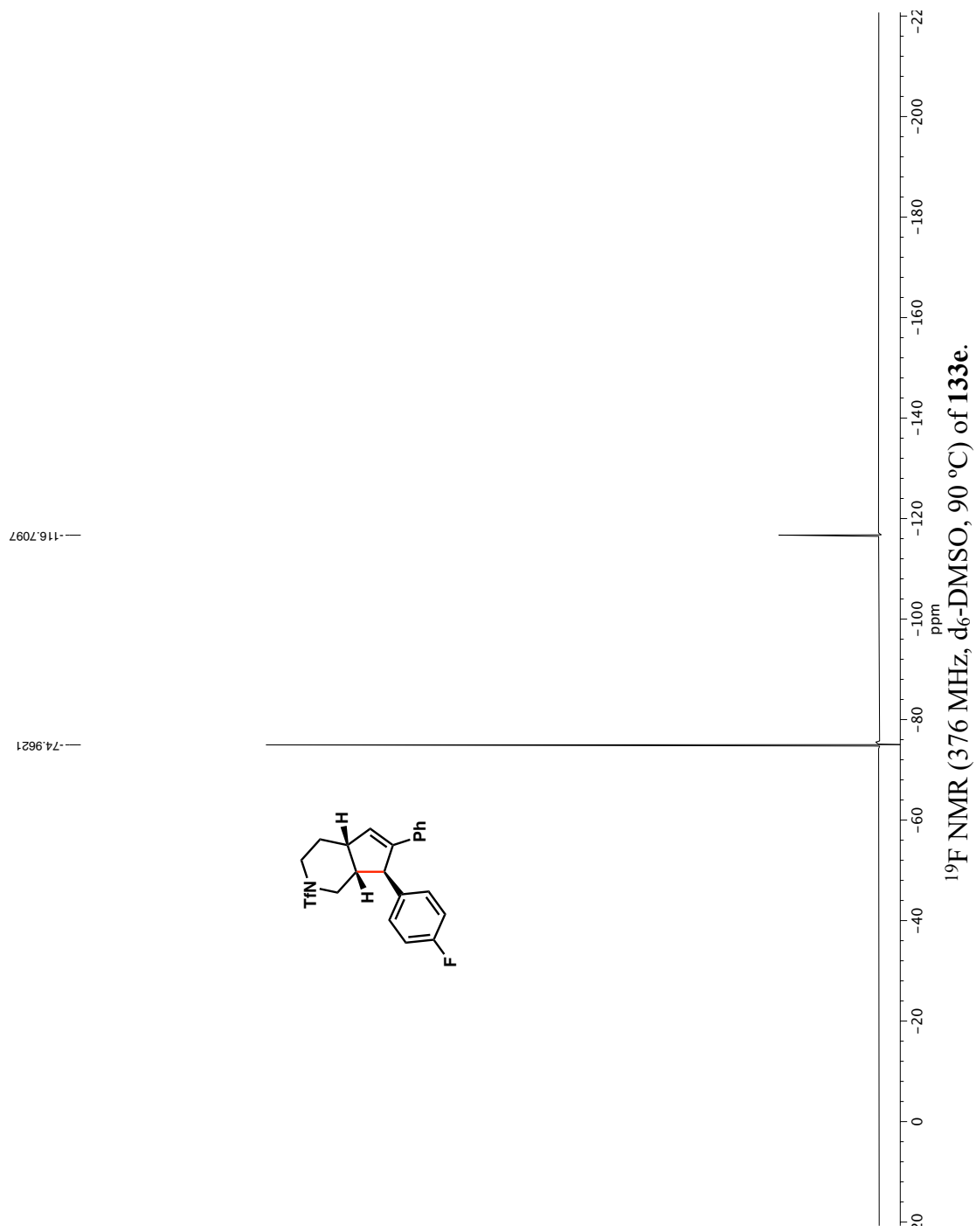


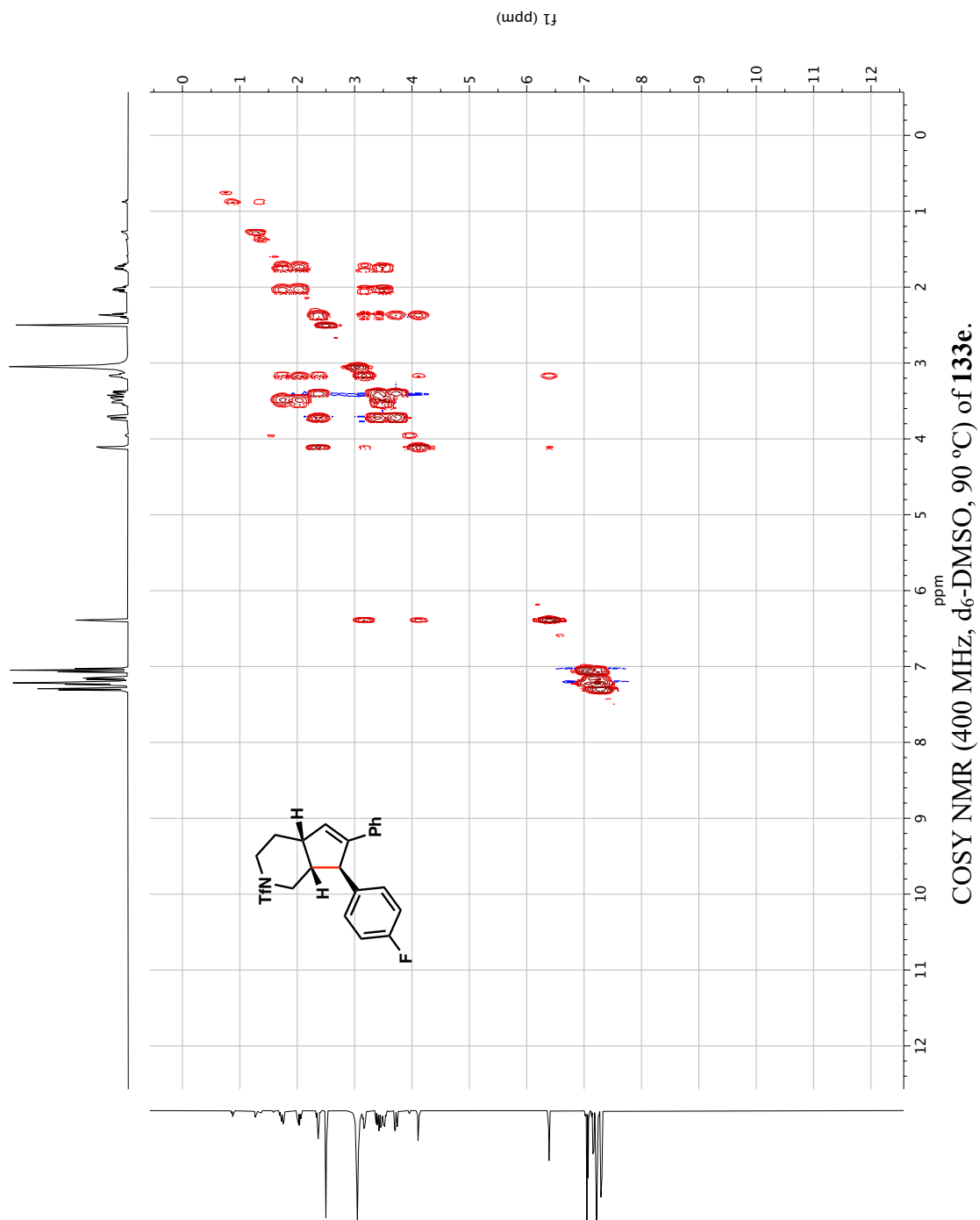


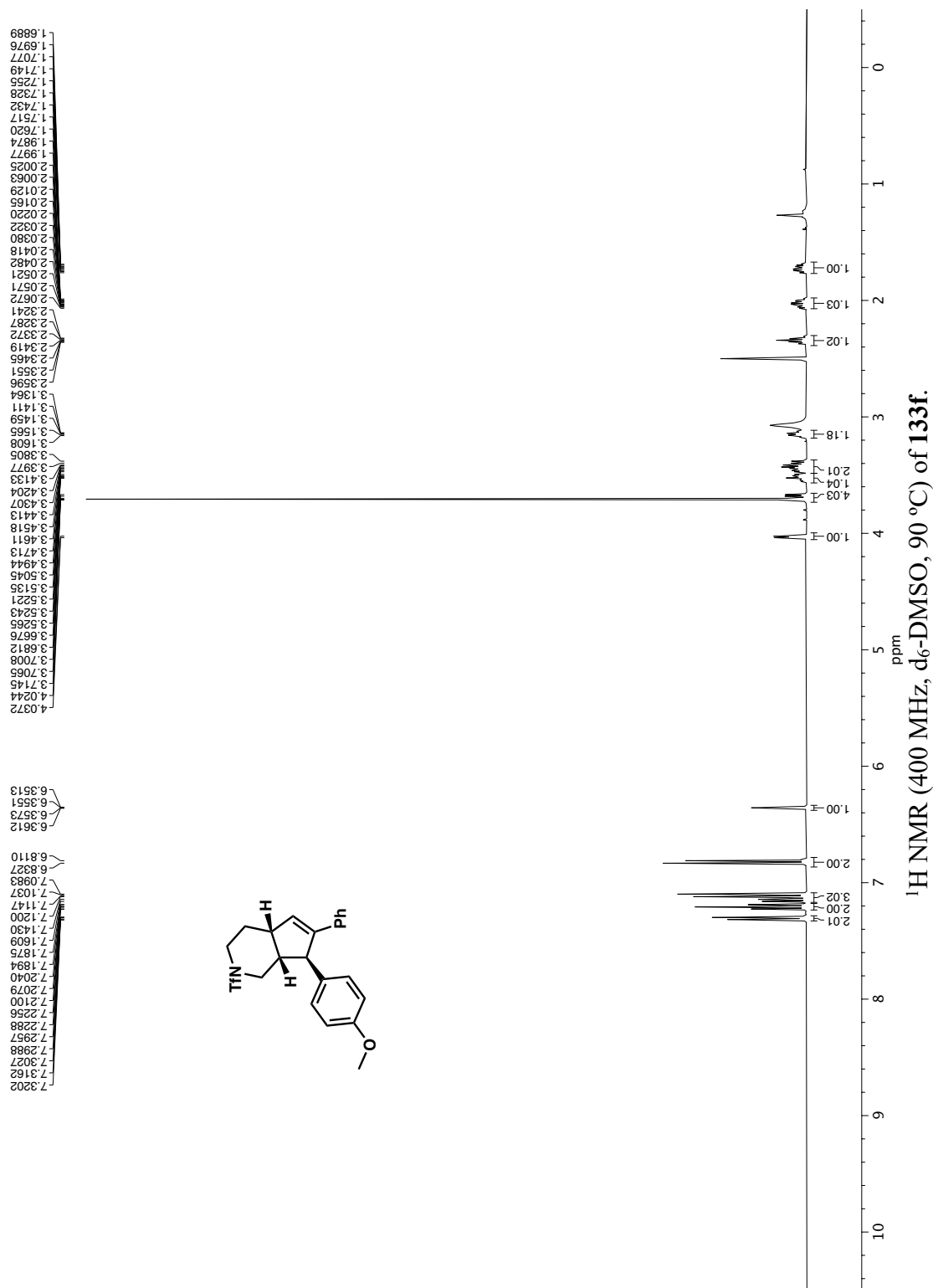


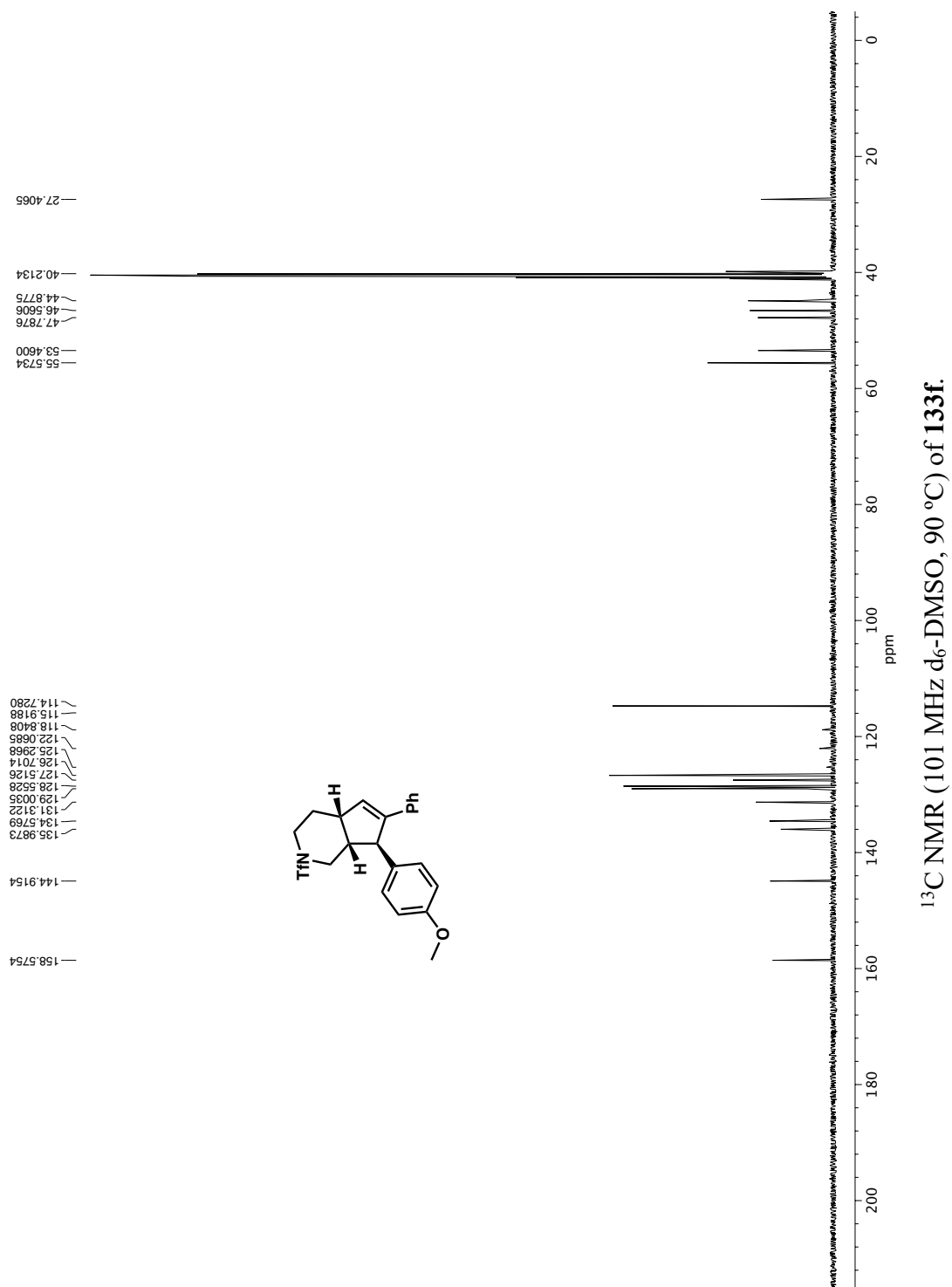


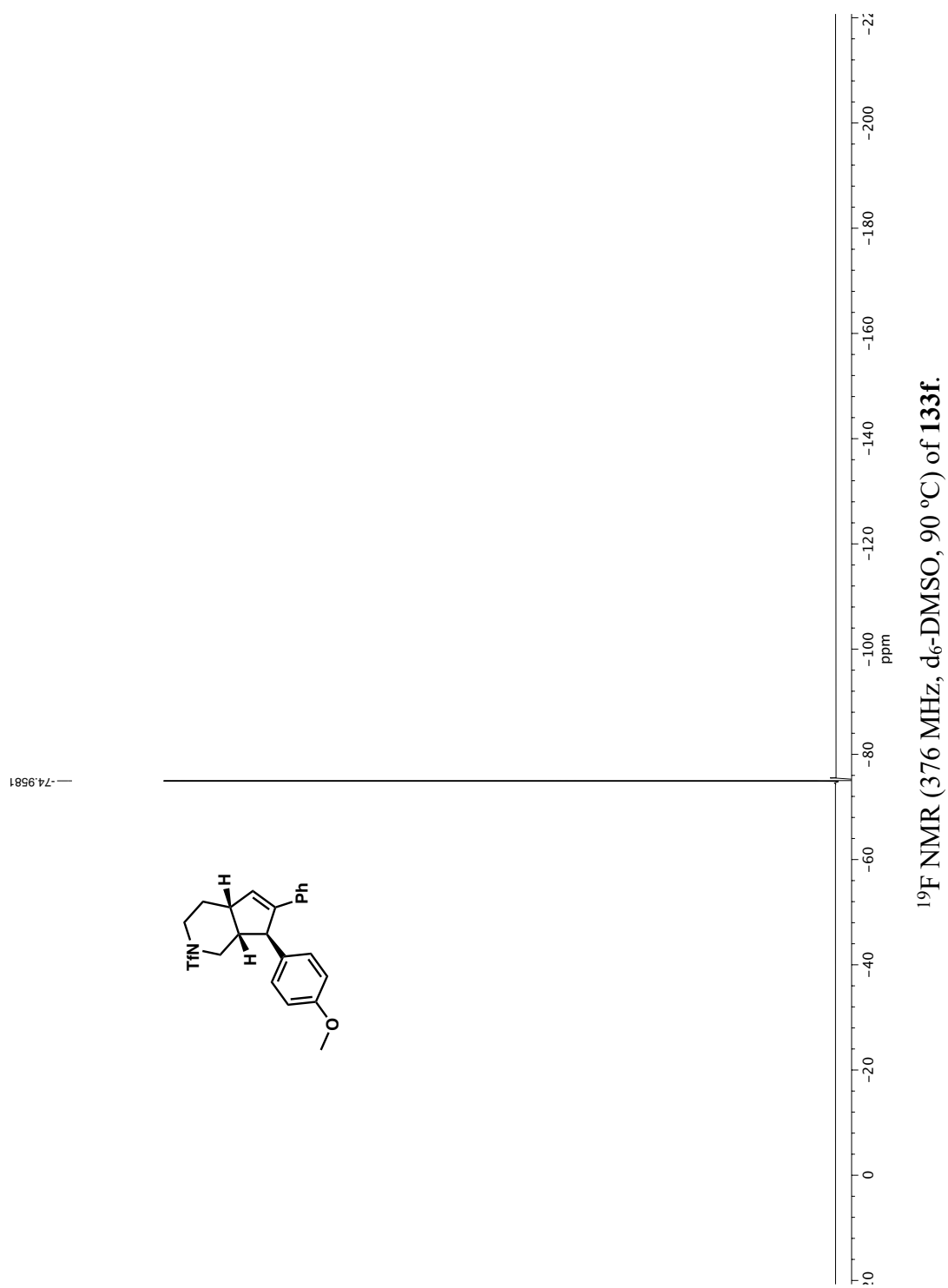


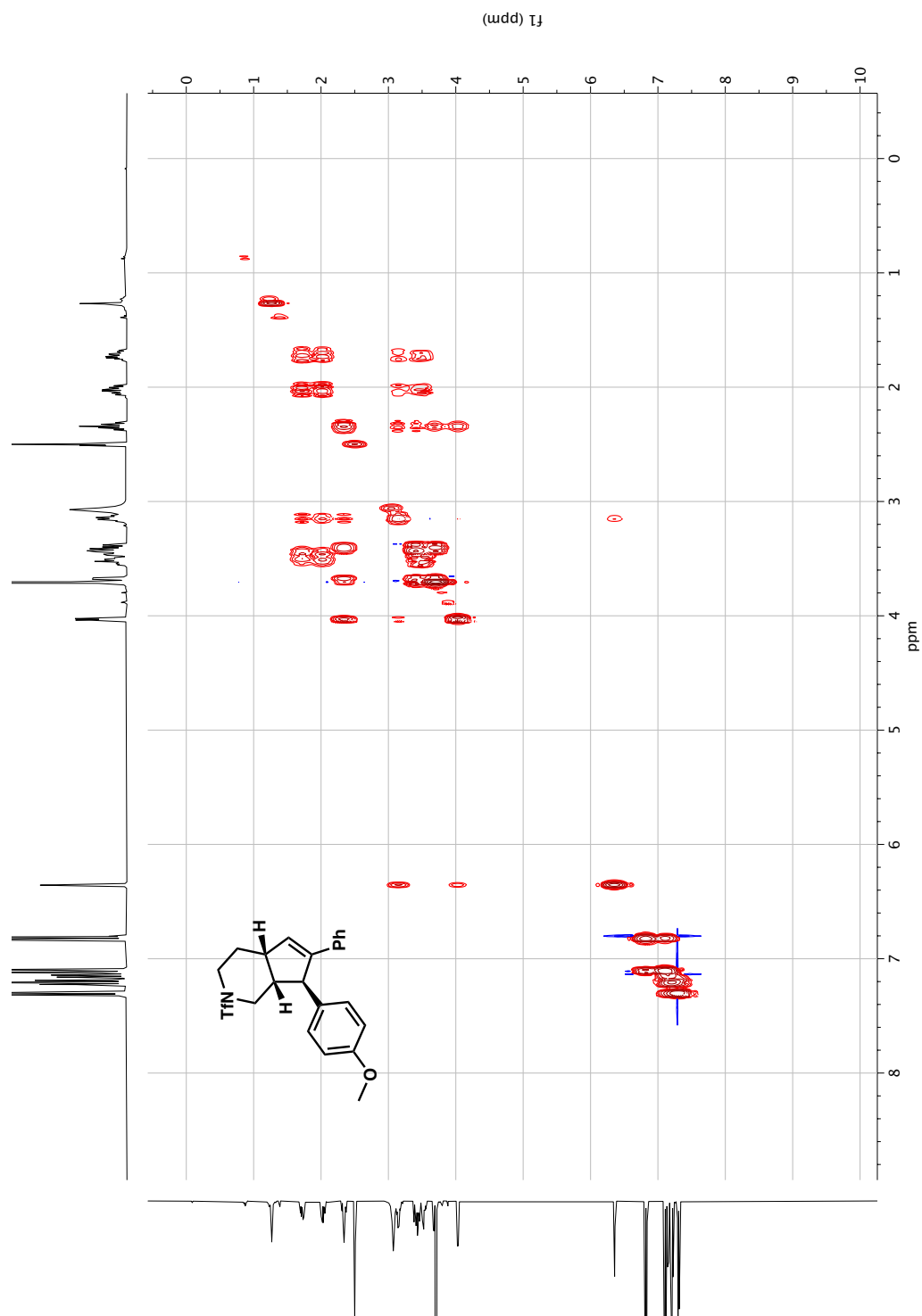




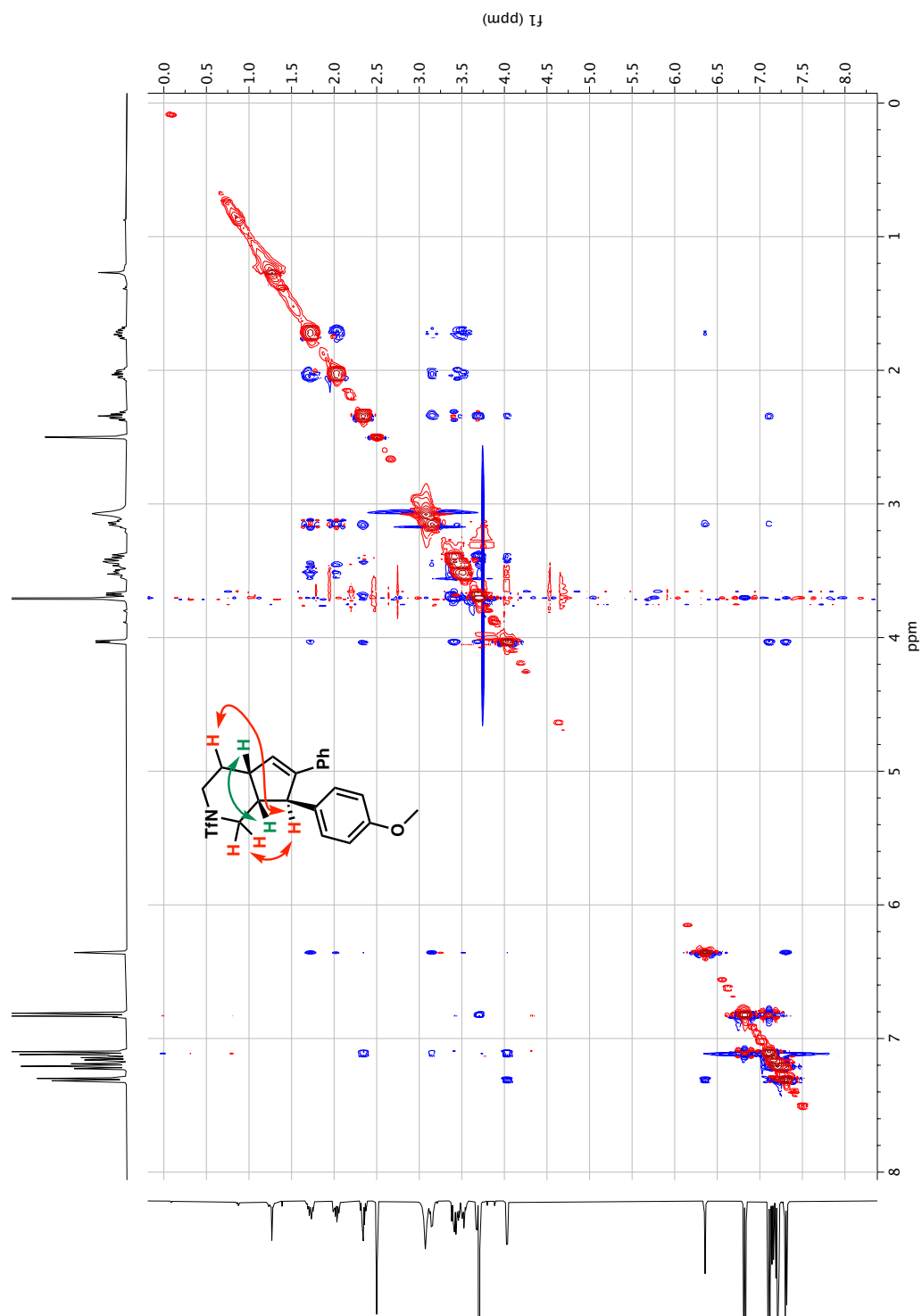




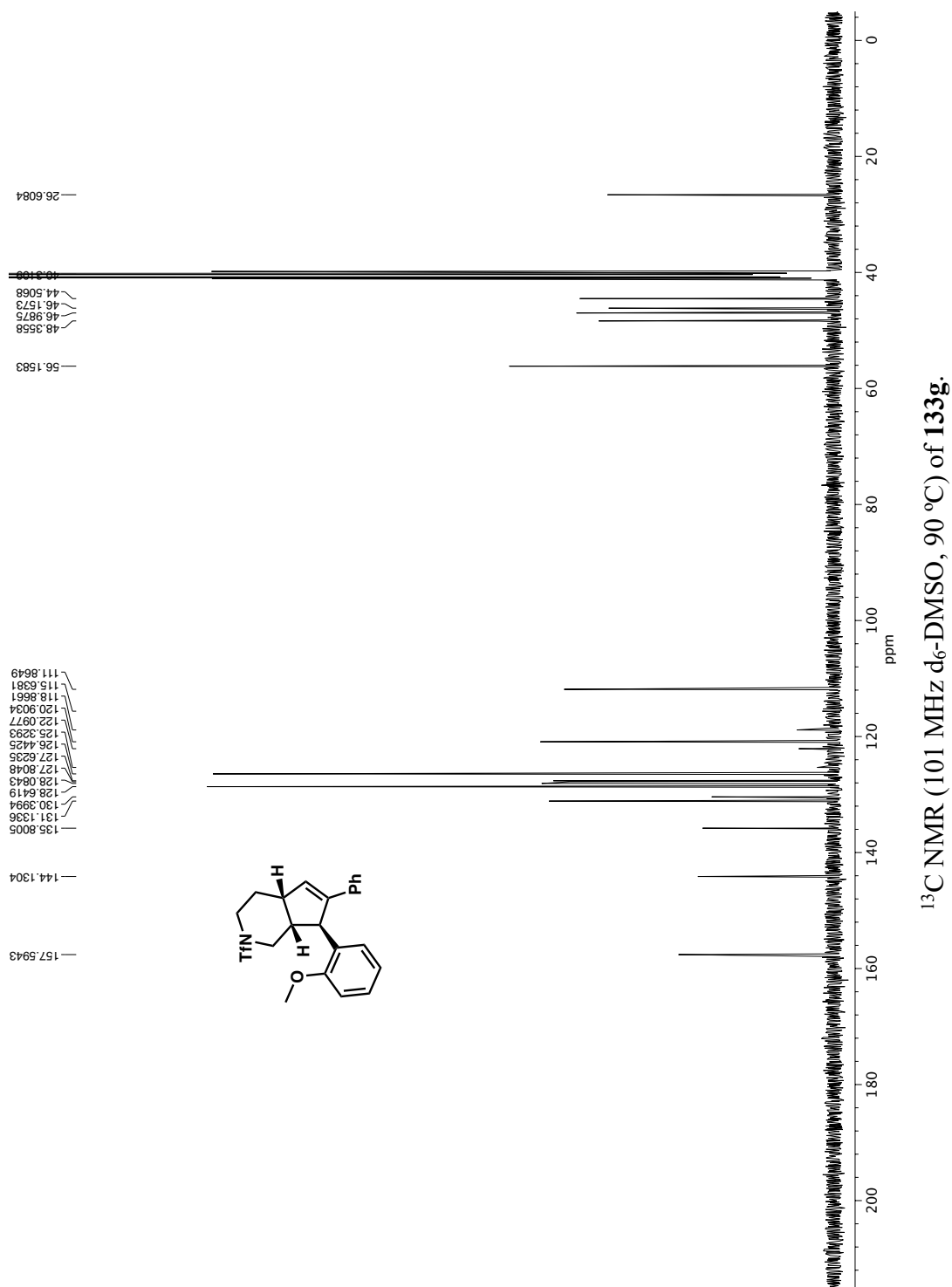


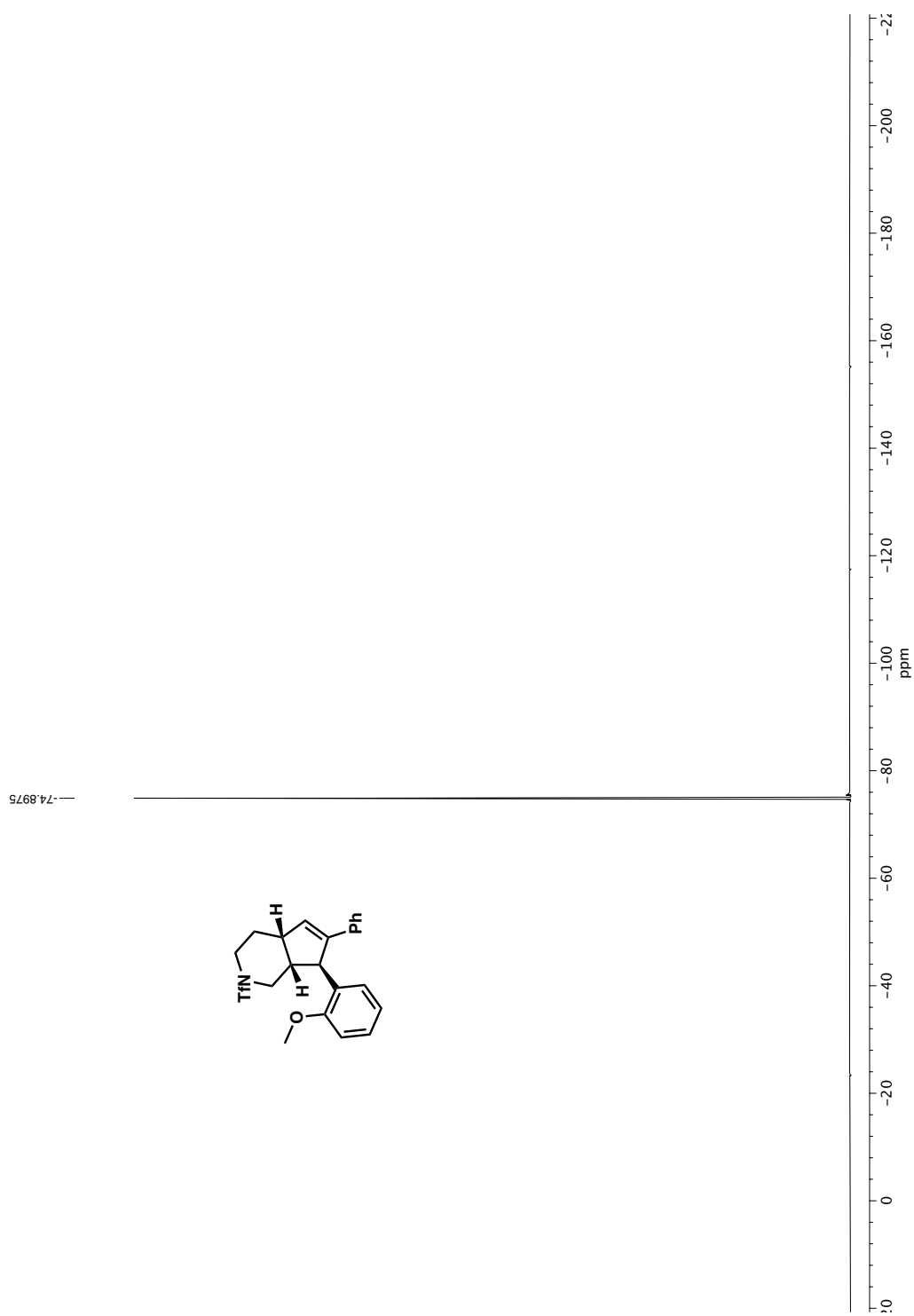


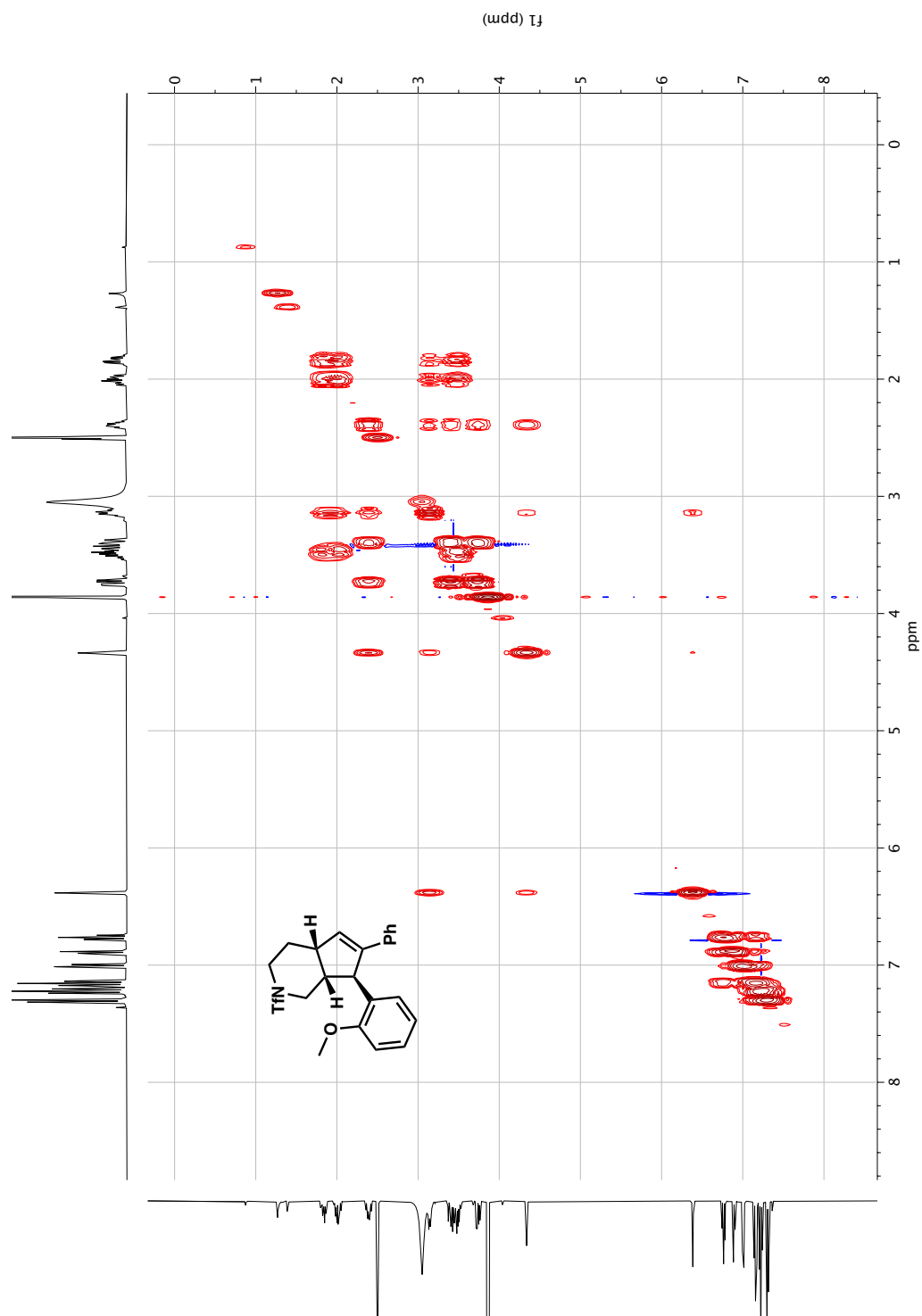
COSY NMR (400 MHz, d_6 -DMSO, 90 °C) of 133f.

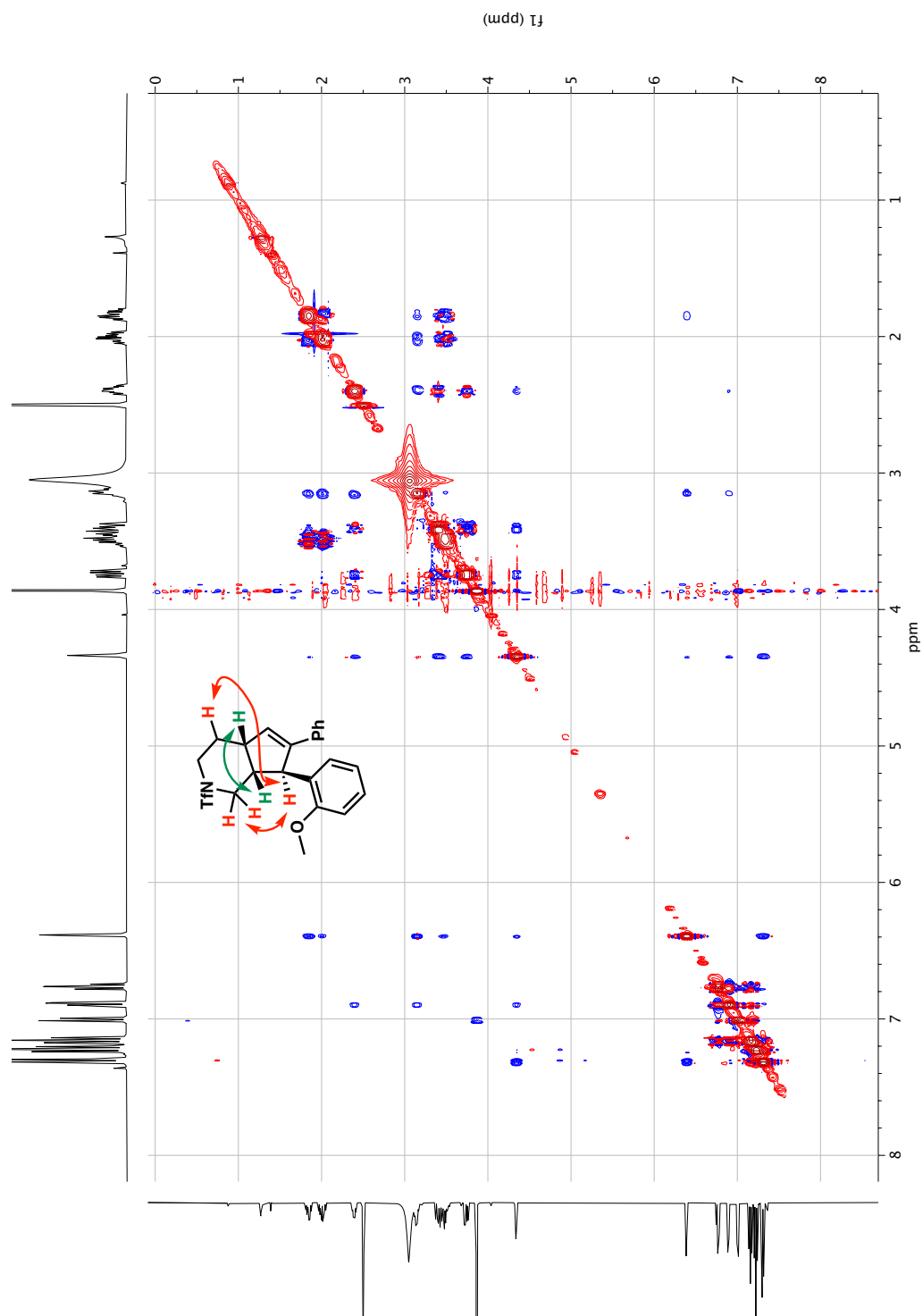


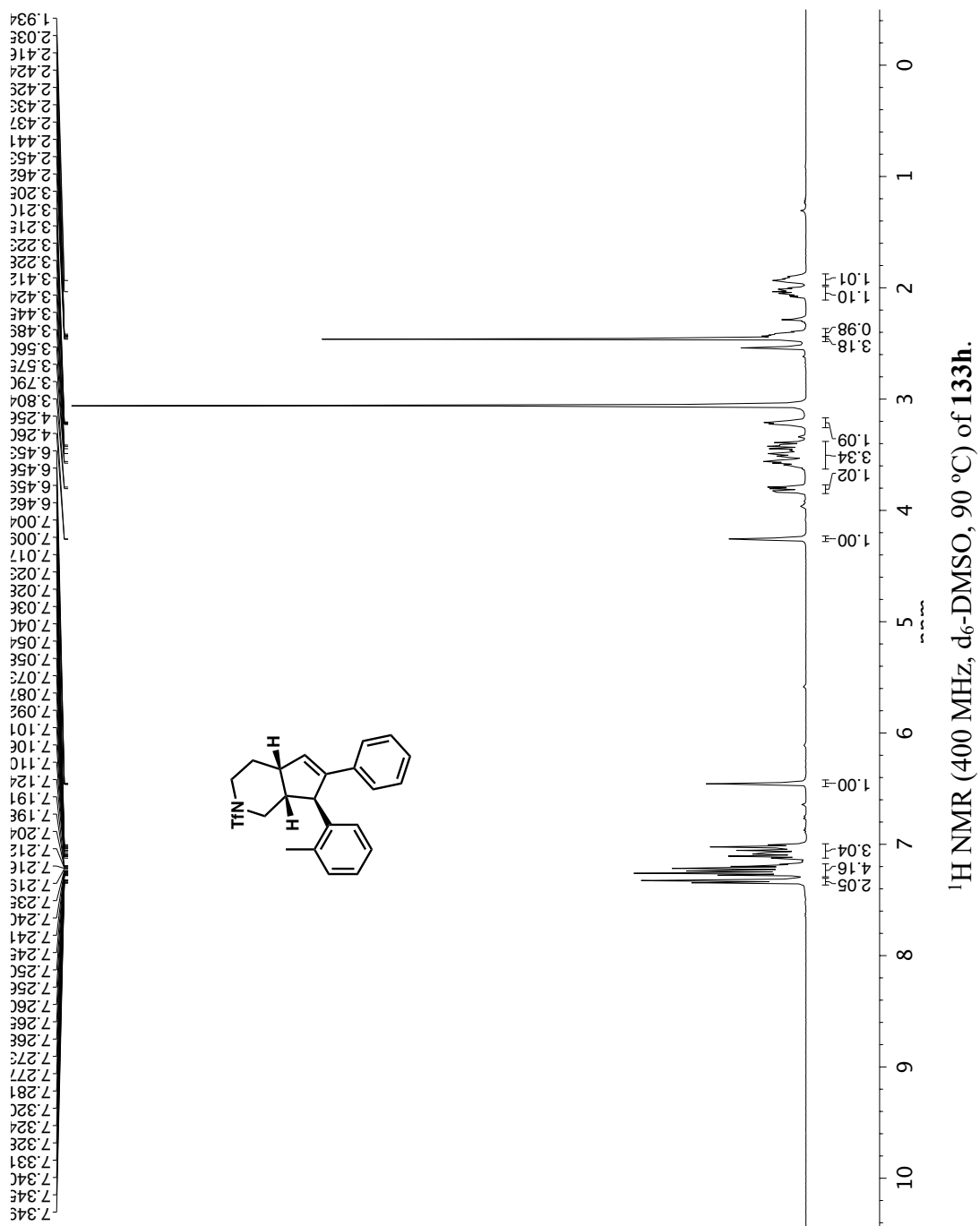
NOESY NMR (400 MHz, d₆-DMSO, 90 °C) of **133f**.

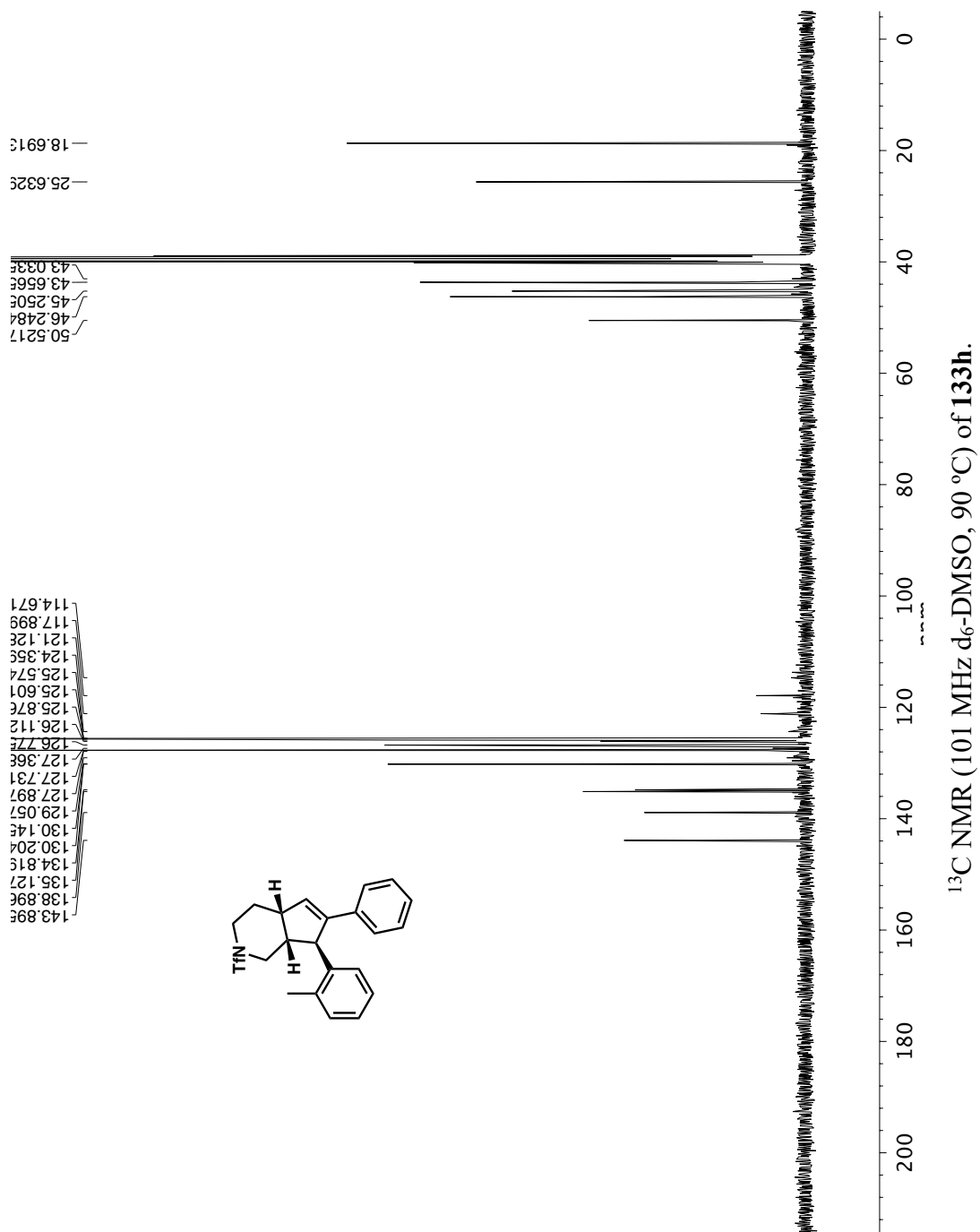


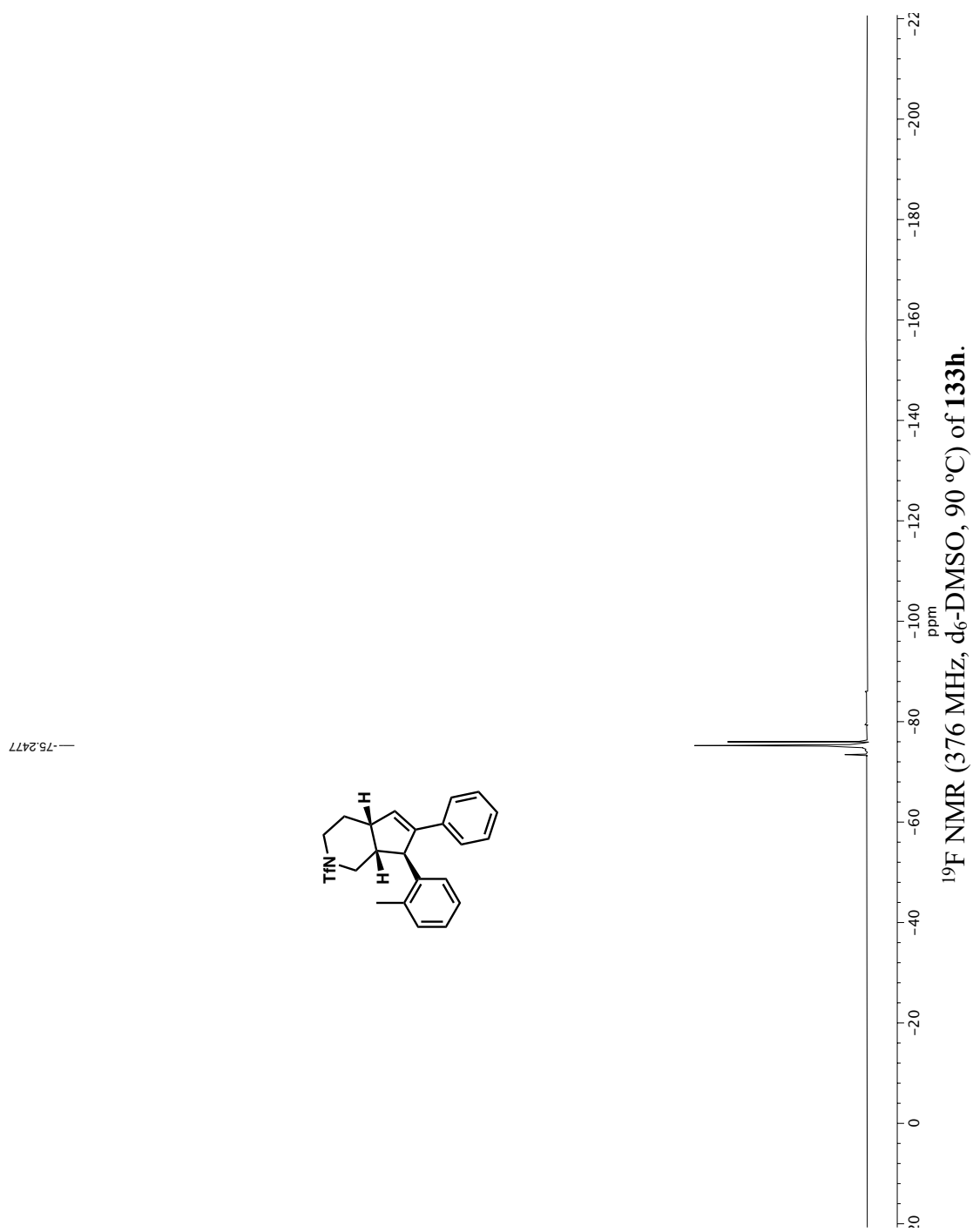


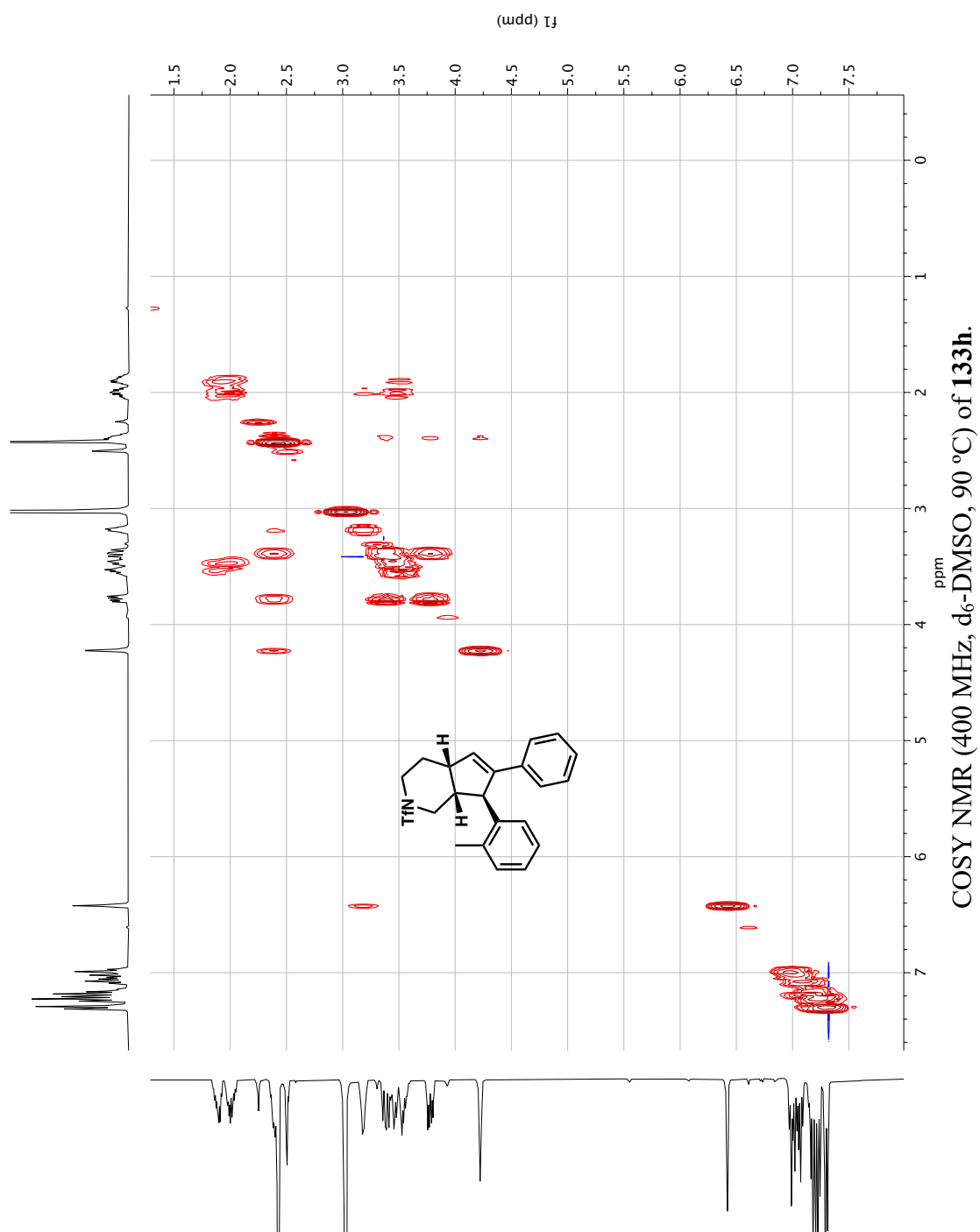


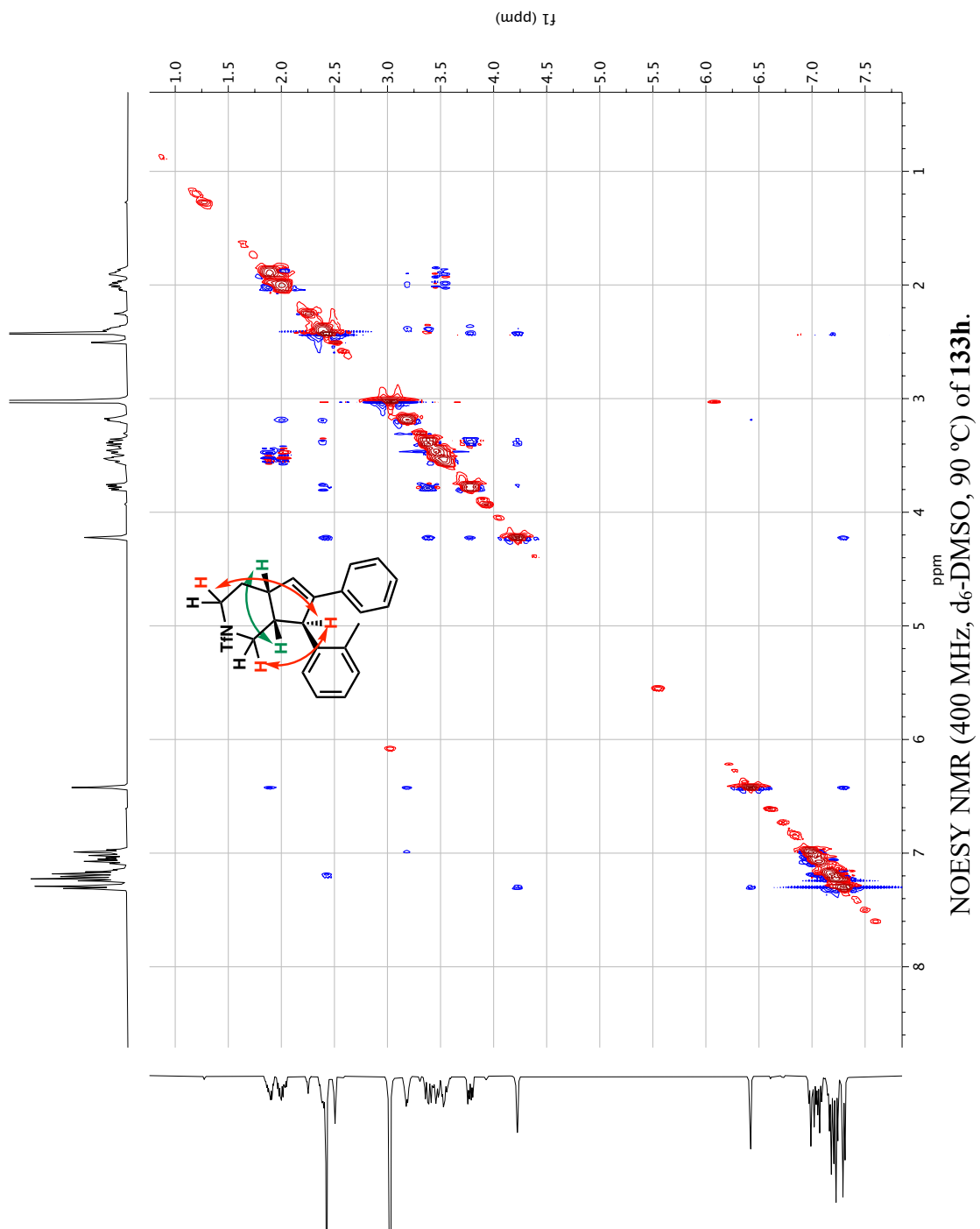


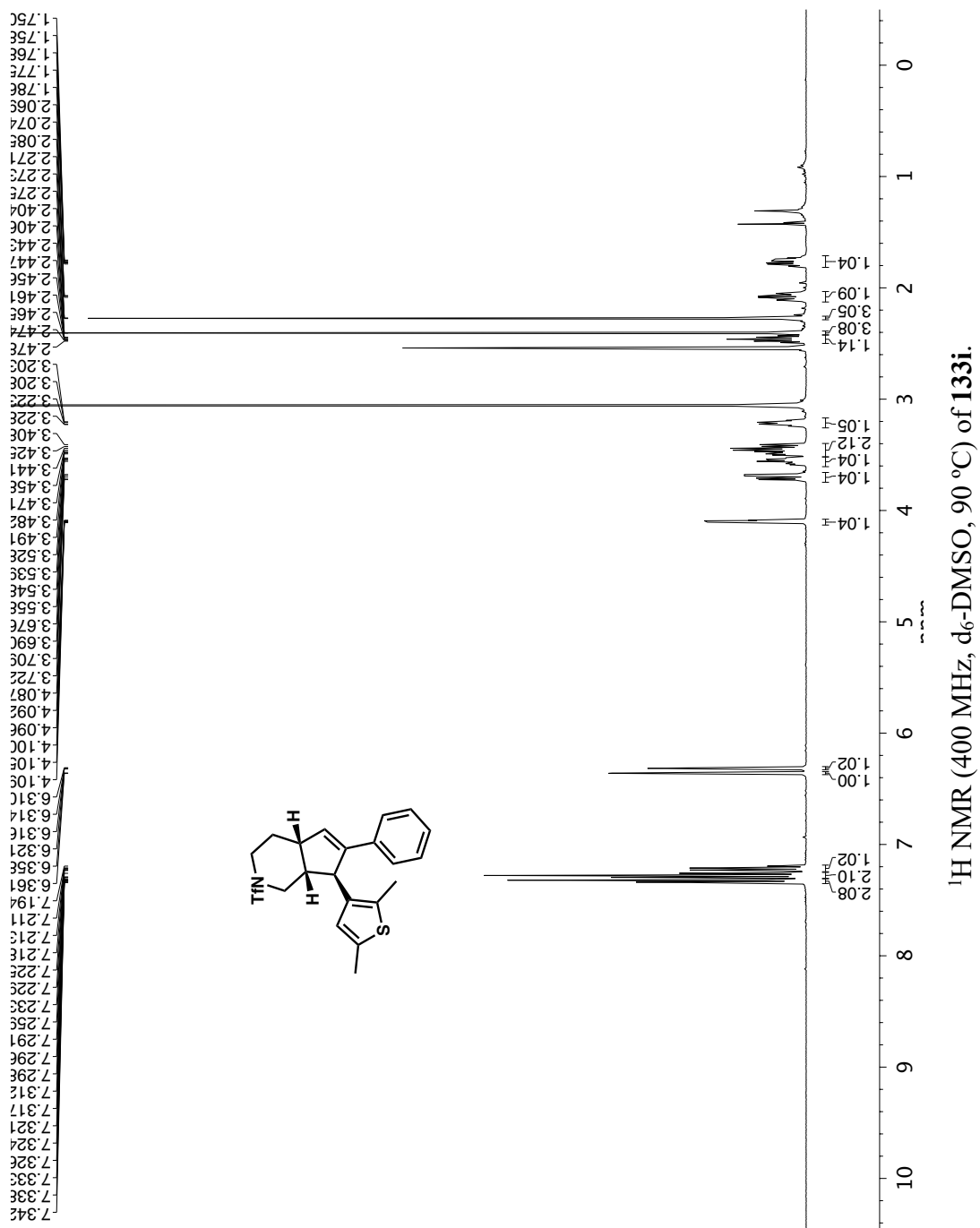


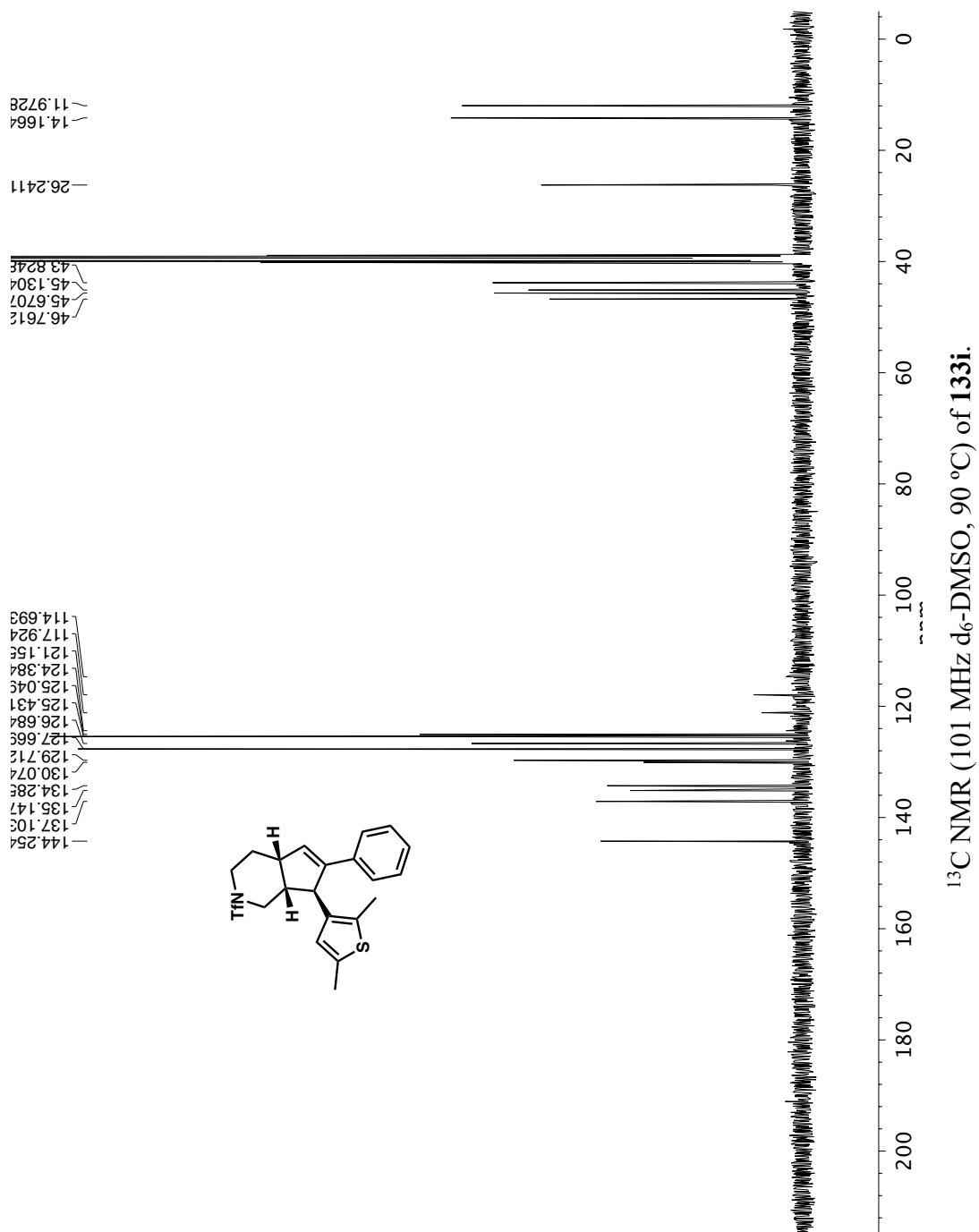




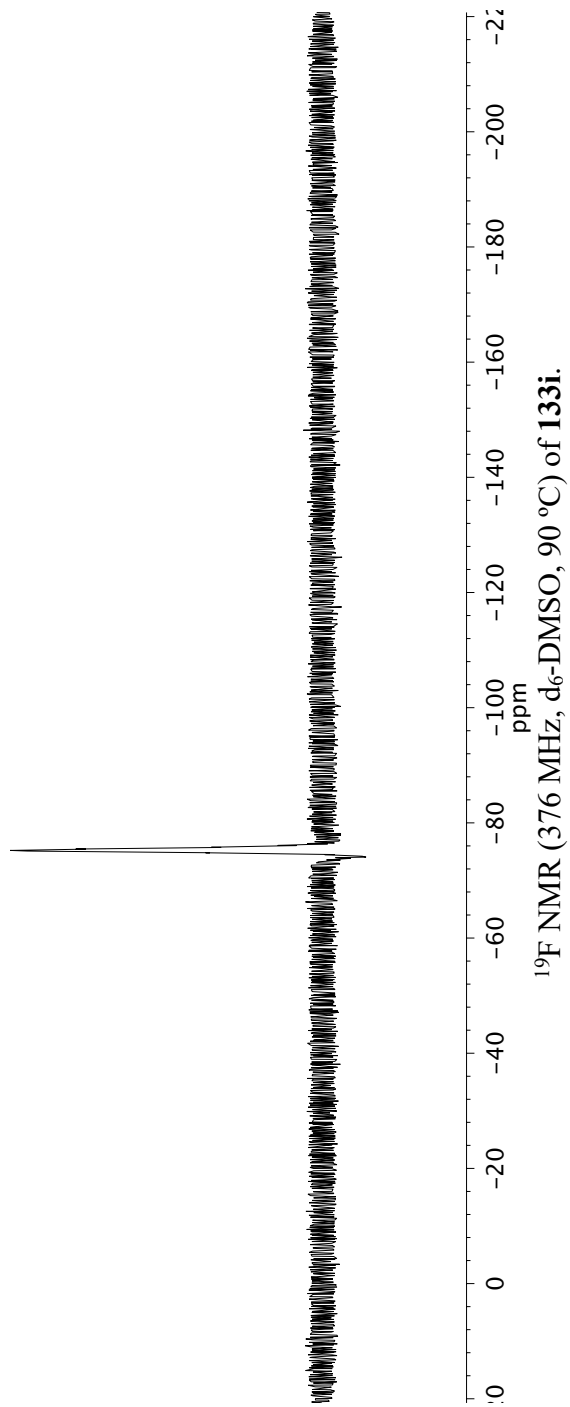
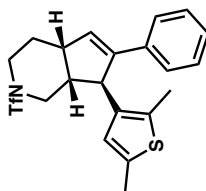


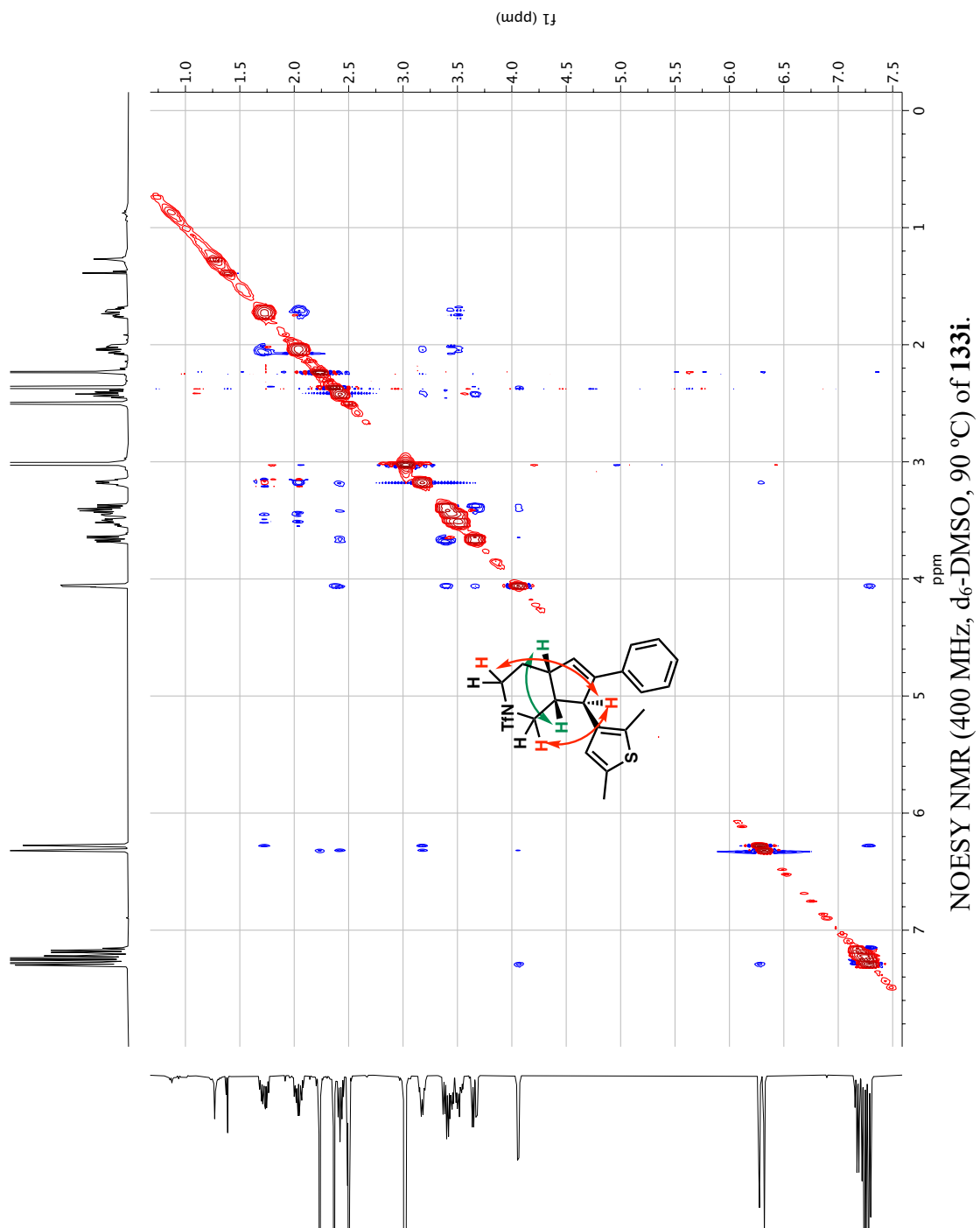


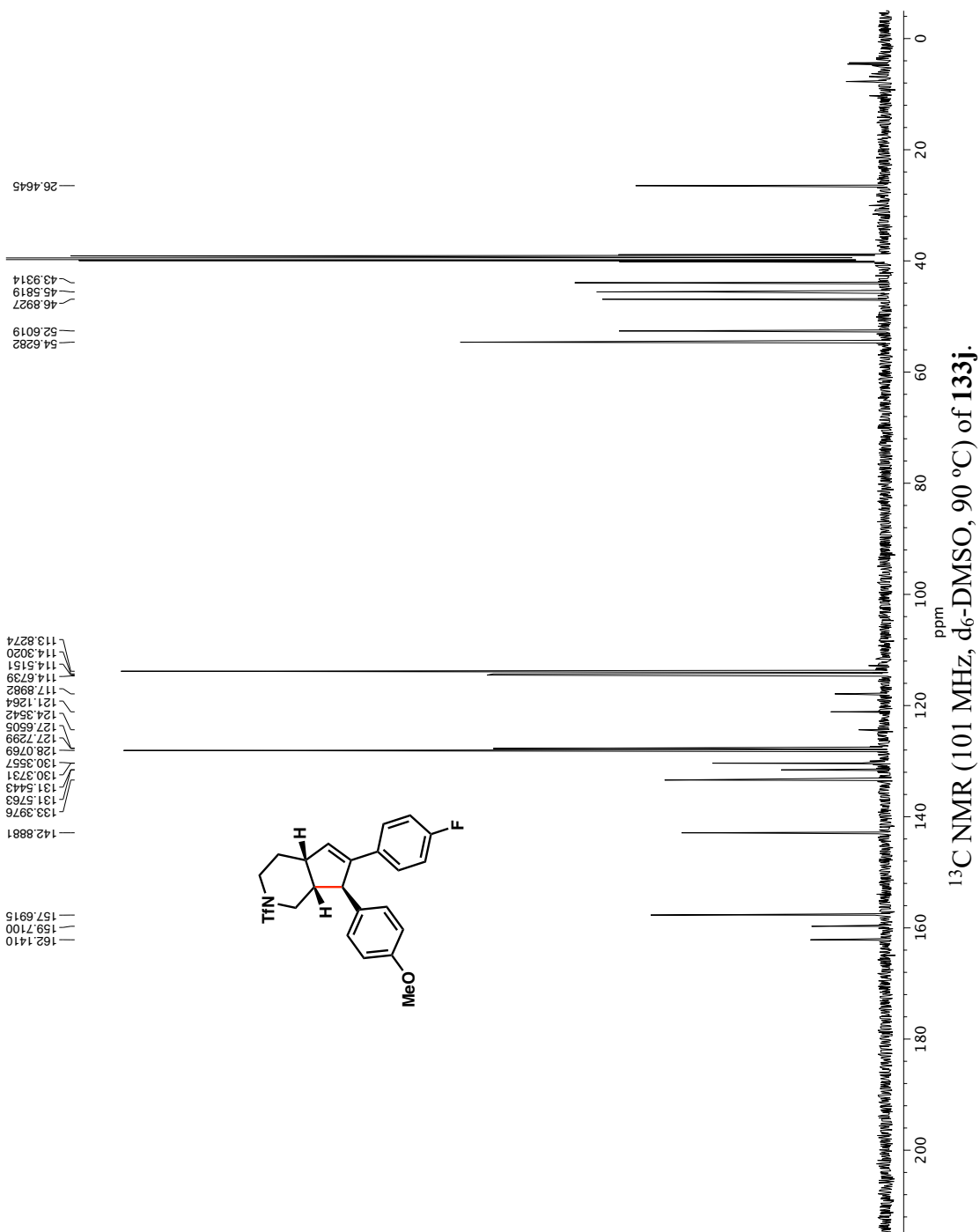


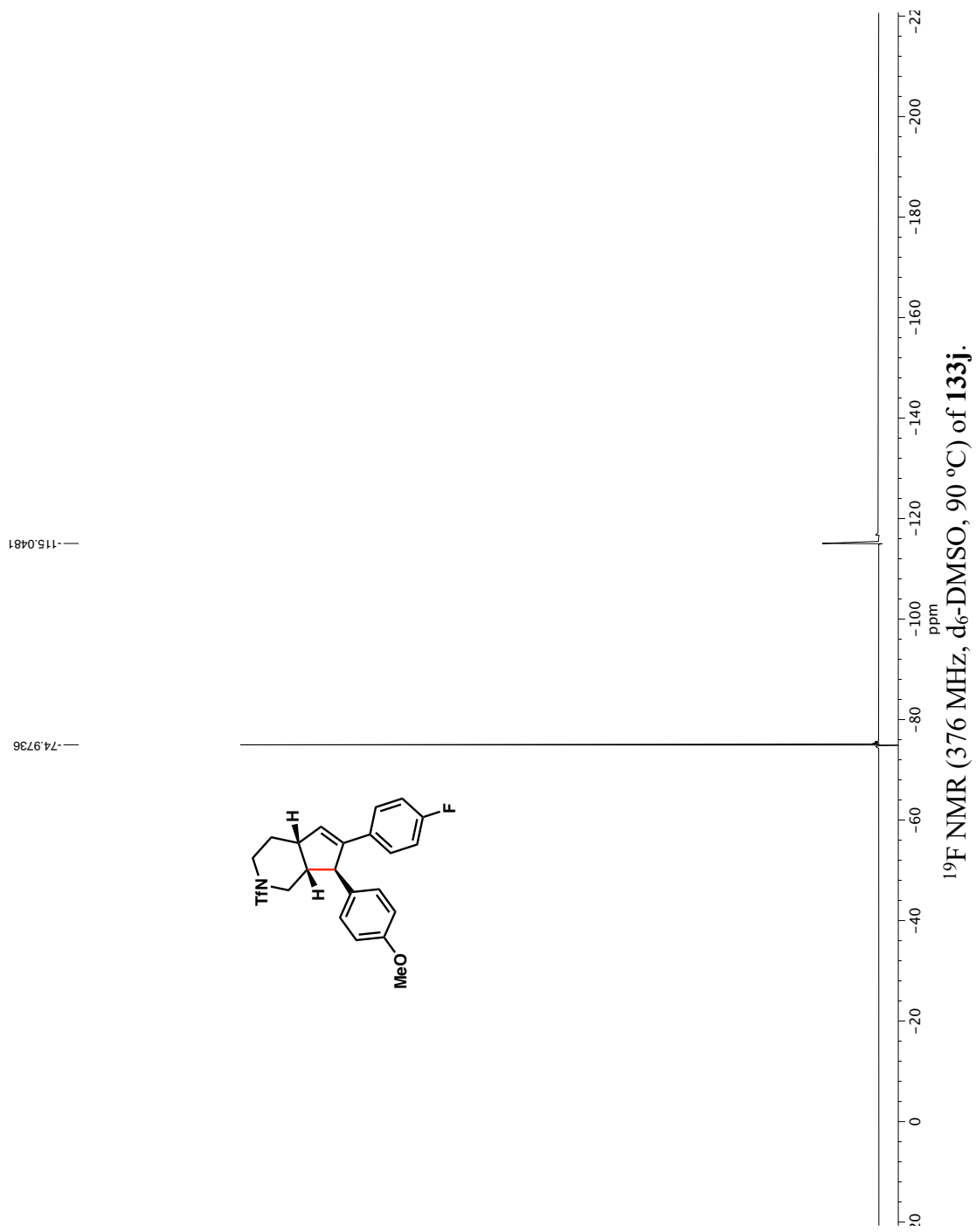


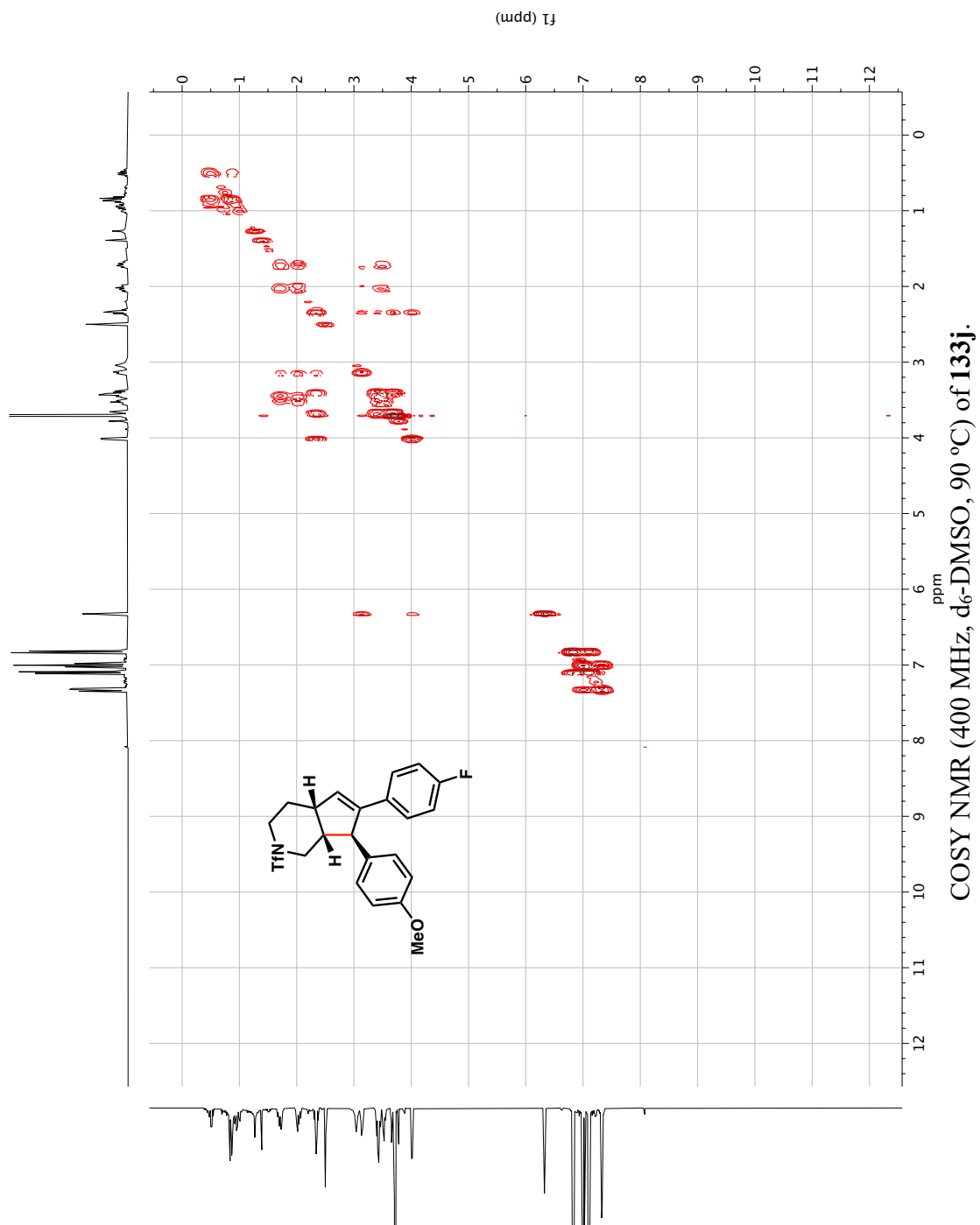
—75.2389

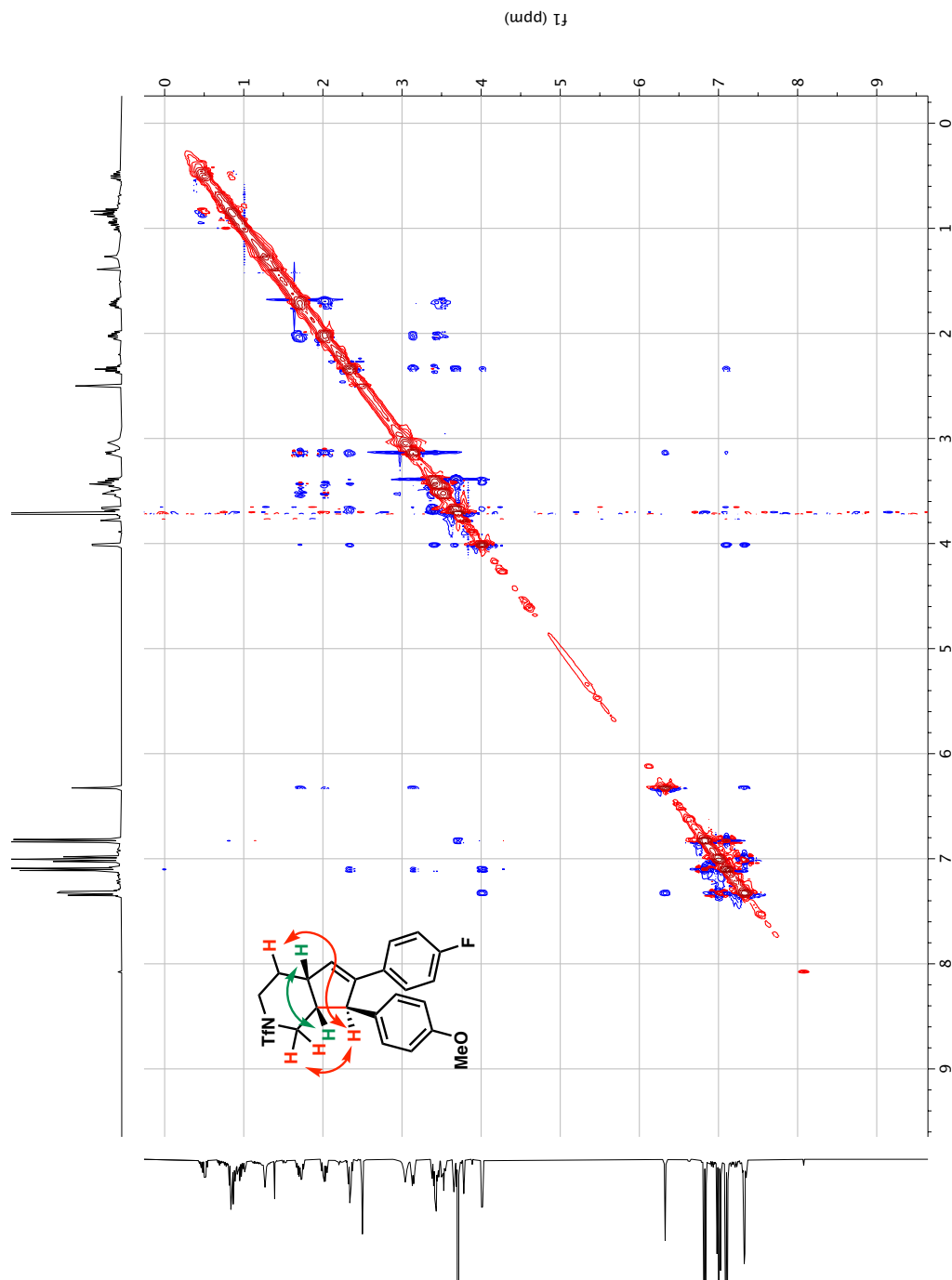


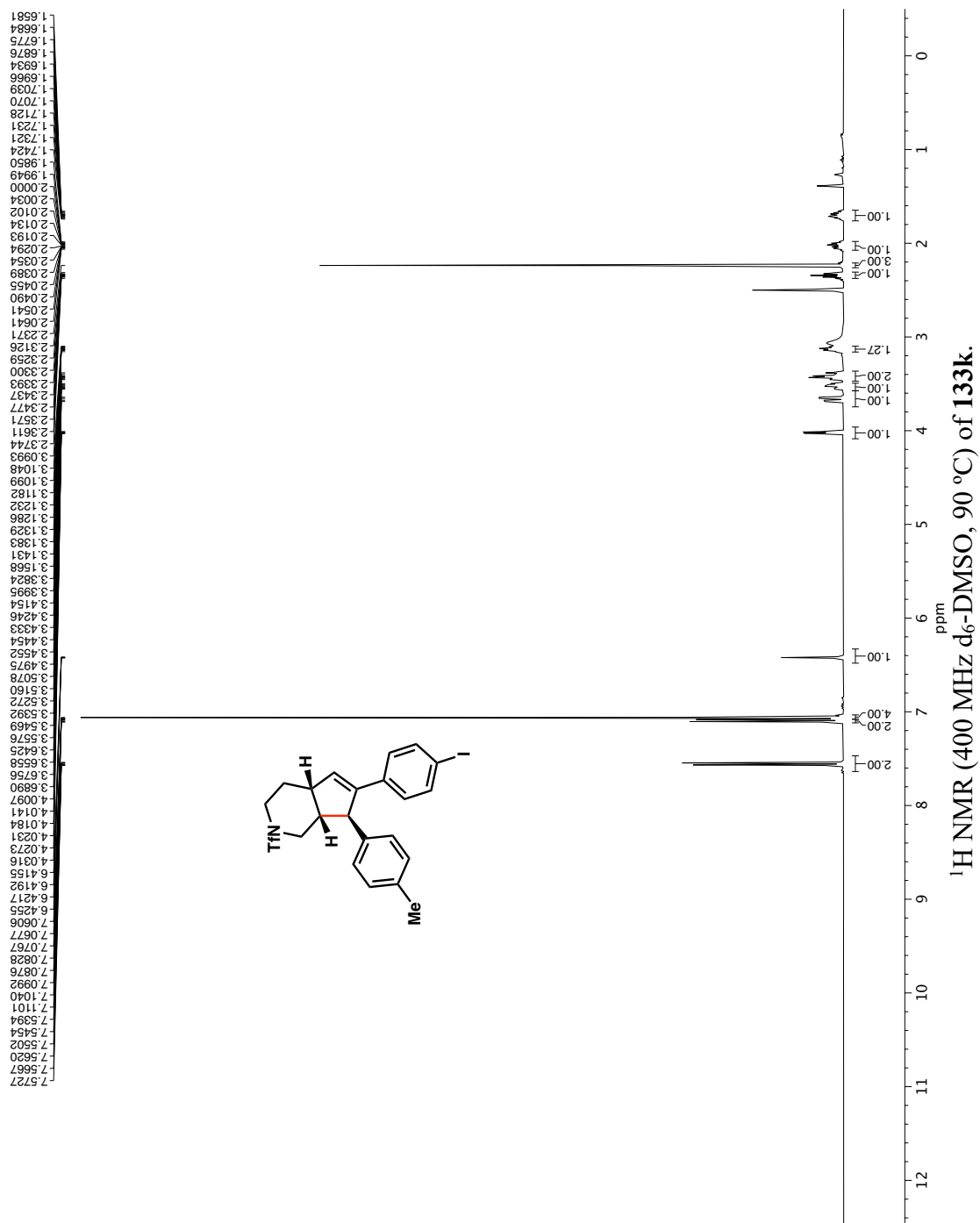


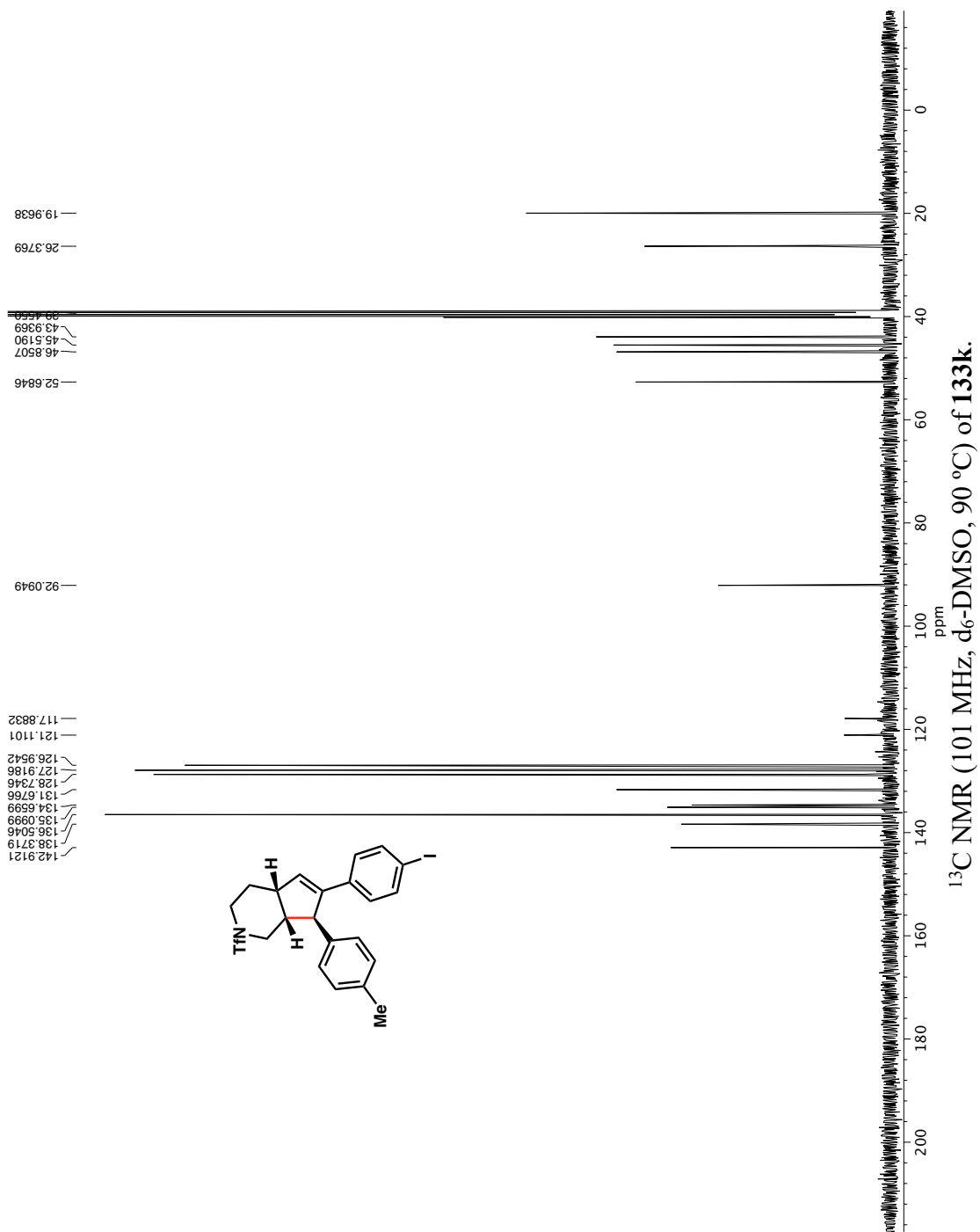


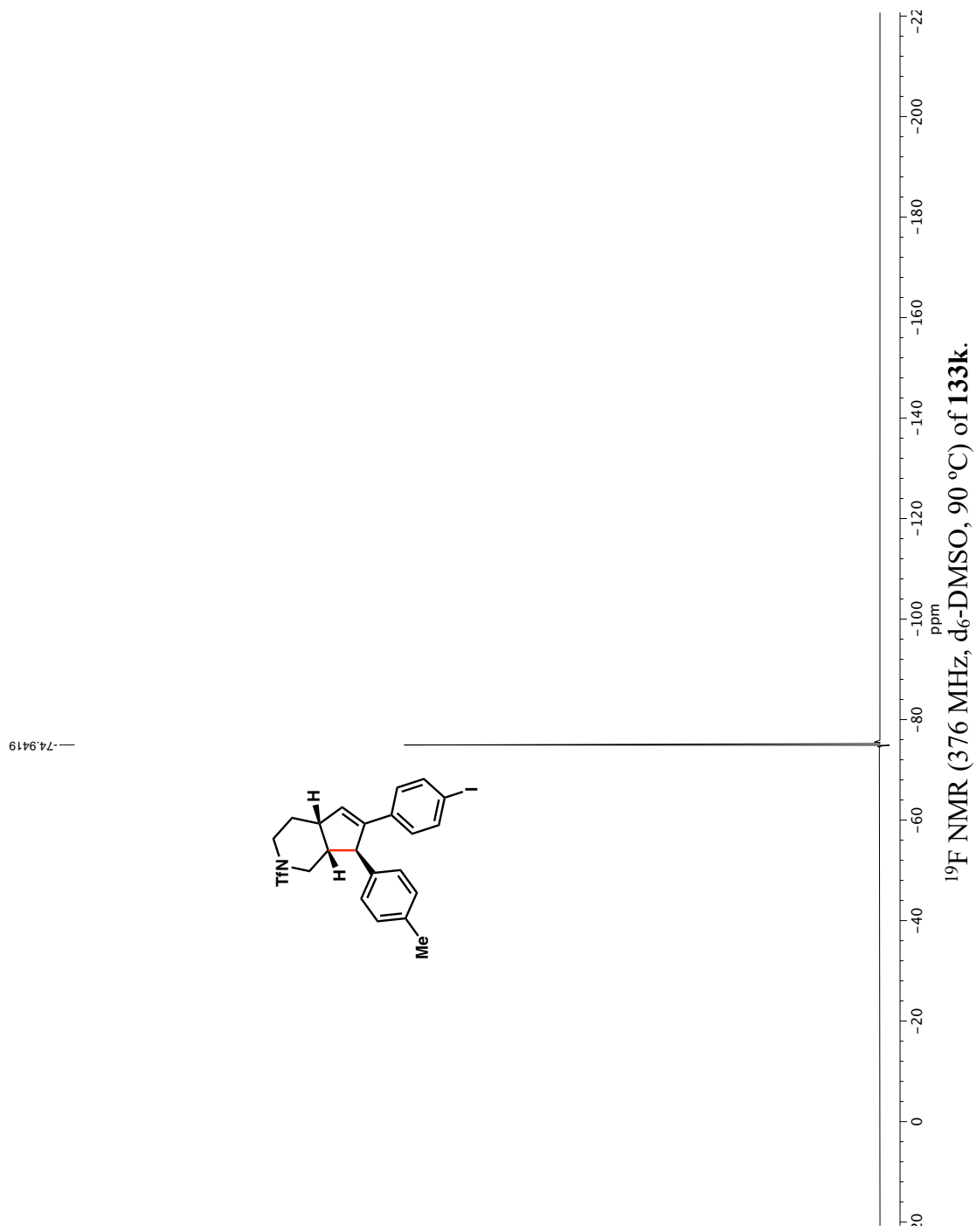


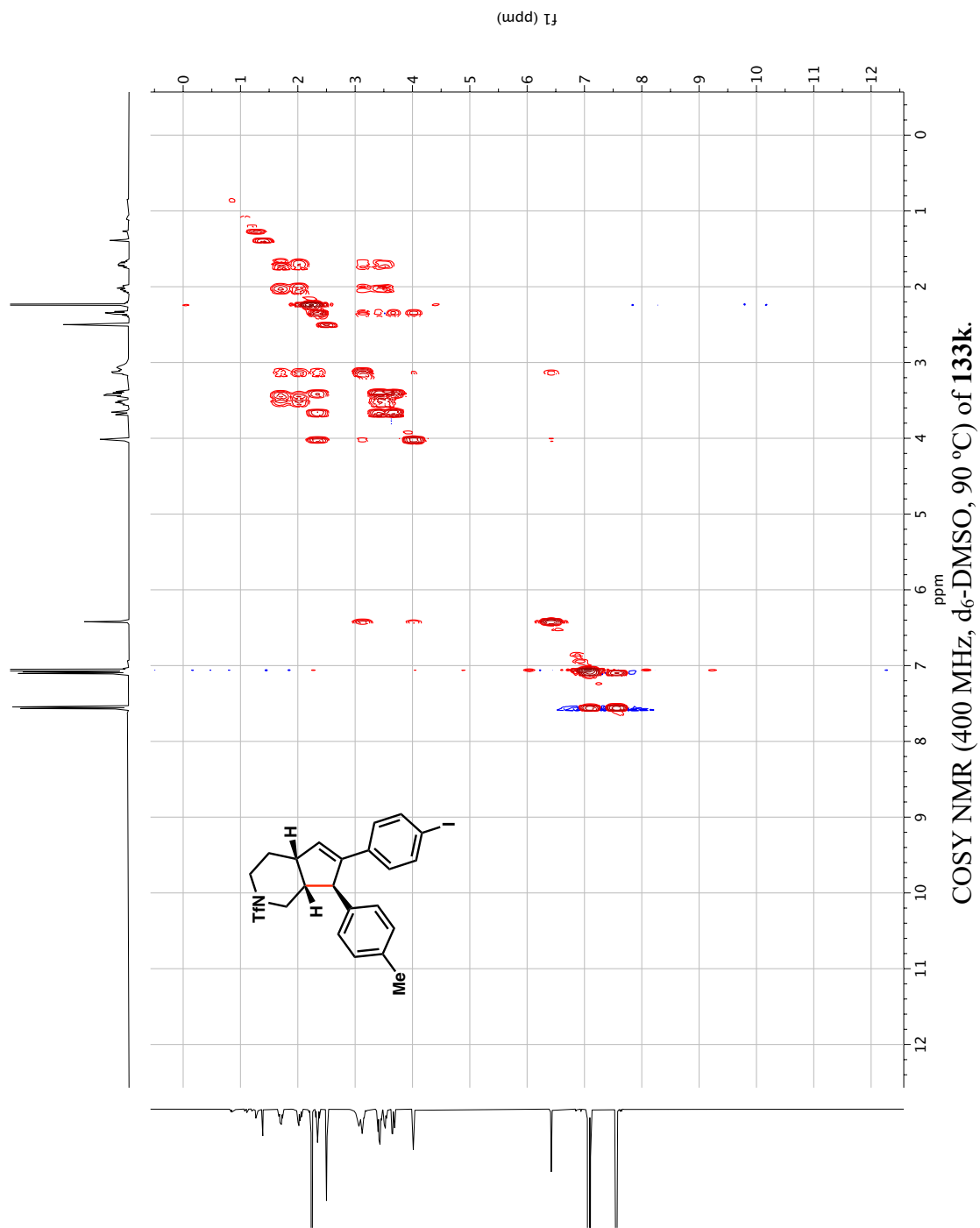


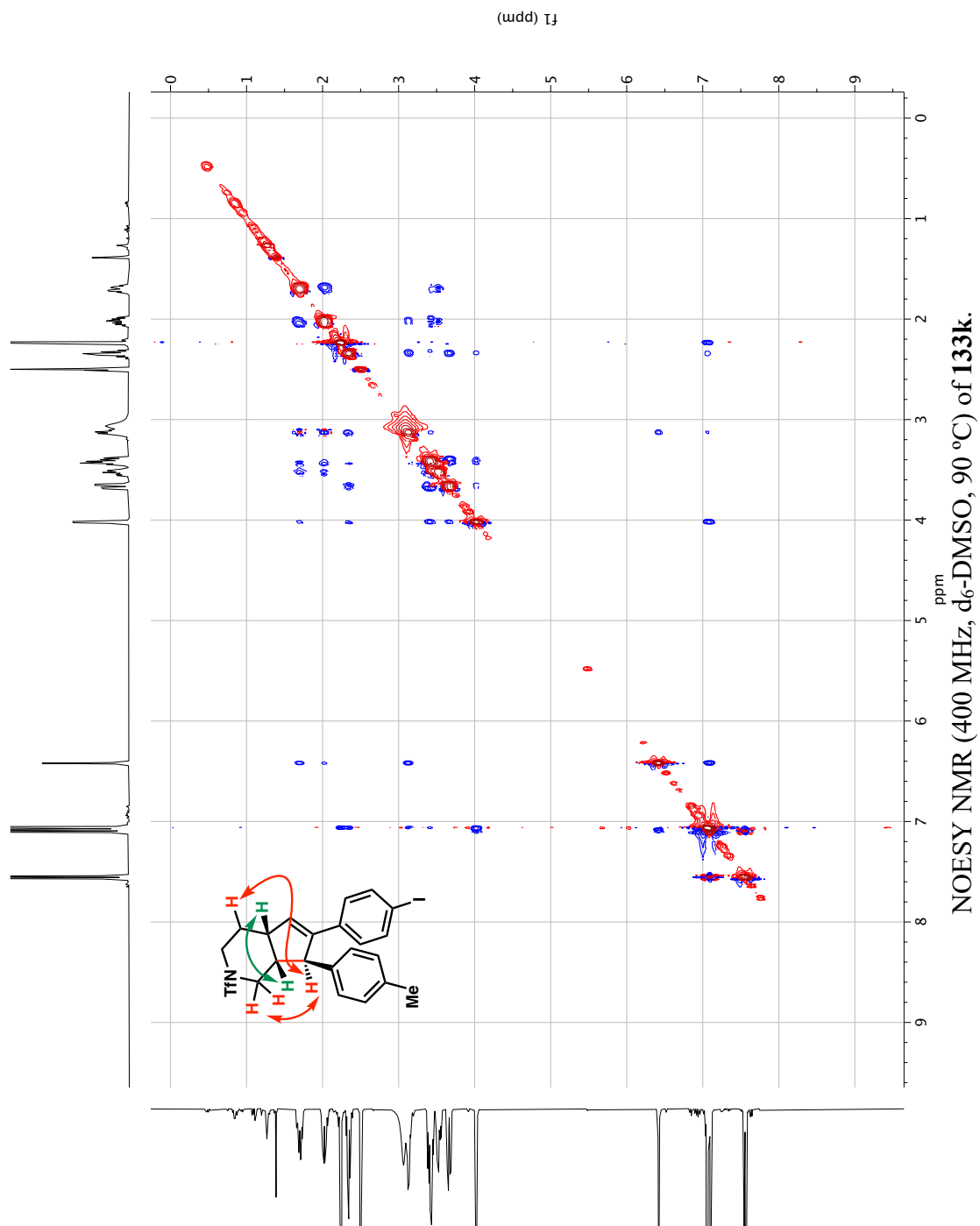


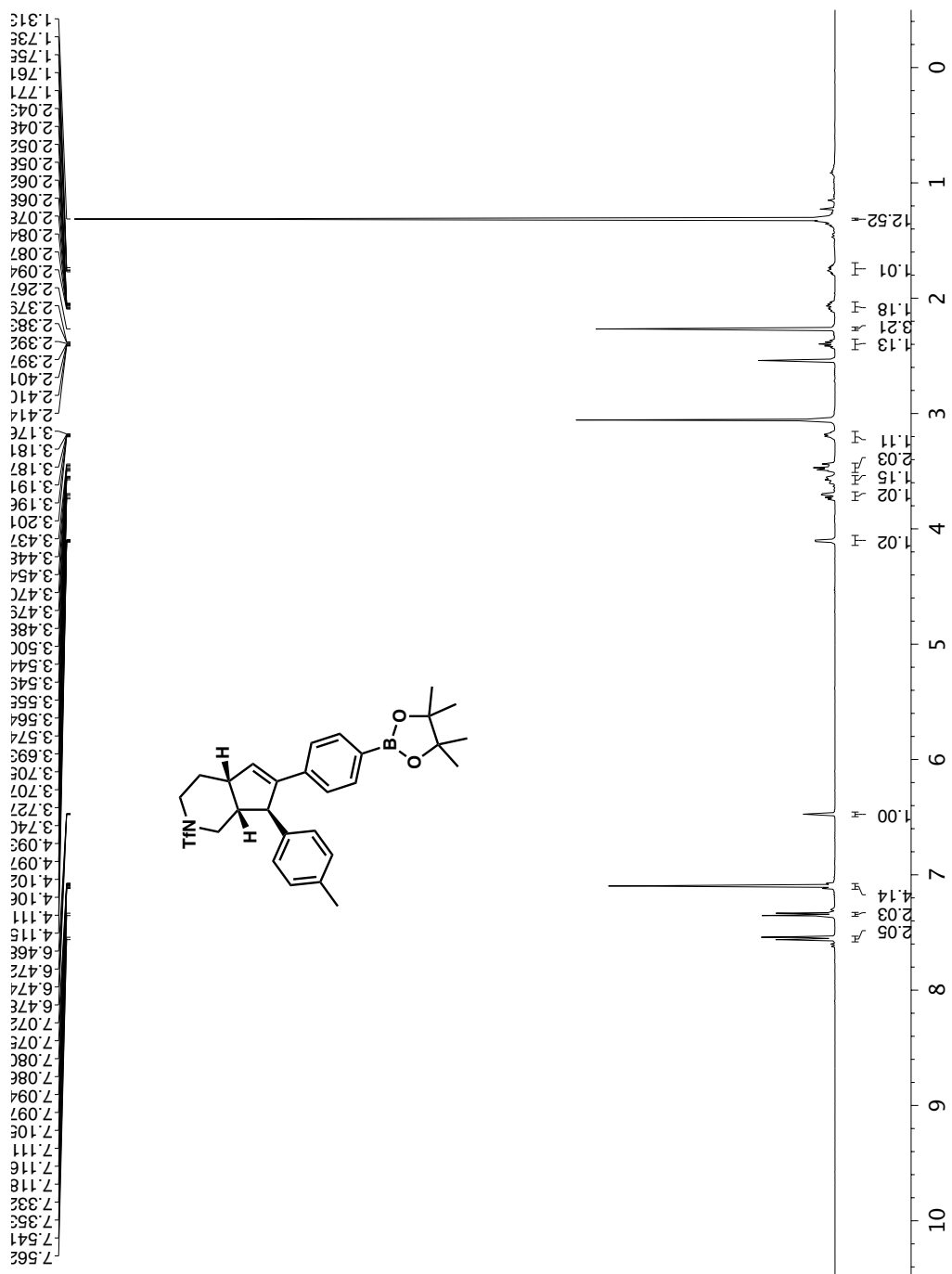


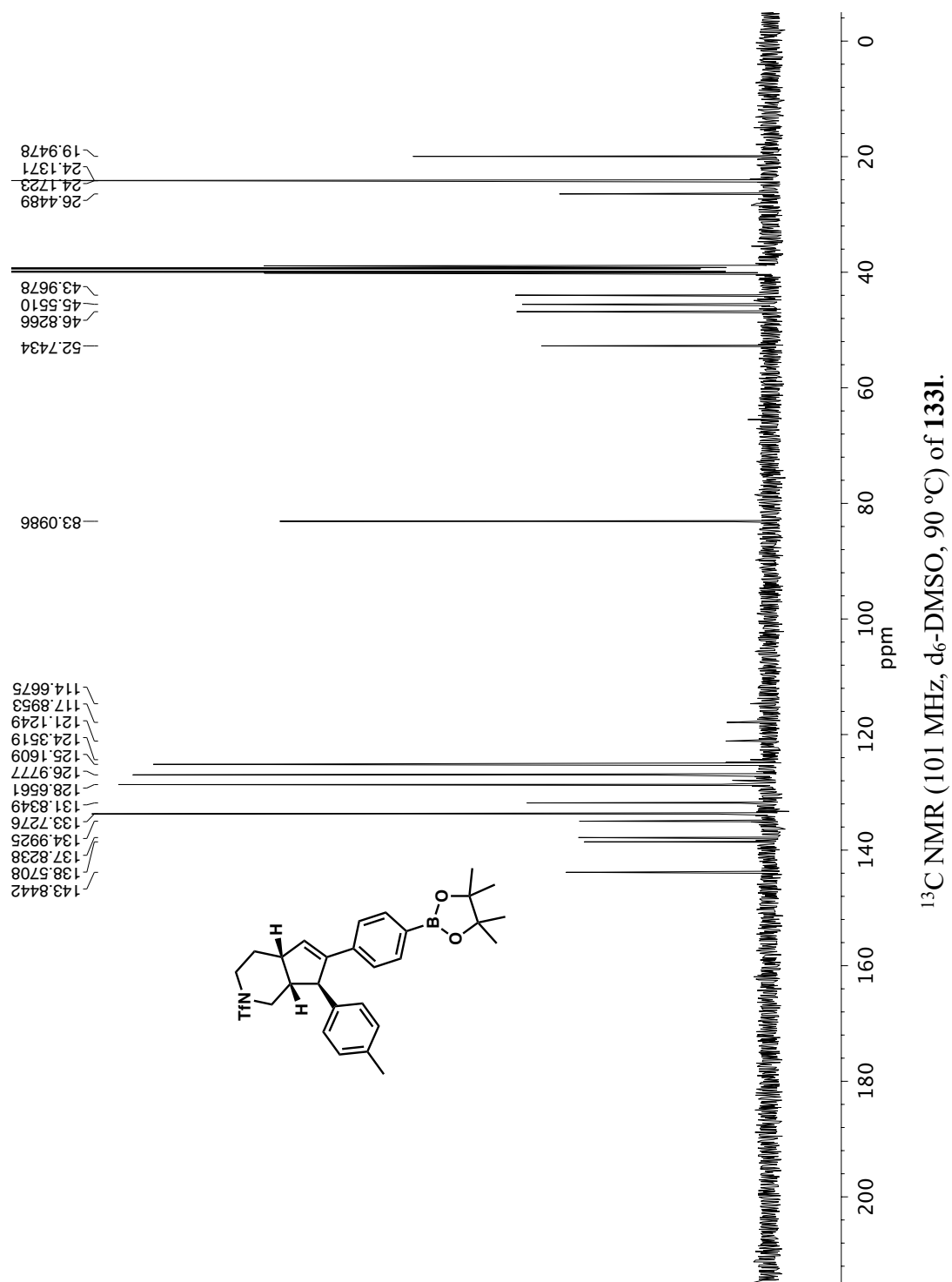




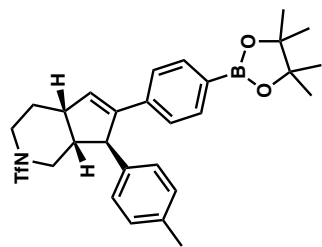






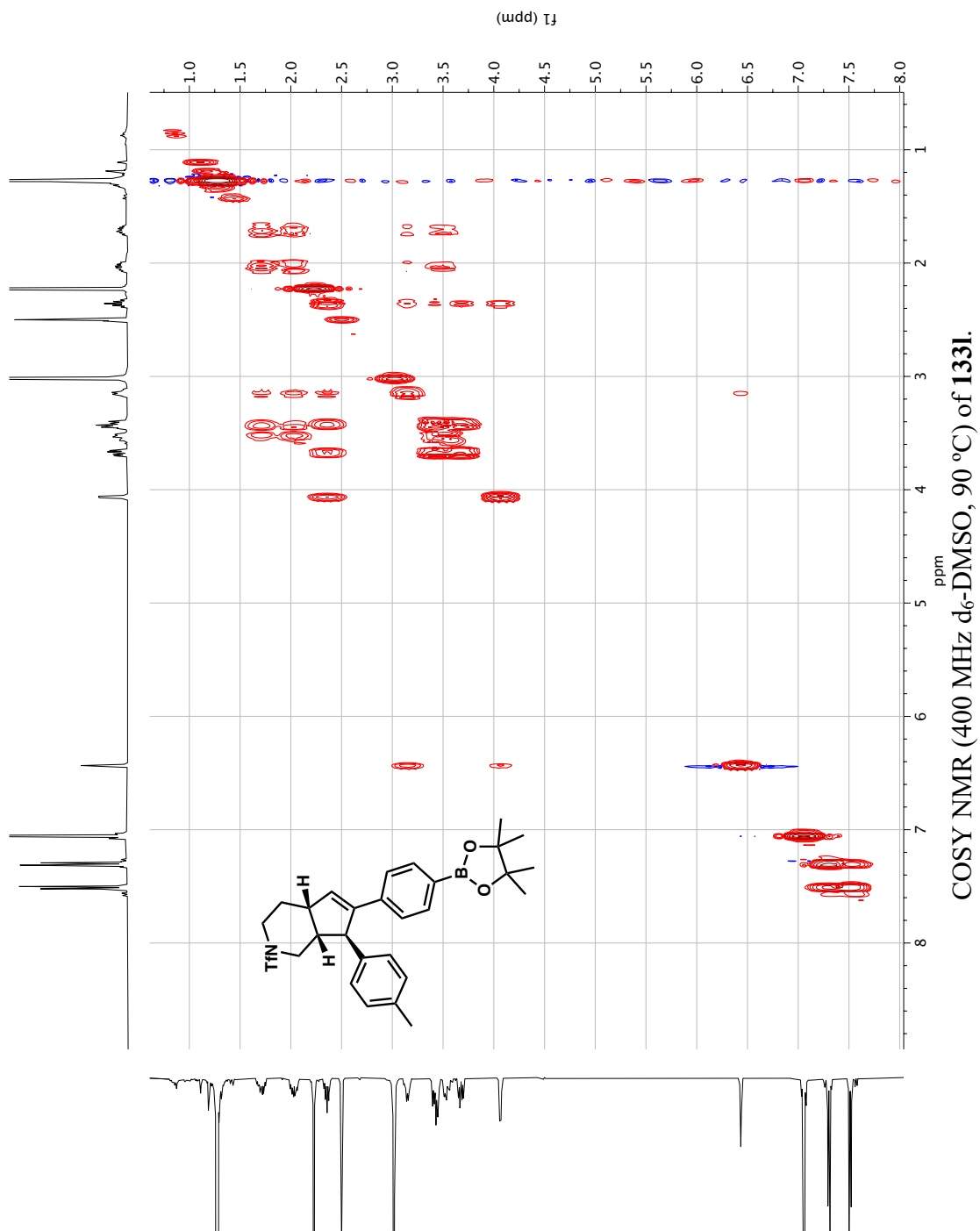


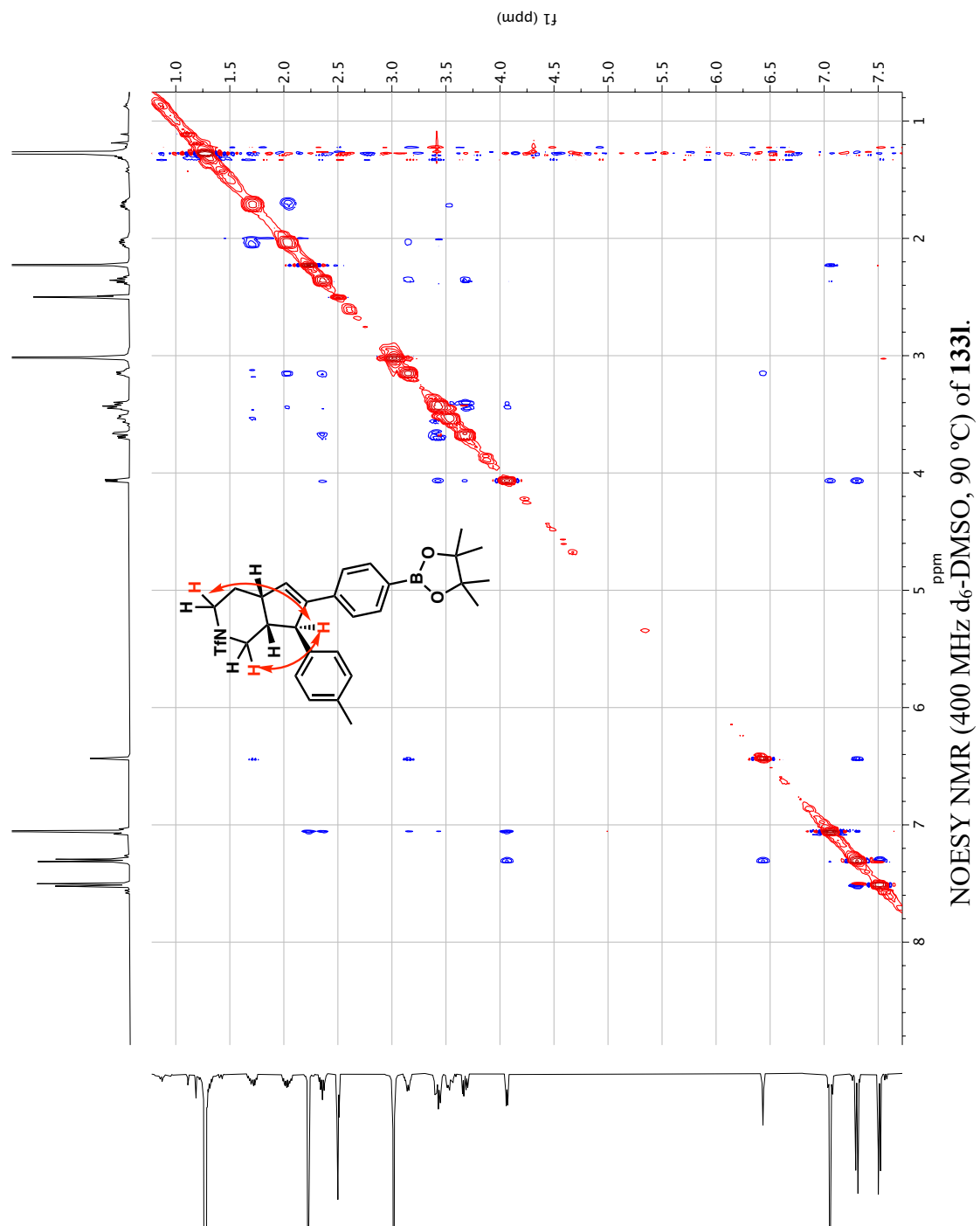
-32.3971

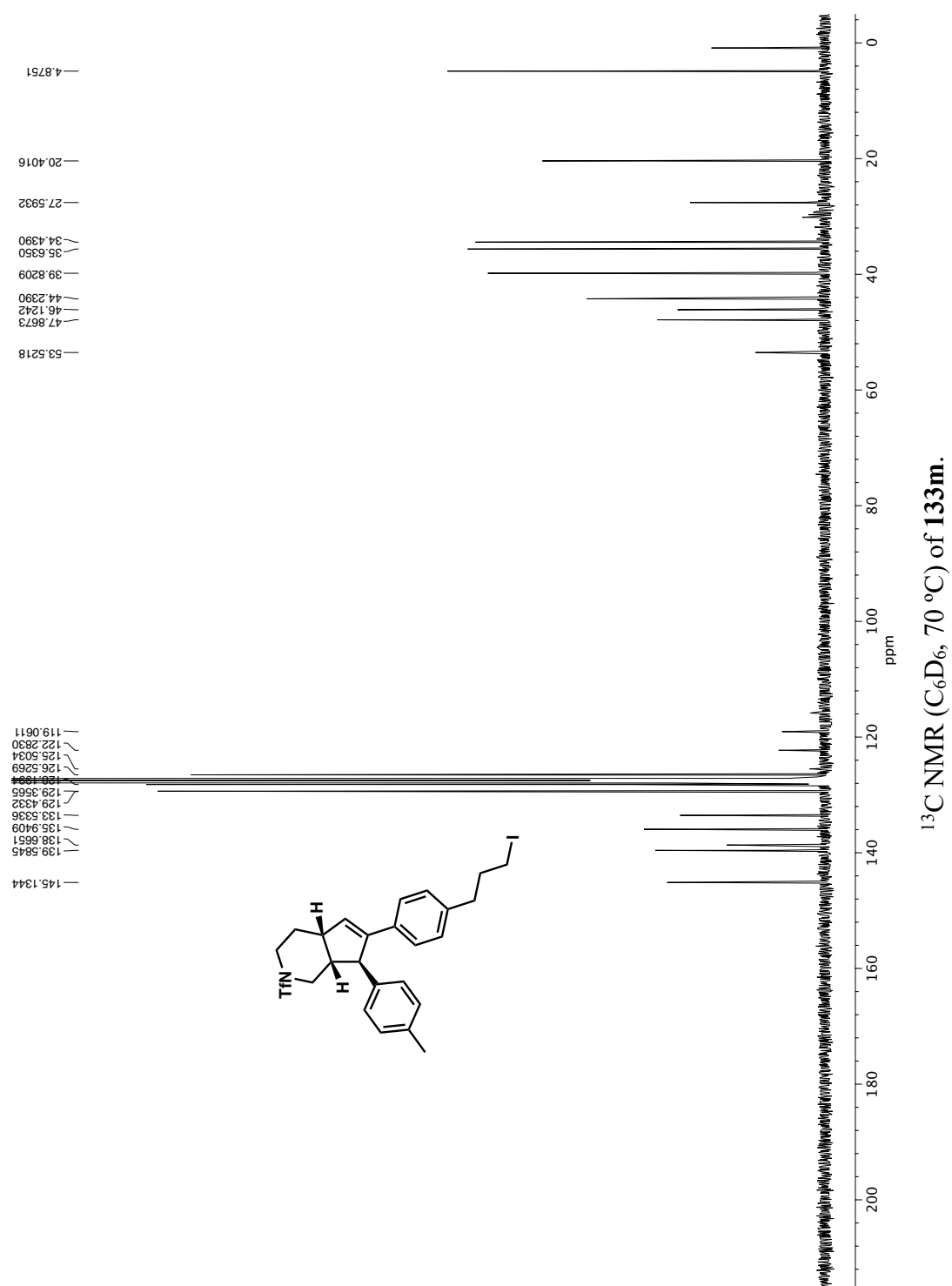


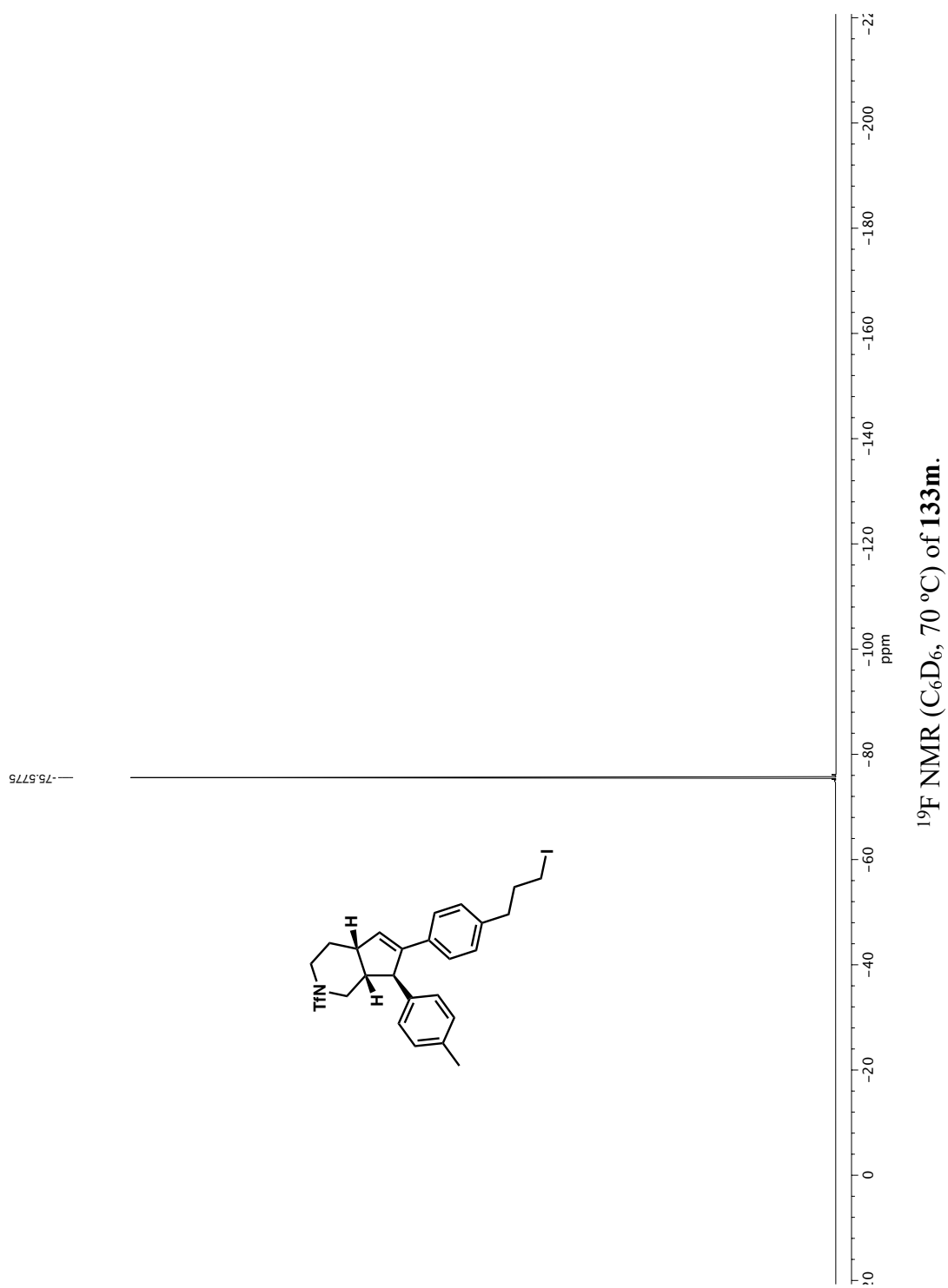
150 100 50 0 -50 -100 -150
ppm

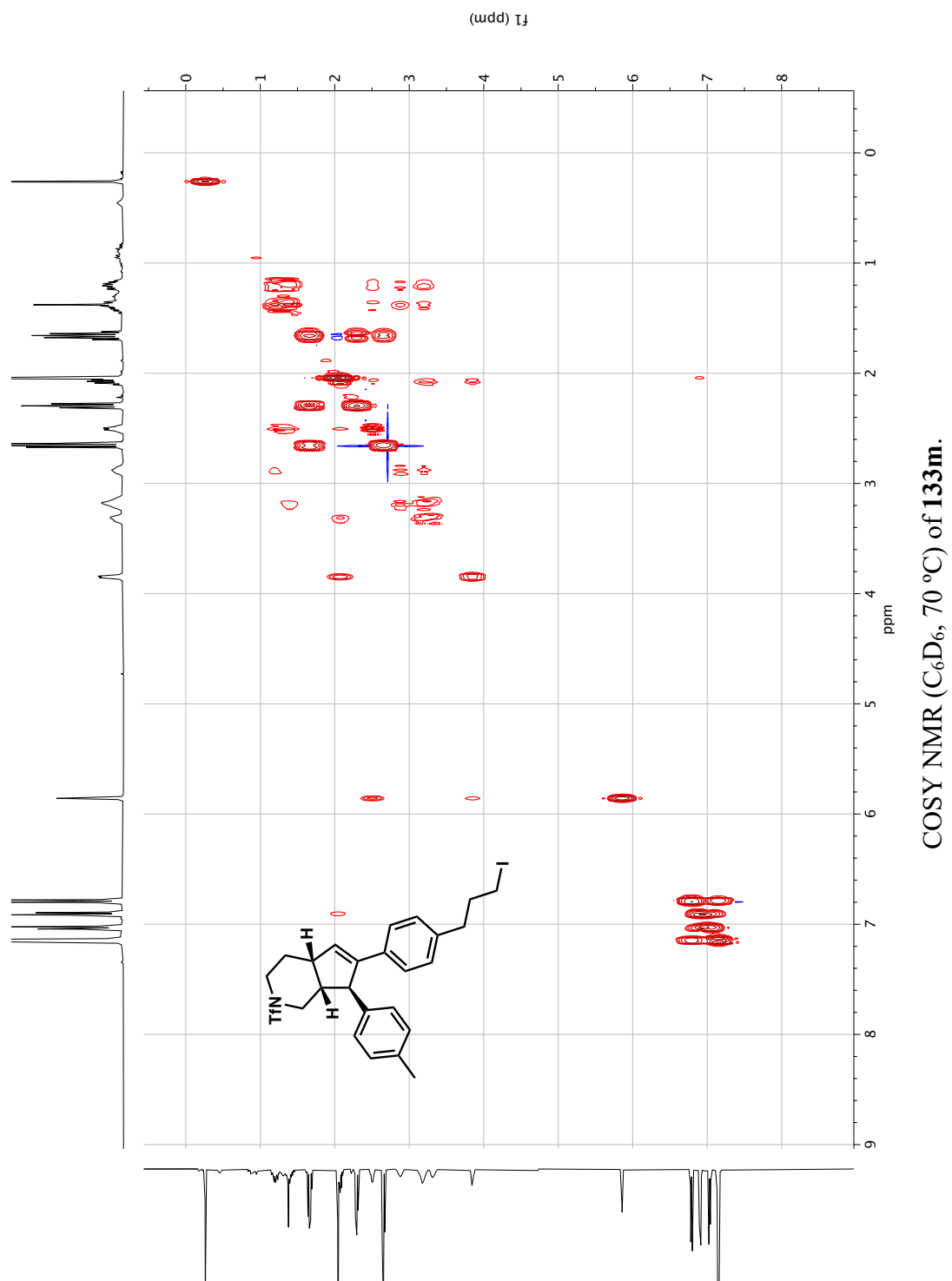
¹¹B NMR (128 MHz, CDCl₃) of **133I**.

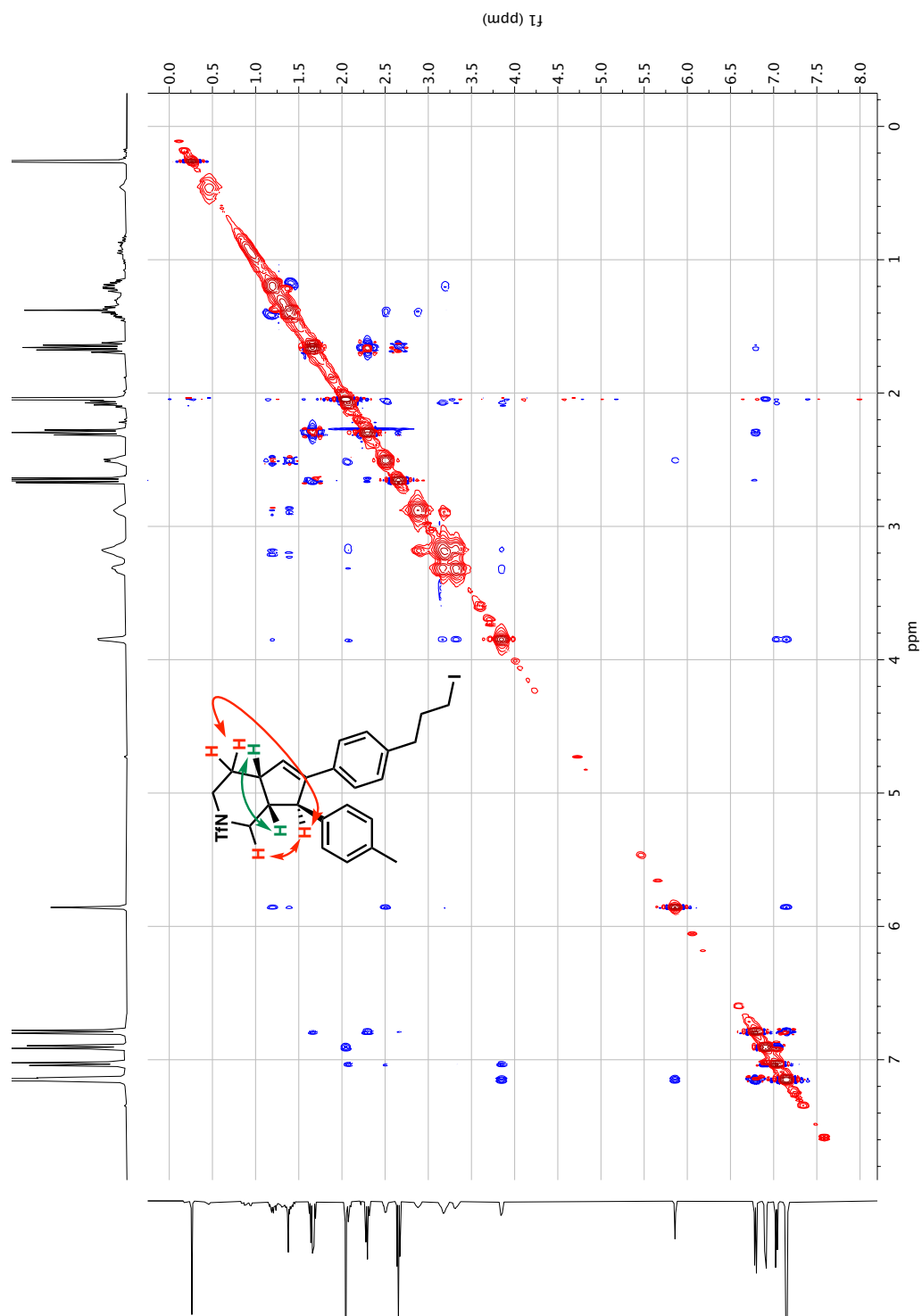




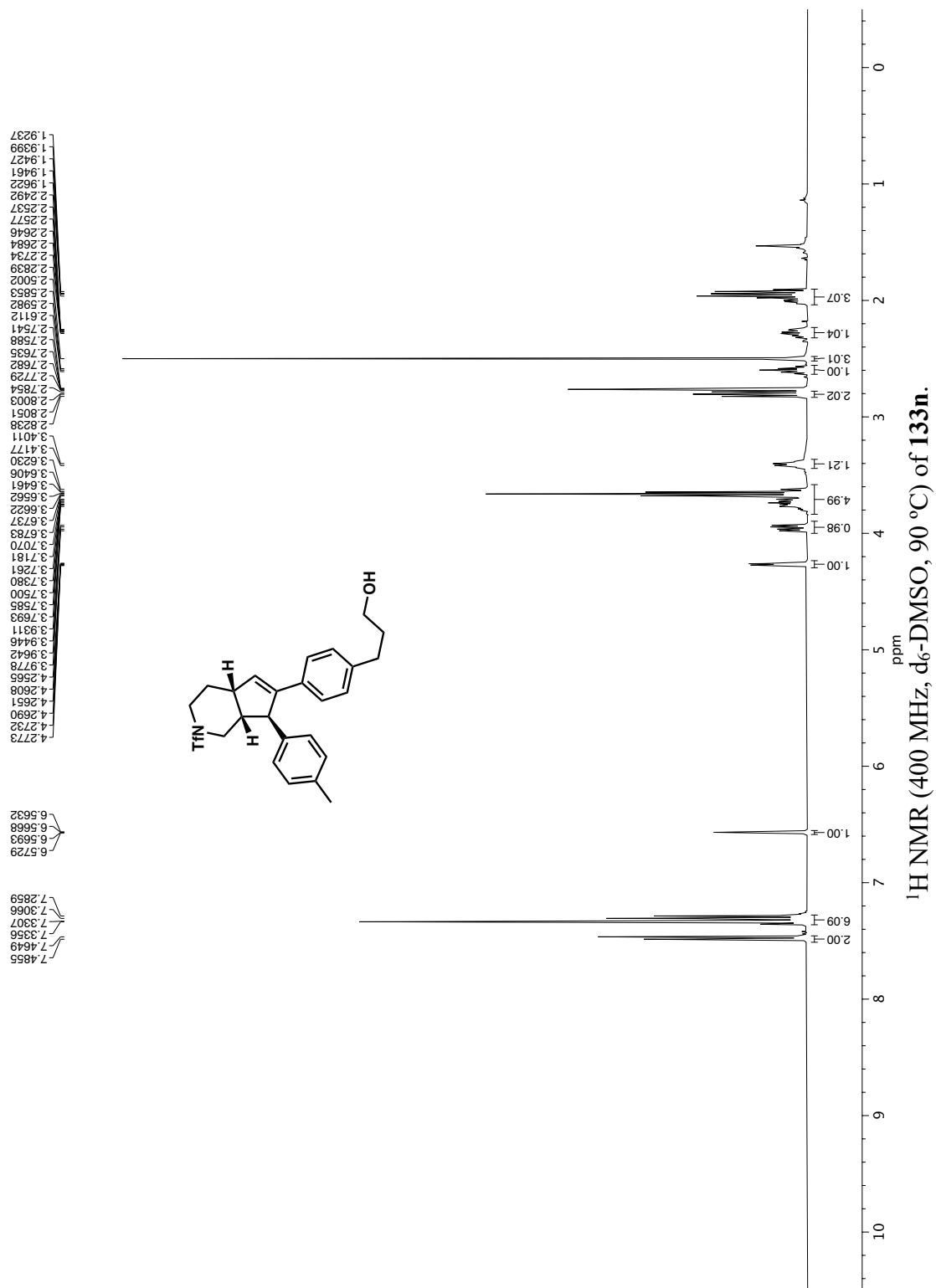


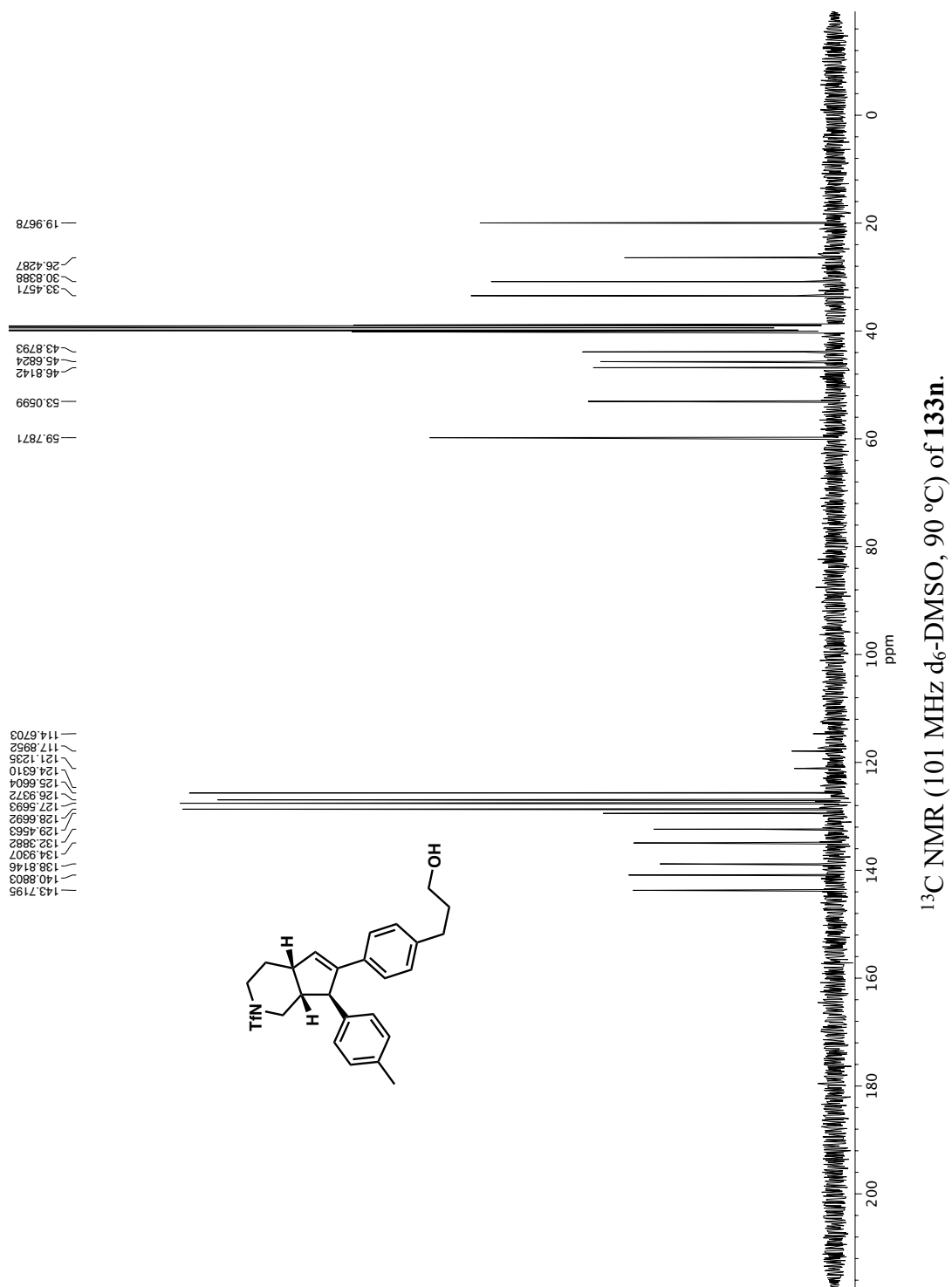


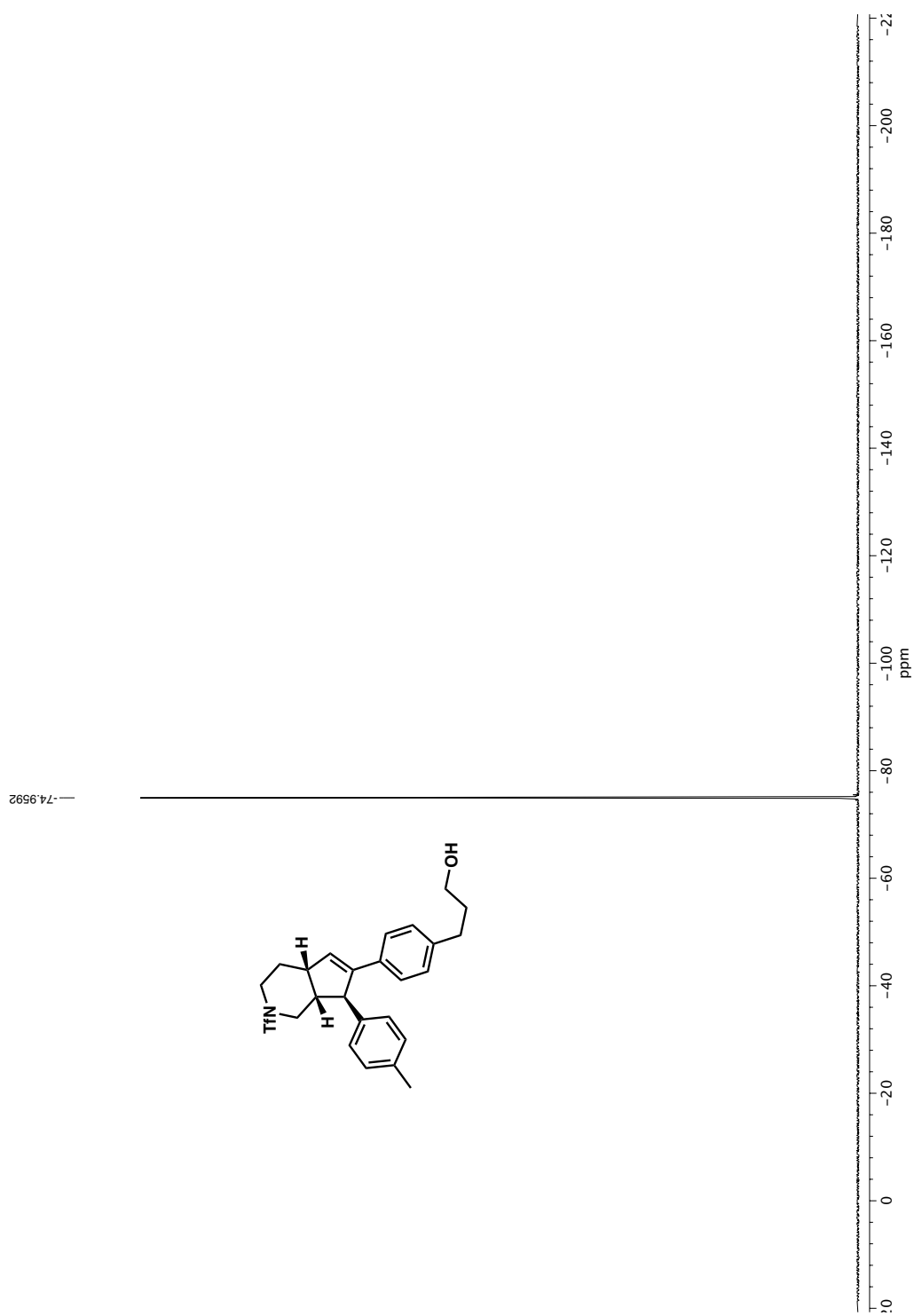


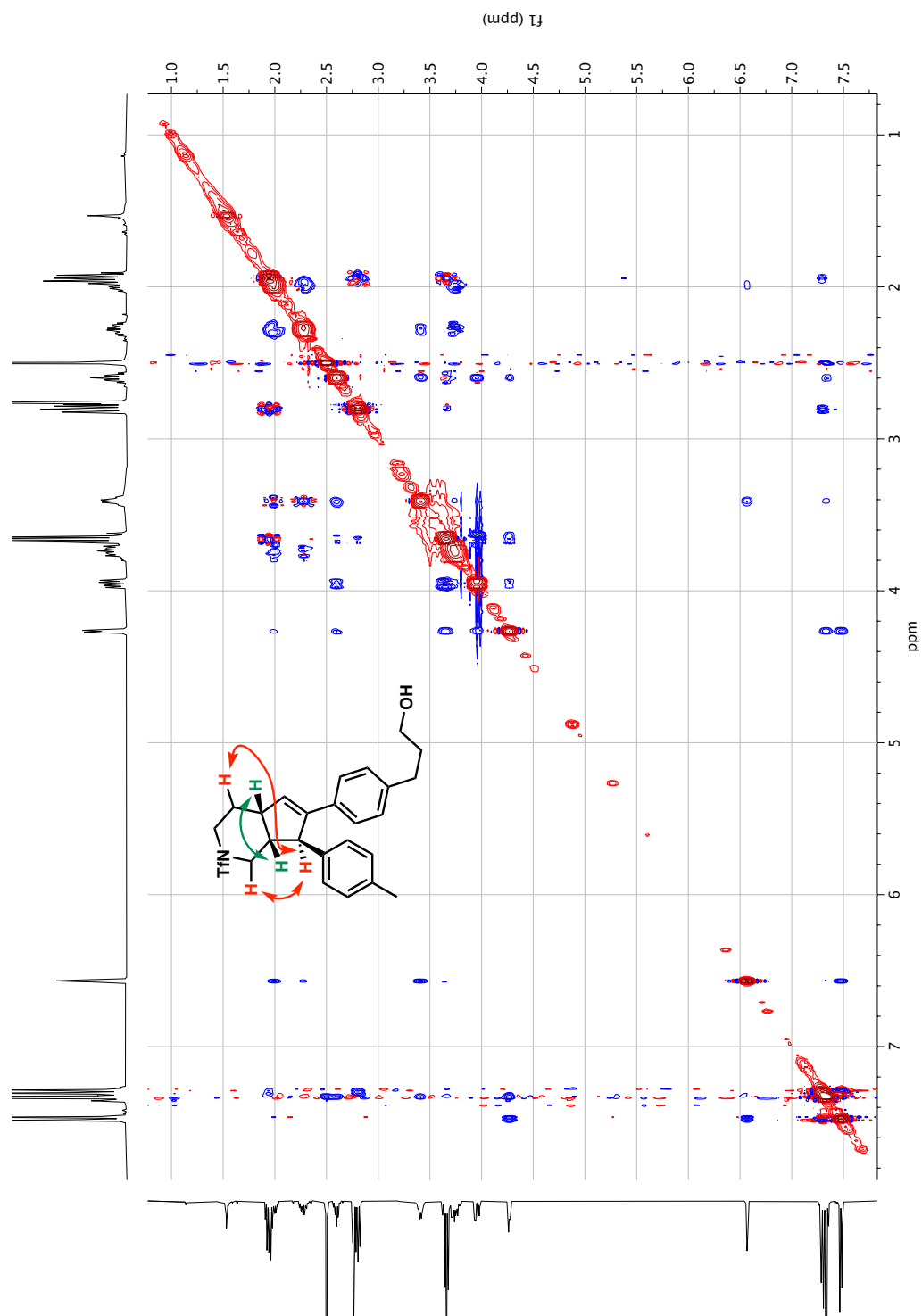


NOESY NMR (C₆D₆, 70 °C) of 133m.

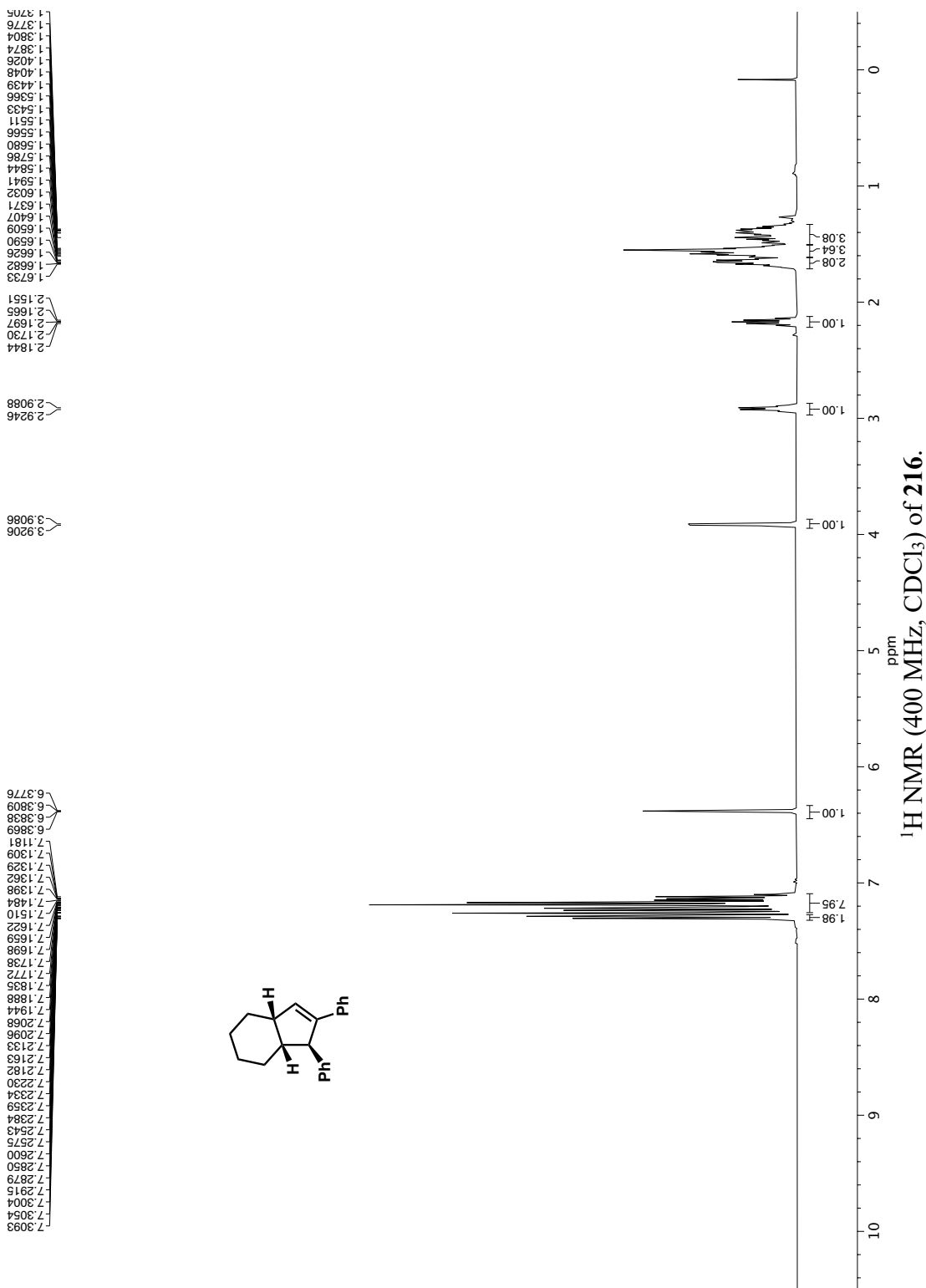


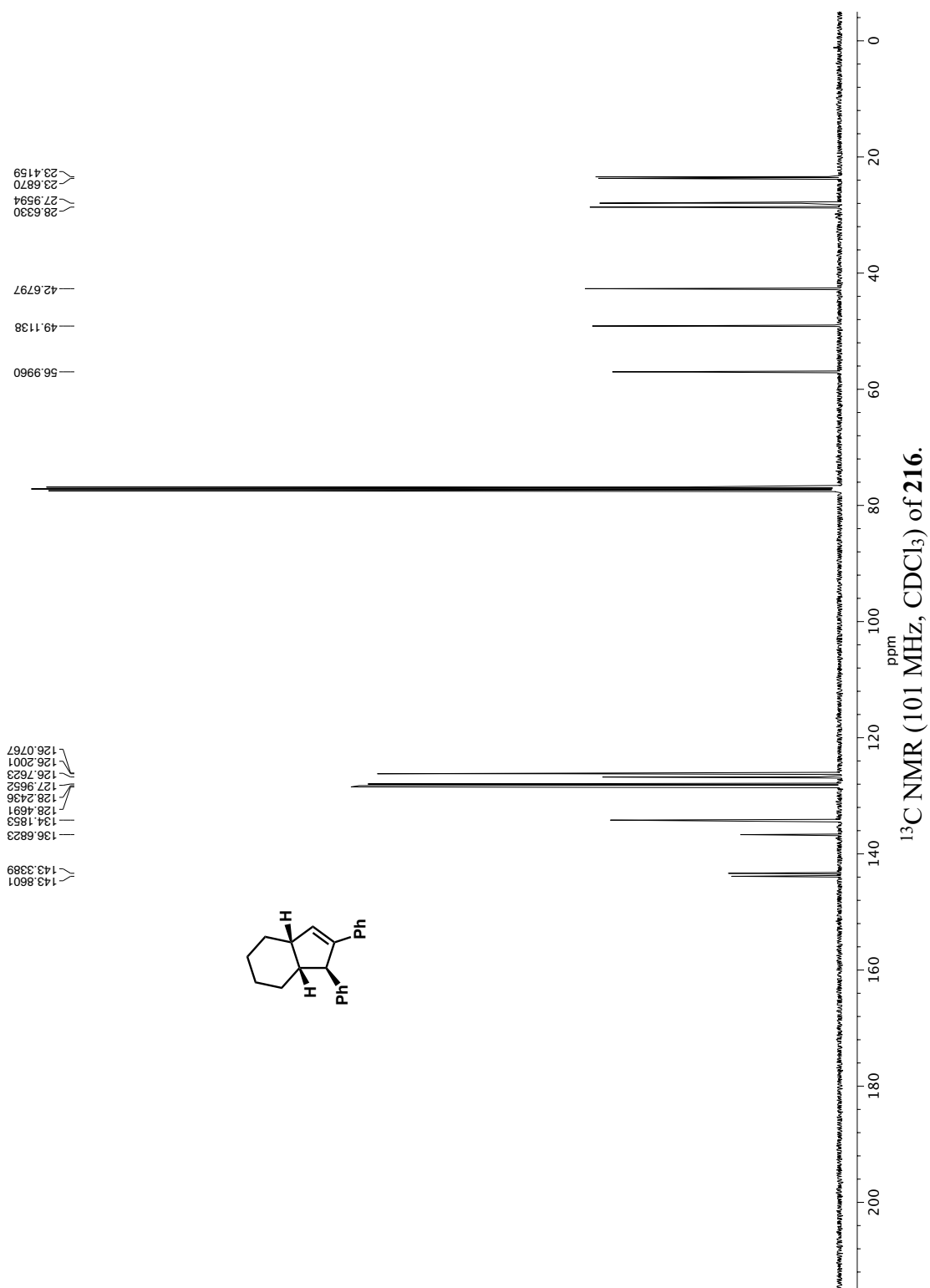


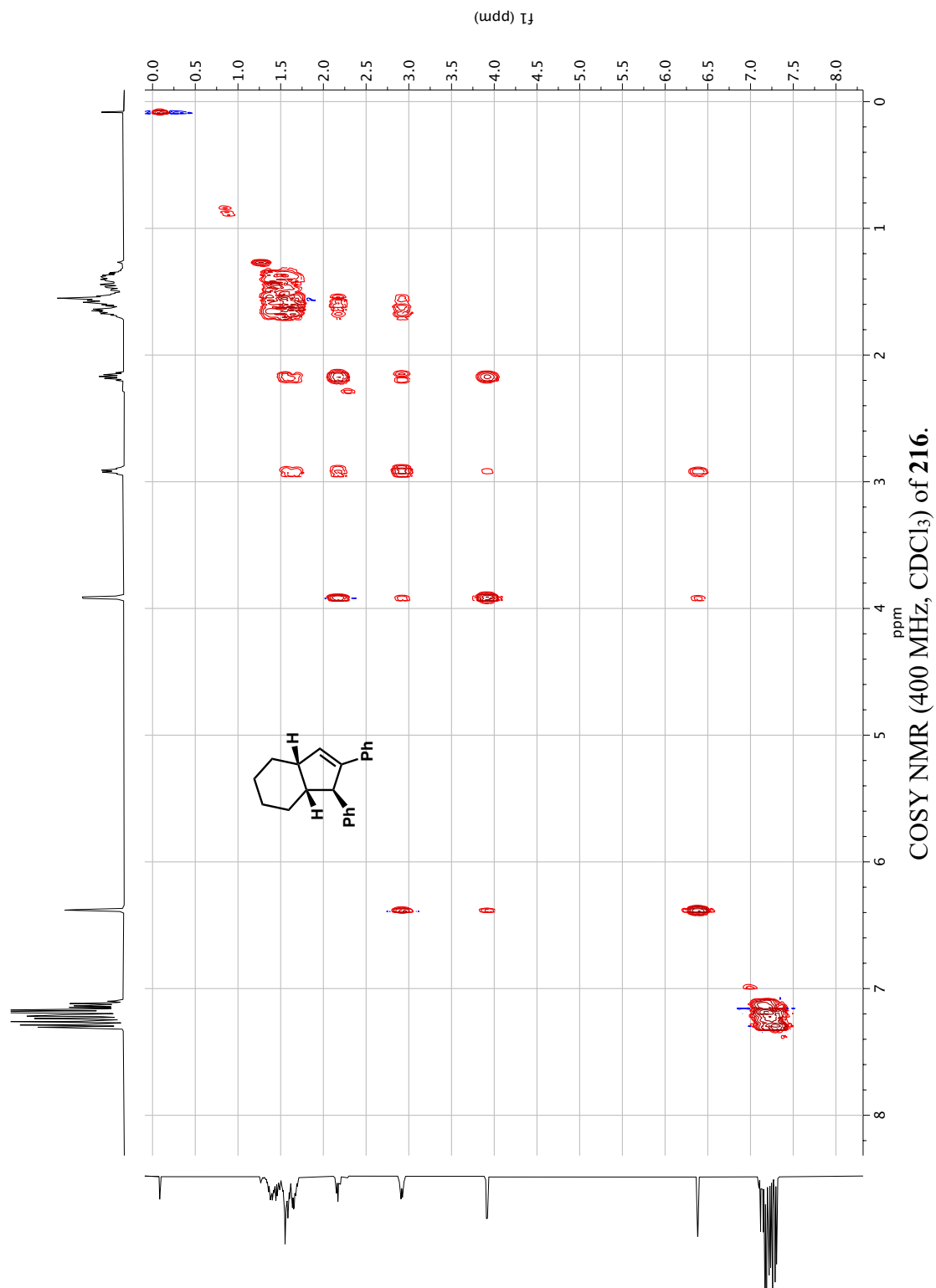


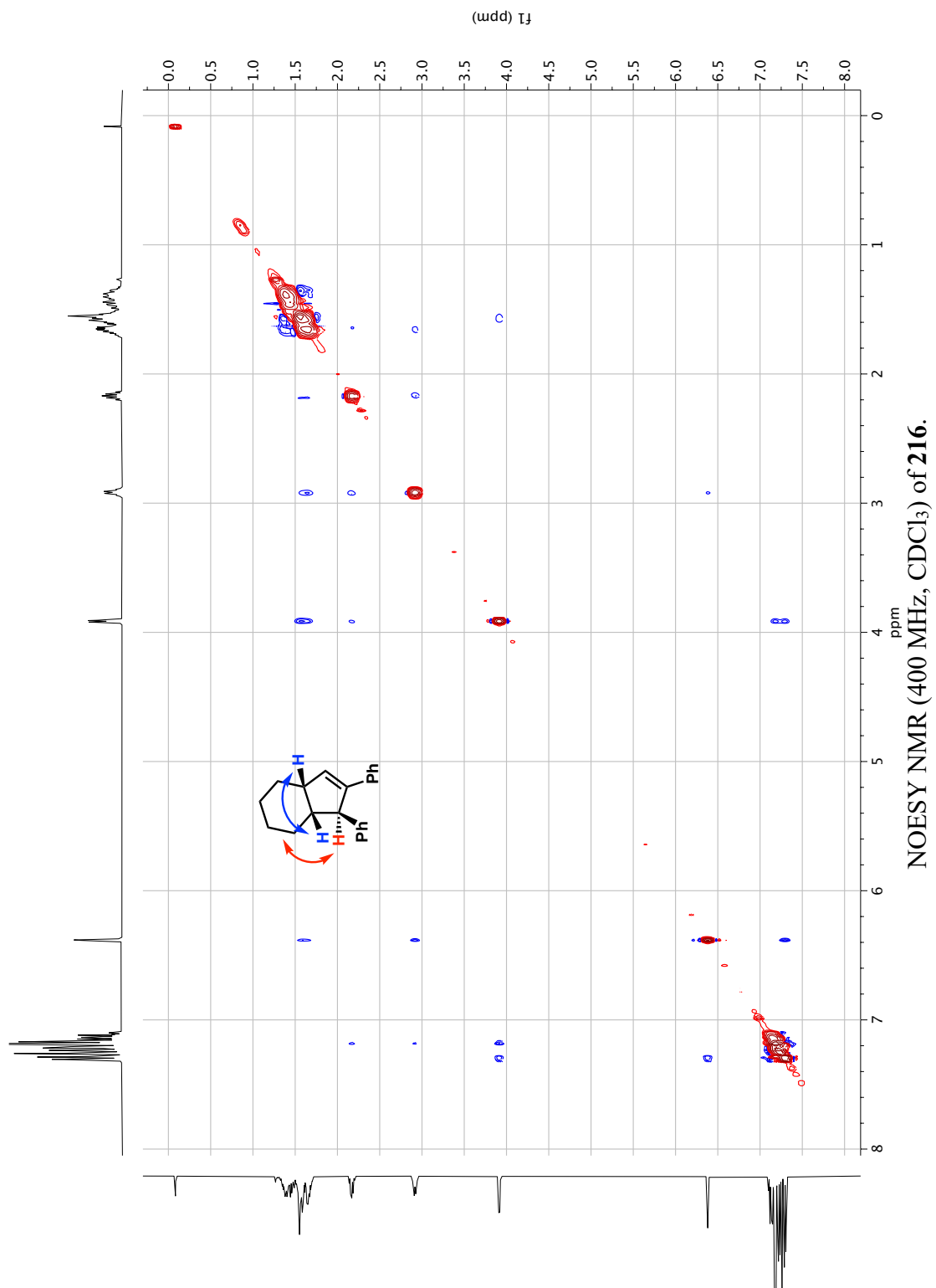


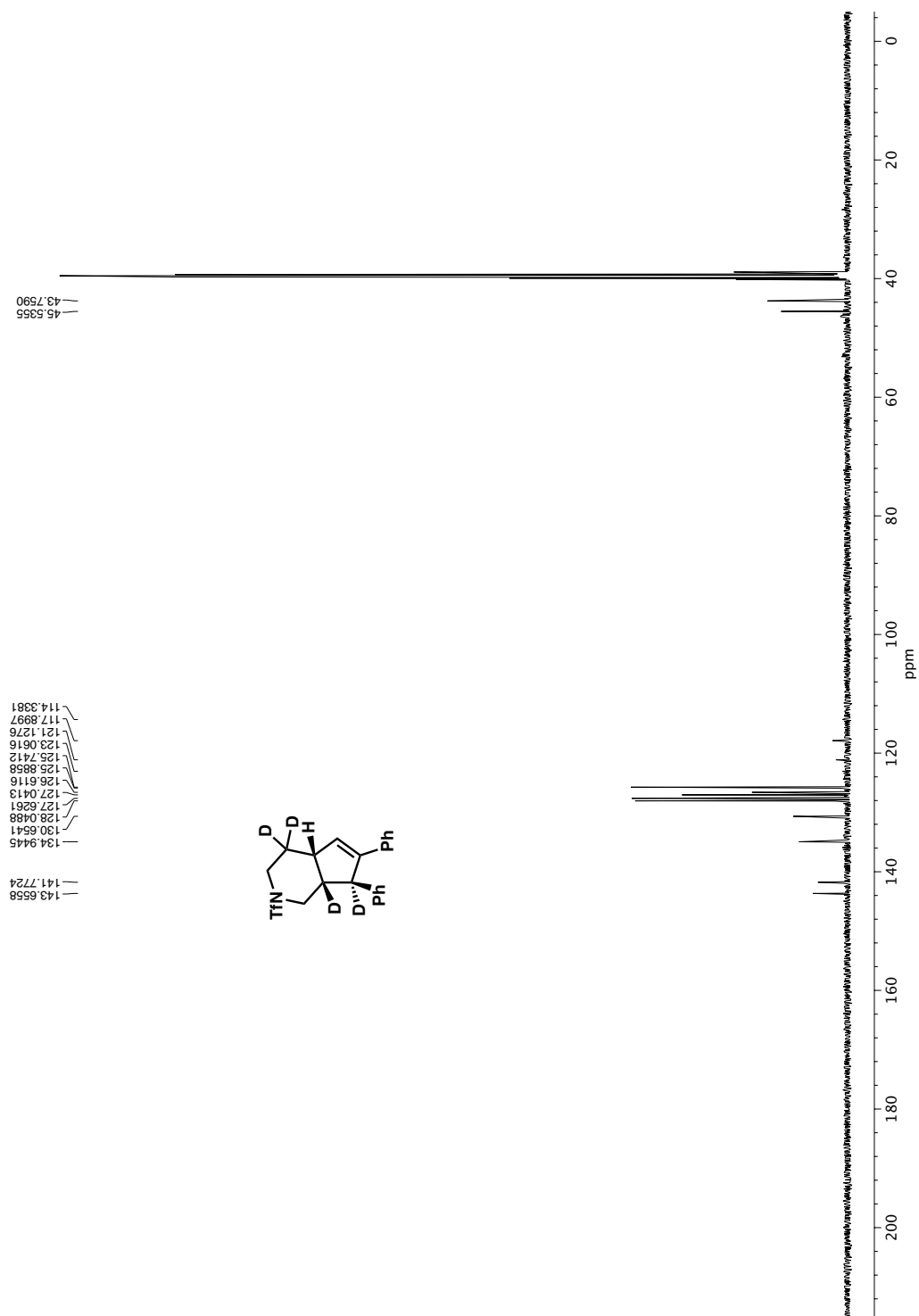
NOESY NMR (400 MHz, d₆-DMSO, 90 °C) of **133n**.

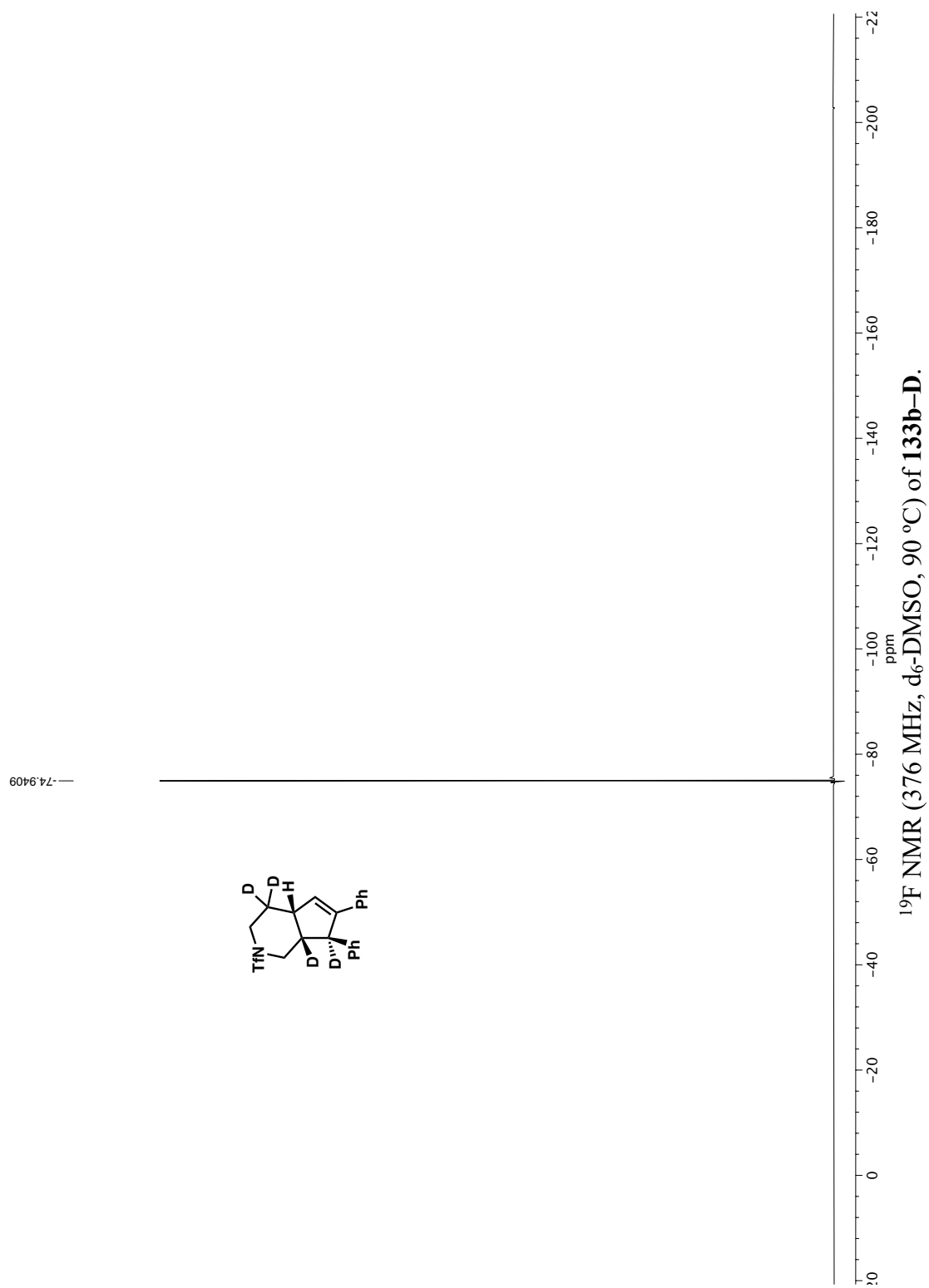


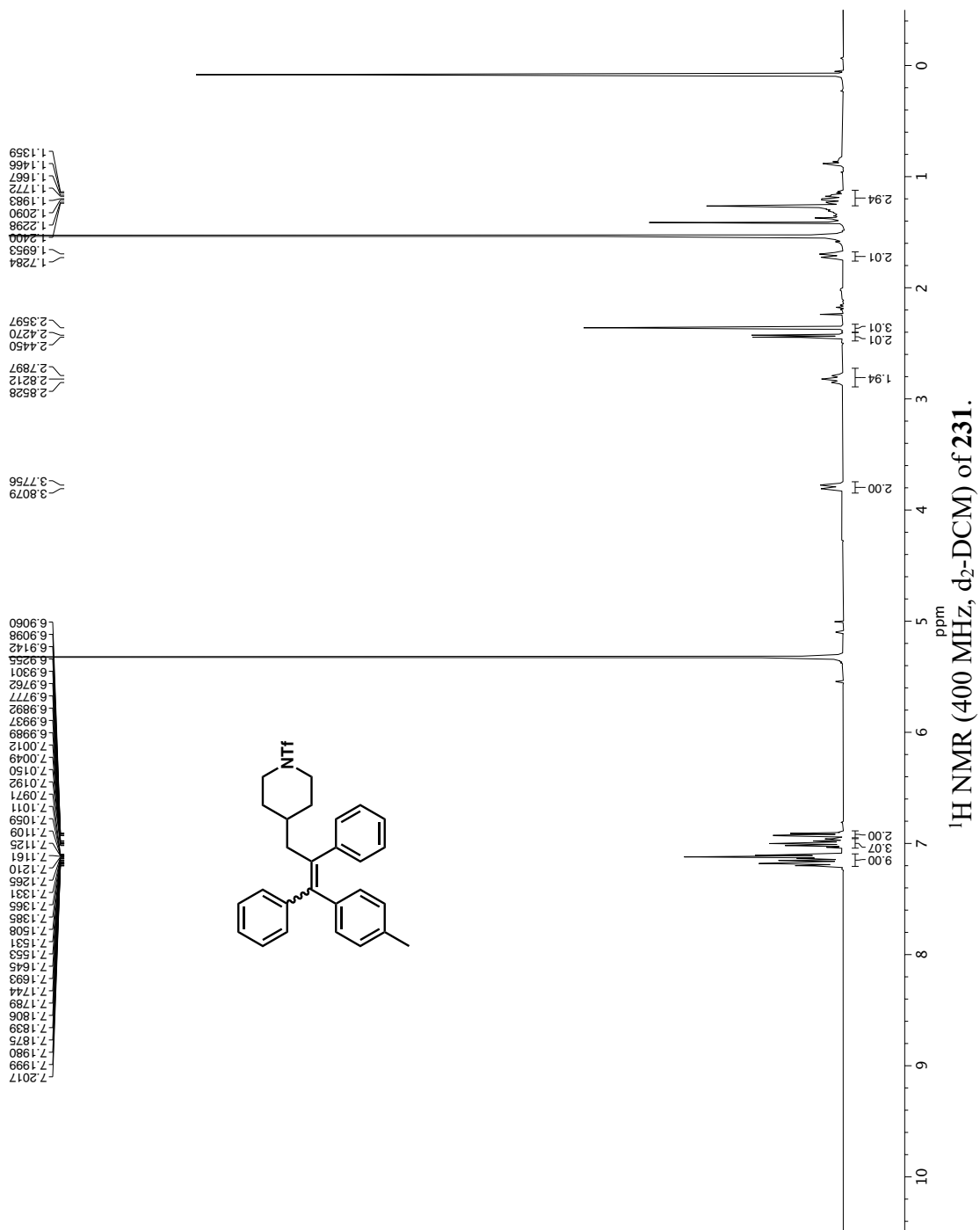


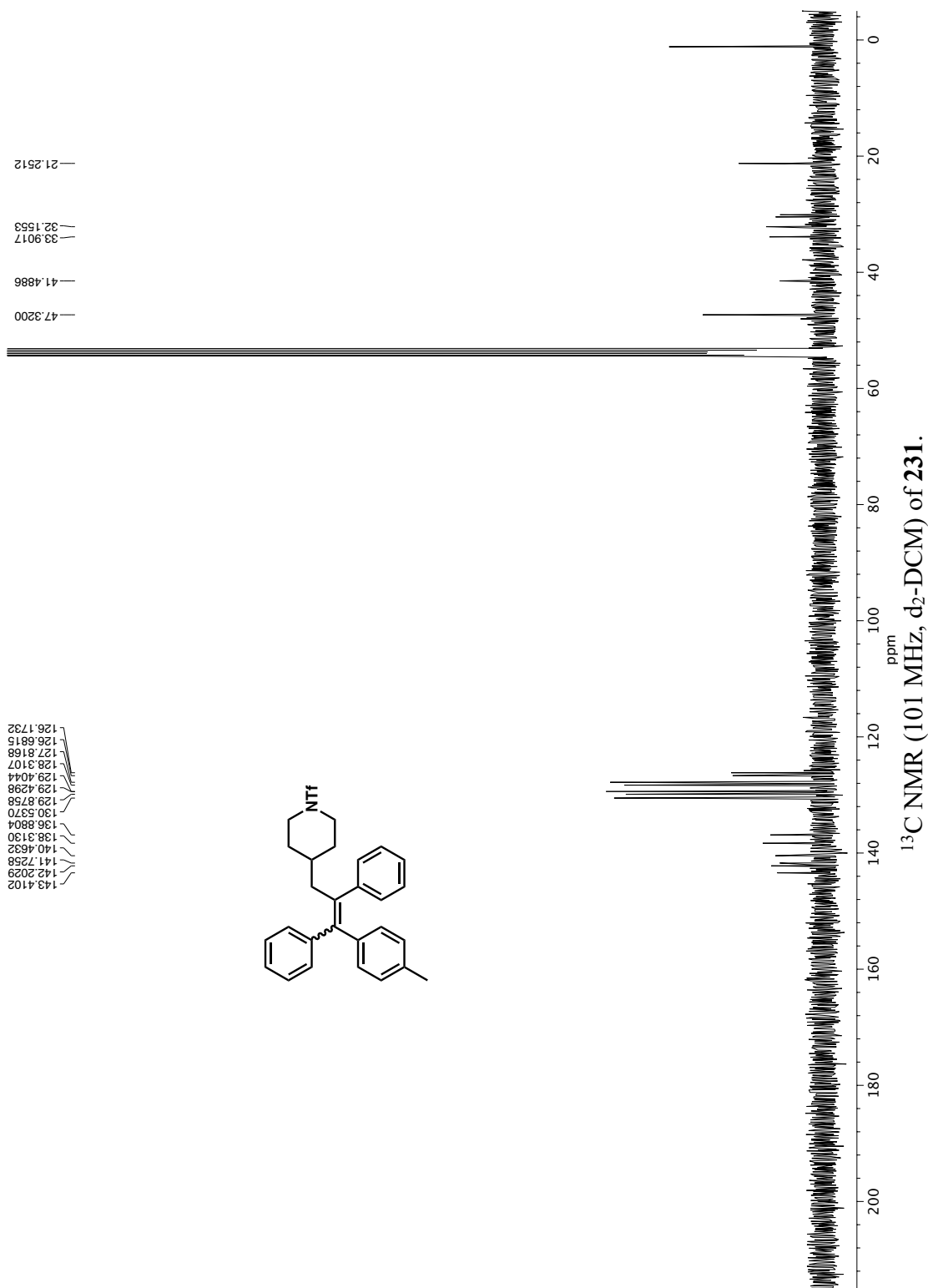




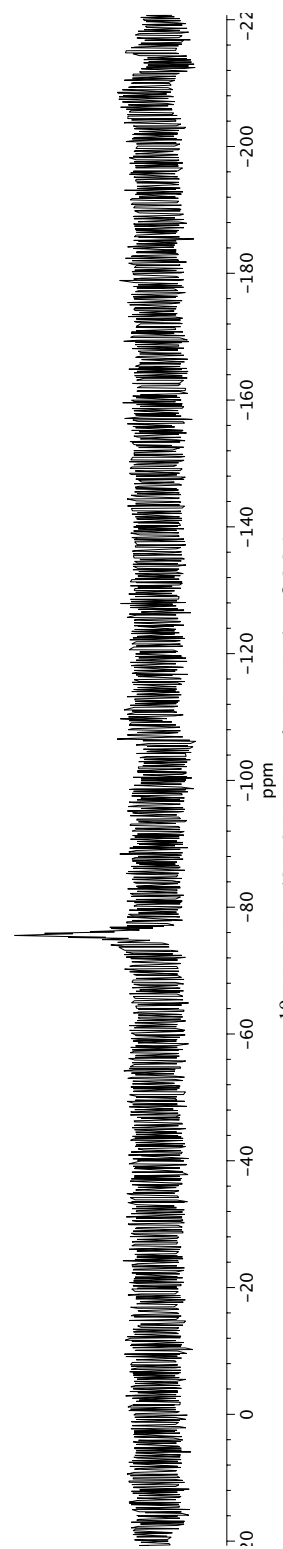
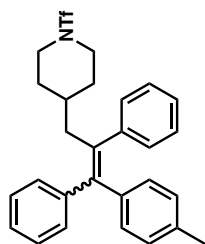


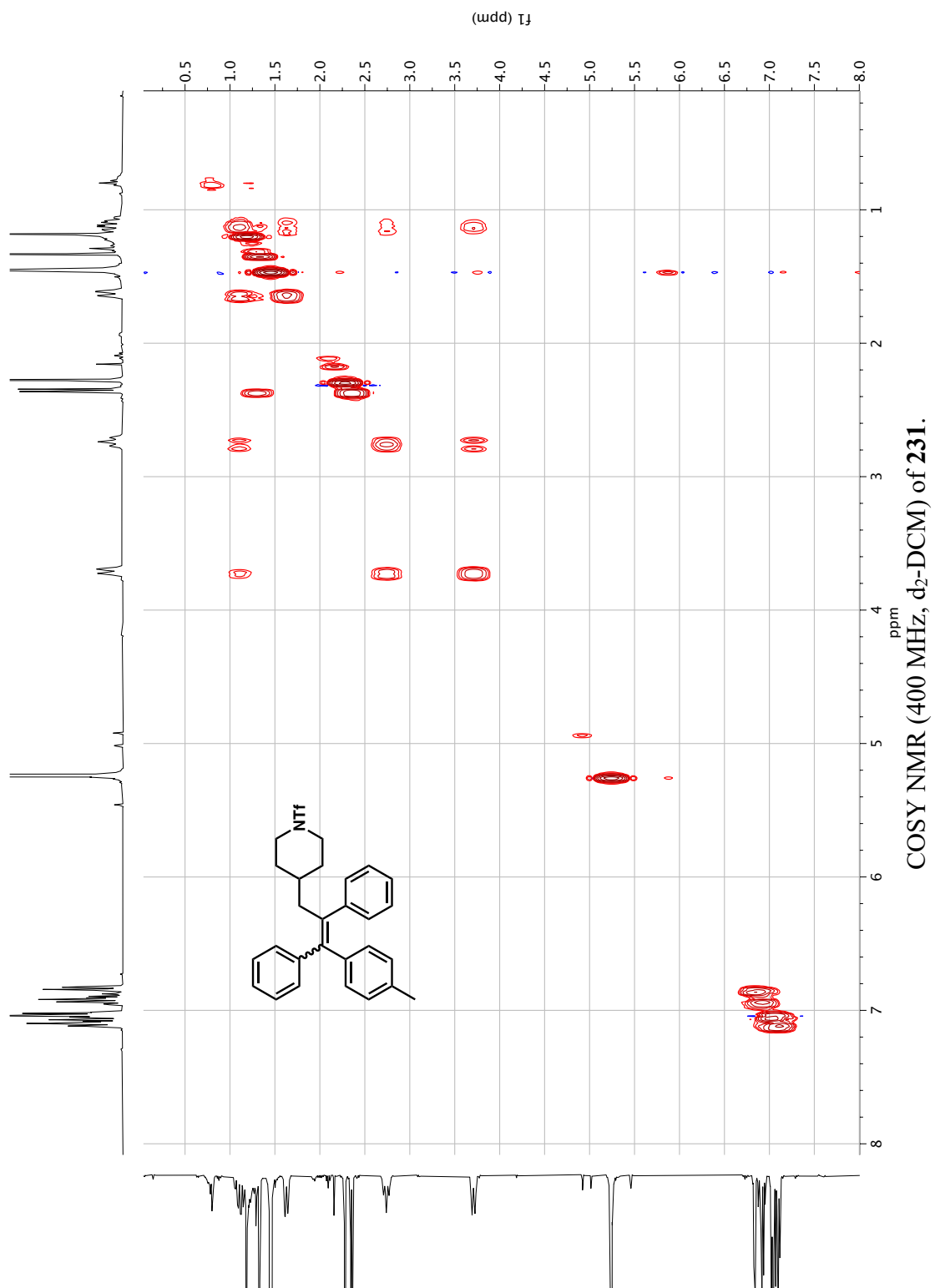






—75.5406





Appendix 5

X-Ray Data Relevant to Chapter 4: Catalytic Asymmetric C–H Insertion

Reactions of Vinyl Carbocations

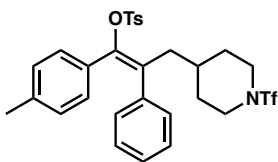
A5.1. GENERAL EXPERIMENTAL

For compounds **132a** and **132h** low-temperature diffraction data (ϕ - and ω -scans) were collected on a Bruker AXS D8 VENTURE KAPPA diffractometer coupled to a PHOTON II CPAD detector with Cu K_{α} radiation ($\lambda = 1.54178 \text{ \AA}$) from an I μ S micro-source for the structure of compound V22166. The structure was solved by direct methods using SHELXS¹ and refined against F^2 on all data by full-matrix least squares with SHELXL-2017² using established refinement techniques³. All non-hydrogen atoms were refined anisotropically. All hydrogen atoms were included into the model at geometrically calculated positions and refined using a riding model. The isotropic displacement parameters of all hydrogen atoms were fixed to 1.2 times the U value of the atoms they are linked to (1.5 times for methyl groups). All disordered atoms were refined with the help of similarity restraints on the 1,2- and 1,3-distances and displacement parameters as well as enhanced rigid bond restraints for anisotropic displacement parameters. Structures were solved by Dr. Michael Takase (Caltech).

For compound **133a**: A colorless tablet shaped crystal with approximate dimensions of 0.40mm x 0.40mm x 0.20mm, was used for intensity data. The diffraction data were measured at 100K(2) on a Bruker Smart Apex2 CCD-based X-ray diffractometer system equipped with a Cu-K α radiation ($\lambda = 1.54178 \text{ \AA}$). The frames were integrated with the Bruker SAINT software package using a narrow-frame integration algorithm. The structure was solved and refined using the Bruker SHELXTL Software Package. All atoms were refined anisotropically, and hydrogen atoms were placed at calculated positions. Structure was solved by Dr. Saeed Khan (UCLA).

All crystallographic data are available free of charge from the Cambridge Crystallographic Data Centre under CCDC 2201597, CCDC 2201599, and CCDC 2201600.

A5.1.1 X-Ray Crystal Structure Analysis for **132a**



Compound **132a** (V22166) crystallizes in the orthorhombic space group $Pna2_1$ with two molecules in the asymmetric unit. One of the CF_3 groups was disordered over two positions.

Figure A5.1 X-Ray Crystal Structure for **132a**

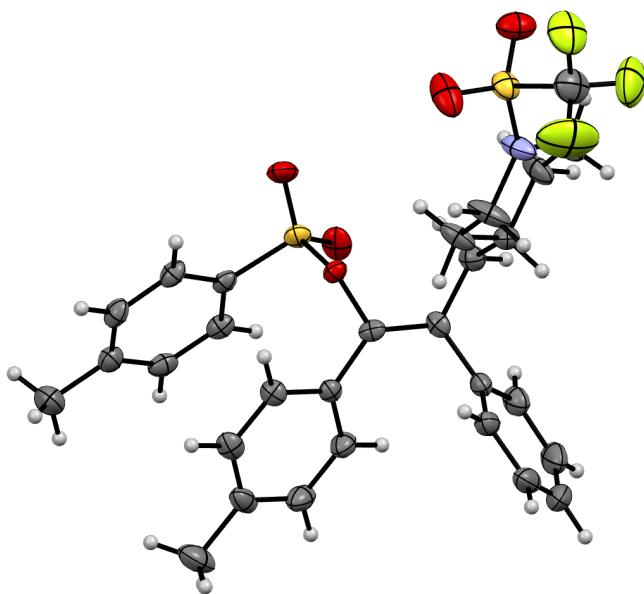
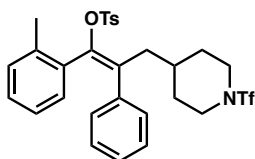


Table A5.1 Crystal Data and Structure Refinement for **132a**

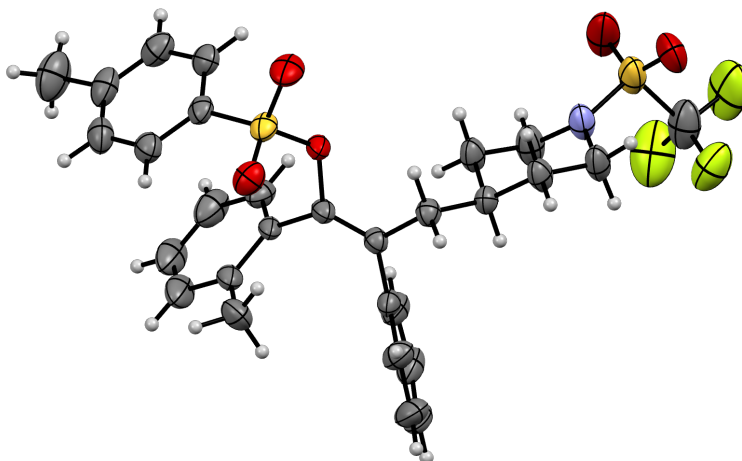
Identification code	V22166	
Empirical formula	C ₂₉ H ₃₀ F ₃ N O ₅ S ₂	
Formula weight	593.66	
Temperature	100(2) K	
Wavelength	1.54178 Å	
Crystal system	Orthorhombic	
Space group	Pna2 ₁	
Unit cell dimensions	a = 24.629(4) Å	a = 90°.
	b = 6.9845(8) Å	b = 90°.
	c = 34.431(4) Å	g = 90°.
Volume	5922.9(13) Å ³	
Z	8	
Density (calculated)	1.332 Mg/m ³	
Absorption coefficient	2.128 mm ⁻¹	
F(000)	2480	
Crystal size	0.200 x 0.150 x 0.050 mm ³	
Theta range for data collection	2.566 to 74.614°.	
Index ranges	-29 ≤ h ≤ 30, -8 ≤ k ≤ 8, -43 ≤ l ≤ 42	
Reflections collected	78494	
Independent reflections	11943 [R(int) = 0.0742]	
Completeness to theta = 67.679°	100.0 %	
Absorption correction	Semi-empirical from equivalents	

Max. and min. transmission	0.7538 and 0.5322
Refinement method	Full-matrix least-squares on F^2
Data / restraints / parameters	11943 / 213 / 762
Goodness-of-fit on F^2	1.056
Final R indices [$I > 2\sigma(I)$]	$R_1 = 0.0658$, $wR_2 = 0.1730$
R indices (all data)	$R_1 = 0.0746$, $wR_2 = 0.1767$
Absolute structure parameter	0.180(10)
Extinction coefficient	n/a
Largest diff. peak and hole	1.287 and $-0.540 \text{ e.}\text{\AA}^{-3}$

A5.1.2 X-Ray Crystal Structure Analysis for **132h**



Compound **132h** (V22190) crystallizes in the monoclinic space group $P2_1/c$ with one molecule in the asymmetric unit along with half a molecule of dichloromethane. One of the aromatic groups is disordered over two positions. The dichloromethane molecule is located near a crystallographic inversion center and disordered over two positions which are pairwise related by the inversion center.

Figure A5.2 X-Ray Crystal Structure for **132h****Table A5.2** Crystal Data and Structure Refinement for **132h**

Identification code	V22190	
Empirical formula	C _{29.50} H ₃₁ Cl F ₃ N O ₅ S ₂	
Formula weight	636.12	
Temperature	100(2) K	
Wavelength	1.54178 Å	
Crystal system	Monoclinic	
Space group	P2 ₁ /c	
Unit cell dimensions	a = 15.2375(14) Å	a = 90°.
	b = 11.9989(13) Å	b = 100.458(7)°.
	c = 16.7908(12) Å	g = 90°.
Volume	3018.9(5) Å ³	
Z	4	
Density (calculated)	1.400 Mg/m ³	

Absorption coefficient	2.920 mm ⁻¹
F(000)	1324
Crystal size	0.150 x 0.150 x 0.100 mm ³
Theta range for data collection	4.555 to 74.715°.
Index ranges	-18<=h<=19, -15<=k<=14, -20<=l<=20
Reflections collected	51642
Independent reflections	6155 [R(int) = 0.0363]
Completeness to theta = 67.679°	99.9 %
Absorption correction	Semi-empirical from equivalents
Max. and min. transmission	0.7538 and 0.5203
Refinement method	Full-matrix least-squares on F ²
Data / restraints / parameters	6155 / 509 / 456
Goodness-of-fit on F ²	1.096
Final R indices [I>2sigma(I)]	R1 = 0.0630, wR2 = 0.1737
R indices (all data)	R1 = 0.0644, wR2 = 0.1751
Extinction coefficient	n/a
Largest diff. peak and hole	0.312 and -0.867 e.Å ⁻³

A5.1.3 X-Ray Crystal Structure Analysis for **133a**

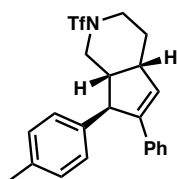
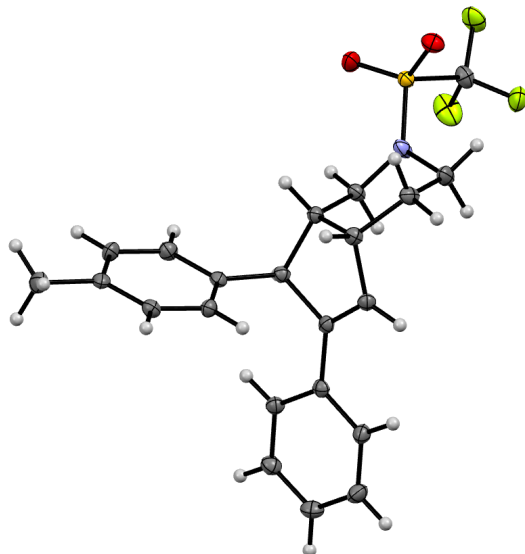


Figure A5.3 X-Ray Crystal Structure for **133a****Table A5.3** Crystal Data and Structure Refinement for **133a**

Identification code	cu_hosea2102s_a
Empirical formula	C ₂₂ H ₂₂ NO ₂ F ₃ S
Formula weight	421.46
Temperature/K	100(2)
Crystal system	orthorhombic
Space group	P2 ₁ 2 ₁ 2 ₁
a/Å	8.9578(2)
b/Å	10.0455(2)
c/Å	21.9822(5)
α /°	90

$\beta/^\circ$	90
$\gamma/^\circ$	90
Volume/ \AA^3	1978.08(7)
Z	4
$\rho_{\text{calc}}/\text{g}/\text{cm}^3$	1.415
μ/mm^{-1}	1.868
F(000)	880.0
Crystal size/ mm^3	$0.4 \times 0.4 \times 0.2$
Radiation	CuK α ($\lambda = 1.54178$)
2Θ range for data collection/ $^\circ$	8.044 to 144.114
Index ranges	$-10 \leq h \leq 11$, $-12 \leq k \leq 12$, $-25 \leq l \leq 26$
Reflections collected	27398
Independent reflections	3863 [$R_{\text{int}} = 0.0205$, $R_{\text{sigma}} = 0.0235$]
Data/restraints/parameters	3863/0/265
Goodness-of-fit on F^2	1.057
Final R indexes [$I \geq 2\sigma(I)$]	$R_1 = 0.0215$, $wR_2 = 0.0556$
Final R indexes [all data]	$R_1 = 0.0217$, $wR_2 = 0.0558$
Largest diff. peak/hole / $e \text{\AA}^{-3}$	0.27/-0.22
Flack parameter	0.028(14)

A5.2 REFERENCES

- (1) Sheldrick, G. M. Phase Annealing in SHELX-90: Direct Methods for Larger Structures. *Acta Crystallogr. A* **1990**, *46*, 467–473.
- (2) Sheldrick, G. M. Crystal Structure Refinement with *SHELXL*. *Acta Crystallogr. Sect. C Struct. Chem.* **2015**, *71*, 3–8.
- (3) Müller, P. Practical Suggestions for Better Crystal Structures. *Crystallogr. Rev.* **2009**, *15*, 57–83.

ABOUT THE AUTHOR

Sepand K. Nistanaki was born on September 30th, 1993 in Neuchâtel, Switzerland and was raised in Tustin, California by his Iranian parents along with his younger brother. He attended Arnold O. Beckman High School and graduated in 2012. He then began his undergraduate studies at UC Berkeley and ultimately earned a B.S. in Chemistry in 2016. While at UC Berkeley, he pursued undergraduate research in the lab of professor Christopher Chang on the synthesis of transition metal complexes for electrocatalytic CO₂ reduction.

In the summer of 2017, Sepand returned to Southern California to begin his PhD studies under Professor Hosea Nelson at UCLA. In 2021, he transferred with the Nelson group to Caltech to continue his PhD studies. During his graduate career, Sepand has worked on several projects involving the application of Dewar heterocycles and vinyl carbocations to organic synthesis. Following the completion of his PhD, Sepand will be moving to Cambridge, MA to begin his postdoctoral fellowship in the lab of Professor Eric Jacobsen at Harvard University.